IDENTIFICATION OF *bptA* (*bbe16*) AS AN ESSENTIAL GENE FOR THE PERSISTENCE OF THE LYME DISEASE SPIROCHETE, *BORRELIA BURGDORFERI*, IN ITS NATURAL TICK VECTOR

APPROVED BY SUPERVISORY COMMITTEE

_____
Michael V. Norgard, Ph. D., Professor, Chairman
Department of Microbiology,
U.T. Southwestern Medical Center at Dallas, Dallas, Texas

_____
Eric J. Hansen, Ph. D., Professor
Department of Microbiology,
U.T. Southwestern Medical Center at Dallas, Dallas, Texas

_____
Kevin McIver, Ph. D., Assistant Professor
Department of Microbiology,
U.T. Southwestern Medical Center at Dallas, Dallas, Texas

_____
Vanessa Sperandio, Ph. D., Assistant Professor
Department of Microbiology,
U.T. Southwestern Medical Center at Dallas, Dallas, Texas

DEDICATION

To my parents James and Louise Revel, my sister and brother-in-law
Lori and Scott Harrison, and my nephews Colin and Braden Harrison.
For your unconditional love, support, and encouragement;
I will be eternally grateful.

Also in memory of my namesakes Dr. Vernon Andrew Suydam, Ph. D.
and Mrs. Lorraine Thomas Revel.

IDENTIFICATION OF *bptA* (*bbe16*) AS AN ESSENTIAL GENE FOR THE PERSISTENCE OF THE LYME DISEASE SPIROCHETE, *BORRELIA BURGDORFERI*, IN ITS NATURAL TICK VECTOR

by

ANDREW THOMAS REVEL, M.S.

DISSERTATION

Presented to the Faculty of the Graduate School of Biomedical Sciences

The University of Texas Southwestern Medical Center at Dallas

In Partial Fulfillment of the Requirements

For the Degree of

DOCTOR OF PHILOSOPHY

The University of Texas Southwestern Medical Center at Dallas

Dallas, Texas

March 9, 2005

Copyright

by

Andrew Thomas Revel, M.S., 2005

All Rights Reserved

IDENTIFICATION OF *bptA* (*bbe16*) AS AN ESSENTIAL GENE FOR THE PERSISTENCE OF THE LYME DISEASE SPIROCHETE, *BORRELIA BURGDORFERI*, IN ITS NATURAL TICK VECTOR

Publication No. _____

Andrew Thomas Revel, M. S.

The University of Texas Southwestern Medical Center at Dallas, 2005

Mentor: Dr. Michael V. Norgard, Ph. D., Chair

Borrelia burgdorferi (*B. burgdorferi*), the agent of Lyme disease, is a zoonotic spirochetal bacterium that depends on both arthropod (*Ixodes* ticks) and mammalian (rodent) hosts for its persistence in nature. To more broadly survey *B. burgdorferi*'s adaptive responses to these two diverse environmental niches, DNA microarrays were constructed and utilized to identify potential virulence factors contributing to *B. burgdorferi*'s infectivity, pathogenesis, host range, and/or maintenance in its complex life cycle. Specifically, the microarray data provided a basis for formulating new testable hypotheses regarding the life cycle of *B. burgdorferi*. Recent advancements in borrelial genetics, some of which were developed in this study, provided us with the tools to genetically manipulate *B. burgdorferi*. Mutational analysis of two differentially regulated genes (*bba36* and *bbe16*) targeted from microarray data was performed in an attempt to ascribe a function to each gene. Although no phenotype could be found for *bba36*, *bbe16* was found to potentiate the virulence of *B. burgdorferi* in the mouse model of Lyme borreliosis and was essential for the persistence of *B. burgdorferi* in *Ixodes scapularis* ticks. As such, we have renamed *bbe16* as a gene encoding borrelial persistence in ticks (*bptA*). Protease accessibility experiments indicated that BptA was a putative lipoprotein and was surface-exposed on the outer membrane of *B. burgdorferi*. Moreover, BptA also was shown to be highly conserved in all *B. burgdorferi sensu lato* strains tested, suggesting that BptA may be widely utilized by Lyme borreliosis spirochetes for persistence in nature. Given *B. burgdorferi*'s absolute dependence on and intimate association with both its arthropod and mammalian hosts, this study has provided evidence that *bptA* is a virulence factor critical for *B. burgdorferi*'s overall parasitic strategy.

Table of Contents

Page

PREVIOUS PUBLICATIONS..... xiii

LIST OF FIGURES..... xiv

LIST OF TABLES..... xvi

LIST OF APPENDICES..... xviii

LIST OF ABBREVIATIONS..... xix

ACKNOWLEDGEMENTS..... xxv

CHAPTER 1. *B. BURGDORFERI* LITERATURE REVIEW..... 1

I. Historical Perspective..... 1

II. Epidemiology..... 3

III. Clinical Presentation, Sequelae, and Diagnosis……..... 5

IV. Histopathology..... 9

V. Immune Involvement and Evasion..... 10

VI. Treatment..... 12

VII. Vaccinology..... 13

VIII. Animal Models..... 15

IX. Taxonomy..... 16

Page

X. Borrelial Structure..... 17

XI. Metabolism..... 19

XII. Genetic Content and Manipulation..... 20

XIII. Virulence Factors..... 22

A. OspA/B..... 22

B. OspC..... 23

C. DbpA/B..... 24

D. VlsE..... 26

E. OspE/OspF/Erps..... 27

F. RpoN/RpoS..... 28

G. PncA..... 30

H. BBK32 (P35, P47)..... 31

I. P66..... 32

CHAPTER 2. OVERALL OBJECTIVE AND SYNOPSIS..... 33

CHAPTER 3. MATERIALS AND METHODS..... 36

I. Bacterial Strains and Cultivation..... 36

A. *E. coli* strains, plasmids, and *in vitro* cultivation..... 36

B. *B. burgdorferi* strains and *in vitro* cultivation..... 36

C. Cultivation of *B. burgdorferi* within dialysis membrane chambers (DMC's). 37

Page

II. Transformation of Bacterial Strains..... 49

A. Electroporation of *E. coli*..... 49

B. Electroporation of virulent *B. burgdorferi*..... 50

III. DNA and RNA Isolation..... 52

IV. Microarray Technology..... 53

A. Microarray construction..... 53

B. Fluorescent probe labeling and hybridization for microarray analysis..... 54

C. Microarray data acquisition and analysis..... 56

D. Hierarchical cluster analysis of microarray data..... 57

V. Real Time RT-PCR..... 57

VI. Protein Expression, Purification, and Analysis Methodologies..... 58

A. Protein expression and purification..... 58

B. Generation of polyclonal antisera raised against recombinant proteins..... 63

C. Sodium dodecyl sulfate-polyacrylamide gel electrophoresis (SDS-PAGE)..... 64

D. Proteinase-K accessibility assay..... 66

E. Gene building..... 66

VII. Generation of Genetically-Engineered *B. burgdorferi* Strains..... 68

A. Generation of BBA36 mutants..... 69

Page

B. Construction of BbDTR630..... 72

C. Construction of pJD shuttle plasmids..... 74

D. Construction of BBE16 and BBE16/17 mutants and Complementation strains..... 78

VIII. Plasmid Profiling of *B. burgdorferi* Strains..... 84

IX. Methodologies Concerning *Ixodes scapularis*……..... 85

A. Generation of infected ticks and other tick studies..... 85

C. Evaluation of *B. burgdorferi* DNA in *Ixodes scapularis* ticks..... 87

C. Immunofluorescence Assays (IFAs) of *B. burgdorferi* in *Ixodes scapularis*..... 88

X. Histopathological and Serological Evaluation for *Borrelia burgdorferi* Infection Via Tick Infestation..... 89

CHAPTER 4. DNA MICROARRAY ANALYSIS OF DIFFERENTIAL GENE EXPRESSION IN *B. BURGDORFERI*..... 91

I. Introduction..... 91

II. Results and Discussion..... 92

A. B31 MI growth conditions for comparative transcriptional analyses…..... 92

B. Use of GDPs for cDNA labeling..... 93

Page

C. Global gene expression profiling..... 95

D. Concordance between microarray and Real-Time RT-PCR data..... 115

E. Distribution of expression patterns among the B31 MI replicons..... 115

F. Paralogous families..... 122

G. Functional classification of differentially expressed genes..... 123

H. Genes encoding putative signal sequences..... 129

I. Summary and implications..... 129

CHAPTER 5. DEVELOPMENT OF A NEW GENETIC COMPLEMENTATION STRATEGY REVEALS AN OCCULT DEFECT IN *B. BURGDORFERI*'S ABILITY TO BE TICK-TRANSMITTED..... 131

I. Introduction..... 131

II. Results..... 132

A. Marking of lp25 with *aph[3']-IIIa* (Kan^r) in strain BbDTR630..... 132

B. BbDTR630 has wild-type growth characteristics and differentially regulates its surface lipoproteins in a normal fashion..... 133

C. BbDTR630 retains infectivity for mice..... 139

D. BbDTR630 colonizes and is maintained within *Ixodes scapularis* ticks..... 141

E. Spirochete transmission from ticks to mice..... 142

III. Summary and Implications..... 143

Page

CHAPTER 6. *bptA* (*bbe16*) IS ESSENTIAL FOR THE PERSISTENCE OF *B. BURGDORFERI* IN ITS NATURAL TICK VECTOR..... 149

I. Introduction..... 149

II. Results..... 150

A. Cloning and disruption of *bba36* and *bptA*..... 150

B. Evaluation of the *bba36* and *bptA* mutants for virulence and pathogenesis after needle-inoculation of mice..... 152

C. Evaluation of the roles for *bba36* or *bptA* in ticks..... 162

D. BptA is protease-accessible and highly conserved in *B. burgdorferi sensu lato* strains..... 165

III. Summary and Implications..... 167

CHAPTER 7. DISCUSSION……..... 174

Appendix A. 190

Appendix B. 234

Appendix C. 281

Appendix D. 282

Appendix E. 283

REFERENCES..... 284

Page

VITA..... 324

PREVIOUS PUBLICATIONS

Revel AT, Talaat AM & Norgard MV. (2002). DNA microarray analysis of differential gene expression in *Borrelia burgdorferi*, the Lyme disease spirochete. Proc. Natl. Acad. Sci. U S A 99:1562-7.

Blick JS, **Revel AT** & Hansen EJ. (2003). FindGDPs: Identification of primers for labeling microbial transcriptomes for DNA microarray analysis. Bioinformatics 19:1718-9.

Hubner A, **Revel AT**, Nolen DM, Hagman KE & Norgard MV. (2003). Expression of a *luxS* gene is not required for *Borrelia burgdorferi* infection of mice via needle inoculation. Infect. Immun. 71:2892-6.

Blevins JS, **Revel AT**, Caimano MJ, Yang XF, Richardson JA, Hagman KE & Norgard MV. (2004). The *luxS* gene is not required for *Borrelia burgdorferi* tick colonization, transmission to a mammalian host, or induction of disease. Infect. Immun. 72:4864-7.

Revel AT, Blevins JS, Almazán C, Neil, L, Kocan KM, de la Fuente J, Hagman KE, and Norgard MV. *bptA* (*bbe16*) is essential for the persistence of the Lyme disease spirochete, *Borrelia burgdorferi*, in its natural tick vector. Proc. Natl. Acad. Sci. U S A, in press.

Revel AT, Blevins JS, Hagman KE, and Norgard MV. (submitted). Development of a new genetic strategy reveals an occult defect in *Borrelia burgdorferi*'s ability to be tick-transmitted.

Yang XF, Lybecker MC, Pal U, Alani SM, Blevins JS, **Revel AT**, Samuels DS, Fikrig E, and Norgard MV. (submitted). Analysis of the *ospC* regulatory element controlled by the Rrp2-RpoN-RpoS regulatory pathway in *Borrelia burgdorferi*.

LIST OF FIGURES

Page

1. *B. burgdorferi* life cycle in nature..... 6

2. Schematic of the construction of pDTR599..... 70

3. Schematic of the construction of pDTR630..... 73

4. Construction of the various pJD shuttle vectors……... 77

5. Construction of pDTR596..... 79

6. Construction of the complementation construct for the *bptA*-deficient mutant (BbDTR596)..... 82

7. Mouse chambers for isolation of infected ticks during tick infestation..... 86

8. SDS-PAGE and immunoblot analysis of whole-cell lysates of B31 MI..... 94

9. Correlation of cDNA labeling efficiencies..... 96

10. Number of genes differentially expressed during various B31 MI culture conditions..... 109

11. Cluster analysis of Microarray data (*chpAI* cluster)..... 110

12. Cluster analysis of Microarray data (*groES* cluster)..... 111

13. Cluster analysis of Microarray data (*hslV* cluster)..... 112

14. Cluster analysis of Microarray data (*ospA* cluster)..... 113

15. Cluster analysis of Microarray data (*ospC* cluster)..... 114

16. Correlation between microarray and real-time RT-PCR data..... 117

Page

17. Number and distribution of differentially expressed genes among B31 MI genetic replicons..... 118

18. Number of differentially expressed genes grouped by putative protein functions..... 125

19. Genetic (PCR) analysis of *B. burgdorferi* strains PL133 and BbDTR630..... 134-35

20. *In vitro* growth analysis of BbDTR630..... 137

21. Immunoblot analysis of differential expression profiles for BbDTR630..... 138

22. Histopathological analysis of mice infected with BbDTR630..... 140

23. Genetic analysis of *B. burgdorferi* strain BbDTR599..... 153-55

24. Genetic analysis of *B. burgdorferi* strain BbDTR596 and complemented strains..... 156-58

25. In vitro growth analysis of the insertional mutants (*bba36*$^-$ and *bptA*$^-$) and complemented strains of *B. burgdorferi*..... 159

26. Histopathological analysis of mice infected with either the *bba36*- or *bptA*-deficient *B. burgdorferi* strains..... 160

27. Spirochete loads of *I. scapularis* larvae infected with either PL133 or BbDTR596..... 164

28. Protease accessibility of BptA in *B. burgdorferi* grown under various culture conditions..... 166

LIST OF TABLES

Page

1. Strains used in this study..... 38-41

2. Plasmids used in this study..... 42-47

3. Genome-directed primers specific for *B. burgdorferi* B31 MI..... 58

4. Real-time RT-PCR primers for B31 MI gene detection..... 59

5. Oligonucleotides used to clone protein expression constructs..... 61

6. Oligonucleotides used in the construction and validation of BbDTR599..... 69

7. Oligonucleotides used in the construction and validation of BbDTR630..... 72

8. Oligonucleotides used in the construction of the pJD shuttle vectors..... 76

9. Oligonucleotides used in the construction and validation of BbDTR596..... 80

10. Gene expression variations greater than 1.8-fold comparing *in vitro* 23°C, pH7.5 (UT) to *in vito* 37°C, pH6.8 (FT)..... 97-101

11. Gene expression variations greater than 1.8-fold comparing *in vitro* 37°C, pH6.8 (FT) to DMCs..... 102-105

12. Gene expression variations greater than 1.8-fold comparing *in vitro* 23°C, pH7.5 (UT) to DMCs..... 106-108

13. Concordance between Real-Time RT-PCR and microarray data..... 116

14. Determination of ID_{50} values for PL133 and BbDTR630 in C3H mice..... 139

15. Acquisition and maintenance of *B. burgdorferi* strains by *I. scapularis* and subsequent tick transmission of spirochetes to mice..... 143

Page

16. Determination of ID_{50} values for PL133 and various mutant and complemented strains of *B. burgdorferi* in C3H mice..... 161

17. IFA- and PCR-detection of various *B. burgdorferi* clones harbored within larval and nymphal forms of *I. scapularis* over time..... 163

18. Percent amino acid similarities and identities (in parentheses) of BptA homologs present among *B. burgdorferi sensu lato* strains tested…….. 167

LIST OF APPENDICES

Page

A. Microarray data for all genes grown under the following conditions: UT, FT, and DMCs (204)..... 190-233

B. Microarray data from the following conditions (unpublished data): room temperature, pH 6.8, room temperature, pH 8.0; 37°C, pH 7.5; and 37°C, pH 8.0..... 234-280

C. Proteinase K accessibility data for selected *B. burgdorferi* proteins..... 281

D. Evaluation of protective capabilities of selected immunogens from *B. burgdorferi* when mice are needle-challenged with 1 x 10^3 spirochetes..... 282

E. Evaluation of protective capabilities of BptA as a vaccinogen when mice are challenged with *B. burgdorferi*-infected ticks..... 283

LIST OF ABBREVIATIONS

297	*Borrelia burgdorferi* strain 297
21038	*Borrelia andersonii* strain 21038
aa	amino acids
A	adenine
B. burgdorferi	*Borrelia burgdorferi*
B31 MI	*B. burgdorferi* strain B31 MI
Bb	*B. burgdorferi*
B. afzelii	*Borrelia afzelii*
B. andersonii	*Borrelia andersonii*
B. bissettii	*Borrelia bissettii*
B. garinii	*Borrelia garinii*
B. hermsii	*Borrelia hermsii*
B. japonica	*Borrelia japonica*
B. valaisiana	*Borrelia valaisiana*
BID	Bis In Die (Twice Daily)
BME	β-mercaptoethanol
BO23	*Borrelia afzelii* strain BO23
bp	base pair
bpt	borrelial persistance in ticks
BSK-H	Barbour Stoenner-Kelley-H complete media

C	cytosine
CDC	Centers for Disease Control
CFA	Complete Freund's Adjuvant
CFU	colony-forming unit
CNS	Central Nervous System
Collab.	collaboration
cp	circular plasmid
Dbp	decorin binding protein
DMC	dialysis membrane chambers
DMSO	Dimethyl Sulfoxide
DN127	Borrelia bissettii strain DN127
°C	degrees Celcius
DNA	Deoxyribonucleic acid
DEPC	diethyl pyrocarbonate
dNTP	dideoxy-nucleotide triphosphate
DTT	Dithiothreitol
EBP	enhancer-binding protein
ECM	Erythemous Chronicum Migrans
E. coli	*Escherichia coli*
EDTA	Ethylenediamine-Tetraacetic Acid
EM	Erythemous Migrans
EPS	Electroporation Solution

Erm	Erythromycin
Erp	OspEF Related Protein
FITC	fluorescein isothiocyanate
Fla	Flagellar
FPLC	Fast Performance Liquid Chromotography
FT	Fed Tick
g	gravity
G	guanine
GDP	genome directed primers
GST	glutathione S-transferase
h	hour(s)
H&E	Hemotoxylin and Eosin
ICFA	Incomplete Freund's Adjuvant
ID	Intradermal
ID50	50% infectious Dose
IFA	immunofluorescence assay
IKA2	*Borrelia japonica* strain IKA2
IP	intraperitoneal
IP90	*Borrelia garinii* strain IP90
IPTG	β-D-thiogalactopyranoside
I. pacificus	*Ixodes pacificus*
I. ricinus	*Ixodes ricinus*

I. scapularis	*Ixodes scapularis*
JRA	Juvenile Rhuematoid Arthritis
Kan	kanamycin
kB	kilobase
kVolt	kilovolt
kD	kilodaltons
LB	Luria-Bertani
lp	linear plasmid
Lp	lipoprotein
LPS	Lipopolysaccharide
mA	milliampere
MAb	monoclonal antibody
mlp	multicopy lipoprotein
MWCO	Molecular weight cut-off
N40	*Borrelia burgdorferi* strain N40
OD	Optical density
OM	Outer Membrane
OMP	outer membrane protein
ORF	open reading frame
Osp	outer surface protein/outer surface (lipo)protein
PAGE	polyacrylamide gel electrophoresis
PBi	*Borrelia garinii* strain PBi

PBS	phosphate-buffered saline
PBS-Tween	phosphate-buffered saline-tween-20
PCR	polymerase chain reaction
pI	isoelectric point
PMSF	phenylmethylsulfonylfluoride
PG	peptidoglycan
QID	Quarter In Die (Four times a day)
RNA	Ribonucleic acid
rpm	revolutions per minute
Rpo	RNA polymerase
Rrp	response regulator protein
RT-PCR	real time PCR
SD	standard deviation
SDS	sodium dodecyl sulfate
SDS-PAGE	sodium dodecyl sulfate-polyacrylamide gel
SOC	super optimal catabolite
SPI	signal peptidase I
SPII	signal peptidase II
Spec	spectinomycin
Strep	streptomycin
SQ	subcutaneous
SSC	saline-sodium citrate

T	thymine
UT	unfed tick
V	volt
Vls	*vmp*-like sequence
VS116	*Borrelia valaisiana* strain VS116
X-gal	5-bromo-4-chloro-3-indolyl β-galactopyranoside

ACKNOWLEDGEMENTS

I first want to thank my mentor, Dr. Michael V. Norgard, for his unwavering support for me as an individual as well as my research on Lyme disease. His desire to foster free thought and scientific independence resulted in a productive, enlightening, and pleasant environment in which to grow as a scientist while performing my graduate research.

Additionally, I am indebted to my dissertation committee members, Drs. Eric Hansen, Kevin McIver, and Vanessa Sperandio, for taking time to assist in my training. Their support as well as constructive criticism of my research is greatly appreciated.

As with any venture in one's life, success is the result of a concerted effort by many parties working together for a common goal. Therefore, I must acknowledge three key co-workers for their exceptional day-to-day guidance, collaborations, and friendship. Most notably is Dr. Kayla Hagman, whom I had the privilege of working with when I rotated though the Norgard lab. She spent much personal time getting me oriented and indoctrinated into the Norgard lab. Over the years, she has been one of my greatest supporters and has become a valued friend. Her unselfish devotion of her time and effort warrants very special recognition and appreciation. Even though Dr. Jon Blevins joined the lab only during my last two years at UT-Southwestern, he has quickly become a trusted colleague that I will sorely miss. Our synergism in discussions and in the execution of ideas will be hard to

reproduce elsewhere. I must also recognize Jason Mock for his helpful scientific discussions, friendship, and putting up with my dog, Sophie, and me as roommates. Collectively, all three helped keep me sane and positive throughout my tenure here at UTSW.

My cousin, Dr. Molly Isbell Lewis, was invaluable in the statistical analysis of the complex microarray data. With her help, statistics finally made sense. Many thanks go to Lori Neil for her expertise with protein chemistry. She made the tasks of protein purification enjoyable. I also want to thank the anaplasmosis group at Oklahoma State University for collaborating with us on our studies to uncover the role that *bptA* plays in *B. burgdorferi*. Without them, we would have had difficulties in obtaining larvae loaded with the various borrelial strains. Additionally, I want to thank the microarray core facility at UT-Southwestern for providing the scanning equipment and analysis software packages.

Finally, I would be remiss to not mention others who have been supportive in many different facets of this endeavor. Thanks goes to the other members of the Norgard lab: Dr. Xaiofeng Yang, Dr. Jeanne Sheffield, Dr. Jason Huntley, Dr. Ranjit Deka, Dr. Carson Harrod, Patrick Coneley, and Martin Goldberg. Former members of the lab, which I must acknowledge, are Drs. Anette Hübner, Deborah Bouis, and Ms. Dena Nolen. I also thank the remaining faculty and graduate students of the Molecular Microbiology Graduate Program for making my time at UTSW a very enjoyable and fruitful experience.

CHAPTER ONE.

BORRELIA BURGDORFERI LITERATURE REVIEW

I. Historical perspective

Borrelia burgdorferi (*B. burgdorferi*), the etiological agent of Lyme disease (Lyme borreliosis), subsists within a complex enzootic life cycle that involves arthropod (*Ixodes* ticks) and mammalian (rodent) hosts (230). Whereas this syndrome was recognized on the North American continent only 25 years ago (230), a Lyme disease-like syndrome was reported in Europe in the early 1900's (122), which subsequently was shown to be caused by either of the European Lyme disease spirochetes, *Borrelia afzelii* (*B. afzelii*) or *Borrelia garinii* (*B. garinii*). These and other reports (2) from European sources described an erythemous annular skin lesion (acrodermatitis chronica atrophicans) following a tick bite. Although many European researchers studied these skin lesions, which were later termed either erythema migrans (EM) for short term rashes or erythema chronicum migrans (ECM) if they persisted for greater than a month (44), it was not until the 1950's that research indicated that EM lesions were possibly of bacterial origin (28, 124). It was eventually shown that EM lesions were abrogated by the administration of low doses of penicillin. Even though researchers used the EM and ECM data to hypothesize that the EM lesions were the result of the transmission of spirochetes from infected ticks, it was not until 1982 that the causative agent of Lyme disease in North America was successfully isolated (45).

Although reports of EM lesions in North America were documented as early as the 1970's (220), it took nearly a decade for the discovery of the causative agent and its zoonotic life cycle. These series of events were precipitated by the action of worried parents of children stricken with juvenile rheumatoid arthritis (JRA) in Lyme, Connecticut. The number of cases of JRA in this quaint township in Connecticut was unusual in that JRA is quite rare and cases do not typically cluster to geographical locales. The concerned parents contacted the Connecticut State Health Department, which then initiated an investigation of the JRA cases in Lyme township to be headed by the Yale University School of Medicine section of rheumatology. Even though EM lesions were evident in a large proportion of the children, similar to disorders involving EM lesions in Europe, the Lyme cases featured the sequelae of late onset arthritis leading to the previously discussed misdiagnosis of JRA. By the late 1970's, researchers proposed that the geographical clustering and seasonality of the cases were indicative of an infectious agent, possibly transmitted by an arthropod vector (237). It was in the early 1980's when Dr. William Burgdorfer demonstrated that sera from Lyme disease infected patients reacted with spirochetes (*B. burgdorferi*) isolated from *Ixodes scapularis* (*I. scapularis*) ticks (45), Jorge Benach isolated spirochetes from the blood of two patient (26), and Alan Steere isolated spirochetes from human EM lesions (235). Shortly thereafter, researchers were able to isolate *B. afzelii* and/or *B. garinii* from European patients with EM lesions, Bannwarth's syndrome, meningoencephalitis (swelling of the meninges), or acrodermatitis (1, 14, 194, 226). Moreover, the efforts of Alan Barbour in the elucidation of growth medium (BSK-II) suitable for *in vitro* cultivation of *B. burgdorferi* were critical for

these historical discoveries listed above, as well as the many others concerning *B. burgdorferi* that have followed (19, 45).

II. Epidemiology

Globally, the geographical range of the Lyme disease spirochetes*, B. burgdorferi sensu lato* (Lyme disease spirochetes in the large sense, *includes B. burgdorferi, B. garinii, and B. afzelii*), is in the upper latitudes of North America, Europe, and Asia which coincides with the location of the terminal moraine of glaciers around 15,000 years ago (232). The geographical range of the North American Lyme disease spirochete*, B. burgdorferi sensu stricto* (*B. burgdorferi* in the strict sense), is localized to three foci centering in the northeastern to mid-Atlantic states, the upper mid-west, and the pacific northwest (230-232). However, even though 49 states and the District of Columbia have reported cases of Lyme disease, ninety-five percent of all cases come from 13 states in the northeastern US (60). After the CDC formally recognized Lyme disease in 1982, there has been nearly a 600% increase in the number of annually reported cases in the US with greater than 157,000 cases in total. These sharp increases in incidence rates have made Lyme disease the most prevalent vector-borne disease in the US (230). Moreover, there is a growing body of evidence of an emerging Lyme disease-like syndrome (Southern tick-associated rash illness [STARI]) in the southeastern US (47, 171, 174, 257); however, recent results indicate that this bacterium, *Borrelia lonestari* (*B. lonestari*), is more closely related to the relapsing fever spirochete,

Borrelia hermsii (*B. hermsii*) (15). The increased rates of infection of these and other zoonotic diseases (i.e., erlichiosis, babesiosis, relapsing fever, and Rocky Mountain spotted fever) has prompted the CDC to classify them as emerging diseases.

In North America, *B. burgdorferi* is transmitted by various hard ticks of the *Ixodes ricinus* complex, including *I. scapularis* and *Ixodes pacificus*, whereas for the European/Asian spirochetes, *B. afzelii* and *B. garinii*, are primarily transmitted by *Ixodes ricinus* and *Ixodes persulcatus*, respectively (45, 46, 229, 231). The higher prevalence of Lyme disease in the northeastern US is a result of the ecology of *B. burgdorferi* (231). In the northeastern US, the natural reservoir of the spirochete is the white-footed mouse (*Peromyscus leucopus*), whereas in the Pacific Northwest, the natural reservoir is the dusky-footed woodrat (*Neotoma fuscipes)*. *I. scapularis* feeds on both small rodents like the white-footed mouse and humans, whereas *Ixodes pacificus* feeds primarily on lizards and humans. Therefore in the Pacific Northwest, only a small percentage of the *Ixodes pacificus* ticks contain *B. burgdorferi* (1-3% as compared to 20-80% of *I. scapularis* ticks in the northeast) and thus are less able to transmit the spirochetes to humans (222), resulting in a lower incidence of disease. The primary vector for transmission *of B. burgdorferi* within the dusky-footed woodrat population is *Ixodes neotomae*, which rarely feed on humans.

Irrespective of the specific *Ixodes* tick, all ticks require a blood meal at each of their three stages of tick development (larval, nymphal, and adult) over their two-year life span. Typically, the larval and nymphal ticks feed upon a small rodent (or lizard in the case of the *Ixodes neotomae*) in late spring/early summer, whereas the adult tick feeds on larger mammals such as the white-tailed deer. This latter host has given rise to the popular

reference of *Ixodes* ticks as the "deer tick". Of note, there is no vertical transmission (i.e., trans-ovarian transmission) of the spirochete from adult female to offspring (169, 222, 231); therefore, horizontal transmission from an infected nymphal ticks to a sterile mammalian host and back to a sterile larval tick is essential for maintenance of the spirochete in nature (Figure 1). The deer is an insufficient reservoir for *B. burgdorferi* (74).

The relatively recent emergence of Lyme disease in the US is a result of two factors: federal protection of deer populations and urban population expansion into historically rural areas (267). Increased deer populations have resulted in an increase of the Ixodid populations, as the deer is an important host for the last (adult) stage of the tick's three-stage life cycle. Typically, the spirochete is transmitted to the incidental human host when an infected nymph comes in contact and feeds upon a human subject.

III. Clinical Presentation, Sequelae, and Diagnosis

Lyme disease is a progressive disorder consisting of three distinct, yet sometimes overlapping, stages: (i) localized infection resulting in a characteristic "bull's-eye lesion" (erythema migrans, EM) presenting 3-14 days post tick bite, (ii) early (acute) disseminated infection persisting for days to weeks involving the nervous system, heart, and joints, and (iii) late (chronic) disseminated infection persisting for months to years (222, 230, 231).

Transmission of *B. burgdorferi* from the tick to mammalian host occurs over a minimum of 48-72 hours after the tick has attached for a blood meal (70, 182, 222, 231).

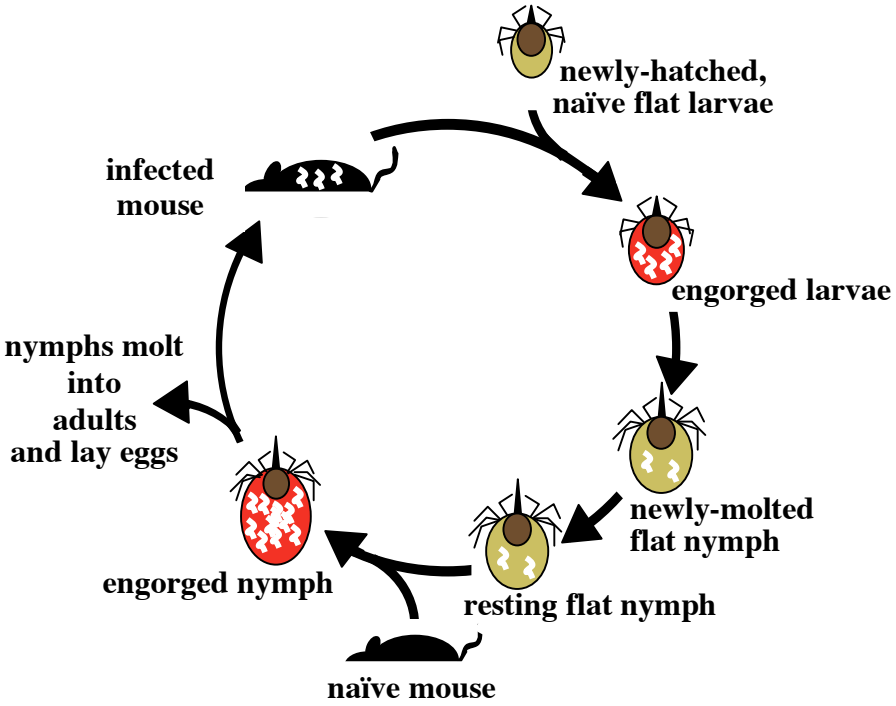


Fig. 1. *B. burgdorferi* life cycle in nature. Sterile larvae become infected after feeding upon infected mice or small rodents. The repleted larvae proceed through the molting process to emerge as nymphs. After a period of weeks to months, the nymphal ticks feed to repletion upon a naive mammalian host, thus transmitting the spirochetes to the new host and completing the bacterial life cycle. Of note, the spirochetal load represented graphically in this figure correlates with the observed bacterial loads at each phase of *B. burgdorferi*'s life cycle in nature.

Once transmission has occurred, localized inflammation, likely due to an innate immune response by macrophages and dendritic cells to spirochetal lipoproteins (164, 165, 181, 203, 205, 231, 248, 258, 260) results in a red macule or papule at the site of tick bite (222, 230, 231). If untreated, 60-90% of patents will develop a lesion that can expand to up to 70 cm in diameter (median 15 cm) to form a large, annular erythemous lesions consisting of concentric rings of variable degrees of clearing. Other sequelae including general malaise, myalgia, arthralgia, headaches, regional lymphoadenopathy, and fever may develop during the primary (localized infection) and secondary (early dissemination) stages of infection.

Early dissemination of *B. burgdorferi* in the mammalian host (stage two) is characterized by the progression of disease to include the nervous and musculoskeletal systems, as well as the aforementioned symptoms of the primary stage (i.e., general malaise, myalgia, arthralgia, headaches, etc). Nearly 50% of untreated patients develop secondary EM lesions anywhere on the body, which typically are smaller in size as compared to the primary EM lesion at the site of inoculation. Resolution of epidermal involvement (EM lesions) occurs usually within one month, but if untreated, the disease typically progresses to other organs. Neurological involvement ($\geq$15%) can result in optic neuritis, meningitis, and radiculoneuritis, but more commonly is typified by facial palsy (Bell's palsy). Inflammation of the cardiac tissues and aortic root resulting in a high-degree atrioventricular block (heart block) and subtle myocarditis can occur in up to 10% of patients, yet it usually resolves spontaneously. The most notable sequelae of secondary Lyme disease is acute inflammatory arthritis, which is either monoarticular or oligoarticular in nature affecting the large joints

(i.e., the knees). Even though spirochetes can be cultured from infected tissues, spirochetes are not reliably cultured from the blood (only 40-50%).

If the disease remains untreated, patients progress to chronic Lyme disease, which usually becomes a life-long disease with a high degree of morbidity. Erythematous lesions are not typical in stage three; however, neurological (sensory polyneuropathy, cognitive disturbances, subtle encephalopathy, insomnia) and musculoskeletal (oligoarticular arthritis) involvements remain hallmark symptoms. The observed concordance between *B. burgdorferi*-infected patients that develop antibiotic treatment-resistant arthritis ($\geq$10%) and those patients with certain HLA-DR4 alleles has lead some researchers to postulate that chronic inflammatory arthritis might be an autoimmune disorder (111, 179, 234, 236). Moreover, some researchers have presented evidence that certain epitopes on the borrelial protein, OspA, may mimic a protein that is expressed on T cells in synovium (mammalian protein, LFA-1), thus inducing an autoimmunity-based arthritis (111, 261). Even though rheumatological manifestations are more prevalent in the United States, neurological complications are most frequent in European cases, depending on the borrelial genospecies responsible for infection. In either case, neuroborreliosis occurs in about 5% of Lyme disease patients, progresses slowly over the course of months to years and, responds inconsistently to treatment. There have been no reports of transplacental infection during pregnancy (3, 89).

Clinical diagnosis of Lyme disease is typically formulated by (i) recognition of characteristic clinical findings (i.e., EM lesions), (ii) history of exposure to an area endemic for *B. burgdorferi* or Ixodid ticks, and (iii) in some cases, reactive antibodies to borrelial antigens by ELISA and/or Immunoblot analysis (61, 222, 231). Whereas presentation with

an EM lesion is the most reliable and preferred clinical indicator for Lyme disease, 20% of patients do not develop EM lesions and the other two criteria are necessary for diagnosis. Moreover, serological testing within the first few weeks of infection is unreliable due to the slow development of a borrelial-specific humoral response. Typically, only 20-30% of patients exhibit a strong serological response within the first two weeks after infection. Serological diagnosis is more reliable after two weeks when 70-80% of patients will test positive for borrelial-specific antibodies. However, serological testing will not differentiate between active and inactive infection. Culturing of the spirochete from tissues is not typically a criteria for diagnosis of Lyme disease for several reasons: (i) culturing of *B. burgdorferi* is expensive, (ii) growth rate of the spirochete *in vitro* is prohibitively slow, (iii) sample collection from the patient is invasive, and (iv) culturing of the spirochete from tissue or blood samples is not reliable. PCR has been utilized in some cases for the detection of spirochetal DNA in synovial fluid when spirochetes are not culturable (179), but this practice is not recommended and interpretations are controversial.

IV. Histopathology

The histopathology underlying the EM lesions is remarkably similar in all three stages of infection. The primary EM lesions are the result of moderate perivascular cellular infiltrate composed of macrophages, lymphocytes, plasma cells, and mast cells (76, 77, 233). Mild vasculitis and hypercellular vascular occlusions may be evident in some patients. Acute

disseminated borreliosis in the distant tissues (heart, joint, CNS, etc) exhibits similar infiltrate profiles to that observed in the primary EM lesion. However, the pathology elicited during chronic disease is markedly different. The persistent infiltration of macrophages, lymphocytes, neutrophils, plasma cells, and mast cells in the joints results in chronic arthritis and synovitis. Some patients may develop varied degrees of proliferative synovitis, which can lead to endarteritis obliterans (76, 77).

V. Immune Involvement and Evasion

Upon infection of the skin, it is believed that Langerhans dendritic cells are the first line of defense for the innate immunity of the host and help lead to the infiltration of phagocytic cells such as macrophages (233). Langerhans cells likely detect the plentiful lipoproteins (34, 135, 201, 202) through the pathogen-associated molecular pattern (PAMP) receptor, TLR-2. In fact, TLR-2 (-/-) mice harbored 100-fold more *B. burgdorferi* in infected tissues as compared to their TLR-2 (+/+) littermates. Moreover, the TLR (-/-) mice showed greater degrees of arthritis suggesting that TLR-2 is an important mediator of the innate immune response to *B. burgdorferi* infection. Activation of Langerhans cells and macrophages result in the release of the proinflamatory cytokines TNF-α and IFN-γ (105, 176) which is vital for the development of the Th1-dependent humoral response (112). Severe combined immunodeficiency disease (SCID) mice infected with *B. burgdorferi* had greater degrees of arthritis and carditis (213) suggesting that the innate immunity-induced

infiltration of macrophages and neutrophils is largely responsible for the immunopathogenesis of disease. Another arm of the early innate immune response to infection by *B. burgdorferi* is the role of host complement and subsequent lysis of the spirochete. Several bacterial lipoproteins have been shown to bind complement host factor H and factor H-like protein 1 (147), and the presence of these bacterial proteins correlates with higher spirochetal loads in infected tissues (156).

With observed disease sequelae thought to be mediated through cytokines (i.e., IL-1β, IL-6 and TNF-α), a role for T cells in disease progression is plausible, however the contribution of T cells is unclear. Cytokine profiles from Lyme disease patients indicate that there is a higher Th1 to Th2 T cell response, a finding that correlates with greater disease severity (112, 276). In support of the observed disparity of the Th1/Th2 response, C3H/HeJ mice (higher Th1 to Th2) are susceptible to infection while Balb/C mice (higher Th2 to Th1) are resistant (144). However, it also has been shown that a Th1 response is necessary for natural regression of Lyme carditis (32). Even though the involvement of T cells is unknown, it was shown very early that the development of a humoral response is vital for clearance of the bacterial infection (23). Antibodies elicited to two major lipoproteins (OspA & B) account for the majority of the protective antibodies produced when *in vitro* propagated, heat-killed *B. burgdorferi* are injected into mice (65, 94, 208).

Further support for the importance of a humoral response to Lyme disease is that the bacterium expends much energy and genomic content for what researchers presume to be antigenic variation/modulation strategies so the spirochete can stay ahead of the adaptive immune response in the mammalian host (120, 159, 243, 264, 277). Although not

definitively proven, antigenic variation is thought to be operative in *B. burgdorferi*, and is hypothesized to be accomplished by the *vmp*-like sequence (Vls) antigenic variation system (278). This system is thought to be primarily active during mammalian infection (279). Antigenic modulation is thought to be accomplished by the expression of certain members of various paralogous families (i.e., *erp*s) throughout mammalian infection resulting in a heterogeneous population of *B. burgdorferi* (120, 243). Another example of antigenic modulation in *B. burgdorferi* is a mechanism that suppresses expression of OspC in the presence of anti-OspC antibodies (161). However, it must be pointed out that neither antigenic variation nor antigenic modulation have been proven to operative during evasion of the immune system by *B. burgdorferi*. A third mechanism employed by this spirochete, yet at a much lower level, is dissemination into immune privileged sites such as the CNS (87, 177, 184).

VI. Treatment

Typically, a 10- to 20-day course of 100 mg doxycycline BID (or 500 mg ampicillin TID) is prescribed for patients with early-localized disease, while a 20- to 30-day course of antibiotics is recommended for patients with disseminated disease (233). For patients allergic to penicillins or tetracyclins, cefuroxime, axetil or erythromycin (500 mg BID) can be used successfully. Neuroborreliosis requires intravenous antibiotic treatment with 2 grams ceftriaxone (QID) or a total of 20-million units penicillin-G daily (four equal doses

daily) for up to four weeks. Pregnant women and children under the age of eight are typically treated with 500 mg amoxicillin TID for 21-days instead of doxycycline. Within the first 24 hours of antibiotic treatment, approximately 15% of patients may develop a Jarisch-Herxheimer-like reaction, for reasons not totally clear since *B. burgdorferi* does not produce endotoxin. However, there are many lines of evidence to suggest that the release of the many lipoproteins of *B. burgdorferi* may be the cause of the observed Jarisch-Herxheimer-like reaction (180, 181, 200, 203, 205, 221). For treatment-resistant borreliosis (>60 days of antibiotics), anti-inflammatory treatments can be employed, as well as arthroscopic synovectomy in extreme cases (222, 231).

VII. Vaccinology

As mentioned previously, early experiments documented the importance of antibodies against the major lipoproteins of *B. burgdorferi* in the clearance of the bacterium from the mammalian host (23, 34, 92, 208). Both of the two outer surface lipoproteins (Osp) OspA & B were capable of eliciting antibodies with the ability to kill the spirochete *in vitro* and *in vivo* (when used in passsive immunization experiments) (65, 208). Research showed that antibodies elicited to these major lipoproteins were protective against infections; however, they were only protective if they were present prior to infection (31, 92). Moreover, even though OspA & B antibodies develop late in infection, they fail to clear the existing infection (3). Together, these data suggested, and later proved (96), that OspA & B are expressed

within the feeding tick (71, 218), and therefore are targets for antibodies during natural tick transmission. Further studies validated the efficacy of OspA as a vaccine target (188, 251), and in 1998, the FDA approved LYMErix as a vaccine against Lyme disease. The mode of protection was unique, in that the vaccine does not work like a classical vaccine (by inducing an immune attack upon the antigen within the human host). Instead, the anti-OspA antibodies, which are ingested during tick engorgement, (i) target OspA located on the surface of *B. burgdorferi* residing in the tick midgut, and (ii) inhibit the transmission of the spirochete from the tick to the human by destabilizing the bacterial outer membrane leading to cell death (65, 141). The vaccine is not universally protective, allowing for natural escape mutants with antigenically distinct OspA variants (95, 97, 207, 208, 262). Moreover, studies had shown that there was a large degree of heterogeneity within the OspA locus among natural isolates, especially within the three borrelia species (i.e., *B. burgdorferi, B. afzelii*, and *B. garinii*) (20, 138, 173, 263, 264, 282). Additionally, there were reports of potential autoimmunity-induced arthritis caused by the cross-reaction of antibodies elicited against OspA to certain HLA-DR4 alleles (111, 179, 234, 236). Due to these complications with the vaccine, the manufacturer (SmithKline Beecham) voluntary removed LYMErix from the market in 2002. One group has made attempts to modify the cross-reactive epitopes of OspA to reduce the induction of autoimmunity, but even they concede that a multi-valent vaccine would be optimal for controlling the incidence of Lyme disease (261).

Other vaccine targets have shown efficacy to varying degrees, including, DbpA (59, 114, 116-118), P35/BBK32 (91), Vra (BB0116) (151), and OspC (281). DbpA has gained the most attention since it was nearly 80% protective when tested in mice (116); however,

researchers went on to show that this protection was only achieved when DbpA-immunized mice were challenged with *in vitro*-propagated *B. burgdorferi* (117). DbpA-immunized mice infested with *B. burgdorferi*-infected ticks became infected with *B. burgdorferi*. With the growing number of Lyme disease cases annually, as well as the lack of a vaccine on the market, there is a renewed interest to identify new vaccine targets to combat this growing problem (233).

VIII. Animal Models

In nature, *B. burgdorferi* infects most warm-blooded animals that can harbor *Ixodes* ticks such as small rodents (i.e., mice, rats, rabbits), birds, and large mammals (8). Therefore, most animals used for biological research are amenable to Lyme borreliosis investigation. The mouse model is most widely used to investigate the host response as well as evaluation of viable vaccine targets (22-24, 238). However, infection rates are dependent on mouse strains (24). Studies indicate that 3-week old C3H mice are most susceptible to infection-induced carditis and arthritis (22, 24) and thus these are typically employed for virulence/pathogenesis studies. Additionally, even though mice develop acute arthritis and carditis, they do not develop chronic arthritis or carditis. Thus, non-human primates are typically used for chronic Lyme borreliosis studies (24, 185). Moreover, since mice fail to present with neuroborreliosis, rhesus monkeys are typically employed to investigate neurological complications to infection (185).

Since Lyme borreliosis is a paucibacillary disease, isolating large number of bacteria from a mammalian host is not plausible. As a result, a model was developed where bacterial suspensions are cultivated in dialysis membrane chambers (DMCs) implanted into the peritoneal cavities of either rats or rabbits, allowing for mammalian-specific antigenic modulation of the spirochete's expression pattern to occur (5). One drawback of this model is the inaccessibility of the immune system to the bacteria and thus an inability to study immune evasion.

IX. Taxonomy

In addition to the genera *Borrelia* (causing either Lyme disease or relapsing fever), the family *Spirochaetaceae* includes the genera *Leptospira* (causing leptospirosis) and *Treponema* (causing treponematoses like syphilis or gingivitis). Collectively, all bacteria that cause Lyme disease are classified as *B. burgdorferi sensu lato* (in the broad sense). In the US, *B. burgdorferi sensu stricto* (in the strict sense) is the only virulent Lyme disease spirochete, however, *B. afzelii* and *B. garinii* are responsible for illness in Europe and Asia. The European and Asian strains are quite different from the North American strain as noted earlier (see epidemiology). Moreover, differences in (i) rRNA gene restriction patterns, (ii) reactivity patterns with murine monoclonal antibodies, and (iii) protein electrophoresis patterns assist in the distinction between strains. *B. burgdorferi sensu lato* is thus divided

into three main groups: (i) *B. burgdorferi sensu stricto* (referred to as *B. burgdorferi* from this point forward), (ii) *B. garinii* (group 2), and (iii) *B. afzelii* (group 3) (17, 18, 238).

X. Borrelial Structure

A prominent characteristic of the family Spirochaetaceae is the slender, helically coiled, corkscrew structure of the bacteria. Unlike the treponemes, which have true spiral morphology, borreliae have a flat, planar wave structure (107). Unstained *B. burgdorferi* are visualized by either dark field or phase-contrast microscopy and measure 20-30 μm long by 0.2-0.3 μm wide (238). As with the other spirochetes, *B. burgdorferi* has a dual membrane structure akin to Gram-negative bacteria. However, unlike Gram-negative bacteria, borreliae contain no lipopolysaccharide (LPS) and also have a unique linkage of the thin peptidoglycan (PG) layer to the cytoplasmic membrane (rather than the outer membrane (101, 102, 249). This unusual linkage of the thin PG layer allows for space within the periplasm for the endoflagella, which are the organelles of spirochetal motility. The endoflagella originate at either pole of the bacteria and wrap around the protoplasmic cylinder toward the longitudinal midpoint (where they overlap). Each bacterium contains between 7-11 endoflagella composed almost entirely of the major flagella subunit protein, FlaB. Insertional mutagenesis of *flaB*, however, has revealed that the endoflagella serve not only for motility, but also for structural purposes (175). FlaB mutants lost their "spiral" morphology and became "rod" shaped, whereas the complemented strain regained motility and normal

morphology (211). Further evaluation of the flagellar motors has revealed that the two polar motors actually have asymmetrical rotation during translational motility (158). A unique result of the spirochetal structure and periplasmic flagella is the ability to swim in viscous fluids as well as to traverse tight junctions of cells (115). For this reason, the endoflagella are considered bacterial virulence factors and vital for dissemination within the host.

As mentioned previously, the outer membrane (OM) of the spirochete is devoid of LPS, which might account for the relative fragility of the bacterium to physical manipulation (i.e., centrifugation, electroporation, etc.). Whereas it is known that the bacteria does contain glycolipids, the cellular location, concentration, and immuno-stimulatory capacities of these glycolipids are unknown (25, 125). Another unique characteristic of *B. burgdorferi* is the abundance of lipoprotein genes in the genome of the bacterium (57, 101, 102). Bacterial lipoproteins are modified proteins with an amino-terminal N-acyl-S-diacylglycerylcysteine that is added post-translationally by the enzymes glyceryl transferase, O-acyl transferase, signal peptidase II, and N-acyl transferase (119). Most bacteria have relatively few lipoproteins encoded in their genomes (i.e., 3-4% for *Escherichia coli* [*E. coli*]; ref. 29), however, nearly 12% of the putative ORFs for *B. burgdorferi* are believed to be lipoproteins. Freeze-fracture/freeze-etch electron microscopy, surface protease accessibility, and OM fractionation analysis of the spirochetal OM has revealed an abundance of lipoproteins that decorate the surface of the bacteria (34, 37, 66-68, 135, 201, 202, 225). With the observation that bacterial clearance is almost entirely antibody mediated, many researchers are actively investigating the OM antigenic components, their potential as vaccine candidates, and their possible role in immune evasion.

XI. Metabolism

B. burgdorferi is a fastidious microaerophilic organism requiring a specialized, complex medium (Barbour-Stoenner-Kelley [BSK]) and low oxygen tension for *in vitro* cultivation (101, 102). The doubling time for the bacteria is extremely long, ranging from 10 to 50 hrs when grown at 37°C and ambient temperature (23°C), respectively (191). Bioinformatics analysis of the spirochete's genome indicates that many metabolic pathways are incomplete and thus unable to support bacterial viability *ex vivo* without supplementation with complex fatty acids, enzyme cofactors, nucleotides, and all amino acids (101, 102). *B. burgdorferi* does encode a complete glycolytic pathway and is hypothesized to primarily utilize glucose, but could also metabolize glycerol, glucosamine, fructose, and maltose as primary carbon sources. None of the gene products necessary for the tricarboxylic acid (TCA) cycle or oxidative phosphorylation pathways are present. The spirochete also lacks a respiratory electron transport chain to produce ATP, thus researchers believe that the bacterium utilizes substrate-level phosphorylation for the production of energy. These analyses support the hypothesis that *B. burgdorferi* has streamlined its metabolic capabilities to only those genes that are necessary for its parasitic survival within the environmental niches of the Ixodid tick and mammalian hosts.

XII. Genetic Content and Gene Manipulation

The *B. burgdorferi* genome was one of the first bacterial genomes to be sequenced by The Institute for Genomic Research (TIGR) in the mid-1990's (101, 102). Even though the genome is considered to be of relatively small size (1.4 Mb compared to 4.6 Mb for *Escherichia coli* [*E. coli*] and 6.2 Mb *for Pseudomonas aeruginosa*), *B. burgdorferi* has an extremely complex genetic organization. There are 853 predicted ORFs on the 0.9 Mb linear chromosome (21, 27), with an additional 970 predicted ORFs on the 20 linear and circular plasmids ranging in size from 5 kB to 56 kB (101, 102). Several studies from the Chaconas laboratory has elucidated the resolution of the unique terminal telomeres on the linear plasmids. First, they have shown that an essential, plasmid-encoded gene (ResT) is responsible for the catalytic cleavage and religation of the covalently-closed, ssDNA during cell replication (16, 48, 146, 255). The genome has a low G + C content overall (28.6%), with the chromosome at 28.6% and the plasmids ranging from 23.1% to 32.3%. The genome appears to be in a period of rapid collapse and selective pressure to evolve (57), which is apparent from the multitude of paralogous families (175) and pseudogenes. Much research has led to the contention that the majority of the virulence factors are plasmid-encoded because the loss of certain plasmids render the bacterium avirulent (108, 198, 199, 217, 269). It has been shown that the loss of at least two of the linear plasmids, lp25 and lp28-1, are detrimental to survival within a mammalian host (108, 198), yet nothing is known concerning chromosomal genomic loci that are essential for survival within the *Ixodes* tick.

A contemporary tenet in bacterial pathogenesis research is that one must be able to fulfill molecular Koch's postulates to confirm the involvement of a specific gene product in the virulence of the pathogen (88, 98). Genetic manipulation of infectious isolates of *B. burgdorferi* is in its infancy, but there has been great progress in the past several years. Even though there have been no reports of conjugation occurring in the spirochete, there is limited evidence of lateral gene transfer with a transducing phage, phiBB-1 (80, 81). There has been no progress to date in manipulating this phage for use in genetic studies of *B. burgdorferi*. Unlike some other bacteria, such as *Morexella catarrhalis* or *Streptococcus pneumoniae*, borreliae does not appear to be naturally competent. However, a low level of transformation can be achieved by electroporation of large concentrations of DNA.

In 1996, the first report of transformation of *B. burgdorferi* was presented when a mutated *gyrB* allele from borreliae conferring coumermycin resistance was transformed into a sensitive strain (206). The first report of targeted insertional gene disruption was performed two years later (240). Both studies utilized the *gyrB* allele that was sub-optimal due to the high rate of development of spontaneous coumermycin resistant non-mutant spirochetes. In 2000, two additional resistance markers, *ermC* from *Staphylococcus aureus* and *kan* from *Tn903* conferring erythromycin and kanamycin resistance, respectively, were introduced as genetic tools to study borrelial gene function (33, 210). Then in 2001, two vital advancements in *B. burgdorferi* genetics were reported: (i) development of the shuttle plasmid pBSV2 derived from the endogenous cp9 plasmid and (ii) transformation of an infectious isolate of *B. burgdorferi* (129, 246). Along with these two relatively recent advancements, other shuttle plasmids (78, 100), resistance markers (85, 100, 212), and

reporters (53, 78) have been developed and employed to uncover the molecular components contributing to *B. burgdorferi*'s host range and/or Lyme disease pathogenesis. To date, OspA has been shown to be essential for survival within the tick host (275). OspC and PncA have been shown to be essential for survival within the mammalian host (110, 187, 198). Also, a novel regulatory network involving the two alternative sigma factors RpoN and RpoS has been elucidated (129). Progress within the past decade thus has positioned the field to answer many more questions concerning the pathogenesis of Lyme disease.

XIII. Virulence Factors

A. OspA/B

The gene that codes for OspA is unarguably the most studied gene in *B. burgdorferi* to date, culminating in over 600 citations. This gene was identified in 1985 as the first gene in a two-gene operon with *ospB* (127). Researchers discovered that the protein encoded by *ospA* is a surface lipoprotein prominently expressed during growth *in vitro*, expressed in almost all natural isolates, elicits protective antibodies, and hypothesized to be a potential virulence factor (34, 214). These data prompted researchers to investigate and subsequently corroborate the utility of OspA as a vaccine (90, 214).

In a pivotal study in 1995, Schwan *et al.* discovered that OspA and OspB were preferentially expressed during growth of the bacteria within the tick host, rather than in the

mammalian host (216), placing into question the role of OspA as a virulence factor within the mammalian host. However, even though natural OspA-deficient clones have been isolated, none are infectious in the mouse, suggesting a role for OspA as a virulence factor (10). Conclusive evidence for OspA as a virulence factor came in 2004 when a deletion mutant of OspAB was shown to be infectious in mice, yet unable to colonize feeding ticks (275). This was the first description of a borrelial gene encoding a virulence factor for the tick, *I. scapularis*.

B. OspC

The outer surface lipoprotein OspC is an immunodominant protein encoded by the first circular plasmid-encoded gene to be identified in *B. burgdorferi* (103, 166). *ospC* resides on cp26, which also contains the gene that encodes the telomere resolvase (*resT*) (48). Even though the sequence of *ospC* is quite variable among various isolates, the primary amino acid sequence is much less heterogeneous than that of OspA (219). An early report of possible similarities between OspC and VlsE (see below) (167) prompted speculation that OspC might be involved in immune evasion; however, no antigenic variation has been observed for OspC (239). Schwan *et al.* and others discovered that OspC was reciprocally regulated with respect to OspA and that OspC was expressed during tick engorgement and growth within the mammalian host (182, 216). Both increased temperature (242) and decreased pH (52, 270) were later identified as environmental parameters influencing the

expression of OspC. Although multiple studies have implicated OspC as a component vital to the virulence of *B. burgdorferi* and as having a potential role in carditis (123), only recently has OspC been proven to be a virulence factor (110, 187). Experiments with an OspC mutant proved the necessity of this gene for infection of the mammalian host; however, the role of OspC in the migration of the bacteria from the tick midgut to the salivary glands during tick engorgement is controversial. One study concluded that OspC was essential for bacterial binding to the salivary glands (no mutants were detected in engorged tick salivary glands) (187), whereas another study was able to identify *ospC* mutants within the salivary glands (110). Ongoing studies will likely investigate (i) the potential tick receptor for OspC, (ii) the target of OspC in the mammalian host, and (iii) the regulatory cascade resulting in OspC induction (see RpoN/RpoS below).

C. DbpA/B

Once *B. burgdorferi* is transmitted from the tick to mammalian host, the spirochete must disseminate from the primary EM dermal lesion to secondary sites throughout the body. Within the dermal tissues, the bacterium must navigate through the extracellular matrix and connective tissues, which are composed of many complex molecules including collagen types I & III. Researchers were able to determine that virulent strains of the spirochete bind the small dermatan sulfate proteoglycan molecule decorin, which decorates collagen fibers, in a concentration-dependant manner (114). Two groups were then able to show that the

binding of mammalian decorin was due to a two-gene operon, which they designated decorin binding proteins B & A (113, 116). They were able to show that both gene products were surface exposed on *in vitro*-cultivated spirochetes. Further research found that *B. burgdorferi*-infected mice elicited DbpA-specific antibodies, suggesting that this gene product was expressed during natural infection (59). Mice passively-immunized with sera from DbpA-immunized mice were protected from infection when the mice were subsequently challenged intradermally with *B. burgdorferi* (118). Moreover, it was found that decorin-deficient mice (Dcn -/-) infected with wild-type *B. burgdorferi* had less severe arthritis, as well as fewer bacteria in all tissues (36), suggesting that DbpA accentuates virulence and pathogenesis possibly by interacting with the mammalian host directly. Other studies found that DbpA and DbpB bind different mammalian glycosaminoglycans, suggesting that each gene product potentially targets distinct cell types and thus each may influence pathogenesis differently (99). However, Hagman *et al.* discovered that DbpA was not a protective antigen when mice were infested with *B. burgdorferi*-infected *Ixodes* ticks (117). This result suggested that DbpA was not expressed by spirochetes within ticks, which was later proven (117). DbpA is expressed at an early time after tick-inoculation of the spirochete into the mouse tissues, as evidenced by antibodies to DbpA within two weeks after challenge. Perhaps DbpA is not surface-localized during natural infection, and thus would not interact directly with the host or be a target of bactericidal antibodies as other studies have suggested. This remains to be more completely elucidated. To date, no evidence has been reported to conclusively identify the role of DbpA in either the virulence or pathogenesis of *B. burgdorferi*.

D. VlsE

In 1997, a putative recombination-based immune evasion system, akin to the variable major protein system of *B. hermsii*, was first reported and denoted as the *vmp*-like sequences (*vls*) system in *B. burgdorferi* (277). This system employs one expression and fifteen donor cassette loci, whereby promiscuous recombination between the expression and donor cassettes could theoretically result in over a million different coding sequences within the expression loci (278, 279). The expression cassette, located on the linear plasmid lp28-1, is composed of six invariable and six variable regions (regions undergoing recombination with donor cassettes). Although VlsE is expressed *in vitro* at low levels, it was shown that VlsE is expressed at higher concentrations in (i) *in vitro* cultures co-cultivated with human endothelial cells (130), (ii) engorging ticks (133), and (iii) within the mammalian host (279). It has also been shown that the unknown recombinase responsible for the observed recombination is active only during growth within the mammalian host (133, 279). Moreover, antigenic variation of VlsE occurs at a higher rate in immunocompetent mice as compared with SCID mice, further suggesting a role for VlsE in immune evasion under immunological pressures. Furthermore, it is believed that VlsE is essential because lp28-1-deficient *B. burgdorferi* strains are avirulent in mice (152, 199). A recent report described the restoration of virulence after electroporation of the entire lp28-1 plasmid into an avirulent, genetically engineered lp28-1-deficient strain (108), thus providing further proof of a virulence-essential locus on lp28-1. However, no definitive study has been performed to

rule out the possibility of a second gene, other than *vlsE*, residing on lp28-1 that could also be necessary for virulence.

X-ray crystallographic analysis of VlsE supports earlier contentions that the six invariable regions play a role in overall structure of the protein (82). These regions were found to lie deep within the protein core, whereas the variable regions formed the surface-exposed loops. During infection of the mammalian host, all regions elicit antibodies. However, none produce protective antibodies due to the inaccessibility of antibodies to the buried invariable regions and the antigenic variation of the surface-exposed variable regions (i.e., immune evasion). Recently, the FDA has approved a diagnostic kit for the diagnosis of Lyme disease that uses the invariable-region six (IR6) peptide as a diagnostic reagent for the detection of VlsE antibodies (162).

E. OspE/OspF/Erp's

OspE, OspF, and the OspEF-related proteins (Erp's) are a family of membrane lipoproteins with high degrees of homology with one another (101). The *ospEF* transcript encodes two proteins that are accessible to antibodies in the engorging tick and mammalian hosts (6, 154, 178). The *erp*'s are comprised of six ORFs in four different operons on the circular plasmids cp32 (243). Most members of these families are differentially regulated similarly to OspC (i.e., higher expression in the engorged tick and mammalian host) (6, 120, 242, 270) and are believed to inhibit complement activity by binding factor H (7, 126, 147,

148, 172). Additional experiments have shown that even though OspE and OspF are expressed similarly to OspC, only OspF appears to be regulated by RpoS in the same manner as OspC (79, 270). However, no studies have conclusively proven a role for or the necessity of these genes in the virulence *of B. burgdorferi* or the progression of Lyme disease.

F. RpoN (σ^N, σ^{54})/RpoS (σ^S)

When sequencing the genome of *B. burgdorferi*, very little insight into potential regulatory pathways was garnered. The genome consists of only two sensor kinase/histidine kinase cognate two-component system pathway proteins (*rrp1/hk1* and *rrp2/hk2*) and two alternative sigma factors (*rpoN/rpoS*) (101). One group developed an insertional mutant of RpoS in an avirulent *B. burgdorferi* strain B31 MI and discovered that (i) the mutant displayed different protein profiles than that of wild-type bacteria in the stationary phase of growth and (ii) the mutant was less resistant to osmotic shock (84). Another group successfully produced an RpoS insertional mutant in an infectious strain of *B. burgdorferi* and determined that expression of the surface-localized lipoproteins OspC and DbpA were dependent on RpoS (129). Moreover, this study also determined that the only other alternative sigma factor of *B. burgdorferi*, RpoN, directly regulated RpoS. Although the researchers were able to restore the expression of OspC and DbpA upon complementation of RpoS in the mutants, virulence was not re-established. This is the first report of a regulatory pathway in *B. burgdorferi*, and the first report of the alternative sigma factor RpoN directly

regulating a second alternative sigma factor in a pathogenic bacterium. Another lab was able to successfully complement an *rpoS*⁻ mutant and restore virulence (51), thus confirming the central role of the RpoN-RpoS regulatory pathway for the virulence of *B. burgdorferi*.

In these initial reports, the only indication for a direct interaction of RpoS with the promoter of *ospC* and *dbpA* was based on bioinformatic predictions. A recent report now has shown that the expression of ospC in a surrogate RpoS-deficient *E. coli* system was dependent on the presence of RpoS from *B. burgdorferi* (79). Moreover, they have described a model similar to *E. coli* where an extended -10 promoter element is instrumental in the specificity and regulation of RpoS-dependent gene expression.

Even though RpoS is central to the general stress response in *E. coli*, there is no evidence that this gene provides the same function in *B. burgdorferi*. An RpoS-deficient mutant of *B. burgdorferi* was proficient in adaptation to various environmental stressors such as temperature shift, serum starvation, increased osmolarity, reactive oxygen intermediates, and changes in oxygen tension (51). The researchers did report a defect in survival of extreme pH (6.0) for the mutant. However, this analysis was performed in duplicate, had a *p*-value of 0.051, and was not performed on the complemented strain. Moreover, the role of RpoS at the low pH tested (6.0) is unclear since there is no indication that *B. burgdorferi* encounters such environmental parameters within its enzootic life cycle. Taken together, further research investigating the role for RpoS in the survivability of the spirochetes in extremely low pH environmental conditions is not worthwhile. Nonetheless, the researchers suggest that RpoS probably "serves as a stress-responsive activator of a subset of virulence determinants" (51).

With RpoN being classified as a regulator of the virulence factors OspC and DbpA, further research has been conducted to ascertain the enhancer-binding protein (EBP) that is also involved in this pathway. Bioinformatic analysis predicted and site-directed mutagenesis confirmed the involvement of Rrp2 as the accessory EBP for σ^N-dependent expression of RpoS (273). Moreover, it was determined that Rrp2 likely performs a second essential function as a negative regulator of other unknown proteins, inasmuch that RpoN mutants were lethal. Taken together, studies have determined that the Rrp2/RpoN/RpoS signaling pathway regulates at least two virulence factors (OspC and DbpA), and potentially more. Yang *et al.* reported that certain members of the multicopy lipoprotein (*mlp*'s) family appear to be either directly or indirectly regulated by this RpoN/RpoS pathway to some degree (274). Eggers *et al.* have gone on to show that even though OspE and OspF are members of the OspEF-related protein (Erp) paralogous family, only OspF is regulated by RpoS (79).

G. PncA

Plasmid content evaluations of avirulent and virulent *B. burgdorferi* strains indicated that the loss of lp25 resulted in the loss of mammalian infectivity (152, 199, 269). Purser *et al.* then identified a single lp25 ORF that restored virulence when provided on a shuttle plasmid in an avirulent, lp25-deficient strain (198). However, ID_{50} experiments suggested that complementation of only *pncA* from lp25 was not sufficient to restore wild-type levels of

infection (restored to within 1.5 logs of wild type). Evaluation of the involvement of PncA during the tick phase of the spirochete's life cycle was not evaluated. Biochemical analysis identified *pncA* as a nicotinamidase involved in the biosynthesis of NAD. Thus, PncA is classified as an essential gene product for virulence in the mammalian host and was the first confirmed virulence factor for *B. burgdorferi*.

H. BBK32 (P35, P47)

BBK32 was first identified as a lipoprotein that is reactive with antisera from infected mice (4, 91). This protein was also shown to expressed at higher levels in stationary phase *in vitro* (134) and in engorging ticks (93). Vaccination studies with BBK32 resulted in almost 90% protection of mice as well as in decreasing spirochete loads in engorging ticks (by 75%) (93). Biochemical analysis indicates that BBK32 may be a fibronectin-binding protein similar to the F1 protein of *Streptococcus pyogenes* (196, 197) and thus may be vital to the early invasiveness of *B. burgdorferi*. However, no conclusive data have been presented to validate the contention that this gene is a virulence factor for *B. burgdorferi*.

I. P66

The first chromosomal-encoded, surface-localized protein (P66) (195) is hypothesized to be either a porin (224) or an integrin-binding protein (62, 72). Bunikis *et al*. first identified P66 and utilized bioinformatic predictions to hypothesize that P66 was a lipoprotein containing a single transmembrane region (43). Skare *et al*. then presented evidence to suggest that P66 was an outer membrane spanning porin (Oms66) with limited single channel conductance (224). Proteinase-K accessibility and formaldehyde cross-linking analysis provided experimental evidence that P66 was surface-localized (41). Surprisingly, proteinase accessibility of P66 was hindered by the expression of OspA suggesting that these two proteins associate with each other on the surface of *B. burgdorferi* (41). However, the interaction between these two proteins is unclear considering that P66 is not expressed in flat ticks when OspA levels are high (69). Further experiments have described a surface-exposed carboxy-terminal fragment of P66 that is thought to undergo antigenic variation, inasmuch that this carboxy-terminal region is immunogenic and hypervariable between strains (42). However, *in vitro* analysis of a P66 mutant derived from an avirulent *B. burgdorferi* clearly identifies P66 as an integrin $\alpha_v\beta_3$-binding protein (63). Thus, the disparity in the data concerning P66 makes the elucidation of the precise function of this protein in *B. burgdorferi* difficult. Moreover, the role of P66 *in vivo* has yet to be elucidated.

CHAPTER TWO.

OVERALL OBJECTIVE AND SYNOPSIS

B. burgdorferi, the agent of Lyme disease, is a zoonotic spirochetal bacterium that depends on both arthropod (*Ixodes* ticks) and mammalian (rodent) hosts for its sustenance in nature. In nature, the spirochete must dramatically alter its proteome to adapt to the two diverse niches of the tick midgut and the tissue compartments of small mammals. Two of the proteins involved in this adaptive process are the well-characterized, reciprocally-regulated outersurface (lipo)proteins (Osp) A and C (71, 216, 218). However, the paucibacillary nature of *B. burgdorferi* in both hosts has hampered a more thorough examination of the spirochete's differential gene expression profiles. As such, the underlying tenet of this dissertation was to identify novel *B. burgdorferi* genes critical for the subsistence of the spirochete in nature.

To more broadly survey *B. burgdorferi*'s adaptive tendencies, DNA microarrays were utilized to identify genes encoding potential virulence factors contributing to *B. burgdorferi*'s infectivity, pathogenesis, host range, and/or persistence in its complex life cycle in ticks and mammals. Growth of *B. burgdorferi* B31 MI under conditions analogous to those found in (i) unfed ticks (UTs), (ii) fed ticks (FTs), or (iii) during mammalian host adaptation (*B. burgdorferi* cultivated in dialysis membrane chambers implanted into rats) were used to survey the adaptive transcriptional genetic responses of *B. burgdorferi*. A substantial proportion (46%) of the differentially regulated genes encoded proteins with predicted export signals (29% from predicted lipoproteins), emphasizing the importance to *B. burgdorferi* of

modulating its extracellular proteome. For B31 MI cultivated at the more restrictive UT condition, microarray data provided the first documented experimental evidence of a bacterial stringent response and factors that restrict cell division. The microarray data thus provide a basis for formulating new testable hypotheses regarding the life cycle of *B. burgdorferi* and attaining a more complete understanding of many aspects of *B. burgdorferi*'s complex parasitic strategies.

Upon evaluating the microarray data, *bba36* and *bbe16* were obvious candidates for genetic inactivation studies to identify their roles in the life cycle of *B. burgdorferi*. However, genetic manipulation of virulent strains of *B. burgdorferi* is hindered by the inherent plasticity of the bacterium. As such, the development of new genetic systems for improving the ability to genetically manipulate virulent strains of *B. burgdorferi* is an important goal of contemporary Lyme disease research. To this end, herein we describe a method that increases the efficiency of recovering *B. burgdorferi* clones that retain a key virulence-associated linear plasmid, lp25, after genetic manipulation. The major features of this approach include (i) the use of kanamycin selection to maintain lp25, (ii) reliance on homologous recombination to achieve genetic complementation, thereby circumventing a putative restriction barrier (*bbe02*) to shuttle plasmids, and (iii) integration of the complementation construct(s) into lp25, thus ensuring native gene dosage.

Inasmuch that the genetic tools were now available to further evaluate the differentially regulated *B. burgdorferi* genes identified via microarray analysis, we report herein that we were successful in the inactivation of both *bba36* and *bbe16* to assess their role in the virulence, pathogenesis, and survival of *B. burgdorferi* during its natural life cycle. Although no

phenotype could be ascribed to *bba36*, *bbe16* was found to potentiate the virulence of *B. burgdorferi* in the murine model of Lyme borreliosis and was essential for the persistence of *B. burgdorferi* in *Ixodes scapularis* (*I. scapularis*) ticks. As such, we have renamed *bbe16* as a gene encoding borrelial persistence in ticks (*bptA*). Although protease accessibility experiments suggested that BptA as a putative lipoprotein is surface-exposed on the outer membrane of *B. burgdorferi*, the molecular mechanism(s) by which BptA promotes *B. burgdorferi*'s persistence within its tick vector remains to be elucidated. BptA also was shown to be highly conserved (>88% similarity and >74% identity at the deduced amino acid levels) in all *B. burgdorferi sensu lato* strains tested, suggesting that BptA may be widely utilized by Lyme borreliosis spirochetes for persistence in nature. Given *B. burgdorferi*'s absolute dependence on and intimate association with both its arthropod and mammalian hosts, BptA should be considered as a virulence factor critical for *B. burgdorferi*'s overall parasitic strategy. These results prove the utility of coupling transcriptional profiling and genetic inactivation approaches to identify novel bacterial genes essential for the persistence of *B. burgdorferi* in nature.

CHAPTER THREE.

MATERIALS AND METHODS

I. Bacterial Strains and Cultivation

A. *E. coli* strains, plasmids, and *in vitro* cultivation

A list of *E. coli* strains used is shown in Table 1. Typically, overnight cultures were grown in Luria-Bertani broth (LB) with shaking at 37°C with appropriate antibiotic (*β-lac* confers ampicillin resistance at 100 μg/ml; P_{FlgB}*::aadA* confers spectinomycin resistance at 100 μg/ml; *aph[3']-IIIa* & P_{FlgB}*::kan* confer kanamycin resistance at 30 μg/ml; *ermC* confers erythromycin resistance at 400 μg/ml; and *cam* confers chloramphenicol resistance at 33 μg/ml). Induction of recombinant protein expression was performed between 23-37°C for 4-14 hours with 0.4-0.6 mM IPTG. A list of *E. coli* plasmids and shuttle plasmids is given in Table 2.

B. *B. burgdorferi* strains and *in vitro* cultivation conditions

Low-passage *B. burgdorferi* strain B31 MI (101) was kindly provided by Dr. Mark Hanson (MedImmune, Gaithersburg, MD) and strain 297 (235) was provided by Dr. Russell Johnson (University of Minnesota) (Table 1). *B. burgdorferi sensu lato* strains IP90, BO23,

VS116, DN127, 21038, IKA2 and relapsing-fever strains HS-1 and OZ-1 were kindly provided by Richard Marconi (Medical College of Virginia, Table 1). *B. lonestari* DNA was provided by Susan Little (University of Georgia). Strain PL133 (Table 1) is a virulent derivative of strain 297, has been propagated in mice and *in vitro*, retains all conventional 297-specific plasmids, and is identical to 297 as determined by all known means to differentiate borreliae strains. Virulence was confirmed for all three strains by culturability of spirochetes from infected mouse tissues two weeks after intradermal (ID) injection of 1×10^3 borreliae in C3H mice (22, 24).

Spirochetes from not more than three *in vitro* serial passages were cultivated at 37°C to the mid-logarithmic phase (ca. 5×10^6 B31 MI per ml) in complete Barbour-Stoenner-Kelly (BSK-H) medium (Sigma Chemical Co.) (191). For *in vitro* cultivation, the initial culture was diluted to 1×10^3 spirochetes per ml in either BSK-H medium held at 23°C (adjusted to pH 7.5) or in BSK-H medium pre-warmed to 37°C (adjusted to either pH 6.8, 7.0), 7.5 or 8.0 (270). To obtain *B. burgdorferi* in a mammalian host-adapted state, spirochetes were diluted (as above) in BSK-H medium and cultivated for two, 14-day cycles in DMCs (see below) (5, 272); spirochetes were harvested and pooled for protein evaluations and total RNA extraction.

C. Cultivation of *B. burgdorferi* within dialysis membrane chambers (DMCs)

The generation of *B. burgdorferi* in a mammalian host-adapted state was performed using a modified technique developed by Darrin Akins (5). Briefly, SpectraPor-7 dialysis

Table 1. Strains used in this study

Organism	Strain	Description	Reference
E. coli	Rosetta Blue	*endA1 hsdR17(r K12–mK12) supE44 thi-1 recA1 gyrA96 relA1 lac[F' proAB lacI^{q}ZΔM15::Tn10 (Tet^r)] pRARE::cam^r*	EMD Biosciences (Novagen)
	M15	*lac ara gal mtl recA uvr* [pREP4, lacI, kan^r]	Qiagen
	XL1-Blue	*recA1 endA1 gyrA96 thi-1 hsdR17 supE44 relA1 lac[F' proAB lacI^{q}ZΔM15::Tn10 (Tet^r)]*	Stratagene
	BL21	*E. coli B F$^-$ dcm ompT hsdS(r_B-m_B-) gal*	Stratagene
Borrelia burgdorferi	297	Non-clonal, infectious human strain	(131)
	B31 MI	Non-clonal, infectious tick strain (sequenced)	(57, 101)
	PL133	Transformable, non-clonal, infectious derivative of 297	This study
	BbDTR599A	Clonal derivative of PL133, infectious *bba36*$^-$ mutant clone P1C5; cp32-6$^-$	This study

Table 1. (Continued) Strains used in this study

Organism	Strain	Description	Reference
	BbDTR599B	Clonal derivative of PL133, infectious *bba36*$^-$ mutant clone P2D6; lp5$^-$, cp32-4$^-$, cp18-2$^-$	This study
	BbDTR596A	Clonal derivative of PL133, infectious *bptA*$^-$ mutant clone P1C5; cp18-2$^-$, cp32-4$^-$ Note: This is the strain used for complementation studies.	This study
	BBDTR596B	Clonal derivative of PL133, infectious *bptA*$^-$ mutant clone P2D6; cp18-2$^-$	This study
	BbDTR651	Non-clonal, infectious isolate of BbDTR596A complemented with *bbe17* & *bptA*$^-$ operon, cp18-2$^-$, cp32-4$^-$	This study
	BbDTR652	Non-clonal, infectious isolate of BbDTR596A complemented with *bbe17*; cp18-2$^-$, cp32-4$^-$	This study
	BbDTR653	Non-clonal, infectious isolate of BbDTR596A complemented with pomoterless *bptA*; cp18-2$^-$, lp5$^-$	This study
	BbDTR654	Non-clonal, infectious isolate of BbDTR596A complemented with *bptA* fused to *bbe17* promoter; cp18-2$^-$, cp32-4$^-$	This study
	BbDTR597	Clonal derivative of PL133, infectious *bptA* & *bbe17* double mutant; cp32-3$^-$, cp32-6$^-$, cp18-2$^-$	This study

Table 1. (Continued) Strains used in this study

Organism	Strain	Description	Reference
	BbDTR630	Clonal derivative of PL133, infectious isolate with *aph[3']-IIIa* marker on lp25; cp18-2$^-$	This study
Borrelia garinii	IP90	Lyme borreliosis strain IP90	(149)
Borrelia afzelii	BO23	Lyme borreliosis strain BO23	(265)
Borrelia andersonii	21038	Lyme borreliosis strain 21038	(11)
Borrelia Valaisiana	VS116	Lyme borreliosis strain VS116	(193)
Borrelia japonica	IKA2	Lyme borreliosis strain IKA2	(142)
Borrelia bissettii	DN127	Lyme borreliosis strain DN127	(193)
Borrelia Hermsii	HS-1	relapsing fever strain HS-1	(253)
Borrelia turicatae	Oz1	relapsing fever strain Oz1	(50)
Ixodes scapularis			Oklahoma State University
Mus muscularis	C3H/HeJ		Jackson Labs

Table 1. (Continued) Strains used in this study

Organism	Strain	Description	Reference
	C3H/HeN		Charles River Labs
Ratus rat	Sprague-Dawley		Harlan

Table 2. Plasmids used in this study.

Plasmid	Description	Reference
pGEM-Teasy	TA cloning vector, high-copy-number; Amp^r	Promega
pPROEX-HtA	Expression vector with N-terminal 6-his tag; Amp^r	Invitrogen (Gibco)
pPROEX-HtB	Expression vector with N-terminal 6-his tag; Amp^r	Invitrogen (Gibco)
pPROEX-1	Expression vector with N-terminal 6-his tag; Amp^r	Invitrogen (Gibco)
pHAT20	Expression vector with N-terminal 6-his tag; Amp^r	BD Biosciences
pRARE	Provides rare codons *proL, lueW, metT, argW, thrT, glyT, tyrU, argU, and ilex*; Cam^r	Novagen
pRep4	Provides repressor of expression to control leaky expression; Kan^r	Qiagen
pBSV2	*B. burgdorferi/E. coli* shuttle plasmid (*cp9/colE1* ori); P_{flgB}::*Kan*; Kan^r	(246)
pKSSF1	*B. burgdorferi/E. coli* shuttle plasmid, P_{flgB}*::aadA* ($Strep^r$/$Spec^r$, respectively); derivative of pBSV2	(100)
pKH400	pPROEX-1Ω::(297-specific *dbpA*, *NcoI*/*Kpn*I [500 bp]); Amp^r	(116)
pKH523	pHAT20Ω::(297-specific *pncA* [550bp]); Amp^r	This study Collab. w/ KE Hagman
pMS2	*B. B. burgdorferi/E. coli* shuttle plasmid, *aph[3']-IIIa* under native promoter; Kan^r/$Gent^r$	(212)
pFlaB-297	pPROEX-HtBΩ::(297-specific *flaB*, *BamHI/XhoI* [~ 1000bp]); Amp^r	This study Collab. w/KE Hagman

Table 2. (Continued) Plasmids used in this study.

Plasmid	Description	Reference
pJSB166	pPROEX-HtAΩ::(297-specific *bbk32*, *NcoI*/*Kpn*I [~980bp]); Amp^r	This study Collab. w/JS Blevins
pJD1	pBSV2Ω::P$_{flgB}$*::aadA* (*Hind*III-*Blg*II); Spec^r/Strep^r	This study Collab. w/JS Blevins
pJD7	pJD1Ω::sythetic *B. burgdorferi* term (*Eag*I-*Kpn*I); Spec^r/Strep^r	This study Collab. w/JS Blevins
pJD39	pJD1Ω::*ermC* (*Bgl*II-*Bsp*HI); Erm^r	This study Collab. w/JS Blevins
pJD44	pJD7Ω::*aph[3']-IIIa* (from pMS2); dual *Asc*I sites; Kan^r	This study Collab. w/JS Blevins
pSpec-SmaI	pGEM-TeasyΩ::*P$_{flgB}$*::aadA with *Sma*I sites on both ends; Amp^r, Spec^r/Strep^r	This study
pErmC-SmaI	pGEM-TeasyΩ::*ermC* with *Sma*I sites on both ends; Amp^r, Erm^r	This study
pKan-SmaI	pGEM-TeasyΩ::*ermC* with *Sma*I sites on both ends; Amp^r, Erm^r	This study
pSpec-AscI	pGEM-TeasyΩ::P$_{flgB}$*::aadA* with *Asc*I sites on both ends; Amp^r, Spec^r/Strep^r	This study
pErmC-AscI	pGEM-TeasyΩ::*ermC* with *Asc*I sites on both ends; Amp^r, Erm^r	This study
pKan-AscI	pGEM-TeasyΩ::*aph[3']-IIIa* from pMS2 with *Asc*I sites on both ends; Amp^r, Kan^r	This study

Table 2. (Continued) Plasmids used in this study.

Plasmid	Description	Reference
pDTR203	pPROEX-HtAΩ::BBA07 (B31 MI, *Nco*I/*Kpn*I [~500 bp]); Amp^r	This study
pDTR204	pPROEX-HtAΩ::BBQ03 (B31 MI, *Nco*I/*Kpn*I [500 bp]); Amp^r	This study
pDTR205	pPROEX-HtAΩ::BBI42/BBK53 (B31 MI, *Nco*I/*Kpn*I [500 bp]); Amp^r	This study
pDTR247	pPROEX-HtAΩ::BBE17 (B31 MI, *Nco*I/*Kpn*I [430 bp]); Amp^r	This study
pDTR261	pPROEX-HtAΩ::BB0664 (B31 MI, *Nco*I/*Kpn*I [600 bp]); Amp^r	This study
pDTR299	pPROEX-HtAΩ::(B31 MI-specific *bba36*, *NcoI*/*Kpn*I [600 bp]); Amp^r	This study
pDTR317	pQE40Ω::BBK07 (B31 MI, *Nco*I/*Kpn*I [840 bp]); Amp^r	This study
pDTR320	pQE40Ω::BB0070 (B31 MI, *Nco*I/*Kpn*I [420 bp]); Amp^r	This study
pDTR401	pQE40Ω::BBK47 (B31 MI, *Nco*I/*Kpn*I [1570 bp]); Amp^r	This study
pDTR402	pQE40Ω::BBE08 (B31 MI, *Nco*I/*Kpn*I [96 bp]); Amp^r	This study
pDTR414	pQE40Ω::BBE16(B31 MI, *Nco*I/*Kpn*I [580 bp]); Amp^r	This study
pDTR420	pPROEX-HtAΩ::OspA (297, *Nco*I/*Kpn*I [850 bp]); Amp^r	This study
pDTR421	pPROEX-HtAΩ::(297-specific *bba36*, *Nco*I/*Kpn*I [600 bp]); Amp^r	This study

Table 2. (Continued) Plasmids used in this study.

Plasmid	Description	Reference
pDTR501	pBSV2Ω::P*flgB*::*sacB*; Kan^r	This study
pDTR594	pGEM-TeasyΩ::3542bp fragment centered around *bba36*; Amp^r	This study
pDTR595	pGEM-TeasyΩ::2442bp around *bbe17*; Amp^r	This study
pDTR596	pDTR595Ω::P*flgB*::*aadA* (inserted into unique *Swa*I site within *bptA*); Amp^r, Strep^r /Spec^r	This study
pDTR596F	pDTR595Ω:: P*flgB*::*aadA* (inserted into unique *Swa*I site within *bptA*); reverse orientation of pDTR596; Amp^r, Strep^r /Spec^r	This study
pDTR597	pDTR595Ω:: P*flgB*::*aadA* (inserted into unique *Swa*I & *Hpa*I sites within *bptA* &*bbe17*, respectively); Amp^r, Strep^r /Spec^r	This study
pDTR598	pDTR595Ω:: P*flgB*::*aadA* (inserted into unique *Swa*I & *Hpa*I sites within *bptA* &*bbe17*, respectively); reverse orientation of pDTR597; Amp^r, Strep^r /Spec^r	This study
pDTR599	pDTR594Ω:: P*flgB*::*aadA* (inserted into unique *Hpa*I site within *bba36*); Amp^r, Strep^r /Spec^r	This study
pDTR620	pGEM-TeasyΩ::Downstream region of *pncA* (*Asc*I & *Bss*H II sites), Amp^r	This study
pDTR621	pGEM-TeasyΩ::Downstream region of *pncA* (*Asc*I & *Bss*H II sites); reverse of pDTR620; Amp^r	This study
pDTR622	pJD1Ω::pDTR621 (*Nco*I-*Bsp*HI), Spec^r/Strep^r	This study Collab. w/ KE Hagman

Table 2. (Continued) Plasmids used in this study.

Plasmid	Description	Reference
pDTR623	pGEM-TeasyΩ::*pncA* & *bbe23* (unique *Asc*I site downstream of *pncA*); Amp^r	This study
pDTR627	pDTR623Ω::pDTR620 (inserted into unique *Asc*I site); Amp^r	This study
pDTR628	pDTR627Ω::pSpec (inserted into unique *Asc*I site); Amp^r, $Spec^r$/$Strep^r$	This study
pDTR629	pDTR627Ω::pErmC (inserted into unique *Asc*I site); Amp^r, Erm^r	This study
pDTR630	pDTR627Ω::pKan (inserted into unique *Asc*I site); Amp^r, Kan^r	This study
pDTR640	pJD44Ω:: P_{flgB}*::bptA* (*Bgl*II-*Hind*III); Kan^r	This study
pDTR641	pJD44Ω::*bbe17-bptA* (*Bgl*II-*Hind*III); Kan^r	This study
pDTR642	pJD44Ω::*bbe17 + 300bp upstream* (*Bgl*II-*Hind*III); Kan^r	This study
pDTR643	pJD44Ω::*bptA + 300bp upstream* (*Bgl*II-*Hind*III); Kan^r	This study
pDTR644	pJD44Ω::P_{bbe17}*::bptA* (*Bgl*II-*Hind*III); Kan^r	This study
pDTR650	pDTR627Ω::pDTR640 (*Asc*I fragment); Amp^r, Kan^r	This study
pDTR651	pDTR627Ω::pDTR641 (*Asc*I fragment); Amp^r, Kan^r	This study
pDTR652	pDTR627Ω::pDTR642 (*Asc*I fragment); Amp^r, Kan^r	This study
pDTR653	pDTR627Ω::pDTR643 (*Asc*I fragment); Amp^r, Kan^r	This study

Table 2. (Continued) Plasmids used in this study.

Description	Reference	
pDTR654	pDTR627Ω::pDTR644 (*Asc*I fragment); Amp^r, Kan^r	This study
pDTR700	pPROEX-HtAΩ:: *bptA* (B31 MI, *Nco*I/*Kpn*I [585bp]); gene-built wild type; Amp^r	This study
pDTR701	pPROEX-HtAΩ:: *bptA* (B31 MI, *Nco*I/*Kpn*I [585bp]); gene-built serine-1 mutant; Amp^r	This study
pDTR702	pPROEX-HtAΩ:: *bptA* (B31 MI, *Nco*I/*Kpn*I [585bp]); gene-built serine-2 mutant; Amp^r	This study
pDTR704	pPROEX-HtAΩ:: *bptA* (B31 MI, NcoI/KpnI [585bp]); gene-built serine-4 mutant; Amp^r	This study
pDTR705	pPROEX-HtAΩ::*bptA* (B31 MI, NcoI/KpnI [585bp]); gene-built serine-5 mutant; Amp^r	This study
pDTR706	pPROEX-HtAΩ:: *bptA* (B31 MI, NcoI/KpnI [585bp]); gene-built serine-6 mutant; Amp^r	This study

membranes (8 kDa molecular weight cut-off, Spectrum Laboratories) were rinsed with Milli-Q water and sterilized by boiling in 1 mM EDTA for 20 minutes. Membranes were then submerged in a 1:1 mixture of BSK-H medium and 1X PBS. Dialysis membranes were then tied at one end, the resulting bag was filled with 10 ml of BSK-H medium (prewarmed to 37°C) containing 1 x 10^3 spirochetes, and the loose end was then tied to form an enclosed chamber. Sprague-Dawley rats (Jackson Laboratory) were anesthetized with 1 ml/kg IP/SQ of rat sedation cocktail (1 mg/ml Acepromazine Maleate, 5 mg/ml Xylazine-20, 50 mg/ml Ketamine). A mid-line excision (~1.5-2 inches) was made through both the dermal and muscle tissue of the abdomen, and connective fasciae between the two layers was separated. Using strict aseptic technique, one DMC was placed intraperitoneally, a running stitch (0.4 silk suture thread) was placed on the muscle layer, and tissue staples were applied to the dermal layer to close the incision. Ten to 14 days post-implantation, rats were euthanized, the chambers were harvested, and were washed in 1x phosphate-buffered saline (PBS); bacteria were aseptically collected and diluted to 1 x 10^3 bacteria/ml in fresh BSK-H medium, and new DMC chambers with this suspension were implanted in new rats for an additional 10-14 days. After two rounds of culturing the spirochetes in DMCs, the bacteria were harvested for analysis. All animal experiments were approved by the U.T. Southwestern Institutional Animal Care and Use Committee.

II. Transformation of Bacterial Strains

A. Electroporation of *E. coli*

All transformations of *E. coli* strains were performed via electroporation. Cells were made electrocompetent using typical protocols with slight modifications. Overnight cultures were diluted 1:50 in fresh LB broth with selection (if needed) and incubated at 37°C until and optical density (OD_{600}) of 0.6 was reached (2-3 hours). Once appropriate cell density was achieved, the culture was placed at 4°C for 30 minutes. Cells were centifuged at 16,000 x g for 10 min. at 4°C. The supernatant was removed and the cell pellet was resuspended in 10 ml of sterile, ice-cold water. Once the cells were resuspended, sterile water was added to a volume equal to that of the original culture. Centrifugation was repeated to pellet cells, then the cells were resuspended with sterile, ice-cold water (half the original culture volume). This process was repeated three more times with decreasing volumes of sterile, ice-cold water at each step in the following volumes (1/4, 1/10, and 1/50, the original culture volume). Two more rounds of centrifugation were repeated, followed by resuspension of the cell pellets in 10 and 2 ml of sterile, ice-cold 10% glycerol each time, respectively. Aliquots were then flash frozen on dry ice and stored at -80°C.

To perform transformation of *E. coli*, an aliquot of electrocompetent *E. coli* was first thawed on ice and then combined with the DNA to be transformed. Typically, super-coiled plasmid DNA in a volume of 1 μl was used to transform cells in a 50-μl volume. An entire DNA-ligation reaction (10 μl) usually was transformed into 50 μl of cells after the DNA

mixture had been desalted. Desalting was performed by placing the DNA on a Type VS 0.025 μm filter (Millipore) floating above sterile DNase-free water. After incubation of the cell-DNA mixture on ice for 5 minutes, the suspension was transferred to a 1-mm gap electrocuvette (MBP Molecular Bioproducts) and subsequently electroporated using a Gene Pulser Xcell (Biorad) with a setting of 1.8 kVolts. Cells were immediately transferred to 200-1000 μl of super optimal catabolite (SOC) medium and incubated at 37°C with shaking for 30-45 minutes. Cells were then placed on LB-agar plates supplemented with appropriate antibiotics and spread with 4.0 millimeter glass beads (Sigma Chemical). Plates were incubated overnight at 37°C. Resultant colonies were patch-plated to fresh LB-agar plates with antibiotics, as well as inoculated into LB broth with antibiotics. All *E. coli* strains were frozen at -70°C in LB broth supplemented with 20% sterile glycerol.

B. Electroporation of virulent *B. burgdorferi*

Virulent *B. burgdorferi* 297-derived strain PL133 was used as the parental strain for all mutational analyses. *B. burgdorferi* electroporation protocols first described by Samuels *et al* (209) were performed with slight modifications. Spirochete cultures were grown to the mid-logarithmic phase of growth (~100 ml of culture with 60-80 bacteria/field = 1.8-2.4 x 10^7 bacteria/ ml) and pelleted at 1,300 x g for 30 minutes. All subsequent steps were performed at 4°C. Cells were washed once in sterile 0.9% normal saline for injection (Braun Medical) and twice in electroporation solution (EPS) (15% Glycerol, 270 mM sucrose), with

centrifugation at 1,300 x g for 30 minutes between washes. Cells were resuspended in an appropriate volume of EPS solution (50 μl cell suspension per 100 ml starting culture). Between 30-50 μg of DNA prepared by Maxiprep (Qiagen) (either suicide or shuttle plasmid), in a maximum volume of 20 μl, was added to 50 μl of electrocompetent *B. burgdorferi* and placed in a 2-mm gap electrocuvette (MBP Molecular Bioproducts). The cells were resuspended in 20 ml BSK-H medium for recovery (for 24 h) after the 2500 kVolt transformation current was applied to the spirochete suspension. The bacterial suspensions were then aliquoted into 200-μl volumes into two 96-well microtiter plates with low evaporation lids (Corning). Plates were wrapped in plastic wrap to limit evaporation and incubated for 2-3 weeks at 37°C (5% CO_2 atmosphere). Outgrowth of clones first was noted by visible yellowing of the culture medium within individual wells (acidification of medium) and then was verified by observation of viable (motile) spirochetes via dark-field microscopy. Selection of clones in liquid medium (limiting dilution) (128, 275) was utilized over the conventional agarose-embedding technique (209) because it is believed that the former technique is less stressful for the spirochetes. Of note, with the low number of recovered clones per plate (typically 10 or fewer), there is a very high probability that positive wells arose from single clones (data not shown). Dark-field positive wells were frozen and a small aliquot was expanded for chromosomal DNA isolation and subsequent PCR verification of gene inactivation and plasmid contents.

Cultivation of mutant strains of *B. burgdorferi* was performed using BSK-H medium supplemented with the appropriate antibiotic (P_{flgB}*::aadA* confers streptomycin resistance at

50 μg/ml; *aph[3']-IIIa* & P_{flgB}*::Kan* confer kanamycin resistance at 160 μg/ml; and *ermC* confers erythromycin resistance at 0.04 μg/ml). All *B. burgdorferi* strains were stored at -70°C in BSK-H medium supplemented with 30% glycerol.

III. DNA and RNA Isolation

B. burgdorferi genomic DNA for use in PCR was isolated from 1 liter of late-logarithmic phase B31 MI or 297 using a Stratagene DNA extraction Kit. Evaluation of genomic DNA from mutants was performed on DNA isolated with the Promega DNA Wizard Plasmid purification kit. Isolation of genomic DNA from mutant strains of *B. burgdorferi* for subsequent electroporation into wild-type 297 was performed using the Qiagen DNA Maxiprep kit. *E. coli* plasmid DNA was purified using either the Promega DNA Wizard plasmid purification kit or the Qiagen DNA Maxiprep kit. All methods are variations of the typical alkaline lysis based procedure for plasmid purification, followed by binding of the DNA to an anion-exchange resin under low salt and pH conditions. Bound DNA was washed on the column followed by elution with either sterile, DNase-free water or Tris-HCl/EDTA (100 mM Tris-HCl/10 mM EDTA) buffer. Isolation of total DNA from *Ixodes* ticks was performed with the DNeasy Tissue DNA extraction kit (Qiagen) following the manufacturer's instructions for "Isolation of Total DNA from Rodent Tails". Total borrelial RNA was isolated utilizing Trizol Reagent (Gibco) according to the manufacturer's protocol. To validate mRNA integrity,

northern blot analysis was carried out (192) using PCR-generated probes for *flaB, ospA*, and *ospC* (192, 272).

IV. Microarray Technology

A. Microarray construction

ORF-specific primer pairs were purchased from Sigma-Genosys and used to PCR-amplify in 96-well plates 1,754 (95.4%) of the 1,838 predicted ORFs from *B. burgdorferi* B31 MI DNA, according to a general protocol provided by the manufacturer. Parameters for PCR amplification were as follows: 95°C for 3 min; 30 cycles of 95°C for 30 s; 50°C for 30 s; 72°C for 2.5 min; and a final extension cycle of 72°C for 10 min. PCR products >150 bp were observed via 1.5% agarose gel electrophoresis. PCR fragments <150 bp were subjected to 10% polyacrylamide gel electrophoresis. Fragments were stained with ethidium bromide and imaged digitally by using a Kodak Image Station. Amplification was scored on a visual scale of 1+ (low) to 4+ (high); amplification was considered acceptable if a single PCR product within 10% of the predicted ORF size was 3+ or better (5). Unsuccessful reactions were characterized as either (*i*) 0 or 1+, (*ii*) DNA smears, (*iii*) multiple bands, or (*iv*) single bands of unexpected size. Primers from unsuccessful PCR reactions were rearrayed into new 96-well plates and reamplified with altered $MgCl_2$ concentrations and annealing temperatures to favor amplification of the desired single products. All PCR products were precipitated with

cold isopropanol, dried, dissolved in 7% DMSO, and rearrayed into 384-well plates for glass-slide printing. The PCR products then were deposited in duplicate on poly-L-lysine-coated glass slides utilizing a MagnaPrinter designed and manufactured by the University of Texas Southwestern Medical Center (microarraycore.swmed.edu). Negative control samples (n = 720) containing vehicle buffer only (7% DMSO) also were deposited on the array for determination of threshold values for both channels. Post-processing of the slides was performed as reported (6). Briefly, to ensure uniformity of DNA features, the slides spotted with DNA were rehydrated by suspension over boiling water for 1 min and then flash-dried on a heating block (100°C). UV crosslinking was performed by using a UV Stratalinker (Stratagene). Removal of unreacted lysine residues on the glass slides was accomplished by submersion in blocking solution (20 mM boric acid (pH 8.0)/55.2 mM succinic anhydride/90% 1-methyl-2- pyrrolidinone) for 30 min with rotation followed by submersion in distilled water (95°C) for 2 min. Slides then were dipped briefly in 95% ethanol and spun dry. Slides were stored, protected from dust and light, and kept at room temperature. Twenty-six of the amplicons also were sequenced to validate their identities; 21 of these amplicons corresponded to genes from 10 paralogous families. For 8 of the 10 families, 2–3 genes were tested and for two families, one representative gene was sequenced. The remaining five amplicons corresponded to nonparalogous genes.

B. Fluorescent probe labeling and hybridization for microarray analysis

Spirochetes from two independent cultivations at each growth condition were harvested at the late-logarithmic phase of growth (ca. 2 x 10^7 B31 MI per ml) for protein evaluation and for total RNA extraction. Ten µg of total *B. burgdorferi* RNA was used to generate Cy3-labeled first-strand cDNA via the SuperScript II reverse transcription kit (GIBCO); in lieu of standard hexamer random priming, 40 genome-directed primers (GDPs; ref. 250) designed for strain B31 MI were used to generate Cy3-labeled cDNA. Each GDP primer was supplied in the reaction to a final concentration of 250 ng/µl. The 40 GDPs were designed as octamers that anneal within the distal 40% of each predicted ORF. On average, each ORF was complementary to three GDPs. To guard against potential bias from spurious enzyme activity, each slide was subjected to hybridization with Cy3-labeled cDNA generated in separate reverse transcription reactions. After cDNA synthesis, the remaining RNA was hydrolyzed by the addition of a 1:10 volume of 10 N NaOH followed by heating at 65°C for 10 min. The solution then was brought to neutral pH by the addition of a 1:10 volume of 10 N HCl. For normalization and data analysis, 1 µg of Cy5-labeled genomic DNA was synthesized by nick translation (Promega; ref. 250). Microcon YM-30 cellulose centrifugal filters (Millipore) were used to remove unincorporated Cy dyes from both Cy5-labeled genomic DNA and Cy3-labeled cDNA. Fifty-microliter hybridization solutions were comprised of 20 ng/µl Cy5-labeled genomic DNA (1.0 µg), 200 ng/µl Cy3-labeled cDNA (10 µg), 0.7 µg/µl yeast tRNA, 0.4% SDS, and 4x SSC buffer (1x SSC = 0.15 M sodium chloride/0.015 M sodium citrate, pH 7). The hybridization solution was heat-denatured for 2 min, allowed to cool to room temperature, and deposited onto the microarray slides. Slides were covered with cover slips (12-544G; Fisher Scientific) and placed into a hybridization

chamber (ArrayIt). Hybridization with both probes was performed at 62.5°C with rotation overnight in a hybridization oven. The slides then were washed twice in buffer A (0.2% SDS + 0.1x SSC; 62.5°C), twice in buffer B (0.1x SSC; 62.5°C), and once in buffer B at 23°C and then spin-dried.

C. Microarray data acquisition and analysis

Data acquisition was performed on a GenePix 4000B scanner using GENEPIX 3 software (Axon Instruments, Foster City, CA). The fluorescence intensity of each feature was measured, and spots with intensity values below threshold (2 SDs above the mean of the negative control features) in the Cy5 (normalizing) channel were omitted from further analysis. Log ratios (Cy3/Cy5) were compared between slides of the same condition, and only slides with a correlation (r) of >0.75 were included in subsequent analyses. To achieve statistical reliability, analyses were performed on a minimum of three slides per condition (157), yielding a possible six data points per condition. For *B. burgdorferi* cultivated *in vitro*, at least two independent cultures were represented in the data sets, whereas spirochetes cultivated in 20 DMCs were pooled to obtain sufficient RNA for microarray analysis. Each feature with Cy3/Cy5 ratios >3 SDs from the mean log ratios for each gene on replicate slides was considered an outlier and omitted. The resultant data set for each slide then was transformed to a mean log ratio of zero, thus allowing the calculation of average log ratios, SD, and uncertainty values for each gene within replicates. Expression changes with 95%

confidence intervals greater than a conservative 1.8-fold threshold were designated as differentially expressed genes. The fold-change threshold was defined as twice the mean of all feature uncertainties (SD) above background, where the average uncertainty was calculated to be 0.4-fold, and background was defined as no change between conditions (i.e., a ratio of 1.0).

D. Hierarchial cluster analysis of microarray data

Cluster analysis utilizing the CLUSTER and TREEVIEW programs (Stanford University; ref. 83) was performed for visual representation and profiling of data. A filter cut-off of 0.4 on log-transformed ratios resulted in 709 genes being selected for inclusion in average linkage clustering analysis.

V. Real-Time RT-PCR

Real-time quantitative RT-PCR was used to validate selected data from microarray experiments. Genome-directed primers (GDPs) (Table 3) were used to prime first-strand cDNA synthesis from DNA-free RNA samples; RT was performed as described (see Fluorescent Probe Labeling below), except without inclusion of Cy-dye. cDNA samples were diluted to 8.0, 0.8, and 0.08 ng/µl. Duplicate quantitative PCR assays were performed on 5 µl of each cDNA

dilution utilizing the SYBR Green Master mix with an ABI 5700 Sequence Detection System according to the manufacturer's protocol (Applied Biosystems); the gene-specific primers (Table 4) were designed using PrimerExpress software (Applied Biosystems). The relative quantitation method (ΔC_T) was used to evaluate quantitative variation between the three *B. burgdorferi* growth conditions relative to each gene examined. 16S rRNA was used as an internal control and normalizer for all data.

Table 3. Genome-Directed Primers specific for *B. burgdorferi* B31 MI. (5'-->3')

TTTTTAAA	TTAAAAAA	AAATCCAA	TTTAGCAA
TTTTTATT	TATTTTAT	TTTTTCAA	TTTCTCAA
TCTTTTAA	TTCTTTTG	ATTTTTGT	TTTACCAA
AAATATTT	TAAAATTT	CTGTGCAG	ATATCCAC
TTTTTATA	AAATAATA	AATAAAAT	TTAACATT
AATTCTTT	TTATCAAA	ATTCTCAT	TTTTTTGG
AAAAATAA	AATCCCAT	ATTGCCAA	TAACACAA
TAAATAAA	CTTTTCAT	TTAATAAT	TGTAAAAA
ATTTAAAA	TTTAATAT	AAAAACAA	TAGAAAAA
TAAATTTA	ATAAAAAT	AATTTCAT	TATAATTC

VI. Protein Expression, Purification, and Analysis

A. Protein expression and purification

All protein expression was performed in *E. coli* (XL1-Blue, Rosetta Blue, or M15) using either the pPROEX-Hta (Invitrogen) or pQE40 (Qiagen) 6-histidine vector systems. The Rosetta Blue strain (Novagen) was used for the expression of some proteins because this

Table 4. Real-Time RT-PCR primers for B31 MI gene detection.

TIGR #	Gene Name	Reverse Primer (5'—>3')	Forward Primer (5'—>3')
16S ribosomal	16S ribosomal	TACGGGAGGCAGCAGCTAAG	CACGCAGTGTCGCTCCG
BB0061	thioredoxin (trxA)	GCTTGCCATCAACAGGAATAAAA	CAAAGTAGATACAGATAAGGAACAAGATATTTC
BB0070	conserved hypothetical protein	AAGGGCAAATGCAAGAGCTATT	ATCAACGGTCACCGCTCTTT
BB0096	V-type ATPase, subunit E, putative	TCAACGCCAATAATTAAATCTCTTATTG	AGCTGCTAGAGTATTAAAGGCAAAATC
BB0147	Flagellar filament core protein (*flaB*)	GCTCCTTCCTGTTGAACACCC	AATCTTTTCTCTGGTGAGGGAGC
BB0296	heat shock protein (hslV)	CAACAAGCATCATAGCCTCAAGC	AAAGGGCGGCTGTTGACC
BB0323	hypothetical protein	TTTCCCACAATGTTCTAGATCTTTCA	TCGCATACGAAGAAAAAGTGGA
BB0466	ABC transporter, ATP-binding protein	AGCAAAAGGTTCATCTAAGAGTAAAAAATAAG	GCGTATACTCTTTCTGGTGGAGAGAG
BB0545	xylulokinase (xylB)	CATTCTATTTGACACAATTCCTTCTTG	GCGTAATTAATGCGGGATCAG
BB0671	chemotaxis operon protein (cheX)	CTTGGCATGCAAAGTGGTAACA	GAAGAAACAAAAGAGATGGTTGCTG
BB0677	ribose/galactose ABC transporter, ATP-binding protein (mglA)	TCAGGATTATCAAAGCTCTTAAGTCCA	CAATATTCCTTCGGACAGGCA
BB0789	cell division protein (ftsH)	TCGTCCAGGCCTAAGCAAAG	TGGAACGCATACCAATGTAATTG
BBA05	antigen, S1	AATCTCCCCACCGCTTTTTT	TGCTCTTGGTGGGTGGCT
BBA07	chpAI protein, putative	GTTTTTTCAACCTGTAGCAATTGC	AAAGAAATGCTTGTTACTGTTGTTAAGTG
BBA15	outer surface protein A (*ospA*)	TGTTTTGCCATCTTCTTTGAAAAC	GGCGTAAAAGCTGACAAAAGTAAAGTA
BBA24	decorin binding protein A (dbpA)	GGCATCAAAATTTACGCCCTT	GATTAGAACGAAGCGCTAAAGACA
BBA36	lipoprotein	AGCCTCCCCTTTGCTATTTTTAA	CAATATTTCTAGCATTGTTTCTAAAGCAGT
BBB19	outer surface protein C (ospC)	CAATAGCTTTAGCAGCAATTTCATCT	CGGATTCTAATGCGGTTTTACTTG

E. coli strain allows the expression of proteins containing codons not typically used by *E. coli*. The pRARE plasmid provides the rare amino acid codons encoded by *proL, lueW, metT, argW, thrT, glyT, tyrU, argU, and ileX.* The M15 strain was utilized for expression of recombinant proteins expressed from the pQE40 vector system because the M15 strain contains the pRep4 expression-repressor plasmid. Primers used to amplify all genes for protein expression are listed in Table 5. Clones derived from pPROEX-Hta vectors that did not express were subcloned into the pQE40 vector by amplification of the gene using a universal (5'GTACAAGATCTGCATGCGATTACGATATCCCAACGACCGAAAAC; *Bgl*II site underlined) and gene-specific primer (*Kpn*I site). Typically, 20 ml of a shaken overnight culture grown in LB broth were inoculated into one liter of LB broth with appropriate antibiotic and grown at 37°C with shaking to an OD of approximately 0.4-0.6 (~2 hours). Recombinant proteins were then induced with 0.4-0.6 mM IPTG at appropriate growth condition (23-37°C) for 4-14 hours. Bacteria were pelleted (8,000 x g for 20 minutes), resuspended in Buffer A (20 mM Tris-HCl-pH 7.5, 100 mM NaCl, 10% Glycerol, 15 mM BME), and lysed with a sonicator (Branson Sonifier 450) set at 50% duty cycle and microtip limit of 7 for 3 x 1-minute cycles on ice. The resultant slurry was supplemented with 1 mM $MgCl_2$ and 150 μg/ml RNase A and then was incubated on ice for one hour. The cell suspension then was pelleted (17-27,000 x g for 30 minutes) to remove cell debris and insoluble proteins.

Soluble recombinant proteins were then applied to a chelating Sepharose Fast Flow (Amersham Biosciences) nickel-affinity chromatography column utilizing the ÄKTA FPLC

Table 5. Oligonucleotides used to clone protein expression constructs.

Plasmid	Gene-Primer Direction	Primer Sequence (restriction sites underlined)
pDTR203	BBA07-5'	GTACACCATGGGTAAAGAATTTAATTATTCTGATCTTAG
	BBA07-3'	CGTAAGGTACCTTAAAACGAAGCAGATGCATCATCATAATTTTTTAC
pDTR204	BBQ03-5'	GTACACCATGGATTTGCCTGATAATCAGGAACAAGCTGTTCAAAC
	BBQ03-3'	CGTAAGGTACCTTATAAAATTTTTCCATTAATTGTATTTCTTTCTATTTCT
pDTR205	BBI42/K53-5'	GTACACCATGGATTTGCCTGATAATCAGGAACAAGCTGTTCAAAC
	BBI42/K53-3'	CGTAAGGTACCTTATGTAGGTAAAATAGGAACTGGTCTATTATAACATAG
PDTR247	BBE17-5'	GTACACCATGGGTGAAATATCTGAAGAAGTTGTTATTTTAAATGATAG
	BBE17-3'	AAGGTACCTTACTTATGAAAAATCATATCAAATGCACTATAAAAATGTG
pDTR261	BB0664-5'	GTACACCATGGGCAATCATAAGAATATACAGTACGACAAG
	BB0664-3'	CGTAAGGTACCTTATTGGGCTTTGATTTCTTGAAGTTCTTC
pDTR299	BBA36-5'	GTACACCATGGTTTGCTATAAAATTAAAAATAGCAAAGGGGAGGC
	BBA36-3'	CGTAAGGTACCTTAAACATTTCCATAATTTTTCAAATTTTTCAATTCG
pDTR317	BBK07-5'	GTACACCATGGAAAATTCAGCGATAAAGGTACCATTAGAAAATGG
	BBK07-3'	ATGCATCCAGGTACTTGGTTAATTATTAAAGCACAAATGTATGGCCATTGCTGCATTCTC
pDTR320	BB0070-5'	GTACACCATGGTATCAGAAAAATTAAAAAAAGAAATAAAAATT
	BB0070-3'	CGTAAGGTACCTTATAGAACCTCTTTCTTTTTGTGCCCCTTG
pDTR401	BBK47-5'	GTACACCATGGGTTCTGGTTTTTCTATCTAAAAAATCTATAG
	BBK47-3'	CGTAAGGGTACCTTATTTTTTGCAAGAATTTCCCTGTTGAAG
pDTR402	BBE08-5'	GTACACCATGGGCAACAATTATGCAAATGATAAAGGCTTA
	BBE08-3'	CGTAAGGTACCTTATAAAACAAAATTTGATAAGCATAAAAATAC
pDTR414	BBE16-5'	GTACACCATGGGTATTTTTTTAGGTTTCTTTTTTTACAAACAAAAAGAAAAC
	BBE16-3'	AAGGTACCTTAAAGATTGTATTTTGGCAAAAAATTTTCTATATCTATTTTATATTC
pDTR420-297	BBA15-5'	CCATGGAAGCAAAATGTTAGCAGCCTTGACGAG
	BBA15-3'	GGTACCTTATTTTAAAGCGTTTTTAATTTCATCAAG
pDTR423	BB0844-5'	GTACATCATGAGTGTAATACAAGTGACCCCAATGAATTAACTCG
	BB0844-3'	CGTAAGGTACCTTATTTACTCGTCTCTAAAAAATCATATAATC
pDTR321	BBA05-5'	GTACACCATGGGTAAGGGCAAATCTTTAGAAGAAGAT
	BBA05-3'	CGTAAGGTACCTTCGCCTGCTAATCTCTTTTATCAAGCTGTT
pDTR323	BBJ34-5'	GTACACCATGGGCAAATTCTATGGAAGTGATGATGATACAAAT
	BBJ34-3'	CGTAAGGTACCTTATTTATCTTTATTTTTAGGCTTAACTG
pJSB166	BBK32-5'	CCATGGATTTATTCATAAGATATGAAAT
	BBK32-3'	GGTACCATTAGTACCAAAGCGCATT
pKH523	BBE22-5'	CTAGACCGGTTACAAACGGGCCTTCAGCTTTATC
	BBE22-3'	ATATGGTACCTTATATATTAAGCTTACTTTGGCTGTC
pFlaB-297	BB0147-5'	TATGGATCCGATGATTATCAATCATAATACATCAGCTATTAA
	BB0147-3'	ATACTCGAGTTATTATCTAAGCAATGACAAAACATATTGGGGAA

chromatography system (Amersham Pharmacia Biotech). Purification was performed using the following protocol: column washing (post sample addition) with 3 column volumes of Buffer A, followed by a step gradient of 8%, 20% and 100% of Buffer B (Buffer B = 20 mM Tris-pH 7.5, 300 mM NaCl, 10% Glycerol, 15 mM BME, 0.5 M Imidazole) in Buffer A, each step with a total of 3 column volumes. Fractions with the desired recombinant protein were pooled, concentrated using a 10,000 molecular weight (MW) exclusion filter system (Centricon, Amicon), and buffer was exchanged into appropriate buffer for size-exclusion chromatography (buffer conditions varied depending on protein – see below). A maximum volume of 2 ml of partially-purified protein suspension was applied to a High Load 16/60 Superdex 75 (Amersham Biosciences) size exclusion column and fractions of monomeric recombinant protein were collected, pooled, and concentrated using a 10,000 MW exclusion device (Centricon). Buffer conditions for size-exclusion chromatography for each recombinant protein were as follows:

Buffer A (20 mM Tris-HCl - pH 7.5, 100 mM NaCl, 10% Glycerol, 15 mM BME). Used for pDTR414 (BBE16[BptA])

Buffer C (20 mM Tris-HCl - pH 6.0, 100 mM NaCl, 10% Glycerol, 15 mM BME). Used for pDTR203 (BBA07), pDTR204 (BBQ03), pDTR205 (BBI42/BBK53), pDTR261 (BB0664), pDTR299 (BBA36), pDTR420 (OspA)

Buffer D (20 mM Tris-HCl – pH 7.5, 100 mM NaCl, 10% Glycerol, 15 mM BME, 2 mM β-octylglucoside). Used for pDTR247 (BBE17)

Recombinant proteins that were not soluble in Buffer A (i.e., located in the cell debris fraction) were resuspended in Buffer A supplemented with 8M urea and then were centrifuged at 17,300 x g for 30 minutes to separate the urea-solubilized proteins from other cellular debris (pDTR317 [BBK07], pDTR320 [BB0070], pDTR401 [BBK47], pDTR402 [BBE08]). The protein solution then was applied to a nickel-affinity chromatography column using a Pharmacia Biotech Gradifrac chromatography system at room temperature. The same protocol as that which was used for the soluble proteins (see above) was utilized, except that Buffer B also was supplemented with 8M urea. Fractions containing the recombinant protein were collected, concentrated using a 10,000 MW exclusion filter [Centricon]), and buffer-exchanged with 0.5M arginine. To further purify the proteins, the samples then were separated via SDS-PAGE, stained with Sypro-tangerine (Molecular Probes) to visualize protein bands, and excised. Gel fragments containing desired recombinant proteins were eluted by electrophoretic microelution into 8,000 MW exclusion dialysis membrane (SpectraPor-7, Spectrum Laboratories) chambers containing SDS-PAGE buffer. The protein solution was then collected and concentrated using a 10,000 MW exclusion filter (Centricon), then buffer exchanged into 0.5M arginine.

B. Generation of polyclonal antisera raised against recombinant proteins

Purified recombinant proteins were used to generate polyclonal antisera (6). Equal volumes of Freund's complete adjuvant was utilized for emulsification of 10 μg of protein before injection into naïve rats via intraperitoneal injection. Two weeks later, a booster consisting of 10 μg protein mixed with equal volumes of Freund's incomplete adjuvant was injected intraperitoneally into the rat. Blood was taken 1-2 weeks later to evaluate antibody titers specific to each recombinant protein. To enhance the detection of low-abundance borrelial proteins within whole-cell lysates via immunoblot analysis, mono-specific polyclonal antisera were generated by purification of protein-specific antibodies from the crude polyclonal antisera using a NHS-activated Hi-Trap column (Amersham Pharmacia) (128) following the manufacturer's protocol.

C. Sodium dodecyl sulfate-polyacrylamide gel electrophoresis (SDS-PAGE)

Purified/partially-purified proteins or whole-cell lysates were boiled for 5-10 minutes in Laemli buffer (62.5 mM Tris-HCL, 2% SDS, 10% glycerol, 2% 2-mercaptoethanol, 0.001% bromophenol blue). For Coomassie blue staining, 2.5 x 10^7 bacteria were loaded per lane, whereas 5.0 x 10^7 bacteria per lane were used for immunoblotting. Samples were electrophoresed through 4.5% stacking (121 mM Tris-HCl pH 6.0, 0.1% SDS, 0.07% APS) and 12.5% resolving gels (373 mM Tris-HCl pH 8.0, 0.1% SDS, 0.07% APS) in SDS-Page running buffer (100 mM Tris-HCl, 750 mM glycine, 15 mM SDS). After electrophoretic

protein separation, gels were stained with Coomasie Brilliant Blue (40% methanol, 10% acetic acid, 0.5 mM Brilliant Blue) followed by destaining (10% methanol, 10% acetic acid, 2% glycerol) and storage in drying buffer (20% methanol, 3% glycerol). Proteins were transferred to either nitrocellulose (hybond-N+, Amersham Pharmacia Biotech) or PVDF (Hybond-P, Amersham Pharmacia Biotech) in Tris-glycine transfer buffer (40 mM Tris-HCl, 300 mM glycine, 20% methanol). Membranes were stained with Ponceau stain (0.5% Ponceau, 1% acetic acid) to verify transfer of the proteins to the membrane. Immunoblots were then incubated in blocking buffer (PBS-Tween; 1.1 M NaCl, 21 mM KCl, 83 mM Na_2HPO_4, 12 mM KH_2PO_4, 0.05% Tween-20, pH 7.4) for at least 1 hour, followed by incubation with primary antibody in blocking buffer (1 h). Blots were washed with blocking buffer three times (15 min each), followed by incubation with secondary antibody in blocking buffer (30 minutes). Membranes were washed again three times (15 min each), in blocking buffer, followed by two washes in sterile water before detection using either chemiluminescence (ECL plus, Amersham Biosciences) or a colorimetric system (4 parts: [50mM Tris, pH 7.6, 200mM NaCl] to 1 part: [3mg/ml 4-chloro-1-napthol] supplemented with 0.003% H_2O_2).

Primary antibodies used were as follows: rat polyclonal antiserum for OspC (5) and monoclonal antibody 8H3-33 for FlaB (5) have been described. A glutathione-*S*-transferase fusion protein (153) was used to prepare rat polyclonal antiserum against OspA (153). A 6-histidine fusion protein (116) was used to prepare rat polyclonal antiserum against BB0070, BB0664, BB0844, BBA05, BBA07, BBA15 (OspA), BBA25 (DbpA), BBA36, BBE08, BBE16 (BptA), BBE17, BBI42/BBK53, BBK07, BBK32 (P35), BBK47. A 6-histidine

fusion protein to FlaB also was generated and sent to Lampire Biologicals (Pipersville, PA) to produce chicken α-FlaB antibodies. Secondary antibodies used were horseradish peroxidase-conjugated antibodies (goat, rabbit, donkey) from Jackson Immunolabs.

D. Proteinase-K accessibility assays

To determine whether certain *B. burgdorferi* proteins may be surface-exposed in *B. burgdorferi*, a proteinase-K accessibility assay was employed (195). In brief, each culture was harvested at the mid-logarithmic phase of growth (~2 x 10^7 bacteria/ml) and washed twice in PBS supplemented with 10mM $MgCl_2$. Spirochetes then were split into mock-treated and proteinase-K-treated suspensions (proteinase-K [Sigma Chemical Co.] supplied in PBS-10 mM $MgCl_2$ buffer at 0.4 mg/ml) and incubated for 30 minutes. The suspensions then were treated with phenylmethylsulfonyl fluoride (PMSF, Sigma Chemical Co.) at a final concentration of 1 mg/ml to inactivate the protease. Samples then were subjected to SDS-PAGE and immunoblot analysis.

E. Gene building

Gene building is a technology where overlapping oligonucleotides are designed to build a synthetic DNA sequence, typically to change codon bias preferences of the original

ORF to that of the host for recombinant protein expression (i.e., a human protein being expressed in *E. coli*). A program (DNA Builder) developed by the Center for Biological Inventions (CBI, http://cbi.swmed.edu/computation/cbu/dnabuilder.html, U. T. Southwestern Medical Center) takes an input protein sequence and produces a list of oligos (of specified length) such that i) there is limited secondary structure within and between oligos, ii) the oligos, once assembled, produce a coding sequence producing a protein analogous to the input protein sequence, and iii) the resulting ORF optimally utilizes codon preferences for the host organism used for protein expression.

B. burgdorferi is a highly AT-rich organism (71.5%) compared *E. coli* (49.3%) (http://www.tigr.org) and thus has a different amino acid codon bias. During recombinant protein expression studies, several proteins were not expressed to high levels in *E. coli*. Although most recombinant protein expression levels increased when induced within an *E. coli* strain harboring the pRARE plasmid, levels achieved were sub-optimal for large-scale production of the respective proteins. Therefore, gene building was utilized to produce a 6-histidine fusion protein to BBE16 in the pPROEX-Hta vector.

Twenty-four desalted 50-base oligonucleotides (oligos) (Midland Certified Reagent Co.) were dissolved individually in sterile, DNase-free water to a concentration of 100 μM. One μl of each oligonucleotide was added together in a fresh tube to make an oligonucleotide stock containing all primers (4 μg each oligonucleotide per μl = 100 μg/μl total). Two μl of this resultant stock was added to a 50-μl PCR mix that contained 1 mM dNTP's, 3 mM $MgCl_2$, 1x PCR buffer, and 5 units of Taq polymerase. The reaction tube was capped and placed into an Eppendorf Gradient Thermocycler with the following cycling conditions: one

initial denaturation cycle of 94°C for 2 minutes; 35 cycles of (i) denaturation at 94°C for 30 seconds, (ii) annealing at 60°C for 30 seconds, and (iii) extension at 72°C for 1 minute; 1 long extension cycle of 72°C for 10 minutes; and one 4°C refrigeration storage cycle. After this initial PCR, 0.5 μl was transferred to a fresh 50-μl reaction containing 1 mM dNTP's, 3 mM $MgCl_2$, 1x PCR buffer, 50 pMoles of each of the outermost two oligos, and 5 units of Taq polymerase. The reaction was capped and placed once again in an Eppendorf Gradient Thermocycler running for the same cycling conditions as carried out earlier. The resultant DNA fragment was gel-purified, TA-tailed (PCR reaction with 1 mM dNTP's, 1x PCR buffer, and 1.5 units of Taq polymerase with the cycling parameters of: 1 cycle at 72°C for 20 minutes followed by a 4°C refrigeration storage cycle), and cloned into pGEM-Teasy vector for propagation and sequencing. DNA fragments found to lack mutations were then sub-cloned into pPROEX-Hta for expression studies. Constructs for protein expression using this gene building appraoch were designated as pDTR700-pDTR706 (Table 2).

VII. Generation of Genetically-Engineered *B. burgdorferi* Strains

An infectious isolate of *B. burgdorferi* strain 297 and all other bacterial strains and plasmid constructs use in this study are listed in Table 1 and 2. The 297 isolate used in this study as the parental strain (hereafter referred to as PL133) is a low-passage isolate of 297 which had been passed multiple times through the mouse model via needle challenge, retains all plasmids, is highly infectious in mice via needle challenge (ID50 ~40 bacteria), induces

typical histopathological sequelae, and is transformable. The strategy for targeted gene inactivation in *B. burgdorferi* via insertional inactivation (homologous recombination) has been previously described (129).

A. Generation of BBA36 mutants.

All PCR oligonucleotide primers (Table 6) were designed on the basis of strain B31 MI sequence information (57, 101) (http://www.tigr.org) and their approximate locale are graphically represented in Figure 2. Expand High Fidelity Taq Polymerase (Roche Diagnostics) was employed for amplification of the 3542-bp region centered around *bba36* using primers 5'GAGAGTGCTTTAGCACTAATTCAAAAATAAG and 5'CTCTACCTTTTAATATTGAAATGCAGAAAATCTAATTAAAAC. The resultant amplicon was ligated into pGEM-Teasy (Promega) to yield pDTR594 (Figure 2). The *bba36* gene was then interrupted by insertion of the streptomycin resistance marker.

Table 6. Oligonucleotides used in the construction and validation of BbDTR599.

Primer	Sequence (restriction sites underlined)
W	GAGAGTGCTTTAGCACTAATTCAAAAATAAG
AB	CGTAAGGTACCTTAAACATTTCCATAATTTTTCAAATTTTTCAATTCG
Y	CCCGGGCGCGCCTAGTCTAAAACAATTCATCCAGTAAAATATAATATTTT
Z	CCCGGGCGCGCCGCAAAACAAACTTTGAAAAAGCTGTTTTCTGG
AA	GTACACCATGGTTTGCTATAAAATTAAAAATAGCAAAGGGGAGGC
X	CTCTACCTTTTAATATTGAAATGCAGAAAATCTAATTAAAAC

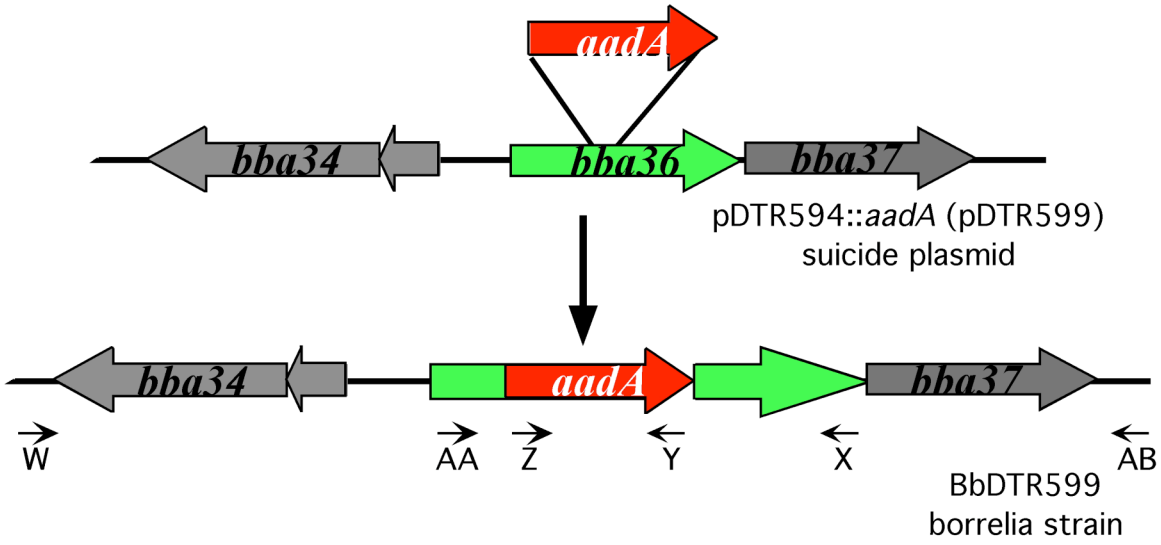


Fig. 2. Plasmid construction strategy for gene inactivation of *bba36* in *Bb* (PL133). The region surrounding *bba36* was amplified using primers W and AB, and cloned into the pGEM-Tez vector to yield pDTR594. *bba36* was disrupted by insertion of an *aadA* cassette (ca. 1 kb conferring streptomycin resistance, amplified with primers Z and Y) into the unique *Hpa*I site to yield the suicide plasmid pDTR599. Primers AA and X are *bba36*-specific primers that were used for PCR-based confirmation of the disruption of *bba36*.

(P_{FlgB}::*aadA*) into the unique *Hpa*I site (blunt cutter) of pDTR594 to generate the suicide plasmid pDTR599. The insertion and orientation of the *aadA* cassette was verified by PCR using primers internal to P_{FlgB}::*aadA* and *bba36* (primers 5'ATGAGCGGATACATATTTGAATG and 5'CGTAAGGTACCTTAAACATTTCCATA ATTTTTCAAATTTTTCAATTCG, respectively or 5'TCATGAGAACCCGAGCCGGTCG GTCCAGAAC and 5'GTACACCATGGTTTGCTATAAAATTAAAAATAGCAAAGGGG AGGC, respectively) (Figure 2).

PL133 was grown to the mid-logarithmic (~1.8 x 10^7/ml) phase of growth and prepared for electroporation using conventional protocols (209) with slight modification (see electroporation of *B. burgdorferi* section above). Thirty to fifty micrograms of pDTR599 DNA (Maxiprep, Qiagen) was used for transformation of PL133 (~2.5 x 10^9 bacteria). The bacteria were allowed to recover in 20 ml of BSK-H medium without selection for 24 hours, after which time the volume was adjusted to 40 ml and supplemented with 50 μg/ml of streptomycin, 1x *Borrelia* Antibiotic Mix (BAM, Sigma Chemical Co.), and 2x phenol red pH indicator (Sigma). The bacterial suspensions were then aliquoted into 200 μl volumes in two 96-well microtiter plates. Plates were wrapped in plastic wrap to limit evaporation and incubated for 2-3 weeks at 37°C under 5% CO_2. Outgrowth of clones first were identified by visible yellowing of the culture medium within individual wells (acidification of media), and then was verified by observation of viable (motile) spirochetes via dark-field microscopy. Two of the clones were selected based on the desired gene inactivation and plasmid contents. These clones then were further evaluated.

B. Construction of BBDTR630

All PCR primers (Table 7) were designed on the basis of strain B31 MI sequence information (57, 101, 198) (http://www.tigr.org) and their approximate locations are graphically represented in Figure 3. Expand High Fidelity Taq Polymerase (Roche Diagnostics) was employed for amplification of the region centered around *bbe22* using primers 5'GGCCATGGCATATGTTTTTATATTGTGAGCCGGTTTAAACAGGTGTTAT TGG (*Nco*I and *Nde*I sites underlined) and 5'GGCGCGCCTACCCGGGTAGTTTTCTAAT TAAATACTATTGAATGATTTT**TTA** (*Asc*I site underlined, stop codon bolded) and the region centered around *bbe21* using the primers 5'GGCGCGCCATTCGCGA**TAA**AAAATC ATTCAATAGTATTTAATTAGAAAACTAC (*Asc*I site underlined, stop codon bolded) and 5'GCGCGCACCCGGGTTTGGAAAATGTATATGATTTTAAAGTGCCATTGATTTTG (*BssH* II site underlined). The resultant amplicons were ligated into pGEM-Teasy (Promega)

Table 7. Oligonucleotides used in the construction and validation of BbDTR630.

Primer	Sequence (restriction sites underlined, stop codons in bold)
A	GCGCGCACCCGGGTTTGGAAAATGTATATGATTTTAAAGTGCCATTGATTTTG
B	TCTTACTAAGAAGTAAAAACCAAGG
C	GGCGCGCCTACCCGGGTAGTTTTCTAATTAAATACTATTGAATGATTTT**TTA**
D	CCCGGGCGCGCCTAGTCTAAAACAATTCATCCAGTAAAATATAATATTTT
E	CCCGGGCGCGCCGCAAAACAAACTTTGAAAAAGCTGTTTTCTGG
F	GGCGCGCCATTCGCGA**TAA**AAAATCATTCAATAGTATTTAATTAGAAAACTAC
G	TATATTAAGCTTACTTTGGCTGTCG
H	AAATTAATTTCTTTGATCAACCAAC
I	GGCCATGGCATATGTTTTTATATTGTGAGCCGGTTTAAACAGGTGTTATTGG

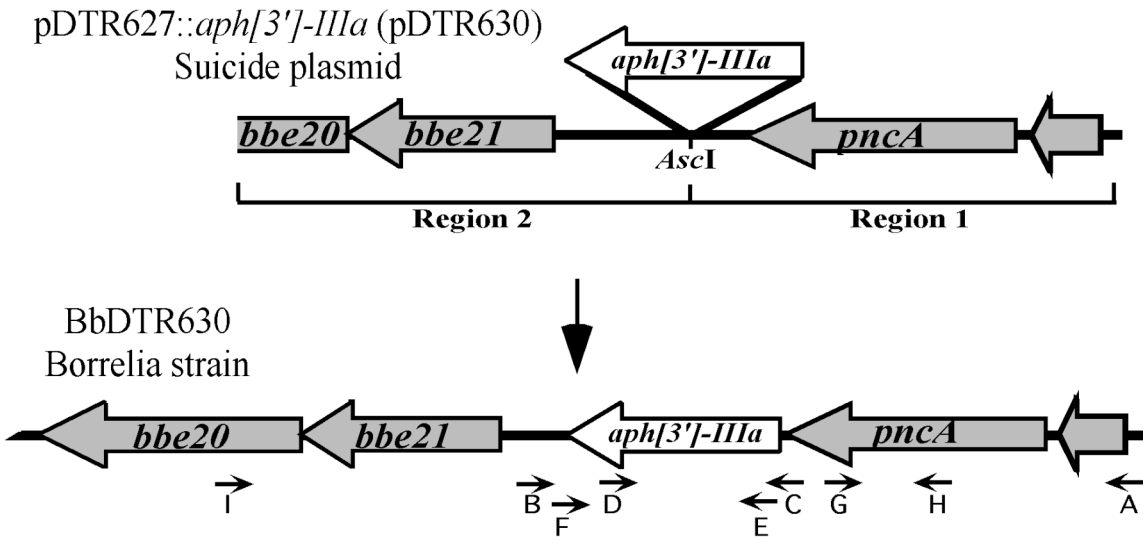


Fig. 3. Schematics outlining the generation of strain BbDTR630 The region encompassing *pncA* on lp25 in *B. burgdorferi* was PCR-amplified and inserted into pGEM-Teasy, yielding pDTR627. An *aph[3']-IIIa* marker encoding Kan resistance was inserted immediately downstream of *pncA* in pDTR627. This resultant suicide plasmid (pDTR630) was then transformed into *B. burgdorferi* PL133. After homologous recombination, strain BbDTR630 (Kan^r) was isolated. Only the relevant regions of each strain or construct are shown.

to yield pDTR623 and pDTR620, respectively (Figure 3). The plasmid pDTR620 was then digested with *Bss*H II and ligated into the unique *Asc*I site in pDTR623 located downstream of *bbe22*. After verification of the correct orientation of the insert relative to the original fragment in pDTR623 containing *bbe22*, the resultant plasmid, pDTR627, contained a unique *Asc*I site immediately downstream of *bbe22* to allow for insertion of exogenous DNA (i.e., resistance markers or complementation constructs). The kanamycin antibiotic resistant marker encoded by *aph[3']-IIIa* (212), from the plasmid, pKan (containing *Asc*I sites on either end), was then inserted into the unique *Asc*I site in pDTR627 to produce the suicide plasmid, pDTR630. The insertion and orientation of the *aph[3']-IIIa* cassette was verified by PCR using primers internal to *aph[3']-IIIa* (5'GGCGCGCCTAGTCTAAAACAATTCATC CAGTAAAATATAATATTTT; *Asc*I site underlined) and *bbe22* (5'AAATTAATTTCTTT GATCAACCAAC) (Figure 3). Two other versions of pDTR627 were generated using P_{FlgB}*::aadA* and *ermC* resistance markers to generate pDTR628 and pDTR629, respectively (not shown).

To generate an lp25-tagged *B. burgdorferi* clone, pDTR630 was transformed into PL133, as described previously, to generate BbDTR630. Resultant clones were frozen, and an aliquot was expanded for genomic DNA evaluations. Mouse infection and tick studies were performed as described herein.

C. Construction of pJD shuttle plasmids

In collaboration with Jon Blevins, a series of shuttle plasmids were developed. Graphical representation of the construction of these plasmids is shown in Figure 4. All primers used in the construction of the various pJD shuttle vectors are listed in Table 8. In general, the *aadA* (100) (PCR-amplified with oligonucleotide primers AL and AM, Table 8) antibiotic resistance marker conferring resistance to spectinomycin and streptomycin in *E. coli* and *B. burgdorferi*, respectively, was introduced into the *BglII* and *BspHI* restriction sites of pKFSS1 (100) (a derivative of pBSV2; ref. 246) shuttle plasmid to yield pJD1 (Figure 4). To remove the *lac* promoter from the multiple cloning site and to introduce a putative borrelial terminator (75), PAGE-purified oligonucleotides were annealed and inserted into the *EagI* and *KpnI* restriction sites of pJD1 to yield pJD7 (Figure 4; Table 8, primers AH-AK). Annealing complementary oligos was performed by placing 100 nmoles of each primer into a reaction mixture containing 15 μl of each oligonucleotide to be annealed, 1μl of 1M Tris-HCl-pH 8.0, 0.5 μl of 1M $MgCl_2$, all in a total volume of 100 μl. The reaction was then heated to 70°C for 10 minutes and then allowed to cool to room temperature slowly over a period of 30 minutes. The reaction was then diluted 1:100 with sterile water and an aliquot of the resultant mixture (containing *EagI* and *KpnI* overhangs) was placed into a ligation reaction containing pJD1 digested with *EagI* and *KpnI* (3 parts insert to 1 part vector). To yield a shuttle plasmid conferring resistance to erythromycin, the *ermC* gene (*BglII* and *BspHI* restriction sites [Table 8, primers AN and AO]) was placed into the same sites within pJD1 to yield pJD39 (Figure 4). To develop a vector compatible with pDTR627 (see Figure 3) for *trans*-complementation, the shuttle plasmid pJD44 was

developed. This was accomplished by exchanging the *aadA* resistance marker in pKFFS1 (*Bam*HI and *BspHI* restriction sites) with *aph[3']-IIIa* (212) (*Bam*HI-*Bgl*II [Table 8, primer AQ] and *Asc*I-*Nco*I [Table 8, primer AP] restriction sites [*Nco*I is compatible with *Bsp*HI]). As with pJD7, primers were also annealed and ligated into this vector at the *Eag*I and *Kpn*I sites to yield pJD44 (Figure 4). This vector is strategic because there are two *AscI* sites on either side of the multiple cloning site/*aph[3']-IIIa* resistance marker, allowing for the one step insertion of complementation constructs into pDTR627.

Table 8. Primers used to construct the various pJD vectors

Primer	Sequence (restriction sites underlined)
AH[a]	GGCCGGCGCGCCAAATAATGCCCGTGTCCCT
AI[a]	TATTCAACAGGGACACGGGCATTATTTGGCGCGCC
AJ[a]	GTTGAATAGGGACACGGTTTTTTAACAATTTTTTTATTCCTAGGCCTTAGTGGCCGGTAC
AK[a]	CGGCCACTAAGGCCTAGGAATAAAAAAATTGTTAAAAAACCGTGTCCC
AL[b]	AAGCTTGATCAGATCTCAGCTTTTTTTTGAAGTGCCTGGCAGTAAGTTG
AM[b]	TCATGAGAACCCGAGCCGGTCGGTCCAGAAC
AN[c]	AGATCTTGCAGTATAAATTTAACGATCACTCATCATG
AO[c]	TCATGAGGCGCGCCTCATGACCCTTAACTTACTTATTAAATAATTTATAG
AP[d]	CCATGGCTAGCGGCGCGCCTAGTCTAAAACAATTCATCCAGTAAATATAATATTTT
AQ[d]	AGATCTCAAAACAAACTTTGAAAAAGCTGTTTTCTGG

[a] primers annealed to produce the *B. burgdorferi* terminator with *Eag*I and *Kpn*I overhangs
[b] primers used to amplify P_{FlgB}*::aadA* for pJD1 and pJD7 vectors
[c] primers used to amplify the *ermC* marker for pJD39
[d] primers used to amplify *aph[3']-IIIa* for pJD44

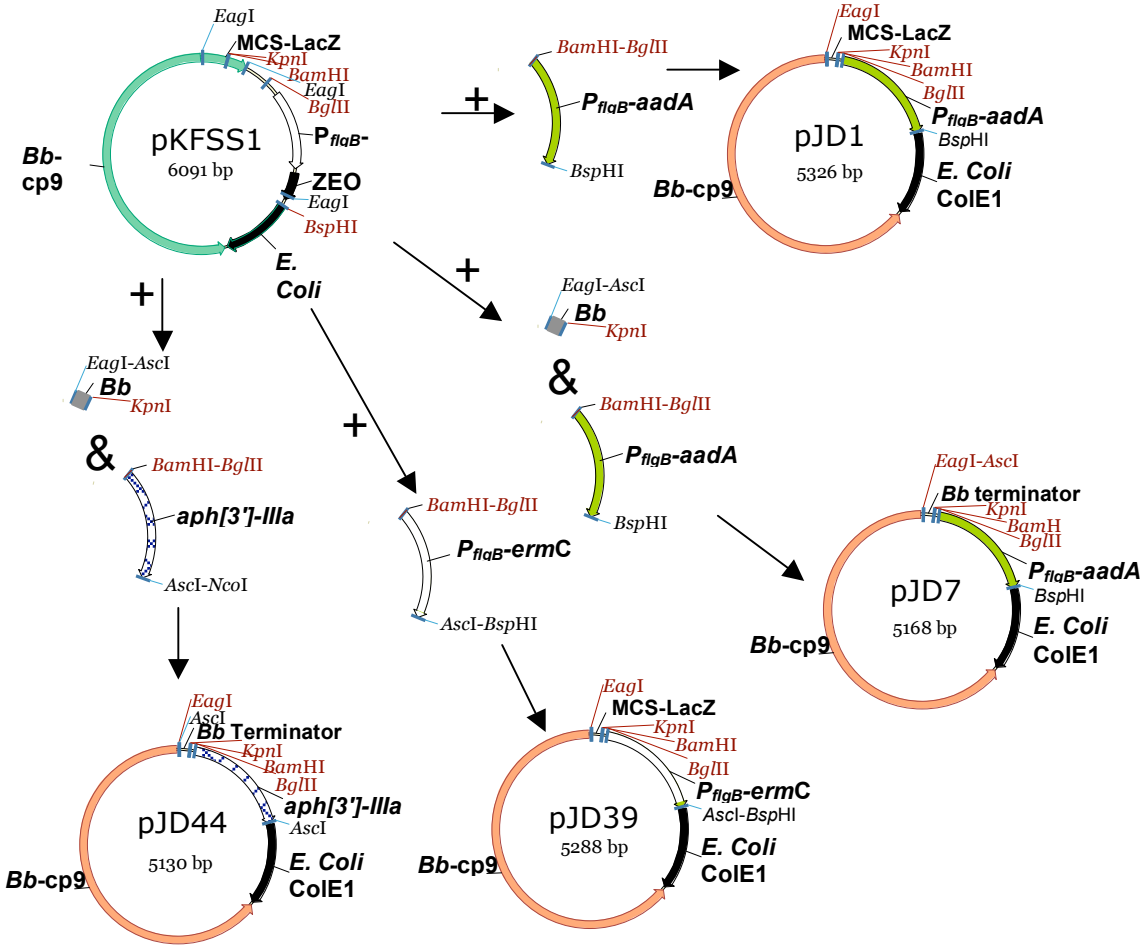


Fig. 4. Construction of the various pJD vectors developed in collaboration with Jon S. Blevins. The shuttle vector pKFSS1 was used as the base vector for all constructions. pJD1 is a smaller version of pKFSS1, whereas pJD7 is the same as pJD1 except the LacZ promoter is replaced with a putative *B. burgdorferi* terminator (75). pJD39 has the *aadA* marker exchanged with the *ermC* marker. Construction of pJD44 was accomplished by replacing (i) the LacZ promoter with the putative *B. burgdorferi* terminator of pKFSS1 and (ii) the *aadA* streptomycin resistance marker from pKFSS1 with the *aph[3']-IIIa* marker. The utility of pJD44 is discussed in Chapter Five.

D. Construction of *bbe16* (*bptA*) and *bbe16/17* mutants and complementation strains

All PCR primers (Table 9) were designed on the basis of strain B31 MI sequence information (57, 101) (http://www.tigr.org) and their approximate locale are graphically represented in Figure 5. Expand High Fidelity Taq Polymerase (Roche Diagnostics) was employed for amplification of the 2,442-bp region centered around *bbe17* using primers 5'CCCGGGCTAATGGATGCAATTTAAAAAAACCTATCCCCTAATTTTAAAAAC and 5'GGCGCCAAAAAGAAATTCACAATAAAATAGAAACAATGAAGATC. The resultant amplicon was ligated into pGEM-Teasy (Promega) to yield pDTR595 (Figure 5). The *bbe16* (*bptA*) gene was then interrupted by insertion of the streptomycin resistance marker (P_{flgB}*::aadA*) into the unique *Swa*I site (blunt cutter) of pDTR595 (Fig. 5) to generate the suicide plasmid pDTR596 (Fig. 5) & pDTR596F (not shown). The insertion and orientation of the P_{flgB}*::aadA* cassette was verified by PCR using primers internal to P_{flgB}*::aadA* and *bptA* (primers 5'CCCGGGCGCGCCGCAAAACAAACTTTGAAAAAAG CTGTTTTCTGG and 5'AAGGTACCTTAAAGATTGTATTTTGGCAAAAAATTTTCTA TATCTATTTTATATTC [*Kpn*I site underlined], respectively or primers 5'CCCGGGCGCGCCTAGTCTAAAACAATTCATCCAGTAAAATATAATATTTT and 5'GTACACCATGGGTATTTTTTTAGGTTTCTTTTTTTACAAACAAAAAGAAAAC [*Nco*I site underlined], respectively) (Fig 5).

As stated previously, PL133 was grown to the mid-logarithmic (~1.8 x 10^7/ml) phase of growth and prepared for electroporation using conventional protocols (209) with slight

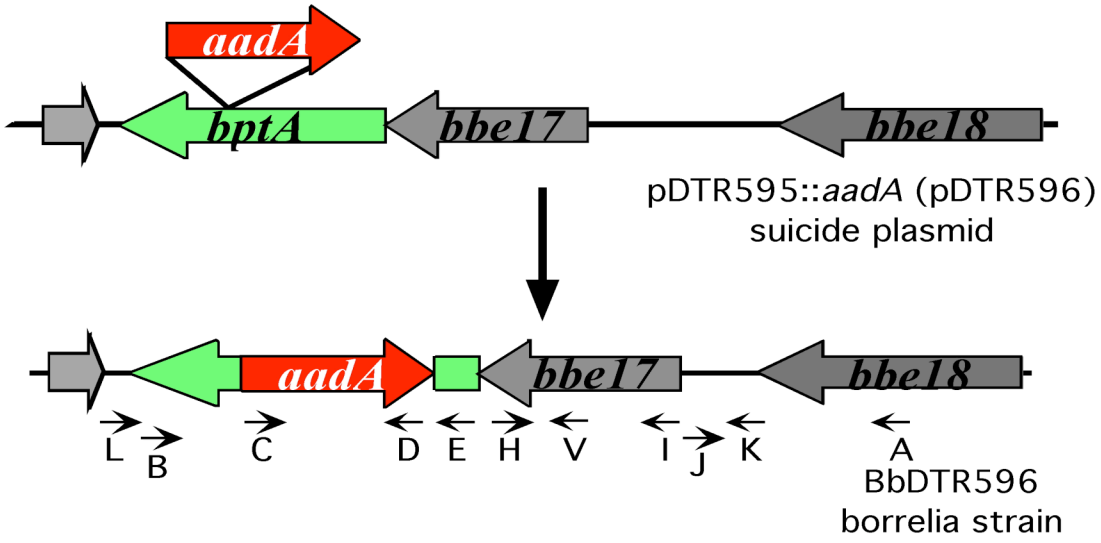


Fig. 5. Strategy for gene inactivation of *bptA* in PL133. The region surrounding *bptA* was amplified using primers A and L, and cloned into the pGEM-Teasy vector to yield pDTR595 in *E. coli*. *bptA* was disrupted by insertion of the *aadA* cassette into the unique *Swa*I site to yield the suicide plasmid pDTR596.

modification (see electroporation of *B. burgdorferi* section above). Thirty to fifty micrograms of pDTR596 or pDTR596F DNA (Maxiprep, Qiagen) was used for transformation of PL133 (~2.5 x 10^9 bacteria). The bacteria were manipulated as stated above for the *bba36* mutants. However, only *B. burgdorferi* clones derived from transformation with pDTR596 were obtained (P_{flgB}*::aadA* inserted on the antisense strand within *bbe16* [*bptA*]). Two clones were selected for initial evaluation, while subsequent complementation analysis was performed on one of these two initial clones.

Table 9. Oligonucleotides used in the construction and validation of BbDTR596-97.

Primer	Sequence (Restriction sites underlined, stop codons in bold)
A	CCCGGGCTAATGGATGCAATTTAAAAAAACCTATCCCCTAATTTTAAAAAC
B	AAGGTACCTTAAAGATTGTATTTTGGCAAAAAATTTTCTATATCTATTTTATAT
C	CCCGGGCGCGCCGCAAAACAAACTTTGAAAAAGCTGTTTTCTGG
D	CCCGGGCGCGCCTAGTCTAAAACAATTCATCCAGTAAAATATAATATTTT
E	GTACACCATGGGTATTTTTTTAGGTTTCTTTTTTTACAAACAAAAAGAAAAC
F	CATATGGGTAAAATATTATTTTTTGGGTTAC
G	AAGGTACCTTACTTATGAAAAATCATATCAAATGCACTAAAAATGTG
H	AAGCTTAGATGAATACTTTTTAGTATAGT
I	GTACACCATGGGTGAAATATCTGAAGAAGTTGTTATTTTAAATGATAG
J	GGGAATTAAAAAAGAAATTAATATTATTATTTTCATATGTTTTATT
K	AGATCTAGTATAGATAATTTTGTGTGCAGAATG
L	GGCGCCAAAAAGAAATTCACAATAAAATAGAAACAATGAAGATC
M	GCGCGCACCCGGGTTTGGAAAATGTATATGATTTTAAAGTGCCATTGATTTTG
N	TCTTACTAAGAAGTAAAAACCAAGG
O	GGCGCGCCTACCCGGGTAGTTTTCTAATTAAATACTATTGAATGATTTT**TTA**
P	CCCGGGCGCGCCTAGTCTAAAACAATTCATCCAGTAAAATATAATATTTT
Q	CCCGGGCGCGCCGCAAAACAAACTTTGAAAAAGCTGTTTTCTGG
R	GGCGCGCCATTCGCGA**TAA**AAAATCATTCAATAGTATTTAATTAGAAAACTAC
S	TATATTAAGCTTACTTTGGCTGTCG
T	AAATTAATTTCTTTGATCAACCAAC
U	GGCCATGGCATATGTTTTTATATTGTGAGCCGGTTTAAACAGGTGTTATTGG
V	AGATCTAAATAACACAGAGATTGTATTTAA

Complementation was performed with several different constructs since knowledge of the upstream promoter elements required for the expression of *bptA* was not known. The promoter for the constitutive flagellar protein, FlgB (primers 5'AAGCTTGATCAGATCTC AGCTTTTTTTTGAAGTGCCTGGCAGTAAGTTG and 5'CATATGGAAACCTCCCTCA TTTAAAATTGC; *Bgl*II and *Nde*I sites underlined, respectively), was fused to *bptA* (5'CATATGGGTAAAATATTATTTTTGGGTTAC and 5'AAGGTACCTTAAAGATTG TATTTTGGCAAAAAATTTTCTATATCTATTTTATAT; *Nde*I and *Hind*III sites underlined, respectively) to guarantee expression in case other constructs did not yield BBE16 [BptA] protein (Figure 6). Additionally, constructs containing either *bbe17* with the putative native promoter, *bptA* without a perceived promoter, *bptA* with the putative *bbe17* promoter, and the putative *bbe17/bptA* operon with native promoter were produced. Attempts at complementation were first performed in the shuttle plasmid pJD44 (derivative of pKFFS1) by insertion of the genes into the unique *Bgl*II and *Hind*III sites of pJD44 (Figure 6). No transformants were obtained using these shuttle plasmids; thus the *Asc*I fragment from these plasmids containing the complementing gene and *aph[3']-IIIa* was excised and placed into pDTR627 (Figure 6). These suicide plasmids were then transformed into pDTR596 using the *B. burgdorferi* transformation protocol listed above. All suicide plasmids generated transformants except for the construct containing *bptA* fused to the constitutive promoter, *flgB* (i.e., pDTR650).

After incubation with antibiotic selection for two weeks, positive clones were frozen and aliquots were expanded for DNA evaluations and infection studies. Clones positive for retention of the original mutation (*bptA* [*bbe16*]) and insertion of complementation construct

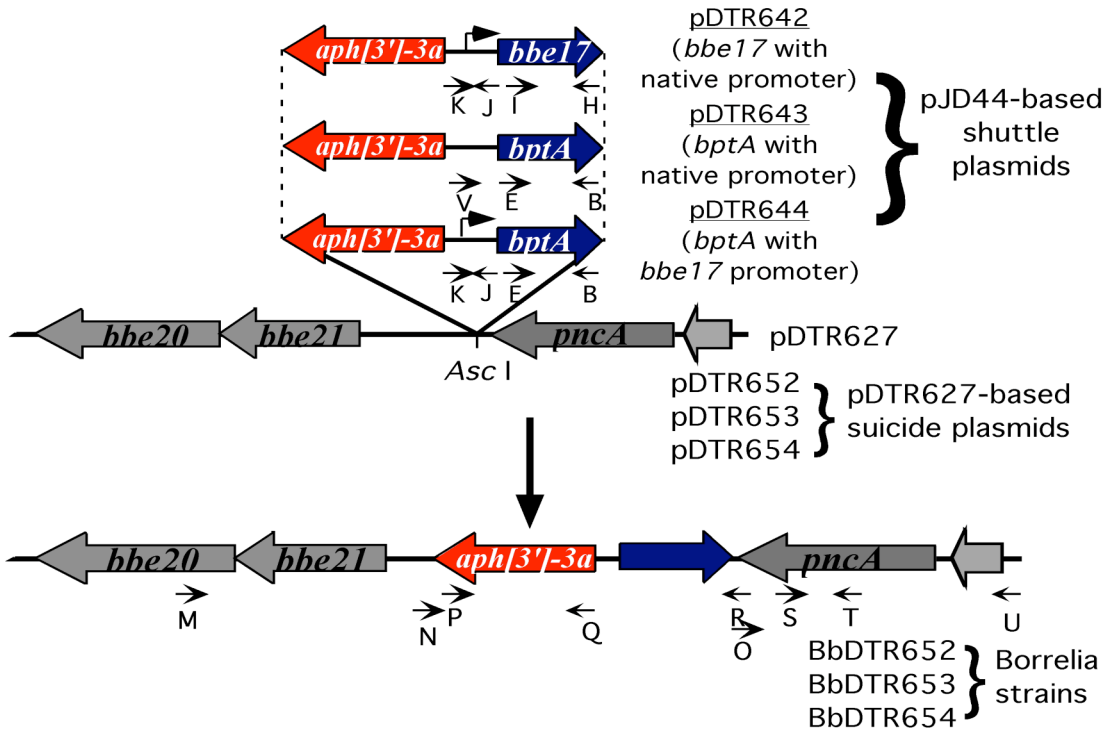


Fig. 6. A *trans*-complementation approach was first employed for complementation of *bptA* or *bbe17* on the pJD44 shuttle plasmid. However, transformants were not produced. Therefore, a *cis*-complementation strategy was employed. The constructs in the pJD44-based vectors were excised (*Asc*I) and inserted into the unique *Asc*I site in pDTR627 (described previously in Fig. 3). This strategy allowed for the wild-type copy of either *bptA* or *bbe17* to be integrated into lp25 downstream of *bbe22* (a site approximately 4 kb removed from the native PCR construction and analysis are listed in Table 9. Only the relevant regions of each construct are shown.

onto lp25 were pooled into groups of four clones each. These pools were ID-injected in C3H mice to ascertain the retention of the virulence phenotype. All ear punch biopsy-positive cultures for each strain were pooled and frozen as the master stock for each complemented strain used in subsequent studies (plasmid profiles not known, nor ascertainable, since it is a pool of clones at this stage).

Evaluation of the genetic organization in the vicinity of *bptA* (*bbe16*) suggests that *bptA* is contained in an operon with *bbe17*; thus, in addition to a single mutation in *bptA*, a double mutant of *bptA* & *bbe17* was also generated. As with the *bptA* mutant, construction of the double mutant utilized pDTR595 as the parental vector. The P_{flgB}*::aadA* resistance marker was inserted into the unique *Swa*I & *Hpa*I sites (blunt cutters) resulting in pDTR597 and pDTR598. Transformation of PL133 and evaluation of resultant clones was performed in the same manner as for the *bptA* single mutants. Verification of insertion of DNA was performed with primers internal to P_{flgB}*::aadA* and *bptA* using primers 5'CCCGGGCGCGCCGCAAAACAAACTTTGAAAAAGCTGTTTTCTGG and 5'AAGGTACCTTAAAGATTGTATTTTGGCAAAAAATTTTCTATATCTATTTTATATTC, while using primers internal to P_{flgB}*::aadA* and *bbe17* using primers 5'CCCGGGCGCGCCTAGTCTAAAACAATTCATCCAGTAAAATATAATATTTT and 5'GTACACCATGGGTGAAATATCTGAAGAAGTTGTTATTTTAAATGATAG, respectively. Complementation of this *bptA/17* mutant was performed in the same manner as for the *bptA* single mutants. However, not a single complemented *bptA/17* mutant retained virulence.

VIII. Plasmid profiling of *B. burgdorferi* strains

Due to the complexity (22 separate replicons) of the *B. burgdorferi* genome and the necessity of certain plasmids for virulence (i.e., lp25 and lp28-1), evaluation of the plasmid content of all genetically-manipulated strains is a vital first-step for the characterization of mutants. This evaluation is performed by PCR-amplification of specific ORFs from each of the known plasmids from strain 297 (78). Most primer pairs used in this study for the detection of each replicon were first described by Eggers *et al.* (78), however, primer-pairs for the detection of lp25, lp38, and *vlsE* (marker for lp28-1) are different from those reported previously. Detection of lp25 was accomplished by using the primers DMN8 (5'AAATTAATTTCTTTGATCAACCAAC) and DMN9 (5'TATATTAAGCTTACTTTGG CTGTCG), while 5'ATGATTATTACCCAAACAACGCCC and 5'TTTTAAATCCATTTT CACAATATG are used for the identification of lp38. Detection of lp28-1 was accomplished by the combination of (i) one of either two sense strand primers designated DMN34 or DMN35 (5'AGTGTTAATGGGATTGCTAGTGGAATAAAGGC [500bp product] or 5'GATGCAGAGAAGGCTGCTGCTGCAGTTAGTGC [300bp product], respectively) and (ii) the antisense primer *vlsE*-full 3' (5'TATAAGCTTTCAGAGAGTCTTATTAACAGCAG TCTCAAC).

Genomic DNA isolated from *in vitro* cultivated *B. burgdorferi* was dissolved in 50 μl of sterile water. One μl of isolated DNA was added to a 50-μl PCR mix (22 reactions in total per strain) with the following cycling conditions: 1 cycle of 95°C for 3 min.; 35 cycles of

95°C denaturation for 20 sec., 45°C annealing for 20 sec., and 72°C extension for 2 min.; 1 cycle of 72°C for 10 min.; and a final 4°C soak.

VIII. Methodologies concerning *I. scapularis*

A. Generation of infected ticks and other tick studies

To obtain ticks harboring the various infectious borrelial strains, mice were intradermally needle-challenged with >5 x 10^5 spirochetes. After two weeks, ear punch biopsies were cultured in BSK-H medium to confirm mouse infections (as above). Infected mice then were infested with approximately 200 pathogen-free *Ixodes scapularis* larvae generously provided by José de la Fuente and Katherine M. Kocan (Oklahoma State University) employing general methods (189). Briefly, mice were restrained for 3-6 h during infestation to allow ticks to attach (Figure 7A). Mice then were removed from restraint and placed into a tick harvesting chamber (Figure 7B). This chamber consisted of a false-bottom grate suspended over water inside a mouse cage; the apparatus allowed for easy collection of engorged ticks from the water reservoir at the bottom of the cage. The water reservoir was inspected and engorged larvae (fed to repletion) were collected twice daily over the 4-7-day infestation period (Figure 7C). Engorged larvae then were washed briefly in distilled water, air dried, and placed into glass vials within an incubator (22°C). Vials were kept over a saturated solution of potassium sulfate (to maintain a high level of relative humidity) and the incubator was adjusted to maintain a

A.



B.



C.

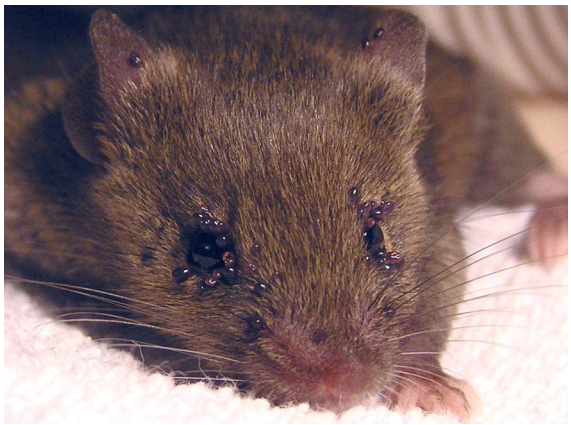


Figure 7. Mouse restraint (A) and engorged tick collection chambers (B) for generation of infected larval ticks. Ticks typically congregate on the head of the mice (C).

photoperiod cycle of 16 h of light and 8 h of dark. Larvae were allowed to molt to the nymphal stage (e.g., about four to five weeks). Nymphal ticks were maintained under these conditions until use either in immunofluorescence assays (IFAs), PCR analysis for spirochetal loads, or mouse infestation experiments.

B. Evaluation of *B. burgdorferi* DNA in *I. scapularis* ticks

The procedure used for the isolation of DNA from either engorged or flat ticks was similar to that previously reported (30). Each tick was washed once sequentially in commercial bleach diluted 1:10, 3.0% hydrogen peroxide, 70% ethanol, and sterile water. Ticks then were placed into a microcentrifuge tube mortal and pestle (Kontes, Vineland, NJ) and flash frozen by submersion of the tube into liquid nitrogen. Ticks were pulverized with the pestle; the process was repeated twice. The DNA from each sample was isolated using the DNeasy Isolation Kit (Qiagen) and was dissolved in 50 μl of sterile water. Five μl of each sample was used in a 50-μl PCR mixture to detect *ospA*. The PCR oligonucleotide primers used to detect *ospA* were 5'CTGCAGCTTGGAATTCAGGCACTT and 5'GTTTTGTAATTTCAACTGCTGACC. PCR was performed using the following amplification conditions: 1 cycle at 94°C for 3 min; 45 cycles at 94°C (denaturation) for 15 sec, 65°C (annealing) for 15 sec, and at 72°C (extension) for 15 sec; and one final cycle of 72°C for 5 min. PCR products were loaded onto and seperated on a 2% Tris-acetate-EDTA agarose gel for resolution of the 156-bp *ospA* fragment. DNA isolated

from naïve ticks was used as a negative control for PCR, whereas 40 ng of genomic DNA extracted from *in vitro*-cultivated PL133 was used as a positive PCR control.

C. Indirect immunofluorescence assay (IFAs) for *B. burgdorferi* in *I. scapularis*

To detect *B. burgdorferi* in ticks via IFAs, total tick contents were dissected free of the tick exoskeleton and placed onto amino-allyl microscope slides (CEL Associates) containing 50 μl of PBS supplemented with 10 mM $MgCl_2$. Slides were then allowed to dry in air. Fixation was performed by placing the slides on a 65°C hotblock for one h, followed by submersion of the slides in acetone for 10 min. Slides were blocked with PBS-Tween supplemented with 5% normal rabbit serum for one h (room temperature) before probing with FITC-conjugated rabbit anti-whole borreliae (diluted 1:100 in PBS-Tween supplemented with 5% normal rabbit serum) (Fitzgerald Industries, Inc.) for one h at 37°C. Samples were then counterstained with 20 μg per ml of propidium iodide (Sigma) and sealed in Slowfade-light (Molecular Probes, Eugene, OR) mounting medium. Ticks were scored as positive for borreliae if more than five spirochetes were detected per tick. An Olympus BH2-RFCA microscope with a 200X objective and filter sets of BP490 and BP545 (for FITC and rhodamine, respectively) was utilized for these evaluations. Slides were protected from light and moisture during storage.

X. Histopathological and Serological Evaluations of Mice After *B. burgdorferi* Infection Via Vick Infestations

Two weeks after mice were infested with *B. burgdorferi*-infected ticks, tissues and blood were harvested for evidence of infection. Blood collection via cardiac puncture was performed with a 23-gauge needle on a 3 ml syringe. Blood was allowed to coagulate for 30 minutes before the sample was centrifuged at 16,000 x g for 10 minutes to separate cellular components from the serum. Serum was aspirated, placed in fresh microcentrifuge tube, and stored at -70°C until needed for serological evaluation.

Detection of antibodies to a number of key borrelial proteins (e.g., P35 and DbpA) has been used as a marker of *B. burgdorferi* infectivity (91, 116). The BBK32 (P35) ORF was cloned into pPROEX-Hta using the ORF-specific primers 5'CCATGGATTTATTCATAAGATATGAAAT and 5'GGTACCATTAGTACCAAACGC CATT. DbpA was also cloned into pPROEX-1 and protein expressed as previously reported (116). A total of 100 ng of each protein was loaded together onto SDS-PAGE preparative gels and subsequently transferred to PVDF membranes. Ten equal-width strips were cut longitudinally from each membrane for evaluation of the elicidation of antibodies specific to DbpA and/or P35 upon successful infection of mice. Serum was used at a dilution of 1:100, while the HRP-conjugated goat α-mouse secondary antibody was used at a dilution of 1:1000. Mice were scored as positive for borrelial infection if antibodies to both antigens were detected. Normal mouse serum was used as a negative control.

Histopathological evaluations were performed on the heart/aortic root, knee joint, and the tibiotarsal joints of mice. Both hind-legs from each mouse were taken by removal of the skin and excision at the hip-joint. Both the legs and heart were placed in 10% buffered formalin (J. T. Baker) for at least two weeks prior to tissue embedding, sectioning, and H&E staining by the UT-Southwestern Pathology core facility. Briefly, all tissues for histology were fixed via transcardial perfusion with 4% paraformaldehyde. Subsequent paraffin processing, embedding, and sectioning were performed by standard protocols (223, 268). Bone tissues were decalcified in 10% formic acid for three days prior to paraffin processing.

CHAPTER FOUR.

DNA MICROARRAY ANALYSIS OF DIFFERENTIAL GENE EXPRESSION IN *B. BURGDORFERI*

I. Introduction

The paucibacillary nature of *B. burgdorferi* in ticks and mammalian hosts has hampered examination of the spirochete's differential gene expression profiles critical to its virulence and host range. To more broadly survey *B. burgdorferi*'s adaptive tendencies, various *in vitro* model systems have been used to mimic certain environmental cues. For example, elevated temperature, reduced pH, and an increase in *B. burgdorferi* cell density, conditions that ostensibly mimic those during tick engorgement, have been shown to induce the reciprocal downregulation of OspA, P22, Lp6.6 (Group II proteins) and the upregulation of OspC, decorin-binding protein A (DbpA), OspF, Mlp-8, and the alternative sigma factor RpoS (Group I proteins) (270). Recently, a novel regulatory pathway involving the control of RpoS by another alternative sigma factor, RpoN, has been strongly implicated in the adaptive changes to these interdependent environmental factors (129). A model system also has been developed in which *B. burgdorferi* is cultivated in dialysis membrane chambers (DMCs) implanted into rat peritoneal cavities to obtain spirochetes in a mammalian host-adapted state (5). However, studies on *B. burgdorferi* differential expression under these or other growth conditions thus far have been practically restricted to examinations of only relatively few proteins at any given time.

A more complete analysis of the adaptive responses occurring during *B. burgdorferi*'s life cycle is invaluable for understanding many aspects of its transmission, virulence expression, immune evasion, and for the potential identification of new Lyme disease vaccine candidates. DNA microarrays (215) are now being applied to survey globally the adaptive gene responses of many pathogenic bacteria (227, 228, 266). The application of microarrays for analysis of the *B. burgdorferi* transcriptome became feasible by the availability of complete genomic sequence information (57, 101). As an initial discovery tool, we pursued the application of DNA microarrays for the global analysis of gene expression patterns in *B. burgdorferi*.

II. Results and Discussion

A. B31 MI growth conditions for comparative transcriptional analyses.

Different B31 MI growth conditions were employed to evaluate transcriptional differences representative of three major stages in the life cycle of *B. burgdorferi*. It currently is infeasible to obtain sufficient quantities of *B. burgdorferi* from ticks for global gene expression studies. Thus, to imitate the unfed tick (UT) condition, spirochetes were cultivated in BSK-H medium (pH 7.5) at 23°C (70, 272); under this condition, *B. burgdorferi* replicates inefficiently, has altered (elongated) morphology, and achieves only modest cell numbers (not shown). To mimic the fed tick (FT) condition, *B. burgdorferi* was cultivated at 37°C to the late logarithmic phase in BSK-H medium adjusted to pH 6.8 (272). These conditions were chosen because

previous studies have indicated that lower pH is critical for the activation of the regulatory cascade(s) that influence the expression of *ospC* and other genes that are thought to be instrumental in transmission to and infectivity of the mammalian host. Finally, mammalian infection by *B. burgdorferi* represents a paucibacillary condition where only very limited numbers of spirochetes are in tissues. Thus, DMCs implanted into the peritoneal cavities of rats were used to obtain mRNA from *B. burgdorferi* in a mammalian host-adapted state (5, 272).

Knowledge of the OspA/OspC paradigm was exploited to validate that RNA used in microarray analysis was derived from spirochetes suitably "adapted" to the various growth conditions. B31 MI cultured under UT conditions showed a high level of OspA expression and a very low expression of OspC, as previously reported (270) (Fig. 8A and 8B). As expected, FT spirochetes showed decreased levels of OspA and markedly elevated levels of OspC (270). Finally, B31 MI cultivated in DMCs virtually lacked OspA but expressed high levels of OspC, consistent with previous studies (5). These protein profiles suggested that each of the *B. burgdorferi* populations used as a source of mRNA for microarray analysis were suitably adapted.

B. Use of GDPs for cDNA labeling.

GDPs (250) were selected for the synthesis of Cy3-labeled cDNA because they increase both the specificity and sensitivity of priming for a targeted mRNA two methods were substantially equivalent (Figure 9). 54.2% of features hybridized with GDP-

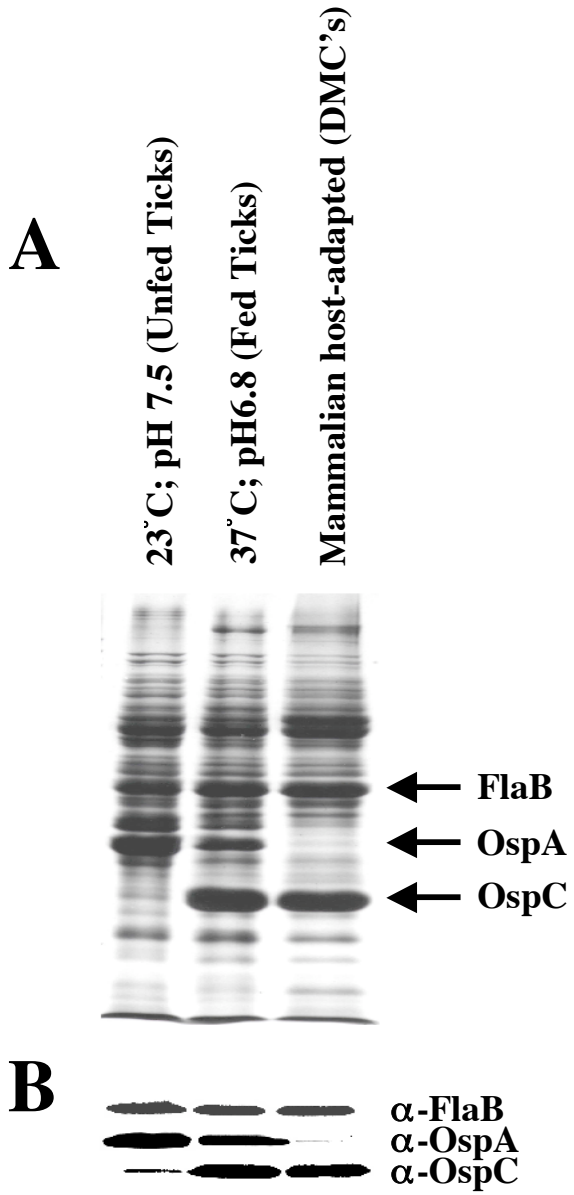


Figure 8. SDS-PAGE (Coomassie blue stain) (A) and immunoblot (B) of whole cell lysates of B31 MI cultivated at the UT, FT, and DMC conditions. The arrows at the right denote the migration of FlaB (loading control), OspA, and OspC.

Cy3:Cy5 ratio being two-fold higher than for random-primed cDNA. Based on these results, all subsequent experiments utilized GDPs.

C. Global gene expression profiling.

An evaluation of mRNA expression profiles of *B. burgdorferi* cultivated under the UT, FT, and DMC conditions was conducted. Although mRNA changes as low as 1.5-fold may have biological relevance (132), the more stringent threshold of 1.8-fold used herein was statistically derived and thus believed to provide a conservative foundation for all interpretations. Using pair-wise analysis among the three B31 MI growth conditions, globally, 8.6% (150) of *B. burgdorferi*'s genes were differentially expressed between the three conditions tested (Tables 10-12). Of these, when *B. burgdorferi* was cultivated under FT conditions, 79 genes (4.5% of the genome) were upregulated whereas 15 genes (0.86% of the genome) were downregulated (relative to UT spirochetes) (Figure 10-I). In contrast, B31 MI cultivated in DMCs upregulated only 6 genes (*vlsE*, *vlsE1*, and four hypothetical genes) and downregulated 60 genes (relative to the FT condition) (Figure 10-II), 30 of which had been upregulated during the FT condition (Figure 10-I). The sharp contrast between the number of genes upregulated during the FT condition (Figure 10-I) but downregulated in DMC spirochetes (Figure 10-II) would lend support to the idea that such differences are a reflection of *B. burgdorferi* subsisting in the two very diverse niches. However, upon further inspection of

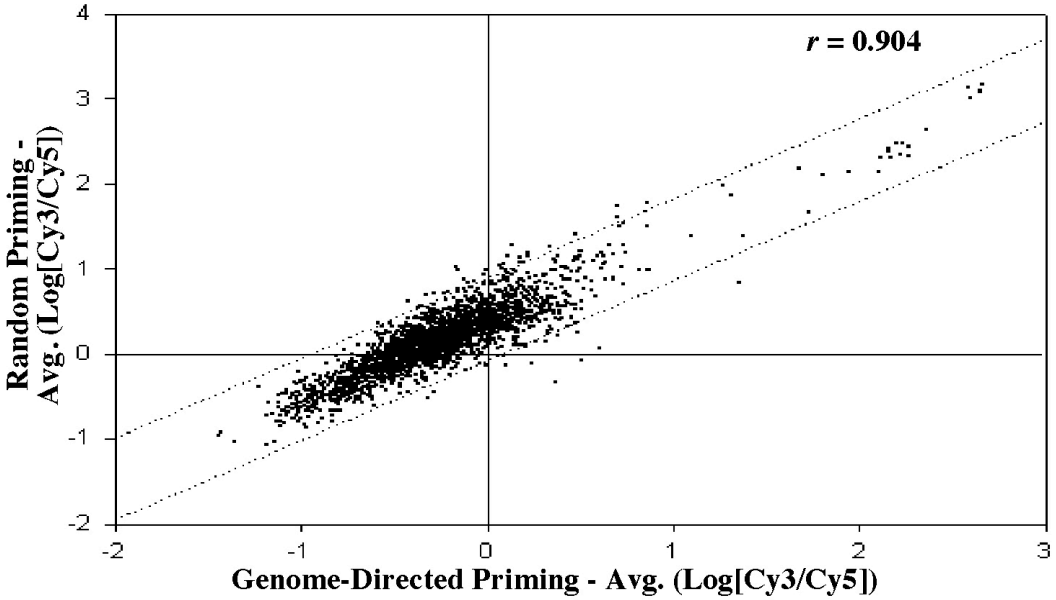


Fig. 9. Correlation of Cy3/Cy5 fluorescence intensities of Cy3-labeled cDNA derived by either random priming or using B31 MI-specific GDPs. The dotted lines represent data within 2 SDs of regression (95% confidence). *r*, correlation coefficient for the similarity between mean log ratios for each feature from the different labeling protocols.

Table 10. Gene expression variations greater than 1.8-fold comparing *in vitro* 23°C, pH7.5 (UT) to in vito37°C, pH6.8 (FT).

TIGR Gene Number and Annotation	Gene Function	Fold Change	Uncertainty	Paralogous Family
BBL29 conserved hypothetical protein		-10.11	0.47	161
BB0191 hypothetical protein		-7.63	0.36	
BB0385 basic membrane protein D (bmpD)	Cell Envelope/Other	-5.96	0.42	36
BB0684 carotenoid biosynthesis protein, putative	Unknown Function/General	-5.42	0.36	
BB0070 conserved hypothetical protein		-5.23	0.4	
BB0545 xylulokinase (xylB)	Energy Metabolism/Sugars	-3.89	0.36	
BB0466 ABC transporter, ATP-binding protein	Transport and binding proteins/Unknown substrate	-3.54	0.34	4
BB0683 3-hydroxy-3-methylglutaryl-CoA synthase	Fatty Acid and Phospholipid Metabolism/Biosynthesis	-3.22	0.38	
BB0686 mevalonate pyrophosphate decarboxylase	Fatty Acid and Phospholipid Metabolism/Biosynthesis	-2.93	0.37	
BB0423 hypothetical protein		-2.84	0.4	
BBF07 hypothetical protein		-2.79	0.4	100
BB0533 phnP protein (phnP)	Central Intermediary Metabolism/Phosphorus compounds	-2.7	0.37	
BBB23 conserved hypothetical protein		-2.64	0.39	94
BB0269 minD-related ATP-binding protein (ylxH-1)	Cellular Processes/Cell division	-2.59	0.36	32
BB0384 basic membrane protein C (bmpC)	Cell Envelope/Other	-2.57	0.34	36
BBO28 lipoprotein (mlpG)	Cell Envelope/Other	2.21	0.39	113
BB0351 hypothetical protein		2.47	0.43	
BB0135 histidyl-tRNA synthetase (hisS)	Protein Synthesis/tRNA aminoacylation	2.51	0.38	
BB0151 N-acetylglucosamine-6-phosphate deacetylase (nagA)	Energy Metabolism/Sugars	2.51	0.39	
BB0195 conserved hypothetical protein		2.55	0.36	123
BBA61 conserved hypothetical protein		2.55	0.39	

Table 10. **(Continued)**
Gene expression variations greater than 1.8-fold comparing *in vitro* 23°C, pH7.5 (UT) to in vito37°C, pH6.8 (FT).

TIGR Gene Number and Annotation	Gene Function	Fold Change	Uncertainty	Paralogous Family
BB0216 phosphate ABC transporter, permease protein (pstC)	Transport and binding proteins/Anions	2.66	0.42	41
BB0561 phosphogluconate dehydrogenase, decarboxylating (gnd)	Energy Metabolism/Pentose phosphate pathway	2.69	0.38	
BB0689 hypothetical protein		2.7	0.36	
BBA03 outer membrane protein	Cell Envelope/Other	2.72	0.35	
BB0365 lipoprotein LA7	Cell Envelope/Other	2.74	0.4	
BBK13 conserved hypothetical protein		2.83	0.37	40
BBM29 conserved hypothetical protein		2.91	0.36	161
BBR36 conserved hypothetical protein		2.93	0.37	165
BBN29 hypothetical protein, paralogous family 161, authentic point mutation		3.03	0.35	161
BB0601 serine hydroxymethyltransferase (glyA)	Amino Acid Biosynthesis/Serine family	3.03	0.39	
BB0037 1-acyl-sn-glycerol-3-phosphate acyltransferase (plsC)	Fatty Acid and Phospholipid Metabolism/Biosynthesis	3.06	0.35	
BBP39 erpB2 protein (erpB2)	Cell Envelope/Other	3.08	0.38	163
BB0330 oligopeptide ABC transporter, periplasmic oligopeptide-binding protein (oppA-3)	Transport and binding proteins/Aminoacids, peptides and amines	3.11	0.42	37
BBO40 erpM protein (erpM)	Cell Envelope/Other	3.16	0.35	163
BB0296 heat shock protein (hslV)	Protein Fate/Protein folding and stabilization	3.2	0.37	
BB0741 chaperonin (groES)	Protein Fate/Protein folding and stabilization	3.2	0.41	
BBA74 outer membrane porin (oms28)	Transport and binding proteins/Porins	3.32	0.4	171
BB0036 DNA topoisomerase IV (parE)	DNA Metabolism/DNA replication, recombination, and repair	3.35	0.37	30
BB0588 5'-methylthioadenosine/S-adenosylhomocysteine nucleosidase, putative (pfs-2)	Purines, Pyrimidines, Nucleosides, and Nucleotides/Salvage of nucleosides and nucleotides	3.35	0.36	26
BBS30 lipoprotein (mlpC)	Cell Envelope/Other	3.38	0.36	113
BB0257 cell division protein, putative	Cellular Processes/Cell division	3.47	0.43	

Table 10. (Continued)

Gene expression variations greater than 1.8-fold comparing *in vitro* 23°C, pH7.5 (UT) to in vito37°C, pH6.8 (FT).

TIGR Gene Number and Annotation	Gene Function	Fold Change	Uncertainty	Paralogous Family
BBA71 hypothetical protein		3.48	0.39	54
BB0646 hypothetical protein		3.57	0.35	
BBI42 outer membrane protein, putative	Cell Envelope/Other	3.61	0.4	52
BBJ34 hypothetical protein		3.62	0.37	92
BB0096 V-type ATPase, subunit E, putative	Energy Metabolism/ATP-proton motive force interconversion	3.66	0.38	
BB0518 heat shock protein 70 (dnaK-2)	Protein Fate/Protein folding and stabilization	3.83	0.39	9
BB0677 ribose/galactose ABC transporter, ATP-binding protein (mglA)	Transport and binding proteins/Carbohydrates, organic alcohols, and acids	3.88	0.41	4
BBK53 outer membrane protein	Cell Envelope/Other	3.95	0.4	52
BBN35 conserved hypothetical protein		4.09	0.4	165
BBK07 hypothetical protein		4.1	0.37	59
BBP35 conserved hypothetical protein		4.2	0.34	165
BB0668 flagellar filament outer layer protein (flaA)	Cellular Processes/Chemotaxis and motility	4.22	0.36	
BBQ47 erpX protein (erpX)	Cell Envelope/Other	4.23	0.4	163
BBO36 conserved hypothetical protein		4.29	0.37	165
BB0669 chemotaxis histidine kinase (cheA-2)	Cellular Processes/Chemotaxis and motility	4.58	0.39	134
BB0094 V-type ATPase, subunit A (atpA)	Energy Metabolism/ATP-proton motive force interconversion	4.58	0.46	39
BB0329 oligopeptide ABC transporter, periplasmic oligopeptide-binding protein (oppA-2)	Transport and binding proteins/Aminoacids, peptides and amines	4.77	0.41	37
BBR29 conserved hypothetical protein		4.99	0.37	161
BBJ23 hypothetical protein		5.12	0.37	106
BB0563 hypothetical protein		5.19	0.35	35
BBC12 conserved hypothetical protein		5.22	0.39	165
BBQ03 outer membrane protein, putative	Cell Envelope/Other	5.29	0.42	52
BBM38 erpK protein (erpK)	Cell Envelope/Other	5.33	0.35	164
BBJ45 hypothetical protein		5.33	0.39	59

Table 10. **(Continued)**
Gene expression variations greater than 1.8-fold comparing *in vitro* 23°C, pH7.5 (UT) to in vito37°C, pH6.8 (FT).

TIGR Gene Number and Annotation	Gene Function	Fold Change	Uncertainty	Paralogous Family
BBL40 erpB2 protein (erpB2)	Cell Envelope/Other	5.58	0.41	163
BBA04 antigen, S2	Cell Envelope/Biosynthesis and degradation of surface polysaccharide	5.69	0.39	44
BB0565 purine-binding chemotaxis protein (cheW-2)	Cellular Processes/Chemotaxis and motility	5.72	0.45	33
BB0567 chemotaxis histidine kinase (cheA-1)	Cellular Processes/Chemotaxis and motility	5.74	0.4	134
BB0671 chemotaxis operon protein (cheX)	Unknown Function/General	6.46	0.41	
BBA72 hypothetical protein		6.56	0.39	
BB0323 hypothetical protein		6.8	0.35	
BB0680 methyl-accepting chemotaxis protein (mcp-4)	Cellular Processes/Chemotaxis and motility	7.14	0.39	13
BBC05 conserved hypothetical protein		7.25	0.38	161
BBA05 antigen, S1	Cell Envelope/Biosynthesis and degradation of surface polysaccharide	9.22	0.4	
BBJ31 hypothetical protein		9.26	0.39	59
BBM28 lipoprotein (mlpF)	Cell Envelope/Other	10.61	0.43	113
BBA73 antigen, P35, putative	Cell Envelope/Biosynthesis and degradation of surface polysaccharide	11.05	0.39	54
BBA07 chpAI protein, putative	Regulatory Functions/Other	11.11	0.45	
BBM27 rev protein (rev)	Unknown Function/General	12.25	0.48	63
BB0844 hypothetical protein		15.1	0.39	12
BB0681 methyl-accepting chemotaxis protein (mcp-5)	Cellular Processes/Chemotaxis and motility	15.15	0.41	13
BBA64 antigen, P35	Cell Envelope/Biosynthesis and degradation of surface polysaccharide	15.35	0.4	54
BBK17 adenine deaminase (adeC)	Purines, Pyrimidines, Nucleosides, and Nucleotides/Salvage of nucleosides and nucleotides	16.02	0.37	61
BBA34 oligopeptide ABC transporter, periplasmic oligopeptide-binding protein (oppAV)	Transport and binding proteins/Aminoacids, peptides and amines	16.1	0.44	37

Table 10. **(Continued)**
Gene expression variations greater than 1.8-fold comparing *in vitro* 23°C, pH7.5 (UT) to in vito37°C, pH6.8 (FT).

TIGR Gene Number and Annotation	Gene Function	Fold Change	Uncertainty	Paralogous Family
BBA65 hypothetical protein		19.52	0.42	54
BBK32 immunogenic protein P35	Cell Envelope/Biosynthesis and degradation of surface polysaccharide	28	0.41	
BBA24 decorin binding protein A (dbpA)	Cell Envelope/Other	46.68	0.38	74
BBA36 lipoprotein	Cell Envelope/Other	58.08	0.37	
BBA66 antigen, P35, putative	Cell Envelope/Biosynthesis and degradation of surface polysaccharide	75.22	0.41	54
BBA25 decorin binding protein B (dbpB)	Cell Envelope/Other	85.69	0.41	74
BBB19 outer surface protein C (ospC)	Cell Envelope/Other	196.29	0.43	

Table 11. Gene expression variations greater than 1.8-fold comparing *in vitro* 37°C, pH6.8 (FT) to DMCs.

TIGR Gene Number and Annotation	Gene Function	Fold Change	Uncertainty	Paralogous Family
BBA66 antigen, P35, putative	Cell Envelope/Biosynthesis and degradation of surface polysaccharide	-31.02	0.43	54
BBK32 immunogenic protein P35	Cell Envelope/Biosynthesis and degradation of surface polysaccharide	-19.31	0.42	
BBA65 hypothetical protein		-18.22	0.43	54
BBA25 decorin binding protein B (dbpB)	Cell Envelope/Other	-18.11	0.47	74
BBA16 outer surface protein B (ospB)	Cell Envelope/Other	-16.01	0.43	53
BBA24 decorin binding protein A (dbpA)	Cell Envelope/Other	-14.77	0.42	74
BBA34 oligopeptide ABC transporter, periplasmic oligopeptide-binding protein (oppAV)	Transport and binding proteins/Aminoacids, peptides and amines	-10.57	0.44	37
BBA07 chpAI protein, putative	Regulatory Functions/Other	-9.05	0.44	
BBA15 outer surface protein A (*ospA*)	Cell Envelope/Other	-8.86	0.42	53
BBK17 adenine deaminase (adeC)	Purines, Pyrimidines, Nucleosides, and Nucleotides/Salvage of nucleosides	-7.58	0.39	61
BBA05 antigen, S1	Cell Envelope/Biosynthesis and degradation of surface polysaccharide	-7.04	0.39	
BBA36 lipoprotein	Cell Envelope/Other	-6.33	0.41	
BBA74 outer membrane porin (oms28)	Transport and binding proteins/Porins	-6.07	0.4	171
BBA64 antigen, P35	Cell Envelope/Biosynthesis and degradation of surface polysaccharide	-6.04	0.41	54
BBC05 conserved hypothetical protein		-5.87	0.4	161
BBM28 lipoprotein (mlpF)	Cell Envelope/Other	-5.77	0.43	113
BBK07 hypothetical protein		-5.67	0.43	59
BBJ08 hypothetical protein		-5.48	0.4	12
BBQ03 outer membrane protein, putative	Cell Envelope/Other	-5.41	0.41	52
BB0323 hypothetical protein		-5.4	0.39	
BBB29 PTS system, maltose and glucose-specific IIABC component (malX)	Transport and binding proteins/Carbohydrates, organic alcohols, and acids	-5.01	0.44	16
BBI42 outer membrane protein, putative	Cell Envelope/Other	-4.81	0.45	52

Table 11. **(Continued)**
Gene expression variations greater than 1.8-fold comparing *in vitro* 37°C, pH6.8 (FT) to DMCs.

TIGR Gene Number and Annotation	Gene Function	Fold Change	Uncertainty	Paralogous Family
BB0563 hypothetical protein		-4.81	0.4	35
BB0631 hypothetical protein		-4.31	0.42	
BB0681 methyl-accepting chemotaxis protein (mcp-5)	Cellular Processes/Chemotaxis and motility	-4.14	0.4	13
BBA04 antigen, S2	Cell Envelope/Biosynthesis and degradation of surface polysaccharide	-4.08	0.4	44
BBK12 hypothetical protein		-4.07	0.39	59
BB0629 PTS system, fructose-specific IIABC component (fruA-2)	Transport and binding proteins/Carbohydrates, organic alcohols, and acids	-4.07	0.36	19
BBK47 hypothetical protein		-4.05	0.4	69
BB0680 methyl-accepting chemotaxis protein (mcp-4)	Cellular Processes/Chemotaxis and motility	-3.83	0.39	13
BB0678 ribose/galactose ABC transporter, permease protein (rbsC-1)	Transport and binding proteins/Carbohydrates, organic alcohols, and acids	-3.78	0.43	130
BB0238 hypothetical protein		-3.76	0.39	
BB0729 glutamate transporter (gltP)	Transport and binding proteins/Amino acids, peptides and amines	-3.71	0.46	
BB0329 oligopeptide ABC transporter, periplasmic oligopeptide-binding protein (oppA-2)	Transport and binding proteins/Aminoacids, peptides and amines	-3.63	0.42	37
BBA67 hypothetical protein		-3.62	0.36	
BBC12 conserved hypothetical protein		-3.56	0.4	165
BB0558 phosphoenolpyruvate-protein phosphatase (ptsI)	Transport and binding proteins/Carbohydrates, organic alcohols, and acids	-3.49	0.41	
BBA62 lipoprotein	Cell Envelope/Other	-3.49	0.37	
BB0603 membrane-associated protein *p66*	Cell Envelope/Other	-3.48	0.42	
BB0366 aminopeptidase I (yscI)	Protein Fate/Degradation of proteins, peptides, and glycopeptides	-3.37	0.38	131

Table 11. **(Continued)**
Gene expression variations greater than 1.8-fold comparing *in vitro* 37°C, pH6.8 (FT) to DMCs.

TIGR Gene Number and Annotation	Gene Function	Fold Change	Uncertainty	Paralogous Family
BB0144 glycine betaine, L-proline ABC transporter, glycine/betaine/L-proline-binding protein (proX)	Transport and binding proteins/Amino acids, peptides and amines	-3.1	0.37	
BB0299 cell division protein (ftsZ)	Cellular Processes/Cell division	-3.09	0.41	
BB0418 hypothetical protein		-3.04	0.36	
BBA73 antigen, P35, putative	Cell Envelope/Biosynthesis and degradation of surface polysaccharide	-3	0.43	54
BB0694 signal recognition particle protein (ffh)	Protein Fate/Protein and peptide secretion and trafficking	-2.99	0.4	10
BB0056 phosphoglycerate kinase (pgk)	Energy Metabolism/Glycolysis & gluconeogenesis	-2.93	0.36	
BBJ09 outer surface protein D (ospD)	Cell Envelope/Other	-2.88	0.38	
BB0057 glyceraldehyde 3-phosphate dehydrogenase (gap)	Energy Metabolism/Glycolysis & gluconeogenesis	-2.87	0.4	
BBR29 conserved hypothetical protein		-2.85	0.38	161
BB0786 general stress protein (ctc)	Cellular Processes/Celldivision	-2.85	0.38	
BBK45 immunogenic protein P37, putative	Cell Envelope/Biosynthesisand degradation of surface polysaccharides	-2.75	0.35	75
BBK48 immunogenic protein P37, putative	Cell Envelope/Biosynthesisand degradation of surface polysaccharides	-2.68	0.38	75
BBP28 lipoprotein	Cell Envelope/Other	-2.67	0.41	113
BB0668 flagellar filament outer layer protein (flaA)	Cellular Processes/Chemotaxis and motility	-2.66	0.39	
BBK13 conserved hypothetical protein		-2.63	0.37	40
BB0691 translation elongation factor G (fus-2)	Protein Synthesis/Translation factors	-2.58	0.39	11
BB0588 5'-methylthioadenosine/S-adenosylhomocysteine nucleosidase, putative (pfs-2)	Purines, Pyrimidines, Nucleosides, and Nucleotides/Salvage of nucleosides and nucleotides	-2.47	0.39	26
BB0789 cell division protein (ftsH)	Cellular Processes/Cell division	-2.43	0.38	
BB0241 glycerol kinase (glpK)	Energy Metabolism/Other	-2.43	0.38	

Table 11. **(Continued)**
Gene expression variations greater than 1.8-fold comparing *in vitro* 37°C, pH6.8 (FT) to DMCs.

TIGR Gene Number and Annotation	Gene Function	Fold Change	Uncertainty	Paralogous Family
BBJ34 hypothetical protein		-2.3	0.38	92
BBS25 conserved hypothetical protein		2.82	0.41	112
BBH13 conserved hypothetical protein		2.83	0.39	80
BBE16 hypothetical protein		2.9	0.51	99
BBF33 surface antigen lipoprotein at right end of lp28-1 (*vlsE*)		2.99	0.41	170
BBF03 conserved hypothetical protein		3.34	0.39	80
BBJ51 *vlsE*1 protein, authentic frameshift (*vlsE*1)	Cell Envelope/Other	4.3	0.44	170

Table 12. Gene expression variations greater than 1.8-fold comparing *in vitro* 23°C, pH7.5 (UT) to DMCs.

TIGR Gene Number and Annotation	Gene Function	Fold Change	Uncertainty	Paralogous Family
BB0191 hypothetical protein		-21.57	0.37	
BBA16 outer surface protein B (ospB)	Cell Envelope/Other	-15.31	0.4	53
BBA15 outer surface protein A (*ospA*)	Cell Envelope/Other	-12.48	0.38	53
BBB29 PTS system, maltose and glucose-specific IIABC component (malX)	Transport and binding proteins/Carbohydrates, organic alcohols, and acids	-10.56	0.42	16
BB0070 conserved hypothetical protein		-7.6	0.41	
BB0684 carotenoid biosynthesis protein, putative	Unknown Function/General	-5.68	0.38	
BB0690 neutrophil activating protein (napA)	Cellular Processes/Detoxification	-5.24	0.4	
BB0423 hypothetical protein		-4.82	0.46	
BB0424 hypothetical protein		-4.78	0.46	
BB0533 phnP protein (phnP)	Central Intermediary Metabolism/Phosphorus compounds	-4.62	0.36	
BB0137 long-chain-fatty-acid CoA ligase	Fatty Acid and Phospholipid Metabolism/Degradation	-4.41	0.38	25
BB0366 aminopeptidase I (yscI)	Protein Fate/Degradation of proteins, peptides, and glycopeptides	-4.37	0.36	131
BB0691 translation elongation factor G (fus-2)	Protein Synthesis/Translation factors	-4.28	0.38	11
BBA62 lipoprotein	Cell Envelope/Other	-4.26	0.36	
BB0144 glycine betaine, L-proline ABC transporter, glycine/betaine/L-proline-binding protein (proX)	Transport and binding proteins/Amino acids, peptides and amines	-4.22	0.4	
BBQ36 hypothetical protein		-3.84	0.39	
BB0789 cell division protein (ftsH)	Cellular Processes/Cell division	-3.57	0.38	
BB0269 minD-related ATP-binding protein (ylxH-1)	Cellular Processes/Cell division	-3.33	0.36	32
BB0683 3-hydroxy-3-methylglutaryl-CoA synthase	Fatty Acid and Phospholipid Metabolism/Biosynthesis	-3.31	0.39	
BBK45 immunogenic protein P37, putative	Cell Envelope/Biosynthesisand degradation of surface polysaccharides	-3.27	0.36	75
BBA38 hypothetical protein		-3.26	0.4	146

Table 12. (Continued)
Gene expression variations greater than 1.8-fold comparing *in vitro* 23°C, pH7.5 (UT) to DMCs.

TIGR Gene Number and Annotation	Gene Function	Fold Change	Uncertainty	Paralogous Family
BBQ42 conserved hypothetical protein		-3.26	0.4	80
BB0149 flagellar hook-associated protein 2 (fliD)	Cellular Processes/Chemotaxis and motility	-3.26	0.38	
BB0271 flagellar biosynthesis protein (flhA)	Cellular Processes/Chemotaxis and motility	-3.25	0.38	
BB0592 hypothetical protein		-3.15	0.4	
BB0061 thioredoxin (trxA)	Energy Metabolism/Electrontransport	-3.08	0.37	
BB0662 hypothetical protein		-3.03	0.4	
BB0156 hypothetical protein		-2.95	0.42	
BB0724 K+ transport protein (ntpJ)	Transport and binding proteins/Cations	-2.93	0.4	
BB0545 xylulokinase (xylB)	Energy Metabolism/Sugars	-2.91	0.4	
BB0067 peptidase, putative	Protein Fate/Degradation of proteins, peptides, and glycopeptides	-2.89	0.36	
BB0241 glycerol kinase (glpK)	Energy Metabolism/Other	-2.74	0.38	
BB0466 ABC transporter, ATP-binding protein	Transport and binding proteins/Unknown substrate	-2.67	0.34	4
BBB22 conserved hypothetical protein		-2.65	0.37	94
BB0805 polyribonucleotide nucleotidyltransferase (pnpA)	Transcription/Degradation of RNA	-2.6	0.36	
BB0824 hypothetical protein		-2.48	0.4	
BB0141 membrane fusion protein (mtrC)	Cellular Processes/Toxinproduction and resistance	-2.45	0.35	
BB0236 hypothetical protein		-2.36	0.39	
BBL15 hypothetical protein		2.32	0.39	156
BB0036 DNA topoisomerase IV (parE)	DNA Metabolism/DNA replication, recombination, and repair	2.41	0.35	30
BB0134 hypothetical protein		2.57	0.36	
BBA72 hypothetical protein		2.8	0.38	
BBL40 erpB2 protein (erpB2)	Cell Envelope/Other	2.85	0.38	163

Table 12. **(Continued)**
Gene expression variations greater than 1.8-fold comparing *in vitro* 23°C, pH7.5 (UT) to DMCs.

TIGR Gene Number and Annotation	Gene Function	Fold Change	Uncertainty	Paralogous Family
BB0741 chaperonin (groES)	Protein Fate/Protein folding and stabilization	2.94	0.4	
BB0096 V-type ATPase, subunit E, putative	Energy Metabolism/ATP-proton motive force interconversion	3.03	0.35	
BB0567 chemotaxis histidine kinase (cheA-1)	Cellular Processes/Chemotaxis and motility	3.19	0.39	134
BB0681 methyl-accepting chemotaxis protein (mcp-5)	Cellular Processes/Chemotaxis and motility	3.66	0.36	13
BBA73 antigen, P35, putative	Cell Envelope/Biosynthesis and degradation of surface polysaccharide	3.68	0.41	54
BB0669 chemotaxis histidine kinase (cheA-2)	Cellular Processes/Chemotaxis and motility	3.71	0.38	134
BBJ23 hypothetical protein		4.09	0.41	106
BBJ31 hypothetical protein		4.42	0.42	59
BBA25 decorin binding protein B (dbpB)	Cell Envelope/Other	4.73	0.46	74
BB0565 purine-binding chemotaxis protein (cheW-2)	Cellular Processes/Chemotaxis and motility	5.72	0.4	33
BBJ51 *vlsE*1 protein, authentic frameshift (*vlsE*1)	Cell Envelope/Other	8.46	0.48	170
BBA36 lipoprotein	Cell Envelope/Other	9.18	0.4	
BB0844 hypothetical protein		14.42	0.39	12
BBB19 outer surface protein C (ospC)	Cell Envelope/Other	119.37	0.42	

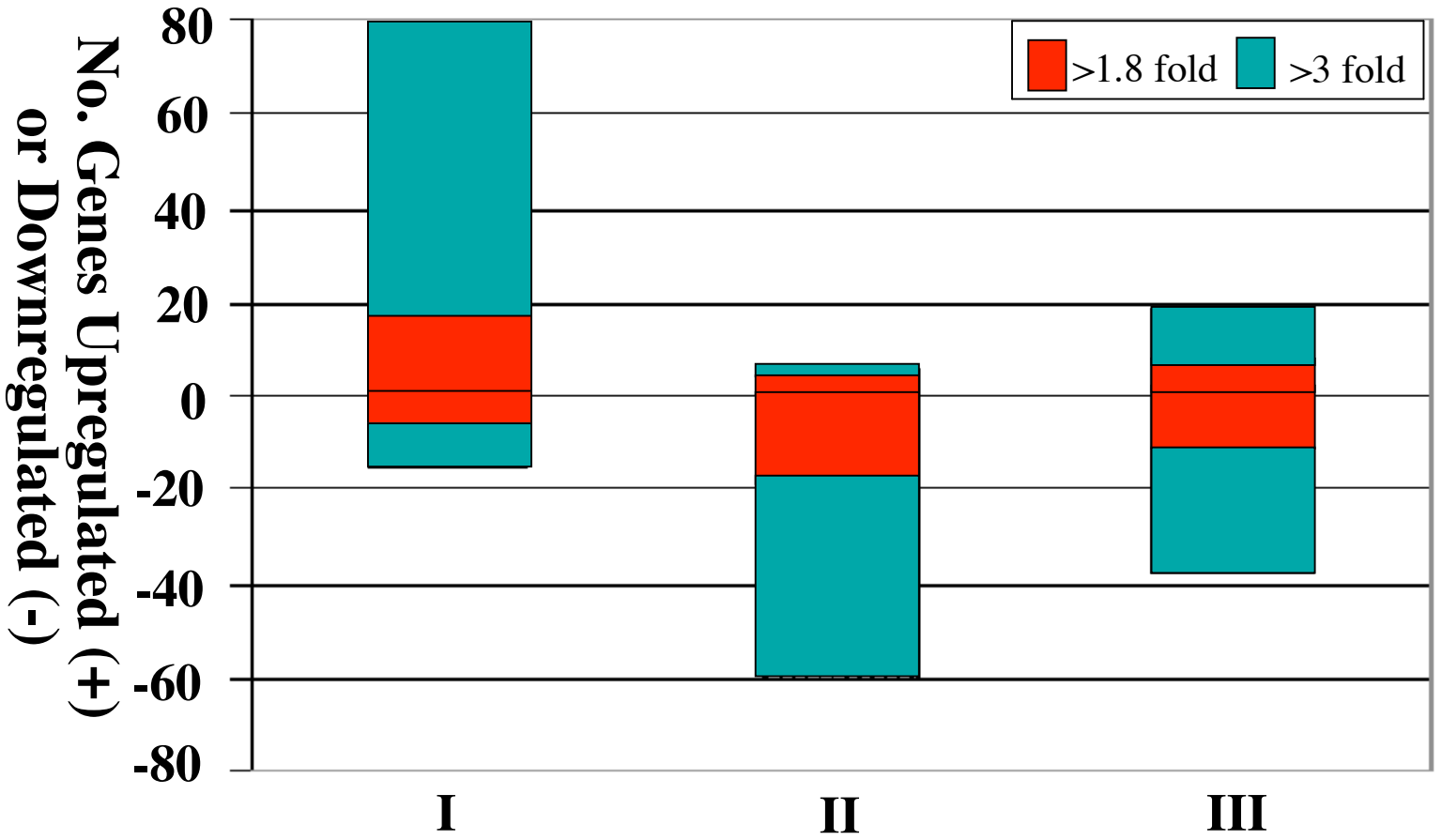


Figure 10. Number of genes differentially expressed during various B31 MI culture conditions. The UT growth condition was used as a baseline reference. The bars reflect comparisons between the UT and FT (I), FT and DMC (II), and UT and DMC (III) growth conditions. The red areas denote gene expression changes of 1.8--3.0-fold, whereas the aqua areas signify changes >3-fold. Individual gene listings are provided in Tables 10-12.

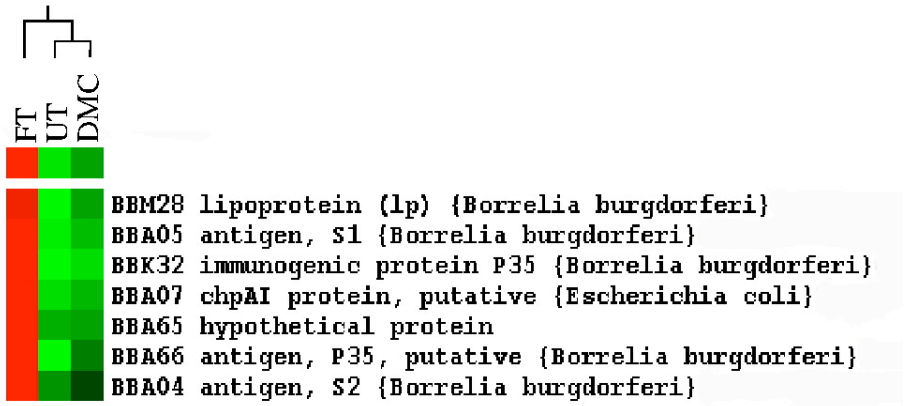


Figure 11. Cluster analysis of Microrray data (*chpAI* cluster).

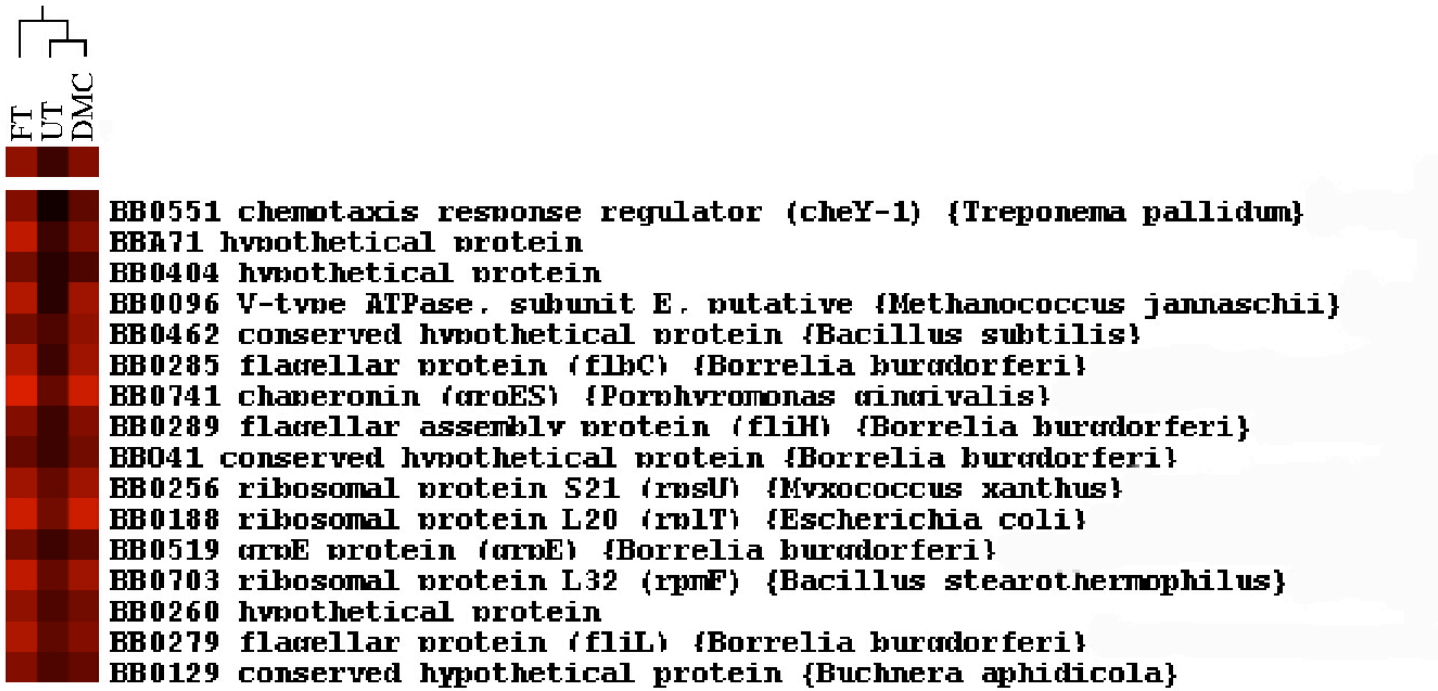


Figure 12. Cluster analysis of Microrray data (*groES* cluster).

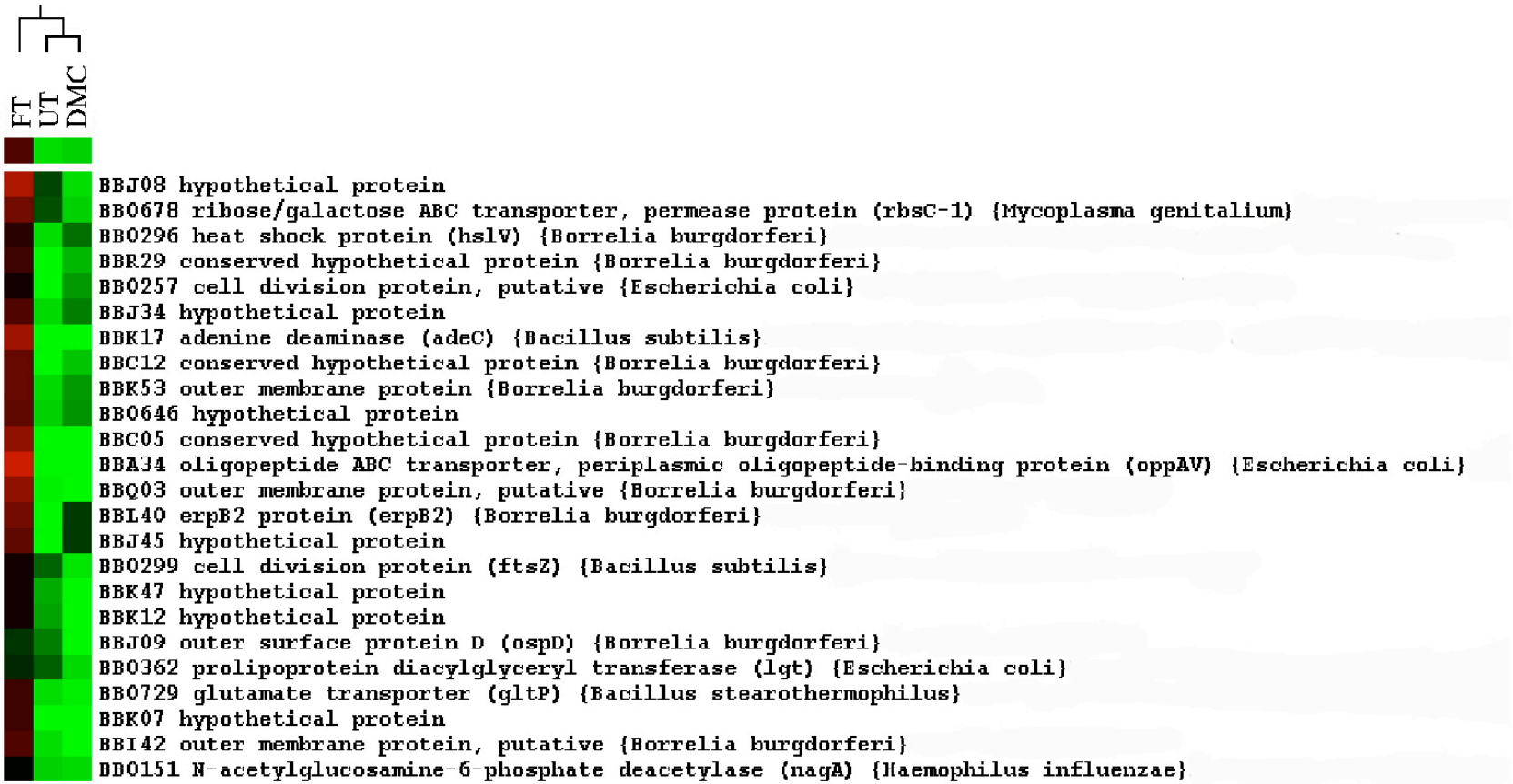


Figure 13. Cluster analysis of Microrray data (*hslV* cluster).

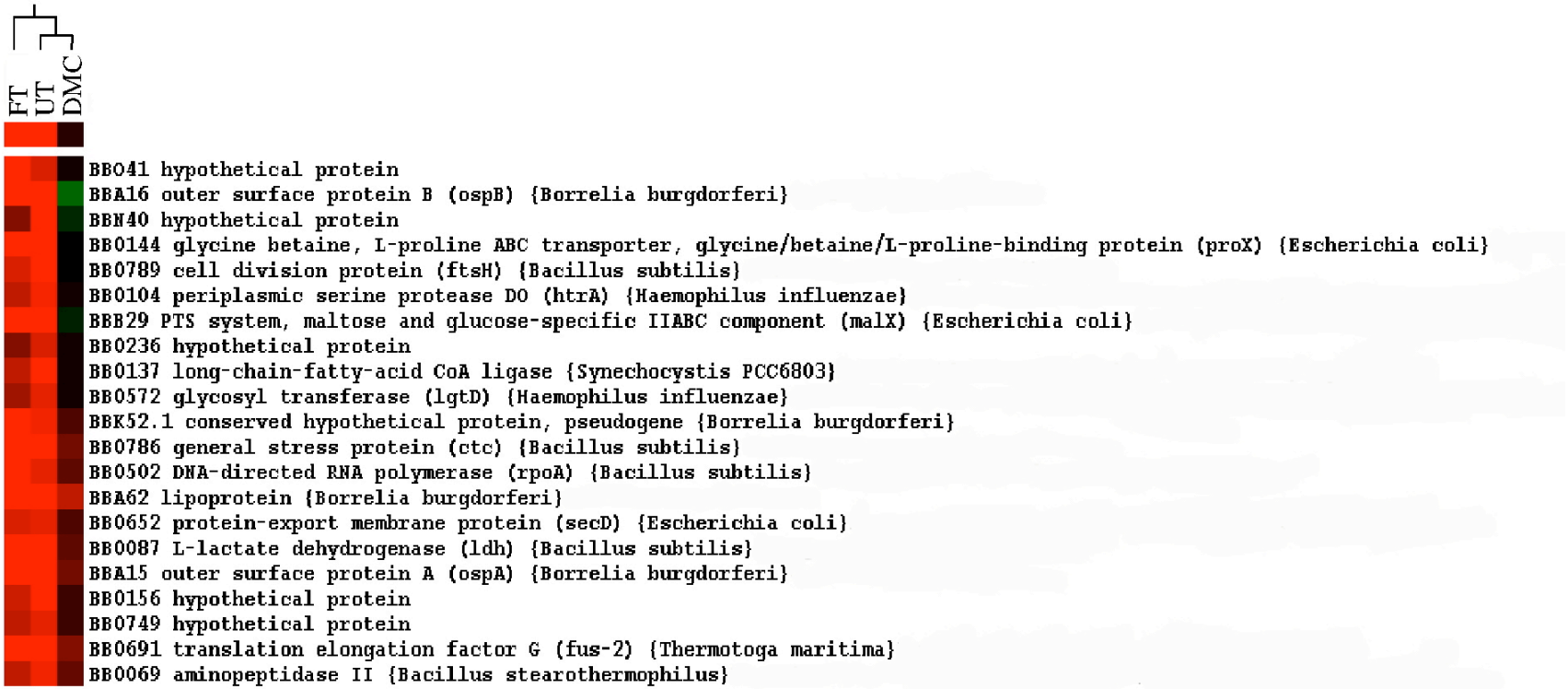


Figure 14. Cluster analysis of Microrray data (*ospA* cluster).



Figure 15. Cluster analysis of Microrray data (*ospC* cluster).

the gene expression profiles between B31 MI cultured under the UT and DMC conditions, DMC-cultured B31 MI showed an upregulation of 19 genes and downregulation of 38 genes (Figure 10-III). From this comparison, and an evaluation of hierarchial cluster analysis (Figure 11-15), it was surprising to find that despite dramatic changes in gene expression occurring between the UT/FT (Figure 10-I) and FT/DMC (Figure 10-II) conditions, growth in the mammalian environment (DMCs) ultimately returns *B. burgdorferi* to a more homeostatic phase (i.e., more akin to the UT condition) (Figure 10-III).

D. Concordance between microarray and real-time RT-PCR data.

Real-time quantitative RT-PCR was used to corroborate selected values from microarrays. Among expression levels compared were those for *ospA*, *ospC*, *dbpA*, *flaB*, and 13 other randomly selected genes (Tables 4 and 13) for which specific PCR primers could be designed. For all three *B. burgdorferi* growth conditions (51 comparisons), there was a high degree of concordance (r=0.883) between data from the two methodologies (Figure 16).

E. Distribution of expression patterns among the B31 MI replicons.

The complex genomic makeup of *B. burgdorferi* includes a linear chromosome and numerous circular and linear plasmids (57, 101); the extent and complexity of the plasmids suggests that they are of enormous importance to the biology of *B. burgdorferi* (57). There was

Table 13. Concordance between Real-Time RT-PCR and microarray data.

TIGR #	Gene Name	Microarray			RT-PCR		
		UT vs FT	FT vs DMC	UT vs DMC	UT vs FT	FT vs DMC	UT vs DMC
16S ribosomal	16S ribosomal	NA	NA	NA	NA	NA	NA
BB0061	thioredoxin (trxA)	1.94	1.59	-3.08	1.06	-9.51	-8.94
BB0070	conserved hypothetical protein	-5.23	1.46	-1.13	-2.85	2.65	-1.08
BB0096	V-type ATPase, subunit E, putative	3.66	-1.21	3.03	2.60	-1.73	1.51
BB0147	Flagellar filament core protein (*flaB*)	2.26	-2.58	-1.14	1.85	-1.99	-1.07
BB0296	heat shock protein (hslV)	3.20	1.82	-1.76	2.16	1.10	-1.05
BB0323	hypothetical protein	6.80	-5.40	1.26	2.47	-3.49	-1.42
BB0466	ABC transporter, ATP-binding protein	-3.54	1.32	-2.67	-2.08	2.33	1.12
BB0545	xylulokinase (xylB)	-3.89	1.34	-2.90	-3.62	1.65	-2.20
BB0671	chemotaxis operon protein (cheX)	6.46	-2.69	2.41	3.25	-1.49	2.17
BB0677	ribose/galactose ABC transporter, ATP-binding protein (mglA)	3.88	-1.54	2.53	2.64	-2.64	1.00
BB0789	cell division protein (ftsH)	1.47	-2.43	-3.57	2.36	-1.77	-1.33
BBA05	antigen, S1	9.22	-7.04	1.31	83.29	-23.40	3.56
BBA07	chpAI protein, putative	11.11	-9.05	1.22	306.55	-27.27	11.24
BBA15	outer surface protein A (*ospA*)	1.41	-8.86	-12.48	-1.16	-3.53	-4.09
BBA24	decorin binding protein A (dbpA)	46.68	-14.77	3.16	108.38	-6.32	17.15
BBA36	lipoprotein	58.08	-6.33	9.18	138.53	-2.99	46.34
BBB19	outer surface protein C (ospC)	196.29	1.62	119.37	121.95	1.20	146.03

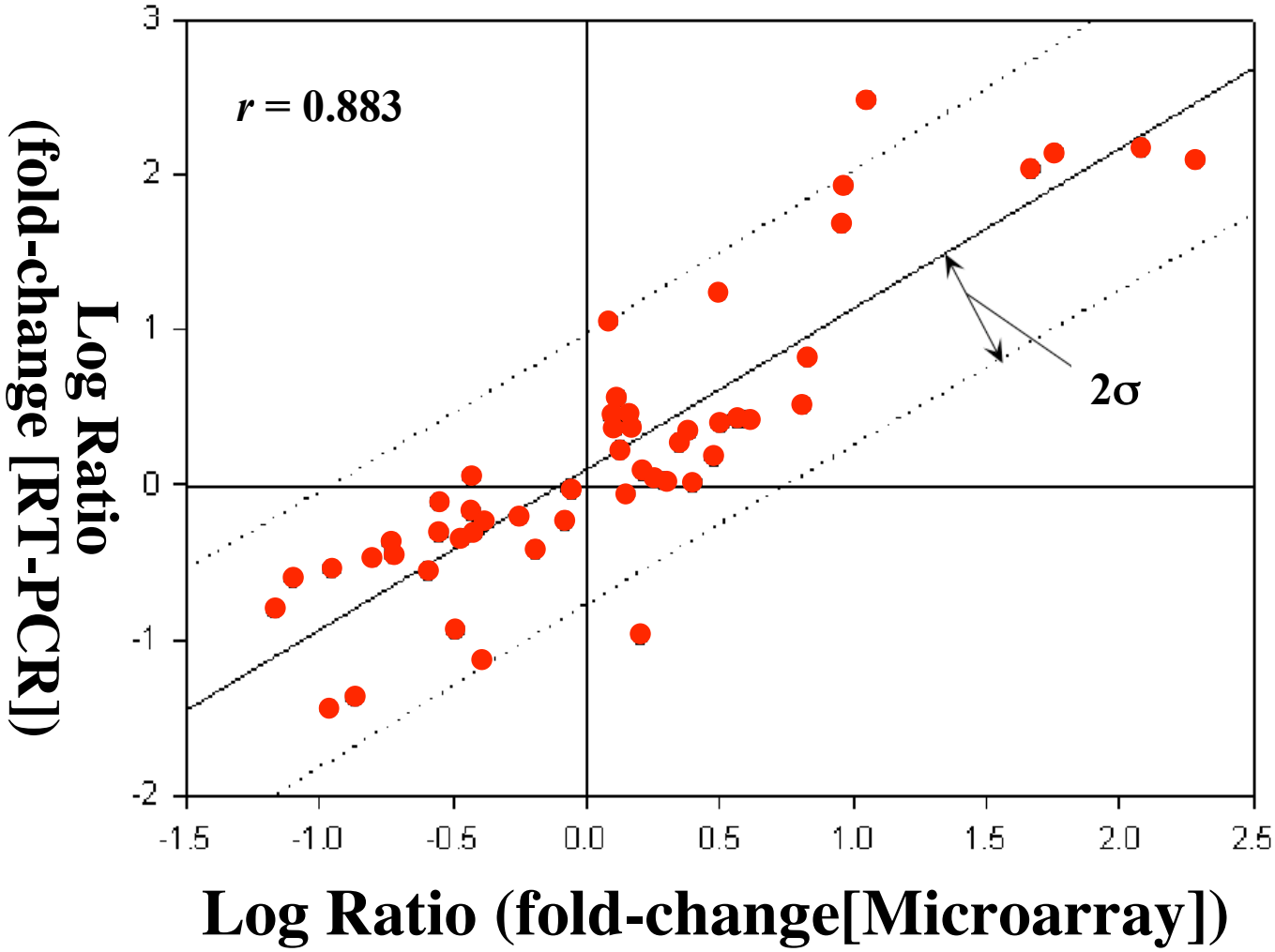


Figure 16. Correlation between microarray and real-time RT-PCR data. Log-transformed fold changes for 16 differentially expressed genes and one constituatively expressed gene (*flaB*; Table 4) were compared at each of the three (UT, FT, DMC) growth conditions. The dotted lines represent data within 2 SDs of regression (95% fonfidence). *r*, correlation coefficient.

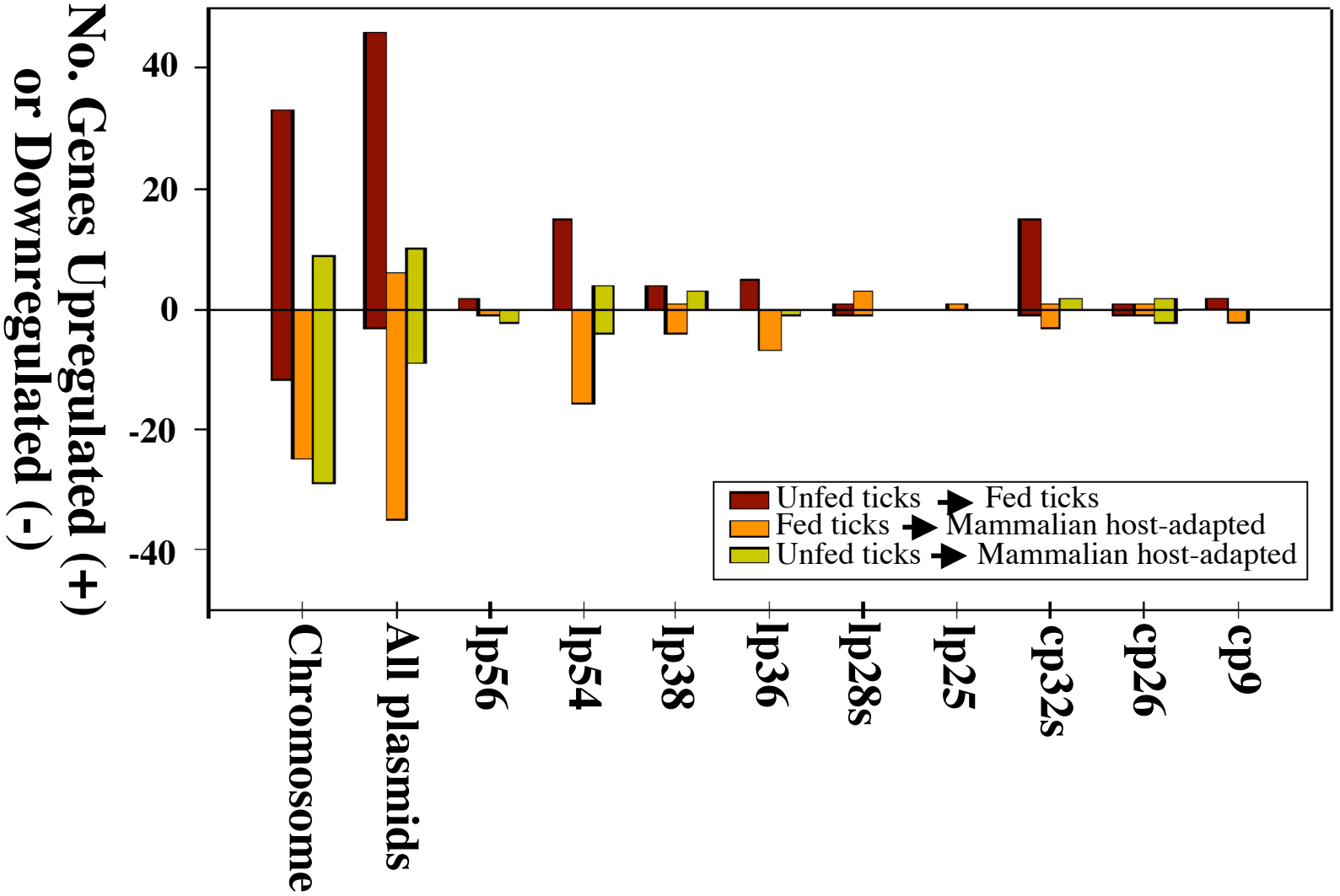


Figure 17. Number and distribution of differentially expressed genes among B31 MI genetic replicons. The UT growth condition was used as a baseline reference. The bars reflect comparisons between the UT and FT (red), FT and DMC (orange), and UT and DMC (yellow) growth conditions. Individual gene listings are provided in Tables 10-12.

nearly an equal distribution of differentially expressed genes between the chromosome (n=78) and the 21 plasmids (n=72) (Figure 17). Seventeen plasmids demonstrated differential expression of their genes; unique genes were detected on linear plasmid (lp) 56, lp54, lp38, lp36, and circular plasmid (cp) 26, whereas only paralogous genes were detected on lp28-1, lp28-3, lp28-4, lp25, cp9, and on all cp32 plasmids (Tables 10-12). Regulated genes were not detected on lp28-2, lp21, lp17, or lp5. The majority of the plasmid-encoded differentially expressed genes were on lp54, lp36, and the family of cp32 plasmids. A number of these genes were upregulated under the FT condition (Figure 17), once again suggesting that shifts in temperature, pH, and spirochete cell density likely are key sensory stimuli. Our data also imply that *B. burgdorferi* genes on diverse replicons can be responsive as a group to a similar constellation of environmental signals. While there are a number of possibilities to explain this, regions of local DNA helicity among the diverse plasmids may be one plausible mechanism. For example, there is evidence that RpoS binding to DNA is adversely affected by negative supercoiling induced by GyrB (150). Topoisomerase IV (ParE) can relax DNA in a replication-independent manner to counteract the effects of GyrB and environmental changes (73), thereby facilitating the accessibility of RpoS to its docking sites. In our studies, *parE* was upregulated under both the FT (3.3-fold) and DMC (2.4-fold) growth conditions (Tables 11-12). From this it is tempting to speculate that ParE activity may play an accessory role in the recently described *B. burgdorferi* RpoN-RpoS pathway, wherein RpoN controls the expression of RpoS (129). In support of the notion that ParE serves an accessory role in the RpoN-RpoS pathway, cluster

analysis revealed that *dbpA*, *ospC*, and 9 other plasmid-encoded genes clustered with *parE* (Figure 15).

lp25 has been closely associated with *B. burgdorferi* infectivity (152, 199, 269). One lp25 gene, BBE16, a putative lipoprotein (57), was upregulated 2.9-fold when B31 MI was cultivated in DMCs (compared with the FT condition) (Table 11). Upstream of BBE16 and separated by only 16 bp is BBE17, which also was upregulated 2.6-fold when B31 MI was cultivated in DMCs. Given the presence of a putative promoter upstream of BBE17 but none for BBE16 (not shown), BBE17 and BBE16 may be operonic; their upregulation during mammalian host adaptation warrants further investigation into their putative roles in *B. burgdorferi* virulence expression.

lp36 also has been implicated in virulence because of its tendency to be present in infectious clones of *B. burgdorferi* (199). This plasmid encodes a P35 homolog, BBK32 (57, 93). BBK32 was upregulated 28-fold under the FT condition and downregulated to near basal level in DMCs. This is consistent with previous observations that BBK32 is sharply upregulated during the transmission of *B. burgdorferi* into mammalian tissue, but decreases to low levels by day 14 in mice (93). Another lp36 gene, BBK17, believed to encode adenine deaminase (AdeC), was upregulated 16-fold in the FT condition (Table 10); this was the only non-chromosomal gene implicated in intermediary (purine) metabolism that was differentially regulated. Thus, lp36, and specifically BBK17, may be vital not only in intermediary metabolism, but also to some poorly understood aspect(s) of *B. burgdorferi* virulence.

lp54 encodes 76 genes, including the *ospAB* and *dbpBA* operons. Consistent with the OspA/C expression paradigm, *ospA* was downregulated about 12-fold from the UT condition

when B31 MI was cultivated in DMCs (Table 12) (real-time RT-PCR showed a 4-fold decrease; Table 13). These levels of *ospA* downregulation were less than anticipated given the degree of OspA reduction in B31 MI cultured within DMCs (Figure 8). While the explanation for the disparity between transcript and protein levels for OspA is unclear, one possibility is some form(s) of post-transcriptional regulation (137). *dbpA* was dramatically upregulated (47-fold) when B31 MI was cultivated at the FT (37°C) condition (Table 3), consistent with the fact that *dbpA* is temperature regulated (59, 117). In contrast, the expression of *dbpA* was 15-fold lower in the DMC versus the FT growth condition; this result is in accord with previous observations that *dbpA* likely is downregulated within days post-mammalian infection (118). Another gene on lp54 with a similar expression pattern to *dbpA* was *bba36*, which was upregulated 58-fold when spriochetes were cultivated in the FT growth condition (relative to the UT condition). *bba36* was subsequently downregulated 6-fold when the spirochetes were cultivated in DMCs (relative to the FT growth condition). This gene has no homology to other genes except for the multicopy lipoproteins (*mlp*) from *B. burgdorferi*. Moreover, similar to *ospC*, the expression of the *mlp* genes have been shown to be regulated (at least partially) by the novel RpoN-RpoS regulatory pathway (51, 129). Taken together, the data suggest that *bba36* may play an essential role in the transmission to and/or infectivity of the mammalian host. Nonetheless, since the majority of the plasmid-encoded genes upregulated during the FT growth condition were subsequently downregulated when spirochetes were cultivated in DMCs (Figure 17), the data indicate that parameters of early *B. burgdorferi* transmission likely trigger a number of plasmid-encoded gene responses that are only transiently necessary (FT). Hence, as noted

earlier (Figure 10-III; Figures 11-15), both the tick (UT) and mammalian (DMCs) environments may largely represent more homeostatic phases in the life cycle of *B. burgdorferi*.

F. Paralogous families.

Gene redundancy (numerous paralogous families) is a salient, yet incompletely understood, feature of *B. burgdorferi* genetic organization (58, 101). The paralogous families potentially complicate the interpretation of microarray data in at least two ways. First, whereas the primer pairs from Sigma-Genosys were intended to amplify specifically each gene of B31 MI, some uncertainty regarding their actual specificities for the paralogous ORFs remained. To examine this, sequencing of amplicons from 21 paralogous ORFs was performed. In every case, the primer pairs specifically amplified their respective genes (not shown), suggesting that target specificity was largely engendered by the set of B31 MI primer pairs.

There was the added possibility of cross-hybridization among related gene family members, thereby masking true differential expression patterns for individual genes. This could have been a limitation in our analyses given that, except in one case (family 161; Table 10), multiple genes of any given paralogous family were similarly regulated at a particular growth condition. However, it is perhaps relevant that of the 49 paralogous families where a subset of member genes showed regulation, 30 families were represented by only a single gene (i.e., 19 families had more than one gene represented). Furthermore, among the 14 genes of the P35 family (#54), although 5 members were differentially regulated similarly as a group, their ranges

varied greatly (3-75-fold upregulation during the FT condition [relative to the UT condition]; 6-31-fold downregulation in DMCs [relative to the FT condition]) (Tables 10-11). Taken together, these data suggest that the arrays, at least to some extent, were capable of distinguishing expression level differences among members of the same paralogous family. Nonetheless, further experiments are neccessary for a more precise analysis of differential regulation among paralogs.

G. Functional classification of differentially expressed genes.

Differential responses of genes within putative functional classes were assessed according to B31 MI genome annotation (58, 101). Given the small B31 MI genome size (ca. 1.5 Mb) and the putative absence of many components of key metabolic pathways (101), it is perhaps not unexpected that genes with essential functions, in general, tended not to show large adaptive changes (Tables 10-11). A logical extension of this is that *B. burgdorferi* utilizes its limited housekeeping genes optimally, even during more static phases of growth. Cluster analysis supported this view in that the majority of the essential genes grouped within the two largest clusters represented by either constitutively high or low levels of gene expression across all conditions (not shown).

Cultivation of *B. burgdorferi* under the FT condition (37°C), where robust spirochete replication occurs, generally led to increased expression of genes associated with the cell envelope, protein synthesis, motility/chemotaxis, transport/binding proteins, and energy

metabolism (Figure 18); these included genes involved in the glycolytic and PTS pathways, as well as others involved in central intermediary metabolism. Additionally, at both the FT and DMC conditions, there were increases in the expression of the V-type ATPase operon (genes BB0090-6) (101) likely responsible for proton efflux (proton motive force) across the cell membrane; such efforts to maintain membrane potential during the more robust periods (FT condition) of cell division are further suggestive that the UT condition represents a more static phase, analogous to the restricted growth of *B. burgdorferi* in unfed ticks (70).

Overall, B31 MI genes associated with cell division tended to be downregulated in the FT and DMC growth conditions (Figure 18), an observation that was seemingly counterintuitive. However, this categorization may be misleading, given that certain gene products serve to inhibit cell division. For example, during the UT growth condition, B31 MI replicated more slowly and displayed a morphology 2-3-fold longer than when cultivated at the FT or DMC condition (not shown). Of potential relevance to this phenotype was the increased expression of the *minD* ortholog *ylxH-1* (BB0269), which was upregulated 2.6- to 3.3-fold in the UT condition (relative to the FT and DMC growth conditions, respectively). In other bacteria, MinD is a cell division inhibitor that, when overexpressed, leads to cell elongation (247). Although the regulation of other cell division genes may contribute to the elongated phenotype of B31 MI grown at room temperature, it is possible that YlxH-1 (MinD) restricts *B. burgdorferi* replication until growth conditions become more favorable. Additionally, these more favorable conditions may induce cell division enhancers that act either as proteases for or suppressors of cell division inhibitors, such as the HslVU dimer (139) or ChpAI (168), respectively. The B31 MI homologs of *hslV* (BB0296) and *chpAI* (BBA07) showed increased

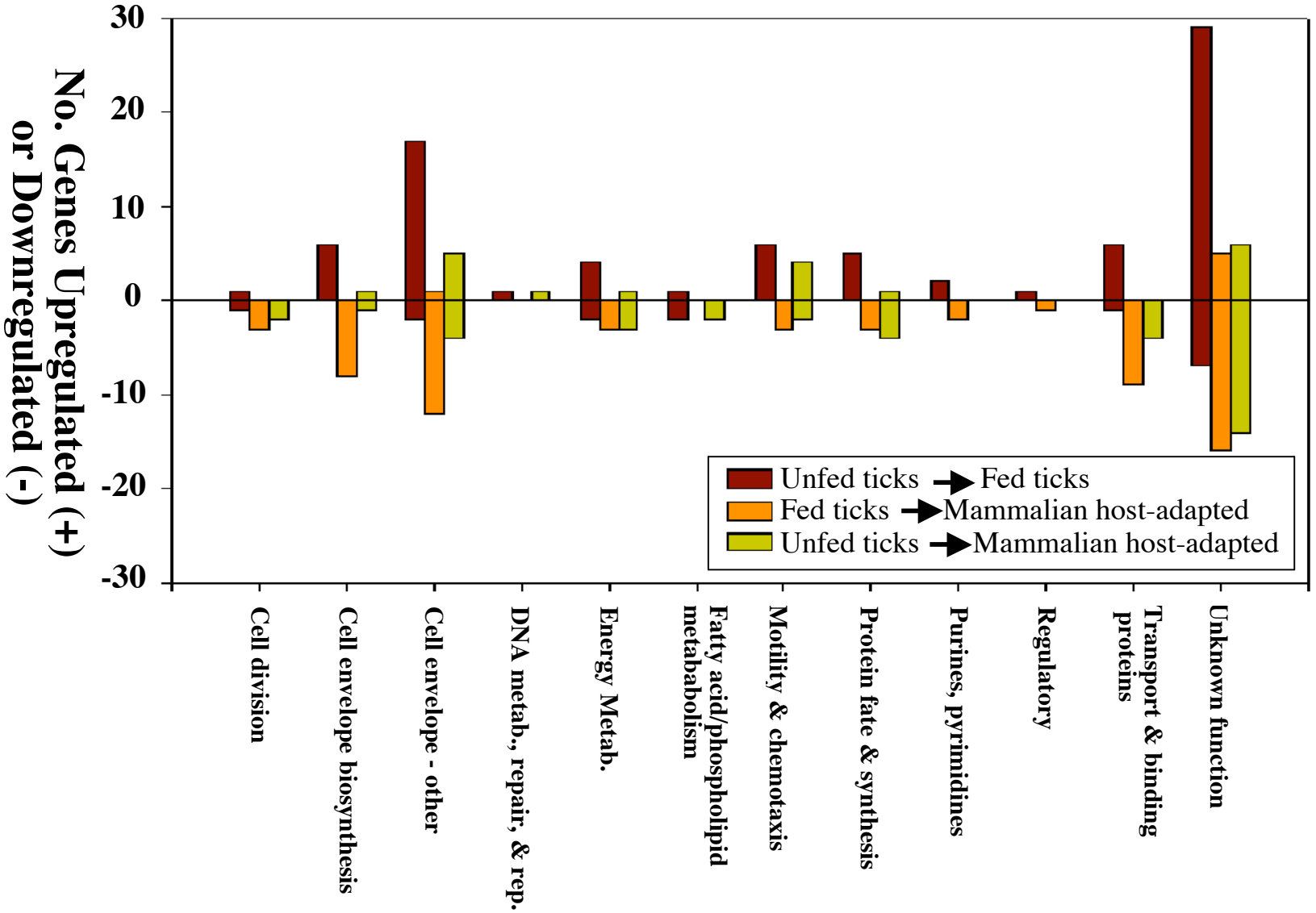


Figure 18. Number of differentially expressed genes grouped by putative protein functions. The UT growth condition was used as a baseline reference. The bars reflect comparisons between the UT and FT (red), FT and DMC (orange), and UT and DMC (yellow) growth conditions. Individual gene listings are provided in Tables 10-12.

expression levels during the FT and DMC conditions (Tables 11-12), implying that inhibitory mechanisms for stasis in *B. burgdorferi* (UT condition) are extant to impede cell division until appropriate growth stimuli are encountered.

A number of genes have been associated with the maintenance of protein stability during periods of bacterial stasis or oxidative stress; among these is *trxA*, which encodes thioredoxin A (163). When B31 MI was cultivated at the suboptimal UT condition, *trxA* (BB0061) increased 2-fold and 3-fold relative to the FT and DMC growth conditions, respectively. In other bacteria, *trxA* is regulated by (p)ppGpp levels that, in turn, are governed via the activities of at least two enzymes, RelA and SpoT (55, 163). RelA has not yet been noted in B31 MI, but SpoT, which can have overlapping function with RelA (55), has been ascribed (BB0198) (101). At the UT growth condition, *spoT* expression was upregulated 1.8-fold and 2.0-fold relative to the FT and DMC growth conditions, respectively. These data, combined with the previously noted genes implicated in inhibition and derepression of cell division (*ylxH-1*, *hslVU*, and *chpAI*), suggest that the steady-state existence of *B. burgdorferi* in unfed ticks (83) may be likened to the bacterial stringent response induced by either limited nutrients or other stress conditions (55). During a stringent response in *B. burgdorferi* (i.e., in unfed ticks), it is conceivable that there is (i) a conservation of energy that assists in cell viability and (ii) a state of cellular readiness that minimizes lags in responsiveness to new sensory information (signifying growth and transmission). While this notion remains hypothetical with present knowledge, it is further supported by the observed upregulation of *B. burgdorferi* genes involved in energy metabolism, protein synthesis, and cell envelope biogenesis during the FT growth condition (Figure 18).

With regard to the cell envelope serving as the principal interface with the host, 17 genes encoding envelope-associated proteins were upregulated in B31 MI cultivated at the FT condition (cell envelope-other; Figure 18). Among these were genes encoding the lipoproteins DbpA, DbpB, OspC, five members of the Erp family, and three members of the Mlp family. Except for OspC, these genes subsequently tended to be downregulated when B31 MI was cultivated in DMCs, consistent with the notion that a more tempered gene response occurs as *B. burgdorferi* adapts to the mammalian environment. Genes associated with cell envelope biogenesis and transport/binding tended to be downregulated by B31 MI cultivated in DMCs (compared with the FT condition), again suggesting a somewhat more controlled growth state perhaps representative of the paucibacillary nature of mammalian infection.

Genes associated with motility/chemotaxis generally were upregulated during the FT growth condition (Figure 18). More specifically, for both chemotaxis (*che*) operons of B31 MI, 3 of 5 genes (*flaA*, *cheA-2*, *cheX*) (104) and 2 genes (*cheW-2*, *cheA-1*) of a second incompletely characterized operon (256) were upregulated in both the FT and DMC growth conditions. Accessory genes encoding methyl-accepting chemotaxis proteins (*mcp4* and *mcp5*) also were upregulated under the FT condition. It thus was not surprising that the majority of these motility/chemotaxis genes clustered with genes associated with mammalian host transmission events (e.g., *ospC* and *dbpA*) (Figures 11-15). The combined data are consistent with the idea that motility and chemotaxis may foster *B. burgdorferi* dissemination processes in both feeding ticks (midgut to salivary glands) and in mammals (spread from dermal tissues), but are less important before transmission events (i.e., within unfed ticks).

Evidence of adaptive changes in B31 MI regulatory genes was sparse in microarrays (Figure 18). This may, in part, be a reflection that only a few homologs of bacterial regulatory proteins have been noted in B31 MI . For example, there is no known heat-shock sigma factor in B31 MI (101), even though a heat-shock response in *B. burgdorferi* has been reported (256). In this study, the heat-shock genes *groES*, *dnaK-2*, and *hslV*, were upregulated during the FT growth condition, suggesting the presence of the relevant regulator(s). However, *groES*, *dnaK-2*, and *hslV* clustered into three different groups (Figures 11-15), suggesting that they may be regulated by different networks. Another possibility for the apparent lack of regulatory gene involvement is that *B. burgdorferi* may be able to exploit only relatively small changes in the expression of its regulatory genes to affect downstream targets. A third possibility may be analogous to the situation for *rpoN*, which is constitutively expressed and post-transcriptionally regulated (38). Consistent with this, the levels of *rpoN* mRNA did not vary in response to the diverse growth conditions. Additionally, in *B. burgdorferi*, RpoN appears to regulate via a novel pathway the expression of *rpoS* (129). Despite this, we did not observe significant changes in *rpoS* mRNA levels under any growth condition, a finding that was surprising given that RpoS levels rise in response to elevated temperature and reduced pH (the FT condition) (270). Although various mechanisms involving post-transcriptional, translational, and post-translational regulation have been described to possibly account for this result, the simplest explanation for this is some form of post-translational regulation over RpoS (i.e., targeted degradation of RpoS) (121).

H. Genes encoding putative signal sequences.

Globally, 46% of the differentially regulated genes of B31 MI were predicted to encode either signal peptidase I (n=25) or signal peptidase II (n=44) leader sequences. This proportion of putative signal peptide-encoding, differentially regulated genes supports the contention that differential expression of the extracellular proteome is of paramount importance to *B. burgdorferi*'s adaptive response(s). Additionally, that 29% of the changing expression patterns represented putative lipoprotein genes likely underscores the dynamic interplay between lipoprotein expression and transitions in the life cycle of *B. burgdorferi*.

I. Summary and implications.

The goal of this study was to examine globally the transcription profile of *B. burgdorferi*, and use the information as a basis for establishing new hypotheses regarding the molecular pathogenesis of Lyme disease. Utilizing B31 MI growth conditions believed to simulate three key phases in the life cycle of *B. burgdorferi*, several valuable insights were garnered. First, a substantial percentage of the differentially regulated genes theoretically encoded export signals, and thus they likely contribute to the extracellular proteome's involvement in host-parasite interactions during strategic *B. burgdorferi* life cycle transitions. Second, while there has been general acceptance that *B. burgdorferi* in unfed ticks represents a form of spirochetal quiescence (70), microarray data provided herein now implicate the bacterial

stringent response (55) and factors that restrain cell division (139, 168, 247) during this *B. burgdorferi* life-cycle phase. Third, a large proportion of genes were responsive to the FT growth environment, wherein increased temperature and reduced pH were prominent environmental conditions analogous to those encountered in feeding ticks (270). Fourth, many of the profound changes in gene expression induced during the FT growth condition were largely ameliorated as B31 MI adapted to the mammalian host; this suggests that once *B. burgdorferi* gains entry and adapts to mammalian tissues, fewer differentially regulated genes are exploited for this phase of survival. Cluster analysis also supported that, despite the disparity between the tick and mammalian hosts, *B. burgdorferi* subjected to conditions analogous to those of unfed ticks and mammalian tissues appeared to induce gene expression profiles more consistent with homeostatic mechanisms. Finally, the microarray data were used as a guide to select genes encoding putative membrane proteins and/or lipoproteins that are differentially regulated during varying growth conditions; these will provide a framework for new avenues of investigation into many aspects of *B. burgdorferi*'s complex parasitic strategy.

CHAPTER FIVE.

DEVELOPMENT OF A NEW GENETIC STRATEGY REVEALS AN OCCULT DEFECT IN *B. BURGDORFERI*'S ABILITY TO BE TICK-TRANSMITTED

I. Introduction

Only recently have the research tools begun to emerge to elucidate the essential nature of selected genes in the natural life cycle of *B. burgdorferi* (110, 187, 275) and other (51, 108, 129, 198). However, attempts to genetically manipulate infectious strains of *B. burgdorferi* often have culminated in a spontaneous loss of virulence (128, 129, 187, 273, 275), thereby hindering one's ability to apply molecular Koch's postulates to substantiate that a given gene encodes a virulence trait (88).

Whereas many aspects surrounding the spontaneous loss of borrelial virulence remain largely undefined, several reports already have pointed to the importance of linear plasmid (lp) 25 (lp25) in the virulence of *B. burgdorferi* (108, 152, 198, 269). lp25 encodes at least one gene (*pncA*, also known as *bbe22*) that has been shown to be essential for conferring on *B. burgdorferi* the ability to infect and persist in a mammalian host (198). However, lp25 also can be lost spontaneously during routine *in vitro* propagation and genetic manipulation of *B. burgdorferi* (109, 217). This prompted me to devise a genetic strategy to efficiently identify clones of *B. burgdorferi* that retain lp25 after genetic manipulation. The attributes of this

approach include (i) the use of antibiotic selection to maintain lp25, thereby increasing the likelihood of obtaining infectious recombinants, (ii) reliance on homologous recombination to achieve genetic complementation, thereby circumventing a putative restriction barrier (*bbe02*) (143, 155) that is particularly deleterious to shuttle plasmids, and (iii) integration of the complementation construct(s) into lp25, thus assuring native copy number (i.e., normal gene dosage).

In my efforts to implement this new strategy, however, I observed that routine laboratory passage of the Lyme disease spirochete in mice led to an occult defect(s) in *B. burgdorferi*'s ability to be transmitted by its tick vector. Such defects serve to undermine advances in borrelial genetics unless comprehensive vector transmission assessments are undertaken for a complete characterization of each *B. burgdorferi* strain used in, or emanating from, genetic manipulation experiments.

II. Results

A. Marking of lp25 with *aph[3']-IIIa* (Kan^r) in strain BbDTR630.

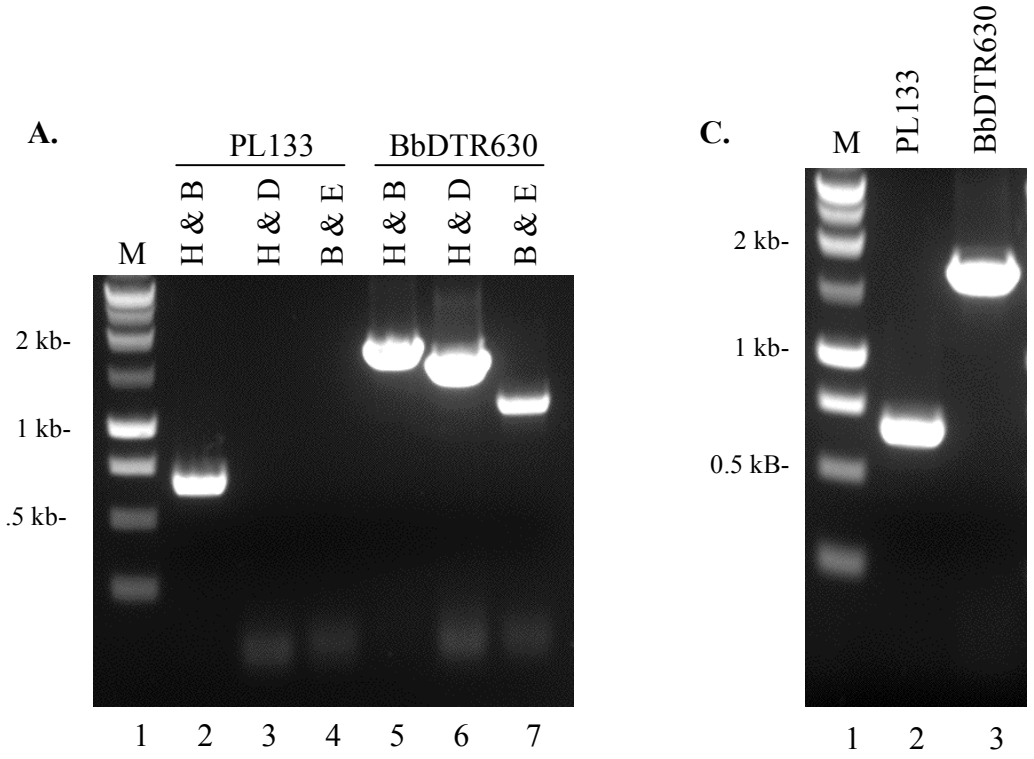
A suicide plasmid was constructed carrying the Kan^r marker within the intergenic region between *pncA* (*bbe22*) and *bbe21* (about 50-bp downstream of *pncA*) (Fig. 3); the Kan^r marker was placed in the same orientation as both *pncA* and *bbe21*. This suicide plasmid then was transformed into strain PL133, yielding approximately 15 Kan^r clones for further evaluations.

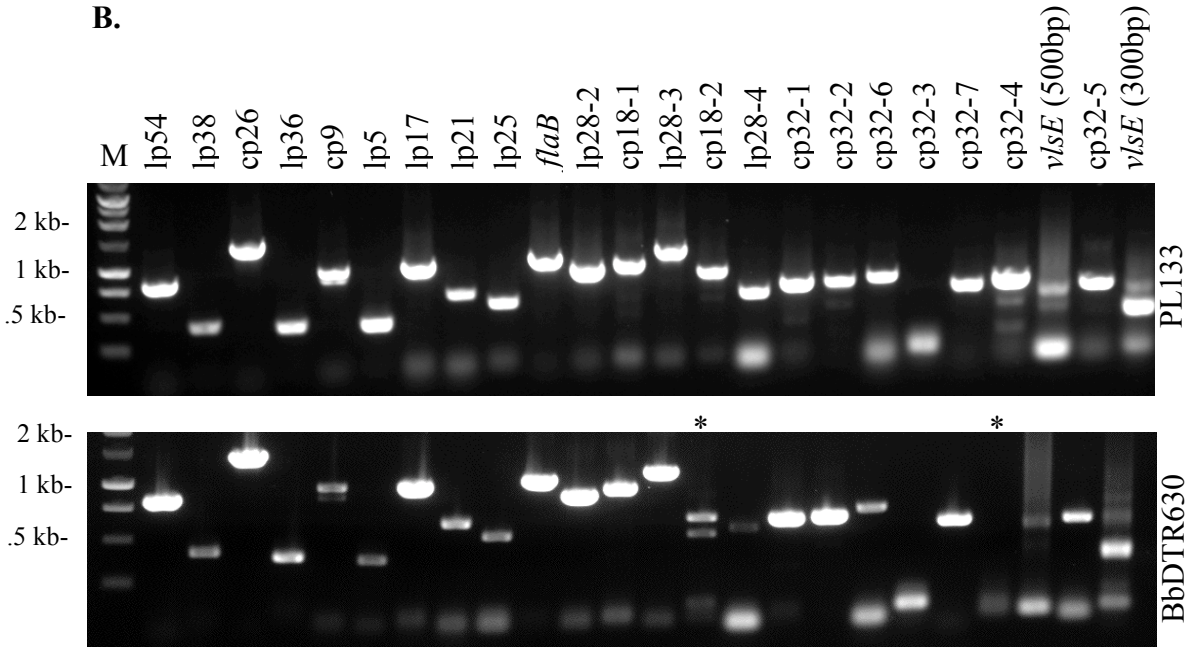
Strain PL133 was chosen for these studies because we have found that PL133 is more amenable to genetic manipulations than strain B31 MI that we previously used for the microarray analysis. One clone was selected based on the desired homologous recombination (double cross-over) event (Fig. 19A); this clone (BbDTR630) was found to possess all but two (cp18-2 and cp32-4) plasmids present in the parental strain (Fig. 19B). Using oligonucleotide primers external to the insertion site (locations of primers H and B shown in Fig. 3) (Table 7), PCR yielded amplicons of predicted size, supporting the fact that Kan^r was due to the insertion of the *aph[3']-IIIa* marker into lp25 (Fig. 19A, lane 5). Presence of the Kan^r marker was further validated by performing PCR with pairs of primers (H and D; B and E) homologous to sequences inside and flanking the inserted *aph[3']-IIIa* gene (Figs. 3 and 19A, lanes 6 and 7). Consistent with the insertion of *aph[3']-IIIa* into lp25, amplicons corresponding to the native (wild-type) gene organization in this region of lp25 were not observed (Fig. 19A, lane 5). Finally, the insertion of *aph[3']-IIIa* into lp25 appeared to be stable; BbDTR630 passaged in C3H mice and recovered from ear punch biopsies cultivated in the absence of Kan retained a gene arrangement in lp25 indicative of the *aph[3']-IIIa* insertion (Fig. 19C, lane 3).

B. BbDTR630 has wild-type growth characteristics and differentially regulates its surface lipoproteins in normal fashion.

Because *B. burgdorferi* has the propensity to lose plasmids spontaneously as well as to manifest spurious secondary mutations, it was essential first to examine the growth phenotype of BbDTR630 as a potential indicator of genetic aberrations. In this regard, there was no

Fig. 19. (Next page) Genetic (PCR) analysis of *B. burgdorferi* strains PL133 and BbDTR630. **A**, confirmation of *aph[3']-IIIa* insertion into lp25 in strain BbDTR630. Lane 1, fragment sizes of DNA markers. Primers H and B flank the insertion site on lp25, thereby signifying the presence of the marker in BbDTR630 (compare lanes 2 and 5). Primers D and E are internal within the *aph[3']-IIIa* marker, and thus primer pairs H+D and B+E were used to verify that the integrant was *aph[3']-IIIa* (lanes 6 and 7). **B**, Analysis of plasmid contents. Approximate plasmid sizes are indicated (in kB) at the left. Amplification of *flaB* was performed as a positive control for PCR. PCR for *vlsE* was used as an indicator for lp28-1. Strain BbDTR630 lacks two plasmids (cp18-2 and cp32-4) (asterisks above lower panel denote absence of expected amplification products). **C**, Evidence (using primers H and B) that *aph[3']-IIIa* was stably integrated into lp25 of BbDTR630. Analysis was as in panel A. BbDTR630 for this analysis was recovered from mouse ear punch biopsies cultured without antibiotic selection.


A.
PL133
BbDTR630
H & B
H & D
B & E
H & B
H & D
B & E
M
2 kb-
1 kb-
.5 kb-
1 2 3 4 5 6 7
C.
M
PL133
BbDTR630
2 kb-
1 kb-
0.5 kB-
1 2 3


B.
M
lp54
lp38
cp26
lp36
cp9
lp5
lp17
lp21
lp25
flaB
lp28-2
cp18-1
lp28-3
cp18-2
lp28-4
cp32-1
cp32-2
cp32-6
cp32-3
cp32-7
cp32-4
vlsE (500bp)
cp32-5
vlsE (300bp)
2 kb-
1 kb-
.5 kb-
PL133
2 kb-
1 kb-
.5 kb-
*
*
BbDTR630

difference in growth rates between BbDTR630 and its parental PL133 when spirochetes were cultivated at 37°C (pH 6.8 or 7.5) (Fig. 20) or when grown at room temperature (not shown). Second, patterns of membrane lipoprotein expression also were evaluated as genetic regulatory processes that typify *B. burgdorferi* (71, 204, 216, 218, 270, 271, 273). *In vitro* culture conditions analogous to those experienced by *B. burgdorferi* within unfed ticks were represented by incubation of the spirochetes at 23°C in BSK-H medium at pH 7.5 (270). To mimic conditions analogous to those experienced by *B. burgdorferi* during tick feeding and transmission into mammalian tissues, spirochetes were cultivated *in vitro* at 37°C in BSK-H medium adjusted to pH 6.8 (270). When cultivated under these diverse conditions and evaluated by immunoblotting, the expression patterns for OspA, OspC, and DbpA in BbDTR630 (Fig. 21) were identical to what has been reported for other wild-type *B. burgdorferi* strains (12, 71, 129, 216, 218, 270). In other words, OspC and DbpA were upregulated when spirochetes were cultivated at elevated temperature and reduced pH, whereas OspA was downregulated under the same conditions. PncA was relatively unchanged within BbDTR630 grown under the two culture conditions (Fig. 21), consistent with prior transcriptional (microarray) analyses (35, 183, 204). The combined results indicate that integration of the Kan^r marker into lp25 did not alter the growth character or the differential expression patterns for OspA, OspC, or DbpA in BbDTR630.

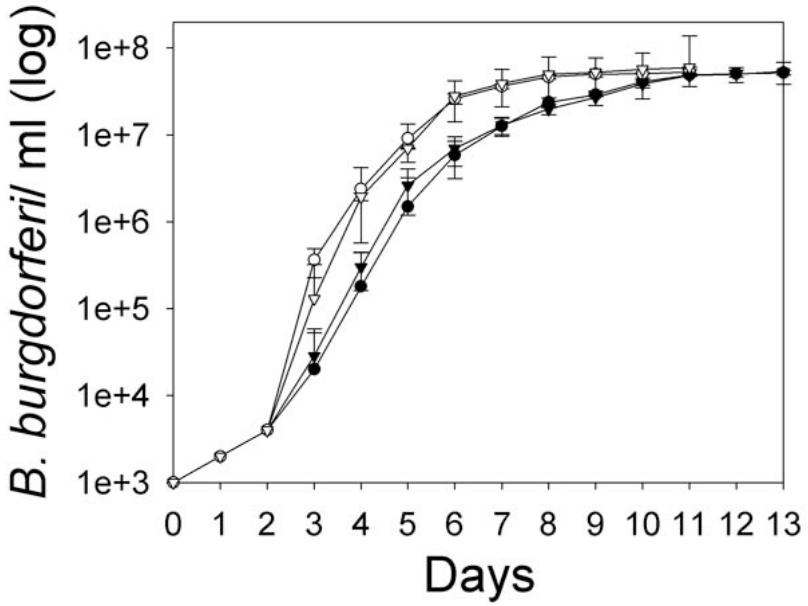


Fig. 20. *In vitro* growth curves of strain BbDTR630 (triangles) and wild-type PL133 (circles) cultivated at 37°C under different pH conditions (pH 7.5 [open features] or pH 6.8 [closed features]). Both strains were grown in triplicate and the average daily cell numbers were determined by darkfield microscopic examinations.

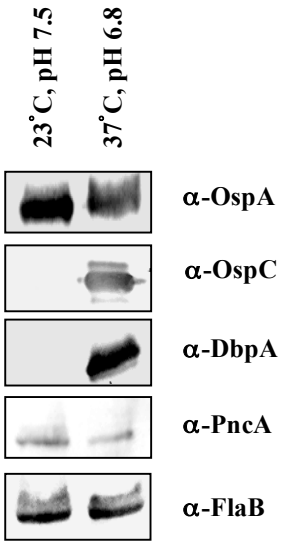


Fig. 21. Expression of proteins by *B. burgdorferi* strain BbDTR630 cultivated under various conditions of temperature and pH (top). SDS-PAGE and immunoblotting were performed using antibody probes (α) specific for OspA, OspC, DbpA, PncA, and FlaB. FlaB was used as a loading control for each gel lane. The modest downregulation of OspA is typical of *B. burgdorferi* cultivated *in vitro* at 37°C (pH 6.8) (204); more pronounced downregulation of OspA occurs when spirochetes are cultivated in a mammalian host-adapted state (5, 204).

C. BbDTR630 retains infectivity for mice.

ID_{50} determinations were performed to assess whether BbDTR630 was attenuated for virulence. BbDTR630 was grown to the mid-logarithmic phase, 10-fold serial dilutions were prepared, and aliquots were intradermally injected into C3H mice (5 mice per group). Ear punch biopsies were collected two weeks later and cultured for the presence of spirochetes. As shown in Table 14, BbDTR630 was infectious for mice at wild-type levels (i.e., comparable to its parental PL133 strain).

Table 14. Determination of ID_{50} values for PL133 and BbDTR630 in C3H mice.

Strain	10^4	10^3	10^2	10^1	ID_{50}
PL133	5/5	5/5	4/5	2/5	31.3 ± 1.61
BbDTR630	3/3[a]	5/5	5/5	2/5	12.8 ± 1.78

[a] two mice died before the completion of experiment

Previous studies have indicated that the virulence and pathogenesis of *B. burgdorferi* are dissociable (9, 252). As such, it was also necessary to evaluate the pathogenicity of BbDTR630. Two weeks after ID injection of mice with 1×10^3 spirochetes, infected mice were euthanized and tissues were harvested for histopathological evaluations (24, 30) of cardiac muscle (carditis) and knee joints (arthritis). As shown in Fig. 22, there were comparable degrees of carditis and arthritis in mice infected with either BbDTR630 or the parental PL133. These results suggest

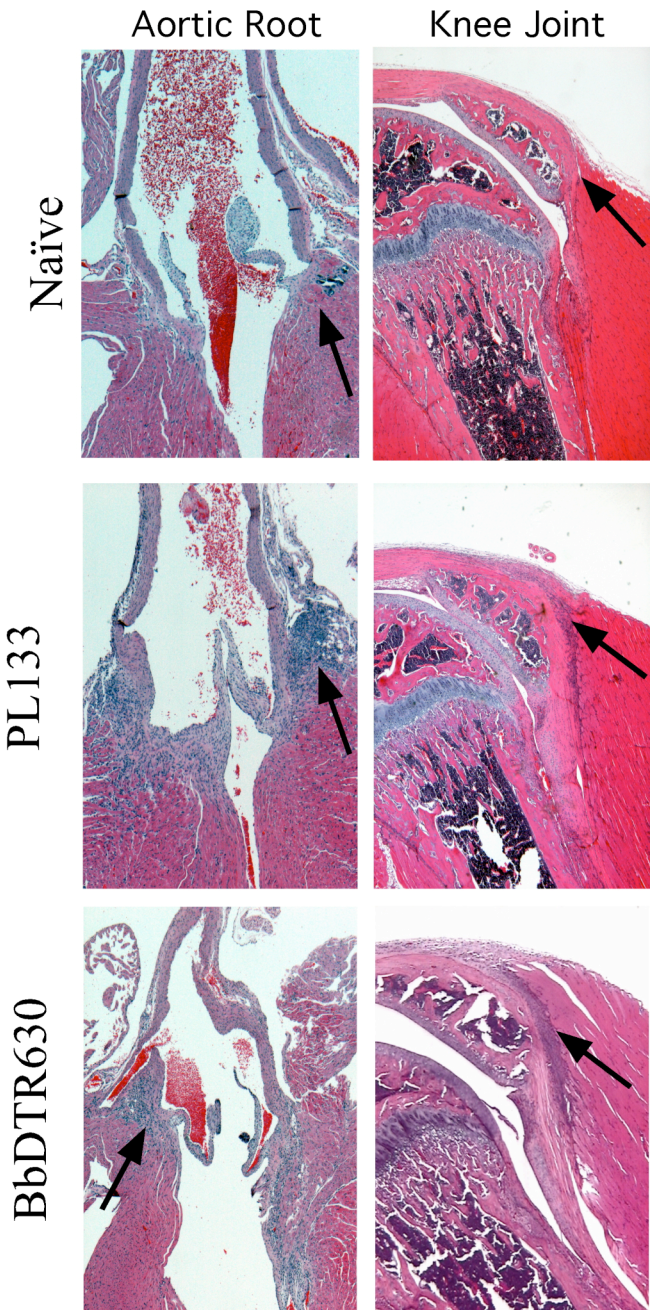


Fig. 22. Histopathological (carditis/arthritis) analysis of knee joints and aortic roots from either naïve mice (3-weeks old) or animals needle-inoculated intradermally with 1 x 10^3 spirochetes. Representative tissue sections are shown for normal tissue, as well as for tissues from mice infected with PL133 or BbDTR630. Arrows denote areas of pronounced immune cell infiltration.

that insertion of the *aph[3']-IIIa* marker into lp25 did not adversely affect dissemination, tissue tropism, or disease progression typical of virulent strains of *B. burgdorferi*.

D. BbDTR630 colonizes and is maintained within *I. scapularis* ticks.

The importance of the tick vector to the life cycle of *B. burgdorferi* prompted us to examine whether BbDTR630 remained competent for colonization and survival within ticks. Comparable to its parental PL133, 100% of larvae that fed on mice infected with BbDTR630 acquired wild-type levels of spirochetes (Table 15). Larval ticks then were allowed to molt to the nymphal stage, at which time the newly molted nymphs were evaluated for bacterial loads. Again, there were no differences in the number of ticks infected or the number of spirochetes per tick for either BbDTR630 or PL133 (Table 15).

Two months after molting, naïve C3H mice were infested each with six nymphs harboring either BbDTR630 or PL133. Nymphal ticks were allowed to feed for 72 h, at which time one tick per mouse was removed for IFAs; 73% or more of engorged nymphal ticks contained either BbDTR630 or PL133, showing that both strains were maintained equally throughout the nymphal stage (Table 15). PCR analysis (to detect the *ospA* gene) of *B. burgdorferi* performed on additional repleted nymphs yielded comparable results (not shown). Taken together, there was no discernable defect in BbDTR630's ability to colonize and persist in ticks.

E. Spirochete transmission from ticks to mice.

To assess tick-to-mammal transmission, BbDTR630- or PL133-infected nymphs were allowed to feed to repletion on naive mice. Two weeks later, ear punch biopsies were harvested from each infested mouse and were cultured for up to two weeks in BSK-H medium (without Kan). In two separate experiments, none of the biopsies from mice, including those mice infested with PL133-loaded nymphs, yielded cultures that were darkfield-positive for spirochetes (Table 15). Given that this result was not anticipated for wild-type PL133, and inasmuch as cultivation of spirochetes from tissue biopsies is an indirect assessment of transmission, mice also were evaluated for serological (93, 116) and histopathological evidence of infection (24, 30). In such evaluations, none of the mice had serological evidence of infection when sera diluted 1:100 were tested by immunoblotting for antibodies directed against the borrelial marker antigens P35 (BBK32) or DbpA (not shown). Moreover, none of the mice showed histopathological evidence of either carditis or arthritis (not shown). These unexpected findings suggested that PL133 was naturally deficient in its transmissibility from ticks to mammals.

To assess further the apparent defect in PL133's ability to be tick-transmitted, and for additional comparative purposes, sterile larvae were allowed to feed on mice infected with either *B. burgdorferi* strain 297 (the parent of PL133) or strain B31 (a wild strain recovered from *I. scapularis*). Fed larvae were allowed to molt to the nymphal stage. Five 297- or B31 MI-infected nymphs were then placed on each of five naïve mice and allowed to feed to repletion. After two weeks, ear punch biopsies were taken and cultivated in BSK-H medium. Upon

darkfield microscopic examination of the cultures, motile spirochetes were observed in all cultures from mice infested with ticks harboring either strain 297 or B31 MI (Table 15). Thus, strain 297, the parent of PL133, was fully competent for tick transmission into mice.

Table 15. Acquisition and maintenance of *B. burgdorferi* strains by *I. scapularis* and subsequent tick transmission of spirochetes to mice.

Strain	Larvae (engorged) % pos. by IFA	Nymphs (flat)		Nymphs (engorged)	Transmission to mice
		% pos. by IFA	# spirochetes/ tick	% pos. by IFA	# mice pos./# tested
297	100%	90%	2196 ± 1075	90%	5/5
B31 MI	100%	90%	1993 ± 1106	100%	5/5
PL133	92%[a]	80%[a]	2146 ± 1049	73%[a]	0/10[b]
BbDTR630	100%[a]	90%[a]	2065 ± 1098	100%[a]	0/10[b]

[a] $p \geq 0.21$ compared to 297- or B31 MI-infected ticks as calculated by chi-square test
[b] $p = 0.0001$ compared to 297- or B31 MI-infected tick infestations, as calculated by chi-square test

III. Summary and Implications.

The primary objective of this study was to design a new genetic system in which the expression of Kan resistance was used to select for *B. burgdorferi* retaining lp25 after genetic manipulation. To achieve this, we employed the *aph[3']-IIIa* Kan^r marker that has been used successfully in *B. burgdorferi* by others (212). We also chose to use this marker under the control of its own (native) *Enterococcus faecalis* promoter, in lieu of being driven by constitutive borrelial promoters such as P_{flgB} or P_{flaB} (33, 85, 100, 240, 246, 254). We assumed

that in so doing, undesirable allelic exchange between the endogenous *flg* or *fla* genes would be obviated. Additionally, inasmuch as linear replicons are known to recombine naturally in *B. burgdorferi* (57, 101, 277), we also reasoned that insertion of an antibiotic resistance marker would be more advantageous if it were in close proximity to the lp25 replication genes (*bbe18-21*) (56, 57, 101, 245). This should assist in maintaining the resistance marker on autonomously replicating lp25, a situation consistent with our findings herein. Another attractive feature of this overall approach was that the intergenic insertion site chosen was proximal to the virulence gene *pncA* (*bbe22*), thereby ensuring the coupling of antibiotic resistance expression to lp25-mediated virulence.

Upon implementing the above strategy, all resultant Kan^r clones retained lp25 but lacked at least one of the other endogenous 21 plasmids described for *B. burgdorferi* (57, 101). Such spontaneous loss of plasmids commonly occurs in *B. burgdorferi* (109, 152, 199, 244, 269) as a feature of the *B. burgdorferi*'s inherent genetic plasticitiy. Clones lacking one plasmid had lost either the virulence-associated plasmid lp28-1 (encoding *vlsE*) (57, 101) or the capacity to infect mice for reasons (unknown) other than the loss of lp28-1 or lp25; such clones were excluded from further characterization. Only 40% of the Kan^r clones that contained both lp25 and lp28-1 remained virulent in the mouse model. Therefore, while plasmid profiling of *B. burgdorferi* isolates is an important first step towards minimizing the labor-intensive process of evaluating genetically manipulated clones, the presence of both lp25 and lp28-1 plasmids does not, in itself, ensure the retention of virulence.

Clone BbDTR630 retained both lp25 and lp28-1 but lacked two other circular plasmids (cp18-2 and cp32-4). However, no reports have indicated adverse effects on the virulence of *B.*

burgdorferi upon the loss of either cp18-2 or cp32-4 (152, 199, 269). Consistent with these findings for cp18-2 and cp32-4 (152, 199, 269), BbDTR630 retained virulence in the murine model of Lyme borreliosis. In addition, the insertion of the Kan^r marker into lp25 did not adversely affect spirochetal growth *in vitro* or the differential expression patterns of the surface lipoproteins OspA, OspC, and DbpA. Inasmuch as passage of BbDTR630 in mice gave rise to populations of BbDTR630 that remained Kan^r and retained the *aph[3']-IIIa* marker, the Kan^r determinant appeared to be stably integrated into lp25. Regarding pathogenesis potential, the ability of BbDTR630 to cause disease in mice was indistinguishable from its parental PL133. The combined data thus suggest that the insertion of exogenous DNA onto lp25 did not adversely affect the virulence, adaptation, dissemination, or pathogenesis of *B. burgdorferi* infection within a mammalian host.

Given *B. burgdorferi*'s absolute dependence on and intimate association with both of its mammalian and arthropod hosts, it was essential also to examine the phenotype of BbDTR630 within *I. scapularis*. BbDTR630 appeared to colonize sterile larvae normally and persisted in wild-type fashion throughout both the larval and nymphal stages of tick development. Further tick infestation experiments with naive mice initially suggested that BbDTR630 was deficient in transmission from feeding nymphs to normal mice. However, additional experiments subsequently revealed that not a single mouse became infected when infested with ticks harboring either the parental strain PL133 or BbDTR630. The defect in the ability of PL133 to be transmitted from infected nymphs to mice was not the result of a failure of the strain to subsist within nymphs. Namely, more than 70% of nymphs contained PL133 at normal levels, results comparable to its parental strain 297. These surprising findings prompted us to re-

examine the ability of strain 297 to be tick transmitted. As expected, strain 297 was fully competent for nymphal transmission to mice, even though BbDTR630 and its parent PL133 were both deficient in the ability to be transmitted by ticks.

The data presented herein suggest that some occult defect exists in PL133, thereby resulting in its inability to be tick transmitted. Elias et al. (86) reported a similar phenomenon for a clonal isolate of B31 MI, which they designated as clone B1. They found that this clone was devoid of lp28-4 and speculated that some gene located on this plasmid likely conferred tick transmissibility to the spirochete. While a direct comparison between clone B1 and strain 297 cannot be made at this time (the latter has not been sequenced), our data indicate that lp28-4 is present in PL133 or, at the very least, PL133 contains all plasmids believed to be present in strain 297. However, our data do not rule out the possibility that an unidentified portion of lp28-4 has been lost, or that some other spurious mutation on lp28-4 resulted in altered protein expression. Regardless, it is apparent that PL133 is genetically distinct from its parental strain 297. Although the mutation(s) culminating in PL133's inability to be transmitted from a tick vector to a mammalian host remains obscure, the deficiency appears not to be due to defects in the expression of OspC, which is critical for the transmission of *B. burgdorferi* from the tick to a mammalian host (187).

That the parental strain PL133 used for genetic experiments was deficient in tick transmissibility sounds a cautionary note. The existence of inapparent defects that can spontaneously arise in *B. burgdorferi* serves to undermine further advances in borrelial genetics. In addition to the conventional genotypic and phenotypic characterizations typically applied to *B. burgdorferi* (e.g., plasmid profiling, infectivity testing, assessments of pathogenesis),

comprehensive phenotypic evaluations should include a complete analysis of vector transmission. Such characterizations should be performed not only on borrelial mutants or recombinants arising from genetic manipulation experiments, but also on the parental strains to be used in such studies. On the more positive side, PL133 described in this report may be invaluable in the future for identifying a new virulence gene(s) that confers tick transmissibility to *B. burgdorferi*. The result described herein that routine laboratory passage of the Lyme disease spirochete strain 297 in mice can result in an occult defect(s) in *B. burgdorferi*'s (strain PL133) ability to be transmitted by its tick vector sends a cuationary note to the borrelial research field. Such defects serve to undermine advances in borrelial genetics unless comprehensive vector transmission assessments are undertaken for a complete characterization of each *B. burgdorferi* strain used in, or emanating from, genetic manipulation experiments.

The unanticipated finding that strain PL133 (parent of BbDTR630) was not competent for tick transmission does not detract from the potential importance of the genetic approach described herein: namely, the tagging of lp25 with an antibiotic resistance marker to ensure its maintenance among desired recombinant clones. A logical extension is to use this strategy not only for generating *B. burgdorferi* mutants that retain lp25 (tagged with the antibiotic resistance determinant), but also when creating various types of complemented strains. For example, we have incorporated the Kan^r marker into a shuttle plasmid derivative of pKFSS1 (100), wherein two *Asc*I sites flank a cassette containing the *aph[3']-IIIa* marker and MCS. The resultant shuttle plasmid, pJD44 (Fig. 4), provides a platform for incorportating genes for episomal *trans*-complementation in *B. burgdorferi*. Alternatively, the cassette containing the *aph[3']-IIIa* marker and the MCS (along with the complementation gene of interest) in this shuttle vector

(Fig. 4**)** can be conveniently subcloned into the unique *Asc*I site within pDTR627 (Fig. 3). The resulting suicide plasmid derivative of pDTR627 then can be used for genetic complementation via homologous recombination with lp25. This approach was used to establish the essential nature of a plasmid-encoded gene that confers to *B. burgdorferi* the ability to persist within its natural tick vector (Chapter Six).

CHAPTER SIX.

bptA (*bbe16*) IS ESSENTIAL FOR THE PERSISTENCE OF *B. BURGDORFERI* IN ITS NATURAL TICK VECTOR

I. Introduction

Although it is clear that the survival and virulence of *B. burgdorferi* is dependent upon certain of its numerous plasmids (i.e., linear plasmid (lp) 54, lp25, lp28-1, circular plasmid 26) (106, 146, 152, 199, 269, 275), other than OspA and OspC, little is known regarding additional plasmid-encoded proteins that are essential for *B. burgdorferi*'s transition between, or survival within, its tick or mammalian hosts. Attempts to elucidate plasmid loci that confer virulence or survival within each host have been hampered by the intractability of virulent strains of *B. burgdorferi* to genetic manipulation (49, 254). Nonetheless, with recent advancements in genetic tools for borrelial research, I report here the genetic inactivation of two plasmid-encoded loci (*bba36* and *bbe16*) to assess their respective roles in the virulence, pathogenesis, and/or survival of *B. burgdorferi* during its natural life cycle. *bba36* and *bbe16* were targeted for study because (i) they reside on the two virulence-associated plasmids lp54 and lp25, respectively and (ii) they both were differentially regulated when assessed in microarray analyses (Chapter 4) (204). *bba36* was differentially regulated to a high degree (up to 58-fold), whereas *bbe16* (bptA) was more moderately regulated (up to 2.9-fold). Moreover, the expression of these genes was greater during growth under the FT condition (37°C, pH 6.8) or within DMCs,

suggesting their potential involvement in transmission to and/or infectivity in the mammalian host. Herein, we provide experimental evidence that, not only does one of these genes (*bbe16*) potentiates virulence of the spirochete in the mammalian host, but it also subserves an essential function for the maintenance of *B. burgdorferi* within the *Ixodes* tick vector. This study thus has identified a gene responsible for borrelial persistence in ticks (*bptA*) that is critical for survival of the bacterium within the tick host and therefore within the natural life cycle of the Lyme disease spirochete. Whereas our data demonstrate that *bptA* (*bbe16*) is essential for the survival of *B. burgdorferi sensu stricto* in ticks, we also show that *bptA* is conserved among *sensu lato* strains of *B. burgdorferi*; this widespread conservation among *sensu lato* strains suggests that *bptA* may be widely utilized by Lyme disease spirochetes for persistence in nature.

II. Results

A. Cloning and disruption of *bba36* and *bptA*.

An infectious, non-clonal isolate of 297 (PL133) that was isolated from ear punch biopsies after repeated rounds of needle-inoculation of mice was used as the parental strain for all mutant constructions. This strain was selected because it (i) was transformable, (ii) contained all known 297-specific plasmids, (iii) was virulent at wild-type levels (ID50 <100), and (iv) elicited histopathological sequelae typical of disease progression in mice. Although we have presented data previously (Chapter Five) that indicates that strain PL133 is a naturally-

derived, transmission-deficient *B. burgdorferi* strain, the studies described here (Chapter Six) were initiated prior to the identification of PL133's deficiency. Consequently, strain PL133 was used as the parental strain for genetic inactivation studies performed on *bba36* and *bbe16*. However, PL133 derivitives can still be evaluated for survival within every stage of the borrelial life cycle except for the ability of these spirochetes to be transmitted from the tick to mammalian host.

To assess the role of BBA36 or BptA in the life cycle of *B. burgdorferi*, each cognate gene and its appropriate flanking regions were PCR-amplified (based on B31 MI sequence information), inserted into pGEM-Teasy, and disrupted by insertion of the streptomycin resistance marker (*aadA*) into unique restriction enzyme sites within each gene. The constructs (*bba36* [pDTR599], Fig. 5; *bptA* [pDTR596], Fig. 6) were electroporated into PL133. Clones for each mutation were obtained and confirmed for insertional inactivation of the respective gene and retention of endogenous plasmids (Figs. 23A and 24A). Two *bba36*-deficient mutants (with different plasmid profiles; clone P1C5 lacked cp32-6, clone P2D6 lacked lp5, cp18-2, and cp32-4) and one *bptA* mutant (lacking cp18-2 and cp32-4) were selected and further evaluated (Figs. 23B and 24B). All *B. burgdorferi* mutants displayed normal growth kinetics in BSK-H medium when grown *in vitro* at two different conditions (pH 7.5 or 6.8, both at 37°C) (Fig. 25) and displayed spirochetal morphology identical to PL133 (not shown).

B. Evaluation of the *bba36* and *bptA* mutants for virulence and pathogenesis after needle-inoculation of mice.

To evaluate whether the loss of *bba36* or *bptA* adversely affected the virulence or pathogenicity of *B. burgdorferi*, all mutants were subjected to 50% infectious dose (ID_{50}) analysis (Table 16). Mice were needle-challenged intradermally with 10^1-10^4 mutant or wild-type bacteria. After two weeks, ear punch biopsies were taken, tissues were placed into BSK-H medium without selection, and the outgrowth of bacteria was assessed two weeks later. Whereas the *bba36* mutant did not show an increase in the ID_{50} in comparison with its parental PL133, the ID_{50} for the *bptA* mutant was reproducibly 1-2 logs higher than that of PL133 ($p<0.05$), suggesting a significant attenuation of virulence. However, upon histopathological analysis of those mice inoculated with 10^3 bacteria that were positive for spirochetes, there were no discernable differences in the levels of carditis or arthritis for any of the mutants (*bba36* or *bptA*) compared to PL133-infected mice (Fig. 26). Of note, spirochetes from ear punch biopsies of mice used for histopathological assessments (and that were cultivated in the absence of antibiotic selection) maintained their mutant genotypes, indicating that histopathology elicited was not due to genotypic reversion to wild-type character (Figs. 23C and 24C).

To establish that the loss of virulence in the *bptA* mutant was the result of *bptA* gene disruption and not due to spurious mutations, the deficiency was restored via complementation with a wild-type copy of *bptA*. Initial *trans*-complementation attempts with a shuttle plasmid failed to yield transformants (not shown). Therefore, we developed and employed a new method of *cis*-complementation that utilized a suicide vector for the integration of exogenous

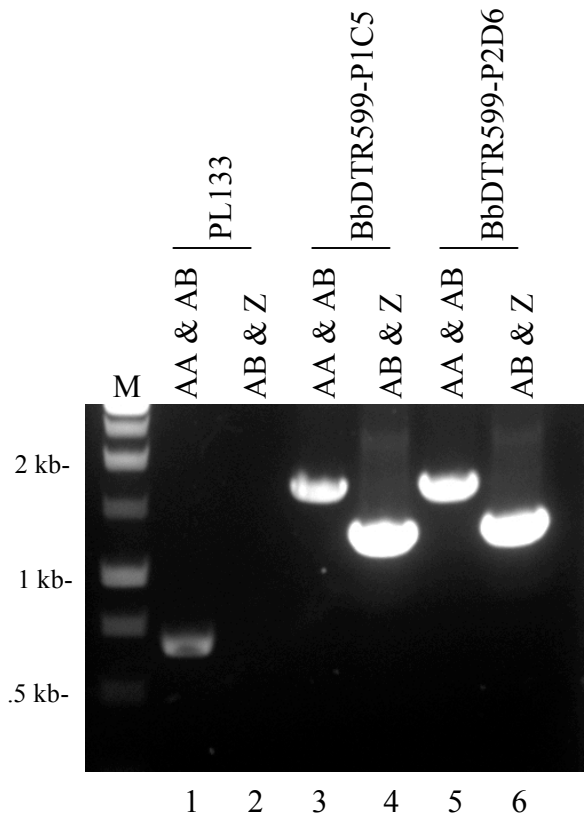


Fig. 23A. Analysis of *bba36*-deficient mutants. PCR confirmation of *bba36* inactivation. The fragment sizes of the DNA ladder markers (M) are denoted on the left. Primers AA and AB flank the insertion site on lp54 to verify insertion, whereas primers AB and Z were used to validate the integration of *aadA*.

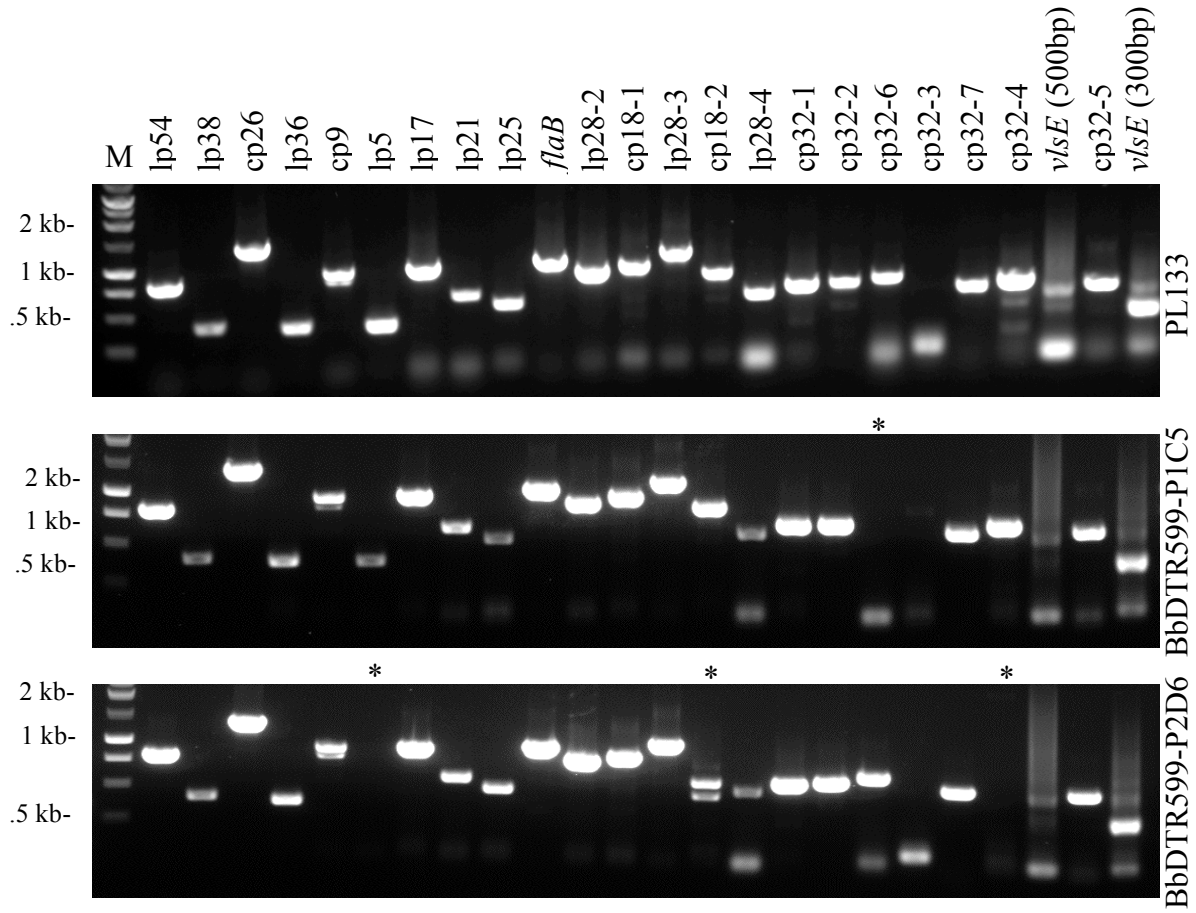


Fig. 23B. Analysis of *bba36*-deficient mutants. Plasmid contents of two *bba36*-deficient mutants (P1C5 and P2D6). Primers used for PCR detection of plasmids have been described (78), except for the detection of lp25 (primers S and T), lp38 (primers AC and AD), and lp28-1 (primers AE and AG [500-bp fragment of *vlsE*] or primers AE and AF [300-bp fragment of *vlsE*]). PCR analysis of the plasmids in each mutant indicated the loss of one plasmid (cp32-6) in P1C5 and three plasmids (lp5, cp18-2, and cp32-4) in P2D6 (asterisks above each panel denote lanes devoid of amplification products or having spurious products).

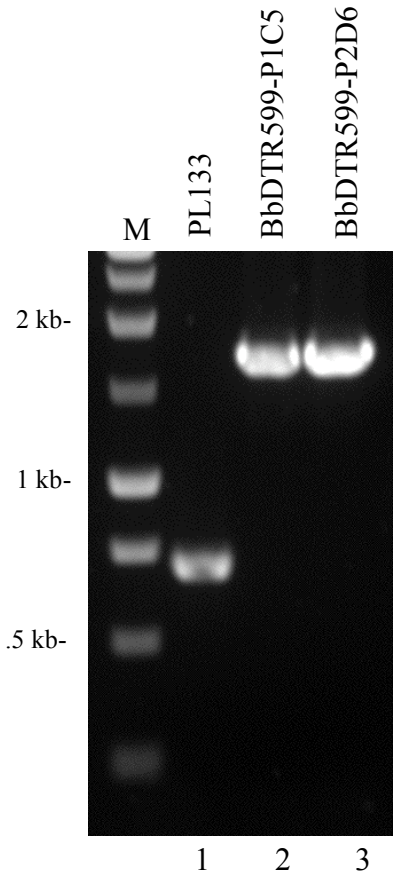


Fig. 23C. Analysis of *bba36*-deficient mutants. PCR evidence (using primers AA and AB) that *aadA* was stably integrated into lp54 of both clones P1C5 and P2D6. Of note, P1C5 and P2D6 were recovered from ear punch biopsies of mice cultured without antibiotic selection.

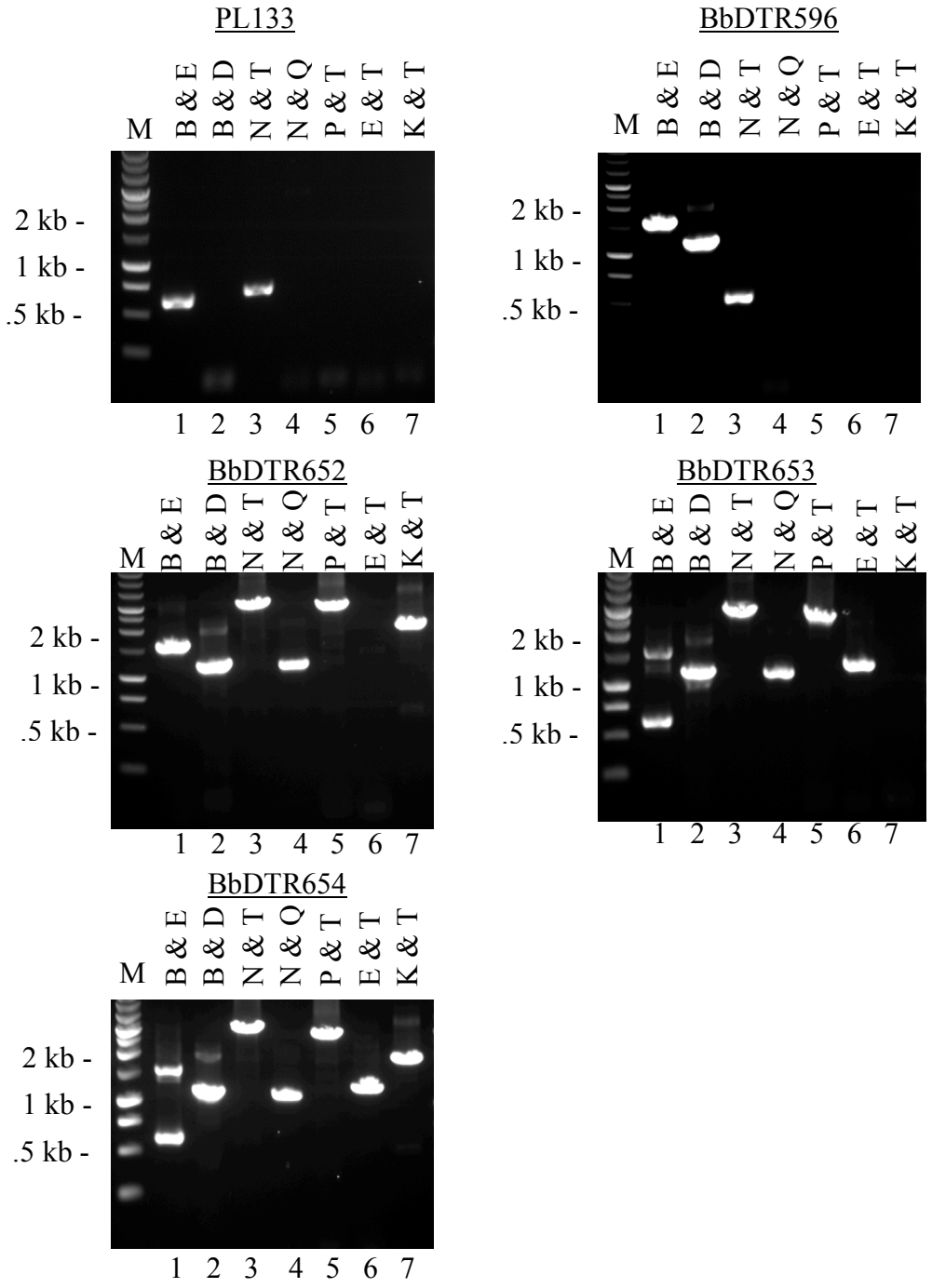


Fig. 24A. Analysis of *bptA* mutant and complemented strains. PCR confirmation of *bptA* inactivation and *cis*-complementation. The fragment sizes of the DNA ladder markers (M) are denoted on the left. Lanes 1 and 2 of each panel confirm insertion of the *aadA* marker into *bptA*. Lanes 3-7 confirm *cis*-complementation by the various constructs (pDTR652-654) with insertions downstream of *pncA* on lp25. The two bands observed in lanes 1 for strains BbDTR653 and BbDTR654 denote the disrupted form of *bptA* and the *cis*-complemented integrant (primers B and E are ORF-specific for *bptA*; see Fig. 5 and 6).

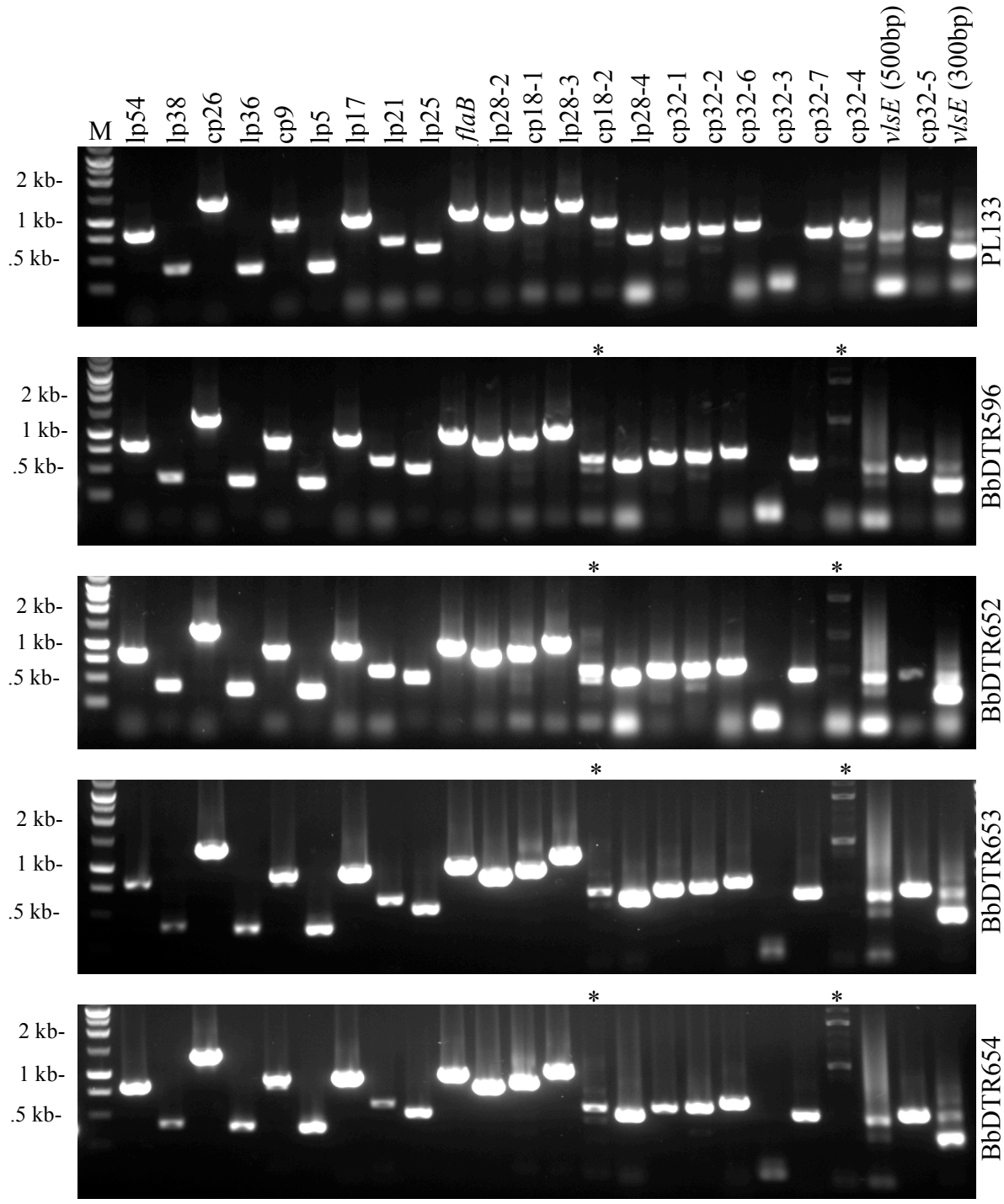


Fig. 24B. Plasmid contents of the *bptA* mutant and *cis*-complemented strains. All mutants and complemented strains were devoid of cp18-2 and cp32-4 (asterisks above each panel denote lanes devoid of amplification products or having spurious products).

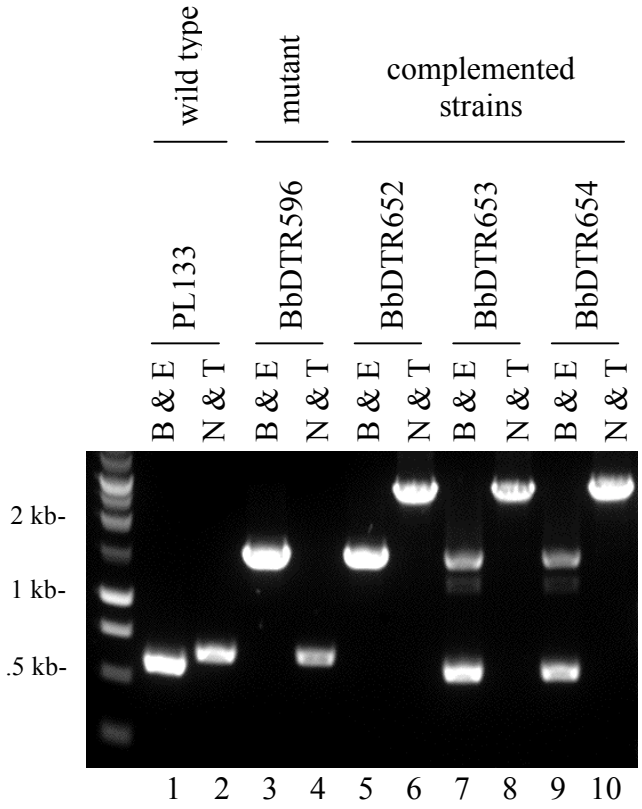


Fig. 24C. Analysis of *bptA* mutant and complemented strains. PCR evidence that spirochetes cultivated from mouse ear punch biopsies (in the absence of antibiotic selection) maintained stable integration of selectable markers. Lanes 3, 5, 7, and 9 demonstrate the integration of *aadA*, whereas lanes 6, 8, and 10 show the integration of *aph[3']-IIIa*.

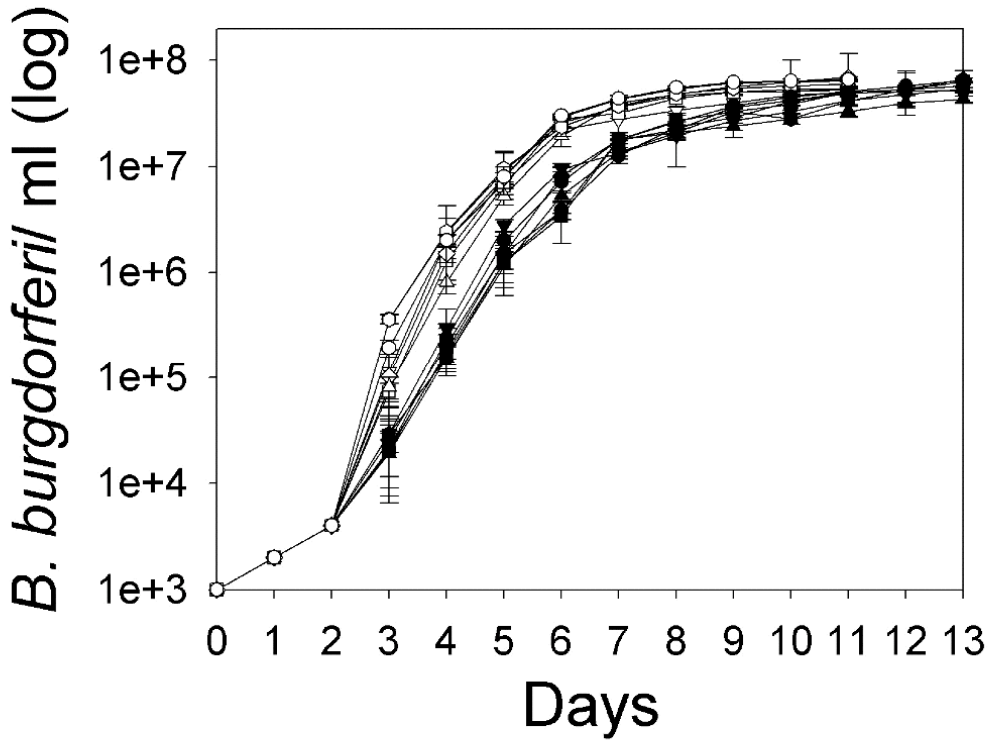


Fig. 25. *In vitro* growth curves of *B. burgdorferi* insertional mutants, complemented strains, and wild-type PL133 cultivated at either 37°C, pH 7.5 (open features) or 37°C, pH 6.8 (closed features). Cultures were grown in triplicate and average daily cell numbers were enumerated by darkfield microscopy. PL133, circle; BbDTR599-P1C5, hexagon; BbDTR596, triangle pointed down; BbDTR652, square; BbDTR653, diamond; BbDTR654, triangle pointed up.

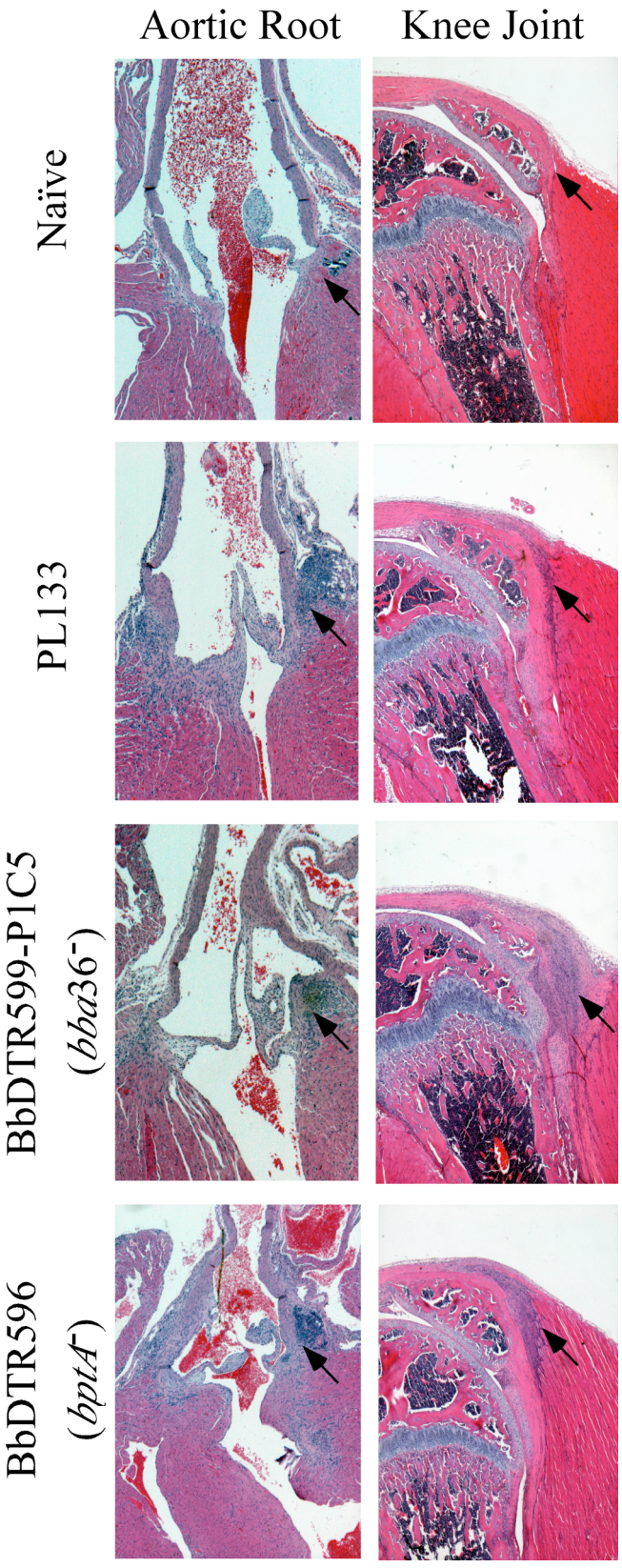


Fig. 26. Histopathological (carditis/arthritis) analysis of knee joints and aortic roots from either naïve mice (3-weeks old) or animals needle-challenged with 1 x 10^3 spirochetes. Representative tissue sections are shown for normal tissue, as well as for PL133 (wild-type *B. burgdorferi*), BbDTR599 (*bba36*-deficient mutant), and BbDTR596 (*bptA* mutant). Arrows denote areas of pronounced immune cell infiltration.

DNA into an innocuous site in lp25 distant (ca. 4 kB) from the native *bptA* (*bbe16*) gene (Fig. 6). Advantages to this approach are two-fold: (i) integration minimized undesirable gene dosage (i.e., copy number) effects and (ii) integration simultaneously assured retention of lp25. Transformants arising from the recombination of the *bptA*-complementation constructs into lp25 (Fig. 5) were assessed for appropriate insertions and plasmid profiles (Figs. 24A and 24B). As a result of complementation, the virulence of clone BbDTR653 (*bptA* mutant complemented with *bptA* under its native promoter) was restored to wild-type levels (Table 16). To confirm that the restoration of virulence in BbDTR653 was due to reestablishing *bptA* expression and not due to the insertion of extraneous DNA into lp25, a construct of *bbe17* driven by its native promoter (BbDTR652) was transformed into BbDTR596 in lieu of *bptA*. The ID_{50} of BbDTR652 was similar to the *bptA* mutant and statistically lower than that for either PL133 or BbDTR653 ($p<0.05$), indicating that virulence was restored only by the integration of a wild-type copy of *bptA*. To show that the *bbe17* native promoter was active, the *bbe17* promoter was fused to *bptA* in another construct (BbDTR654). As for BbDTR653, the virulence of clone BbDTR654 was restored to a level similar to PL133 (data not shown).

Table 16. Determination of 50% infectious dose (ID_{50}) values for PL133 and various mutants and complemented strains of *B. burgdorferi* in C3H mice.

Strain	10^4	10^3	10^2	10^1	ID_{50}
PL133 (*wt*)	10/10	10/10	7/10	3/10	44.9 ± 1.41
BbDTR599-P1C5 (*bba36*$^-$)	5/5	2/2[†]	4/5	0/5	51.3 ± 1.75
BbDTR-P2D6 (*bba36*$^-$)	5/5	5/5	4/5	0/5	53.3 ± 1.72
BbDTR596 (*bptA*$^-$)	10/10	7/10	0/10	0/10	659 ± 1.48*
BbDTR652 (*bptA*$^{-/-}$, *bbe17*$^{+/+}$)	10/10	9/10	4/10	0/10	238 ± 1.41*
BbDTR653 (*bptA*$^{-/+}$)	10/10	10/10	8/10	4/10	31.3 ± 1.39

[*] statistically significant difference from PL133 and BbDTR653 (*p*-values reported in text)
[†] three mice died before completion of experiment

C. Evaluation of the roles for *bba36* or *bptA* in ticks.

Inasmuch as infection of and survival within the mammalian host represents only one facet of the spirochete's enzootic life cycle, a more comprehensive evaluation of the behavior of these *B. burgdorferi* mutants in the tick vector was warranted. To approach this, sterile larval ticks were allowed to feed upon mice that were infected at high spirochete levels ($0.5\text{-}1x10^6$) with either the wild-type, mutant, or complemented strains. Upon larval repletion, the majority of the ticks were allowed to proceed naturally through the month-long molting process, whereas a subset was dissected for immunofluorescence assay (IFA). For each bacterial strain, a large proportion ($\geq$70%) of all repleted larvae was positive for spirochetes (Table 17). There was no statistical difference in the average number of bacteria per fed larva for all strains (data not shown). Upon subsequent evaluation of newly molted nymphs, *bba36* deficiency did not affect survival of the spirochetes at any point within the tick host, including when nymphs were allowed to take a blood meal (Table 17). In contrast, the *bptA* mutant displayed a dramatic defect for survival within newly-molted flat nymphal ticks; IFA analysis showed a sharp reduction in both the number of infected ticks ($p<0.016$) as well as the number of spirochetes per tick ($p<0.0001$) in comparison with PL133 (Table 17). Complementation of the *bptA* mutant (BbDTR596) with wild-type *bptA* (BbDTR653) resulted in the restoration to wild-type levels in both the percent of ticks infected ($p<0.001$), as well as the number of bacteria per tick ($p<0.044$) (Table 17). Of note, levels of wild-type PL133 dropped normally (190) in fed larvae during the 4-5-week time frame between larval tick engorgement and metamorphosis to the

nymphal form (Fig. 27), whereas the *bptA* deficiency resulted in an accelerated loss of spirochetes within the first two weeks post repletion (Fig. 27).

Table 17. IFA- and PCR-detection of various *B. burgdorferi* clones harbored within larval and nymphal forms of *I. scapularis* ticks over time.

strain	genotype	larvae (engorged)	newly molted nymphs (flat)		2 month-old nymphs (flat)	2 month-old nymphs (engorged)	
		% pos. by IFA[*†]	% pos. by IFA[†]	# bacteria/tick[†]	% pos. by IFA[†]	% pos. by IFA[†]	# pos. by PCR[‡]
PL133	wild-type	92%	90%	2146 ± 1049	100%	73%	70%
BbDTR599-P1C5	*bba36*$^-$	70%	60%	1683 ± 1202	62%	50%	48%
BbDTR599-P2D6	*bba36*$^-$	100%	90%	2057 ± 1108	88%	92%	90%
BbDTR596	*bptA*$^-$	90%	20%[§]	1.4 ± 3.8[¶]	16%[§]	0%[§]	0%[§]
BbDTR652	*bptA*$^{-/-}$,*bbe17*$^{+/+}$	93%	6.6%[§]	2 ± 7.75[¶]	10%[§]	0%[§]	ND
BbDTR653	native promoter *bptA*$^{-/+}$	100%	93%	415 ± 609	80%	70%	ND
BbDTR654	*bbe17* promoter::*bptA*$^{-/+}$	100%	80%	486 ± 582	90%	70%	ND

[*]No statistically significant differences between strains for bacterial loading within ticks
[†]n = 6-15
[‡]n = 20-25
[§]Statistically different from PL133, BbDTR653, and BbDTR654 or just PL133 (PCR data) as calculated by χ^2 goodness of fit test (*p*-values listed in text)
[¶]Statistically different from PL133, BbDTR653, and BbDTR654 or PL133 as calculated by unpaired Student's t-test (*p*-values listed in text)
ND, not determined; pos., positive

At two months (Table 17) and up to five months (data not shown) post molting to the nymphal form (about three and six months post larval repletion), the number of flat (unfed) nymphal ticks infected with each *B. burgdorferi* strain remained similar to that which was observed upon molting. Only 16% of ticks harboring the *bptA* mutant (BbDTR596) retained spirochetes ($p<0.02$) (Table 17). Similar results were found for a *bptA* mutant *cis*-complemented with an irrelevant gene (*bbe17*) (BbDTR652) (Table 17). Based on these data, we hypothesized that any *bptA*-deficient *B. burgdorferi* that had survived the larval engorgement process would not survive a second repletion during the nymphal stage. Indeed,

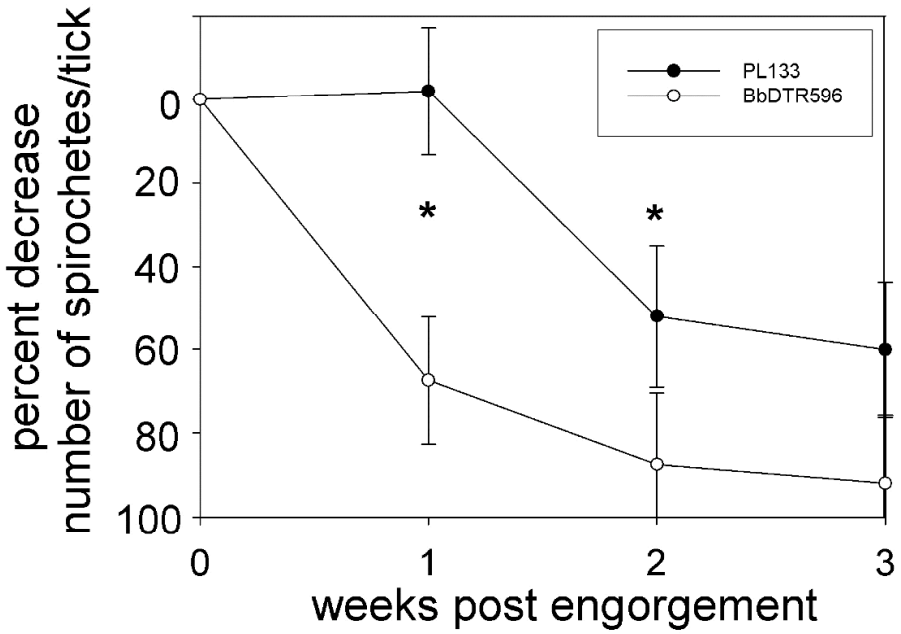


Fig. 27. Spirochete loads of *I. scapularis* larvae infected with either PL133 (closed features) or BbDTR596 (*bptA* mutant) (open features). Repleted ticks were assessed for spirochetes by IFAs performed at weekly intervals. The % decrease in spirochete loads for the *bptA* mutant were most marked within the first two weeks post-repletion ($p<0.05$, Mann-Whitney-U test, denoted by asterisks).

whereas >70% of the engorged nymphal ticks harboring either PL133 (wild-type), complemented strain BbDTR653 (*bptA* under its own promoter), or complemented strain BbDTR654 (*bptA* fused to the *bbe17* promoter) were positive for spirochetes via IFA (Table 17), not a single spirochete was detected within engorged nymphal ticks initially harboring the *bptA* mutants ($p<0.0016$, $p<0.01$, $p<0.01$, respectively). Moreover, PCR amplification of the borrelial gene, *ospA*, also was negative from all ticks initially harboring the *bptA* mutant, BbDTR596 ($p<4.7 \times 10^{-7}$). In contrast, PCR analysis showed that 70% of fed nymphs contained PL133 (Table 17).

D. BptA is protease-accessible and highly conserved in *B. burgdorferi sensu lato* strains.

From the deduced amino acid sequence (using SignalP and PSort), BptA appears to contain a putative cleavable amino-terminal leader sequence (signal peptidase II [lipoprotein-specific] consensus). Proteinase-K accessibility assays were employed as an initial assessment of whether BptA might be surface-exposed on the outer membrane of wild-type *B. burgdorferi* (like other borrelial lipoproteins). Proteinase-K treatment of *B. burgdorferi* under conditions that did not digest periplasmic FlaB (control for outer membrane integrity) removed BptA detectable by immunoblotting (Fig. 28, lanes 4 and 6). These findings held true regardless of whether the spirochetes were cultivated under conditions analogous to those present in feeding ticks (i.e., 37°C, pH 6.8) or within DMCs (to mimic mammalian host adaptation) (Fig. 28). Of

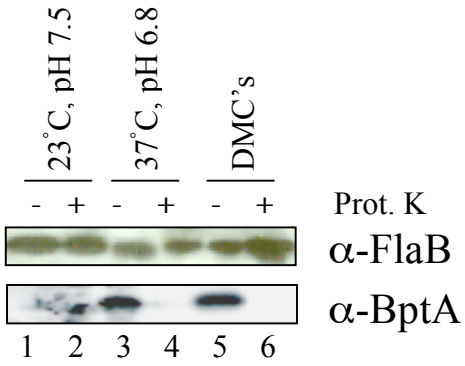


Fig. 28. Protease accessibility of BptA in *B. burgdorferi* grown under various culture conditions (top). Each lane was loaded with 5 x 10^7 bacteria that had been subjected to either Proteinase K (Prot. K) (+) or mock treatment (-). Detection (immunoblotting) of the endoflagellar (periplasmic) protein FlaB was used as an indicator of *B. burgdorferi* outer membrane integrity and as a loading control.

note, BptA was not detected among spirochetes cultivated under conditions that mimic the flat (unfed) tick (i.e., 23°C, pH 7.5).

With the discovery of the essential nature of *bptA* for the survival of *B. burgdorferi* within *I. scapularis*, we hypothesized that BptA may be conserved in *B. burgdorferi sensu lato* isolates in general. PCR-analysis of the entire ORF indicated that all seven *sensu lato* strains tested contained *bptA*. Moreover, there was a high degree of conservation (>74% identity, >88% similarity) between strains at the amino acid level (Table 18). Further evaluation of the deduced amino acid sequence indicated that the putative signal peptidase II consensus motif (LXXC) at amino acid 13 in BptA was conserved in all *sensu lato* isolates tested (not shown).

Table 18. Percent amino acid similarities and identities (in parentheses) of BptA homologs present among *B. burgdorferi sensu lato* strains tested. Strain designations are in bold.

	B.burgdorferi			*B. garinii*		*B. afzelii*	*B. valaisiana*	*B. bissettii*	*B. andersonii*	*B. japonica*
	B31 MI	**297**	**N40**	**IP90**	**PBi**	**BO23**	**VS116**	**DN127**	**21038**	**IKA2**
B31 MI		99 (97)	99 (97)	96 (91)	89 (76)	98 (95)	91 (80)	97 (92)	97 (91)	98 (96)
297			99 (95)	97 (93)	89 (75)	98 (94)	91 (78)	97 (92)	98 (90)	98 (95)
N40				96 (92)	89 (76)	100 (98)	90 (77)	98 (92)	97 (88)	100 (99)
IP90					89 (75)	96 (91)	89 (77)	97 (95)	97 (89)	96 (91)
PBi						89 (74)	89 (77)	89 (76)	89 (78)	89 (75)
BO23							90 (80)	98 (92)	96 (88)	100 (99)
VS116								88 (78)	90 (78)	90 (79)
DN127									97 (89)	98 (93)
21038										96 (89)
IKA2										

III. **Summary and Implications**

Previous microarray analyses performed on *B. burgdorferi* have revealed a large number of differentially-regulated genes that encodee products whose function(s) remain largely unknown (35, 183, 204). Whereas many of these differentially-regulated genes likely represent physiological "housekeeping" genes typically not thought of as virulence-associated, others have been noted in separate studies to encode virulence factors essential for *B. burgdorferi*'s infection of or survival within its arthropod or mammalian hosts (51, 110, 129, 187, 198, 275). Regardless, the testing of Koch's molecular postulates to ascertain whether a gene encodes a virulence trait (88) has been hindered greatly by a paucity of systems for genetically manipulating virulent *B. burgdorferi* (49, 254). Despite the refractory nature of *B. burgdorferi* to genetic manipulation, we applied recent advancements in borrelial insertional mutagenesis and genetic complementation to study two genes of interest. *bba36* was selected for study because (i) expression levels (35, 183, 204) were higher when *B. burgdorferi* was cultivated under conditions analogous to those of the feeding tick (37°C, pH 6.8) and within the mammalian host (DMCs) and (ii) it had an expression pattern similar to that of the known virulence factor *ospC* (chapter 4) (204). Despite these features, ID_{50} analysis indicated that *bba36*-deficient mutants were virulent at wild-type levels (Table 16) and elicited histopathological sequelae typical of the murine model of Lyme borrelosis (Fig. 26). Moreover, tick studies indicated that spirochetes deficient in *bba36* had no discernable defect on the presence of *B. burgdorferi* within either the larval or nymphal stages of *I. scapularis* infection (Table 17). Consequently, we have not yet ascribed a function to BBA36.

bptA was targeted for study because it was the only gene differentially regulated in our global transcriptional analysis that was encoded on the virulence-associated lp25 plasmid (204).

Microarray analysis indicated that *bptA* was more highly expressed when the spirochetes were cultivated in a mammalian host-adapted state (DMCs) as compared to cultivation at either the UT (23°C, pH 7.5) or FT (37°C, pH 6.8) growth conditions. Inasmuch as many lines of evidence now point to the importance of lp25 to virulence expression by *B. burgdorferi* (108, 152, 198, 199, 269), we hypothesized that this gene might play a pivotal role in the infectious life cycle of the spirochete. We garnered experimental evidence to support this hypothesis by creating an insertional mutant of *bptA* as well as *cis*-complemented strains. The loss of *bptA* resulted in a reproducible attenuation of *B. burgdorferi* infectivity for mice by 1-2 logs (Table 16). Whereas it was possible that this loss of virulence by the *bptA* mutant was due to spurious mutations or the spontaneous loss of a plasmid(s) (129, 187, 273, 275), virulence was restored to wild-type levels upon complementation of the *bptA* mutant with an intact *bptA* gene (Table 1), suggesting that the attenuation of infectivity was a direct result of the inactivation of *bptA*. Of note, when Purser *et al.* (198) complemented a lp25-deficient (i.e., lacking *bptA*), avirulent strain of *B. burgdorferi* with a wild-type copy of *pncA* on a shuttle plasmid, virulence was restored, albeit not completely. In our case, the *bptA* mutant contained lp25 (i.e., it contained *pncA*), and hence the restoration of virulence to wild-type levels in the *bptA*-complemented strain likely was due to the contributions of both *bptA* and *pncA*. Also, as in the case of the lp25-deficient strain complemented with *pncA* (198), we found no differences in mouse histopathology elicited by either the *bptA* mutant or wild-type *B. burgdorferi* (Fig. 26), suggesting that dissemination and tissue tropism (i.e., pathogenesis) were not impaired by the loss of *bptA*. The combined data presented herein suggest that although BptA likely is an accessory molecule for borrelial infectivity, it too, along with PncA, is required for achieving

natural levels of *B. burgdorferi* infectivity. On the other hand, our data do not rule out the possibility that other as yet unidentified lp25-encoded gene(s) work in concert with BptA and PncA for maximal infectivity of *B. burgdorferi* in its mammalian host.

Assessing borrelial gene function in both ticks and mice is of paramount importance given the absolute dependence on and intimate association of *B. burgdorferi* with both its arthropod and mammalian hosts. Prior studies to assess borrelial gene function have led to circumstances in which desired mutants lost infectivity for mice (110, 187, 198), thereby revealing important aspects of virulence expression by *B. burgdorferi* in the mammalian host. When such studies identify *B. burgdorferi* genes that are unequivocally essential for mammalian infectivity/pathogenesis, it is more challenging, and perhaps of lesser importance, to investigate a role for the respective gene(s) in the arthropod phase of *B. burgdorferi*'s life cycle. On the other hand, when loss of a gene leads to no discernable phenotype relative to mammalian infectivity/pathogenesis, or results in attenuation, it should be considered that the gene in question may impact *B. burgdorferi*'s survival within its arthropod vector. Such logic prompted us to investigate the *bptA* mutant, which was only attenuated for infectivity in mice, for its ability to survive within various phases of tick morphogenesis.

When sterile tick larvae were allowed to feed on mice infected with the *bptA* mutant, there was a severe defect in the ability of the *bptA* mutant to maintain normal bacterial loads within ticks. In fact, there was a 92% decrease in spirochetal numbers in newly molted nymphs as compared with those found in larvae fed to repletion (Fig. 27). Most of this decline occurred within the first two weeks after larval repletion (Fig. 27), a time in which large amounts of blood meal remnants were observed within the midguts of the dissected ticks (not shown).

There also were significantly fewer newly molted nymphs that harbored any *bptA* mutant spirochetes (Table 17). Spirochete loads within these flat (unfed) nymphs did not change significantly during the subsequent (2-month) resting period (Table 17). An interesting *in vitro* corollary to this observation may be found in the fact that BptA was not expressed by *B. burgdorferi* under *in vitro* culture conditions analogous to those of flat ticks (Fig. 28), suggesting that BptA is not required when ticks are resting (i.e., not feeding). On the other hand, the same *in vitro* experiments showed that BptA was expressed when *B. burgdorferi* was cultivated under conditions that mimic tick feeding, implying that BptA functions to sustain the spirochete during tick feeding. Consistent with this notion, when mature nymphs were allowed to feed on naive mice (i.e., second feeding of tick life cycle), *bptA* mutant spirochetes were completely cleared. Taken together, *bptA* appears to be essential for the persistence of *B. burgdorferi* throughout the tick phase(s) of its life cycle, and thus BptA can be considered as a virulence factor essential to the overall parasitic strategy of *B. burgdorferi* (54).

Lyme borreliosis can be caused by three different *sensu lato* strains (*B. burgdorferi, B. garinii,* and *B. afzelii*) in humans, whereas seven additional strains are thought to cause disease in animals (*Borrelia andersonii, Borrelia bissettii, Borrelia valaisiana, Borrelia japonica, Borrelia turdae, Borrelia tunukii,* and *Borrelia lusitaniae*) (259). PCR amplification using oligonucleotide primers designed from *B. burgdorferi* strain B31 MI sequence information (57, 101) revealed that BptA homologs were present in all borrelial strains tested. Moreover, there was a high degree of similarity (>88%) and identity (>74%) at the deduced amino acid level among all *B. burgdorferi sensu lato* isolates (Table 18). Whereas the relapsing fever borreliae are closely related to *B. burgdorferi*, they cause disease clinically distinct from that of Lyme

borreliosis, suggesting that certain molecular determinants are specific to the different etiological agents. In this regard, *bptA* homologs were not detected by PCR among the two relapsing fever isolates tested (*B. hermsii* and *Borrelia turicatae*) (data not shown), suggesting that *bptA* may be generally conserved for the survival of Lyme borreliosis strains in arthropod hosts. Although sequence divergence between isolates could account for our inability to detect *bptA* homologs in relapsing fever borreliae, that *bptA* may be specific to Lyme borreliosis organisms is supported by microarray analysis of the *B. hermsii* genome; namely, no hybridization signal for any lp25-encoded gene, including *bptA*, was detected on *B. burgdorferi* B31 MI-based microarrays (280). Moreover, *bptA* was not detected in *B. lonestari*, the putative agent of Southern tick-associated rash illness (257) (data not shown), further supporting the contention that *B. lonestari* is more closely related to relapsing fever strains than to Lyme borreliosis agents (15). Taken together, this implies that strong selective pressure(s) are operative for maintaining *bptA* among Lyme borreliosis strains in nature.

Earlier work called attention to another lp25-encoded gene product, PncA (BBE22), as essential for the survival of *B. burgdorferi* in a mammalian host (198). However, PncA as a virulence factor may be unique to *sensu stricto* stains of *B. burgdorferi*. For example, Glockner *et al.* found that *B. garinii* does not appear to contain a homolog of *pncA*, whereas it does contain all other B31 MI-specific lp25-encoded genes (including *bptA*) (106). In fact, we detected *pncA* homologs via PCR in only four of the seven strains tested (*B. burgdorferi, Borrelia valaisiana, Borrelia andersonii,* and *Borrelia bissettii*; data not shown), even though all seven strains yielded a homolog of *bptA*. Although observations made to date (108, 198) may lead one to assume that selective pressure(s) to sustain *pncA* in *B. burgdorferi* in nature is

the driving force that maintains lp25 in wild-type strains, our data raise the provocative possibility that *bptA* may be what maintains virulence-associated lp25 in nature, at least in *B. burgdorferi* and *B. garinii*, and possibly in other *sensu lato* strains.

GenBank searches did not identify proteins with homologies to BptA and thus did not yield theoretical predictions of BptA function. However, sequence analysis predicts that BptA is a membrane lipoprotein, and protease-accessibility experiments suggested that it is surface-exposed in *B. burgdorferi*. Only two other outer membrane lipoproteins of *B. burgdorferi*, OspA and OspC, thus far have been shown, via genetic studies, to play major roles in the tick phase of the Lyme disease spirochete. OspA is essential for tick midgut colonization by *B. burgdorferi* (275), and OspC facilitates *B. burgdorferi* invasion of tick salivary glands (187). Although the precise mechanism by which *bptA* serves to maintain *B. burgdorferi* in ticks remains unclear, data presented herein support the contention that *bptA* should be considered a virulence factor and be included among those genes that impact tick-associated events crucial to *B. burgdorferi*'s persistence in nature.

CHAPTER SEVEN:

DISCUSSION

Although Lyme disease (Lyme borreliosis) has an extremely low mortality rate (60), it is a disease with a high rate of morbidity in individuals not diagnosed early in the course of infection. Moreover, the marked increase in the number of reported cases annually is linked closely to the persistent encroachment of suburbia into the natural habitats of the small rodents and deer that harbor the Lyme disease spirochete in nature (267). As a result, there has been an overwhelming public outcry to provide both private and federal funds to investigate potential medical and/or environmental avenues in which to combat this public health threat. Pursuant to this goal, the identification and characterization of novel borrelial proteins that could be potential vaccine and/or pharmaceutical targets is the underlying tenet to this dissertation.

Armed with the genomic sequence of *B. burgdorferi* strain B31 MI and the relatively new global transcriptional profiling technology embodied in gene microarrays, we sought first to identify previously uncharacterized borrelial genes that were preferentially expressed in the mammalian host and could thus be potential targets for either bactericidal antibodies or chemotherapeutics. In line with this goal, microarray analysis identified 150 genes that were differentially regulated when the spirochetes were grown either *in vitro* under conditions analogous to growth parameters within the flat tick and feeding tick (270) or when grown within DMCs implanted within rat peritoneal cavities (as a surrogate for the mammalian host

adapted state) (Chapter Four) (5, 204). Moreover, greater than a third of these differentially regulated genes lacked homology to any other known gene, suggesting that these genes are specific to the Lyme disease spirochete for transmission between and/or survival within each of its enzootic hosts. In addtion, a large proportion (46%) of the differentially regulated genes contained a putative signal peptidase I (n=25) or signal peptidase II (n=44) leader sequence. The large proportion of genes identified by microarray analyses that contained putative cleavable leader sequences likely underscores the dynamic interplay between the spirochete's outer surface and its two diverse enzootic hosts.

One of the most interesting results from the microarray analyses (Chapter Four) was the identification of what appeared to be an operative bacterial stringent response. This system was thought not to be functional in *B. burgdorferi*, inasmuch as several components appear to be lacking in *B. burgdorferi* strain B31 MI (57, 101). In our analysis, a gene central to this stress response pathway (*spoT)* was differentially regulated by up to 2.0-fold in certain growth conditions. Moreover*, trxA, hslVU, ylxH-1*, and *chpAI* were all regulated in a fashion that supports the hypothesis that a bacterial stringent response is operative in *B. burgdorferi*. Other groups have gone on to obtain direct experimental evidence that *B. burgdorferi* has an operative stringent response. For example, Budrysheva *et al.* were able to show a decrease in the expression of *spoT,* as well as a decrease in (p)ppGpp levels when *B. burgdorferi* strain N40 was co-cultured with tick cells (39). Although interpretations made by this other group were contrary to our hypothesis of *spoT* expression and activity, the data do appear to be in close agreement upon further evaluations. The co-culturing experiments performed by Bugrysheva *et al.* were carried out at a lower pH (6.8) than when *B.*

burgdorferi was cultured alone in BSK-H medium (pH 7.5). The fact that I also saw decreased levels of spoT levels when spirochetes were cultivated at pH 6.8 suggests that the fluctuations in (p)ppGpp levels observed by Bugrysheva *et al.* may in fact be due to changes in pH instead of the co-culturing of the spirochetes with tick cells. Bugrysheva *et al.* went on to show in a subsequent paper that two other *B. burgdorferi* strains (297 and B31 MI) also were capable of producing (p)ppGpp, indicating that a stringent response was operative in these strains as well (40). Although the precise mechanism of *spoT* activation was not elucidated in this latter study, the data suggested, however, that SpoT does not provide the classic role of growth rate control as it does for *E. coli*. Further experiments are warranted to determine what role(s) this gene plays in the life cycle of *B. burgdorferi*.

A major problem with microarray analysis is how effectively to mine the plethora of data generated (data are shown in Appendices A and B). We chose to approach this problem in two ways: (i) identify putative surface-associated gene products that could be potential vaccine candidates (Appendices C-E) and (ii) perform insertional mutagenesis analysis on potential virulence factors (Chapter Six). Taking the applied approach to the microarray data, we sought to identify candidate vaccine targets with potential protective capabilities (Appendices C, D, and E, unpublished data). One approach to the analysis of these potential vaccine targets included protease accessibility of surface-localized proteins on intact *B. burgdorferi*. To accomplish this, polyclonal antibodies specific to each protein were generated for detection in immunoblot analyses. All genes were cloned into expression vectors (pQE40 and/or pPROEX-Hta) as 6His-tagged recombinant proteins. Proteins then were purified via nickel-affinity chromatography to homogeneity, then mixed with Freund's

adjuvant for the production of antibodies specific to each protein to be evaluated via immunoblotting of proteinase K treated *B. burgdorferi* (BB0070, BB0664, BBA07, BBA36, BptA [BBE16], BBE17, BBI42/BBK53, BBK07, and BBQ03). Initial immunoblot analysis (Appendix C) indicated that all proteins were potential targets for bactericidal antibodies, inasmuch that all proteins were proteinase K-accessible and thus likely surface exposed. We then attempted to assay directly for the production of bactericidal antibodies characteristic of a protective immune response. After mice generated high titers against the respective borrelial antigens, mice were needle-challenged with *B. burgdorferi* to assess protective capabilities of each potential vaccinogen (Appendix C). Although the data suggested that the majority of the proteins were not protective, mice immunized with either BBE17 or BptA (BBE16) appeared to be partially protected against super-infection with *B. burgdorferi* via needle-challenge (Appendix D). However, when vaccinated mice were challenged with ticks harboring *B. burgdorferi* strain 297, all mice became infected, suggesting that immunization with BptA did not produce an immune response that could be protective for mice upon tick challenge (Appendix E).

Even though BptA was shown to be immunogenic (i.e., eliciting antibodies in mice either naturally [during natural infection, data not shown] or after immunization with recombinant protein) and surface-associated, there are several explanations for the vaccinology data. First, the surface-localization studies were performed on *in vitro*-cultivated spirochetes, thus, there is no evidence that BptA is surface-localized in *B. burgdorferi* strains replicating *in vivo*. BptA could be sub-surface in spirochetes within the mammalian and *Ixodes* tick hosts, much like what is believed to occur for DbpA (117).

Immunofluorescence analysis of spirochetes in ticks thus is warranted to discern when (and where) BptA is expressed by *B. burgdorferi* during its natural life cycle.

There is another potential explanation for the disparity concerning the protective capabilities of BptA-specific antibodies against *B. burgdorferi* when mice are challenged via needle- (Appendix D) versus tick-inoculation (Appendix E). Previous experiments have indicated that clearance of *B. burgdorferi* in the mammalian host is dependent solely upon protective antibodies, without involvement of other cellular or complement factors (31, 92). Moreover, researchers have found that bactericidal antibodies specific to OspB work by destabilizing the outer membrane of the spirochete, thus resulting in outer membrane blebbing and cell death (141). Taken together, it is possible that the *in vivo* expression levels of BptA in spirochetes are low enough (at least less than *in vitro* cultivated spirochetes) such that the level of membrane destabilization necessary for bactericidal antibody-dependant cell death is not reached in mice immunized against BptA. Further tests are warranted to determine whether the BptA-mediated killing observed in mice needle-challenged with *in vitro* cultivated *B. burgdorferi* can be heightened or whether BptA could be used in conjunction with other partially-protective antigens (e.g., BBK32) to produce a more completely protective vaccine cocktail.

Although we were unsuccessful in identifying borrelial proteins that could be efficacious vaccines, we were successful in utilizing the microarray data to garner insight into the basic biology of the spirochete. The preferential expression of two genes when the spirochetes were grown under conditions analogous to the mammalian host-adaptated state (*bba36* and *bptA*) prompted us to initiate insertional mutagenesis studies in an attempt to

elucidate their roles in the life cycle of *B. burgdorferi* (Chapter Six). However, until recently, the quest to identify borrelial genes that account for *B. burgdorferi*'s complex parasitic dependence on both the mammalian and arthropod hosts has been hampered by the intractability of virulent strains of *B. burgdorferi* to genetic manipulation. Additionally, the quest to functionally annotate virulence genes via Koch's molecular postulates (88) has been hindered by the spontaneous loss of virulence due to spurious mutations or loss of key virulence-associated plasmids (i.e., lp25 and lp28-1) (128, 129, 187, 273, 275).

In an attempt to circumvent the problem of spontaneous plasmid loss, we chose to develop a complementation system that targets the virulence-associated lp25 for integration of exogenous DNA (i.e., antibiotic marker and complementation constructs) and thus utilizing antibiotic selection to ease the labor-intensive process of screening clones for their retention of lp25 (Chapter Five). As such, we sought to identify a locus on the virulence-associated plasmid that was amenable to innocuous introduction of exogenous DNA. We were successful in introducing the kanamycin resistance marker encoded by *aph[3']-IIIa* into lp25 immediately downstream of *pncA* (*bbe22*). Moreover, we were able to customize this approach for complementation of *bptA* in a *bptA*-deficient strain (Chapter Six), thus proving the utility of targeting the virulence-associated plasmid lp25 for complementation. However, lp25 is not the only virulence-associated plasmid that is lost during repeated *in vitro* propagation or genetic manipulation. lp28-1, which encodes *vlsE* as a putative antigenic variation locus, has also been shown to be essential for infectivity of mice (108, 277, 279). It is thus plausible to apply the lp25-targeting approach to other virulence-associated plasmids lp28-1, such that targeted insertion of either an antibiotic resistance marker or

complementation construct would result in the isolation of only those strains with the desired integrant (i.e., containing the virulence plasmid).

One caveat with targeting a virulence-associated plasmid for integration of a complementation and/or antibiotic marker construct (Chapter Five) via homologous recombination is that selection for the retained plasmid does not guarantee retention of an infectious phenotype. In other words, other spurious mutations can still accumulate, thus generating avirulent *B. burgdorferi* clones. The majority of the mutants generated over the course of my studies contained all virulence-associated plasmids. However, most were avirulent due to occult mutations. Although the loss of virulence may be multi-factorial and thus difficult to ascertain, it is also possible that these avirulent mutants all arose from the same secondary mutation. If the latter hypothesis is correct, a comparative transcriptional analysis of avirulent and virulent mutants having identical plasmid profiles may prove fruitful for identifying genes essential for virulence of the mammalain host. This approach is based upon the assumption that the defect will affect the transcript level(s) of downstream gene(s), and thus be detectable via microarray analysis.

While developing the lp25-targeting system for complementation (Chapter Five), we were surprised to discover that the parental strain PL133 was naturally deficient in transmissibility from the tick to mammalian hosts. As mentioned earlier, this finding suggests that routine laboratory passage of the Lyme disease spirochete in mice can lead to occult defects in the ability of *B. burgdorferi* to be transmitted from the vector to mammal host. This result is remarkably similar to previous studies (252) wherein it was discovered that serial *in vitro* passage of *B. burgdorferi* could lead to the loss of infectivity in the mouse

model of Lyme borreliosis. Taken together, these results indicate that routine passage of *B. burgdorferi* outside either host of the bacterial life cycle (i.e., restricting growth to either the tick or mammalian host only) can result in the deleterious genetic adaptation of the spirochete to one host at the expense of the other. This further underscores the genomic plasticity of *B. burgdorferi*, as well as the absolute dependence on and intimate association with both its arthropod and mammalian hosts. The implication of these data are that clones utilized for genetic studies must be verified to be competent for survival within and transmission between both hosts prior to insertional mutagenesis studies.

Whereas the discovery of this natural defect was after the development of lp25-targeting complementation system, I was unable to conclusively prove the utility of this system in every stage of the *B. burgdorferi* life cycle (i.e., transmission studies). Nonetheless, we were successful in identifying a locus on lp25 that appears to be amenable to the innocuous integration of exogenous DNA without obvious untoward effects. Moreover, we utilized this system to successfully complement *bptA* in a *bptA*-deficient mutant and show that this gene is essential for natural progression in the spirochete's life cycle (Chapter Seven, discussed below). Nonetheless, the serendipitous finding of a natural tick-transmission deficiency in PL133 provides a unique opportunity to discover a factor essential for the subsistence of the spirochete in nature, and more specifically, transmission to the mammalian host. The identification of a strain that is naturally a mammal transmission-deficient strain is not unique to my studies, inasmuch that one such clone was identified in strain B31 MI (86). Unlike PL133, which contains all plasmids that are found in its parental strain 297, the transmission-deficient B31 MI clone (B31 B) was lacking lp28-4, prompting

speculation that this plasmid encodes a tick transmission factor. Even though B31 B and PL133 have different plasmid profiles, the simplest explanation for the similarity of phenotypes could be that both strains have a defect in either the same gene or pathway. Thus, a pair-wise, comparative transcriptional profile analysis of each mutant (PL133 and B31 B) to its parental strains (297 and B31 MI, respectively) may provide vital clues to the genetic circuitry responsible for a key defect in tick-to-mammal transmission.

Additionally, although transformation efficiencies for *B. burgdorferi* are low, one could perform a screen of a 297 library in a PL133 clone that had been inactivated in *bbe02* (i.e., inactivation of the DNA-restriction modification system that acts as a transformation barrier). A recent report describing the transformation of *B. burgdorferi* with intact, whole borrelial plasmids would also help in this process (108). With this approach, the search for the gene(s) responsible for this transmission deficiency of PL133 could be easily pinpointed to the 297-specific plasmid that restores tick-transmissibility when transformed into strain PL133. Although this approach is based on the assumption that the defect is attributed to only one of the plasmids, all of the virulence-associated genes (*ospC, ospA, pncA*, and *bptA* [Chapter Six]) identified to date in borreliae (except for *rpoS*) have been found to be encoded on one of the twenty-one extra-chromosomal replicons (110, 187, 198, 275). Conversely, if one assumes that the mutation could be anywhere in the genome (even on the chromosome) and a genomic library approach was utilized, a library screen of approximately 3,500 clones would be necessary (297 DNA fragments cloned into shuttle vector and transformed into PL133, in attempts to recover tick transmissibility). The size of this library is based on the assumption that constructs would contain inserts roughly 2,000 bp each (calculation based on

N=ln(1-Probability)/ln[1-(Insert size/Genome size)]). Irrespective of the approach taken, discovery of the genetic locus responsible for this transmission defect will unfortunately be a labor-intensive endeavor given the present genetic systems available for *B. burgdorferi*. However, until bold new steps such as the one above are undertaken, little progress will be made in further elucidating the genetics of *B. burgdorferi*.

With the development of the lp25-targeting complementation system in hand (Chapter Five), the role(s) that certain genes play in the life cycle of *B. burgdorferi* could be evaluated and assessed for their fulfillment of molecular Koch's postulates (88). Upon assessment of the microarray data (Chapter Four), two genes (*bba36* and *bbe16* [*bptA*]) were chosen for insertional mutagenesis studies because they were (i) encoded on virulence-associated plasmids and (ii) differentially regulated in a fashion similar to the virulence factor OspC. Although *bptA* mutants were shown to have a severe defect in propagation through the enzootic life cycle of the spirochete (Chapter Six, summarized below), the loss of *bba36* did not result in a discernable phenotype. This was somewhat surprising given the magnitude (up to 58-fold) of differential regulation displayed by *bba36*. Given that these mutagenesis studies were performed in the 297-derived strain PL133, assessment of transmissibility from the tick to mammalian host was not feasible. It is thus entirely possible that *bba36* may play a role in the transition between hosts (i.e., tick to mammal), and as a result, further experiments are warranted to discern whether *bba36* is functional during this phase of the enzootic life cycle.

bba36 has an additional characteristic that makes analysis of the insertional mutant difficult. *bba36* is potentially a divergent member of the well-characterized multicopy

lipoprotein (*mlp*) family of genes. Although some members of the *mlp* family appear to be regulated (at least partially) by the novel RpoN-RpoS alternative sigma factor regulatory cascade in *B. burgdorferi* (204, 274), the function of the Mlp's have yet to be elucidated, cluster analysis (204) (Chapter Four) indicated that *bba36* was regulated similar to several members of the *mlp* paralogous family (as well as *ospC*). Taken together, the data would suggest that *bba36* potentially is a new member of the RpoN-RpoS regulon; however, no differences in the expression of BBA36 protein levels were discernable between either the *rpoS*-deficient mutant or wild-type strain 297 (unpublished data, not shown). These data thus suggest that *bba36* is regulated independently of at least some members of the *mlp* paralogous family (as well as *ospC*). However, given that only some members of the *mlp* family are regulated by the RpoN-RpoS regulatory cascade, the data do not rule out the possibility that *bba36* still is a divergent member of the *mlp* family.

It is possible that the *mlp*s might represent a group of redundant genes that are preferentially active in only certain small mammal hosts. This possibility is not unprecidented in *B. burgdorferi*, inasmuch that another well-characterized family of highly similar proteins in *B. burgdorferi* (OspEF [Erps] family [paralogous families 162-164]) has been shown to encode factor H-binding proteins that inhibit complement-mediated killing of *B. burgdorferi* (7, 126, 147, 148, 172). Certain members of the *B. burgdorferi* Erp proteins bind factor H molecules of various organisms with different relative binding affinities (147, 148, 170, 172, 241), suggesting different roles for each member of this family (e.g., depending on the specific mammal acting as a host for the spirochetes). Therefore, to functionally assess the role(s) of the various members of a paralogous family, one would

have to evaluate each paralog in the absence of the other paralogous family members. A consequence of this notion is that the role for a certain paralogous family member in the enzootic life cycle would be difficult, if not impossible, to ascertain unless all other paralogous family members were also depleted from the *B. burgdorferi* strain.

Although *bba36* has not been shown to be essential in the life cycle of *B. burgdorferi* at this time, results from insertional mutagenesis studies on *bbe16* (*bptA*) were drastically different (Chapter Six). Even though histopathological analysis indicated that spirochetes deficient in *bptA* were able to disseminate appropriately and produce typical disease sequelae, these mutants were attenuated for virulence by 1-2 logs. More importantly, *bptA* was shown to subserve an essential function for the maintenance *of B. burgdorferi* within the *I. scapularis* tick vector. BptA also was shown to be highly conserved (>88% similarity and >74% identity at the deduced amino acid levels) in all *B. burgdorferi sensu lato* strains tested. However, GeneBank analysis indicates that even though BptA may be highly conserved, BptA is unique to the Lyme borreliosis borreliae; thus suggesting that BptA provides a conserved mechanism for these spirochetes' persistence in nature. The lack of sequence homology between BptA and any other protein with known function, however, will make elucidation of the molecular mechanism(s) by which *bptA* promotes persistence within its tick host challenging.

Closer evaluation of the deduced amino acid sequences of BptA indicates that this protein is lysine-rich (15.05%) and basic (pI = 9.30); these traits possibly explain the observed faster migration of BptA in SDS-PAGE analysis. Bioinformatics predict that a mature BptA lipoprotein should migrate around 23 kDa, however, it migrates at

approximately 17 kDa. These features are of interest because they are defining characteristic of both DNA-binding proteins (e.g., histone-like proteins and DNA uptake/competence proteins) and plasminogen-binding proteins (e.g., urokinase and streptokinase) (13, 136, 140, 145). In considering these other lysine-rich molecules, as well as the proteinase-accessibility data provided herein (indicating that BptA is surface-associated), it is possible that BptA could be either a DNA-uptake or plasminogen-binding protein. Whereas *B. burgdorferi* is not a naturally competent bacterium, the need for a DNA-uptake protein is not known. Moreover, transformation efficiencies of the *bptA*-deficient strains were not different from wild-type strains (personal observations). Therefore, it is highly improbable that BptA is a molecule involved in DNA uptake. Although previous studies performed by Coleman *et al.* indicate that mammalian plasminogen plays a role in the efficient dissemination of *B. burgdorferi* within ticks (as well as enhancing spirochetemia in mice) (64), a direct connection, if any, between this previously published data and the data presented herein concerning *bptA* is not apparent. However, since BptA has some characteristics of plasminogen-binding proteins, it is possible that *bptA* plays a role in the plasminogen-mediated survival and dissemination of *B. burgdorferi* described by Coleman *et al* (64). As such, further studies are necessary to elucidate the precise mechanism by which BptA functions to maintain *B. burgdorferi* in the tick vector and to facilitate virulence in a mammalian host.

Mutational analyses indicated that BptA is functional in both the mammalian and *Ixodes* tick hosts (Chapter Six). Furthermore, BptA appears to be expressed in *B. burgdorferi* when the spirochete is cultivated *in vitro* at 37°C, pH 6.8. Thus, *in vitro* growth

conditions can be used to evaluate both the expression of *bptA* as well as the upstream gene(s) necessary for the expression of *bptA*. With the genetic arrangement of *bptA* and *bbe17* suggesting that they may be co-transcribed from a common promoter, RT-PCR analysis is warranted to determine whether this hypothesis is true. However, the complementation data from strain BbDTR653 (*bptA* with its native 300-bp upstream region) indicate that *bptA* may have its own cryptic internal promoter. In support of this hypothesis, data have suggested that the expression of the *ospAB* operon may be from an operonic promoter as well as from an unidentified internal promoter for the expression of *ospB* (separate from *ospA*) (160). As such, primer extension experiments should be performed to help identify the putative promoters of *bptA*. Once the promoter(s) are known, one can perform DNA affinity purification techniques to isolate the DNA-binding protein(s) that are operative in regulating the expression of *bptA*.

Although we were successful in showing that the primary role of *bptA* is to allow *B. burgdorferi* to persist within feeding *Ixodes* ticks (Chapter Six), the precise mechanism by which *bptA* provides this function is unclear. Since proteinase accessibility studies indicate that BptA is surface-associated, it is plausible that BptA is a receptor for either a mammalian or tick host protein. Alternatively, *bptA* may encode a protein involved in either binding small organic/inorganic molecules or interacting with other borrelial proteins. To investigate these possibilities, one could screen a tick cDNA expression library (186) to discover tick proteins that are unable to bind *bptA*-deficient mutants but that bind wild-type *B. burgdorferi*. Conversely, a mouse blood cDNA expression library could be used to investigate whether BptA binds to a mammalian host factor. Finding small molecules that bind BptA would

prove more difficult to accomplish. One other possibility is that BptA actually binds and works in concert with another borrelial protein. Protein cross-linking studies or immunoprecipitation of BptA followed by mass spectrophotometric and/or protein sequencing analysis could be employed to detect proteins that interact with BptA in *B. burgdorferi*. The type of studies listed above would identify proteins that interact with or bind to BptA. However, these studies would not elucidate downstream events that lead to spirochetal persistence. Thus, microarray or two-dimensional SDS-PAGE analysis of both wild-type *B. burgdorferi* and the *bptA*-deficient mutant extracted from engorged larvae may be instrumental in elucidating these downstream events. Taken together, these experiments could potentially lead to the elucidation of the precise mechanism of *B. burgdorferi*'s *bptA*-dependent persistence within the arthropod vector.

Appendix A. Microarray data for all genes grown under the following conditions: room temperature, pH 7.5; 37°C, pH 6.8; and within DMCs (204).

	Log Ratios			Percentile Rank			Uncertainty		
Gene	DMC	RT-7.5	37-6.8	DMC	RT-7.5	37-6.8	DMC	RT-7.5	37-6.8
BB0001	0.363	0.457	0.113	0.860	0.860	0.620	0.060	0.107	0.242
BB0002	-0.104	-0.067	-0.061	0.350	0.390	0.400	0.078	0.048	0.047
BB0003	-0.021	0.588	0.087	0.450	0.930	0.600	0.045	0.473	0.152
BB0004	0.137	0.115	-0.017	0.620	0.590	0.460	0.016	0.051	0.064
BB0005	-0.382	-0.278	-0.342	0.130	0.210	0.160	0.078	0.131	0.088
BB0006	-0.020	0.069	-0.076	0.450	0.540	0.390	0.052	0.046	0.048
BB0007	0.229	0.239	0.080	0.740	0.710	0.590	0.025	0.064	0.024
BB0008	0.032	0.065	0.011	0.510	0.530	0.490	0.107	0.116	0.111
BB0009	0.003	-0.032	-0.309	0.480	0.430	0.190	0.079	0.082	0.065
BB0010	0.543	0.497	0.393	0.950	0.890	0.860	0.048	0.033	0.046
BB0011	0.038	0.101	-0.047	0.520	0.570	0.420	0.032	0.088	0.038
BB0012	0.099	-0.066	-0.048	0.590	0.390	0.420	0.080	0.083	0.093
BB0013	0.234	0.159	-0.013	0.750	0.640	0.460	0.028	0.079	0.069
BB0014	-0.344	-0.439	-0.358	0.160	0.120	0.150	0.068	0.045	0.086
BB0015	0.133	0.065	0.040	0.620	0.530	0.540	0.071	0.115	0.067
BB0016	0.622	0.582	0.640	0.960	0.930	0.940	0.055	0.062	0.065
BB0017	-0.472	-0.425	-0.186	0.080	0.120	0.280	0.071	0.088	0.045
BB0018	-0.183	-0.401	-0.189	0.280	0.130	0.270	0.092	0.046	0.024
BB0019	0.141	0.069	0.236	0.630	0.540	0.760	0.087	0.039	0.038
BB0020	-0.062	0.071	0.321	0.400	0.540	0.830	0.061	0.022	0.054
BB0021	-0.008	-0.023	-0.023	0.460	0.430	0.460	0.089	0.093	0.077
BB0022	0.033	-0.043	0.149	0.520	0.410	0.670	0.071	0.021	0.051
BB0023	0.327	0.208	0.308	0.840	0.680	0.820	0.040	0.049	0.045
BB0024	-0.214	0.023	0.028	0.250	0.480	0.520	0.061	0.043	0.070
BB0025	-0.081	0.101	0.071	0.380	0.570	0.570	0.055	0.035	0.045
BB0026	-0.071	0.028	0.030	0.390	0.490	0.520	0.063	0.040	0.051
BB0027	0.303	0.757	0.393	0.820	0.970	0.860	0.066	0.074	0.079
BB0028	-0.053	0.282	0.004	0.410	0.750	0.490	0.066	0.015	0.059
BB0029	0.117	0.083	-0.037	0.610	0.550	0.440	0.092	0.077	0.104
BB0030	0.344	0.176	0.079	0.850	0.650	0.590	0.040	0.047	0.106
BB0031	0.113	0.106	0.188	0.600	0.580	0.710	0.046	0.067	0.034
BB0032	0.143	0.123	0.192	0.630	0.600	0.720	0.056	0.032	0.089

BB0033	0.036	0.233	-0.038	0.520	0.700	0.430	0.050	0.078	0.043
BB0034	0.015	0.389	0.320	0.500	0.820	0.830	0.074	0.057	0.041
BB0035	0.314	0.409	0.373	0.830	0.840	0.860	0.051	0.033	0.043
BB0036	0.279	-0.103	0.422	0.790	0.350	0.880	0.035	0.040	0.059
BB0037	0.085	-0.119	0.367	0.570	0.340	0.850	0.029	0.059	0.043
BB0038	0.158	-0.038	0.169	0.660	0.420	0.690	0.049	0.067	0.061
BB0039	0.113	-0.035	0.235	0.600	0.420	0.760	0.054	0.121	0.024
BB0040	0.190	-0.049	0.138	0.700	0.410	0.650	0.054	0.101	0.017
BB0041	0.419	0.351	0.222	0.890	0.800	0.740	0.165	0.143	0.057
BB0042	0.420	0.151	0.077	0.890	0.630	0.580	0.041	0.014	0.082
BB0043	0.208	0.142	0.197	0.720	0.620	0.720	0.025	0.063	0.043
BB0044	0.634	0.477	0.531	0.970	0.880	0.910	0.040	0.077	0.025
BB0045	-0.049	-0.191	-0.108	0.420	0.280	0.360	0.056	0.078	0.052
BB0046	-0.097	-0.095	-0.070	0.360	0.360	0.400	0.097	0.050	0.035
BB0047	0.712	0.751	0.614	0.970	0.970	0.930	0.083	0.049	0.039
BB0048	0.219	0.200	0.066	0.730	0.670	0.570	0.051	0.074	0.096
BB0049	0.622	1.294	0.938	0.970	0.990	0.980	0.080	0.192	0.207
BB0050	-0.169	-0.331	-0.354	0.290	0.180	0.160	0.099	0.031	0.045
BB0051	-0.288	-0.137	-0.331	0.190	0.330	0.170	0.081	0.050	0.091
BB0052	-0.047	-0.191	-0.049	0.420	0.280	0.420	0.075	0.050	0.021
BB0053	-0.269	-0.163	-0.255	0.210	0.310	0.220	0.142	0.041	0.083
BB0054	0.261	0.253	0.457	0.770	0.720	0.890	0.100	0.087	0.092
BB0055	0.269	0.459	0.445	0.780	0.870	0.890	0.044	0.052	0.032
BB0056	0.447	0.694	0.914	0.910	0.960	0.980	0.086	0.029	0.053
BB0057	0.601	0.635	1.059	0.960	0.940	0.990	0.053	0.077	0.059
BB0058	0.015	-0.002	0.088	0.490	0.450	0.600	0.120	0.062	0.068
BB0059	0.226	0.452	0.200	0.740	0.860	0.720	0.032	0.042	0.018
BB0060	0.314	0.612	0.525	0.830	0.940	0.910	0.086	0.075	0.060
BB0061	0.446	0.934	0.647	0.910	0.980	0.940	0.048	0.045	0.069
BB0062	-0.088	0.031	-0.180	0.370	0.490	0.290	0.068	0.079	0.120
BB0063	0.202	0.372	0.232	0.720	0.810	0.750	0.063	0.018	0.028
BB0064	0.256	0.395	0.415	0.770	0.830	0.870	0.062	0.045	0.034
BB0065	0.398	0.622	0.524	0.880	0.940	0.910	0.040	0.081	0.077
BB0066	0.544	0.542	0.462	0.950	0.910	0.900	0.077	0.054	0.042
BB0067	0.311	0.772	0.428	0.820	0.970	0.880	0.025	0.049	0.039
BB0068	0.260	0.339	0.363	0.770	0.790	0.850	0.037	0.057	0.072
BB0069	0.167	0.458	0.347	0.670	0.870	0.840	0.034	0.031	0.015
BB0070	-0.008	0.873	0.154	0.460	0.980	0.670	0.086	0.059	0.049
BB0071	-0.150	0.011	-0.057	0.310	0.470	0.410	0.061	0.056	0.019

BB0072	-0.205	-0.129	-0.041	0.260	0.330	0.430	0.053	0.082	0.077
BB0073	-0.007	0.080	-0.053	0.460	0.550	0.410	0.102	0.044	0.066
BB0074	-0.153	-0.136	0.074	0.310	0.330	0.580	0.047	0.033	0.044
BB0075	0.420	0.557	0.252	0.890	0.920	0.780	0.071	0.075	0.050
BB0076	-0.083	-0.087	-0.163	0.370	0.370	0.300	0.046	0.046	0.113
BB0077	0.086	0.084	0.022	0.570	0.560	0.500	0.079	0.071	0.170
BB0078	0.430	0.340	0.121	0.900	0.790	0.630	0.058	0.038	0.163
BB0079	0.168	0.188	-0.022	0.670	0.660	0.460	0.059	0.077	0.108
BB0080	0.012	0.034	-0.125	0.490	0.500	0.340	0.035	0.044	0.117
BB0081	-0.275	-0.118	-0.304	0.200	0.340	0.190	0.040	0.064	0.054
BB0082	0.124	-0.009	0.207	0.610	0.450	0.730	0.059	0.058	0.061
BB0083	0.503	0.392	0.532	0.940	0.820	0.920	0.048	0.050	0.049
BB0084	0.190	0.131	0.242	0.700	0.600	0.770	0.068	0.034	0.047
BB0085	0.117	0.224	0.076	0.610	0.700	0.580	0.078	0.096	0.063
BB0086	-0.057	-0.156	-0.213	0.410	0.310	0.260	0.077	0.045	0.098
BB0087	0.153	0.581	0.559	0.650	0.930	0.920	0.041	0.085	0.098
BB0088	-0.057	0.285	0.368	0.410	0.750	0.850	0.059	0.064	0.079
BB0089	-0.194	0.069	0.209	0.270	0.540	0.740	0.051	0.047	0.094
BB0090	-0.046	0.098	0.183	0.420	0.570	0.710	0.073	0.074	0.081
BB0091	-0.030	0.149	0.297	0.440	0.620	0.810	0.054	0.099	0.177
BB0092	0.590	0.469	0.459	0.960	0.870	0.890	0.038	0.027	0.076
BB0093	-0.009	-0.196	0.309	0.460	0.270	0.820	0.040	0.043	0.128
BB0094	-0.543	-0.722	-0.061	0.050	0.020	0.400	0.100	0.047	0.129
BB0095	0.302	0.170	0.470	0.820	0.650	0.900	0.051	0.080	0.213
BB0096	0.614	0.132	0.695	0.960	0.610	0.950	0.033	0.038	0.067
BB0097	0.101	0.163	0.494	0.590	0.640	0.900	0.113	0.081	0.089
BB0098	-0.301	-0.536	-0.414	0.180	0.080	0.130	0.083	0.037	0.071
BB0099	-0.043	-0.049	-0.302	0.430	0.410	0.190	0.067	0.087	0.099
BB0100	0.197	0.192	0.089	0.710	0.660	0.600	0.055	0.044	0.036
BB0101	-0.357	-0.397	-0.165	0.150	0.140	0.300	0.076	0.037	0.044
BB0102	0.221	0.055	0.050	0.740	0.520	0.550	0.094	0.049	0.096
BB0103	0.166	0.244	-0.038	0.670	0.720	0.430	0.064	0.037	0.072
BB0104	0.022	0.480	0.345	0.500	0.880	0.840	0.089	0.080	0.066
BB0105	0.194	0.401	0.245	0.710	0.830	0.770	0.050	0.044	0.033
BB0106	0.152	0.177	0.244	0.650	0.650	0.770	0.040	0.059	0.066
BB0107	0.184	0.201	0.139	0.690	0.670	0.650	0.077	0.118	0.098
BB0108	-0.021	-0.112	0.125	0.450	0.340	0.640	0.063	0.027	0.034
BB0109	0.023	0.117	0.108	0.500	0.590	0.620	0.078	0.047	0.039
BB0110	-0.141	-0.069	-0.274	0.320	0.390	0.210	0.077	0.059	0.048

BB0111	0.039	0.282	0.297	0.520	0.750	0.810	0.065	0.029	0.030
BB0112	0.483	0.597	0.521	0.930	0.930	0.910	0.075	0.060	0.036
BB0113	0.668	0.726	0.918	0.970	0.960	0.980	0.052	0.129	0.105
BB0114	0.783	0.708	0.640	0.980	0.960	0.940	0.031	0.054	0.049
BB0115	0.920	0.921	0.660	0.990	0.980	0.950	0.070	0.074	0.061
BB0116	-0.405	-0.448	-0.341	0.120	0.110	0.160	0.094	0.076	0.078
BB0117	-0.081	-0.031	-0.042	0.380	0.430	0.430	0.060	0.066	0.083
BB0118	-0.289	-0.363	-0.191	0.190	0.160	0.270	0.087	0.089	0.076
BB0119	-0.070	0.159	0.056	0.390	0.640	0.550	0.060	0.057	0.066
BB0120	0.526	0.464	0.584	0.940	0.870	0.930	0.045	0.031	0.050
BB0121	0.456	0.507	0.544	0.910	0.890	0.920	0.042	0.032	0.085
BB0122	0.591	0.625	0.584	0.960	0.940	0.930	0.041	0.041	0.051
BB0123	0.588	0.776	0.674	0.960	0.970	0.950	0.050	0.039	0.059
BB0124	0.321	0.612	0.350	0.830	0.940	0.840	0.059	0.115	0.120
BB0125	0.463	0.503	0.496	0.910	0.890	0.910	0.043	0.078	0.042
BB0126	0.577	0.420	0.524	0.960	0.840	0.910	0.075	0.038	0.058
BB0127	0.494	0.513	0.560	0.930	0.900	0.920	0.019	0.037	0.047
BB0128	0.534	0.378	0.518	0.940	0.810	0.910	0.045	0.033	0.016
BB0129	0.352	0.269	0.494	0.860	0.740	0.900	0.077	0.030	0.065
BB0130	0.483	0.402	0.436	0.930	0.830	0.880	0.034	0.044	0.071
BB0131	0.336	0.493	0.419	0.840	0.880	0.880	0.038	0.046	0.034
BB0132	0.547	0.344	0.488	0.950	0.790	0.900	0.059	0.061	0.073
BB0133	0.941	0.943	0.960	0.990	0.980	0.980	0.049	0.042	0.069
BB0134	0.080	-0.330	-0.240	0.570	0.180	0.230	0.045	0.042	0.080
BB0135	0.049	-0.157	0.243	0.530	0.310	0.770	0.051	0.018	0.061
BB0136	0.077	-0.118	-0.223	0.570	0.340	0.250	0.067	0.030	0.104
BB0137	0.038	0.682	0.353	0.520	0.960	0.850	0.034	0.073	0.068
BB0138	0.640	0.503	0.343	0.970	0.890	0.840	0.045	0.088	0.103
BB0139	-0.377	0.110	-0.168	0.130	0.580	0.300	0.169	0.060	0.038
BB0140	0.326	0.596	0.208	0.830	0.930	0.730	0.116	0.133	0.082
BB0141	-0.055	0.335	0.158	0.410	0.780	0.670	0.035	0.035	0.038
BB0142	-0.312	-0.275	-0.221	0.170	0.210	0.250	0.063	0.045	0.070
BB0143	-0.037	0.215	-0.052	0.430	0.690	0.410	0.142	0.057	0.085
BB0144	-0.001	0.624	0.490	0.480	0.940	0.900	0.068	0.069	0.025
BB0145	-0.243	-0.017	-0.128	0.230	0.440	0.340	0.065	0.074	0.060
BB0146	0.274	0.410	0.338	0.790	0.840	0.840	0.039	0.056	0.025
BB0147	1.203	1.262	1.615	0.990	0.990	0.990	0.074	0.101	0.079
BB0148	0.090	0.307	0.262	0.580	0.770	0.780	0.021	0.163	0.405
BB0149	0.299	0.811	0.416	0.810	0.970	0.880	0.043	0.067	0.033

BB0150	0.276	0.555	0.201	0.790	0.920	0.720	0.142	0.130	0.135
BB0151	-0.425	-0.409	-0.009	0.100	0.130	0.470	0.075	0.044	0.043
BB0152	-0.482	-0.693	-0.369	0.080	0.030	0.150	0.075	0.044	0.066
BB0153	-0.125	0.218	0.312	0.330	0.690	0.820	0.054	0.078	0.091
BB0154	0.071	0.089	0.287	0.560	0.560	0.800	0.089	0.045	0.055
BB0155	0.194	0.271	0.169	0.710	0.740	0.690	0.047	0.051	0.031
BB0156	0.080	0.550	0.374	0.570	0.920	0.860	0.063	0.040	0.037
BB0157	0.433	0.456	0.156	0.900	0.860	0.670	0.053	0.104	0.051
BB0158	0.325	0.521	0.253	0.830	0.900	0.780	0.058	0.043	0.029
BB0159	0.114	0.248	-0.077	0.600	0.720	0.390	0.055	0.110	0.081
BB0160	0.241	0.305	0.022	0.760	0.770	0.510	0.093	0.087	0.069
BB0161	0.005	0.080	-0.047	0.480	0.550	0.420	0.066	0.063	0.042
BB0162	0.398	0.250	0.306	0.880	0.720	0.820	0.089	0.069	0.047
BB0163	0.499	0.691	0.418	0.940	0.960	0.880	0.033	0.123	0.034
BB0164	-0.098	-0.242	-0.160	0.360	0.240	0.310	0.116	0.106	0.111
BB0165	-0.236	0.002	-0.141	0.230	0.460	0.330	0.091	0.070	0.047
BB0166	-0.216	-0.226	-0.044	0.250	0.250	0.430	0.100	0.059	0.036
BB0167	0.046	0.209	-0.045	0.530	0.680	0.420	0.094	0.078	0.086
BB0168	0.130	0.088	0.093	0.620	0.560	0.600	0.119	0.046	0.050
BB0169	0.418	0.547	0.349	0.890	0.910	0.840	0.037	0.135	0.079
BB0170	-0.044	0.075	-0.176	0.430	0.540	0.290	0.104	0.066	0.024
BB0171	0.319	0.544	0.283	0.830	0.910	0.800	0.031	0.045	0.044
BB0172	0.216	0.171	0.025	0.730	0.650	0.510	0.062	0.064	0.073
BB0173	0.101	0.347	0.208	0.590	0.790	0.740	0.062	0.023	0.052
BB0174	0.021	0.041	-0.092	0.500	0.500	0.370	0.101	0.077	0.172
BB0175	-0.132	-0.022	-0.064	0.330	0.430	0.400	0.091	0.063	0.049
BB0176	-0.328	-0.364	-0.208	0.170	0.160	0.260	0.114	0.057	0.067
BB0177	0.110	0.023	0.230	0.600	0.480	0.750	0.068	0.062	0.082
BB0178	-0.369	-0.327	-0.216	0.140	0.180	0.250	0.072	0.049	0.048
BB0179	-0.163	-0.101	0.032	0.300	0.360	0.520	0.044	0.064	0.041
BB0180	0.349	0.304	0.217	0.850	0.770	0.740	0.041	0.058	0.062
BB0181	0.347	0.525	0.385	0.850	0.900	0.860	0.136	0.105	0.057
BB0182	-0.150	-0.236	0.066	0.310	0.240	0.570	0.018	0.030	0.061
BB0183	-0.003	0.063	0.130	0.470	0.530	0.650	0.069	0.068	0.035
BB0184	0.362	0.193	-0.049	0.860	0.670	0.420	0.060	0.044	0.064
BB0185	0.043	0.110	-0.147	0.530	0.590	0.320	0.053	0.094	0.094
BB0186	0.273	0.082	0.059	0.790	0.550	0.560	0.047	0.030	0.065
BB0187	0.352	0.436	0.295	0.850	0.850	0.810	0.065	0.083	0.053
BB0188	0.822	0.426	0.779	0.990	0.850	0.960	0.098	0.057	0.061

BB0189	0.722	0.533	0.873	0.980	0.910	0.970	0.183	0.102	0.141
BB0190	0.815	0.533	0.861	0.980	0.910	0.970	0.065	0.031	0.075
BB0191	-0.329	1.005	0.123	0.160	0.990	0.640	0.257	0.262	0.132
BB0192	0.186	-0.043	-0.030	0.700	0.410	0.450	0.027	0.064	0.055
BB0193	-0.058	0.155	0.024	0.400	0.630	0.510	0.051	0.060	0.085
BB0194	0.085	-0.063	0.003	0.570	0.400	0.490	0.084	0.099	0.050
BB0195	0.264	0.010	0.416	0.780	0.470	0.880	0.032	0.051	0.048
BB0196	-0.523	-0.741	-0.563	0.060	0.020	0.070	0.089	0.047	0.048
BB0197	-0.037	0.243	-0.012	0.430	0.710	0.470	0.065	0.034	0.052
BB0198	-0.485	-0.171	-0.431	0.080	0.300	0.120	0.087	0.041	0.059
BB0199	-0.530	-0.376	-0.685	0.060	0.150	0.030	0.112	0.066	0.046
BB0200	-0.311	-0.162	-0.228	0.180	0.310	0.240	0.056	0.100	0.061
BB0201	-0.286	-0.147	-0.246	0.190	0.320	0.230	0.078	0.060	0.029
BB0202	-0.271	-0.332	-0.141	0.210	0.180	0.330	0.073	0.047	0.027
BB0203	0.054	0.109	-0.020	0.540	0.580	0.460	0.064	0.093	0.049
BB0204	-0.144	-0.089	0.001	0.320	0.370	0.480	0.076	0.051	0.033
BB0205	-0.126	-0.211	-0.298	0.330	0.260	0.200	0.036	0.085	0.052
BB0206	-0.168	-0.238	0.055	0.300	0.240	0.550	0.094	0.038	0.022
BB0207	0.053	-0.077	0.036	0.540	0.380	0.530	0.067	0.120	0.020
BB0208	-0.016	-0.157	-0.033	0.450	0.310	0.440	0.094	0.053	0.072
BB0209	0.139	0.362	0.106	0.630	0.800	0.610	0.022	0.050	0.023
BB0210	-0.306	-0.227	-0.122	0.180	0.250	0.350	0.065	0.025	0.099
BB0211	-0.223	-0.047	-0.033	0.240	0.410	0.440	0.107	0.059	0.020
BB0212	0.298	0.392	0.196	0.810	0.820	0.720	0.051	0.048	0.019
BB0213	-0.048	0.082	-0.176	0.420	0.550	0.290	0.055	0.051	0.081
BB0214	-0.122	-0.310	-0.181	0.340	0.190	0.290	0.092	0.073	0.055
BB0215	0.236	0.133	0.275	0.750	0.610	0.800	0.074	0.062	0.044
BB0216	-0.088	-0.244	0.180	0.370	0.240	0.700	0.120	0.050	0.023
BB0217	-0.032	0.133	0.083	0.440	0.610	0.590	0.155	0.073	0.085
BB0218	-0.358	-0.413	-0.385	0.150	0.130	0.140	0.053	0.022	0.083
BB0219	-0.321	-0.108	-0.083	0.170	0.350	0.380	0.067	0.064	0.082
BB0220	0.053	0.034	0.120	0.540	0.500	0.630	0.046	0.051	0.045
BB0221	-0.121	-0.070	-0.147	0.340	0.390	0.320	0.060	0.067	0.024
BB0222	-0.213	-0.206	-0.440	0.250	0.270	0.120	0.122	0.042	0.061
BB0223	0.301	0.279	0.242	0.810	0.750	0.760	0.040	0.069	0.052
BB0224	0.282	0.128	-0.131	0.800	0.600	0.340	0.125	0.058	0.061
BB0225	0.028	0.003	0.129	0.510	0.460	0.640	0.090	0.122	0.089
BB0226	0.013	-0.096	0.024	0.490	0.360	0.510	0.046	0.059	0.043
BB0227	0.059	0.086	0.176	0.550	0.560	0.700	0.073	0.064	0.095

BB0228	-0.062	0.190	0.023	0.400	0.660	0.510	0.038	0.038	0.067
BB0229	0.406	0.498	0.431	0.880	0.890	0.880	0.047	0.078	0.060
BB0230	0.294	0.212	0.182	0.800	0.680	0.710	0.062	0.098	0.041
BB0231	0.706	0.678	0.699	0.970	0.950	0.950	0.034	0.070	0.081
BB0232	0.824	1.025	0.814	0.990	0.990	0.970	0.089	0.096	0.083
BB0233	0.567	0.944	0.662	0.950	0.980	0.950	0.036	0.178	0.157
BB0234	0.279	0.155	0.153	0.790	0.630	0.670	0.034	0.038	0.051
BB0235	-0.251	0.010	-0.047	0.220	0.470	0.420	0.038	0.055	0.072
BB0236	0.031	0.405	0.209	0.510	0.830	0.740	0.024	0.047	0.056
BB0237	-0.446	-0.304	-0.404	0.090	0.200	0.140	0.065	0.065	0.072
BB0238	0.202	0.535	0.778	0.720	0.910	0.960	0.045	0.053	0.048
BB0239	0.000	0.025	-0.045	0.480	0.490	0.430	0.031	0.081	0.034
BB0240	-0.199	0.051	0.021	0.260	0.510	0.500	0.045	0.062	0.047
BB0241	-0.457	-0.020	-0.072	0.090	0.440	0.390	0.034	0.069	0.042
BB0242	0.126	0.236	0.010	0.610	0.710	0.490	0.096	0.089	0.070
BB0243	-0.158	-0.011	0.017	0.300	0.440	0.500	0.082	0.075	0.025
BB0244	-0.001	0.044	-0.027	0.470	0.510	0.450	0.089	0.051	0.046
BB0245	-0.070	0.144	0.128	0.390	0.620	0.640	0.065	0.052	0.059
BB0246	-0.305	-0.133	-0.241	0.180	0.330	0.230	0.048	0.060	0.098
BB0247	-0.005	0.053	-0.255	0.470	0.520	0.220	0.090	0.091	0.060
BB0248	-0.376	-0.401	-0.318	0.140	0.130	0.180	0.107	0.041	0.056
BB0249	-0.439	-0.300	-0.330	0.090	0.200	0.170	0.072	0.035	0.065
BB0250	0.184	0.012	0.075	0.700	0.470	0.580	0.085	0.098	0.061
BB0251	0.160	0.567	0.267	0.660	0.920	0.790	0.062	0.070	0.037
BB0252	-0.289	-0.164	-0.141	0.190	0.300	0.330	0.094	0.074	0.053
BB0253	-0.036	0.293	0.165	0.430	0.760	0.680	0.047	0.040	0.025
BB0254	-0.328	-0.306	-0.327	0.170	0.190	0.170	0.019	0.104	0.043
BB0255	-0.196	-0.398	-0.182	0.270	0.130	0.280	0.095	0.062	0.056
BB0256	0.629	0.350	0.601	0.970	0.800	0.930	0.078	0.049	0.082
BB0257	-0.275	-0.506	0.035	0.200	0.090	0.530	0.098	0.094	0.085
BB0258	0.126	0.108	0.048	0.610	0.580	0.550	0.056	0.112	0.009
BB0259	0.148	-0.177	0.205	0.640	0.290	0.730	0.065	0.029	0.064
BB0260	0.401	0.243	0.522	0.880	0.710	0.910	0.031	0.039	0.071
BB0261	0.138	0.127	0.165	0.630	0.600	0.680	0.096	0.037	0.060
BB0262	-0.123	0.159	-0.089	0.330	0.640	0.380	0.116	0.063	0.131
BB0263	0.058	0.016	0.059	0.540	0.470	0.560	0.087	0.059	0.035
BB0264	-0.174	0.032	-0.009	0.290	0.500	0.470	0.031	0.072	0.051
BB0265	0.492	0.562	0.610	0.930	0.920	0.930	0.021	0.030	0.043
BB0266	0.479	0.524	0.489	0.920	0.900	0.900	0.040	0.043	0.028

BB0267	0.333	0.646	0.437	0.840	0.950	0.880	0.031	0.035	0.024
BB0268	0.453	0.619	0.535	0.910	0.940	0.920	0.059	0.056	0.110
BB0269	0.087	0.610	0.197	0.580	0.940	0.720	0.031	0.050	0.044
BB0270	0.260	0.157	0.147	0.770	0.630	0.670	0.024	0.052	0.081
BB0271	-0.196	0.316	0.031	0.270	0.780	0.520	0.017	0.081	0.066
BB0272	0.010	0.343	0.238	0.490	0.790	0.760	0.074	0.077	0.042
BB0273	0.055	0.140	0.147	0.540	0.610	0.670	0.122	0.086	0.065
BB0274	0.113	0.209	-0.011	0.600	0.680	0.470	0.101	0.061	0.058
BB0275	-0.026	0.023	0.161	0.440	0.480	0.680	0.086	0.091	0.033
BB0276	0.482	0.425	0.444	0.920	0.840	0.890	0.039	0.086	0.052
BB0277	0.447	0.549	0.618	0.910	0.910	0.940	0.022	0.040	0.060
BB0278	0.189	0.122	0.340	0.700	0.600	0.840	0.030	0.042	0.077
BB0279	0.473	0.314	0.650	0.920	0.770	0.940	0.036	0.052	0.062
BB0280	0.160	-0.009	0.412	0.660	0.450	0.870	0.086	0.060	0.088
BB0281	-0.082	0.065	0.176	0.380	0.530	0.700	0.073	0.029	0.081
BB0282	0.577	0.490	0.707	0.960	0.880	0.950	0.044	0.032	0.085
BB0283	0.243	0.416	0.657	0.760	0.840	0.940	0.039	0.047	0.078
BB0284	0.712	0.460	0.783	0.980	0.870	0.960	0.070	0.057	0.084
BB0285	0.597	0.215	0.639	0.960	0.690	0.940	0.078	0.059	0.101
BB0286	0.236	0.143	0.163	0.750	0.620	0.680	0.057	0.066	0.035
BB0287	-0.035	-0.038	0.001	0.430	0.420	0.480	0.097	0.055	0.066
BB0288	0.037	-0.095	0.167	0.520	0.360	0.690	0.073	0.031	0.078
BB0289	0.467	0.197	0.486	0.920	0.670	0.900	0.055	0.056	0.088
BB0290	0.236	0.053	0.460	0.750	0.520	0.890	0.046	0.034	0.081
BB0291	0.037	0.007	0.439	0.520	0.460	0.890	0.034	0.034	0.091
BB0292	0.020	-0.060	0.081	0.500	0.400	0.590	0.066	0.037	0.111
BB0293	0.263	0.174	0.434	0.780	0.650	0.880	0.104	0.044	0.075
BB0294	0.584	0.553	0.546	0.960	0.920	0.920	0.052	0.118	0.186
BB0295	-0.149	-0.363	-0.068	0.310	0.160	0.400	0.097	0.058	0.079
BB0296	-0.191	-0.436	0.069	0.270	0.120	0.570	0.061	0.035	0.036
BB0297	-0.182	-0.288	-0.038	0.280	0.200	0.440	0.086	0.060	0.070
BB0298	0.215	0.108	0.208	0.730	0.580	0.730	0.074	0.047	0.104
BB0299	-0.460	-0.172	0.030	0.090	0.300	0.520	0.054	0.047	0.094
BB0300	-0.007	0.279	0.322	0.460	0.750	0.830	0.068	0.051	0.060
BB0301	0.216	0.275	0.187	0.730	0.740	0.710	0.049	0.121	0.087
BB0302	-0.172	-0.253	-0.171	0.290	0.230	0.300	0.097	0.095	0.103
BB0303	-0.263	0.022	-0.332	0.210	0.480	0.170	0.058	0.087	0.074
BB0304	0.473	0.490	0.432	0.920	0.880	0.880	0.032	0.103	0.021
BB0305	0.143	0.282	0.079	0.640	0.750	0.580	0.058	0.084	0.098

BB0306	-0.129	-0.250	-0.177	0.330	0.230	0.290	0.074	0.022	0.034
BB0307	0.251	0.335	0.153	0.760	0.780	0.670	0.037	0.069	0.037
BB0308	0.128	-0.044	-0.085	0.620	0.410	0.380	0.074	0.036	0.058
BB0309	-0.073	-0.087	-0.124	0.380	0.370	0.340	0.064	0.051	0.118
BB0310	0.266	0.215	0.029	0.780	0.690	0.520	0.080	0.056	0.059
BB0311	-0.094	0.084	0.026	0.360	0.560	0.510	0.068	0.052	0.025
BB0312	0.208	0.050	0.266	0.720	0.510	0.790	0.042	0.072	0.025
BB0313	0.289	0.164	0.458	0.800	0.640	0.890	0.050	0.043	0.069
BB0314	-0.283	-0.345	-0.298	0.200	0.170	0.200	0.099	0.054	0.041
BB0315	0.078	0.215	-0.144	0.570	0.690	0.320	0.053	0.059	0.113
BB0316	-0.229	-0.134	-0.441	0.240	0.330	0.120	0.072	0.058	0.059
BB0317	0.030	0.144	0.060	0.510	0.620	0.560	0.086	0.054	0.067
BB0318	0.242	0.063	0.090	0.760	0.530	0.600	0.052	0.059	0.041
BB0319	-0.141	0.009	-0.089	0.320	0.470	0.380	0.047	0.065	0.036
BB0320	0.156	0.576	0.171	0.650	0.930	0.700	0.088	0.024	0.107
BB0321	0.163	0.307	0.087	0.660	0.770	0.600	0.064	0.121	0.095
BB0322	0.058	0.152	-0.067	0.540	0.630	0.400	0.089	0.069	0.027
BB0323	0.375	0.275	1.107	0.870	0.740	0.990	0.044	0.033	0.093
BB0324	0.149	0.110	-0.022	0.640	0.590	0.460	0.038	0.089	0.027
BB0325	-0.318	-0.035	-0.106	0.170	0.420	0.360	0.082	0.046	0.074
BB0326	0.090	-0.032	0.118	0.580	0.420	0.630	0.050	0.084	0.065
BB0327	0.476	0.637	0.690	0.920	0.950	0.950	0.061	0.056	0.073
BB0328	-0.235	-0.356	0.008	0.230	0.160	0.490	0.059	0.044	0.072
BB0329	0.034	-0.085	0.593	0.520	0.370	0.930	0.030	0.068	0.100
BB0330	-0.285	-0.308	0.185	0.200	0.190	0.710	0.087	0.045	0.084
BB0331	0.455	0.573	0.359	0.910	0.930	0.850	0.033	0.108	0.078
BB0332	0.043	0.067	0.292	0.530	0.540	0.810	0.043	0.054	0.079
BB0333	-0.132	-0.322	-0.036	0.330	0.180	0.440	0.052	0.078	0.048
BB0334	-0.153	-0.218	0.032	0.310	0.260	0.530	0.040	0.064	0.092
BB0335	-0.185	-0.291	-0.215	0.280	0.200	0.250	0.027	0.045	0.051
BB0336	0.219	0.156	0.328	0.740	0.630	0.830	0.042	0.079	0.033
BB0337	0.152	0.381	0.554	0.650	0.820	0.920	0.039	0.093	0.083
BB0338	0.881	0.986	1.018	0.990	0.990	0.990	0.062	0.055	0.066
BB0339	0.805	0.676	0.925	0.980	0.950	0.980	0.051	0.071	0.112
BB0340	-0.195	0.145	-0.115	0.270	0.620	0.350	0.069	0.110	0.057
BB0341	-0.130	-0.314	-0.054	0.330	0.190	0.410	0.049	0.051	0.056
BB0342	-0.318	-0.255	0.013	0.170	0.230	0.500	0.022	0.034	0.108
BB0343	0.181	0.067	0.201	0.690	0.540	0.730	0.067	0.037	0.098
BB0344	-0.023	0.145	-0.043	0.450	0.620	0.430	0.048	0.100	0.050

BB0345	0.022	0.122	-0.005	0.500	0.600	0.470	0.087	0.066	0.133
BB0346	-0.016	0.019	-0.068	0.450	0.480	0.400	0.067	0.060	0.123
BB0347	-0.192	-0.121	-0.243	0.270	0.340	0.230	0.150	0.070	0.067
BB0348	0.065	0.209	0.386	0.550	0.680	0.860	0.047	0.034	0.068
BB0349	-0.027	-0.026	-0.112	0.440	0.430	0.350	0.126	0.061	0.088
BB0350	0.218	-0.012	0.116	0.730	0.440	0.630	0.072	0.032	0.062
BB0351	-0.063	-0.313	0.080	0.400	0.190	0.590	0.081	0.024	0.062
BB0352	-0.025	-0.199	-0.049	0.440	0.270	0.420	0.098	0.060	0.076
BB0353	0.070	0.096	-0.056	0.560	0.570	0.410	0.037	0.047	0.039
BB0354	0.208	0.320	0.207	0.720	0.780	0.730	0.090	0.082	0.080
BB0355	0.487	0.712	0.500	0.930	0.960	0.910	0.037	0.053	0.043
BB0356	0.336	0.381	0.167	0.850	0.810	0.690	0.025	0.045	0.024
BB0357	0.422	0.254	0.121	0.890	0.720	0.630	0.032	0.054	0.065
BB0358	0.055	-0.177	0.001	0.540	0.290	0.480	0.064	0.052	0.039
BB0359	0.088	0.054	0.081	0.580	0.520	0.590	0.024	0.075	0.029
BB0360	0.152	0.190	0.178	0.650	0.660	0.700	0.067	0.056	0.036
BB0361	-0.058	0.220	0.065	0.410	0.690	0.570	0.054	0.048	0.033
BB0362	-0.419	-0.164	-0.059	0.110	0.300	0.410	0.064	0.062	0.070
BB0363	-0.249	-0.214	-0.173	0.220	0.260	0.300	0.076	0.076	0.023
BB0364	0.112	-0.038	0.125	0.600	0.420	0.640	0.037	0.061	0.085
BB0365	0.181	0.011	0.448	0.690	0.470	0.890	0.079	0.043	0.055
BB0366	-0.348	0.292	0.179	0.150	0.760	0.700	0.034	0.044	0.061
BB0367	0.127	0.208	0.116	0.610	0.680	0.630	0.079	0.041	0.025
BB0368	-0.089	0.090	0.034	0.370	0.560	0.530	0.032	0.048	0.021
BB0369	-0.097	-0.247	-0.263	0.360	0.230	0.220	0.035	0.043	0.048
BB0370	-0.049	-0.190	0.186	0.420	0.280	0.710	0.060	0.066	0.029
BB0371	-0.229	-0.412	-0.037	0.240	0.130	0.440	0.047	0.045	0.062
BB0372	-0.160	-0.218	0.085	0.300	0.250	0.590	0.046	0.036	0.023
BB0373	0.256	0.121	0.120	0.770	0.600	0.630	0.031	0.061	0.049
BB0374	0.046	-0.124	0.298	0.530	0.340	0.810	0.049	0.045	0.093
BB0375	-0.068	-0.129	-0.038	0.390	0.330	0.430	0.041	0.040	0.025
BB0376	-0.271	-0.269	0.100	0.210	0.210	0.610	0.048	0.063	0.046
BB0377	0.095	0.078	0.118	0.590	0.550	0.630	0.070	0.055	0.034
BB0378	0.158	0.229	0.169	0.660	0.700	0.690	0.070	0.037	0.036
BB0379	0.153	0.204	0.170	0.650	0.670	0.690	0.035	0.062	0.072
BB0380	-0.419	-0.194	-0.288	0.110	0.280	0.200	0.036	0.036	0.045
BB0381	0.542	0.499	0.510	0.940	0.890	0.910	0.033	0.041	0.056
BB0382	-0.092	0.153	0.182	0.360	0.630	0.700	0.039	0.047	0.036
BB0383	0.211	0.126	0.411	0.730	0.600	0.870	0.050	0.036	0.055

BB0384	0.171	0.316	-0.094	0.680	0.780	0.370	0.035	0.033	0.023
BB0385	-0.064	0.481	-0.294	0.400	0.880	0.200	0.114	0.086	0.018
BB0386	0.921	0.691	1.012	0.990	0.960	0.990	0.075	0.099	0.124
BB0387	1.170	0.838	1.064	0.990	0.980	0.990	0.090	0.070	0.084
BB0388	0.229	0.403	0.286	0.740	0.830	0.800	0.035	0.043	0.066
BB0389	-0.083	0.251	0.133	0.370	0.720	0.650	0.060	0.094	0.085
BB0390	-0.069	0.213	0.139	0.390	0.680	0.650	0.049	0.089	0.074
BB0391	0.231	0.283	0.256	0.750	0.750	0.780	0.012	0.047	0.036
BB0392	0.616	0.757	0.612	0.960	0.970	0.930	0.067	0.074	0.046
BB0393	0.683	0.795	0.655	0.970	0.970	0.940	0.031	0.060	0.074
BB0394	0.495	0.677	0.611	0.930	0.950	0.930	0.094	0.078	0.103
BB0395	0.440	0.459	0.569	0.900	0.870	0.920	0.072	0.086	0.113
BB0396	0.635	0.821	0.585	0.970	0.970	0.930	0.042	0.062	0.075
BB0397	-0.175	-0.467	-0.043	0.290	0.110	0.430	0.079	0.030	0.040
BB0398	-0.299	-0.106	-0.153	0.190	0.350	0.310	0.091	0.070	0.078
BB0399	-0.023	0.054	-0.145	0.450	0.520	0.320	0.105	0.080	0.051
BB0400	0.024	-0.260	-0.075	0.510	0.220	0.390	0.043	0.063	0.102
BB0401	-0.037	-0.070	-0.105	0.430	0.390	0.360	0.066	0.045	0.040
BB0402	-0.357	-0.485	-0.094	0.150	0.100	0.370	0.078	0.048	0.053
BB0403	-0.073	-0.082	0.142	0.380	0.380	0.660	0.147	0.051	0.073
BB0404	0.282	0.106	0.410	0.790	0.580	0.870	0.043	0.052	0.128
BB0405	-0.107	0.064	0.256	0.350	0.530	0.780	0.040	0.034	0.037
BB0406	0.028	-0.006	0.078	0.510	0.450	0.580	0.095	0.080	0.052
BB0407	-0.171	-0.387	0.040	0.290	0.140	0.540	0.108	0.069	0.087
BB0408	0.433	0.480	0.291	0.900	0.880	0.810	0.030	0.116	0.027
BB0409	0.001	0.022	0.129	0.480	0.480	0.640	0.094	0.070	0.058
BB0410	0.416	0.449	0.207	0.890	0.860	0.730	0.058	0.160	0.061
BB0411	0.067	0.059	0.071	0.550	0.520	0.570	0.079	0.082	0.060
BB0412	0.075	0.077	-0.091	0.560	0.550	0.370	0.065	0.084	0.089
BB0413	-0.147	-0.141	-0.180	0.310	0.330	0.290	0.079	0.052	0.052
BB0414	0.013	0.050	-0.011	0.490	0.510	0.470	0.055	0.095	0.064
BB0415	-0.212	-0.353	-0.263	0.250	0.160	0.220	0.077	0.036	0.028
BB0416	-0.001	0.142	0.093	0.470	0.610	0.610	0.073	0.050	0.040
BB0417	0.070	0.059	0.084	0.550	0.520	0.590	0.089	0.065	0.045
BB0418	-0.314	-0.004	0.168	0.170	0.450	0.690	0.059	0.052	0.066
BB0419	0.107	0.009	0.095	0.600	0.470	0.610	0.045	0.035	0.046
BB0420	-0.114	0.008	-0.009	0.340	0.470	0.470	0.045	0.062	0.049
BB0421	0.234	0.254	0.287	0.750	0.720	0.810	0.079	0.072	0.038
BB0422	-0.020	0.228	0.061	0.450	0.700	0.560	0.067	0.042	0.033

BB0423	0.165	0.848	0.394	0.670	0.980	0.860	0.089	0.080	0.053
BB0424	0.430	1.110	0.725	0.900	0.990	0.960	0.053	0.150	0.082
BB0425	0.946	1.221	0.835	0.990	0.990	0.970	0.130	0.085	0.040
BB0426	0.809	0.945	0.896	0.980	0.980	0.980	0.046	0.165	0.109
BB0427	-0.179	0.018	-0.225	0.280	0.480	0.240	0.033	0.067	0.050
BB0428	0.220	0.497	0.275	0.740	0.890	0.800	0.062	0.052	0.047
BB0429	0.128	0.217	-0.028	0.620	0.690	0.450	0.070	0.086	0.036
BB0430	0.063	0.223	0.042	0.550	0.700	0.540	0.069	0.058	0.060
BB0431	0.173	0.135	0.003	0.680	0.610	0.490	0.052	0.109	0.043
BB0432	0.204	0.306	0.206	0.720	0.770	0.730	0.047	0.037	0.044
BB0433	0.639	0.624	0.423	0.970	0.940	0.880	0.047	0.090	0.040
BB0434	0.008	0.179	-0.062	0.490	0.650	0.400	0.054	0.049	0.041
BB0435	0.763	0.810	0.663	0.980	0.970	0.950	0.020	0.094	0.078
BB0436	0.773	1.001	0.753	0.980	0.990	0.960	0.079	0.099	0.086
BB0437	-0.129	-0.005	-0.108	0.330	0.450	0.360	0.060	0.029	0.044
BB0438	0.395	0.336	0.087	0.870	0.790	0.600	0.077	0.053	0.044
BB0439	0.484	0.447	0.276	0.930	0.860	0.800	0.031	0.058	0.027
BB0440	0.785	0.834	0.971	0.980	0.980	0.980	0.052	0.130	0.094
BB0441	0.436	0.339	0.466	0.900	0.790	0.900	0.058	0.047	0.063
BB0442	0.064	0.241	0.236	0.550	0.710	0.760	0.052	0.070	0.098
BB0443	0.707	0.544	0.525	0.970	0.910	0.910	0.050	0.086	0.092
BB0444	0.258	0.377	0.329	0.770	0.810	0.840	0.039	0.080	0.091
BB0445	0.403	0.674	0.772	0.880	0.950	0.960	0.045	0.115	0.094
BB0446	-0.206	-0.149	-0.144	0.260	0.320	0.320	0.071	0.075	0.044
BB0447	-0.240	-0.246	-0.198	0.230	0.240	0.270	0.081	0.066	0.060
BB0448	0.156	0.186	0.186	0.660	0.660	0.710	0.057	0.107	0.104
BB0449	0.329	0.200	0.214	0.840	0.670	0.740	0.034	0.031	0.061
BB0450	0.038	-0.003	-0.030	0.520	0.450	0.450	0.097	0.061	0.053
BB0451	-0.303	-0.537	-0.403	0.180	0.080	0.140	0.083	0.022	0.079
BB0452	-0.309	-0.151	-0.215	0.180	0.320	0.250	0.091	0.055	0.068
BB0453	-0.148	-0.167	-0.038	0.310	0.300	0.440	0.069	0.054	0.082
BB0454	-0.022	0.341	-0.059	0.450	0.790	0.410	0.079	0.115	0.088
BB0455	0.047	-0.149	-0.075	0.530	0.320	0.390	0.113	0.063	0.068
BB0456	-0.106	-0.053	-0.341	0.350	0.400	0.160	0.090	0.066	0.036
BB0457	-0.410	-0.562	-0.491	0.110	0.070	0.100	0.112	0.042	0.065
BB0458	0.293	0.438	0.273	0.800	0.850	0.790	0.024	0.104	0.123
BB0459	0.178	0.030	0.166	0.690	0.490	0.680	0.081	0.043	0.045
BB0460	0.366	0.388	0.126	0.860	0.820	0.640	0.022	0.060	0.102
BB0461	0.218	0.035	0.224	0.730	0.500	0.750	0.078	0.033	0.030

BB0462	0.559	0.276	0.410	0.950	0.740	0.870	0.023	0.123	0.056
BB0463	0.044	0.064	0.113	0.530	0.530	0.620	0.098	0.073	0.056
BB0464	0.103	0.039	-0.051	0.590	0.500	0.420	0.056	0.071	0.108
BB0465	0.438	0.509	0.325	0.900	0.890	0.830	0.051	0.054	0.015
BB0466	0.089	0.516	-0.033	0.580	0.900	0.440	0.031	0.026	0.024
BB0467	0.291	0.039	0.110	0.800	0.500	0.620	0.076	0.053	0.028
BB0468	0.153	0.285	0.072	0.650	0.750	0.570	0.071	0.021	0.049
BB0469	0.407	0.343	0.174	0.880	0.790	0.700	0.050	0.056	0.059
BB0470	0.296	0.455	0.308	0.810	0.860	0.820	0.047	0.107	0.054
BB0471	0.164	0.301	0.269	0.670	0.770	0.790	0.057	0.076	0.070
BB0472	-0.209	-0.160	-0.313	0.250	0.310	0.180	0.023	0.074	0.078
BB0473	-0.370	-0.333	-0.331	0.140	0.170	0.170	0.089	0.057	0.050
BB0474	0.434	0.708	0.357	0.900	0.960	0.850	0.051	0.170	0.107
BB0475	0.297	0.424	0.111	0.810	0.840	0.620	0.030	0.050	0.081
BB0476	0.769	0.969	0.922	0.980	0.990	0.980	0.046	0.076	0.068
BB0477	0.814	0.934	0.935	0.980	0.980	0.980	0.083	0.083	0.108
BB0478	0.767	0.966	0.913	0.980	0.990	0.980	0.037	0.047	0.071
BB0479	0.711	0.737	0.828	0.970	0.960	0.970	0.017	0.055	0.089
BB0480	0.727	0.701	0.817	0.980	0.960	0.970	0.049	0.115	0.140
BB0481	0.505	0.573	0.650	0.940	0.930	0.940	0.087	0.044	0.079
BB0482	0.641	0.761	0.699	0.970	0.970	0.950	0.037	0.048	0.067
BB0483	0.335	0.400	0.476	0.840	0.830	0.900	0.052	0.069	0.130
BB0484	0.511	0.581	0.698	0.940	0.930	0.950	0.018	0.052	0.118
BB0485	0.574	0.445	0.615	0.960	0.860	0.940	0.046	0.041	0.092
BB0486	0.535	0.524	0.624	0.940	0.900	0.940	0.107	0.058	0.107
BB0487	0.482	0.416	0.521	0.920	0.840	0.910	0.025	0.057	0.099
BB0488	0.323	0.448	0.585	0.830	0.860	0.930	0.027	0.036	0.056
BB0489	0.556	0.438	0.545	0.950	0.850	0.920	0.039	0.037	0.036
BB0490	0.465	0.595	0.687	0.910	0.930	0.950	0.040	0.051	0.091
BB0491	0.655	0.537	0.729	0.970	0.910	0.960	0.044	0.051	0.107
BB0492	0.584	0.558	0.752	0.960	0.920	0.960	0.058	0.084	0.121
BB0493	0.438	0.255	0.466	0.900	0.720	0.900	0.043	0.043	0.087
BB0494	0.465	0.398	0.602	0.910	0.830	0.930	0.084	0.076	0.083
BB0495	0.312	0.272	0.546	0.830	0.740	0.920	0.052	0.063	0.093
BB0496	0.427	0.621	0.823	0.900	0.940	0.970	0.231	0.079	0.149
BB0497	0.873	0.649	0.788	0.990	0.950	0.960	0.076	0.039	0.060
BB0498	-0.137	0.004	0.184	0.320	0.460	0.710	0.034	0.053	0.129
BB0499	-0.077	0.030	0.175	0.380	0.490	0.700	0.049	0.133	0.326
BB0500	0.562	0.391	0.615	0.950	0.820	0.940	0.048	0.057	0.041

BB0501	0.175	0.233	0.450	0.680	0.700	0.890	0.033	0.048	0.120
BB0502	0.148	0.441	0.509	0.640	0.850	0.910	0.098	0.085	0.102
BB0503	0.573	0.583	0.659	0.950	0.930	0.950	0.027	0.058	0.121
BB0504	0.132	0.292	0.249	0.620	0.760	0.770	0.091	0.069	0.072
BB0505	-0.006	0.024	-0.127	0.470	0.490	0.340	0.071	0.097	0.077
BB0506	-0.008	-0.126	-0.244	0.460	0.340	0.230	0.077	0.064	0.079
BB0507	0.188	0.027	0.006	0.700	0.490	0.490	0.055	0.115	0.026
BB0508	0.092	0.209	0.317	0.580	0.680	0.830	0.038	0.043	0.034
BB0509	-0.091	-0.130	0.094	0.360	0.330	0.610	0.075	0.061	0.024
BB0510	0.303	0.240	0.200	0.820	0.710	0.720	0.047	0.083	0.067
BB0511	0.034	-0.179	0.038	0.520	0.290	0.530	0.080	0.055	0.046
BB0512	0.170	0.027	0.125	0.680	0.490	0.640	0.040	0.088	0.038
BB0513	-0.352	-0.483	-0.175	0.150	0.100	0.290	0.104	0.084	0.093
BB0514	0.041	-0.080	0.077	0.530	0.380	0.580	0.027	0.049	0.036
BB0515	-0.200	-0.317	-0.230	0.260	0.190	0.240	0.078	0.055	0.044
BB0516	-0.180	0.042	-0.194	0.280	0.510	0.270	0.071	0.059	0.050
BB0517	-0.140	-0.265	-0.002	0.320	0.220	0.480	0.026	0.062	0.062
BB0518	0.157	-0.062	0.521	0.660	0.400	0.910	0.054	0.070	0.070
BB0519	0.329	0.221	0.407	0.840	0.690	0.870	0.049	0.026	0.092
BB0520	0.370	0.337	0.137	0.860	0.790	0.650	0.100	0.046	0.074
BB0521	0.340	0.393	0.460	0.850	0.820	0.890	0.075	0.042	0.043
BB0522	0.026	0.066	0.191	0.510	0.540	0.710	0.089	0.058	0.085
BB0523	0.352	0.373	0.245	0.860	0.810	0.770	0.060	0.097	0.035
BB0524	-0.111	-0.217	-0.399	0.350	0.260	0.140	0.072	0.030	0.035
BB0525	0.337	0.348	0.300	0.850	0.790	0.810	0.061	0.075	0.018
BB0526	-0.026	-0.014	0.047	0.440	0.440	0.540	0.069	0.046	0.049
BB0527	-0.230	-0.063	-0.247	0.240	0.390	0.230	0.086	0.055	0.060
BB0528	-0.112	-0.187	-0.324	0.350	0.290	0.170	0.105	0.046	0.022
BB0529	0.492	0.434	0.314	0.930	0.850	0.820	0.054	0.088	0.052
BB0530	-0.085	-0.250	-0.203	0.370	0.230	0.260	0.058	0.019	0.049
BB0531	0.006	-0.073	0.003	0.480	0.380	0.490	0.081	0.108	0.081
BB0532	0.106	0.063	0.025	0.600	0.530	0.510	0.017	0.082	0.044
BB0533	0.094	0.758	0.327	0.580	0.970	0.830	0.042	0.043	0.053
BB0534	0.071	0.154	0.034	0.560	0.630	0.530	0.045	0.060	0.037
BB0535	0.160	0.134	0.038	0.660	0.610	0.530	0.064	0.069	0.036
BB0536	0.000	-0.143	0.018	0.480	0.320	0.500	0.055	0.053	0.029
BB0537	0.179	0.176	0.161	0.690	0.650	0.680	0.072	0.052	0.073
BB0538	0.254	0.110	0.154	0.770	0.590	0.670	0.036	0.060	0.049
BB0539	0.294	0.511	0.453	0.800	0.900	0.890	0.057	0.063	0.065

BB0540	0.092	0.026	0.372	0.580	0.490	0.860	0.034	0.049	0.117
BB0541	0.862	1.215	0.896	0.990	0.990	0.980	0.036	0.097	0.069
BB0542	0.343	0.487	0.014	0.850	0.880	0.500	0.045	0.117	0.027
BB0543	0.492	0.872	0.575	0.930	0.980	0.930	0.062	0.080	0.074
BB0544	0.139	0.316	0.026	0.630	0.780	0.510	0.060	0.113	0.068
BB0545	-0.005	0.459	-0.131	0.470	0.870	0.340	0.054	0.077	0.021
BB0546	-0.065	0.011	-0.194	0.400	0.470	0.270	0.064	0.080	0.077
BB0547	-0.162	-0.169	-0.124	0.300	0.300	0.340	0.054	0.040	0.063
BB0548	-0.381	-0.481	-0.355	0.130	0.100	0.150	0.051	0.071	0.107
BB0549	0.222	0.042	0.052	0.740	0.510	0.550	0.110	0.097	0.101
BB0550	0.208	0.117	0.160	0.720	0.590	0.670	0.066	0.023	0.091
BB0551	0.301	0.073	0.455	0.810	0.540	0.890	0.050	0.047	0.075
BB0552	-0.298	-0.554	-0.314	0.190	0.070	0.180	0.028	0.047	0.075
BB0553	-0.200	-0.098	-0.134	0.260	0.360	0.330	0.088	0.100	0.079
BB0554	-0.199	-0.233	-0.044	0.260	0.240	0.430	0.066	0.060	0.080
BB0555	-0.129	-0.110	-0.281	0.330	0.350	0.210	0.091	0.047	0.056
BB0556	0.094	-0.012	-0.009	0.580	0.440	0.470	0.054	0.062	0.071
BB0557	0.739	0.836	0.929	0.980	0.980	0.980	0.074	0.076	0.089
BB0558	0.089	0.302	0.632	0.580	0.770	0.940	0.085	0.063	0.084
BB0559	0.598	0.699	0.939	0.960	0.960	0.980	0.060	0.034	0.066
BB0560	0.083	0.099	0.315	0.570	0.570	0.820	0.047	0.056	0.095
BB0561	-0.200	-0.378	0.052	0.260	0.150	0.550	0.067	0.020	0.049
BB0562	0.176	-0.031	0.081	0.690	0.430	0.590	0.041	0.082	0.054
BB0563	-0.355	-0.389	0.327	0.150	0.140	0.830	0.091	0.073	0.107
BB0564	0.253	0.257	0.112	0.770	0.730	0.620	0.039	0.088	0.036
BB0565	0.699	-0.058	0.699	0.970	0.400	0.950	0.092	0.042	0.114
BB0566	0.484	0.428	0.461	0.930	0.850	0.900	0.021	0.073	0.015
BB0567	0.172	-0.332	0.427	0.680	0.180	0.880	0.060	0.072	0.084
BB0568	-0.063	0.083	0.077	0.400	0.550	0.580	0.049	0.048	0.030
BB0569	-0.080	-0.184	0.028	0.380	0.290	0.520	0.068	0.047	0.061
BB0570	0.337	0.666	0.359	0.850	0.950	0.850	0.043	0.048	0.062
BB0571	0.170	0.073	0.122	0.680	0.540	0.630	0.049	0.033	0.015
BB0572	0.023	0.440	0.268	0.500	0.850	0.790	0.056	0.060	0.050
BB0573	0.136	0.022	0.155	0.620	0.480	0.670	0.061	0.057	0.042
BB0574	0.261	0.346	0.159	0.780	0.790	0.670	0.085	0.040	0.019
BB0575	-0.111	-0.034	0.135	0.350	0.420	0.650	0.042	0.027	0.046
BB0576	0.027	0.089	-0.024	0.510	0.560	0.450	0.071	0.084	0.037
BB0577	0.144	-0.067	0.159	0.640	0.390	0.670	0.109	0.051	0.058
BB0578	0.063	-0.005	0.207	0.550	0.450	0.730	0.037	0.020	0.053

BB0579	0.312	0.041	0.247	0.830	0.500	0.770	0.080	0.045	0.100
BB0580	0.036	0.096	0.032	0.520	0.570	0.530	0.092	0.075	0.048
BB0581	-0.198	-0.243	-0.165	0.270	0.240	0.300	0.040	0.095	0.064
BB0582	0.040	0.219	0.170	0.520	0.690	0.690	0.055	0.054	0.046
BB0583	-0.083	-0.101	0.019	0.370	0.360	0.500	0.047	0.043	0.116
BB0584	-0.431	-0.368	-0.250	0.100	0.150	0.220	0.047	0.050	0.066
BB0585	0.252	0.260	0.110	0.770	0.730	0.620	0.044	0.062	0.051
BB0586	0.294	0.567	0.405	0.800	0.920	0.870	0.039	0.055	0.040
BB0587	-0.217	-0.362	-0.245	0.250	0.160	0.230	0.030	0.076	0.060
BB0588	-0.068	-0.201	0.324	0.390	0.270	0.830	0.018	0.069	0.056
BB0589	-0.158	-0.396	-0.123	0.300	0.140	0.340	0.054	0.094	0.070
BB0590	0.047	-0.113	-0.011	0.530	0.340	0.470	0.094	0.063	0.070
BB0591	-0.116	-0.229	-0.200	0.340	0.250	0.270	0.065	0.055	0.033
BB0592	0.118	0.617	0.303	0.610	0.940	0.820	0.062	0.099	0.134
BB0593	-0.211	-0.038	0.130	0.250	0.420	0.650	0.045	0.089	0.082
BB0594	-0.207	-0.292	0.092	0.260	0.200	0.600	0.059	0.054	0.067
BB0595	0.253	0.144	0.170	0.770	0.620	0.690	0.044	0.091	0.035
BB0596	-0.624	-0.488	-0.283	0.030	0.100	0.210	0.128	0.048	0.035
BB0597	-0.180	-0.098	0.078	0.280	0.360	0.580	0.029	0.059	0.043
BB0598	-0.268	-0.102	-0.202	0.210	0.350	0.260	0.086	0.068	0.075
BB0599	-0.226	-0.240	0.050	0.240	0.240	0.550	0.052	0.045	0.070
BB0600	-0.297	-0.398	-0.114	0.190	0.130	0.350	0.078	0.050	0.073
BB0601	-0.412	-0.562	-0.080	0.110	0.070	0.380	0.024	0.047	0.082
BB0602	0.174	0.137	0.209	0.680	0.610	0.740	0.065	0.126	0.045
BB0603	0.048	0.105	0.590	0.530	0.580	0.930	0.055	0.087	0.088
BB0604	-0.240	-0.040	-0.060	0.230	0.420	0.400	0.101	0.108	0.085
BB0605	-0.168	-0.083	-0.189	0.290	0.380	0.280	0.068	0.063	0.072
BB0606	-0.140	-0.077	-0.013	0.320	0.380	0.460	0.061	0.045	0.081
BB0607	-0.231	-0.467	-0.302	0.240	0.110	0.190	0.037	0.043	0.120
BB0608	0.057	-0.202	0.150	0.540	0.270	0.670	0.070	0.054	0.061
BB0609	0.311	0.389	0.247	0.820	0.820	0.770	0.073	0.204	0.119
BB0610	0.481	0.531	0.461	0.920	0.900	0.890	0.066	0.084	0.085
BB0611	0.279	0.358	0.397	0.790	0.800	0.870	0.038	0.076	0.057
BB0612	0.295	0.462	0.317	0.800	0.870	0.830	0.043	0.056	0.067
BB0613	0.116	0.071	0.168	0.600	0.540	0.690	0.056	0.043	0.057
BB0614	0.223	0.461	0.361	0.740	0.870	0.850	0.146	0.137	0.102
BB0615	0.920	0.897	1.024	0.990	0.980	0.990	0.059	0.085	0.037
BB0616	-0.332	-0.191	-0.244	0.160	0.280	0.230	0.070	0.090	0.019
BB0617	0.070	0.157	-0.022	0.560	0.630	0.460	0.004	0.109	0.075

BB0618	0.382	0.292	0.299	0.870	0.760	0.810	0.084	0.116	0.061
BB0619	-0.113	0.226	-0.059	0.350	0.700	0.410	0.052	0.035	0.016
BB0620	-0.379	-0.260	-0.415	0.130	0.220	0.130	0.088	0.031	0.040
BB0621	0.181	0.117	0.265	0.690	0.590	0.790	0.078	0.054	0.050
BB0622	-0.381	-0.241	-0.324	0.130	0.240	0.180	0.114	0.098	0.067
BB0623	-0.355	-0.200	-0.315	0.150	0.270	0.180	0.090	0.061	0.083
BB0624	0.151	0.083	0.325	0.640	0.550	0.830	0.062	0.028	0.039
BB0625	-0.140	-0.082	-0.156	0.320	0.380	0.310	0.034	0.046	0.037
BB0626	0.311	0.772	0.303	0.820	0.970	0.820	0.078	0.127	0.070
BB0627	-0.369	-0.140	-0.339	0.140	0.330	0.170	0.075	0.046	0.017
BB0628	-0.071	-0.276	0.005	0.390	0.210	0.490	0.099	0.034	0.057
BB0629	-0.170	0.153	0.439	0.290	0.630	0.880	0.035	0.037	0.049
BB0630	-0.438	-0.515	-0.523	0.100	0.090	0.080	0.061	0.058	0.073
BB0631	0.215	0.450	0.850	0.730	0.860	0.970	0.050	0.038	0.087
BB0632	-0.061	-0.192	-0.186	0.400	0.280	0.280	0.054	0.052	0.105
BB0633	-0.136	-0.100	-0.238	0.330	0.360	0.240	0.100	0.075	0.063
BB0634	0.014	-0.058	-0.084	0.490	0.400	0.380	0.038	0.069	0.095
BB0635	-0.223	-0.188	-0.214	0.240	0.290	0.260	0.056	0.049	0.043
BB0636	-0.063	-0.203	-0.122	0.400	0.270	0.340	0.063	0.030	0.046
BB0637	-0.243	-0.174	0.075	0.230	0.300	0.580	0.086	0.063	0.092
BB0638	-0.285	-0.371	-0.234	0.200	0.150	0.240	0.057	0.069	0.093
BB0639	-0.214	0.158	0.046	0.250	0.640	0.540	0.080	0.029	0.041
BB0640	0.000	0.011	0.027	0.480	0.470	0.520	0.026	0.071	0.040
BB0641	-0.183	0.007	-0.007	0.280	0.470	0.470	0.067	0.051	0.055
BB0642	0.027	-0.296	-0.003	0.510	0.200	0.480	0.047	0.074	0.038
BB0643	-0.072	-0.082	-0.241	0.390	0.380	0.230	0.128	0.078	0.039
BB0644	0.023	-0.386	-0.130	0.500	0.140	0.340	0.068	0.042	0.075
BB0645	-0.501	-0.551	-0.300	0.070	0.070	0.190	0.064	0.032	0.093
BB0646	-0.260	-0.410	0.143	0.210	0.130	0.660	0.022	0.020	0.082
BB0647	0.176	0.078	0.250	0.680	0.550	0.770	0.013	0.082	0.045
BB0648	-0.219	-0.128	-0.264	0.240	0.330	0.210	0.070	0.096	0.051
BB0649	0.758	0.886	0.963	0.980	0.980	0.980	0.053	0.091	0.054
BB0650	0.438	0.811	0.756	0.900	0.970	0.960	0.033	0.092	0.123
BB0651	0.531	0.743	0.680	0.940	0.960	0.950	0.039	0.071	0.094
BB0652	0.137	0.447	0.416	0.630	0.860	0.880	0.037	0.078	0.101
BB0653	-0.097	0.053	0.111	0.360	0.520	0.620	0.046	0.017	0.086
BB0654	-0.279	0.032	-0.074	0.200	0.500	0.390	0.074	0.100	0.114
BB0655	-0.034	-0.226	-0.230	0.440	0.250	0.240	0.057	0.059	0.049
BB0656	-0.576	-0.510	-0.613	0.040	0.090	0.050	0.121	0.068	0.074

BB0657	-0.037	-0.050	-0.166	0.430	0.410	0.300	0.068	0.143	0.036
BB0658	-0.151	-0.271	0.092	0.310	0.210	0.600	0.054	0.040	0.035
BB0659	0.029	0.422	0.007	0.510	0.840	0.490	0.152	0.183	0.183
BB0660	-0.110	-0.152	0.035	0.350	0.310	0.530	0.057	0.067	0.090
BB0661	-0.081	0.236	0.200	0.380	0.710	0.720	0.073	0.057	0.069
BB0662	0.174	0.655	0.299	0.680	0.950	0.810	0.041	0.088	0.107
BB0663	-0.019	0.058	-0.014	0.450	0.520	0.460	0.091	0.026	0.021
BB0664	0.299	0.492	0.284	0.810	0.880	0.800	0.020	0.103	0.054
BB0665	0.096	-0.045	0.012	0.590	0.410	0.490	0.086	0.063	0.050
BB0666	0.087	0.017	-0.005	0.580	0.480	0.480	0.072	0.075	0.021
BB0667	0.406	0.264	0.709	0.880	0.730	0.960	0.060	0.068	0.073
BB0668	0.298	0.098	0.723	0.810	0.570	0.960	0.047	0.081	0.032
BB0669	0.213	-0.356	0.305	0.730	0.160	0.820	0.035	0.068	0.087
BB0670	0.159	0.093	0.486	0.660	0.560	0.900	0.039	0.056	0.101
BB0671	0.142	-0.240	0.571	0.630	0.240	0.920	0.084	0.044	0.067
BB0672	0.180	0.239	0.293	0.690	0.710	0.810	0.065	0.048	0.063
BB0673	0.148	0.100	0.049	0.640	0.570	0.550	0.085	0.030	0.055
BB0674	0.081	0.182	0.129	0.570	0.660	0.640	0.053	0.041	0.063
BB0675	0.089	0.094	0.132	0.580	0.560	0.650	0.044	0.085	0.035
BB0676	-0.041	-0.016	-0.034	0.430	0.440	0.440	0.073	0.078	0.047
BB0677	0.219	-0.183	0.405	0.740	0.290	0.870	0.077	0.059	0.073
BB0678	-0.402	-0.129	0.176	0.120	0.330	0.700	0.075	0.068	0.113
BB0679	-0.358	-0.339	-0.226	0.150	0.170	0.240	0.085	0.068	0.061
BB0680	0.126	-0.145	0.709	0.610	0.320	0.950	0.038	0.039	0.078
BB0681	0.197	-0.367	0.813	0.710	0.160	0.970	0.053	0.032	0.095
BB0682	0.108	0.043	0.224	0.600	0.510	0.750	0.047	0.061	0.016
BB0683	0.152	0.671	0.163	0.650	0.950	0.680	0.052	0.074	0.056
BB0684	-0.154	0.600	-0.134	0.310	0.930	0.330	0.038	0.070	0.039
BB0685	0.167	0.205	0.030	0.670	0.670	0.520	0.040	0.044	0.073
BB0686	-0.003	0.370	-0.097	0.470	0.810	0.370	0.048	0.056	0.053
BB0687	-0.005	0.131	0.091	0.470	0.600	0.600	0.077	0.094	0.062
BB0688	-0.007	0.219	0.075	0.460	0.690	0.580	0.095	0.049	0.091
BB0689	0.187	-0.035	0.396	0.700	0.420	0.870	0.045	0.044	0.049
BB0690	0.732	1.451	1.073	0.980	1.000	0.990	0.045	0.086	0.073
BB0691	0.219	0.850	0.630	0.730	0.980	0.940	0.045	0.062	0.059
BB0692	0.307	0.414	0.377	0.820	0.840	0.860	0.149	0.060	0.095
BB0693	0.275	0.169	0.449	0.790	0.640	0.890	0.056	0.070	0.100
BB0694	0.414	0.657	0.890	0.890	0.950	0.970	0.034	0.064	0.078
BB0695	0.698	0.494	0.720	0.970	0.880	0.960	0.052	0.036	0.106

BB0696	0.116	0.294	0.243	0.610	0.760	0.770	0.027	0.067	0.067
BB0697	0.108	0.255	0.198	0.600	0.730	0.720	0.049	0.067	0.044
BB0698	0.234	0.373	0.399	0.750	0.810	0.870	0.031	0.085	0.103
BB0699	0.951	0.715	0.956	0.990	0.960	0.980	0.077	0.039	0.056
BB0700	0.235	0.615	0.204	0.750	0.940	0.730	0.158	0.205	0.074
BB0701	0.307	0.315	0.185	0.820	0.780	0.710	0.032	0.034	0.054
BB0702	-0.088	0.114	0.057	0.370	0.590	0.550	0.035	0.085	0.098
BB0703	0.575	0.353	0.709	0.960	0.800	0.950	0.063	0.054	0.093
BB0704	0.184	0.141	0.432	0.690	0.610	0.880	0.073	0.049	0.136
BB0705	0.058	-0.007	0.276	0.540	0.450	0.800	0.029	0.040	0.078
BB0706	-0.131	-0.238	-0.226	0.330	0.240	0.240	0.137	0.055	0.050
BB0707	-0.144	-0.085	0.175	0.320	0.370	0.700	0.065	0.039	0.096
BB0708	0.269	0.274	0.241	0.780	0.740	0.760	0.071	0.065	0.045
BB0709	-0.012	-0.094	0.123	0.460	0.360	0.640	0.073	0.119	0.031
BB0710	-0.015	0.017	-0.006	0.460	0.470	0.470	0.033	0.176	0.087
BB0711	0.496	0.492	0.485	0.930	0.880	0.900	0.064	0.082	0.087
BB0712	0.222	0.136	0.270	0.740	0.610	0.790	0.053	0.038	0.056
BB0713	0.429	0.456	0.396	0.900	0.860	0.870	0.084	0.034	0.033
BB0714	0.973	0.961	0.975	0.990	0.990	0.990	0.073	0.127	0.053
BB0715	-0.107	0.055	0.195	0.350	0.520	0.720	0.075	0.019	0.046
BB0716	0.116	0.100	0.039	0.610	0.570	0.540	0.041	0.075	0.082
BB0717	0.395	0.385	0.291	0.880	0.820	0.810	0.045	0.051	0.048
BB0718	-0.265	-0.227	-0.135	0.210	0.250	0.330	0.074	0.072	0.053
BB0719	0.279	0.216	0.171	0.790	0.690	0.700	0.071	0.060	0.045
BB0720	0.069	0.031	0.204	0.550	0.490	0.730	0.023	0.032	0.016
BB0721	0.377	0.452	0.298	0.870	0.860	0.810	0.045	0.110	0.098
BB0722	0.336	0.375	0.115	0.840	0.810	0.620	0.030	0.151	0.032
BB0723	0.482	0.781	0.332	0.920	0.970	0.840	0.059	0.173	0.088
BB0724	-0.314	0.153	-0.111	0.170	0.630	0.350	0.035	0.093	0.073
BB0725		0.539	0.254		0.910	0.780		0.238	0.136
BB0726	-0.031	0.147	0.077	0.440	0.620	0.580	0.075	0.044	0.054
BB0727	-0.168	0.080	-0.009	0.300	0.550	0.470	0.103	0.049	0.060
BB0728	0.258	0.372	0.352	0.770	0.810	0.850	0.038	0.060	0.042
BB0729	-0.475	-0.444	0.095	0.080	0.110	0.610	0.088	0.121	0.099
BB0730	0.030	-0.199	0.088	0.510	0.270	0.600	0.037	0.069	0.032
BB0731	0.246	0.240	0.043	0.760	0.710	0.540	0.044	0.054	0.068
BB0732	0.372	0.324	0.104	0.870	0.780	0.610	0.101	0.135	0.057
BB0733	0.514	0.619	0.341	0.940	0.940	0.840	0.072	0.049	0.058
BB0734	0.156	0.366	0.120	0.650	0.810	0.630	0.089	0.141	0.077

BB0735	0.300	0.550	0.475	0.810	0.910	0.900	0.100	0.044	0.055
BB0736	0.410	0.529	0.212	0.880	0.900	0.740	0.032	0.115	0.082
BB0737	0.089	0.101	-0.024	0.580	0.580	0.450	0.072	0.066	0.046
BB0738	-0.177	-0.078	-0.023	0.290	0.380	0.460	0.032	0.041	0.037
BB0739	0.270	0.420	-0.004	0.790	0.840	0.480	0.042	0.045	0.111
BB0740	0.063	0.331	-0.033	0.550	0.780	0.440	0.054	0.062	0.047
BB0741	0.828	0.359	0.865	0.990	0.800	0.970	0.079	0.057	0.076
BB0742	-0.115	-0.285	0.087	0.340	0.210	0.600	0.037	0.055	0.057
BB0743	-0.117	-0.304	-0.192	0.340	0.190	0.270	0.053	0.029	0.049
BB0744	0.356	0.405	0.556	0.860	0.830	0.920	0.048	0.045	0.072
BB0745	0.138	0.039	0.018	0.630	0.500	0.500	0.047	0.066	0.021
BB0746	-0.110	-0.056	-0.090	0.350	0.400	0.370	0.072	0.055	0.046
BB0747	-0.045	-0.070	-0.120	0.420	0.390	0.350	0.051	0.044	0.044
BB0748	0.187	0.229	0.143	0.700	0.700	0.660	0.123	0.102	0.069
BB0749	0.102	0.445	0.346	0.590	0.850	0.840	0.024	0.045	0.087
BB0750	0.052	0.320	0.025	0.540	0.780	0.510	0.074	0.246	0.131
BB0751	-0.075	-0.248	-0.110	0.380	0.230	0.360	0.083	0.027	0.066
BB0752	-0.337	-0.353	-0.157	0.160	0.170	0.310	0.120	0.057	0.111
BB0753	-0.208	-0.281	-0.099	0.260	0.210	0.370	0.108	0.030	0.132
BB0754	-0.158	-0.314	0.085	0.300	0.190	0.590	0.098	0.044	0.089
BB0755	-0.209	-0.320	-0.184	0.250	0.190	0.280	0.043	0.068	0.078
BB0756	-0.464	-0.431	-0.465	0.080	0.120	0.110	0.122	0.048	0.066
BB0757	0.057	0.043	0.163	0.540	0.510	0.680	0.048	0.044	0.026
BB0758	0.011	0.063	-0.018	0.490	0.530	0.460	0.067	0.067	0.060
BB0759	-0.052	-0.145	-0.003	0.410	0.320	0.480	0.072	0.032	0.014
BB0760	0.304	0.174	0.316	0.820	0.650	0.820	0.036	0.066	0.017
BB0761	-0.308	-0.313	-0.278	0.180	0.190	0.210	0.120	0.117	0.140
BB0762	0.362	0.576	0.299	0.860	0.930	0.810	0.052	0.094	0.033
BB0763	-0.171	-0.037	-0.153	0.290	0.420	0.310	0.055	0.039	0.037
BB0764	-0.140	0.021	-0.229	0.320	0.480	0.240	0.088	0.103	0.080
BB0765	0.143	0.191	0.088	0.630	0.660	0.600	0.091	0.072	0.070
BB0766	-0.002	0.008	-0.113	0.470	0.470	0.350	0.097	0.037	0.103
BB0767	-0.235	-0.395	-0.164	0.230	0.140	0.300	0.097	0.043	0.044
BB0768	-0.023	0.094	-0.081	0.450	0.570	0.380	0.051	0.089	0.030
BB0769	-0.171	0.005	-0.037	0.290	0.460	0.440	0.079	0.047	0.066
BB0770	-0.050	-0.138	-0.116	0.420	0.330	0.350	0.016	0.071	0.030
BB0771	0.566	0.531	0.533	0.950	0.900	0.920	0.121	0.157	0.113
BB0772	0.076	-0.020	0.002	0.560	0.440	0.480	0.020	0.096	0.047
BB0773	0.094	0.037	0.014	0.580	0.500	0.500	0.087	0.063	0.071

BB0774	0.142	0.419	0.211	0.630	0.840	0.740	0.057	0.076	0.034
BB0775	0.519	0.647	0.581	0.940	0.950	0.930	0.050	0.040	0.045
BB0776	0.513	0.697	0.982	0.940	0.960	0.990	0.035	0.143	0.120
BB0777	-0.044	0.213	0.254	0.430	0.680	0.780	0.049	0.042	0.050
BB0778	0.832	0.626	0.838	0.990	0.940	0.970	0.049	0.062	0.073
BB0779	0.107	0.131	0.296	0.600	0.600	0.810	0.046	0.056	0.059
BB0780	0.441	0.485	0.446	0.900	0.880	0.890	0.044	0.038	0.037
BB0781	0.185	0.244	0.270	0.700	0.720	0.790	0.042	0.061	0.041
BB0782	0.152	0.114	0.004	0.650	0.590	0.490	0.052	0.040	0.046
BB0783	0.237	0.145	0.056	0.750	0.620	0.550	0.044	0.066	0.037
BB0784	0.157	0.169	0.024	0.660	0.640	0.510	0.060	0.032	0.080
BB0785	0.271	0.401	0.300	0.790	0.830	0.820	0.038	0.024	0.020
BB0786	0.185	0.562	0.639	0.700	0.920	0.940	0.031	0.057	0.050
BB0787	-0.002	0.085	0.080	0.470	0.560	0.590	0.090	0.072	0.060
BB0788	0.072	0.225	0.114	0.560	0.700	0.620	0.046	0.044	0.048
BB0789	0.014	0.567	0.400	0.490	0.920	0.870	0.041	0.068	0.044
BB0790	-0.005	0.170	0.081	0.470	0.650	0.590	0.052	0.045	0.049
BB0791	0.160	0.283	0.160	0.660	0.750	0.680	0.029	0.033	0.039
BB0792	-0.120	0.177	-0.061	0.340	0.650	0.400	0.061	0.068	0.048
BB0793	0.069	-0.020	-0.054	0.550	0.430	0.410	0.079	0.058	0.097
BB0794	-0.560	-0.248	-0.348	0.050	0.230	0.160	0.067	0.067	0.050
BB0795	0.147	0.312	0.230	0.640	0.770	0.750	0.056	0.097	0.086
BB0796	-0.031	0.166	0.048	0.440	0.640	0.540	0.058	0.051	0.047
BB0797	0.065	0.094	0.249	0.550	0.560	0.770	0.043	0.054	0.094
BB0798	0.238	0.071	0.146	0.750	0.540	0.660	0.029	0.050	0.010
BB0799	0.442	0.405	0.251	0.910	0.830	0.780	0.075	0.087	0.079
BB0800	0.239	0.186	0.117	0.760	0.660	0.630	0.037	0.042	0.074
BB0801	0.080	0.240	0.117	0.570	0.710	0.630	0.040	0.042	0.039
BB0802	0.375	0.892	0.370	0.870	0.980	0.850	0.059	0.123	0.083
BB0803	-0.072	0.260	-0.127	0.380	0.730	0.340	0.099	0.100	0.133
BB0804	0.577	0.763	0.735	0.960	0.970	0.960	0.066	0.153	0.167
BB0805	0.335	0.750	0.647	0.840	0.970	0.940	0.032	0.053	0.041
BB0806	0.180	0.212	0.290	0.690	0.680	0.810	0.014	0.075	0.106
BB0807	-0.143	-0.201	-0.075	0.320	0.270	0.390	0.094	0.061	0.072
BB0808	-0.312	-0.235	-0.300	0.180	0.240	0.200	0.090	0.035	0.057
BB0809	-0.339	-0.448	-0.344	0.160	0.110	0.160	0.108	0.087	0.064
BB0810	-0.027	-0.020	-0.151	0.440	0.440	0.310	0.060	0.084	0.023
BB0811	-0.415	-0.391	-0.261	0.110	0.140	0.220	0.076	0.042	0.045
BB0812	0.499	0.687	0.408	0.930	0.960	0.870	0.031	0.104	0.036

BB0813	0.379	0.476	0.361	0.870	0.870	0.850	0.077	0.060	0.058
BB0814	0.086	0.155	-0.056	0.570	0.630	0.410	0.038	0.109	0.052
BB0815	-0.019	0.085	-0.052	0.450	0.560	0.410	0.057	0.068	0.047
BB0816	0.189	0.444	0.193	0.700	0.850	0.720	0.037	0.081	0.073
BB0817	0.018	-0.165	0.057	0.500	0.300	0.550	0.065	0.027	0.063
BB0818	0.030	0.064	0.039	0.510	0.530	0.530	0.097	0.081	0.035
BB0819	0.104	-0.094	0.002	0.590	0.370	0.480	0.093	0.042	0.027
BB0820	0.504	0.623	0.547	0.940	0.940	0.920	0.031	0.090	0.054
BB0821	0.170	0.017	0.073	0.680	0.480	0.570	0.063	0.044	0.014
BB0822	0.385	0.520	0.139	0.870	0.900	0.650	0.062	0.084	0.062
BB0823	0.124	0.280	0.263	0.610	0.750	0.780	0.062	0.050	0.044
BB0824	0.066	0.460	0.158	0.550	0.870	0.670	0.053	0.035	0.054
BB0825	0.448	0.450	0.229	0.910	0.860	0.750	0.060	0.079	0.123
BB0826	0.475	0.462	0.273	0.920	0.870	0.790	0.063	0.037	0.119
BB0827	0.414	0.339	0.338	0.890	0.790	0.840	0.296	0.215	0.196
BB0828	-0.408	-0.284	-0.135	0.110	0.210	0.330	0.065	0.064	0.060
BB0829	-0.019	-0.007	0.036	0.450	0.450	0.530	0.040	0.025	0.053
BB0830	0.003	0.000	-0.095	0.480	0.460	0.370	0.076	0.066	0.041
BB0831	0.220	0.318	0.325	0.740	0.780	0.830	0.066	0.078	0.073
BB0832	0.019	0.109	0.063	0.500	0.580	0.560	0.070	0.050	0.023
BB0833	0.194	0.382	0.163	0.710	0.820	0.680	0.083	0.090	0.068
BB0834	0.041	0.034	0.047	0.530	0.500	0.540	0.027	0.038	0.052
BB0835	-0.257	-0.359	-0.453	0.220	0.160	0.110	0.076	0.122	0.078
BB0836	0.877	0.818	0.887	0.990	0.970	0.970	0.279	0.305	0.247
BB0837	-0.359	-0.399	-0.287	0.150	0.130	0.200	0.044	0.109	0.050
BB0838	0.044	0.143	0.008	0.530	0.620	0.490	0.108	0.109	0.046
BB0839	0.186	0.112	0.073	0.700	0.590	0.570	0.024	0.059	0.066
BB0840	0.245	0.440	0.105	0.760	0.850	0.610	0.109	0.133	0.091
BB0841	-0.116	0.061	-0.184	0.340	0.530	0.280	0.131	0.080	0.027
BB0842	-0.102	-0.102	0.312	0.350	0.360	0.820	0.054	0.061	0.114
BB0843	-0.455	-0.410	-0.141	0.090	0.130	0.330	0.070	0.107	0.114
BB0843.1	0.387	0.353	0.362	0.870	0.800	0.850	0.066	0.073	0.031
BB0844	0.574	-0.585	0.594	0.960	0.060	0.930	0.051	0.053	0.078
BB0845.1			1.742			0.990			0.001
BB0845.2	-0.326	-0.433	-0.313	0.170	0.120	0.180	0.041	0.086	0.033
BB0847	0.207	0.264	0.018	0.720	0.740	0.500	0.102	0.121	0.051
BB0848	0.136	0.126	0.106	0.620	0.600	0.610	0.074	0.058	0.058
BB0848.1	0.167	0.533	0.227	0.670	0.910	0.750	0.062	0.068	0.063

BB0849.1	-0.051	-0.123	-0.256	0.410	0.340	0.220	0.088	0.110	0.065
BB0849.2	0.350	0.532	0.353	0.850	0.910	0.850	0.039	0.052	0.150
BB0852	-0.200	-0.332	-0.433	0.260	0.170	0.120	0.055	0.074	0.070
BB0853	0.251	0.334	0.199	0.770	0.780	0.720	0.077	0.154	0.164
BB0853.1	0.426	0.559	0.203	0.890	0.920	0.730	0.055	0.087	0.133
Bb2.36	0.002	0.047	0.265	0.480	0.510	0.790	0.046	0.055	0.065
BB764	-0.278	-0.329	-0.558	0.200	0.180	0.070	0.162	0.118	0.081
BBA01	0.017	0.162	-0.043	0.500	0.640	0.430	0.058	0.154	0.037
BBA01	-0.457	-0.637	-0.465	0.090	0.040	0.110	0.088	0.044	0.084
BBA02	0.353	0.673	0.330	0.860	0.950	0.840	0.066	0.045	0.056
BBA03	0.204	-0.075	0.360	0.720	0.380	0.850	0.033	0.071	0.035
BBA04	-0.116	-0.260	0.495	0.340	0.220	0.910	0.075	0.094	0.040
BBA05	-0.361	-0.478	0.486	0.140	0.100	0.900	0.065	0.051	0.068
BBA06	0.149	0.139	0.275	0.640	0.610	0.790	0.088	0.102	0.104
BBA07	-0.346	-0.435	0.611	0.150	0.120	0.930	0.075	0.048	0.129
BBA08	0.365	0.287	0.328	0.860	0.760	0.830	0.036	0.062	0.051
BBA09	-0.488	-0.495	-0.484	0.070	0.090	0.100	0.093	0.049	0.030
BBA10	-0.325	-0.162	-0.297	0.170	0.310	0.200	0.042	0.051	0.066
BBA11	-0.390	-0.259	-0.462	0.120	0.220	0.110	0.032	0.077	0.082
BBA12	0.245	0.129	0.259	0.760	0.600	0.780	0.051	0.181	0.088
BBA13	-0.019	-0.110	-0.203	0.450	0.350	0.260	0.053	0.091	0.121
BBA14	-0.140	-0.101	-0.210	0.320	0.360	0.260	0.085	0.136	0.078
BBA15	0.203	1.300	1.151	0.720	0.990	0.990	0.043	0.071	0.100
BBA16	-0.179	1.006	1.025	0.280	0.990	0.990	0.056	0.077	0.098
BBA17	0.348	0.403	0.169	0.850	0.830	0.690	0.049	0.063	0.077
BBA18	0.072	-0.064	-0.174	0.560	0.390	0.290	0.074	0.069	0.062
BBA19	0.057	-0.024	0.049	0.540	0.430	0.550	0.063	0.034	0.040
BBA20	0.200	-0.042	0.022	0.710	0.410	0.510	0.046	0.045	0.049
BBA21	0.151	0.128	-0.038	0.640	0.600	0.440	0.053	0.089	0.043
BBA22	0.370	0.530	0.392	0.860	0.900	0.860	0.046	0.131	0.082
BBA23	-0.003	-0.226	0.059	0.470	0.250	0.560	0.087	0.126	0.071
BBA24	0.331	-0.169	1.500	0.840	0.300	0.990	0.063	0.114	0.043
BBA25	0.227	-0.448	1.485	0.740	0.110	0.990	0.070	0.146	0.084
BBA26	0.151	0.205	-0.076	0.640	0.680	0.390	0.069	0.079	0.088
BBA27	0.393	0.311	0.279	0.870	0.770	0.800	0.039	0.043	0.065
BBA28	0.132	0.033	-0.182	0.620	0.500	0.280	0.048	0.029	0.092
BBA29	0.371	0.255	0.327	0.870	0.730	0.830	0.023	0.087	0.030
BBA30	-0.011	-0.190	-0.085	0.460	0.280	0.380	0.073	0.066	0.030

BBA31	-0.533	-0.511	-0.522	0.060	0.090	0.090	0.061	0.066	0.076
BBA32	0.169	0.079	-0.043	0.670	0.550	0.430	0.081	0.076	0.090
BBA33	0.238	0.363	0.000	0.760	0.800	0.480	0.058	0.083	0.133
BBA34	-0.637	-0.820	0.387	0.020	0.010	0.860	0.061	0.041	0.128
BBA35	0.153	0.280	-0.025	0.650	0.750	0.450	0.092	0.132	0.048
BBA36	0.509	-0.453	1.311	0.940	0.110	0.990	0.036	0.089	0.053
BBA37	0.094	-0.138	0.063	0.580	0.330	0.560	0.097	0.119	0.060
BBA38	-0.562	-0.049	-0.252	0.040	0.410	0.220	0.053	0.091	0.048
BBA39	-0.248	-0.168	-0.333	0.220	0.300	0.170	0.037	0.087	0.091
BBA40	-0.532	-0.263	-0.372	0.060	0.220	0.150	0.071	0.060	0.078
BBA41	-0.248	-0.178	-0.290	0.220	0.290	0.200	0.052	0.059	0.104
BBA42	-0.191	0.022	-0.316	0.270	0.480	0.180	0.112	0.040	0.098
BBA43	0.050	-0.019	-0.247	0.530	0.440	0.230	0.049	0.071	0.066
BBA44	0.175	0.210	0.112	0.680	0.680	0.620	0.047	0.054	0.080
BBA45	-0.170	-0.253	-0.324	0.290	0.230	0.180	0.046	0.091	0.082
BBA46	-0.724	-0.501	-0.588	0.010	0.090	0.060	0.101	0.036	0.051
BBA47	-0.230	-0.323	-0.352	0.240	0.180	0.160	0.056	0.076	0.078
BBA48	-0.240	-0.299	-0.422	0.230	0.200	0.130	0.123	0.129	0.074
BBA49	0.080	-0.063	-0.090	0.570	0.390	0.370	0.046	0.102	0.098
BBA50	-0.552	-0.329	-0.444	0.050	0.180	0.120	0.060	0.074	0.083
BBA51	-0.436	-0.636	-0.636	0.100	0.040	0.050	0.061	0.058	0.119
BBA52	-0.268	-0.292	-0.072	0.210	0.200	0.390	0.058	0.063	0.041
BBA53	-0.304	-0.261	-0.351	0.180	0.220	0.160	0.083	0.047	0.128
BBA54	-0.113	-0.085	-0.113	0.340	0.370	0.350	0.212	0.057	0.030
BBA55	-0.692	-0.728	-0.672	0.010	0.020	0.040	0.100	0.050	0.033
BBA56	-0.565	-0.547	-0.505	0.040	0.080	0.090	0.098	0.063	0.074
BBA57	-0.610	-0.515	-0.362	0.030	0.090	0.150	0.107	0.118	0.077
BBA58	-0.141	-0.088	-0.266	0.320	0.370	0.210	0.111	0.118	0.034
BBA59	0.194	0.285	0.395	0.710	0.750	0.860	0.060	0.038	0.071
BBA60	-0.330	-0.286	-0.341	0.160	0.200	0.160	0.105	0.055	0.055
BBA61	-0.247	-0.388	0.019	0.220	0.140	0.500	0.084	0.044	0.029
BBA62	0.330	0.959	0.873	0.840	0.990	0.970	0.039	0.044	0.048
BBA63	0.408	0.304	0.239	0.880	0.770	0.760	0.018	0.201	0.084
BBA64	0.141	-0.264	0.922	0.630	0.220	0.980	0.058	0.081	0.079
BBA65	-0.293	-0.323	0.968	0.190	0.180	0.980	0.045	0.062	0.113
BBA66	-0.212	-0.597	1.280	0.250	0.050	0.990	0.037	0.083	0.103
BBA67	0.109	0.260	0.667	0.600	0.730	0.950	0.018	0.069	0.075
BBA68	-0.216	-0.050	0.179	0.250	0.410	0.700	0.071	0.032	0.051
BBA69	-0.143	0.105	-0.042	0.320	0.580	0.430	0.029	0.067	0.039

BBA70	-0.359	-0.400	-0.434	0.150	0.130	0.120	0.082	0.078	0.050
BBA71	0.498	0.169	0.711	0.930	0.640	0.960	0.045	0.078	0.044
BBA72	0.436	-0.011	0.805	0.900	0.440	0.970	0.051	0.058	0.077
BBA73	0.336	-0.231	0.813	0.840	0.250	0.970	0.044	0.096	0.078
BBA74	-0.061	0.201	0.722	0.400	0.670	0.960	0.059	0.063	0.081
BBA75	0.193	0.373	0.139	0.700	0.810	0.660	0.037	0.226	0.096
BBA76	0.059	-0.275	-0.163	0.540	0.210	0.310	0.086	0.060	0.022
BBB01	0.207	0.257	0.285	0.720	0.730	0.800	0.049	0.081	0.034
BBB02	0.071	0.192	-0.053	0.560	0.660	0.410	0.064	0.027	0.044
BBB03	-0.193	-0.104	-0.240	0.270	0.350	0.230	0.063	0.059	0.054
BBB04	-0.470	-0.252	-0.567	0.080	0.230	0.070	0.041	0.093	0.062
BBB05	-0.244	0.041	-0.226	0.230	0.500	0.240	0.075	0.082	0.033
BBB06	-0.368	-0.079	-0.307	0.140	0.380	0.190	0.025	0.087	0.064
BBB07	-0.410	-0.175	-0.437	0.110	0.300	0.120	0.093	0.030	0.059
BBB08	0.004	0.096	-0.258	0.480	0.570	0.220	0.039	0.052	0.076
BBB09	-0.007	-0.027	0.003	0.470	0.430	0.480	0.060	0.122	0.019
BBB10	0.154	0.139	-0.034	0.650	0.610	0.440	0.078	0.071	0.068
BBB11	0.301	0.321	0.144	0.810	0.780	0.660	0.065	0.046	0.019
BBB12	-0.052	0.146	-0.274	0.410	0.620	0.210	0.141	0.161	0.128
BBB13	0.212	0.042	-0.156	0.730	0.510	0.310	0.033	0.059	0.073
BBB14	0.660	0.025	-0.038	0.970	0.490	0.430	0.077	0.078	0.034
BBB15	0.563	0.521	0.233	0.950	0.900	0.760	0.033	0.090	0.072
BBB16	-0.273	0.067	-0.255	0.210	0.540	0.220	0.037	0.057	0.031
BBB17	-0.373	-0.089	-0.322	0.140	0.370	0.180	0.067	0.081	0.022
BBB18	-0.078	0.194	-0.061	0.380	0.670	0.400	0.036	0.035	0.072
BBB19	1.716	-0.361	1.932	1.000	0.160	1.000	0.092	0.073	0.091
BBB20	0.268	0.442	0.202	0.780	0.850	0.730	0.082	0.106	0.120
BBB21	0.562	0.636	0.442	0.950	0.950	0.890	0.040	0.053	0.062
BBB22	-0.203	0.220	0.197	0.260	0.690	0.720	0.057	0.036	0.079
BBB23	-0.248	0.108	-0.314	0.220	0.580	0.180	0.069	0.037	0.054
BBB24	0.174	0.291	0.075	0.680	0.760	0.580	0.026	0.072	0.024
BBB25	0.062	0.010	-0.148	0.550	0.470	0.320	0.047	0.041	0.064
BBB26	0.017	0.277	-0.074	0.500	0.740	0.390	0.068	0.157	0.054
BBB27	0.254	0.127	-0.034	0.770	0.600	0.440	0.017	0.086	0.064
BBB28	0.095	0.060	-0.047	0.590	0.520	0.420	0.094	0.116	0.050
BBB29	-0.050	0.974	0.650	0.410	0.990	0.940	0.044	0.113	0.075
BBC01	-0.194	-0.142	0.080	0.270	0.330	0.590	0.110	0.053	0.094
BBC02	-0.021	-0.196	-0.208	0.450	0.270	0.260	0.053	0.123	0.062
BBC03	-0.122	-0.091	-0.299	0.340	0.370	0.200	0.067	0.075	0.032

BBC04	0.476	0.672	0.510	0.920	0.950	0.910	0.036	0.076	0.046
BBC05	-0.531	-0.623	0.237	0.060	0.050	0.760	0.039	0.071	0.064
BBC06	-0.184	-0.060	-0.270	0.280	0.400	0.210	0.197	0.073	0.139
BBC07	-0.025	-0.098	-0.151	0.440	0.360	0.310	0.120	0.055	0.079
BBC08	-0.183	-0.163	-0.335	0.280	0.300	0.170	0.103	0.072	0.028
BBC10	-0.439	-0.549	-0.565	0.090	0.070	0.070	0.093	0.105	0.043
BBC11	-0.421	-0.361	-0.509	0.110	0.160	0.090	0.069	0.086	0.076
BBC12	-0.381	-0.548	0.170	0.130	0.070	0.690	0.063	0.081	0.061
BBD001	-0.051	-0.084	-0.139	0.410	0.380	0.330	0.075	0.085	0.059
BBD01	-0.606	-0.498	-0.775	0.030	0.090	0.010	0.042	0.078	0.109
BBD02	0.202	0.174	0.049	0.720	0.650	0.550	0.062	0.066	0.071
BBD03	0.014	0.119	-0.121	0.490	0.590	0.350	0.050	0.144	0.071
BBD04	0.021	0.161	-0.050	0.500	0.640	0.420	0.068	0.091	0.080
BBD05	0.125	0.214	-0.088	0.610	0.680	0.380	0.065	0.116	0.098
BBD05.1	-0.041	-0.100	-0.226	0.430	0.360	0.240	0.071	0.022	0.034
BBD06.1	0.237	0.152	-0.106	0.750	0.630	0.360	0.044	0.081	0.105
BBD07	0.443	0.294	0.248	0.910	0.760	0.770	0.068	0.072	0.047
BBD08	0.271	0.341	0.143	0.790	0.790	0.660	0.080	0.095	0.065
BBD09	0.106	0.089	-0.066	0.590	0.560	0.400	0.050	0.063	0.093
BBD10	-0.067	-0.038	-0.195	0.400	0.420	0.270	0.060	0.056	0.086
BBD11	0.031	0.036	-0.144	0.510	0.500	0.320	0.034	0.039	0.097
BBD12	0.054	0.131	-0.200	0.540	0.600	0.270	0.087	0.058	0.086
BBD13	0.016	0.189	0.031	0.500	0.660	0.520	0.053	0.048	0.029
BBD14	0.154	0.179	0.061	0.650	0.650	0.560	0.040	0.036	0.034
BBD15	0.220	0.160	-0.027	0.740	0.640	0.450	0.049	0.038	0.067
BBD15.1	0.313	0.372	0.220	0.830	0.810	0.740	0.036	0.097	0.080
BBD16	0.116	0.393	0.108	0.610	0.820	0.610	0.059	0.051	0.114
BBD17	0.267	0.304	0.103	0.780	0.770	0.610	0.026	0.195	0.074
BBD18	-0.263	0.002	-0.168	0.210	0.460	0.300	0.033	0.063	0.055
BBD19	0.230	0.390	0.212	0.750	0.820	0.740	0.153	0.105	0.071
BBD20	-0.031	-0.078	-0.305	0.440	0.380	0.190	0.081	0.039	0.071
BBD21	0.001	0.049	0.134	0.480	0.510	0.650	0.031	0.036	0.054
BBD22	0.072	-0.005	0.064	0.560	0.450	0.560	0.106	0.064	0.060
BBD23	-0.064	-0.001	-0.337	0.400	0.460	0.170	0.096	0.094	0.133
BBD24	0.297	0.239	0.044	0.810	0.710	0.540	0.044	0.043	0.085
BBD25	0.264	0.297	0.015	0.780	0.760	0.500	0.074	0.060	0.073
BBE01	0.519	0.496	0.228	0.940	0.880	0.750	0.042	0.057	0.102
BBE02	-0.200	0.408	0.026	0.260	0.840	0.520	0.077	0.164	0.125
BBE03	0.210	0.435	0.117	0.730	0.850	0.630	0.070	0.131	0.060

BBE04	0.332	0.270	0.072	0.840	0.740	0.570	0.060	0.056	0.064
BBE04.1	0.297	0.215	0.026	0.810	0.690	0.510	0.041	0.060	0.103
BBE06	0.416	0.302	0.282	0.890	0.770	0.800	0.030	0.058	0.040
BBE07	0.275	0.166	0.066	0.790	0.640	0.570	0.070	0.088	0.106
BBE08	0.367	0.277	0.219	0.860	0.740	0.740	0.037	0.045	0.034
BBE09	-0.289	-0.269	-0.403	0.190	0.210	0.140	0.104	0.068	0.057
BBE10	0.422	0.345	0.258	0.890	0.790	0.780	0.058	0.040	0.041
BBE11	-0.146	0.349	0.171	0.310	0.800	0.700	0.422	0.121	0.068
BBE12	0.255	0.208	0.129	0.770	0.680	0.640	0.047	0.063	0.039
BBE13	0.342	0.511	0.089	0.850	0.890	0.600	0.072	0.080	0.072
BBE14	0.423	0.450	0.162	0.890	0.860	0.680	0.060	0.050	0.065
BBE15	0.213	0.297	0.114	0.730	0.770	0.620	0.200	0.077	0.039
BBE16	0.571	0.502	0.108	0.950	0.890	0.620	0.037	0.039	0.091
BBE17	0.555	0.506	0.146	0.950	0.890	0.660	0.072	0.148	0.147
BBE17.1	0.223	0.233	0.026	0.740	0.710	0.510	0.082	0.131	0.136
BBE18	0.161	0.368	0.362	0.660	0.810	0.850	0.113	0.149	0.126
BBE19	0.033	-0.108	-0.102	0.520	0.350	0.370	0.046	0.048	0.095
BBE20	0.175	0.243	0.253	0.680	0.720	0.780	0.085	0.054	0.095
BBE21	0.350	0.198	0.263	0.850	0.670	0.790	0.054	0.046	0.112
BBE21.1	0.011	0.147	-0.028	0.490	0.620	0.450	0.244	0.048	0.059
BBE22	-0.049	0.104	0.024	0.420	0.580	0.510	0.061	0.136	0.128
BBE23	0.555	0.480	0.395	0.950	0.880	0.860	0.050	0.065	0.032
BBE23.1	0.403	0.708	0.250	0.880	0.960	0.770	0.125	0.091	0.092
BBE23.2	0.326	0.352	0.218	0.830	0.800	0.740	0.064	0.054	0.042
BBE24	0.230	0.244	-0.045	0.750	0.720	0.430	0.121	0.146	0.151
BBE24.1	0.492	0.407	0.239	0.930	0.830	0.760	0.065	0.035	0.014
BBE25	0.475	0.507	0.252	0.920	0.890	0.780	0.048	0.142	0.054
BBE26	0.267	0.382	0.245	0.780	0.820	0.770	0.065	0.040	0.031
BBE27	0.469	0.481	0.221	0.920	0.880	0.740	0.064	0.155	0.099
BBE28	0.450	0.469	0.276	0.910	0.870	0.800	0.025	0.086	0.019
BBE29	-0.141	-0.151	-0.273	0.320	0.310	0.210	0.075	0.051	0.038
BBE29.1	0.304	0.354	0.069	0.820	0.800	0.570	0.060	0.102	0.080
BBE30	0.557	0.557	0.379	0.950	0.920	0.860	0.016	0.081	0.041
BBE31	-0.185	-0.246	-0.073	0.280	0.230	0.390	0.060	0.091	0.091
BBE31	0.260	0.416	0.225	0.770	0.840	0.750	0.085	0.087	0.047
BBE32	0.239	0.223	0.043	0.760	0.700	0.540	0.051	0.073	0.035
BBE33	0.315	0.527	0.227	0.830	0.900	0.750	0.056	0.064	0.082
BBF001	0.398	0.281	0.144	0.880	0.750	0.660	0.041	0.098	0.037
BBF001.1	0.321	0.575	0.123	0.830	0.930	0.640	0.036	0.095	0.067

BBF01	-0.071	-0.103	-0.181	0.390	0.350	0.290	0.071	0.054	0.076
BBF02	0.128	0.246	-0.028	0.620	0.720	0.450	0.043	0.096	0.063
BBF03	0.555	0.280	0.032	0.950	0.750	0.520	0.107	0.066	0.053
BBF04	0.154	0.195	-0.149	0.650	0.670	0.310	0.072	0.108	0.141
BBF05	-0.079	-0.114	-0.302	0.380	0.340	0.190	0.054	0.070	0.106
BBF06	0.236	0.288	0.057	0.750	0.760	0.550	0.055	0.110	0.103
BBF07	0.380	0.573	0.127	0.870	0.930	0.640	0.054	0.026	0.060
BBF08	0.204	0.261	0.183	0.720	0.730	0.710	0.089	0.140	0.047
BBF09	0.225	0.243	-0.034	0.740	0.710	0.440	0.047	0.057	0.049
BBF10	-0.384	-0.354	-0.593	0.130	0.160	0.060	0.076	0.064	0.104
BBF11.1	0.439	0.499	0.259	0.900	0.890	0.780	0.060	0.064	0.066
BBF12	-0.047	0.103	-0.216	0.420	0.580	0.250	0.055	0.072	0.072
BBF13	0.288	0.173	-0.014	0.800	0.650	0.460	0.040	0.041	0.102
BBF14	0.192	0.197	-0.062	0.700	0.670	0.400	0.074	0.038	0.141
BBF14.1	0.441	0.481	0.286	0.900	0.880	0.800	0.041	0.104	0.053
BBF16	0.230	0.248	0.207	0.750	0.720	0.730	0.070	0.083	0.085
BBF17	0.145	0.070	-0.163	0.640	0.540	0.300	0.060	0.044	0.057
BBF18	-0.057	0.006	-0.310	0.410	0.460	0.180	0.107	0.079	0.053
BBF19	0.008	-0.054	-0.184	0.490	0.400	0.280	0.071	0.049	0.063
BBF19.1	-0.265	0.118	-0.066	0.210	0.590	0.400	0.202	0.108	0.056
BBF20	0.328	0.221	0.088	0.840	0.690	0.600	0.043	0.035	0.060
BBF21	0.070	0.446	0.137	0.560	0.860	0.650	0.088	0.116	0.099
BBF22	0.330	0.265	0.105	0.840	0.740	0.610	0.057	0.030	0.045
BBF23	0.177	0.100	-0.117	0.690	0.570	0.350	0.069	0.085	0.053
BBF24	0.201	-0.105	-0.236	0.710	0.350	0.240	0.038	0.053	0.086
BBF25	-0.088	-0.256	-0.401	0.370	0.220	0.140	0.123	0.090	0.061
BBF26	-0.004	-0.042	-0.127	0.470	0.420	0.340	0.088	0.037	0.037
BBF26.1	-0.123	-0.109	-0.447	0.340	0.350	0.120	0.077	0.080	0.048
BBF29	0.166	0.271	0.084	0.670	0.740	0.590	0.086	0.097	0.074
BBF30	0.028	0.044	-0.059	0.510	0.510	0.410	0.063	0.091	0.036
BBF31	0.269	0.238	-0.086	0.780	0.710	0.380	0.091	0.045	0.091
BBF31.1	0.336	0.438	0.063	0.840	0.850	0.560	0.087	0.051	0.041
BBF32	-0.902	-1.121	-1.132	0.000	0.000	0.000	0.081	0.043	0.060
BBF33	-0.368	-0.441	-0.844	0.140	0.120	0.000	0.069	0.146	0.048
BBG01	-0.425	-0.319	-0.412	0.100	0.190	0.130	0.124	0.073	0.079
BBG02	-0.152	-0.301	-0.369	0.310	0.200	0.150	0.071	0.031	0.080
BBG03	0.075	0.017	-0.182	0.560	0.480	0.280	0.080	0.071	0.072
BBG03	0.014	-0.020	-0.016	0.490	0.430	0.460	0.082	0.090	0.089
BBG04	0.239	0.265	0.138	0.760	0.740	0.650	0.120	0.042	0.073

BBG05	-0.074	-0.193	-0.210	0.380	0.280	0.260	0.061	0.064	0.081
BBG06	0.255	0.388	0.051	0.770	0.820	0.550	0.030	0.061	0.057
BBG07	0.182	0.271	0.143	0.690	0.740	0.660	0.082	0.063	0.020
BBG08	-0.200	0.075	-0.219	0.260	0.550	0.250	0.026	0.045	0.022
BBG09	0.334	0.264	0.158	0.840	0.730	0.670	0.051	0.049	0.054
BBG10	-0.403	-0.582	-0.786	0.120	0.060	0.010	0.047	0.055	0.062
BBG11	-0.174	-0.254	-0.295	0.290	0.230	0.200	0.119	0.046	0.082
BBG12	0.019	-0.054	-0.165	0.500	0.400	0.300	0.074	0.057	0.105
BBG13	-0.379	-0.625	-0.576	0.130	0.050	0.060	0.087	0.049	0.089
BBG14	-0.104	0.061	-0.222	0.350	0.530	0.250	0.072	0.072	0.070
BBG15	-0.055	-0.193	-0.206	0.410	0.280	0.260	0.055	0.065	0.107
BBG16	0.207	0.177	-0.075	0.720	0.650	0.390	0.087	0.072	0.057
BBG17	-0.201	-0.374	-0.470	0.260	0.150	0.110	0.062	0.050	0.118
BBG18	-0.251	-0.418	-0.570	0.220	0.130	0.070	0.063	0.121	0.092
BBG19	-0.373	-0.709	-0.685	0.140	0.030	0.030	0.104	0.072	0.041
BBG20	-0.288	-0.251	-0.360	0.190	0.230	0.150	0.086	0.078	0.162
BBG21	-0.417	-0.551	-0.659	0.110	0.070	0.040	0.051	0.049	0.101
BBG22	-0.422	-0.401	-0.492	0.100	0.130	0.100	0.069	0.074	0.105
BBG23	-0.608	-0.721	-0.845	0.030	0.020	0.000	0.042	0.031	0.139
BBG24	-0.693	-0.742	-0.939	0.010	0.020	0.000	0.072	0.092	0.087
BBG25	0.279	0.193	-0.017	0.790	0.660	0.460	0.103	0.061	0.133
BBG26	-0.251	-0.109	-0.408	0.220	0.350	0.130	0.100	0.097	0.071
BBG27	-0.072	-0.162	-0.412	0.390	0.310	0.130	0.066	0.050	0.032
BBG28	-0.091	0.055	-0.052	0.360	0.520	0.410	0.071	0.084	0.144
BBG29	-0.113	-0.483	-0.375	0.340	0.100	0.150	0.047	0.049	0.047
BBG30	-0.025	-0.103	-0.135	0.440	0.350	0.330	0.046	0.071	0.102
BBG31	0.052	0.025	-0.086	0.540	0.490	0.380	0.037	0.060	0.067
BBG32	-0.408	-0.417	-0.505	0.110	0.130	0.090	0.066	0.072	0.061
BBG33	0.216	0.208	0.013	0.730	0.680	0.500	0.031	0.032	0.040
BBG34	-0.187	-0.001	-0.245	0.280	0.460	0.230	0.097	0.059	0.047
BBH01	0.028	-0.196	-0.353	0.510	0.280	0.160	0.071	0.057	0.091
BBH02	-0.330	-0.151	-0.573	0.160	0.310	0.060	0.138	0.162	0.044
BBH03	0.203	0.110	-0.047	0.720	0.590	0.420	0.042	0.066	0.066
BBH04	-0.378	-0.196	-0.477	0.130	0.270	0.110	0.106	0.070	0.061
BBH05	0.184	0.029	-0.141	0.690	0.490	0.330	0.039	0.087	0.098
BBH06	-0.155	-0.144	-0.301	0.300	0.320	0.190	0.116	0.077	0.062
BBH07	0.288	0.150	0.032	0.800	0.630	0.530	0.074	0.065	0.096
BBH08	-0.048	-0.007	-0.154	0.420	0.450	0.310	0.112	0.043	0.128
BBH09	-0.219	-0.336	-0.337	0.240	0.170	0.170	0.037	0.034	0.087

BBH09.1	0.115	0.188	-0.036	0.600	0.660	0.440	0.095	0.067	0.065
BBH10.1	0.281	0.352	0.284	0.790	0.800	0.800	0.074	0.107	0.059
BBH11.1	-0.053	-0.043	-0.183	0.410	0.410	0.280	0.088	0.045	0.071
BBH12	0.022	-0.110	-0.133	0.500	0.350	0.340	0.023	0.079	0.047
BBH13	0.519	0.260	0.067	0.940	0.730	0.570	0.067	0.065	0.061
BBH14	0.421	0.524	0.425	0.890	0.900	0.880	0.070	0.075	0.031
BBH15	0.350	0.288	0.258	0.850	0.760	0.780	0.060	0.127	0.084
BBH16	0.293	0.287	0.212	0.800	0.760	0.740	0.076	0.085	0.056
BBH16.1	0.411	0.408	0.271	0.890	0.840	0.790	0.090	0.099	0.044
BBH17	0.370	0.452	0.272	0.870	0.860	0.790	0.056	0.064	0.047
BBH18	0.492	0.551	0.227	0.930	0.920	0.750	0.121	0.133	0.025
BBH18.1	0.112	0.209	0.085	0.600	0.680	0.600	0.076	0.057	0.054
BBH20	-0.182	-0.064	-0.306	0.280	0.390	0.190	0.056	0.105	0.098
BBH20.1	0.309	0.286	0.198	0.820	0.760	0.720	0.155	0.135	0.059
BBH24.1	0.473	0.601	0.349	0.920	0.940	0.840	0.039	0.095	0.035
BBH25.1	0.302	0.445	0.144	0.820	0.860	0.660	0.033	0.166	0.090
BBH26	0.273	0.326	0.226	0.790	0.780	0.750	0.101	0.113	0.073
BBH27	0.403	0.560	0.331	0.880	0.920	0.840	0.053	0.105	0.024
BBH28	0.468	0.476	0.221	0.920	0.870	0.740	0.052	0.063	0.039
BBH29	0.222	0.548	0.236	0.740	0.910	0.760	0.099	0.173	0.033
BBH30	0.543	0.471	0.336	0.950	0.870	0.840	0.078	0.090	0.023
BBH31	0.249	0.432	0.147	0.760	0.850	0.670	0.110	0.148	0.111
BBH32	0.384	0.682	0.064	0.870	0.960	0.560	0.079	0.154	0.115
BBH33	-0.067	0.034	-0.084	0.390	0.500	0.380	0.088	0.108	0.026
BBH34	0.212	0.111	-0.213	0.730	0.590	0.260	0.173	0.051	0.074
BBH35	0.173	0.230	0.169	0.680	0.700	0.690	0.072	0.064	0.122
BBH36.1	0.165	0.057	0.002	0.670	0.520	0.480	0.081	0.083	0.053
BBH36.2	0.298	0.102	0.189	0.810	0.580	0.710	0.055	0.114	0.077
BBH37	-0.275	-0.067	-0.297	0.200	0.390	0.200	0.051	0.140	0.072
BBH38	0.306	0.358	0.094	0.820	0.800	0.610	0.029	0.111	0.094
BBH39	0.501	0.444	0.345	0.940	0.850	0.840	0.047	0.092	0.060
BBH40	0.009	-0.057	-0.224	0.490	0.400	0.250	0.074	0.095	0.073
BBH41	-0.066	0.294	0.030	0.400	0.760	0.520	0.245	0.074	0.100
BBH41	-0.013	-0.235	-0.298	0.460	0.240	0.200	0.111	0.098	0.031
BBI01	0.059	0.156	-0.062	0.550	0.630	0.400	0.134	0.067	0.103
BBI02	0.193	0.098	-0.107	0.710	0.570	0.360	0.030	0.058	0.103
BBI02.1	0.377	0.422	0.392	0.870	0.840	0.860	0.069	0.048	0.073
BBI02.2	0.352	0.279	0.202	0.850	0.750	0.730	0.047	0.064	0.061
BBI03	0.135	0.199	-0.018	0.620	0.670	0.460	0.067	0.079	0.118

BBI04	0.475	0.322	0.289	0.920	0.780	0.810	0.027	0.043	0.051
BBI05	0.198	0.567	0.133	0.710	0.920	0.650	0.041	0.096	0.110
BBI06	-0.024	0.057	-0.175	0.440	0.520	0.290	0.077	0.081	0.021
BBI07	0.369	0.239	0.071	0.860	0.710	0.570	0.020	0.049	0.064
BBI08.1	-0.229	-0.127	-0.227	0.240	0.340	0.240	0.108	0.058	0.086
BBI11	0.302	0.408	0.268	0.820	0.840	0.790	0.043	0.067	0.030
BBI12	0.092	0.231	0.165	0.580	0.700	0.680	0.125	0.119	0.059
BBI13	0.449	0.377	0.409	0.910	0.810	0.870	0.050	0.047	0.028
BBI14	0.040	0.282	-0.051	0.520	0.750	0.420	0.105	0.068	0.064
BBI15	0.387	0.145	0.074	0.870	0.620	0.580	0.077	0.107	0.054
BBI16	-0.592	-0.373	-0.610	0.040	0.150	0.060	0.124	0.093	0.072
BBI17	-0.169	-0.162	-0.319	0.290	0.310	0.180	0.077	0.050	0.100
BBI17.1	-0.093	0.079	-0.213	0.360	0.550	0.260	0.105	0.089	0.049
BBI18	0.269	0.305	0.183	0.780	0.770	0.710	0.046	0.085	0.085
BBI19	0.303	0.217	0.135	0.820	0.690	0.650	0.125	0.134	0.181
BBI20	-0.087	0.007	-0.139	0.370	0.470	0.330	0.080	0.052	0.075
BBI21	0.338	0.339	0.226	0.850	0.790	0.750	0.075	0.151	0.024
BBI22	0.159	0.205	0.095	0.660	0.670	0.610	0.062	0.083	0.050
BBI23	0.238	0.544	0.222	0.760	0.910	0.750	0.125	0.062	0.099
BBI24	0.296	0.257	0.238	0.800	0.730	0.760	0.118	0.039	0.042
BBI25	0.166	0.524	0.185	0.670	0.900	0.710	0.245	0.116	0.056
BBI26	-0.045	-0.028	-0.231	0.420	0.430	0.240	0.088	0.139	0.125
BBI27	-0.046	-0.144	-0.266	0.420	0.320	0.210	0.088	0.073	0.035
BBI28	-0.143	-0.218	-0.337	0.320	0.250	0.170	0.127	0.118	0.117
BBI29	-0.361	-0.180	-0.177	0.140	0.290	0.290	0.111	0.039	0.047
BBI30	0.331	0.266	0.043	0.840	0.740	0.540	0.051	0.089	0.065
BBI31	-0.151	-0.267	-0.185	0.310	0.220	0.280	0.144	0.078	0.032
BBI31.1	0.412	0.408	0.303	0.890	0.830	0.820	0.063	0.132	0.085
BBI33	0.264	0.093	0.035	0.780	0.560	0.530	0.090	0.090	0.082
BBI34	-0.134	-0.085	-0.319	0.330	0.370	0.180	0.085	0.042	0.107
BBI35	0.164	0.075	-0.028	0.670	0.550	0.450	0.076	0.037	0.053
BBI36	-0.103	-0.063	-0.047	0.350	0.390	0.420	0.141	0.068	0.080
BBI37	0.290	0.225	0.071	0.800	0.700	0.570	0.106	0.106	0.072
BBI38	-0.208	-0.010	-0.119	0.260	0.450	0.350	0.071	0.055	0.052
BBI39	-0.291	-0.250	-0.181	0.190	0.230	0.290	0.029	0.044	0.060
BBI40	0.259	0.181	0.237	0.770	0.650	0.760	0.041	0.124	0.074
BBI41	0.289	0.132	-0.038	0.800	0.610	0.430	0.077	0.059	0.099
BBI42	-0.571	-0.446	0.111	0.040	0.110	0.620	0.073	0.127	0.072
BBI43	-0.235	-0.100	-0.324	0.230	0.360	0.170	0.124	0.112	0.087

BBJ001	-0.157	-0.099	0.040	0.300	0.360	0.540	0.086	0.112	0.050
BBJ02.1	-0.376	-0.346	-0.589	0.140	0.170	0.060	0.065	0.032	0.090
BBJ04	0.168	-0.011	-0.060	0.670	0.440	0.410	0.060	0.130	0.132
BBJ05	-0.017	-0.069	-0.297	0.450	0.390	0.200	0.025	0.062	0.104
BBJ07.1	0.101	0.242	0.129	0.590	0.710	0.640	0.100	0.104	0.019
BBJ08	-0.432	-0.107	0.307	0.100	0.350	0.820	0.038	0.066	0.071
BBJ09	-0.532	-0.226	-0.072	0.060	0.250	0.390	0.083	0.061	0.055
BBJ10	-0.058	0.150	-0.143	0.400	0.630	0.320	0.102	0.038	0.079
BBJ11	0.007	-0.172	-0.215	0.480	0.300	0.250	0.029	0.061	0.090
BBJ12.1	0.211	0.248	0.009	0.730	0.720	0.490	0.052	0.063	0.165
BBJ13	0.097	-0.072	-0.189	0.590	0.380	0.280	0.026	0.064	0.037
BBJ15.1	0.003	0.032	-0.065	0.480	0.490	0.400	0.103	0.048	0.085
BBJ16	0.170	-0.066	-0.081	0.670	0.390	0.380	0.036	0.078	0.043
BBJ17	0.033	-0.050	-0.148	0.520	0.400	0.320	0.087	0.057	0.042
BBJ18	0.319	0.099	0.059	0.830	0.570	0.560	0.051	0.080	0.063
BBJ19	-0.085	-0.143	-0.144	0.370	0.320	0.320	0.087	0.057	0.062
BBJ20	0.045	-0.193	-0.402	0.530	0.280	0.140	0.079	0.086	0.130
BBJ20.1	-0.069	-0.175	-0.298	0.390	0.290	0.200	0.066	0.055	0.077
BBJ21.1	0.268	0.056	-0.027	0.780	0.520	0.450	0.020	0.068	0.119
BBJ23	0.231	-0.381	0.328	0.750	0.150	0.830	0.038	0.081	0.074
BBJ24	-0.047	-0.275	-0.104	0.420	0.210	0.360	0.059	0.089	0.044
BBJ25	-0.211	-0.535	-0.071	0.250	0.080	0.400	0.032	0.068	0.109
BBJ26	0.135	-0.218	0.087	0.620	0.250	0.600	0.048	0.098	0.045
BBJ27	-0.428	-0.712	-0.217	0.100	0.030	0.250	0.062	0.077	0.111
BBJ28	0.175	-0.192	0.061	0.680	0.280	0.560	0.069	0.102	0.083
BBJ29	-0.614	-0.730	-0.731	0.030	0.020	0.020	0.057	0.103	0.044
BBJ30	-0.084	0.089	0.085	0.370	0.560	0.590	0.087	0.078	0.204
BBJ31	-0.400	-1.045	-0.079	0.120	0.000	0.390	0.038	0.047	0.052
BBJ32	-0.003	0.034	-0.241	0.470	0.500	0.230	0.071	0.099	0.055
BBJ33	-0.052	0.004	0.121	0.410	0.460	0.630	0.140	0.064	0.085
BBJ34	-0.221	-0.418	0.141	0.240	0.120	0.660	0.035	0.065	0.036
BBJ35	0.195	0.283	0.179	0.710	0.750	0.700	0.062	0.069	0.036
BBJ36	-0.171	-0.328	-0.193	0.290	0.180	0.270	0.081	0.071	0.054
BBJ37	-0.248	-0.306	-0.292	0.220	0.190	0.200	0.090	0.043	0.034
BBJ38	0.140	0.219	0.022	0.630	0.690	0.500	0.050	0.070	0.074
BBJ39	0.242	0.191	0.117	0.760	0.660	0.630	0.068	0.052	0.038
BBJ39.1	0.194	0.262	0.019	0.710	0.730	0.500	0.063	0.061	0.081
BBJ40	0.388	0.510	0.235	0.870	0.890	0.760	0.092	0.218	0.038
BBJ41	-0.321	0.063	-0.077	0.170	0.530	0.390	0.080	0.040	0.052

BBJ42	0.245	0.186	0.060	0.760	0.660	0.560	0.077	0.082	0.066
BBJ43	-0.336	-0.156	-0.328	0.160	0.310	0.170	0.106	0.107	0.062
BBJ44	0.096	-0.004	0.026	0.590	0.450	0.510	0.060	0.054	0.044
BBJ45	-0.086	-0.582	0.145	0.370	0.060	0.660	0.074	0.099	0.045
BBJ45.1	0.100	0.004	-0.085	0.590	0.460	0.380	0.082	0.061	0.028
BBJ46	0.178	0.226	0.278	0.690	0.700	0.800	0.064	0.052	0.022
BBJ47	-0.002	-0.317	0.163	0.470	0.190	0.680	0.073	0.054	0.111
BBJ48	0.012	-0.039	0.316	0.490	0.420	0.820	0.072	0.089	0.097
BBJ49	0.191	0.111	0.071	0.700	0.590	0.570	0.016	0.070	0.114
BBJ50	-0.079	-0.006	-0.142	0.380	0.450	0.330	0.088	0.062	0.087
BBJ51	-0.114	-1.041	-0.748	0.340	0.000	0.020	0.126	0.128	0.046
BBK001	0.485	0.354	0.324	0.930	0.800	0.830	0.064	0.032	0.064
BBK01	-0.243	-0.332	-0.155	0.230	0.180	0.310	0.033	0.028	0.067
BBK02.1	-0.363	-0.389	-0.559	0.140	0.140	0.070	0.090	0.125	0.142
BBK04.1	0.132	0.029	-0.172	0.620	0.490	0.300	0.077	0.109	0.100
BBK05	0.364	0.636	0.376	0.860	0.950	0.860	0.054	0.078	0.042
BBK06	0.470	0.495	0.356	0.920	0.880	0.850	0.026	0.066	0.025
BBK07	-0.658	-0.517	0.096	0.020	0.080	0.610	0.112	0.099	0.060
BBK08	0.464	0.396	0.242	0.910	0.830	0.770	0.042	0.115	0.056
BBK09	0.247	0.252	0.039	0.760	0.720	0.540	0.081	0.093	0.176
BBK10	0.464	0.504	0.236	0.910	0.890	0.760	0.036	0.042	0.060
BBK12	-0.572	-0.293	0.038	0.040	0.200	0.530	0.068	0.072	0.055
BBK13	0.175	0.143	0.595	0.680	0.620	0.930	0.027	0.031	0.059
BBK14	0.141	0.477	0.269	0.630	0.870	0.790	0.118	0.072	0.070
BBK15	0.066	-0.016	-0.108	0.550	0.440	0.360	0.041	0.091	0.134
BBK16	-0.046	0.198	0.310	0.420	0.670	0.820	0.059	0.078	0.100
BBK17	-0.608	-0.933	0.272	0.030	0.000	0.790	0.025	0.053	0.068
BBK18	0.406	0.197	0.161	0.880	0.670	0.680	0.070	0.096	0.084
BBK19	-0.176	-0.372	-0.047	0.290	0.150	0.420	0.053	0.070	0.031
BBK20	0.083	0.379	-0.096	0.570	0.810	0.370	0.009	0.335	0.222
BBK21	-0.156	-0.257	-0.101	0.300	0.220	0.370	0.108	0.071	0.086
BBK22	-0.086	-0.035	-0.085	0.370	0.420	0.380	0.106	0.069	0.086
BBK23	-0.254	-0.191	-0.170	0.220	0.280	0.300	0.087	0.045	0.038
BBK24	-0.011	0.140	-0.197	0.460	0.610	0.270	0.073	0.060	0.026
BBK25	-0.118	-0.045	-0.166	0.340	0.410	0.300	0.047	0.095	0.047
BBK25.1	-0.422	-0.159	-0.346	0.100	0.310	0.160	0.139	0.109	0.069
BBK31	0.158	0.160	-0.096	0.660	0.640	0.370	0.038	0.057	0.046
BBK32	-0.435	-0.596	0.851	0.100	0.050	0.970	0.081	0.098	0.072
BBK33	0.139	0.599	0.109	0.630	0.930	0.620	0.172	0.292	0.132

BBK34	0.206	0.218	0.170	0.720	0.690	0.690	0.069	0.119	0.069
BBK35	-0.111	0.105	-0.267	0.350	0.580	0.210	0.067	0.115	0.163
BBK36	-0.010	-0.018	-0.129	0.460	0.440	0.340	0.093	0.054	0.063
BBK37	-0.238	-0.057	-0.352	0.230	0.400	0.160	0.061	0.124	0.064
BBK38	-0.314	-0.305	0.062	0.170	0.190	0.560	0.086	0.054	0.023
BBK39	-0.211	-0.109	-0.148	0.250	0.350	0.320	0.042	0.104	0.029
BBK40	-0.080	0.143	0.215	0.380	0.620	0.740	0.082	0.022	0.053
BBK41	-0.215	-0.208	-0.535	0.250	0.260	0.080	0.094	0.078	0.092
BBK42	0.079	0.117	-0.105	0.570	0.590	0.360	0.062	0.069	0.087
BBK42.1	0.108	0.111	0.116	0.600	0.590	0.630	0.087	0.051	0.080
BBK44	0.075	0.090	-0.010	0.560	0.560	0.470	0.070	0.019	0.035
BBK45	-0.194	0.321	0.245	0.270	0.780	0.770	0.052	0.032	0.034
BBK46	-0.602	-0.629	-0.290	0.030	0.050	0.200	0.097	0.063	0.039
BBK47	-0.562	-0.314	0.045	0.050	0.190	0.540	0.065	0.086	0.044
BBK48	-0.675	-0.593	-0.247	0.010	0.060	0.230	0.057	0.071	0.046
BBK49	-0.562	-0.387	-0.134	0.050	0.140	0.330	0.107	0.105	0.068
BBK50	-0.342	-0.208	0.001	0.160	0.260	0.480	0.044	0.107	0.027
BBK51	0.450	0.507	0.178	0.910	0.890	0.700	0.083	0.251	0.115
BBK52	-0.361	-0.227	-0.261	0.140	0.250	0.220	0.111	0.066	0.077
BBK52.1	0.135	0.470	0.499	0.620	0.870	0.910	0.040	0.255	0.194
BBK53	-0.286	-0.430	0.166	0.200	0.120	0.690	0.073	0.056	0.070
BBK54	0.087	0.056	0.037	0.570	0.520	0.530	0.047	0.071	0.094
BBL01	-0.343	-0.537	-0.544	0.160	0.080	0.080	0.068	0.060	0.042
BBL02	-0.449	-0.711	-0.644	0.090	0.030	0.050	0.057	0.137	0.065
BBL03	-0.348	-0.418	-0.530	0.150	0.120	0.080	0.051	0.045	0.051
BBL04	-0.593	-0.455	-0.644	0.040	0.110	0.050	0.059	0.051	0.062
BBL05	-0.298	-0.403	-0.298	0.190	0.130	0.200	0.037	0.086	0.104
BBL06	-0.826	-0.656	-0.682	0.000	0.040	0.030	0.009	0.078	0.060
BBL07	-0.566	-0.735	-0.729	0.040	0.020	0.020	0.061	0.049	0.052
BBL08	-0.300	-0.260	-0.481	0.180	0.220	0.100	0.084	0.146	0.097
BBL09	-0.395	-0.457	-0.506	0.120	0.110	0.090	0.046	0.070	0.172
BBL10	-0.413	-0.467	-0.555	0.110	0.110	0.070	0.072	0.085	0.089
BBL11	-0.784	-0.747	-0.696	0.000	0.020	0.030	0.031	0.035	0.086
BBL12	-0.756	-0.485	-0.749	0.000	0.100	0.020	0.042	0.065	0.056
BBL13	-0.307	-0.362	-0.487	0.180	0.160	0.100	0.081	0.117	0.096
BBL14	-0.344	0.002	-0.345	0.160	0.460	0.160	0.218	0.119	0.074
BBL15	-0.758	-1.124	-1.017	0.000	0.000	0.000	0.036	0.038	0.020
BBL16	-0.519	-0.419	-0.611	0.060	0.120	0.060	0.079	0.045	0.069
BBL17	-0.559	-0.737	-0.752	0.050	0.020	0.010	0.026	0.093	0.084

BBL18	-0.600	-0.424	-0.689	0.030	0.120	0.030	0.065	0.081	0.080
BBL19	-0.071	-0.181	-0.180	0.390	0.290	0.290	0.056	0.052	0.056
BBL20	-0.597	-0.354	-0.687	0.040	0.160	0.030	0.028	0.072	0.020
BBL21	-0.596	-0.396	-0.565	0.040	0.140	0.070	0.112	0.078	0.081
BBL22	-0.719	-0.483	-0.621	0.010	0.100	0.050	0.128	0.076	0.101
BBL23	-0.199	-0.217	-0.212	0.270	0.260	0.260	0.056	0.033	0.068
BBL24	-0.578	-0.441	-0.648	0.040	0.120	0.040	0.095	0.078	0.071
BBL25	0.030	0.298	0.031	0.510	0.770	0.520	0.063	0.176	0.171
BBL26	-0.048	0.188		0.420	0.660		0.074	0.248	
BBL27	0.201	0.240	-0.026	0.710	0.710	0.450	0.089	0.043	0.087
BBL28	-0.248	-0.179	0.057	0.220	0.290	0.550	0.058	0.053	0.066
BBL29		0.948	-0.057		0.980	0.410		0.048	0.170
BBL30	-0.008	0.093	0.027	0.460	0.560	0.520	0.039	0.037	0.051
BBL31	-0.133	-0.189	-0.241	0.330	0.290	0.230	0.040	0.059	0.115
BBL32	-0.118	-0.246	-0.102	0.340	0.240	0.360	0.106	0.086	0.061
BBL33		0.498	0.324		0.890	0.830		0.176	0.080
BBL34	0.061	-0.063	0.044	0.550	0.400	0.540	0.104	0.090	0.043
BBL35	0.022	-0.171	-0.281	0.500	0.300	0.210	0.073	0.083	0.105
BBL36	-0.387	-0.522	-0.191	0.120	0.080	0.270	0.051	0.109	0.029
BBL37	-0.270	-0.328	-0.439	0.210	0.180	0.120	0.104	0.059	0.104
BBL38	-0.238	-0.137	-0.399	0.230	0.330	0.140	0.041	0.074	0.055
BBL39	-0.001	-0.086	0.075	0.470	0.370	0.580	0.056	0.090	0.062
BBL40	-0.100	-0.555	0.192	0.360	0.070	0.710	0.076	0.036	0.073
BBL41	0.099	0.151	-0.016	0.590	0.630	0.460	0.045	0.068	0.036
BBL42	-0.159	-0.331	-0.249	0.300	0.180	0.220	0.053	0.065	0.037
BBL43	-0.608	-0.706	-0.599	0.030	0.030	0.060	0.058	0.126	0.048
BBM01	-0.383	-0.559	-0.456	0.130	0.070	0.110	0.025	0.076	0.063
BBM02	-0.423	-0.673	-0.744	0.100	0.030	0.020	0.069	0.124	0.100
BBM03	-0.386	-0.349	-0.499	0.120	0.170	0.100	0.048	0.076	0.084
BBM04	-0.488	-0.527	-0.628	0.070	0.080	0.050	0.104	0.112	0.109
BBM05	-0.728	-0.671	-0.726	0.010	0.030	0.020	0.067	0.075	0.106
BBM06	-0.751	-0.693	-0.658	0.000	0.030	0.040	0.053	0.083	0.077
BBM07	-0.543	-0.759	-0.676	0.050	0.020	0.030	0.045	0.034	0.077
BBM08	-0.304	-0.396	-0.532	0.180	0.140	0.080	0.076	0.157	0.134
BBM09	-0.193	-0.359	-0.390	0.270	0.160	0.140	0.036	0.066	0.131
BBM10	-0.513	-0.497	-0.489	0.070	0.090	0.100	0.089	0.083	0.115
BBM11	-0.829	-0.709	-0.733	0.000	0.030	0.020	0.025	0.043	0.076
BBM12	-0.787	-0.657	-0.845	0.000	0.040	0.000	0.104	0.088	0.102
BBM13	-0.279	-0.449	-0.522	0.200	0.110	0.090	0.069	0.054	0.078

BBM14	-0.224	-0.193	-0.340	0.240	0.280	0.160	0.047	0.098	0.106
BBM15	-0.710	-0.964	-0.853	0.010	0.000	0.000	0.033	0.041	0.061
BBM16	-0.549	-0.484	-0.682	0.050	0.100	0.030	0.081	0.043	0.097
BBM17	-0.528	-0.579	-0.515	0.060	0.070	0.090	0.057	0.076	0.113
BBM18	-0.823	-0.620	-0.730	0.000	0.050	0.020	0.023	0.124	0.149
BBM19	-0.126	-0.191	-0.201	0.330	0.280	0.270	0.061	0.062	0.035
BBM20	-0.698	-0.696	-0.636	0.010	0.030	0.050	0.033	0.080	0.053
BBM21	-0.359	-0.548	-0.564	0.150	0.070	0.070	0.038	0.059	0.075
BBM22	-0.657	-0.593	-0.730	0.020	0.060	0.020	0.045	0.076	0.087
BBM23	0.074	-0.013	-0.092	0.560	0.440	0.370	0.065	0.078	0.038
BBM24	-0.380	-0.244	-0.503	0.130	0.240	0.090	0.135	0.090	0.056
BBM25	-0.161	-0.215	-0.285	0.300	0.260	0.210	0.059	0.094	0.051
BBM26	-0.473	-0.267	-0.496	0.080	0.220	0.100	0.101	0.109	0.075
BBM27	0.116	-0.516	0.572	0.610	0.090	0.920	0.129	0.154	0.124
BBM28	-0.300	-0.564	0.462	0.180	0.070	0.900	0.099	0.093	0.085
BBM29	-0.512	-0.815	-0.351	0.070	0.010	0.160	0.047	0.054	0.037
BBM30	-0.140	-0.179	-0.172	0.320	0.290	0.300	0.087	0.039	0.050
BBM31	-0.179	-0.260	-0.278	0.280	0.220	0.210	0.055	0.057	0.074
BBM32	-0.282	-0.331	-0.364	0.200	0.180	0.150	0.111	0.075	0.050
BBM33	-0.252	-0.116	-0.306	0.220	0.340	0.190	0.077	0.055	0.078
BBM34	-0.011	-0.145	-0.417	0.460	0.320	0.130	0.031	0.088	0.149
BBM35	-0.193	-0.393	-0.187	0.270	0.140	0.280	0.188	0.072	0.021
BBM36	-0.326	-0.152	-0.386	0.170	0.310	0.140	0.037	0.112	0.093
BBM37	-0.274	-0.251	-0.301	0.210	0.230	0.190	0.069	0.073	0.065
BBM38	0.101	-0.324	0.403	0.590	0.180	0.870	0.041	0.092	0.017
BBM39	0.194	0.280	0.074	0.710	0.750	0.570	0.103	0.175	0.109
BBM40	0.096	0.541	0.192	0.590	0.910	0.720	0.078	0.084	0.097
BBM41	-0.382	-0.519	-0.407	0.130	0.080	0.130	0.084	0.051	0.040
BBM42	-0.513	-0.455	-0.485	0.070	0.110	0.100	0.054	0.118	0.040
BBN01	-0.444	-0.590	-0.560	0.090	0.060	0.070	0.054	0.078	0.031
BBN02	-0.430	-0.505	-0.690	0.100	0.090	0.030	0.036	0.084	0.037
BBN03	-0.468	-0.659	-0.569	0.080	0.040	0.070	0.090	0.083	0.085
BBN04	-0.511	-0.591	-0.613	0.070	0.060	0.050	0.025	0.112	0.045
BBN05	-0.518	-0.385	-0.611	0.060	0.140	0.050	0.088	0.068	0.068
BBN06	-0.704	-0.591	-0.649	0.010	0.060	0.040	0.077	0.115	0.095
BBN07	-0.682	-0.980	-0.801	0.010	0.000	0.010	0.104	0.032	0.043
BBN08	-0.297	-0.226	-0.511	0.190	0.250	0.090	0.065	0.082	0.078
BBN09	-0.561	-0.383	-0.448	0.050	0.140	0.120	0.129	0.092	0.098
BBN10	-0.442	-0.145	-0.502	0.090	0.320	0.090	0.077	0.067	0.077

BBN11	-0.778	-0.811	-0.880	0.000	0.010	0.000	0.082	0.092	0.040
BBN12	-0.519	-0.591	-0.665	0.060	0.060	0.040	0.062	0.094	0.114
BBN13	-0.189	-0.190	-0.371	0.270	0.280	0.150	0.044	0.059	0.111
BBN14	-0.247	-0.032	-0.364	0.220	0.430	0.150	0.071	0.047	0.090
BBN15	-0.741	-0.768	-0.985	0.010	0.020	0.000	0.057	0.100	0.028
BBN16	-0.378	-0.374	-0.365	0.130	0.150	0.150	0.085	0.115	0.087
BBN17	-0.495	-0.491	-0.733	0.070	0.100	0.020	0.054	0.081	0.082
BBN18	-0.501	-0.549	-0.531	0.070	0.070	0.080	0.068	0.101	0.060
BBN19	-0.019	-0.053	-0.138	0.450	0.400	0.330	0.029	0.090	0.083
BBN20	-0.536	-0.482	-0.493	0.050	0.100	0.100	0.048	0.053	0.071
BBN21	-0.284	-0.303	-0.261	0.200	0.200	0.220	0.028	0.075	0.116
BBN22	-0.531	-0.212	-0.509	0.060	0.260	0.090	0.067	0.111	0.106
BBN23	0.074	-0.082	-0.146	0.560	0.380	0.320	0.038	0.063	0.034
BBN24	-0.369	-0.362	-0.408	0.140	0.160	0.130	0.044	0.092	0.099
BBN25	-0.039	-0.116	-0.205	0.430	0.340	0.260	0.032	0.071	0.058
BBN26	-0.380	-0.203	-0.458	0.130	0.270	0.110	0.091	0.094	0.066
BBN27	0.151	-0.024	-0.178	0.640	0.430	0.290	0.057	0.048	0.058
BBN28	-0.154	0.146	0.126	0.300	0.620	0.640	0.048	0.121	0.057
BBN29	-0.173	-0.338	0.143	0.290	0.170	0.660	0.027	0.054	0.041
BBN30	-0.092	-0.087	-0.008	0.360	0.370	0.470	0.052	0.097	0.089
BBN31	-0.076	-0.213	-0.255	0.380	0.260	0.220	0.035	0.051	0.066
BBN32	-0.143	0.084	-0.063	0.320	0.550	0.400	0.035	0.082	0.053
BBN33	0.238	0.250	0.250	0.750	0.720	0.780	0.048	0.037	0.034
BBN34	-0.023	-0.003	-0.142	0.440	0.450	0.320	0.088	0.133	0.066
BBN35	-0.500	-0.870	-0.259	0.070	0.000	0.220	0.092	0.067	0.025
BBN36	-0.605	-0.568	-0.558	0.030	0.070	0.070	0.114	0.059	0.087
BBN37	-0.631	-0.529	-0.548	0.020	0.080	0.080	0.076	0.058	0.100
BBN38	-0.172	-0.038	0.013	0.290	0.420	0.500	0.116	0.166	0.126
BBN39	-0.278	-0.420	-0.029	0.200	0.120	0.450	0.061	0.086	0.079
BBN40	-0.066	0.523	0.227	0.400	0.900	0.750	0.044	0.252	0.093
BBN41	-0.068	-0.031	-0.108	0.390	0.430	0.360	0.095	0.092	0.038
BBN42	-0.438	-0.001	-0.174	0.100	0.460	0.290	0.137	0.096	0.144
BBN43	-0.665	-0.820	-0.598	0.020	0.010	0.060	0.097	0.079	0.032
BBO01	-0.393	-0.595	-0.518	0.120	0.050	0.090	0.036	0.108	0.086
BBO02	-0.508	-0.629	-0.609	0.070	0.040	0.060	0.067	0.054	0.038
BBO03	-0.414	-0.621	-0.554	0.110	0.050	0.070	0.050	0.059	0.088
BBO04	-0.655	-0.992	-0.655	0.020	0.000	0.040	0.091	0.042	0.038
BBO05	-0.426	-0.395	-0.598	0.100	0.140	0.060	0.076	0.045	0.046
BBO06	-0.787	-0.952	-0.627	0.000	0.000	0.050	0.088	0.143	0.041

BBO07	-0.562	-0.509	-0.673	0.040	0.090	0.030	0.033	0.106	0.083
BBO08	-0.184	-0.332	-0.473	0.280	0.170	0.110	0.072	0.062	0.077
BBO09	-0.287	-0.177	-0.317	0.190	0.290	0.180	0.057	0.093	0.066
BBO10	-0.277	-0.336	-0.350	0.200	0.170	0.160	0.047	0.087	0.110
BBO11	-0.938	-0.956	-0.931	0.000	0.000	0.000	0.050	0.086	0.068
BBO12	-0.471	-0.700	-0.599	0.080	0.030	0.060	0.102	0.045	0.041
BBO13	-0.110	-0.025	-0.214	0.350	0.430	0.260	0.037	0.066	0.099
BBO14	-0.089	-0.296	-0.439	0.360	0.200	0.120	0.135	0.069	0.108
BBO15	-0.417	-0.316	-0.504	0.110	0.190	0.090	0.056	0.079	0.034
BBO16	-0.282	-0.134	-0.440	0.200	0.330	0.120	0.035	0.043	0.104
BBO17	-0.318	-0.201	-0.361	0.170	0.270	0.150	0.071	0.144	0.078
BBO18	0.013	0.173	0.019	0.490	0.650	0.500	0.048	0.098	0.048
BBO19	-0.230	-0.218	-0.396	0.240	0.250	0.140	0.048	0.096	0.136
BBO20	-0.238	-0.182	-0.402	0.230	0.290	0.140	0.148	0.062	0.077
BBO21	-0.255	-0.286	-0.423	0.220	0.200	0.130	0.039	0.108	0.096
BBO22	-0.560	-0.449	-0.728	0.050	0.110	0.020	0.075	0.056	0.079
BBO23	0.012	0.023	-0.111	0.490	0.480	0.350	0.041	0.075	0.060
BBO24	0.003	-0.125	-0.235	0.480	0.340	0.240	0.080	0.094	0.064
BBO25	-0.069	0.043	-0.167	0.390	0.510	0.300	0.047	0.076	0.054
BBO26	-0.091	-0.180	-0.373	0.360	0.290	0.150	0.079	0.064	0.068
BBO27	-0.040	-0.204	-0.215	0.430	0.270	0.250	0.028	0.056	0.096
BBO28	0.128	-0.143	0.201	0.620	0.320	0.730	0.069	0.016	0.031
BBO29	-0.381	-0.227	-0.151	0.130	0.250	0.310	0.065	0.054	0.056
BBO30	-0.055	0.183	-0.013	0.410	0.660	0.470	0.056	0.053	0.084
BBO31	-0.121	-0.142	-0.196	0.340	0.320	0.270	0.052	0.057	0.039
BBO32	-0.049	-0.085	-0.103	0.420	0.370	0.360	0.040	0.050	0.045
BBO33	-0.040	-0.114	-0.113	0.430	0.340	0.350	0.066	0.059	0.031
BBO34	0.066	0.103	-0.002	0.550	0.580	0.480	0.061	0.057	0.062
BBO35	-0.387	0.257	-0.244	0.120	0.730	0.230	0.178	0.262	0.050
BBO36	-0.469	-0.808	-0.176	0.080	0.010	0.290	0.052	0.059	0.042
BBO37	-0.481	-0.266	-0.435	0.080	0.220	0.120	0.028	0.052	0.040
BBO38	-0.286	-0.516	-0.450	0.190	0.080	0.110	0.024	0.122	0.084
BBO39	-0.272	-0.371	-0.012	0.210	0.150	0.470	0.095	0.079	0.048
BBO39	-0.103	0.227	0.082	0.350	0.700	0.590	0.058	0.233	0.157
BBO40	0.129	-0.050	0.450	0.620	0.410	0.890	0.040	0.117	0.025
BBO41	0.036	0.403	0.545	0.520	0.830	0.920	0.030	0.305	0.381
BBO42	0.169	0.139	0.038	0.670	0.610	0.530	0.055	0.059	0.126
BBO43	-0.328	-0.274	-0.359	0.170	0.210	0.150	0.101	0.040	0.061
BBO44	-0.692	-0.784	-0.636	0.010	0.010	0.050	0.073	0.087	0.035

BBP01	-0.441	-0.453	-0.546	0.090	0.110	0.080	0.075	0.124	0.093
BBP02	-0.515	-0.670	-0.635	0.060	0.030	0.050	0.035	0.072	0.046
BBP03	-0.562	-0.476	-0.586	0.040	0.100	0.060	0.068	0.057	0.063
BBP04	-0.768	-0.872	-0.762	0.000	0.000	0.010	0.052	0.045	0.053
BBP05	-0.605	-0.507	-0.694	0.030	0.090	0.030	0.076	0.094	0.070
BBP06	-0.719	-1.045	-0.645	0.010	0.000	0.040	0.089	0.115	0.040
BBP07	-0.539	-0.520	-0.702	0.050	0.080	0.030	0.031	0.102	0.077
BBP08	-0.514	-0.473	-0.506	0.060	0.110	0.090	0.086	0.100	0.103
BBP09	-0.292	-0.304	-0.456	0.190	0.200	0.110	0.047	0.168	0.141
BBP10	-0.633	-0.808	-0.672	0.020	0.010	0.040	0.095	0.061	0.060
BBP11	-0.775	-0.885	-0.833	0.000	0.000	0.010	0.081	0.094	0.049
BBP12	-0.613	-0.896	-0.805	0.030	0.000	0.010	0.126	0.074	0.108
BBP13	-0.284	-0.370	-0.490	0.200	0.150	0.100	0.060	0.122	0.104
BBP14	-0.199	-0.348	-0.465	0.260	0.170	0.110	0.123	0.077	0.132
BBP15	-0.670	-0.870	-0.858	0.020	0.010	0.000	0.041	0.104	0.080
BBP16	-0.442	-0.580	-0.628	0.090	0.060	0.050	0.053	0.091	0.138
BBP17	-0.630	-0.666	-0.769	0.030	0.040	0.010	0.052	0.129	0.096
BBP18	-0.629	-0.859	-0.745	0.030	0.010	0.020	0.097	0.058	0.060
BBP19	-0.033	-0.142	-0.203	0.440	0.320	0.260	0.062	0.127	0.128
BBP20	-0.455	-0.606	-0.573	0.090	0.050	0.070	0.082	0.076	0.069
BBP21	-0.352	-0.363	-0.500	0.150	0.160	0.100	0.085	0.113	0.143
BBP22	-0.531	-0.581	-0.673	0.060	0.060	0.040	0.061	0.055	0.049
BBP23	-0.091	-0.017	-0.117	0.360	0.440	0.350	0.097	0.145	0.066
BBP24	-0.227	-0.454	-0.468	0.240	0.110	0.110	0.070	0.051	0.089
BBP25	-0.125	-0.170	-0.268	0.330	0.300	0.210	0.063	0.139	0.054
BBP26	-0.637	-0.278	-0.712	0.020	0.210	0.030	0.159	0.106	0.137
BBP27	0.184	0.569	0.282	0.700	0.920	0.800	0.140	0.095	0.105
BBP28	0.116	0.128	0.542	0.610	0.600	0.920	0.045	0.091	0.067
BBP29	-0.298	-0.419	-0.001	0.190	0.120	0.480	0.042	0.095	0.046
BBP30	0.298	0.130	0.079	0.810	0.600	0.580	0.062	0.066	0.055
BBP31	-0.070	-0.193	-0.109	0.390	0.280	0.360	0.045	0.098	0.039
BBP32	0.179	-0.020	0.008	0.690	0.430	0.490	0.028	0.049	0.071
BBP33	0.248	0.258	0.188	0.760	0.730	0.710	0.043	0.071	0.063
BBP34	0.420	0.052	0.084	0.890	0.510	0.590	0.023	0.086	0.078
BBP35	-0.468	-0.775	-0.152	0.080	0.020	0.310	0.020	0.068	0.031
BBP36	-0.402	-0.661	-0.631	0.120	0.040	0.050	0.077	0.068	0.111
BBP37	-0.437	-0.283	-0.428	0.100	0.210	0.130	0.063	0.049	0.142
BBP38	0.049	-0.202	0.183	0.530	0.270	0.710	0.029	0.072	0.050
BBP39	-0.101	-0.350	0.139	0.360	0.170	0.660	0.046	0.077	0.066

BBP40	-0.050	-0.091	-0.254	0.410	0.370	0.220	0.126	0.104	0.051
BBP41	-0.257	-0.150	-0.221	0.220	0.320	0.250	0.059	0.036	0.044
BBP42	-0.584	-0.804	-0.783	0.040	0.010	0.010	0.047	0.070	0.137
BBQ01	-0.067	0.058	-0.156	0.400	0.520	0.310	0.067	0.087	0.075
BBQ02	0.155	0.212	0.160	0.650	0.680	0.680	0.090	0.022	0.062
BBQ03	-0.496	-0.487	0.237	0.070	0.100	0.760	0.076	0.046	0.096
BBQ04	-0.246	-0.494	-0.451	0.230	0.100	0.110	0.034	0.060	0.102
BBQ05	-0.334	0.074	-0.302	0.160	0.540	0.190	0.137	0.083	0.058
BBQ06	-0.047	-0.379	-0.120	0.420	0.150	0.350	0.032	0.082	0.063
BBQ07	-0.407	0.132	-0.023	0.110	0.610	0.460	0.093	0.164	0.118
BBQ08	0.021	-0.064	-0.303	0.500	0.390	0.190	0.109	0.060	0.065
BBQ09	-0.094	0.042	-0.234	0.360	0.510	0.240	0.105	0.059	0.066
BBQ10	-0.330	-0.348	-0.526	0.160	0.170	0.080	0.131	0.060	0.091
BBQ12	-0.847	-0.679	-0.771	0.000	0.030	0.010	0.048	0.036	0.097
BBQ13	-0.931	-1.194	-0.998	0.000	0.000	0.000	0.036	0.042	0.043
BBQ14	-0.850	-0.861	-0.945	0.000	0.010	0.000	0.059	0.043	0.074
BBQ15	-0.579	-0.693	-0.746	0.040	0.030	0.020	0.086	0.059	0.067
BBQ16	-0.621	-0.622	-0.661	0.030	0.050	0.040	0.089	0.099	0.057
BBQ17	-0.455	-0.591	-0.543	0.090	0.060	0.080	0.068	0.089	0.057
BBQ18	-0.666	-0.675	-0.690	0.020	0.030	0.030	0.037	0.142	0.069
BBQ19	-0.472	-0.601	-0.545	0.080	0.050	0.080	0.083	0.135	0.080
BBQ20	-0.311	-0.254	-0.537	0.180	0.230	0.080	0.055	0.148	0.056
BBQ21	-0.341	-0.514	-0.575	0.160	0.090	0.060	0.119	0.072	0.040
BBQ22	-0.721	-0.893	-0.855	0.010	0.000	0.000	0.034	0.135	0.042
BBQ23	-0.620	-0.838	-0.760	0.030	0.010	0.010	0.103	0.077	0.092
BBQ24	-0.543	-0.588	-0.665	0.050	0.060	0.040	0.048	0.079	0.103
BBQ25	-0.502	-0.490	-0.533	0.070	0.100	0.080	0.079	0.085	0.034
BBQ26	-0.163	-0.076	-0.183	0.300	0.380	0.280	0.061	0.078	0.055
BBQ27	-0.386	-0.493	-0.442	0.120	0.100	0.120	0.050	0.086	0.055
BBQ28	-0.413	-0.428	-0.650	0.110	0.120	0.040	0.066	0.101	0.123
BBQ29	-0.801	-1.020	-0.840	0.000	0.000	0.010	0.088	0.053	0.033
BBQ30	0.180	0.052	0.075	0.690	0.510	0.580	0.038	0.103	0.085
BBQ31	-0.542	-0.505	-0.572	0.050	0.090	0.070	0.128	0.053	0.044
BBQ32	-0.219	-0.143	-0.307	0.250	0.320	0.190	0.060	0.096	0.090
BBQ33	-0.334	-0.381	-0.624	0.160	0.150	0.050	0.081	0.039	0.070
BBQ34	0.055	-0.094	-0.132	0.540	0.370	0.340	0.063	0.138	0.026
BBQ34	0.120		-0.150	0.610		0.310	0.195		0.365
BBQ35	0.092	0.108	0.012	0.580	0.580	0.490	0.103	0.069	0.145
BBQ36	-0.001	0.583	0.131	0.480	0.930	0.650	0.052	0.065	0.153

BBQ37	-0.466	-0.518	-0.301	0.080	0.080	0.190	0.077	0.043	0.031
BBQ38	0.001	-0.211	-0.179	0.480	0.260	0.290	0.105	0.038	0.050
BBQ39	-0.035	-0.159	-0.029	0.430	0.310	0.450	0.029	0.113	0.050
BBQ40	0.133	-0.053	-0.006	0.620	0.400	0.470	0.073	0.039	0.006
BBQ41	0.429	0.189	0.361	0.900	0.660	0.850	0.056	0.109	0.025
BBQ42	0.048	0.561	0.167	0.530	0.920	0.690	0.083	0.060	0.096
BBQ42	0.357	0.005	0.128	0.860	0.460	0.640	0.053	0.080	0.037
BBQ43	-0.332	-0.483	-0.092	0.160	0.100	0.370	0.058	0.072	0.036
BBQ44	-0.085	-0.232	-0.208	0.370	0.250	0.260	0.025	0.073	0.128
BBQ45	-0.135	-0.163	-0.328	0.330	0.300	0.170	0.090	0.102	0.152
BBQ46	0.196	0.393	0.085	0.710	0.820	0.600	0.117	0.052	0.048
BBQ47	0.141	-0.382	0.244	0.630	0.150	0.770	0.052	0.135	0.083
BBQ48	0.107	0.167	-0.088	0.600	0.640	0.380	0.060	0.068	0.155
BBQ49	-0.258	-0.533	-0.201	0.220	0.080	0.270	0.075	0.098	0.055
BBQ50	-0.658	-0.666	-0.512	0.020	0.040	0.090	0.049	0.098	0.088
BBQ51	-0.422	-0.665	-0.598	0.100	0.040	0.060	0.021	0.070	0.045
BBQ52	-0.571	-0.789	-0.811	0.040	0.010	0.010	0.052	0.075	0.038
BBQ53	-0.319	-0.584	-0.449	0.170	0.060	0.110	0.063	0.085	0.097
BBQ54	-0.560	-0.595	-0.684	0.050	0.050	0.030	0.114	0.054	0.077
BBQ56	-0.013	0.350	0.168	0.460	0.800	0.690	0.156	0.200	0.120
BBQ60	-0.591	-0.621	-0.657	0.040	0.050	0.040	0.074	0.055	0.057
BBQ63	-0.316	-0.634	-0.549	0.170	0.040	0.080	0.025	0.082	0.066
BBQ65	-0.088	-0.049	-0.216	0.370	0.410	0.250	0.056	0.032	0.040
BBQ66	0.401	0.405	0.160	0.880	0.830	0.680	0.060	0.044	0.053
BBQ67	0.365	0.347	0.029	0.860	0.790	0.520	0.083	0.073	0.074
BBQ69	-0.163	-0.007	-0.287	0.300	0.450	0.200	0.171	0.060	0.045
BBQ71	-0.035	-0.039	-0.187	0.430	0.420	0.280	0.076	0.019	0.062
BBQ72	-0.217	0.369	-0.135	0.250	0.810	0.330	0.149	0.154	0.095
BBQ73	0.139	0.040	0.010	0.630	0.500	0.490	0.039	0.081	0.070
BBQ74	-0.531	-0.268	-0.494	0.060	0.210	0.100	0.132	0.051	0.049
BBQ75	0.171	0.263	0.200	0.680	0.730	0.720	0.100	0.053	0.064
BBQ76	0.410	0.429	0.192	0.890	0.850	0.720	0.065	0.031	0.054
BBQ77	0.160	0.062	0.023	0.660	0.530	0.510	0.070	0.030	0.048
BBQ79	0.322	0.532	0.117	0.830	0.910	0.630	0.086	0.085	0.130
BBQ80	-0.150	-0.230	-0.191	0.310	0.250	0.270	0.086	0.050	0.087
BBQ81	0.307	0.260	0.140	0.820	0.730	0.660	0.035	0.150	0.073
BBQ82	0.360	0.354	0.285	0.860	0.800	0.800	0.070	0.032	0.038
BBQ83	0.297	0.273	0.240	0.810	0.740	0.760	0.084	0.064	0.057
BBQ84	-0.007	0.000	-0.087	0.460	0.460	0.380	0.041	0.054	0.060

BBQ84.1	0.269	0.297	0.061	0.780	0.760	0.560	0.040	0.095	0.060
BBQ85	-0.061	-0.173	-0.309	0.400	0.300	0.190	0.076	0.062	0.087
BBQ86	0.497	0.613	0.389	0.930	0.940	0.860	0.061	0.092	0.041
BBQ87	0.144	0.076	-0.026	0.640	0.550	0.450	0.044	0.053	0.105
BBQ88	-0.351	-0.217	-0.455	0.150	0.260	0.110	0.085	0.100	0.108
BBQ89	0.042	0.031	-0.095	0.530	0.490	0.370	0.040	0.043	0.109
BBR01	-0.407	-0.587	-0.557	0.110	0.060	0.070	0.054	0.107	0.070
BBR02	-0.480	-0.795	-0.735	0.080	0.010	0.020	0.078	0.069	0.030
BBR03	-0.229	-0.324	-0.362	0.240	0.180	0.150	0.053	0.066	0.095
BBR04	-0.152	-0.296	-0.398	0.310	0.200	0.140	0.179	0.136	0.127
BBR05	-0.598	-0.541	-0.507	0.030	0.080	0.090	0.071	0.077	0.106
BBR06	-0.744	-0.780	-0.787	0.010	0.020	0.010	0.043	0.052	0.045
BBR07	-0.498	-0.555	-0.543	0.070	0.070	0.080	0.083	0.102	0.092
BBR08	-0.134	-0.249	-0.324	0.330	0.230	0.180	0.063	0.080	0.139
BBR09	-0.486	-0.549	-0.418	0.080	0.070	0.130	0.078	0.086	0.058
BBR10	-0.460	-0.438	-0.746	0.090	0.120	0.020	0.070	0.065	0.116
BBR11	-0.684	-0.717	-0.667	0.010	0.020	0.040	0.057	0.101	0.101
BBR12	-0.439	-0.611	-0.747	0.090	0.050	0.020	0.081	0.070	0.102
BBR13	-0.232	-0.067	-0.152	0.230	0.390	0.310	0.102	0.124	0.133
BBR14	-0.093	-0.121	-0.323	0.360	0.340	0.180	0.036	0.079	0.104
BBR15	-0.633	-0.647	-0.742	0.020	0.040	0.020	0.052	0.116	0.081
BBR16	-0.187	-0.267	-0.350	0.270	0.220	0.160	0.043	0.072	0.142
BBR17	-0.632	-0.594	-0.750	0.020	0.060	0.010	0.067	0.075	0.082
BBR18	-0.487	-0.749	-0.868	0.070	0.020	0.000	0.073	0.049	0.148
BBR19	-0.073	0.002	-0.148	0.380	0.460	0.320	0.039	0.082	0.085
BBR20	-0.528	-0.702	-0.694	0.060	0.030	0.030	0.036	0.049	0.029
BBR21	0.053	0.070	-0.142	0.540	0.540	0.320	0.161	0.156	0.182
BBR22	-0.648	-0.856	-0.861	0.020	0.010	0.000	0.038	0.082	0.066
BBR23	0.030	0.019	-0.092	0.510	0.480	0.370	0.048	0.128	0.056
BBR24	-0.270	-0.397	-0.444	0.210	0.130	0.120	0.057	0.076	0.065
BBR25	-0.259	-0.238	-0.430	0.210	0.240	0.130	0.102	0.069	0.068
BBR26	-0.389	-0.653	-0.671	0.120	0.040	0.040	0.046	0.066	0.083
BBR27	0.229	0.162	-0.108	0.740	0.640	0.360	0.110	0.085	0.062
BBR28	-0.154	-0.270	-0.074	0.310	0.210	0.390	0.081	0.030	0.059
BBR29	-0.348	-0.591	0.107	0.150	0.060	0.610	0.053	0.064	0.045
BBR30	0.409	0.362	0.134	0.880	0.800	0.650	0.087	0.066	0.113
BBR31	0.073	0.045	-0.033	0.560	0.510	0.440	0.107	0.126	0.101
BBR32	-0.186	-0.205	-0.216	0.280	0.270	0.250	0.050	0.077	0.028
BBR33	-0.213	-0.161	-0.321	0.250	0.310	0.180	0.087	0.110	0.054

BBR34	0.145	-0.050	-0.186	0.640	0.410	0.280	0.027	0.067	0.084
BBR35	0.123	0.100	-0.079	0.610	0.570	0.390	0.044	0.091	0.084
BBR36	-0.397	-0.652	-0.185	0.120	0.040	0.280	0.052	0.062	0.038
BBR37	-0.265	-0.201	-0.333	0.210	0.270	0.170	0.070	0.120	0.084
BBR38	-0.177	-0.316	-0.219	0.280	0.190	0.250	0.085	0.096	0.104
BBR39	0.139	0.205	-0.039	0.630	0.670	0.430	0.024	0.109	0.072
BBR40	0.163	0.292	0.109	0.660	0.760	0.620	0.027	0.025	0.031
BBR41	-0.151	-0.213	0.053	0.310	0.260	0.550	0.065	0.169	0.036
BBR42	0.151	-0.079	0.124	0.640	0.380	0.640	0.051	0.088	0.022
BBR43	-0.032	0.029	-0.272	0.440	0.490	0.210	0.060	0.092	0.092
BBR44	-0.311	-0.518	-0.144	0.180	0.080	0.320	0.068	0.069	0.039
BBR45	-0.559	-0.661	-0.548	0.050	0.040	0.080	0.029	0.147	0.058
BBS01	-0.452	-0.671	-0.565	0.090	0.030	0.070	0.072	0.068	0.057
BBS02	-0.378	-0.546	-0.576	0.130	0.080	0.060	0.049	0.072	0.057
BBS03	0.399	0.370	0.202	0.880	0.810	0.730	0.078	0.103	0.046
BBS04	-0.392	-0.506	-0.614	0.120	0.090	0.050	0.161	0.062	0.044
BBS05	-0.345	-0.501	-0.462	0.160	0.090	0.110	0.047	0.061	0.075
BBS06	-0.671	-0.609	-0.653	0.020	0.050	0.040	0.065	0.078	0.060
BBS07	-0.666	-0.864	-0.854	0.020	0.010	0.000	0.090	0.044	0.070
BBS08	-0.235	-0.095	-0.404	0.230	0.360	0.130	0.063	0.083	0.092
BBS09	-0.281	-0.376	-0.477	0.200	0.150	0.100	0.071	0.070	0.094
BBS10	-0.364	-0.301	-0.376	0.140	0.200	0.150	0.067	0.099	0.052
BBS11	-0.741	-0.814	-0.845	0.010	0.010	0.000	0.093	0.071	0.058
BBS12	-0.510	-0.559	-0.493	0.070	0.070	0.100	0.075	0.121	0.062
BBS13	-0.309	-0.347	-0.484	0.180	0.170	0.100	0.051	0.054	0.088
BBS14	-0.203	-0.114	-0.406	0.260	0.340	0.130	0.125	0.106	0.059
BBS15	-0.489	-0.633	-0.803	0.070	0.040	0.010	0.075	0.056	0.052
BBS16	-0.351	-0.391	-0.426	0.150	0.140	0.130	0.080	0.102	0.155
BBS17	-0.525	-0.726	-0.688	0.060	0.020	0.030	0.045	0.085	0.101
BBS18	-0.384	-0.235	-0.431	0.130	0.240	0.120	0.104	0.099	0.127
BBS19	-0.040	-0.104	-0.197	0.430	0.350	0.270	0.040	0.060	0.047
BBS20	-0.426	-0.369	-0.484	0.100	0.150	0.100	0.058	0.097	0.085
BBS21	-0.198	-0.267	-0.399	0.270	0.220	0.140	0.048	0.067	0.129
BBS22	-0.631	-0.620	-0.758	0.020	0.050	0.010	0.047	0.041	0.062
BBS23	0.075	-0.094	-0.125	0.560	0.360	0.340	0.043	0.069	0.070
BBS24	-0.370	-0.216	-0.386	0.140	0.260	0.140	0.057	0.084	0.078
BBS25	-0.068	-0.371	-0.519	0.390	0.150	0.090	0.040	0.100	0.031
BBS26	-0.413	-0.342	-0.418	0.110	0.170	0.130	0.096	0.144	0.095
BBS27	0.323	0.061	0.035	0.830	0.530	0.530	0.082	0.103	0.037

BBS28	0.165	0.286	-0.142	0.670	0.760	0.320	0.118	0.160	0.154
BBS29	0.148	-0.052	-0.238	0.640	0.400	0.240	0.050	0.068	0.041
BBS30	-0.164	-0.255	0.275	0.300	0.230	0.800	0.094	0.048	0.063
BBS31	-0.486	-0.713	-0.433	0.080	0.020	0.120	0.027	0.090	0.049
BBS32	0.269	0.326	0.160	0.780	0.780	0.680	0.085	0.087	0.033
BBS33	0.036	0.019	0.024	0.520	0.480	0.510	0.014	0.058	0.062
BBS34	-0.231	-0.273	-0.252	0.240	0.210	0.220	0.077	0.066	0.053
BBS35	-0.104	-0.211	-0.238	0.350	0.260	0.230	0.060	0.067	0.037
BBS36	0.200	0.068	-0.030	0.710	0.540	0.450	0.123	0.072	0.061
BBS37	0.721	1.174	0.799	0.980	0.990	0.960	0.232	0.086	0.104
BBS37	0.177	-0.210	-0.046	0.690	0.260	0.420	0.064	0.070	0.070
BBS38	-0.403	-0.408	-0.326	0.120	0.130	0.170	0.120	0.077	0.159
BBS39	-0.389	-0.611	-0.614	0.120	0.050	0.050	0.048	0.053	0.067
BBS40	-0.305	-0.223	-0.395	0.180	0.250	0.140	0.074	0.114	0.116
BBS41	0.156	-0.138	0.226	0.650	0.330	0.750	0.048	0.118	0.051
BBS42	0.342	0.230	0.178	0.850	0.700	0.700	0.066	0.081	0.032
BBS43	0.272	0.651	0.400	0.790	0.950	0.870	0.046	0.061	0.079
BBS44	-0.151	-0.014	-0.284	0.310	0.440	0.210	0.082	0.108	0.089
BBS45	-0.542	-0.659	-0.529	0.050	0.040	0.080	0.071	0.096	0.059
BBT01	0.205	0.228	-0.139	0.720	0.700	0.330	0.109	0.173	0.075
BBT02	0.293	0.389	0.259	0.800	0.820	0.780	0.052	0.057	0.060
BBT03	0.193	0.138	-0.114	0.700	0.610	0.350	0.040	0.126	0.087
BBT04	0.306	0.416	0.228	0.820	0.840	0.750	0.079	0.107	0.130
BBT05	0.159	0.173	-0.052	0.660	0.650	0.420	0.099	0.106	0.059
BBT06	-0.087	-0.087	-0.395	0.370	0.370	0.140	0.092	0.107	0.092
BBT07	0.323	0.016	0.042	0.830	0.470	0.540	0.060	0.060	0.042
BBU01	0.210	0.312	-0.059	0.730	0.770	0.410	0.069	0.129	0.070
BBU02	0.164	-0.020	0.000	0.670	0.430	0.480	0.033	0.119	0.070
BBU03	0.288	0.255	0.059	0.800	0.720	0.560	0.081	0.103	0.038
BBU04	-0.056	-0.217	-0.224	0.410	0.260	0.250	0.093	0.058	0.053
BBU05	0.077	0.064	-0.107	0.570	0.530	0.360	0.037	0.044	0.052
BBU06	0.300	0.402	0.147	0.810	0.830	0.660	0.042	0.178	0.049
BBU07	0.267	0.095	-0.108	0.780	0.570	0.360	0.041	0.064	0.047
BBU08	0.156	0.062	0.026	0.650	0.530	0.520	0.037	0.103	0.088
BBU09	0.080	-0.042	-0.173	0.570	0.410	0.300	0.077	0.053	0.068
BBU10	0.301	0.394	0.105	0.810	0.820	0.610	0.103	0.088	0.103
BBU11	-0.376	-0.334	-0.599	0.140	0.170	0.060	0.087	0.076	0.066
BBU12	0.289	0.020	0.114	0.800	0.480	0.620	0.052	0.194	0.093
BBU-63	0.200	0.094	-0.127	0.710	0.570	0.340	0.039	0.042	0.103

Appendix B. Microarray data from the following conditions (unpublished data): room temperature, pH 6.8; room temperature, pH 8.0; 37°C, pH 7.5; and 37°C, pH 8.0.

	Log Ratios				Percentile Rank				Uncertainty			
gene	RT-6.8	RT-8.0	37-7.5	37-8.0	RT-6.8	RT-8.0	37-7.5	37-8.0	RT-6.8	RT-8.0	37-7.5	37-8.0
BB0001	0.632	0.697	0.583	0.624	0.950	0.980	0.940	0.940	0.067	0.125	0.123	0.094
BB0002	-0.194	-0.263	-0.210	-0.319	0.290	0.210	0.270	0.190	0.060	0.078	0.036	0.063
BB0003		0.601	0.480	0.703		0.950	0.880	0.960		0.215	0.122	0.115
BB0004	0.323	0.245	0.195	0.291	0.790	0.750	0.710	0.770	0.116	0.115	0.018	0.105
BB0005	-0.264	-0.133	-0.279	-0.370	0.220	0.340	0.210	0.160	0.117	0.077	0.069	0.084
BB0006	0.187	0.059	0.020	-0.095	0.680	0.570	0.530	0.420	0.043	0.068	0.081	0.028
BB0007	-0.180	-0.198	-0.118	-0.145	0.310	0.270	0.380	0.360	0.034	0.040	0.052	0.044
BB0008	-0.029	-0.328	-0.059	0.010	0.460	0.160	0.440	0.530	0.158	0.051	0.061	0.061
BB0009	0.144	0.028	-0.080	-0.031	0.650	0.540	0.420	0.490	0.011	0.132	0.091	0.050
BB0010	0.593	0.376	0.404	0.547	0.940	0.840	0.840	0.900	0.073	0.041	0.076	0.109
BB0011	-0.227	-0.265	-0.150	0.110	0.260	0.210	0.330	0.630	0.060	0.021	0.055	0.105
BB0012	0.183	-0.121	-0.010	0.094	0.680	0.360	0.490	0.610	0.135	0.069	0.048	0.043
BB0013	0.017	-0.055	-0.091	0.012	0.520	0.430	0.410	0.530	0.015	0.079	0.040	0.025
BB0014	-0.110	-0.407	-0.214	-0.160	0.370	0.110	0.270	0.340	0.117	0.042	0.047	0.081
BB0015	-0.160	-0.237	0.010	0.029	0.320	0.230	0.520	0.550	0.107	0.066	0.054	0.055
BB0016	0.578	0.620	1.113	1.105	0.930	0.960	0.990	0.990	0.144	0.077	0.029	0.051
BB0017	-0.483	-0.268	-0.264	-0.189	0.070	0.210	0.220	0.320	0.120	0.063	0.069	0.073
BB0018	0.098	-0.270	-0.091	-0.154	0.600	0.200	0.410	0.350	0.095	0.058	0.063	0.054
BB0019	-0.062	-0.067	0.137	0.174	0.420	0.420	0.670	0.680	0.057	0.070	0.052	0.080
BB0020	0.052	-0.009	-0.051	-0.062	0.560	0.490	0.450	0.450	0.069	0.076	0.038	0.060
BB0021	-0.182	-0.136	0.026	0.010	0.300	0.340	0.540	0.530	0.080	0.101	0.049	0.055
BB0022	-0.309	-0.354	-0.125	-0.121	0.180	0.140	0.370	0.390	0.134	0.159	0.046	0.127
BB0023	0.099	0.151	0.462	0.306	0.600	0.660	0.870	0.780	0.083	0.043	0.035	0.033
BB0024	-0.058	-0.157	0.074	0.291	0.430	0.320	0.600	0.770	0.040	0.100	0.017	0.090
BB0025	-0.309	-0.125	0.062	-0.018	0.180	0.350	0.580	0.500	0.033	0.094	0.053	0.113
BB0026	-0.140	-0.103	0.034	-0.088	0.340	0.380	0.540	0.430	0.026	0.096	0.069	0.109
BB0027	-0.128	0.216	0.307	0.204	0.350	0.720	0.780	0.700	0.043	0.223	0.072	0.152
BB0028	-0.014	-0.012	0.042	0.245	0.480	0.490	0.560	0.730	0.041	0.102	0.025	0.114
BB0029	-0.048	0.027	-0.097	-0.039	0.440	0.530	0.400	0.480	0.039	0.095	0.032	0.055

BB0030	0.042	0.013	0.080	0.097	0.540	0.520	0.600	0.620	0.196	0.092	0.060	0.046
BB0031	0.179	0.223	0.483	0.291	0.680	0.730	0.890	0.770	0.035	0.051	0.067	0.075
BB0032	0.017	-0.091	0.275	0.221	0.520	0.390	0.760	0.720	0.137	0.092	0.020	0.076
BB0033	0.092	0.261	0.268	0.210	0.590	0.760	0.750	0.710	0.081	0.047	0.053	0.085
BB0034	-0.097	0.112	0.269	0.222	0.390	0.630	0.760	0.720	0.094	0.210	0.055	0.031
BB0035	0.451	0.545	0.424	0.425	0.860	0.930	0.850	0.840	0.092	0.052	0.044	0.076
BB0036	-0.072	-0.129	-0.010	-0.078	0.420	0.350	0.490	0.440	0.070	0.070	0.030	0.057
BB0037	-0.026	-0.079	-0.028	-0.115	0.460	0.400	0.470	0.400	0.049	0.084	0.061	0.043
BB0038	0.003	-0.109	0.026	-0.150	0.500	0.370	0.540	0.350	0.171	0.065	0.079	0.047
BB0039	-0.013	-0.032	0.059	-0.058	0.480	0.460	0.570	0.460	0.108	0.083	0.029	0.064
BB0040	0.008	-0.088	-0.028	-0.278	0.510	0.390	0.470	0.230	0.100	0.048	0.095	0.066
BB0041	0.525	0.597	0.593	0.616	0.910	0.950	0.940	0.930	0.001	0.047	0.093	0.071
BB0042	0.128	0.110	0.034	0.049	0.630	0.630	0.550	0.570	0.261	0.082	0.090	0.031
BB0043	-0.095	0.074	0.071	0.036	0.390	0.590	0.590	0.560	0.031	0.062	0.069	0.062
BB0044	0.454	0.338	0.676	0.619	0.860	0.820	0.960	0.930	0.153	0.044	0.046	0.053
BB0045	-0.061	0.081	-0.018	-0.097	0.430	0.600	0.480	0.410	0.053	0.063	0.035	0.070
BB0046	-0.055	-0.104	-0.039	-0.297	0.430	0.370	0.460	0.210	0.131	0.057	0.019	0.049
BB0047	0.196	0.450	0.413	0.422	0.690	0.880	0.850	0.840	0.061	0.099	0.106	0.107
BB0048	0.270	0.173	0.147	-0.042	0.750	0.680	0.670	0.480	0.076	0.035	0.014	0.035
BB0049	0.678	0.857	0.871	0.715	0.970	0.990	0.980	0.960	0.127	0.147	0.076	0.150
BB0050	0.029	-0.246	-0.182	-0.352	0.530	0.220	0.300	0.170	0.143	0.080	0.042	0.074
BB0051	-0.063	0.106	0.007	-0.065	0.420	0.630	0.510	0.450	0.068	0.064	0.036	0.034
BB0052	-0.008	-0.171	-0.033	-0.312	0.490	0.300	0.460	0.200	0.114	0.061	0.032	0.056
BB0053	-0.038	0.019	0.074	-0.051	0.450	0.520	0.600	0.470	0.088	0.058	0.035	0.045
BB0054	0.290	0.213	0.542	0.709	0.760	0.720	0.920	0.960	0.031	0.047	0.061	0.062
BB0055	-0.354	-0.098	0.203	0.054	0.150	0.380	0.710	0.580	0.064	0.134	0.097	0.123
BB0056	0.032	0.208	0.726	0.599	0.530	0.710	0.970	0.920	0.064	0.153	0.121	0.147
BB0057	-0.198	0.087	0.886	0.624	0.280	0.600	0.980	0.940	0.155	0.193	0.178	0.228
BB0058	0.146	-0.056	0.249	0.263	0.650	0.430	0.740	0.750	0.108	0.042	0.076	0.079
BB0059	-0.027	0.079	0.190	0.243	0.460	0.600	0.710	0.730	0.127	0.072	0.112	0.124
BB0060	0.774	0.774	1.113	1.317	0.990	0.990	0.990	0.990	0.234	0.070	0.056	0.082
BB0061	0.120	0.442	0.703	1.030	0.630	0.880	0.960	0.990	0.167	0.134	0.108	0.110
BB0062	0.090	0.105	0.127	0.050	0.590	0.620	0.660	0.570	0.036	0.099	0.044	0.068
BB0063	-0.126	0.117	0.279	0.384	0.360	0.640	0.760	0.820	0.074	0.072	0.044	0.093
BB0064	0.031	0.297	0.396	0.472	0.530	0.790	0.840	0.860	0.072	0.219	0.059	0.075
BB0065	-0.222	0.223	0.330	0.310	0.260	0.730	0.790	0.780	0.060	0.109	0.080	0.145
BB0066	0.505	0.397	0.608	0.529	0.890	0.860	0.940	0.890	0.135	0.093	0.043	0.073

BB0067	-0.059	0.303	0.241	0.384	0.430	0.790	0.740	0.820	0.090	0.167	0.114	0.133
BB0068	0.197	0.199	0.767	0.967	0.690	0.710	0.970	0.990	0.033	0.055	0.095	0.110
BB0069	-0.329	0.035	0.291	0.490	0.170	0.540	0.770	0.870	0.039	0.080	0.075	0.169
BB0070	0.032	0.155	0.192	0.383	0.530	0.670	0.710	0.820	0.075	0.159	0.081	0.153
BB0071	-0.128	-0.006	0.171	0.314	0.350	0.500	0.690	0.780	0.068	0.060	0.040	0.097
BB0072	-0.022	-0.124	0.014	0.051	0.470	0.350	0.520	0.580	0.059	0.064	0.033	0.088
BB0073	0.051	0.198	0.164	0.226	0.560	0.710	0.690	0.720	0.079	0.079	0.036	0.110
BB0074	-0.260	-0.363	0.041	0.080	0.220	0.140	0.550	0.600	0.039	0.094	0.044	0.092
BB0075	0.758	0.434	0.581	0.565	0.980	0.880	0.930	0.900	0.086	0.102	0.081	0.049
BB0076	-0.052	-0.232	-0.042	0.116	0.440	0.240	0.460	0.630	0.060	0.061	0.058	0.041
BB0077	0.059	0.101	0.182	0.170	0.560	0.620	0.700	0.680	0.125	0.059	0.039	0.045
BB0078	0.145	-0.002	-0.009	0.014	0.650	0.500	0.490	0.530	0.212	0.110	0.064	0.085
BB0079	0.207	0.387	-0.016	0.022	0.700	0.850	0.490	0.540	0.134	0.094	0.041	0.034
BB0080	-0.094	-0.013	-0.191	-0.124	0.390	0.490	0.290	0.390	0.079	0.071	0.029	0.083
BB0081	0.102	0.204	0.169	0.117	0.600	0.710	0.690	0.630	0.127	0.082	0.121	0.074
BB0082	-0.061	-0.107	0.090	-0.049	0.430	0.370	0.620	0.470	0.109	0.058	0.027	0.056
BB0083	0.360	0.165	0.325	0.238	0.810	0.680	0.790	0.730	0.058	0.055	0.063	0.077
BB0084	-0.028	-0.070	0.049	-0.010	0.460	0.410	0.570	0.510	0.167	0.096	0.027	0.071
BB0085	0.115	0.102	0.006	0.154	0.620	0.620	0.510	0.670	0.074	0.047	0.025	0.081
BB0086	-0.253	-0.231	-0.127	-0.221	0.230	0.240	0.370	0.290	0.170	0.087	0.010	0.056
BB0087	0.040	0.306	0.532	0.358	0.540	0.800	0.920	0.800	0.173	0.086	0.096	0.114
BB0088	0.067	0.050	0.222	0.100	0.570	0.560	0.730	0.620	0.162	0.166	0.076	0.079
BB0089	0.123	0.331	0.217	0.204	0.630	0.810	0.720	0.700	0.023	0.082	0.069	0.116
BB0090	-0.301	-0.098	-0.025	-0.140	0.190	0.380	0.480	0.370	0.110	0.140	0.071	0.081
BB0091	-0.297	0.081	0.176	0.169	0.190	0.600	0.700	0.680	0.074	0.128	0.078	0.091
BB0092	0.447	0.413	0.500	0.354	0.850	0.870	0.900	0.800	0.146	0.035	0.027	0.016
BB0093	-0.397	-0.169	0.085	-0.176	0.110	0.300	0.610	0.330	0.034	0.071	0.046	0.092
BB0094	-0.390	-0.283	-0.291	-0.260	0.120	0.190	0.210	0.250	0.129	0.071	0.102	0.043
BB0095	0.209	0.238	0.389	0.112	0.700	0.740	0.840	0.630	0.072	0.087	0.083	0.069
BB0096	0.028	0.145	0.365	0.016	0.530	0.660	0.820	0.530	0.048	0.094	0.112	0.037
BB0097	0.168	0.104	0.261	0.149	0.670	0.620	0.750	0.660	0.026	0.039	0.061	0.063
BB0098	-0.217	-0.322	-0.342	-0.482	0.260	0.170	0.170	0.090	0.102	0.037	0.024	0.038
BB0099	-0.271	-0.243	-0.116	-0.264	0.210	0.230	0.380	0.250	0.062	0.071	0.026	0.020
BB0100	0.080	0.059	0.139	-0.147	0.580	0.570	0.670	0.360	0.130	0.075	0.054	0.101
BB0101	-0.144	-0.228	0.074	0.041	0.340	0.240	0.600	0.570	0.067	0.041	0.107	0.089
BB0102	0.390	0.154	0.370	0.247	0.830	0.670	0.830	0.740	0.103	0.034	0.059	0.049
BB0103	0.143	0.091	-0.061	0.099	0.640	0.610	0.440	0.620	0.013	0.045	0.066	0.051

BB0104	-0.011	0.211	0.381	0.341	0.490	0.720	0.830	0.800	0.114	0.135	0.107	0.115
BB0105	-0.265	0.034	0.351	0.277	0.220	0.540	0.810	0.760	0.106	0.093	0.078	0.076
BB0106	0.225	0.160	0.408	0.310	0.720	0.670	0.840	0.780	0.049	0.033	0.095	0.077
BB0107	0.460	0.295	0.068	0.317	0.860	0.790	0.590	0.780	0.092	0.097	0.093	0.148
BB0108	-0.089	-0.171	-0.089	-0.278	0.400	0.300	0.410	0.230	0.045	0.067	0.047	0.040
BB0109	-0.155	-0.148	-0.170	-0.214	0.330	0.330	0.310	0.290	0.038	0.099	0.068	0.052
BB0110	0.193	0.062	-0.027	-0.134	0.690	0.580	0.470	0.370	0.037	0.055	0.046	0.062
BB0111	-0.370	0.032	0.094	0.039	0.130	0.540	0.620	0.560	0.071	0.264	0.075	0.099
BB0112	0.343	0.183	0.343	0.268	0.800	0.690	0.810	0.750	0.153	0.149	0.050	0.114
BB0113	0.391	0.558	0.749	0.700	0.830	0.940	0.970	0.960	0.110	0.080	0.132	0.132
BB0114	0.198	0.226	0.615	0.634	0.690	0.730	0.950	0.940	0.129	0.131	0.129	0.120
BB0115	0.035	0.315	0.545	0.487	0.540	0.800	0.920	0.870	0.068	0.189	0.116	0.181
BB0116	-0.189	-0.212	0.008	-0.123	0.300	0.260	0.520	0.390	0.062	0.159	0.045	0.064
BB0117	-0.212	0.019	-0.108	-0.159	0.270	0.520	0.390	0.340	0.043	0.215	0.062	0.062
BB0118	-0.026	-0.134	-0.076	-0.185	0.460	0.340	0.430	0.320	0.044	0.063	0.037	0.063
BB0119	-0.048	0.036	0.036	0.063	0.440	0.540	0.550	0.590	0.039	0.094	0.025	0.093
BB0120	0.298	0.287	0.335	0.491	0.770	0.780	0.800	0.870	0.072	0.066	0.048	0.098
BB0121	0.105	0.253	0.331	0.533	0.610	0.750	0.800	0.890	0.095	0.086	0.105	0.144
BB0122	-0.016	0.078	0.273	0.219	0.480	0.600	0.760	0.720	0.080	0.154	0.061	0.118
BB0123	-0.034	0.204	0.424	0.401	0.450	0.710	0.850	0.820	0.041	0.154	0.095	0.146
BB0124	0.557	0.470	0.552	0.622	0.920	0.890	0.930	0.930	0.034	0.047	0.071	0.059
BB0125	0.149	0.198	0.418	0.478	0.650	0.700	0.850	0.860	0.058	0.120	0.074	0.128
BB0126	0.468	0.406	0.785	0.824	0.870	0.860	0.980	0.980	0.040	0.040	0.070	0.076
BB0127	0.092	0.266	0.495	0.539	0.590	0.760	0.890	0.890	0.021	0.074	0.090	0.105
BB0128	0.212	0.194	0.481	0.468	0.710	0.700	0.880	0.860	0.117	0.057	0.021	0.042
BB0129	0.215	0.249	0.376	0.369	0.710	0.750	0.830	0.810	0.062	0.021	0.038	0.049
BB0130	0.114	0.159	0.305	0.247	0.620	0.670	0.780	0.740	0.231	0.086	0.021	0.056
BB0131	-0.265	0.139	0.162	0.137	0.220	0.660	0.680	0.650	0.083	0.176	0.056	0.087
BB0132	-0.016	0.043	0.278	0.252	0.480	0.550	0.760	0.740	0.049	0.110	0.068	0.109
BB0133	0.577	0.784	1.009	0.907	0.930	0.990	0.990	0.980	0.048	0.088	0.108	0.101
BB0134	-0.138	-0.169	0.128	-0.057	0.340	0.300	0.660	0.460	0.241	0.061	0.053	0.079
BB0135	-0.079	-0.102	0.087	-0.071	0.410	0.380	0.610	0.440	0.071	0.093	0.042	0.072
BB0136	-0.169	-0.094	0.008	-0.134	0.320	0.380	0.520	0.370	0.220	0.087	0.034	0.068
BB0137	0.368	0.633	0.247	0.377	0.820	0.960	0.740	0.810	0.261	0.072	0.047	0.059
BB0138	0.425	0.289	0.461	0.291	0.850	0.780	0.870	0.760	0.184	0.064	0.099	0.052
BB0139	-0.040	-0.005	-0.006	-0.003	0.440	0.500	0.500	0.520	0.051	0.067	0.047	0.051
BB0140	0.622	0.454	0.604	0.721	0.950	0.890	0.940	0.960	0.045	0.091	0.044	0.179

BB0141	0.015	-0.048	-0.007	-0.023	0.510	0.440	0.500	0.500	0.224	0.089	0.088	0.120
BB0142	-0.253	-0.313	-0.131	-0.266	0.230	0.170	0.360	0.240	0.142	0.082	0.037	0.091
BB0143	0.412	0.242	0.375	0.214	0.840	0.740	0.830	0.710	0.130	0.048	0.117	0.051
BB0144	0.113	0.261	0.500	0.564	0.620	0.760	0.900	0.900	0.098	0.131	0.091	0.071
BB0145	-0.029	0.069	-0.052	-0.110	0.460	0.580	0.450	0.400	0.098	0.058	0.066	0.043
BB0146	0.171	0.176	0.170	0.074	0.670	0.690	0.690	0.600	0.087	0.083	0.116	0.070
BB0147	0.238	0.642	0.899	0.779	0.730	0.960	0.990	0.970	0.193	0.215	0.178	0.155
BB0148	0.672	0.639	0.458	0.679	0.970	0.960	0.870	0.950	0.124	0.147	0.030	0.086
BB0149	0.037	0.375	0.531	0.594	0.540	0.840	0.910	0.920	0.156	0.102	0.108	0.105
BB0150	0.602	0.656	0.551	0.644	0.940	0.970	0.930	0.940	0.104	0.079	0.073	0.122
BB0151	-0.645	-0.282	-0.079	-0.179	0.030	0.190	0.420	0.330	0.027	0.148	0.086	0.122
BB0152	-0.386	-0.439	-0.161	-0.290	0.120	0.100	0.320	0.220	0.165	0.067	0.030	0.046
BB0153	0.255	0.246	0.209	0.158	0.750	0.750	0.720	0.670	0.096	0.082	0.024	0.039
BB0154	-0.261	-0.129	0.043	-0.085	0.220	0.350	0.560	0.430	0.073	0.119	0.076	0.063
BB0155	0.136	0.115	0.283	0.312	0.640	0.630	0.770	0.780	0.028	0.051	0.094	0.095
BB0156	0.376	0.350	0.362	0.422	0.820	0.820	0.820	0.830	0.078	0.090	0.082	0.064
BB0157	0.424	0.320	0.306	0.454	0.850	0.810	0.780	0.850	0.098	0.035	0.063	0.105
BB0158	0.307	0.230	0.324	0.476	0.780	0.740	0.790	0.860	0.098	0.053	0.097	0.132
BB0159	0.536	0.635	0.380	0.580	0.910	0.960	0.830	0.910	0.249	0.235	0.123	0.101
BB0160	0.505	0.419	0.232	0.237	0.890	0.870	0.740	0.730	0.109	0.088	0.060	0.058
BB0161	-0.142	-0.010	-0.210	-0.200	0.340	0.490	0.270	0.310	0.077	0.093	0.075	0.033
BB0162	0.508	0.249	0.498	0.177	0.900	0.750	0.900	0.680	0.091	0.037	0.021	0.043
BB0163	0.466	0.503	0.461	0.504	0.870	0.920	0.870	0.880	0.065	0.063	0.032	0.041
BB0164	0.079	-0.226	-0.149	-0.217	0.580	0.240	0.340	0.290	0.132	0.078	0.055	0.045
BB0165	-0.278	0.049	-0.332	-0.233	0.210	0.560	0.180	0.280	0.083	0.089	0.023	0.077
BB0166	-0.057	-0.280	-0.273	-0.223	0.430	0.190	0.220	0.280	0.034	0.035	0.024	0.092
BB0167	-0.296	-0.110	0.116	0.023	0.190	0.370	0.650	0.540	0.048	0.043	0.041	0.024
BB0168	0.299	-0.021	0.102	-0.101	0.770	0.470	0.630	0.410	0.138	0.099	0.062	0.046
BB0169	0.671	0.590	0.615	0.729	0.970	0.950	0.950	0.970	0.080	0.098	0.084	0.066
BB0170	0.172	0.183	-0.083	-0.072	0.670	0.690	0.420	0.440	0.056	0.042	0.109	0.083
BB0171	0.104	0.354	0.111	0.076	0.600	0.830	0.640	0.600	0.040	0.117	0.058	0.055
BB0172	0.151	0.059	0.019	-0.047	0.650	0.570	0.530	0.470	0.065	0.073	0.047	0.021
BB0173	-0.028	0.266	0.203	0.193	0.460	0.760	0.720	0.700	0.130	0.073	0.022	0.048
BB0174	-0.023	-0.166	-0.097	-0.129	0.470	0.310	0.400	0.380	0.091	0.085	0.016	0.043
BB0175	-0.320	-0.063	-0.043	-0.135	0.170	0.420	0.450	0.370	0.049	0.063	0.039	0.040
BB0176	-0.409	-0.387	-0.260	-0.375	0.110	0.130	0.230	0.160	0.036	0.129	0.035	0.113
BB0177	-0.088	-0.123	0.124	0.016	0.400	0.350	0.650	0.530	0.039	0.078	0.024	0.047

BB0178	-0.572	-0.331	-0.285	-0.468	0.040	0.160	0.210	0.100	0.042	0.103	0.061	0.058
BB0179	-0.318	-0.151	-0.078	-0.165	0.170	0.320	0.420	0.340	0.066	0.129	0.055	0.071
BB0180	0.297	0.285	0.276	0.331	0.770	0.780	0.760	0.790	0.037	0.027	0.045	0.076
BB0181	0.772	0.670	0.653	0.626	0.990	0.970	0.960	0.940	0.084	0.100	0.082	0.105
BB0182	-0.531	-0.337	-0.339	-0.307	0.060	0.150	0.170	0.200	0.071	0.079	0.025	0.079
BB0183	0.002	0.008	0.009	-0.005	0.500	0.510	0.520	0.510	0.053	0.055	0.077	0.073
BB0184	0.212	0.130	0.080	0.078	0.710	0.650	0.600	0.600	0.079	0.039	0.076	0.055
BB0185	0.230	0.265	0.044	0.083	0.730	0.760	0.560	0.610	0.071	0.077	0.050	0.072
BB0186	-0.034	0.040	-0.080	-0.056	0.450	0.550	0.420	0.460	0.123	0.069	0.051	0.021
BB0187	0.385	0.405	0.332	0.354	0.820	0.860	0.800	0.800	0.117	0.048	0.039	0.034
BB0188	0.019	0.087	0.042	0.017	0.520	0.610	0.560	0.540	0.241	0.208	0.015	0.055
BB0189	0.624	0.533	0.457	0.579	0.950	0.930	0.870	0.910	0.044	0.066	0.060	0.096
BB0190	0.284	0.315	0.609	0.320	0.760	0.800	0.950	0.780	0.067	0.094	0.127	0.083
BB0191	0.499	0.507	0.481	0.666	0.890	0.920	0.880	0.950	0.127	0.324	0.148	0.075
BB0192	0.100	-0.053	0.055	0.066	0.600	0.440	0.570	0.590	0.140	0.061	0.059	0.065
BB0193	0.597	0.309	0.217	0.447	0.940	0.800	0.720	0.850	0.181	0.147	0.059	0.040
BB0194	0.307	0.213	-0.023	-0.032	0.780	0.720	0.480	0.490	0.075	0.094	0.075	0.079
BB0195	-0.010	-0.067	0.216	-0.123	0.490	0.420	0.720	0.390	0.023	0.084	0.080	0.053
BB0196	-0.415	-0.458	-0.486	-0.605	0.100	0.080	0.090	0.030	0.108	0.058	0.024	0.054
BB0197	-0.039	0.176	0.245	0.379	0.450	0.690	0.740	0.810	0.130	0.047	0.061	0.044
BB0198	-0.385	-0.136	-0.300	-0.292	0.120	0.340	0.200	0.220	0.082	0.087	0.026	0.074
BB0199	0.418	-0.024	-0.126	-0.062	0.840	0.470	0.370	0.450	0.183	0.062	0.043	0.063
BB0200	-0.189	-0.092	-0.069	0.171	0.300	0.390	0.430	0.680	0.162	0.118	0.030	0.033
BB0201	-0.089	0.178	-0.146	0.031	0.400	0.690	0.340	0.560	0.154	0.039	0.022	0.026
BB0202	-0.161	-0.295	-0.144	-0.192	0.320	0.190	0.340	0.310	0.079	0.070	0.070	0.066
BB0203	-0.224	-0.320	-0.183	-0.052	0.260	0.170	0.300	0.460	0.045	0.039	0.069	0.049
BB0204	-0.121	-0.253	-0.010	0.227	0.360	0.220	0.490	0.720	0.064	0.028	0.077	0.097
BB0205	-0.143	-0.231	-0.141	-0.110	0.340	0.240	0.350	0.400	0.024	0.058	0.063	0.085
BB0206	-0.003	-0.152	-0.088	-0.194	0.500	0.320	0.410	0.310	0.079	0.036	0.026	0.052
BB0207	-0.098	-0.198	-0.224	-0.101	0.390	0.270	0.260	0.410	0.019	0.059	0.046	0.064
BB0208	0.209	-0.043	-0.140	-0.185	0.700	0.450	0.350	0.320	0.058	0.055	0.049	0.018
BB0209	-0.087	0.027	-0.082	0.026	0.400	0.530	0.420	0.550	0.101	0.047	0.044	0.044
BB0210	-0.039	-0.066	-0.196	-0.020	0.450	0.420	0.280	0.500	0.077	0.050	0.014	0.050
BB0211	-0.331	-0.246	-0.164	-0.051	0.160	0.230	0.320	0.470	0.043	0.054	0.021	0.064
BB0212	0.572	0.315	0.427	0.901	0.930	0.800	0.850	0.980	0.074	0.077	0.062	0.067
BB0213	-0.135	-0.147	0.101	0.074	0.350	0.330	0.630	0.600	0.080	0.051	0.065	0.065
BB0214	0.088	-0.037	-0.236	-0.235	0.590	0.460	0.250	0.270	0.044	0.078	0.029	0.051

BB0215	0.028	-0.167	0.278	0.261	0.530	0.310	0.760	0.750	0.045	0.025	0.071	0.072
BB0216	0.043	-0.160	0.304	0.145	0.540	0.310	0.780	0.660	0.137	0.063	0.026	0.028
BB0217	-0.354	-0.314	-0.019	-0.020	0.150	0.170	0.480	0.500	0.028	0.047	0.019	0.047
BB0218	-0.276	-0.317	-0.364	-0.364	0.210	0.170	0.160	0.170	0.049	0.114	0.015	0.051
BB0219	-0.542	-0.329	-0.139	-0.208	0.050	0.160	0.350	0.300	0.071	0.128	0.088	0.084
BB0220	-0.375	-0.418	-0.138	-0.153	0.130	0.110	0.350	0.350	0.040	0.135	0.045	0.073
BB0221	-0.190	-0.086	-0.027	0.024	0.290	0.400	0.470	0.550	0.047	0.092	0.061	0.039
BB0222	0.154	0.059	-0.034	0.007	0.660	0.580	0.460	0.520	0.070	0.115	0.103	0.076
BB0223	0.238	0.248	0.061	0.213	0.730	0.750	0.580	0.710	0.069	0.032	0.092	0.056
BB0224	0.329	0.122	0.046	0.232	0.790	0.640	0.560	0.720	0.057	0.043	0.041	0.078
BB0225	-0.085	0.007	-0.037	-0.065	0.400	0.510	0.460	0.450	0.100	0.064	0.049	0.051
BB0226	-0.381	-0.358	-0.149	-0.210	0.120	0.140	0.340	0.290	0.152	0.112	0.023	0.027
BB0227	-0.028	-0.050	0.067	0.045	0.460	0.440	0.590	0.570	0.122	0.088	0.049	0.061
BB0228	-0.124	-0.047	-0.093	-0.083	0.360	0.440	0.400	0.430	0.061	0.104	0.031	0.060
BB0229	0.289	0.347	0.333	0.282	0.760	0.820	0.800	0.760	0.051	0.036	0.057	0.117
BB0230	-0.207	-0.061	0.004	-0.074	0.270	0.430	0.510	0.440	0.041	0.115	0.046	0.092
BB0231	0.447	0.583	0.887	0.958	0.850	0.940	0.980	0.990	0.081	0.032	0.063	0.072
BB0232	0.478	0.653	0.770	0.824	0.880	0.970	0.970	0.980	0.170	0.116	0.091	0.083
BB0233	0.572	0.550	0.659	0.788	0.930	0.930	0.960	0.970	0.128	0.105	0.075	0.111
BB0234	0.226	0.113	0.108	0.053	0.720	0.630	0.640	0.580	0.052	0.032	0.018	0.047
BB0235	-0.376	-0.015	-0.012	-0.002	0.130	0.480	0.490	0.520	0.141	0.081	0.056	0.089
BB0236	-0.043	0.147	0.139	0.107	0.440	0.660	0.670	0.630	0.073	0.103	0.102	0.083
BB0237	-0.259	-0.066	0.050	0.090	0.220	0.420	0.570	0.610	0.014	0.045	0.066	0.080
BB0238	0.033	0.211	0.260	0.395	0.540	0.720	0.750	0.820	0.038	0.139	0.081	0.116
BB0239	0.218	0.071	-0.155	-0.063	0.710	0.590	0.330	0.450	0.207	0.059	0.052	0.095
BB0240	-0.100	-0.243	-0.269	-0.066	0.380	0.230	0.220	0.450	0.084	0.065	0.026	0.093
BB0241	-0.286	-0.373	-0.393	0.041	0.200	0.130	0.140	0.560	0.178	0.081	0.054	0.149
BB0242	0.190	0.032	0.054	0.167	0.690	0.540	0.570	0.670	0.145	0.050	0.059	0.110
BB0243	-0.238	-0.057	-0.178	0.045	0.250	0.430	0.300	0.570	0.192	0.030	0.055	0.131
BB0244	-0.074	-0.087	0.077	-0.117	0.410	0.390	0.600	0.400	0.156	0.072	0.168	0.086
BB0245	0.000	0.062	-0.008	0.036	0.500	0.580	0.490	0.560	0.024	0.057	0.039	0.098
BB0246	-0.294	-0.216	-0.145	-0.193	0.200	0.250	0.340	0.310	0.106	0.079	0.055	0.054
BB0247	0.073	0.049	0.090	0.105	0.580	0.560	0.620	0.620	0.081	0.034	0.050	0.094
BB0248	-0.312	-0.448	-0.179	-0.298	0.180	0.090	0.300	0.210	0.173	0.022	0.011	0.075
BB0249	-0.244	0.078	-0.139	-0.029	0.240	0.600	0.350	0.490	0.044	0.171	0.049	0.072
BB0250	0.213	-0.018	0.041	0.054	0.710	0.480	0.560	0.580	0.134	0.048	0.048	0.026
BB0251	-0.019	0.106	0.153	0.247	0.480	0.630	0.680	0.740	0.123	0.080	0.083	0.124

BB0252	-0.046	-0.179	-0.148	-0.018	0.440	0.290	0.340	0.500	0.105	0.087	0.064	0.065
BB0253	-0.154	-0.045	-0.083	0.014	0.330	0.450	0.420	0.530	0.073	0.104	0.083	0.060
BB0254	-0.335	-0.409	-0.264	-0.319	0.160	0.110	0.220	0.190	0.066	0.030	0.057	0.062
BB0255	0.027	-0.346	-0.139	-0.271	0.530	0.150	0.350	0.240	0.127	0.017	0.051	0.059
BB0256	0.614	0.301	0.736	0.478	0.950	0.790	0.970	0.860	0.035	0.046	0.034	0.056
BB0257	-0.344	-0.514	-0.297	-0.446	0.150	0.060	0.200	0.120	0.132	0.061	0.089	0.059
BB0258	-0.319	-0.318	-0.266	-0.243	0.170	0.170	0.220	0.270	0.038	0.022	0.053	0.066
BB0259	0.117	-0.085	-0.198	-0.220	0.620	0.400	0.280	0.290	0.028	0.047	0.030	0.039
BB0260	0.180	0.179	-0.038	0.010	0.680	0.690	0.460	0.530	0.034	0.065	0.037	0.067
BB0261	0.164	-0.044	0.119	0.172	0.660	0.450	0.650	0.680	0.103	0.089	0.053	0.098
BB0262	-0.320	0.105	0.108	0.121	0.170	0.620	0.640	0.640	0.065	0.059	0.033	0.031
BB0263	0.295	0.107	0.051	-0.131	0.770	0.630	0.570	0.380	0.079	0.043	0.029	0.046
BB0264	-0.083	-0.031	-0.199	-0.180	0.400	0.460	0.280	0.330	0.083	0.110	0.047	0.036
BB0265	0.151	0.012	0.048	0.107	0.650	0.510	0.560	0.630	0.102	0.102	0.039	0.064
BB0266	0.545	0.417	0.453	0.545	0.920	0.870	0.870	0.890	0.092	0.044	0.026	0.044
BB0267	-0.153	0.198	0.360	0.354	0.330	0.700	0.820	0.800	0.072	0.130	0.058	0.078
BB0268	0.299	0.317	0.376	0.467	0.770	0.800	0.830	0.860	0.052	0.119	0.107	0.138
BB0269	-0.189	0.179	0.004	0.025	0.300	0.690	0.510	0.550	0.069	0.144	0.069	0.102
BB0270	-0.022	-0.002	0.033	-0.032	0.470	0.500	0.540	0.490	0.044	0.074	0.039	0.061
BB0271	-0.424	-0.045	0.039	-0.142	0.100	0.450	0.550	0.360	0.128	0.162	0.078	0.107
BB0272	0.008	0.287	0.303	0.158	0.510	0.780	0.780	0.670	0.051	0.090	0.038	0.039
BB0273	0.009	0.139	0.014	-0.065	0.510	0.650	0.520	0.450	0.057	0.025	0.059	0.091
BB0274	0.417	0.379	0.269	0.277	0.840	0.850	0.750	0.760	0.106	0.110	0.092	0.137
BB0275	-0.128	-0.025	0.024	-0.005	0.360	0.470	0.530	0.510	0.054	0.080	0.026	0.042
BB0276	0.537	0.530	0.338	0.428	0.910	0.930	0.800	0.840	0.099	0.051	0.047	0.059
BB0277	0.073	0.366	0.439	0.409	0.580	0.840	0.860	0.830	0.175	0.074	0.075	0.076
BB0278	-0.129	0.016	0.126	0.036	0.350	0.520	0.660	0.560	0.042	0.077	0.063	0.067
BB0279	-0.062	0.166	0.264	0.245	0.420	0.680	0.750	0.730	0.042	0.036	0.060	0.110
BB0280	-0.132	-0.133	0.097	0.040	0.350	0.340	0.630	0.560	0.059	0.070	0.027	0.078
BB0281	-0.309	-0.097	-0.087	-0.193	0.180	0.380	0.410	0.310	0.054	0.111	0.037	0.082
BB0282	0.327	0.155	0.382	0.338	0.790	0.670	0.830	0.790	0.116	0.058	0.058	0.091
BB0283	-0.302	-0.091	0.015	-0.105	0.190	0.390	0.520	0.410	0.074	0.143	0.099	0.123
BB0284	0.179	0.307	0.598	0.629	0.680	0.800	0.940	0.940	0.160	0.046	0.022	0.046
BB0285	0.370	0.323	0.488	0.443	0.820	0.810	0.890	0.850	0.129	0.063	0.059	0.085
BB0286	-0.173	-0.111	0.112	-0.202	0.310	0.370	0.640	0.300	0.094	0.076	0.172	0.066
BB0287	-0.035	0.155	0.001	-0.066	0.450	0.670	0.510	0.450	0.065	0.163	0.031	0.039
BB0288	-0.335	-0.163	-0.211	-0.347	0.160	0.310	0.270	0.180	0.053	0.100	0.040	0.049

BB0289	-0.038	0.121	0.182	0.052	0.450	0.640	0.700	0.580	0.059	0.053	0.098	0.075
BB0290	-0.102	-0.124	0.064	-0.077	0.380	0.350	0.580	0.440	0.137	0.084	0.040	0.064
BB0291	-0.195	-0.063	0.173	-0.085	0.290	0.420	0.700	0.430	0.145	0.089	0.116	0.094
BB0292	-0.150	-0.108	-0.222	-0.326	0.330	0.370	0.260	0.190	0.037	0.025	0.029	0.057
BB0293	0.100	0.160	0.059	0.021	0.600	0.670	0.570	0.540	0.190	0.073	0.046	0.043
BB0294	0.571	0.603	0.800	0.842	0.930	0.950	0.980	0.980	0.211	0.056	0.102	0.076
BB0295	-0.138	-0.104	-0.077	-0.244	0.340	0.380	0.430	0.260	0.052	0.063	0.071	0.076
BB0296	-0.508	-0.380	-0.276	-0.484	0.060	0.130	0.220	0.090	0.119	0.089	0.036	0.006
BB0297	-0.237	-0.053	-0.002	-0.263	0.250	0.440	0.500	0.250	0.086	0.059	0.077	0.035
BB0298	0.028	0.074	0.203	0.003	0.530	0.590	0.720	0.520	0.179	0.052	0.043	0.042
BB0299	-0.603	-0.241	-0.185	-0.348	0.040	0.230	0.290	0.180	0.051	0.131	0.072	0.035
BB0300	-0.343	-0.122	-0.063	-0.278	0.160	0.360	0.440	0.230	0.056	0.183	0.100	0.098
BB0301	0.366	0.215	0.012	0.207	0.810	0.720	0.520	0.700	0.100	0.081	0.062	0.037
BB0302	-0.078	-0.268	-0.212	-0.282	0.410	0.210	0.270	0.230	0.099	0.029	0.050	0.057
BB0303	-0.345	-0.233	-0.124	0.013	0.150	0.240	0.370	0.530	0.122	0.048	0.045	0.059
BB0304	0.693	0.537	0.474	0.545	0.970	0.930	0.880	0.890	0.057	0.082	0.046	0.126
BB0305	0.178	0.123	0.143	0.316	0.680	0.640	0.670	0.780	0.078	0.035	0.058	0.054
BB0306	0.016	-0.074	-0.218	-0.303	0.520	0.410	0.260	0.210	0.054	0.059	0.077	0.036
BB0307	0.226	0.168	0.329	0.322	0.720	0.680	0.790	0.790	0.053	0.072	0.061	0.036
BB0308	0.427	0.228	0.073	0.216	0.850	0.730	0.600	0.710	0.102	0.074	0.078	0.097
BB0309	0.051	0.034	-0.141	0.076	0.560	0.540	0.350	0.600	0.040	0.100	0.045	0.056
BB0310	0.518	0.491	0.304	0.491	0.900	0.910	0.780	0.870	0.048	0.141	0.037	0.087
BB0311	-0.187	-0.046	-0.033	-0.090	0.300	0.450	0.460	0.420	0.051	0.072	0.020	0.027
BB0312	-0.026	0.106	-0.065	-0.013	0.460	0.630	0.430	0.510	0.073	0.179	0.069	0.090
BB0313	0.017	-0.014	0.254	0.174	0.520	0.480	0.750	0.680	0.037	0.078	0.029	0.072
BB0314	-0.028	-0.218	-0.286	-0.350	0.460	0.250	0.210	0.180	0.059	0.031	0.024	0.051
BB0315	0.120	-0.019	-0.042	0.064	0.630	0.480	0.460	0.590	0.027	0.045	0.036	0.051
BB0316	0.059	-0.055	-0.299	-0.189	0.570	0.430	0.200	0.320	0.084	0.077	0.042	0.110
BB0317	-0.016	0.029	0.013	-0.039	0.480	0.540	0.520	0.480	0.031	0.057	0.015	0.069
BB0318	0.122	0.046	-0.021	-0.142	0.630	0.560	0.480	0.360	0.022	0.058	0.018	0.050
BB0319	-0.187	-0.037	-0.162	-0.054	0.300	0.460	0.320	0.460	0.097	0.042	0.030	0.031
BB0320	0.661	0.830	0.723	0.660	0.960	0.990	0.970	0.940	0.243	0.094	0.129	0.254
BB0321	0.528	0.226	0.367	0.539	0.910	0.730	0.820	0.890	0.052	0.137	0.046	0.067
BB0322	0.150	0.140	-0.002	-0.043	0.650	0.660	0.500	0.480	0.059	0.036	0.077	0.029
BB0323	-0.052	-0.025	0.081	-0.006	0.430	0.470	0.610	0.510	0.047	0.089	0.071	0.141
BB0324	0.143	0.167	-0.009	0.035	0.650	0.680	0.490	0.560	0.020	0.066	0.034	0.024
BB0325	-0.447	-0.296	-0.305	-0.226	0.090	0.180	0.190	0.280	0.080	0.114	0.023	0.111

BB0326	-0.022	-0.036	-0.005	-0.125	0.470	0.460	0.500	0.390	0.051	0.038	0.038	0.054
BB0327	0.314	0.464	0.440	0.242	0.780	0.890	0.860	0.730	0.143	0.081	0.121	0.080
BB0328	-0.123	-0.149	-0.222	-0.280	0.360	0.330	0.260	0.230	0.083	0.041	0.050	0.055
BB0329	-0.288	-0.205	-0.242	-0.290	0.200	0.260	0.240	0.220	0.100	0.078	0.065	0.038
BB0330	-0.141	-0.169	-0.225	-0.332	0.340	0.300	0.250	0.190	0.043	0.037	0.046	0.079
BB0331	0.528	0.480	0.491	0.452	0.910	0.900	0.890	0.850	0.024	0.041	0.060	0.064
BB0332	0.048	0.166	0.055	-0.004	0.550	0.680	0.570	0.520	0.047	0.047	0.036	0.093
BB0333	-0.383	-0.204	-0.318	-0.366	0.120	0.260	0.190	0.160	0.043	0.096	0.008	0.044
BB0334	-0.304	-0.199	-0.144	-0.247	0.180	0.270	0.340	0.260	0.042	0.108	0.038	0.077
BB0335	-0.263	-0.200	-0.204	-0.207	0.220	0.270	0.280	0.300	0.073	0.062	0.035	0.072
BB0336	0.129	0.253	0.154	0.031	0.630	0.750	0.680	0.550	0.035	0.022	0.084	0.079
BB0337	-0.194	-0.104	0.065	-0.139	0.290	0.370	0.580	0.370	0.091	0.133	0.092	0.121
BB0338	0.464	0.807	0.858	0.940	0.860	0.990	0.980	0.990	0.190	0.072	0.063	0.078
BB0339	0.371	0.503	0.713	0.842	0.820	0.920	0.970	0.980	0.092	0.104	0.113	0.106
BB0340	0.211	0.368	0.168	0.176	0.710	0.840	0.690	0.680	0.123	0.066	0.015	0.051
BB0341	-0.326	-0.192	-0.239	-0.303	0.170	0.280	0.240	0.210	0.071	0.078	0.044	0.042
BB0342	-0.343	-0.071	-0.127	-0.147	0.160	0.410	0.370	0.360	0.047	0.089	0.056	0.081
BB0343	0.370	0.096	0.032	0.133	0.820	0.620	0.540	0.650	0.103	0.077	0.045	0.080
BB0344	-0.002	0.284	0.004	0.025	0.500	0.770	0.510	0.550	0.182	0.080	0.034	0.058
BB0345	0.130	-0.014	-0.152	-0.146	0.630	0.480	0.330	0.360	0.098	0.080	0.041	0.076
BB0346	0.015	0.051	-0.216	-0.183	0.510	0.560	0.260	0.320	0.103	0.033	0.049	0.066
BB0347	-0.108	-0.107	0.035	-0.212	0.370	0.370	0.550	0.290	0.072	0.014	0.132	0.034
BB0348	-0.304	-0.167	0.260	0.198	0.190	0.310	0.750	0.700	0.044	0.103	0.093	0.144
BB0349	0.172	0.058	0.115	0.279	0.670	0.570	0.650	0.760	0.112	0.049	0.053	0.112
BB0350	0.009	-0.005	-0.182	-0.022	0.510	0.500	0.300	0.500	0.082	0.037	0.024	0.156
BB0351	-0.062	-0.041	-0.098	-0.133	0.420	0.450	0.400	0.380	0.181	0.053	0.052	0.035
BB0352	0.229	-0.071	-0.104	-0.164	0.730	0.410	0.390	0.340	0.079	0.071	0.040	0.045
BB0353	0.179	0.059	0.066	0.150	0.680	0.570	0.580	0.660	0.088	0.052	0.067	0.037
BB0354	0.469	0.426	0.518	0.511	0.870	0.870	0.910	0.880	0.090	0.043	0.081	0.054
BB0355	0.323	0.327	0.445	0.382	0.790	0.810	0.860	0.810	0.170	0.098	0.083	0.060
BB0356	0.341	0.188	0.034	0.102	0.800	0.700	0.540	0.620	0.038	0.066	0.055	0.065
BB0357	0.483	0.318	0.385	0.489	0.880	0.800	0.840	0.870	0.093	0.045	0.078	0.070
BB0358	0.067	-0.117	-0.316	-0.365	0.570	0.360	0.190	0.160	0.043	0.024	0.036	0.049
BB0359	-0.135	-0.144	-0.310	-0.266	0.350	0.330	0.190	0.240	0.107	0.037	0.052	0.073
BB0360	0.475	0.237	0.195	0.347	0.870	0.740	0.710	0.800	0.069	0.056	0.043	0.077
BB0361	-0.222	-0.152	-0.137	-0.043	0.260	0.320	0.360	0.480	0.046	0.087	0.030	0.082
BB0362	-0.295	-0.189	0.071	0.242	0.190	0.280	0.590	0.730	0.155	0.058	0.034	0.053

BB0363	-0.336	-0.044	-0.131	0.023	0.160	0.450	0.360	0.540	0.087	0.055	0.017	0.042
BB0364	-0.250	-0.057	-0.243	-0.055	0.230	0.430	0.240	0.460	0.020	0.194	0.022	0.090
BB0365	-0.026	-0.117	-0.103	-0.229	0.460	0.360	0.400	0.280	0.150	0.076	0.033	0.063
BB0366	-0.529	-0.151	0.102	0.464	0.060	0.320	0.630	0.850	0.173	0.082	0.019	0.171
BB0367	0.326	0.128	0.111	0.236	0.790	0.650	0.640	0.730	0.085	0.037	0.026	0.086
BB0368	-0.225	-0.072	-0.089	-0.068	0.260	0.410	0.410	0.450	0.054	0.074	0.038	0.061
BB0369	-0.034	-0.153	-0.295	-0.213	0.450	0.320	0.200	0.290	0.043	0.055	0.024	0.043
BB0370	-0.247	-0.166	-0.254	-0.159	0.230	0.310	0.230	0.340	0.051	0.040	0.026	0.033
BB0371	-0.307	-0.369	-0.372	-0.344	0.180	0.140	0.150	0.180	0.051	0.053	0.020	0.067
BB0372	-0.421	-0.287	-0.362	-0.327	0.100	0.190	0.160	0.190	0.040	0.056	0.029	0.037
BB0373	0.207	0.140	0.115	0.060	0.700	0.660	0.650	0.580	0.021	0.035	0.060	0.043
BB0374	0.039	-0.021	0.109	0.234	0.540	0.470	0.640	0.730	0.093	0.043	0.013	0.092
BB0375	0.113	-0.085	-0.314	-0.116	0.610	0.400	0.190	0.400	0.120	0.037	0.039	0.037
BB0376	-0.496	-0.443	-0.416	-0.308	0.070	0.090	0.130	0.200	0.028	0.114	0.028	0.076
BB0377	0.009	0.001	-0.065	-0.071	0.510	0.500	0.430	0.440	0.069	0.045	0.085	0.050
BB0378	0.191	0.216	0.045	0.090	0.690	0.720	0.560	0.610	0.048	0.070	0.028	0.042
BB0379	-0.023	0.020	-0.174	-0.105	0.470	0.530	0.310	0.410	0.043	0.059	0.050	0.075
BB0380	-0.391	-0.197	-0.276	-0.308	0.120	0.270	0.220	0.200	0.029	0.107	0.020	0.055
BB0381	0.223	0.389	0.371	0.293	0.720	0.850	0.830	0.770	0.062	0.061	0.078	0.074
BB0382	-0.364	-0.253	-0.223	-0.191	0.140	0.220	0.260	0.320	0.049	0.122	0.032	0.045
BB0383	-0.286	-0.135	-0.194	-0.286	0.200	0.340	0.280	0.220	0.026	0.142	0.064	0.072
BB0384	-0.226	0.064	0.121	-0.021	0.260	0.580	0.650	0.500	0.129	0.079	0.052	0.077
BB0385	-0.174	0.075	-0.199	-0.102	0.310	0.590	0.280	0.410	0.125	0.171	0.069	0.070
BB0386	0.549	0.617	0.817	0.688	0.920	0.960	0.980	0.950	0.121	0.110	0.117	0.135
BB0387	-0.055	0.213	0.493	0.096	0.430	0.720	0.890	0.620	0.060	0.224	0.135	0.119
BB0388	-0.173	0.036	0.109	0.128	0.310	0.550	0.640	0.640	0.092	0.112	0.087	0.113
BB0389	-0.369	-0.052	0.074	-0.027	0.130	0.440	0.600	0.500	0.069	0.162	0.105	0.088
BB0390	-0.373	0.088	-0.288	-0.165	0.130	0.610	0.210	0.340	0.091	0.094	0.076	0.068
BB0391	-0.165	0.054	0.029	-0.069	0.320	0.570	0.540	0.440	0.081	0.117	0.075	0.085
BB0392	0.013	0.265	0.327	0.155	0.510	0.760	0.790	0.670	0.077	0.169	0.068	0.141
BB0393	-0.023	0.129	0.270	0.117	0.470	0.650	0.760	0.630	0.110	0.218	0.131	0.141
BB0394	0.242	0.506	0.539	0.435	0.740	0.920	0.920	0.840	0.053	0.097	0.071	0.142
BB0395	0.218	0.319	0.423	0.328	0.710	0.800	0.850	0.790	0.098	0.102	0.093	0.119
BB0396	0.413	0.582	0.566	0.662	0.840	0.940	0.930	0.950	0.099	0.109	0.072	0.051
BB0397	-0.030	-0.182	-0.026	-0.192	0.460	0.290	0.470	0.310	0.030	0.044	0.114	0.049
BB0398	0.010	0.015	0.338	0.045	0.510	0.520	0.800	0.570	0.272	0.028	0.047	0.071
BB0399	0.214	0.213	0.060	0.154	0.710	0.720	0.580	0.670	0.073	0.119	0.078	0.105

BB0400	-0.006	0.292	-0.017	-0.145	0.490	0.780	0.480	0.360	0.169	0.175	0.060	0.054
BB0401	-0.063	-0.007	0.119	-0.016	0.420	0.490	0.650	0.510	0.049	0.049	0.047	0.055
BB0402	-0.425	-0.358	-0.194	-0.226	0.100	0.140	0.290	0.280	0.061	0.034	0.085	0.058
BB0403	0.246	0.125	0.053	-0.035	0.740	0.640	0.570	0.490	0.038	0.046	0.048	0.080
BB0404	0.552	0.347	0.992	0.709	0.920	0.820	0.990	0.960	0.156	0.080	0.059	0.032
BB0405	-0.337	-0.238	-0.032	-0.137	0.160	0.230	0.470	0.370	0.061	0.071	0.104	0.086
BB0406	0.020	0.062	0.092	-0.128	0.520	0.580	0.620	0.380	0.139	0.096	0.106	0.071
BB0407	-0.186	-0.370	-0.336	-0.445	0.300	0.140	0.180	0.120	0.146	0.040	0.032	0.042
BB0408	0.344	0.273	0.276	0.397	0.800	0.770	0.760	0.820	0.036	0.040	0.054	0.115
BB0409	0.121	-0.116	-0.128	-0.240	0.630	0.360	0.370	0.270	0.076	0.061	0.040	0.036
BB0410	0.390	0.463	0.266	0.501	0.830	0.890	0.750	0.870	0.038	0.103	0.075	0.151
BB0411	0.074	-0.021	-0.151	-0.265	0.580	0.470	0.330	0.240	0.042	0.126	0.058	0.085
BB0412	0.046	-0.176	-0.125	-0.137	0.550	0.290	0.370	0.370	0.137	0.124	0.053	0.060
BB0413	0.190	0.001	-0.063	-0.061	0.690	0.500	0.440	0.450	0.024	0.112	0.061	0.075
BB0414	-0.061	-0.240	-0.193	-0.244	0.430	0.230	0.290	0.260	0.088	0.089	0.124	0.104
BB0415	-0.025	-0.121	-0.117	-0.103	0.470	0.360	0.380	0.410	0.038	0.035	0.061	0.034
BB0416	-0.202	-0.111	-0.106	-0.136	0.280	0.370	0.390	0.370	0.040	0.070	0.035	0.040
BB0417	0.118	-0.011	-0.025	-0.127	0.620	0.490	0.480	0.390	0.103	0.043	0.033	0.023
BB0418	-0.386	-0.008	0.021	-0.058	0.120	0.490	0.530	0.460	0.139	0.070	0.065	0.030
BB0419	-0.140	0.120	-0.032	-0.142	0.340	0.640	0.470	0.360	0.032	0.095	0.059	0.048
BB0420	-0.271	0.058	0.085	-0.030	0.210	0.570	0.610	0.490	0.164	0.100	0.028	0.077
BB0421	0.320	0.589	0.470	0.332	0.790	0.950	0.880	0.790	0.066	0.087	0.039	0.043
BB0422	0.019	0.351	0.296	0.166	0.520	0.830	0.780	0.670	0.143	0.058	0.035	0.030
BB0423	0.222	0.473	0.499	0.331	0.720	0.900	0.900	0.790	0.100	0.153	0.040	0.046
BB0424	0.437	0.767	0.715	0.664	0.850	0.980	0.970	0.950	0.066	0.118	0.043	0.067
BB0425	0.852	0.743	1.188	1.134	0.990	0.980	0.990	0.990	0.093	0.104	0.056	0.072
BB0426	0.442	0.852	1.090	0.914	0.850	0.990	0.990	0.990	0.156	0.089	0.060	0.072
BB0427	0.178	0.282	0.241	0.146	0.670	0.770	0.740	0.660	0.097	0.021	0.040	0.022
BB0428	0.240	0.289	0.353	0.359	0.740	0.780	0.810	0.800	0.080	0.047	0.010	0.102
BB0429	0.144	0.189	0.124	0.017	0.650	0.700	0.650	0.530	0.036	0.048	0.030	0.045
BB0430	0.129	0.171	0.113	0.024	0.630	0.680	0.640	0.540	0.088	0.055	0.029	0.034
BB0431	0.112	0.077	0.004	-0.044	0.610	0.590	0.510	0.470	0.033	0.060	0.029	0.077
BB0432	0.215	0.303	0.311	0.201	0.710	0.790	0.780	0.700	0.092	0.045	0.067	0.068
BB0433	0.648	0.638	0.757	0.713	0.960	0.960	0.970	0.960	0.022	0.023	0.039	0.044
BB0434	0.196	0.227	0.168	0.067	0.690	0.730	0.690	0.590	0.037	0.058	0.060	0.112
BB0435	0.110	0.499	0.546	0.550	0.610	0.910	0.920	0.900	0.149	0.117	0.105	0.107
BB0436	0.169	0.667	0.653	0.731	0.670	0.970	0.960	0.970	0.160	0.126	0.092	0.083

BB0437	-0.118	-0.015	-0.000	-0.095	0.370	0.480	0.510	0.420	0.125	0.019	0.050	0.091
BB0438	0.464	0.252	0.187	0.140	0.870	0.750	0.700	0.650	0.149	0.032	0.035	0.052
BB0439	0.328	0.343	0.155	0.225	0.790	0.820	0.680	0.720	0.085	0.057	0.036	0.078
BB0440	0.450	0.648	0.693	0.621	0.860	0.970	0.960	0.930	0.109	0.109	0.045	0.135
BB0441	0.235	0.260	0.132	0.154	0.730	0.760	0.660	0.670	0.028	0.059	0.027	0.036
BB0442	-0.008	0.169	0.060	0.061	0.490	0.680	0.580	0.590	0.030	0.065	0.046	0.078
BB0443	0.166	0.307	0.490	0.589	0.670	0.800	0.890	0.920	0.085	0.056	0.070	0.083
BB0444	-0.191	0.039	0.164	0.158	0.290	0.550	0.690	0.670	0.099	0.103	0.096	0.132
BB0445	-0.009	0.179	0.345	0.220	0.490	0.690	0.810	0.720	0.062	0.144	0.096	0.088
BB0446	-0.021	-0.056	-0.175	-0.159	0.470	0.430	0.300	0.340	0.211	0.048	0.051	0.100
BB0447	-0.135	-0.201	-0.167	-0.316	0.350	0.270	0.310	0.200	0.198	0.055	0.096	0.049
BB0448	0.223	0.283	0.296	0.248	0.720	0.770	0.770	0.740	0.001	0.081	0.043	0.092
BB0449	0.228	0.199	0.283	0.287	0.730	0.710	0.770	0.760	0.020	0.036	0.049	0.051
BB0450	0.045	0.082	0.040	-0.065	0.550	0.600	0.550	0.450	0.028	0.040	0.033	0.059
BB0451	-0.292	-0.130	-0.426	-0.043	0.200	0.350	0.120	0.480	0.173	0.297	0.059	0.357
BB0452	-0.158	-0.176	0.023	-0.183	0.330	0.290	0.530	0.320	0.074	0.069	0.032	0.089
BB0453	-0.101	-0.170	-0.327	-0.402	0.380	0.300	0.180	0.140	0.089	0.049	0.033	0.041
BB0454	0.214	0.455	0.801	0.908	0.710	0.890	0.980	0.990	0.220	0.092	0.066	0.099
BB0455	-0.001	-0.075	-0.077	-0.234	0.500	0.410	0.420	0.270	0.042	0.020	0.087	0.023
BB0456	0.173	0.130	0.007	0.256	0.670	0.650	0.510	0.750	0.130	0.149	0.069	0.058
BB0457	-0.097	-0.208	-0.116	-0.379	0.390	0.260	0.380	0.150	0.066	0.027	0.063	0.077
BB0458	0.112	0.406	0.503	0.424	0.610	0.860	0.900	0.840	0.105	0.044	0.087	0.045
BB0459	0.079	0.057	-0.060	-0.133	0.580	0.570	0.440	0.380	0.081	0.070	0.066	0.072
BB0460	0.181	0.178	0.103	0.098	0.680	0.690	0.630	0.620	0.073	0.083	0.055	0.043
BB0461	-0.166	-0.088	-0.165	-0.294	0.320	0.390	0.320	0.220	0.054	0.099	0.078	0.045
BB0462	0.113	0.072	0.025	-0.023	0.620	0.590	0.530	0.500	0.096	0.103	0.059	0.077
BB0463	-0.290	-0.305	-0.311	-0.351	0.200	0.180	0.190	0.170	0.049	0.073	0.046	0.087
BB0464	0.076	0.018	0.170	0.236	0.580	0.520	0.690	0.730	0.115	0.067	0.045	0.092
BB0465	0.162	0.122	0.054	-0.017	0.660	0.640	0.570	0.500	0.197	0.116	0.051	0.068
BB0466	-0.242	-0.033	-0.076	-0.051	0.240	0.460	0.430	0.470	0.156	0.140	0.103	0.072
BB0467	0.163	0.246	0.330	0.289	0.660	0.750	0.790	0.760	0.051	0.078	0.039	0.042
BB0468	-0.200	0.011	0.052	0.134	0.280	0.510	0.570	0.650	0.056	0.079	0.034	0.063
BB0469	0.360	0.220	0.126	0.148	0.810	0.730	0.660	0.660	0.076	0.060	0.052	0.025
BB0470	0.249	0.405	0.348	0.491	0.740	0.860	0.810	0.870	0.061	0.051	0.023	0.105
BB0471	0.086	0.291	0.286	0.276	0.590	0.780	0.770	0.750	0.071	0.056	0.061	0.074
BB0472	-0.685	-0.268	-0.123	-0.262	0.020	0.210	0.370	0.250	0.101	0.057	0.035	0.073
BB0473	-0.048	-0.094	-0.089	-0.234	0.440	0.380	0.410	0.270	0.042	0.076	0.048	0.048

BB0474	0.723	0.550	0.725	0.569	0.980	0.930	0.970	0.910	0.020	0.067	0.057	0.177
BB0475	0.413	0.279	0.362	0.299	0.840	0.770	0.820	0.770	0.092	0.065	0.053	0.053
BB0476	0.072	0.657	0.981	0.794	0.580	0.970	0.990	0.980	0.230	0.146	0.081	0.099
BB0477	0.356	0.630	0.810	0.727	0.810	0.960	0.980	0.970	0.082	0.135	0.125	0.138
BB0478	-0.152	0.371	0.580	0.368	0.330	0.840	0.930	0.810	0.093	0.226	0.159	0.176
BB0479	0.121	0.274	0.504	0.252	0.630	0.770	0.900	0.740	0.076	0.129	0.131	0.152
BB0480	0.232	0.491	0.700	0.590	0.730	0.910	0.960	0.920	0.047	0.111	0.097	0.143
BB0481	-0.186	0.216	0.359	0.167	0.300	0.720	0.820	0.680	0.069	0.200	0.098	0.087
BB0482	-0.003	0.400	0.400	0.184	0.500	0.860	0.840	0.690	0.018	0.211	0.120	0.116
BB0483	-0.177	0.075	0.251	0.074	0.310	0.590	0.750	0.600	0.036	0.137	0.126	0.099
BB0484	-0.045	0.326	0.545	0.458	0.440	0.810	0.920	0.850	0.059	0.105	0.083	0.116
BB0485	-0.208	0.070	0.221	0.132	0.270	0.580	0.730	0.640	0.053	0.179	0.109	0.128
BB0486	0.423	0.387	0.646	0.594	0.850	0.850	0.950	0.920	0.101	0.055	0.094	0.153
BB0487	0.375	0.398	0.441	0.466	0.820	0.860	0.860	0.850	0.081	0.080	0.046	0.095
BB0488	-0.262	0.072	0.123	0.134	0.220	0.590	0.650	0.650	0.061	0.097	0.043	0.090
BB0489	0.101	0.041	0.173	0.008	0.600	0.550	0.700	0.520	0.131	0.102	0.045	0.070
BB0490	0.105	0.407	0.818	0.666	0.610	0.860	0.980	0.950	0.087	0.049	0.065	0.087
BB0491	0.218	0.261	0.382	0.372	0.710	0.760	0.830	0.810	0.106	0.090	0.092	0.079
BB0492	0.219	0.357	0.628	0.557	0.720	0.830	0.950	0.900	0.043	0.053	0.113	0.133
BB0493	-0.104	0.023	0.098	0.022	0.380	0.530	0.630	0.540	0.121	0.090	0.060	0.076
BB0494	-0.004	0.188	0.183	0.054	0.500	0.700	0.700	0.580	0.026	0.079	0.076	0.093
BB0495	-0.138	0.025	0.126	0.004	0.340	0.530	0.660	0.520	0.175	0.141	0.077	0.052
BB0496	0.075	0.462	0.668	0.576	0.580	0.890	0.960	0.910	0.067	0.034	0.057	0.179
BB0497	-0.003	0.227	0.335	0.114	0.500	0.730	0.800	0.630	0.128	0.161	0.119	0.102
BB0498	-0.251	0.051	0.120	0.062	0.230	0.560	0.650	0.590	0.032	0.101	0.066	0.104
BB0499	0.489	0.291	0.730		0.880	0.780	0.970		0.343	0.406	0.318	
BB0500	-0.023	0.100	0.286	0.236	0.470	0.620	0.770	0.730	0.133	0.079	0.081	0.142
BB0501	-0.230	-0.031	-0.003	-0.085	0.250	0.460	0.500	0.430	0.018	0.114	0.074	0.099
BB0502	-0.046	0.152	0.102	0.069	0.440	0.660	0.630	0.590	0.117	0.125	0.097	0.122
BB0503	0.188	0.322	0.569	0.561	0.680	0.810	0.930	0.900	0.048	0.086	0.093	0.120
BB0504	-0.174	0.012	0.008	0.025	0.310	0.520	0.510	0.550	0.084	0.123	0.102	0.161
BB0505	0.048	0.128	0.061	-0.097	0.550	0.650	0.580	0.420	0.071	0.046	0.075	0.082
BB0506	-0.137	-0.108	-0.227	-0.262	0.350	0.370	0.250	0.250	0.054	0.025	0.030	0.023
BB0507	0.454	0.151	0.014	-0.088	0.860	0.660	0.520	0.430	0.063	0.071	0.078	0.044
BB0508	-0.056	-0.030	0.088	0.187	0.430	0.470	0.610	0.690	0.071	0.040	0.068	0.042
BB0509	0.027	-0.090	-0.189	-0.351	0.530	0.390	0.290	0.170	0.018	0.086	0.072	0.155
BB0510	0.075	-0.002	0.110	0.150	0.580	0.500	0.640	0.660	0.036	0.074	0.045	0.077

BB0511	0.207	-0.021	0.019	-0.014	0.700	0.470	0.530	0.510	0.056	0.068	0.063	0.072
BB0512	-0.028	-0.138	-0.190	-0.135	0.460	0.340	0.290	0.370	0.035	0.038	0.059	0.045
BB0513	-0.250	-0.369	-0.325	-0.394	0.230	0.140	0.180	0.140	0.049	0.061	0.041	0.024
BB0514	-0.214	-0.163	-0.150	-0.135	0.270	0.310	0.330	0.370	0.042	0.053	0.059	0.057
BB0515	-0.192	-0.320	-0.245	-0.355	0.290	0.170	0.240	0.170	0.097	0.130	0.066	0.046
BB0516	-0.195	-0.200	-0.135	-0.153	0.290	0.270	0.360	0.350	0.042	0.076	0.028	0.035
BB0517	-0.121	-0.127	-0.047	-0.114	0.360	0.350	0.450	0.400	0.039	0.041	0.032	0.074
BB0518	-0.393	-0.238	0.211	-0.160	0.110	0.230	0.720	0.340	0.083	0.048	0.096	0.127
BB0519	-0.095	-0.015	0.335	0.141	0.390	0.480	0.800	0.650	0.052	0.029	0.055	0.067
BB0520	0.607	0.397	0.597	0.418	0.940	0.850	0.940	0.830	0.040	0.054	0.050	0.100
BB0521	0.297	0.195	0.301	0.246	0.770	0.700	0.780	0.740	0.051	0.037	0.050	0.047
BB0522	0.293	0.124	0.188	0.112	0.760	0.640	0.710	0.630	0.051	0.065	0.054	0.040
BB0523	0.471	0.359	0.411	0.421	0.870	0.830	0.850	0.830	0.058	0.069	0.033	0.073
BB0524	-0.104	-0.151	-0.301	-0.256	0.380	0.320	0.200	0.250	0.071	0.058	0.056	0.075
BB0525	0.031	0.039	0.142	0.032	0.530	0.550	0.670	0.560	0.085	0.046	0.058	0.062
BB0526	0.156	0.136	-0.079	-0.084	0.660	0.650	0.420	0.430	0.147	0.043	0.042	0.039
BB0527	-0.289	-0.185	-0.201	-0.115	0.200	0.290	0.280	0.400	0.038	0.039	0.065	0.063
BB0528	-0.016	-0.198	-0.141	-0.207	0.480	0.270	0.350	0.300	0.041	0.058	0.038	0.072
BB0529	0.689	0.534	0.518	0.550	0.970	0.930	0.910	0.900	0.075	0.055	0.063	0.064
BB0530	-0.164	-0.193	-0.119	-0.122	0.320	0.280	0.380	0.390	0.064	0.053	0.016	0.046
BB0531	-0.174	-0.146	-0.151	-0.131	0.310	0.330	0.330	0.380	0.052	0.080	0.030	0.056
BB0532	-0.010	-0.010	0.066	0.105	0.490	0.490	0.580	0.620	0.041	0.029	0.044	0.084
BB0533	0.166	0.435	0.341	0.438	0.660	0.880	0.800	0.840	0.113	0.139	0.086	0.119
BB0534	0.049	0.055	-0.002	0.137	0.560	0.570	0.500	0.650	0.043	0.049	0.061	0.036
BB0535	0.198	0.229	0.159	0.254	0.690	0.740	0.680	0.740	0.017	0.070	0.019	0.083
BB0536	-0.280	-0.263	-0.117	-0.167	0.210	0.210	0.380	0.330	0.132	0.090	0.038	0.069
BB0537	0.019	0.074	0.037	0.124	0.520	0.590	0.550	0.640	0.031	0.071	0.019	0.066
BB0538	0.063	-0.023	0.004	0.030	0.570	0.470	0.510	0.550	0.046	0.019	0.025	0.060
BB0539	0.730	0.682	0.597	0.708	0.980	0.970	0.940	0.960	0.042	0.100	0.044	0.095
BB0540	-0.489	-0.206	0.110	0.057	0.070	0.260	0.640	0.580	0.047	0.097	0.081	0.132
BB0541	0.340	0.771	0.519	0.381	0.800	0.990	0.910	0.810	0.032	0.290	0.052	0.108
BB0542	0.141	0.375	0.199	0.130	0.640	0.840	0.710	0.640	0.065	0.085	0.097	0.062
BB0543	0.014	0.555	0.536	0.402	0.510	0.940	0.920	0.820	0.137	0.160	0.099	0.130
BB0544	-0.076	0.208	0.134	0.145	0.410	0.710	0.660	0.660	0.056	0.097	0.054	0.062
BB0545	0.206	0.227	0.032	0.058	0.700	0.730	0.540	0.580	0.194	0.089	0.054	0.049
BB0546	-0.008	-0.003	-0.076	-0.076	0.490	0.500	0.430	0.440	0.088	0.026	0.014	0.051
BB0547	-0.014	0.003	-0.150	-0.084	0.480	0.500	0.330	0.430	0.024	0.051	0.028	0.039

BB0548	-0.142	-0.272	-0.211	-0.297	0.340	0.200	0.270	0.210	0.036	0.073	0.040	0.048
BB0549	0.151	0.050	0.021	-0.072	0.650	0.560	0.530	0.440	0.118	0.053	0.039	0.039
BB0550	0.093	0.061	0.153	0.023	0.590	0.580	0.680	0.540	0.097	0.025	0.036	0.069
BB0551	0.260	0.155	0.585	0.391	0.750	0.670	0.940	0.820	0.109	0.050	0.032	0.063
BB0552	-0.265	-0.330	-0.267	-0.473	0.220	0.160	0.220	0.100	0.067	0.028	0.030	0.077
BB0553	0.247	-0.039	0.121	-0.034	0.740	0.450	0.650	0.490	0.127	0.065	0.059	0.053
BB0554	0.129	0.054	0.022	-0.265	0.630	0.570	0.530	0.240	0.106	0.097	0.145	0.062
BB0555	-0.017	-0.046	0.037	0.105	0.480	0.450	0.550	0.620	0.047	0.039	0.046	0.059
BB0556	0.308	0.217	-0.071	0.040	0.780	0.720	0.430	0.560	0.036	0.088	0.050	0.018
BB0557	-0.101	0.071	0.173	0.254	0.380	0.590	0.700	0.740	0.039	0.161	0.115	0.129
BB0558	-0.137	0.007	0.081	0.119	0.350	0.510	0.610	0.630	0.082	0.116	0.078	0.075
BB0559	0.245	0.293	0.224	0.341	0.740	0.790	0.730	0.800	0.046	0.160	0.093	0.106
BB0560	-0.006	-0.035	0.001	0.092	0.490	0.460	0.510	0.610	0.204	0.051	0.051	0.148
BB0561	-0.176	-0.209	-0.330	-0.437	0.310	0.260	0.180	0.120	0.035	0.049	0.060	0.025
BB0562	0.016	0.014	-0.337	-0.039	0.510	0.520	0.170	0.480	0.081	0.068	0.050	0.082
BB0563	-0.227	-0.306	-0.445	-0.429	0.260	0.180	0.110	0.120	0.047	0.044	0.025	0.056
BB0564	-0.101	-0.153	0.121	0.268	0.380	0.320	0.650	0.750	0.010	0.019	0.090	0.058
BB0565	0.136	0.016	0.103	-0.053	0.640	0.520	0.630	0.460	0.068	0.067	0.086	0.057
BB0566	0.043	0.001	0.126	0.007	0.540	0.500	0.660	0.520	0.114	0.054	0.079	0.039
BB0567	-0.329	-0.272	-0.281	-0.386	0.170	0.200	0.210	0.150	0.029	0.052	0.014	0.051
BB0568	-0.307	-0.078	-0.208	-0.128	0.180	0.400	0.270	0.380	0.065	0.043	0.021	0.062
BB0569	-0.115	-0.196	-0.277	-0.360	0.370	0.270	0.220	0.170	0.075	0.077	0.031	0.071
BB0570	-0.230	-0.011	-0.023	-0.037	0.250	0.490	0.480	0.480	0.059	0.216	0.073	0.075
BB0571	0.222	0.078	0.080	0.142	0.720	0.600	0.600	0.650	0.062	0.055	0.063	0.069
BB0572	0.012	0.296	0.453	0.585	0.510	0.790	0.870	0.920	0.149	0.078	0.077	0.057
BB0573	0.189	0.303	0.104	0.198	0.680	0.790	0.630	0.700	0.035	0.078	0.022	0.031
BB0574	0.226	0.343	0.125	0.191	0.720	0.820	0.660	0.700	0.042	0.058	0.053	0.074
BB0575	-0.189	-0.131	-0.273	-0.323	0.300	0.350	0.220	0.190	0.142	0.067	0.013	0.033
BB0576	-0.113	-0.019	-0.175	-0.146	0.370	0.480	0.310	0.360	0.034	0.026	0.022	0.067
BB0577	-0.072	-0.044	-0.213	-0.272	0.420	0.450	0.270	0.240	0.085	0.024	0.024	0.026
BB0578	-0.193	-0.091	-0.205	-0.309	0.290	0.390	0.280	0.200	0.058	0.058	0.048	0.048
BB0579	-0.269	-0.045	0.172	-0.027	0.210	0.450	0.690	0.500	0.067	0.107	0.069	0.095
BB0580	-0.029	-0.086	-0.063	-0.119	0.460	0.390	0.440	0.400	0.055	0.090	0.015	0.041
BB0581	-0.246	-0.108	-0.349	-0.376	0.240	0.370	0.170	0.160	0.055	0.023	0.029	0.023
BB0582	0.069	0.185	0.225	0.072	0.570	0.700	0.730	0.600	0.056	0.026	0.042	0.068
BB0583	-0.253	-0.073	-0.105	-0.144	0.230	0.410	0.390	0.360	0.082	0.083	0.015	0.060
BB0584	-0.345	-0.048	-0.342	-0.317	0.150	0.440	0.170	0.200	0.021	0.084	0.030	0.045

BB0585	0.314	0.232	0.170	0.153	0.780	0.740	0.690	0.670	0.018	0.045	0.072	0.036
BB0586	0.272	0.354	0.527	0.394	0.760	0.830	0.910	0.820	0.093	0.104	0.037	0.080
BB0587	-0.230	-0.296	-0.405	-0.332	0.250	0.180	0.130	0.190	0.081	0.033	0.021	0.037
BB0588	-0.201	-0.273	-0.221	-0.262	0.280	0.200	0.260	0.250	0.074	0.053	0.010	0.034
BB0589	-0.350	-0.325	-0.333	-0.438	0.150	0.160	0.180	0.120	0.145	0.049	0.029	0.024
BB0590	-0.200	-0.062	-0.117	-0.239	0.280	0.420	0.380	0.270	0.060	0.064	0.016	0.041
BB0591	-0.224	-0.140	-0.103	-0.376	0.260	0.340	0.400	0.160	0.053	0.033	0.124	0.048
BB0592	0.958	0.868	0.865	0.803	0.990	0.990	0.980	0.980	0.007	0.065	0.044	0.077
BB0593	-0.371	-0.021	-0.153	-0.248	0.130	0.470	0.330	0.260	0.057	0.095	0.042	0.047
BB0594	-0.201	-0.147	-0.262	-0.162	0.280	0.330	0.230	0.340	0.046	0.041	0.024	0.072
BB0595	0.117	-0.024	-0.147	-0.089	0.620	0.470	0.340	0.420	0.209	0.064	0.016	0.050
BB0596	-0.344	-0.089	-0.336	-0.239	0.150	0.390	0.180	0.270	0.142	0.072	0.031	0.066
BB0597	-0.233	-0.173	-0.168	-0.156	0.250	0.300	0.310	0.350	0.096	0.065	0.030	0.064
BB0598	-0.333	0.081	-0.104	-0.105	0.160	0.600	0.390	0.400	0.074	0.137	0.047	0.081
BB0599	-0.228	-0.260	-0.159	-0.356	0.250	0.210	0.320	0.170	0.064	0.052	0.044	0.043
BB0600	-0.224	-0.274	-0.109	-0.179	0.260	0.200	0.390	0.330	0.107	0.058	0.022	0.083
BB0601	-0.515	-0.406	-0.497	-0.544	0.060	0.110	0.090	0.060	0.057	0.051	0.040	0.042
BB0602	0.154	0.089	0.035	0.038	0.660	0.610	0.550	0.560	0.029	0.053	0.029	0.040
BB0603	-0.263	-0.085	0.166	0.315	0.220	0.400	0.690	0.780	0.105	0.082	0.048	0.135
BB0604	-0.017	0.031	0.099	0.059	0.480	0.540	0.630	0.580	0.120	0.136	0.154	0.123
BB0605	-0.234	-0.120	0.037	-0.183	0.250	0.360	0.550	0.320	0.046	0.053	0.044	0.033
BB0606	-0.065	0.003	-0.097	-0.135	0.420	0.500	0.400	0.370	0.084	0.055	0.041	0.024
BB0607	-0.344	-0.313	-0.348	-0.381	0.150	0.170	0.170	0.150	0.036	0.036	0.040	0.058
BB0608	0.116	0.107	0.101	0.130	0.620	0.630	0.630	0.640	0.066	0.057	0.059	0.045
BB0609		0.601	0.596	0.546		0.950	0.940	0.900		0.130	0.152	0.082
BB0610	0.353	0.373	0.554	0.513	0.810	0.840	0.930	0.880	0.045	0.063	0.100	0.093
BB0611	-0.254	0.010	-0.035	-0.082	0.230	0.510	0.460	0.430	0.049	0.145	0.068	0.072
BB0612	0.241	0.219	0.330	0.286	0.740	0.730	0.790	0.760	0.112	0.115	0.066	0.084
BB0613	-0.295	-0.043	-0.024	-0.053	0.190	0.450	0.480	0.460	0.107	0.100	0.107	0.060
BB0614		0.566	0.458	0.634		0.940	0.870	0.940		0.119	0.122	0.098
BB0615	0.107	0.483	0.986	0.761	0.610	0.900	0.990	0.970	0.101	0.122	0.125	0.157
BB0616	0.072	0.040	-0.030	0.049	0.570	0.550	0.470	0.570	0.059	0.048	0.099	0.027
BB0617	0.475	0.267	0.284	0.434	0.870	0.770	0.770	0.840	0.009	0.076	0.071	0.033
BB0618	0.462	0.395	0.433	0.262	0.860	0.850	0.850	0.750	0.135	0.083	0.073	0.042
BB0619	-0.284	0.005	-0.064	-0.004	0.200	0.510	0.440	0.520	0.069	0.053	0.025	0.038
BB0620	-0.074	-0.068	-0.110	-0.133	0.410	0.410	0.390	0.380	0.063	0.121	0.031	0.057
BB0621	-0.197	-0.150	-0.091	-0.194	0.290	0.320	0.410	0.310	0.115	0.097	0.061	0.052

BB0622	0.317	0.131	-0.006	0.184	0.790	0.650	0.500	0.690	0.067	0.098	0.101	0.106
BB0623	-0.478	-0.438	-0.379	-0.382	0.080	0.100	0.150	0.150	0.024	0.060	0.012	0.030
BB0624	0.293	0.141	0.066	0.031	0.760	0.660	0.580	0.550	0.065	0.055	0.038	0.076
BB0625	-0.397	-0.186	-0.202	-0.226	0.110	0.290	0.280	0.280	0.090	0.029	0.016	0.050
BB0626	0.985	0.790	0.610	0.939	1.000	0.990	0.950	0.990	0.287	0.068	0.158	0.071
BB0627	-0.261	-0.193	0.037	0.116	0.220	0.280	0.550	0.630	0.115	0.023	0.027	0.073
BB0628	-0.121	-0.276	-0.117	-0.143	0.360	0.190	0.380	0.360	0.058	0.054	0.038	0.133
BB0629	-0.314	-0.158	0.084	0.049	0.170	0.320	0.610	0.570	0.068	0.139	0.075	0.123
BB0630	-0.307	-0.304	-0.286	-0.243	0.180	0.180	0.210	0.260	0.091	0.070	0.062	0.057
BB0631	0.262	0.155	0.384	0.496	0.750	0.670	0.830	0.870	0.033	0.091	0.072	0.133
BB0632	0.174	0.028	-0.093	-0.150	0.670	0.530	0.400	0.350	0.072	0.025	0.038	0.016
BB0633	0.002	-0.075	-0.091	-0.121	0.500	0.410	0.410	0.400	0.015	0.087	0.053	0.044
BB0634	0.041	-0.049	-0.186	-0.101	0.540	0.440	0.290	0.410	0.022	0.026	0.031	0.075
BB0635	-0.209	-0.125	-0.122	-0.238	0.270	0.350	0.370	0.270	0.035	0.070	0.037	0.038
BB0636	-0.138	-0.028	-0.254	-0.303	0.340	0.470	0.230	0.210	0.037	0.060	0.033	0.065
BB0637	-0.302	-0.220	-0.208	-0.381	0.190	0.250	0.270	0.150	0.055	0.088	0.113	0.013
BB0638	-0.457	-0.370	-0.398	-0.444	0.090	0.140	0.140	0.120	0.132	0.067	0.040	0.027
BB0639	-0.158	0.028	-0.052	0.038	0.330	0.530	0.450	0.560	0.057	0.072	0.027	0.089
BB0640	0.052	0.034	0.023	0.188	0.560	0.540	0.530	0.690	0.051	0.045	0.014	0.065
BB0641	-0.123	-0.016	0.162	-0.000	0.360	0.480	0.680	0.520	0.036	0.056	0.118	0.060
BB0642	-0.406	-0.234	-0.046	-0.208	0.110	0.240	0.450	0.290	0.108	0.087	0.122	0.071
BB0643	-0.034	0.015	0.197	0.109	0.450	0.520	0.710	0.630	0.062	0.052	0.034	0.071
BB0644	-0.245	-0.243	-0.270	-0.290	0.240	0.230	0.220	0.220	0.201	0.123	0.105	0.049
BB0645	-0.312	-0.307	-0.320	-0.489	0.180	0.180	0.190	0.080	0.240	0.084	0.041	0.056
BB0646	-0.364	-0.309	-0.211	-0.208	0.140	0.170	0.270	0.300	0.069	0.065	0.037	0.120
BB0647	0.135	0.032	0.067	0.071	0.640	0.540	0.590	0.600	0.020	0.024	0.049	0.041
BB0648	-0.098	0.053	0.002	-0.131	0.390	0.560	0.510	0.380	0.054	0.062	0.014	0.096
BB0649	0.112	0.454	0.809	0.723	0.610	0.890	0.980	0.970	0.146	0.135	0.093	0.063
BB0650	0.343	0.491	0.891	0.943	0.800	0.910	0.980	0.990	0.070	0.064	0.132	0.146
BB0651	0.219	0.349	0.519	0.484	0.720	0.820	0.910	0.870	0.086	0.112	0.095	0.082
BB0652	-0.140	0.230	0.350	0.250	0.340	0.740	0.810	0.740	0.108	0.149	0.058	0.112
BB0653	0.052	-0.003	0.067	0.017	0.560	0.500	0.590	0.540	0.111	0.086	0.082	0.092
BB0654	0.137	0.056	0.164	0.173	0.640	0.570	0.690	0.680	0.128	0.026	0.023	0.078
BB0655	-0.009	-0.132	0.023	-0.084	0.490	0.350	0.530	0.430	0.165	0.034	0.025	0.102
BB0656	-0.362	-0.272	-0.207	-0.416	0.140	0.200	0.280	0.130	0.083	0.048	0.035	0.019
BB0657	0.095	-0.067	-0.074	-0.114	0.600	0.420	0.430	0.400	0.070	0.043	0.036	0.040
BB0658	-0.223	-0.261	0.045	-0.148	0.260	0.210	0.560	0.350	0.198	0.071	0.087	0.080

BB0659	0.609	0.671	0.494	0.767	0.950	0.970	0.890	0.970	0.394	0.183	0.229	0.017
BB0660	0.195	0.368	0.093	0.217	0.690	0.840	0.620	0.710	0.163	0.128	0.077	0.047
BB0661	0.217	0.074	0.118	0.110	0.710	0.590	0.650	0.630	0.114	0.061	0.125	0.069
BB0662	0.433	0.476	0.608	0.834	0.850	0.900	0.950	0.980	0.234	0.079	0.072	0.089
BB0663	0.249	0.166	0.104	0.183	0.740	0.680	0.640	0.690	0.004	0.026	0.042	0.049
BB0664	0.669	0.451	0.462	0.570	0.960	0.890	0.870	0.910	0.066	0.161	0.040	0.102
BB0665	0.296	-0.222	-0.119	-0.195	0.770	0.250	0.380	0.310	0.102	0.053	0.046	0.043
BB0666	-0.130	-0.196	-0.146	-0.155	0.350	0.270	0.340	0.350	0.091	0.047	0.044	0.037
BB0667	0.354	0.017	0.201	0.142	0.810	0.520	0.710	0.660	0.103	0.044	0.062	0.050
BB0668	-0.337	-0.386	-0.360	-0.380	0.160	0.130	0.160	0.150	0.125	0.131	0.038	0.044
BB0669	-0.142	-0.179	-0.135	-0.243	0.340	0.290	0.360	0.260	0.043	0.044	0.037	0.037
BB0670	-0.011	0.065	0.015	0.057	0.490	0.580	0.520	0.580	0.095	0.046	0.029	0.048
BB0671	-0.095	-0.160	-0.017	-0.229	0.390	0.310	0.480	0.280	0.135	0.068	0.042	0.044
BB0672	-0.105	-0.269	-0.060	-0.102	0.370	0.200	0.440	0.410	0.146	0.083	0.043	0.059
BB0673	0.296	0.023	-0.041	-0.015	0.770	0.530	0.460	0.510	0.135	0.035	0.030	0.059
BB0674	-0.047	0.014	0.108	0.131	0.440	0.520	0.640	0.640	0.060	0.045	0.034	0.048
BB0675	0.077	-0.059	0.022	-0.080	0.580	0.430	0.530	0.440	0.093	0.082	0.038	0.040
BB0676	-0.360	-0.340	-0.097	-0.232	0.140	0.150	0.400	0.280	0.084	0.041	0.023	0.036
BB0677	-0.007	-0.033	0.073	0.021	0.490	0.460	0.590	0.540	0.063	0.048	0.058	0.040
BB0678	-0.460	-0.212	-0.135	-0.122	0.080	0.260	0.360	0.390	0.083	0.078	0.033	0.107
BB0679	-0.203	-0.163	-0.191	-0.324	0.280	0.310	0.290	0.190	0.024	0.101	0.063	0.053
BB0680	-0.396	-0.408	-0.136	-0.361	0.110	0.110	0.360	0.170	0.076	0.110	0.049	0.079
BB0681	-0.252	-0.305	-0.071	-0.265	0.230	0.180	0.430	0.240	0.054	0.103	0.055	0.064
BB0682	-0.083	0.046	0.107	-0.042	0.400	0.560	0.640	0.480	0.038	0.090	0.037	0.067
BB0683	-0.307	0.224	0.353	0.409	0.180	0.730	0.810	0.830	0.101	0.239	0.093	0.084
BB0684	-0.367	0.194	0.114	0.185	0.140	0.700	0.650	0.690	0.050	0.175	0.088	0.119
BB0685	-0.150	0.097	0.089	0.066	0.330	0.620	0.610	0.590	0.044	0.114	0.053	0.060
BB0686	-0.297	0.307	0.075	0.135	0.190	0.800	0.600	0.650	0.199	0.159	0.055	0.099
BB0687	-0.082	0.133	0.225	0.254	0.400	0.650	0.730	0.740	0.110	0.063	0.021	0.033
BB0688	-0.207	-0.072	0.037	-0.085	0.270	0.410	0.550	0.430	0.047	0.104	0.037	0.090
BB0689	0.045	0.093	0.029	-0.048	0.550	0.610	0.540	0.470	0.064	0.065	0.062	0.043
BB0690	0.899	1.190	1.341	1.401	0.990	1.000	1.000	0.990	0.296	0.082	0.115	0.076
BB0691	0.159	0.567	0.709	0.725	0.660	0.940	0.960	0.970	0.262	0.106	0.069	0.047
BB0692	0.478	0.450	0.458	0.503	0.880	0.880	0.870	0.880	0.105	0.047	0.028	0.083
BB0693	-0.099	0.095	0.341	0.241	0.380	0.610	0.800	0.730	0.034	0.082	0.110	0.088
BB0694	0.006	0.338	0.629	0.550	0.500	0.820	0.950	0.900	0.088	0.106	0.102	0.116
BB0695	0.320	0.382	0.765	0.877	0.790	0.850	0.970	0.980	0.033	0.063	0.143	0.084

BB0696	-0.438	-0.136	-0.130	-0.038	0.090	0.340	0.360	0.480	0.052	0.142	0.095	0.073
BB0697	-0.233	-0.122	-0.134	-0.089	0.250	0.360	0.360	0.420	0.095	0.147	0.064	0.098
BB0698	-0.251	0.116	0.367	0.173	0.230	0.640	0.820	0.680	0.064	0.103	0.116	0.116
BB0699	0.634	0.639	1.039	0.747	0.950	0.960	0.990	0.970	0.086	0.077	0.074	0.054
BB0700	0.596	0.493	0.363	0.557	0.940	0.910	0.820	0.900	0.091	0.026	0.030	0.104
BB0701	0.270	0.154	0.087	0.071	0.750	0.670	0.610	0.590	0.052	0.077	0.072	0.038
BB0702	0.412	0.296	0.391	0.307	0.840	0.790	0.840	0.780	0.118	0.087	0.092	0.082
BB0703	0.716	0.480	0.833	0.638	0.980	0.900	0.980	0.940	0.078	0.047	0.052	0.014
BB0704	0.006	0.071	0.096	0.025	0.500	0.580	0.620	0.550	0.037	0.059	0.069	0.059
BB0705	-0.059	-0.030	-0.118	-0.202	0.430	0.470	0.380	0.300	0.041	0.075	0.036	0.044
BB0706	-0.223	-0.047	-0.107	-0.272	0.260	0.440	0.390	0.240	0.118	0.073	0.031	0.052
BB0707	-0.152	-0.164	-0.222	-0.366	0.330	0.310	0.260	0.160	0.107	0.080	0.028	0.049
BB0708	0.373	0.506	0.317	0.421	0.820	0.920	0.780	0.830	0.046	0.114	0.051	0.051
BB0709	-0.056	-0.171	-0.053	-0.135	0.430	0.300	0.450	0.370	0.062	0.032	0.051	0.022
BB0710	0.434	0.219	0.013	0.227	0.850	0.730	0.520	0.720	0.221	0.099	0.050	0.119
BB0711	0.215	0.329	0.493	0.379	0.710	0.810	0.890	0.810	0.053	0.084	0.103	0.088
BB0712	-0.394	-0.039	-0.071	-0.074	0.110	0.460	0.430	0.440	0.086	0.086	0.121	0.079
BB0713	0.265	0.287	0.127	0.095	0.750	0.780	0.660	0.610	0.052	0.058	0.056	0.076
BB0714	0.131	0.487	0.940	0.646	0.640	0.910	0.990	0.940	0.128	0.118	0.127	0.149
BB0715	-0.127	-0.059	-0.180	-0.297	0.360	0.430	0.300	0.210	0.080	0.055	0.061	0.048
BB0716	0.285	0.193	0.070	0.184	0.760	0.700	0.590	0.690	0.007	0.061	0.046	0.089
BB0717	0.675	0.641	0.312	0.271	0.970	0.960	0.780	0.750	0.072	0.131	0.050	0.087
BB0718	-0.490	-0.224	-0.190	-0.258	0.070	0.250	0.290	0.250	0.072	0.040	0.016	0.043
BB0719	0.559	0.475	0.315	0.364	0.920	0.900	0.780	0.810	0.022	0.104	0.068	0.071
BB0720	-0.315	-0.180	-0.044	-0.079	0.170	0.290	0.450	0.440	0.037	0.114	0.060	0.075
BB0721		0.529	0.507	0.597		0.930	0.900	0.920		0.130	0.054	0.102
BB0722	0.480	0.257	0.387	0.297	0.880	0.750	0.840	0.770	0.065	0.128	0.048	0.072
BB0723	0.621	0.653	0.547	0.695	0.950	0.970	0.920	0.960	0.085	0.200	0.044	0.076
BB0724	-0.407	0.077	0.221	0.101	0.110	0.590	0.730	0.620	0.115	0.095	0.075	0.100
BB0725	0.659	0.668			0.960	0.970			0.265	0.312		
BB0726	-0.196	0.036	0.092	0.083	0.290	0.550	0.620	0.600	0.069	0.036	0.045	0.112
BB0727	-0.096	0.115	-0.165	-0.121	0.390	0.630	0.320	0.390	0.181	0.056	0.037	0.060
BB0728	0.489	0.258	0.297	0.382	0.880	0.760	0.780	0.810	0.064	0.075	0.038	0.081
BB0729	-0.314	-0.302	-0.584	-0.572	0.170	0.180	0.050	0.050	0.148	0.070	0.043	0.069
BB0730	-0.336	-0.268	-0.193	-0.253	0.160	0.210	0.290	0.250	0.046	0.091	0.020	0.061
BB0731	0.391	0.207	0.102	0.188	0.830	0.710	0.630	0.690	0.045	0.095	0.055	0.060
BB0732	0.576	0.615	0.783	0.849	0.930	0.950	0.970	0.980	0.102	0.100	0.101	0.086

BB0733	0.574	0.613	0.500	0.573	0.930	0.950	0.900	0.910	0.149	0.047	0.061	0.094
BB0734	0.380	0.462	0.583	0.431	0.820	0.890	0.930	0.840	0.100	0.159	0.122	0.076
BB0735	0.034	0.374	0.584	0.272	0.540	0.840	0.940	0.750	0.120	0.122	0.090	0.089
BB0736	0.774	0.704	0.654	0.585	0.990	0.980	0.960	0.920	0.107	0.065	0.041	0.135
BB0737	0.044	0.012	0.053	-0.080	0.550	0.510	0.570	0.440	0.092	0.066	0.054	0.042
BB0738	-0.094	-0.010	-0.142	-0.201	0.400	0.490	0.350	0.300	0.077	0.050	0.016	0.030
BB0739	0.180	0.169	0.381	0.452	0.680	0.680	0.830	0.850	0.041	0.066	0.090	0.118
BB0740	0.082	0.145	0.096	0.083	0.590	0.660	0.620	0.600	0.079	0.065	0.126	0.070
BB0741	0.465	0.172	0.671	0.469	0.870	0.680	0.960	0.860	0.094	0.059	0.080	0.079
BB0742	-0.024	-0.033	-0.114	-0.129	0.470	0.460	0.380	0.380	0.102	0.099	0.060	0.089
BB0743	-0.201	-0.228	-0.156	-0.305	0.280	0.240	0.330	0.210	0.077	0.053	0.026	0.046
BB0744	0.109	0.293	0.139	0.009	0.610	0.790	0.670	0.520	0.183	0.065	0.095	0.065
BB0745	-0.012	-0.178	-0.141	-0.169	0.490	0.290	0.350	0.330	0.147	0.071	0.016	0.024
BB0746	-0.092	0.060	-0.132	-0.090	0.400	0.580	0.360	0.420	0.043	0.100	0.049	0.074
BB0747	-0.070	-0.145	-0.081	-0.232	0.420	0.330	0.420	0.280	0.064	0.043	0.190	0.043
BB0748	0.167	0.472	0.440	0.285	0.670	0.900	0.860	0.760	0.038	0.069	0.049	0.085
BB0749	-0.013	0.156	0.117	0.087	0.480	0.670	0.650	0.610	0.074	0.160	0.103	0.066
BB0750	0.581	0.910	0.500	0.721	0.930	0.990	0.900	0.960	0.196	0.143	0.239	0.101
BB0751	0.004	-0.165	-0.031	-0.137	0.500	0.310	0.470	0.370	0.106	0.040	0.036	0.093
BB0752	-0.177	-0.224	-0.189	-0.103	0.310	0.240	0.290	0.410	0.048	0.021	0.035	0.077
BB0753	-0.165	-0.261	-0.145	-0.243	0.320	0.210	0.340	0.260	0.095	0.036	0.036	0.059
BB0754	-0.382	-0.272	0.034	-0.045	0.120	0.200	0.550	0.470	0.080	0.068	0.076	0.099
BB0755	-0.425	-0.352	-0.003	-0.306	0.100	0.140	0.500	0.200	0.041	0.052	0.061	0.053
BB0756	-0.139	-0.024	-0.100	-0.175	0.340	0.470	0.400	0.330	0.132	0.120	0.120	0.064
BB0757	0.165	0.305	0.034	0.052	0.660	0.790	0.540	0.580	0.086	0.135	0.077	0.094
BB0758	-0.107	-0.061	0.105	0.045	0.370	0.430	0.640	0.570	0.107	0.038	0.077	0.053
BB0759	-0.026	-0.226	-0.294	-0.391	0.460	0.240	0.200	0.140	0.125	0.063	0.024	0.023
BB0760	-0.189	-0.160	-0.157	-0.229	0.300	0.310	0.330	0.280	0.050	0.070	0.016	0.058
BB0761	-0.272	-0.452	-0.425	-0.468	0.210	0.090	0.120	0.100	0.135	0.086	0.038	0.103
BB0762	0.719	0.549	0.506	0.538	0.980	0.930	0.900	0.890	0.058	0.117	0.077	0.095
BB0763	-0.217	0.005	-0.014	-0.016	0.270	0.510	0.490	0.500	0.029	0.175	0.025	0.079
BB0764	-0.242	-0.164	0.086	0.082	0.240	0.310	0.610	0.600	0.044	0.042	0.039	0.044
BB0765	0.161	0.096	-0.039	0.018	0.660	0.620	0.460	0.540	0.031	0.062	0.047	0.032
BB0766	-0.067	-0.180	-0.172	-0.038	0.420	0.290	0.310	0.480	0.088	0.103	0.062	0.031
BB0767	-0.104	-0.208	-0.341	-0.352	0.380	0.260	0.170	0.170	0.091	0.055	0.021	0.047
BB0768	-0.102	-0.091	-0.172	-0.061	0.380	0.390	0.310	0.460	0.101	0.064	0.045	0.042
BB0769	-0.368	-0.130	-0.135	-0.157	0.130	0.350	0.360	0.350	0.054	0.055	0.024	0.068

BB0770	0.117	0.059	-0.142	-0.062	0.620	0.570	0.340	0.450	0.054	0.076	0.037	0.028
BB0771	0.667	0.814	0.810	0.635	0.960	0.990	0.980	0.940	0.176	0.163	0.187	0.147
BB0772	0.043	-0.078	-0.077	-0.082	0.540	0.400	0.420	0.430	0.023	0.061	0.024	0.023
BB0773	0.291	0.043	-0.041	-0.060	0.760	0.550	0.460	0.460	0.039	0.053	0.049	0.032
BB0774	-0.238	0.021	0.153	0.227	0.250	0.530	0.670	0.720	0.190	0.062	0.077	0.062
BB0775	0.240	0.377	0.590	0.479	0.730	0.840	0.940	0.860	0.043	0.094	0.128	0.122
BB0776	0.279	0.529	1.045	0.979	0.760	0.930	0.990	0.990	0.072	0.108	0.111	0.111
BB0777	-0.097	0.005	-0.006	0.005	0.390	0.510	0.500	0.520	0.034	0.097	0.038	0.049
BB0778	0.033	0.326	0.585	0.441	0.530	0.810	0.940	0.850	0.041	0.119	0.091	0.180
BB0779	0.391	0.259	0.187	0.262	0.830	0.760	0.700	0.750	0.065	0.049	0.023	0.077
BB0780	-0.066	0.116	0.018	-0.090	0.420	0.640	0.520	0.420	0.074	0.106	0.043	0.062
BB0781	-0.203	-0.072	-0.124	-0.283	0.280	0.410	0.370	0.230	0.079	0.162	0.041	0.046
BB0782	-0.089	-0.047	-0.020	0.046	0.400	0.440	0.480	0.570	0.085	0.065	0.028	0.077
BB0783	0.277	0.175	0.191	0.066	0.760	0.690	0.710	0.590	0.045	0.046	0.032	0.050
BB0784	0.070	0.089	0.234	0.217	0.570	0.610	0.740	0.710	0.045	0.039	0.046	0.049
BB0785	0.068	0.187	0.093	0.133	0.570	0.700	0.620	0.650	0.055	0.087	0.051	0.087
BB0786	-0.136	0.319	0.362	0.213	0.350	0.810	0.820	0.710	0.041	0.166	0.073	0.133
BB0787	-0.207	-0.161	-0.047	-0.158	0.270	0.310	0.450	0.340	0.060	0.112	0.071	0.115
BB0788	-0.018	0.120	0.058	0.009	0.480	0.640	0.570	0.530	0.112	0.057	0.046	0.062
BB0789	-0.401	0.011	0.096	0.024	0.110	0.510	0.620	0.540	0.056	0.218	0.119	0.131
BB0790	0.056	0.129	0.035	0.076	0.560	0.650	0.550	0.600	0.037	0.044	0.040	0.090
BB0791	-0.040	0.077	0.067	0.210	0.450	0.590	0.590	0.710	0.032	0.074	0.057	0.075
BB0792	0.447	0.290	0.179	0.207	0.860	0.780	0.700	0.710	0.079	0.066	0.100	0.100
BB0793	0.322	0.039	0.044	-0.143	0.790	0.550	0.560	0.360	0.217	0.017	0.069	0.027
BB0794	-0.155	-0.074	-0.089	-0.086	0.330	0.410	0.410	0.430	0.075	0.026	0.044	0.100
BB0795	0.142	0.302	0.359	0.455	0.640	0.790	0.820	0.850	0.103	0.102	0.088	0.076
BB0796	0.120	0.208	0.101	0.188	0.620	0.710	0.630	0.690	0.062	0.070	0.036	0.054
BB0797	0.199	0.269	0.178	0.119	0.700	0.770	0.700	0.630	0.118	0.047	0.045	0.029
BB0798	0.085	-0.049	-0.162	-0.237	0.590	0.440	0.320	0.270	0.089	0.056	0.026	0.066
BB0799	0.296	0.383	0.327	0.432	0.770	0.850	0.790	0.840	0.040	0.046	0.031	0.092
BB0800	0.055	0.080	0.023	-0.010	0.560	0.600	0.530	0.510	0.191	0.103	0.098	0.088
BB0801	-0.273	0.001	-0.135	-0.121	0.210	0.500	0.360	0.400	0.142	0.130	0.060	0.183
BB0802	0.179	0.556	0.357	0.480	0.680	0.940	0.810	0.860	0.076	0.088	0.026	0.086
BB0803	0.313	0.372	0.319	0.487	0.780	0.840	0.790	0.870	0.065	0.132	0.116	0.053
BB0804	0.270	0.443	0.674	0.509	0.750	0.880	0.960	0.880	0.035	0.138	0.136	0.140
BB0805	-0.199	0.276	0.401	0.068	0.280	0.770	0.840	0.590	0.072	0.194	0.150	0.130
BB0806	0.253	0.456	0.531	0.571	0.740	0.890	0.920	0.910	0.102	0.111	0.050	0.044

BB0807	0.106	0.406	0.026	0.215	0.610	0.860	0.540	0.710	0.226	0.137	0.105	0.133
BB0808	-0.067	0.020	-0.082	-0.215	0.420	0.520	0.420	0.290	0.059	0.074	0.095	0.053
BB0809	-0.214	-0.212	-0.380	-0.241	0.270	0.260	0.150	0.270	0.086	0.088	0.108	0.041
BB0810	-0.009	-0.040	-0.044	-0.065	0.490	0.450	0.450	0.450	0.068	0.055	0.086	0.041
BB0811	-0.198	-0.349	-0.146	-0.257	0.290	0.150	0.340	0.250	0.051	0.036	0.062	0.045
BB0812	0.728	0.432	0.411	0.428	0.980	0.880	0.850	0.840	0.036	0.126	0.077	0.112
BB0813	0.807	0.510	0.368	0.372	0.990	0.920	0.820	0.810	0.027	0.132	0.043	0.080
BB0814	0.260	0.032	-0.134	-0.011	0.750	0.540	0.360	0.510	0.084	0.094	0.053	0.063
BB0815	0.298	0.079	-0.284	-0.222	0.770	0.600	0.210	0.290	0.039	0.084	0.028	0.083
BB0816	-0.079	-0.019	-0.157	0.029	0.410	0.480	0.330	0.550	0.151	0.106	0.044	0.071
BB0817	0.203	0.050	0.009	-0.130	0.700	0.560	0.520	0.380	0.064	0.068	0.103	0.057
BB0818	0.040	-0.115	-0.306	-0.232	0.540	0.360	0.190	0.280	0.053	0.093	0.052	0.060
BB0819	0.009	-0.243	-0.158	-0.212	0.510	0.230	0.330	0.290	0.108	0.067	0.062	0.048
BB0820	0.382	0.362	0.229	0.160	0.820	0.830	0.740	0.670	0.078	0.082	0.039	0.037
BB0821	0.122	-0.001	-0.238	-0.251	0.630	0.500	0.240	0.260	0.082	0.061	0.016	0.043
BB0822	0.522	0.351	0.420	0.352	0.900	0.820	0.850	0.800	0.019	0.128	0.054	0.106
BB0823	0.388	0.256	0.146	0.029	0.830	0.750	0.670	0.550	0.056	0.051	0.050	0.076
BB0824	0.189	0.471	0.624	0.617	0.690	0.890	0.950	0.930	0.170	0.050	0.022	0.063
BB0825	0.548	0.582	0.613	0.568	0.920	0.940	0.950	0.910	0.044	0.080	0.090	0.075
BB0826	0.348	0.256	0.288	0.171	0.810	0.750	0.770	0.680	0.053	0.124	0.027	0.070
BB0827	0.312	0.299	0.452	0.336	0.780	0.790	0.870	0.790	0.319	0.268	0.291	0.265
BB0828	-0.324	-0.290	-0.365	-0.404	0.170	0.190	0.160	0.140	0.062	0.081	0.017	0.057
BB0829	0.114	-0.039	-0.168	-0.256	0.620	0.450	0.310	0.250	0.054	0.050	0.043	0.036
BB0830	-0.017	0.056	-0.140	-0.224	0.480	0.570	0.350	0.280	0.027	0.089	0.027	0.031
BB0831	0.099	0.218	0.266	0.162	0.600	0.720	0.750	0.670	0.112	0.122	0.085	0.063
BB0832	0.091	0.105	-0.026	0.080	0.590	0.620	0.470	0.600	0.087	0.050	0.051	0.066
BB0833	0.675	0.551	0.717	0.470	0.970	0.930	0.970	0.860	0.046	0.091	0.105	0.076
BB0834	0.027	0.158	-0.098	-0.128	0.530	0.670	0.400	0.390	0.051	0.091	0.027	0.063
BB0835	-0.279	-0.331	-0.401	-0.455	0.210	0.160	0.140	0.110	0.094	0.074	0.061	0.045
BB0836	0.905	0.879	1.138	1.090	0.990	0.990	0.990	0.990	0.294	0.310	0.302	0.199
BB0837	-0.497	-0.525	-0.538	-0.597	0.070	0.060	0.060	0.040	0.083	0.067	0.022	0.026
BB0838	0.099	0.110	0.175	0.063	0.600	0.630	0.700	0.590	0.263	0.167	0.239	0.221
BB0839	0.037	-0.078	-0.096	-0.122	0.540	0.400	0.400	0.390	0.132	0.070	0.019	0.054
BB0840	0.723	0.434	0.579	0.487	0.980	0.880	0.930	0.870	0.150	0.126	0.103	0.073
BB0841	0.177	0.267	0.028	-0.124	0.670	0.770	0.540	0.390	0.112	0.074	0.052	0.055
BB0842	-0.313	-0.235	-0.271	-0.352	0.180	0.230	0.220	0.170	0.063	0.047	0.042	0.036
BB0843	-0.421	-0.329	-0.364	-0.479	0.100	0.160	0.160	0.090	0.075	0.055	0.021	0.020

BB0843.1	0.517	0.524	0.477	0.509	0.900	0.920	0.880	0.880	0.115	0.071	0.047	0.054
BB0844	-0.124	-0.377	-0.150	-0.356	0.360	0.130	0.330	0.170	0.189	0.062	0.109	0.078
BB0845.1		0.689		0.692		0.980		0.960		0.714		0.574
BB0845.2	-0.569	-0.589	-0.539	-0.633	0.050	0.030	0.060	0.020	0.164	0.052	0.015	0.034
BB0847	0.422	0.364	0.338	0.292	0.850	0.840	0.800	0.770	0.110	0.069	0.092	0.075
BB0848	0.318	0.225	0.210	0.187	0.790	0.730	0.720	0.690	0.099	0.154	0.043	0.043
BB0848.1	0.603	0.581	0.652	0.687	0.940	0.940	0.960	0.950	0.106	0.097	0.094	0.065
BB0849.1	0.145	0.154	0.132	0.187	0.650	0.660	0.660	0.690	0.071	0.125	0.134	0.150
BB0849.2	0.548	0.760	0.718	0.662	0.920	0.980	0.970	0.950	0.053	0.103	0.141	0.112
BB0852	-0.232	-0.336	-0.182	-0.283	0.250	0.150	0.300	0.230	0.122	0.059	0.040	0.073
BB0853	0.557	0.550	0.525	0.619	0.920	0.930	0.910	0.930	0.109	0.099	0.110	0.103
BB0853.1	0.669	0.552	0.447	0.370	0.960	0.930	0.860	0.810	0.154	0.081	0.103	0.084
Bb2.36	-0.545	-0.218	0.203	-0.096	0.050	0.250	0.710	0.420	0.029	0.159	0.104	0.120
BB764	-0.025	-0.306	-0.202	-0.293	0.470	0.180	0.280	0.220	0.157	0.050	0.053	0.022
BBA01	0.520	0.358	0.253	0.527	0.900	0.830	0.750	0.890	0.170	0.129	0.072	0.135
BBA01	-0.344	-0.653	-0.526	-0.663	0.150	0.010	0.070	0.010	0.087	0.065	0.032	0.066
BBA02	0.690	0.424	0.449	0.522	0.970	0.870	0.870	0.880	0.096	0.085	0.075	0.107
BBA03	-0.034	-0.276	-0.169	-0.238	0.450	0.200	0.310	0.270	0.070	0.047	0.052	0.059
BBA04	-0.362	-0.625	-0.472	-0.523	0.140	0.020	0.100	0.070	0.040	0.092	0.045	0.051
BBA05	-0.186	-0.542	-0.331	-0.403	0.300	0.050	0.180	0.140	0.041	0.119	0.042	0.077
BBA06	0.493	0.304	0.391	0.449	0.880	0.790	0.840	0.850	0.079	0.165	0.147	0.114
BBA07	-0.039	-0.371	-0.291	-0.485	0.450	0.140	0.210	0.090	0.070	0.141	0.086	0.035
BBA08	0.452	0.199	0.161	0.312	0.860	0.710	0.680	0.780	0.129	0.143	0.063	0.080
BBA09	-0.189	-0.388	-0.358	-0.470	0.300	0.120	0.160	0.100	0.046	0.042	0.043	0.016
BBA10	-0.068	-0.311	0.010	0.021	0.420	0.170	0.520	0.540	0.084	0.093	0.134	0.042
BBA11	0.151	0.074	-0.062	-0.002	0.650	0.590	0.440	0.520	0.124	0.164	0.082	0.124
BBA12	0.689	0.482	0.520	0.647	0.970	0.900	0.910	0.940	0.075	0.073	0.101	0.147
BBA13	-0.118	-0.299	-0.175	-0.202	0.360	0.180	0.310	0.300	0.050	0.032	0.038	0.105
BBA14	-0.087	-0.153	-0.026	-0.196	0.400	0.320	0.470	0.310	0.060	0.044	0.050	0.093
BBA15	0.195	0.413	1.161	1.151	0.690	0.870	0.990	0.990	0.128	0.251	0.235	0.188
BBA16	0.416	0.680	1.218	1.429	0.840	0.970	0.990	1.000	0.356	0.108	0.172	0.117
BBA17	0.668	0.417	0.224	0.166	0.960	0.870	0.730	0.670	0.039	0.105	0.041	0.082
BBA18	0.044	-0.145	0.066	-0.083	0.550	0.330	0.580	0.430	0.047	0.025	0.023	0.053
BBA19	-0.153	-0.001	0.029	0.069	0.330	0.500	0.540	0.590	0.050	0.085	0.037	0.097
BBA20	0.198	-0.021	0.142	0.295	0.700	0.470	0.670	0.770	0.151	0.079	0.032	0.062
BBA21	-0.085	-0.162	-0.106	-0.072	0.400	0.310	0.390	0.440	0.047	0.127	0.045	0.049
BBA22	0.737	0.670	0.590	0.666	0.980	0.970	0.940	0.950	0.174	0.134	0.063	0.072

BBA23	-0.163	-0.139	0.070	0.071	0.320	0.340	0.590	0.590	0.065	0.057	0.073	0.055
BBA24	0.021	-0.269	-0.276	-0.337	0.520	0.200	0.220	0.190	0.158	0.089	0.082	0.100
BBA25	-0.240	-0.627	-0.395	-0.531	0.240	0.020	0.140	0.070	0.294	0.051	0.053	0.122
BBA26	0.412	0.116	-0.080	0.012	0.840	0.630	0.420	0.530	0.114	0.063	0.102	0.069
BBA27	0.293	0.248	0.005	0.211	0.760	0.750	0.510	0.710	0.065	0.107	0.060	0.108
BBA28	0.224	-0.094	-0.119	-0.101	0.720	0.390	0.380	0.410	0.084	0.056	0.053	0.025
BBA29	0.575	0.357	0.331	0.253	0.930	0.830	0.800	0.740	0.068	0.095	0.042	0.058
BBA30	-0.180	-0.224	-0.300	-0.355	0.310	0.240	0.200	0.170	0.079	0.068	0.050	0.084
BBA31	-0.465	-0.463	-0.539	-0.534	0.080	0.080	0.060	0.070	0.057	0.064	0.042	0.055
BBA32	0.135	0.017	-0.062	0.001	0.640	0.520	0.440	0.520	0.028	0.029	0.074	0.099
BBA33	0.498	0.408	0.639	0.612	0.890	0.870	0.950	0.930	0.044	0.102	0.084	0.072
BBA34	-0.580	-0.513	-0.653	-0.725	0.040	0.060	0.020	0.000	0.076	0.101	0.036	0.055
BBA35	0.433	0.439	0.271	0.416	0.850	0.880	0.760	0.830	0.063	0.139	0.130	0.155
BBA36	-0.310	-0.641	-0.649	-0.677	0.180	0.020	0.020	0.010	0.200	0.038	0.032	0.075
BBA37	-0.196	-0.330	-0.425	-0.399	0.290	0.160	0.120	0.140	0.143	0.046	0.041	0.035
BBA38	-0.439	-0.236	-0.355	-0.397	0.090	0.230	0.160	0.140	0.056	0.080	0.038	0.031
BBA39	-0.306	-0.397	-0.239	-0.384	0.180	0.120	0.240	0.150	0.074	0.063	0.148	0.057
BBA40	-0.297	-0.331	-0.387	-0.396	0.190	0.160	0.150	0.140	0.147	0.059	0.037	0.046
BBA41	-0.177	-0.349	-0.413	-0.462	0.310	0.150	0.130	0.110	0.125	0.029	0.042	0.083
BBA42	-0.081	-0.081	-0.141	-0.164	0.400	0.400	0.350	0.340	0.091	0.092	0.158	0.093
BBA43	-0.031	-0.164	-0.238	-0.158	0.450	0.310	0.240	0.340	0.053	0.030	0.087	0.055
BBA44	0.400	0.243	0.124	0.195	0.830	0.740	0.660	0.700	0.056	0.061	0.057	0.063
BBA45	-0.151	-0.235	-0.334	-0.351	0.330	0.240	0.180	0.170	0.066	0.053	0.033	0.043
BBA46	-0.519	-0.402	-0.416	-0.451	0.060	0.120	0.130	0.110	0.070	0.060	0.030	0.072
BBA47	-0.371	-0.482	-0.396	-0.450	0.130	0.070	0.140	0.110	0.084	0.034	0.017	0.029
BBA48	-0.242	-0.246	-0.427	-0.378	0.240	0.220	0.120	0.160	0.125	0.081	0.046	0.080
BBA49	0.056	-0.170	-0.067	-0.356	0.560	0.300	0.430	0.170	0.086	0.012	0.120	0.060
BBA50	-0.281	-0.191	-0.289	-0.283	0.200	0.280	0.210	0.230	0.018	0.058	0.140	0.068
BBA51	-0.585	-0.660	-0.686	-0.654	0.040	0.010	0.010	0.020	0.093	0.057	0.047	0.065
BBA52	-0.183	-0.131	-0.267	-0.145	0.300	0.350	0.220	0.360	0.103	0.086	0.068	0.099
BBA53	0.113	-0.292	-0.206	-0.257	0.620	0.190	0.280	0.250	0.120	0.065	0.044	0.117
BBA54	-0.035	-0.049	-0.034	-0.089	0.450	0.440	0.460	0.430	0.011	0.089	0.052	0.129
BBA55	-0.633	-0.503	-0.663	-0.684	0.030	0.060	0.020	0.010	0.081	0.140	0.057	0.105
BBA56	-0.536	-0.581	-0.514	-0.483	0.060	0.040	0.080	0.090	0.109	0.061	0.046	0.184
BBA57	-0.381	-0.425	-0.416	-0.670	0.130	0.100	0.130	0.010	0.045	0.055	0.056	0.120
BBA58	0.104	0.044	-0.004	0.167	0.610	0.550	0.500	0.670	0.049	0.134	0.114	0.121
BBA59	0.012	-0.003	0.241	-0.182	0.510	0.500	0.740	0.330	0.089	0.101	0.082	0.050

BBA60	-0.179	-0.289	-0.240	-0.356	0.310	0.190	0.240	0.170	0.039	0.060	0.038	0.067
BBA61	-0.074	-0.374	-0.179	-0.472	0.410	0.130	0.300	0.100	0.095	0.051	0.039	0.044
BBA62	0.691	0.576	0.835	0.914	0.970	0.940	0.980	0.990	0.072	0.143	0.110	0.108
BBA63	0.497	0.646	0.493	0.605	0.890	0.960	0.890	0.930	0.125	0.182	0.119	0.139
BBA64	-0.046	-0.305	-0.183	-0.433	0.440	0.180	0.300	0.120	0.080	0.084	0.056	0.034
BBA65	-0.194	-0.418	-0.413	-0.467	0.290	0.110	0.130	0.100	0.067	0.121	0.041	0.083
BBA66	-0.288	-0.735	-0.466	-0.626	0.200	0.000	0.100	0.030	0.066	0.091	0.028	0.061
BBA67	0.405	0.109	0.158	0.421	0.830	0.630	0.680	0.830	0.093	0.113	0.132	0.066
BBA68	0.102	-0.153	0.291	-0.160	0.600	0.320	0.770	0.340	0.053	0.029	0.080	0.075
BBA69	-0.159	-0.193	-0.057	-0.154	0.320	0.280	0.450	0.350	0.054	0.022	0.067	0.054
BBA70	-0.148	-0.430	-0.385	-0.538	0.340	0.100	0.150	0.060	0.045	0.046	0.046	0.055
BBA71	-0.116	-0.382	-0.216	-0.294	0.370	0.130	0.260	0.220	0.137	0.068	0.014	0.064
BBA72	0.202	-0.150	-0.150	-0.240	0.700	0.330	0.330	0.270	0.053	0.083	0.067	0.105
BBA73	-0.169	-0.390	-0.214	-0.246	0.320	0.120	0.270	0.260	0.089	0.089	0.008	0.051
BBA74	-0.401	0.023	-0.118	-0.461	0.110	0.530	0.380	0.110	0.109	0.258	0.087	0.104
BBA75	0.659	0.528	0.471	0.684	0.960	0.920	0.880	0.950	0.061	0.117	0.113	0.120
BBA76	-0.257	-0.271	-0.161	-0.532	0.230	0.200	0.320	0.070	0.067	0.095	0.054	0.070
BBB01	0.139	0.167	0.089	0.251	0.640	0.680	0.610	0.740	0.040	0.029	0.029	0.034
BBB02	0.105	0.039	0.091	0.118	0.610	0.550	0.620	0.630	0.045	0.076	0.050	0.094
BBB03	-0.289	-0.124	-0.259	-0.233	0.200	0.350	0.230	0.270	0.105	0.021	0.035	0.081
BBB04	-0.312	-0.253	-0.454	-0.404	0.180	0.220	0.110	0.140	0.068	0.061	0.013	0.061
BBB05	-0.350	-0.242	-0.257	-0.269	0.150	0.230	0.230	0.240	0.067	0.039	0.044	0.067
BBB06	-0.463	-0.301	-0.398	-0.370	0.080	0.180	0.140	0.160	0.038	0.056	0.055	0.060
BBB07	-0.121	-0.136	-0.228	-0.192	0.360	0.340	0.250	0.310	0.219	0.034	0.050	0.066
BBB08	0.028	-0.009	-0.128	-0.176	0.530	0.490	0.370	0.330	0.047	0.072	0.025	0.031
BBB09	0.061	0.106	-0.149	-0.150	0.570	0.620	0.340	0.350	0.056	0.106	0.056	0.075
BBB10	0.055	0.034	0.073	0.150	0.560	0.540	0.590	0.660	0.059	0.015	0.016	0.060
BBB11	0.509	0.474	0.389	0.579	0.900	0.900	0.840	0.910	0.074	0.070	0.036	0.066
BBB12	0.086	0.393	0.204	0.385	0.590	0.850	0.720	0.820	0.025	0.138	0.061	0.144
BBB13	-0.031	-0.073	-0.107	-0.126	0.460	0.410	0.390	0.390	0.092	0.024	0.040	0.036
BBB14	0.024	0.102	0.024	0.044	0.530	0.620	0.530	0.570	0.047	0.049	0.036	0.022
BBB15	0.500	0.360	0.563	0.565	0.890	0.830	0.930	0.900	0.088	0.145	0.078	0.120
BBB16	-0.472	-0.223	-0.255	-0.312	0.080	0.250	0.230	0.200	0.048	0.130	0.050	0.081
BBB17	-0.331	-0.046	-0.245	-0.287	0.160	0.450	0.240	0.220	0.210	0.087	0.052	0.041
BBB18	-0.072	-0.011	-0.115	-0.174	0.420	0.490	0.380	0.330	0.129	0.095	0.098	0.076
BBB19	0.340	-0.317	-0.267	-0.377	0.800	0.170	0.220	0.160	0.249	0.042	0.085	0.056
BBB20	0.813	0.664	0.641	0.786	0.990	0.970	0.950	0.970	0.042	0.077	0.114	0.108

BBB21	0.681	0.599	0.575	0.605	0.970	0.950	0.930	0.930	0.102	0.070	0.081	0.063
BBB22	-0.427	-0.061	0.270	0.210	0.100	0.430	0.760	0.710	0.113	0.094	0.085	0.148
BBB23	-0.433	-0.036	-0.064	-0.288	0.090	0.460	0.440	0.220	0.129	0.115	0.074	0.088
BBB24	0.333	0.168	0.134	0.020	0.800	0.680	0.670	0.540	0.130	0.021	0.045	0.060
BBB25	0.046	-0.042	-0.078	-0.094	0.550	0.450	0.420	0.420	0.097	0.041	0.020	0.052
BBB26	0.228	0.361	0.146	0.324	0.730	0.830	0.670	0.790	0.094	0.095	0.051	0.027
BBB27	0.066	0.023	-0.031	-0.181	0.570	0.530	0.470	0.330	0.072	0.027	0.045	0.068
BBB28	0.285	0.275	0.189	0.235	0.760	0.770	0.710	0.730	0.110	0.043	0.050	0.082
BBB29	0.193	0.590	0.575	0.720	0.690	0.950	0.930	0.960	0.244	0.113	0.074	0.084
BBC01	-0.118	-0.105	-0.188	-0.033	0.360	0.370	0.290	0.490	0.006	0.108	0.080	0.105
BBC02	-0.066	-0.248	-0.395	-0.318	0.420	0.220	0.140	0.200	0.172	0.056	0.027	0.028
BBC03	0.151	0.057	0.038	0.094	0.650	0.570	0.550	0.610	0.026	0.078	0.074	0.064
BBC04	0.502	0.502	0.662	0.596	0.890	0.920	0.960	0.920	0.112	0.043	0.109	0.056
BBC05	-0.355	-0.397	-0.584	-0.506	0.140	0.120	0.050	0.080	0.041	0.049	0.097	0.099
BBC06	0.499	0.164	0.056	0.209	0.890	0.680	0.570	0.710	0.005	0.142	0.146	0.087
BBC07	0.111	0.022	0.154	-0.035	0.610	0.530	0.680	0.490	0.096	0.094	0.052	0.137
BBC08	-0.223	-0.223	-0.299	-0.280	0.260	0.250	0.200	0.230	0.160	0.070	0.059	0.064
BBC10	-0.551	-0.403	-0.611	-0.645	0.050	0.120	0.030	0.020	0.084	0.129	0.069	0.078
BBC11	-0.426	-0.387	-0.488	-0.616	0.100	0.120	0.090	0.030	0.022	0.045	0.079	0.096
BBC12	-0.254	-0.448	-0.537	-0.467	0.230	0.090	0.060	0.100	0.023	0.072	0.066	0.055
BBD001	0.096	-0.078	-0.056	0.050	0.600	0.400	0.450	0.570	0.062	0.114	0.082	0.138
BBD01	-0.442	-0.425	-0.590	-0.447	0.090	0.100	0.040	0.110	0.068	0.120	0.065	0.044
BBD02	0.193	-0.013	-0.166	-0.229	0.690	0.480	0.320	0.280	0.071	0.047	0.037	0.068
BBD03	0.231	0.037	-0.130	0.177	0.730	0.550	0.360	0.680	0.101	0.150	0.109	0.174
BBD04	0.309	0.090	-0.223	-0.094	0.780	0.610	0.260	0.420	0.088	0.133	0.047	0.087
BBD05	0.405	0.237	0.200	0.368	0.830	0.740	0.710	0.810	0.042	0.114	0.162	0.130
BBD05.1	0.159	-0.115	-0.138	0.133	0.660	0.360	0.350	0.650	0.037	0.081	0.041	0.061
BBD06.1	0.241	0.039	-0.019	0.024	0.740	0.550	0.480	0.550	0.058	0.128	0.038	0.100
BBD07	0.573	0.343	0.323	0.286	0.930	0.820	0.790	0.760	0.064	0.070	0.065	0.092
BBD08	0.365	0.318	0.380	0.395	0.810	0.800	0.830	0.820	0.020	0.115	0.078	0.095
BBD09	0.117	-0.145	-0.060	-0.031	0.620	0.330	0.440	0.490	0.143	0.028	0.036	0.035
BBD10	-0.182	-0.178	-0.302	-0.205	0.300	0.290	0.200	0.300	0.051	0.107	0.032	0.094
BBD11	0.046	0.066	0.094	0.139	0.550	0.580	0.620	0.650	0.081	0.085	0.022	0.081
BBD12	-0.075	-0.029	-0.011	0.035	0.410	0.470	0.490	0.560	0.069	0.079	0.083	0.081
BBD13	0.125	0.058	0.085	0.353	0.630	0.570	0.610	0.800	0.032	0.052	0.048	0.144
BBD14	0.204	0.086	0.186	0.496	0.700	0.600	0.700	0.870	0.085	0.062	0.041	0.088
BBD15	0.294	0.206	0.006	0.127	0.770	0.710	0.510	0.640	0.048	0.106	0.054	0.098

BBD15.1	0.393	0.202	0.343	0.340	0.830	0.710	0.810	0.790	0.043	0.137	0.066	0.100
BBD16	0.605	0.506	0.482	0.526	0.940	0.920	0.880	0.890	0.082	0.088	0.134	0.137
BBD17	0.494	0.351	0.292	0.285	0.880	0.830	0.770	0.760	0.107	0.059	0.066	0.065
BBD18	-0.106	-0.175	-0.071	-0.124	0.370	0.290	0.430	0.390	0.064	0.033	0.040	0.033
BBD19	0.430	0.338	0.358	0.359	0.850	0.820	0.810	0.800	0.049	0.104	0.093	0.090
BBD20	0.100	0.030	-0.171	-0.028	0.600	0.540	0.310	0.490	0.060	0.086	0.078	0.068
BBD21	-0.018	0.063	0.019	0.005	0.480	0.580	0.530	0.520	0.075	0.082	0.041	0.073
BBD22	0.218	0.071	0.228	0.168	0.720	0.590	0.740	0.680	0.046	0.058	0.032	0.040
BBD23	0.026	-0.037	-0.212	-0.234	0.530	0.460	0.270	0.270	0.046	0.082	0.038	0.050
BBD24	0.160	0.036	-0.085	0.013	0.660	0.550	0.410	0.530	0.055	0.027	0.091	0.085
BBD25	0.432	0.266	0.206	0.303	0.850	0.760	0.720	0.770	0.097	0.091	0.040	0.093
BBE01	0.626	0.489	0.440	0.581	0.950	0.910	0.860	0.920	0.068	0.050	0.048	0.090
BBE02	0.643	0.478	0.507	0.577	0.960	0.900	0.900	0.910	0.187	0.158	0.110	0.153
BBE03	0.645	0.433	0.443	0.357	0.960	0.880	0.860	0.800	0.164	0.076	0.106	0.085
BBE04	0.327	0.214	0.087	0.160	0.790	0.720	0.610	0.670	0.054	0.048	0.044	0.060
BBE04.1	0.501	0.377	0.091	0.176	0.890	0.840	0.620	0.680	0.102	0.066	0.057	0.092
BBE06	0.551	0.353	0.265	0.260	0.920	0.830	0.750	0.750	0.043	0.068	0.085	0.041
BBE07	0.333	0.333	0.102	0.098	0.800	0.810	0.630	0.620	0.086	0.088	0.033	0.080
BBE08	0.466	0.400	0.368	0.418	0.870	0.860	0.820	0.830	0.037	0.052	0.024	0.068
BBE09	-0.111	0.036	-0.238	-0.142	0.370	0.540	0.250	0.360	0.057	0.095	0.058	0.081
BBE10	0.569	0.479	0.454	0.463	0.930	0.900	0.870	0.850	0.039	0.060	0.037	0.064
BBE11	0.530	0.723	0.608	0.633	0.910	0.980	0.950	0.940	0.008	0.058	0.139	0.066
BBE12	0.455	0.315	0.407	0.425	0.860	0.800	0.840	0.840	0.037	0.062	0.060	0.043
BBE13	0.759	0.701	0.543	0.670	0.980	0.980	0.920	0.950	0.098	0.129	0.103	0.126
BBE14	0.555	0.479	0.278	0.320	0.920	0.900	0.760	0.780	0.044	0.040	0.040	0.041
BBE15	0.704	0.624	0.553	0.619	0.980	0.960	0.930	0.930	0.108	0.059	0.108	0.194
BBE16	0.317	0.329	0.095	0.134	0.780	0.810	0.620	0.650	0.040	0.057	0.047	0.034
BBE17	0.493	0.720	0.809	0.654	0.880	0.980	0.980	0.940	0.202	0.050	0.129	0.087
BBE17.1	0.331	0.257	0.213	-0.007	0.790	0.760	0.720	0.510	0.057	0.066	0.079	0.067
BBE18		0.582	0.360	0.634		0.940	0.820	0.940		0.266	0.106	0.100
BBE19	0.104	-0.047	-0.008	0.179	0.600	0.440	0.490	0.690	0.056	0.068	0.043	0.106
BBE20	0.386	0.488	0.533	0.569	0.820	0.910	0.920	0.910	0.123	0.104	0.082	0.076
BBE21	0.309	0.296	0.359	0.567	0.780	0.790	0.820	0.910	0.051	0.052	0.055	0.133
BBE21.1	0.576	0.578	0.556	0.516	0.930	0.940	0.930	0.880	0.149	0.159	0.089	0.125
BBE22	0.447	0.494	0.533	0.415	0.860	0.910	0.920	0.830	0.164	0.121	0.098	0.106
BBE23	0.721	0.501	0.485	0.299	0.980	0.920	0.890	0.770	0.059	0.077	0.029	0.038
BBE23.1	0.547	0.475	0.446	0.389	0.920	0.900	0.860	0.820	0.053	0.111	0.067	0.092

BBE23.2	0.480	0.231	0.066	0.131	0.880	0.740	0.580	0.640	0.020	0.075	0.028	0.074
BBE24	0.581	0.383	0.331	0.577	0.930	0.850	0.800	0.910	0.078	0.120	0.105	0.060
BBE24.1	0.617	0.383	0.382	0.217	0.950	0.850	0.830	0.710	0.092	0.083	0.032	0.016
BBE25	0.689	0.436	0.524	0.553	0.970	0.880	0.910	0.900	0.154	0.086	0.056	0.087
BBE26	0.599	0.390	0.293	0.281	0.940	0.850	0.770	0.760	0.078	0.074	0.030	0.071
BBE27	0.651	0.607	0.516	0.679	0.960	0.950	0.910	0.950	0.116	0.132	0.056	0.107
BBE28	0.550	0.467	0.365	0.432	0.920	0.890	0.820	0.840	0.061	0.077	0.031	0.073
BBE29	0.234	0.126	-0.107	-0.141	0.730	0.650	0.390	0.360	0.073	0.080	0.058	0.055
BBE29.1	0.235	0.291	0.196	0.256	0.730	0.780	0.710	0.740	0.024	0.129	0.025	0.076
BBE30	0.704	0.714	0.517	0.536	0.970	0.980	0.910	0.890	0.071	0.097	0.066	0.069
BBE31	-0.310	-0.377	-0.172	-0.219	0.180	0.130	0.310	0.290	0.078	0.063	0.079	0.038
BBE31	0.503	0.161	0.328	0.412	0.890	0.670	0.790	0.830	0.168	0.083	0.077	0.066
BBE32	0.463	0.399	0.439	0.206	0.860	0.860	0.860	0.700	0.067	0.102	0.125	0.100
BBE33	0.483	0.393	0.334	0.357	0.880	0.850	0.800	0.800	0.055	0.131	0.022	0.054
BBF001	0.474	0.395	0.329	0.306	0.870	0.850	0.790	0.780	0.032	0.068	0.053	0.083
BBF001.1	0.510	0.422	0.446	0.463	0.900	0.870	0.860	0.850	0.049	0.154	0.073	0.077
BBF01	0.136	-0.032	-0.240	-0.152	0.640	0.460	0.240	0.350	0.085	0.054	0.053	0.122
BBF02	0.061	-0.015	-0.073	-0.071	0.570	0.480	0.430	0.440	0.034	0.051	0.061	0.068
BBF03	0.220	0.211	0.400	0.387	0.720	0.720	0.840	0.820	0.064	0.031	0.023	0.074
BBF04	0.208	0.052	0.082	0.151	0.700	0.560	0.610	0.660	0.102	0.061	0.116	0.086
BBF05	0.082	-0.018	-0.241	-0.218	0.580	0.480	0.240	0.290	0.093	0.055	0.086	0.105
BBF06	0.268	0.234	-0.007	0.092	0.750	0.740	0.500	0.610	0.072	0.072	0.051	0.065
BBF07	0.609	0.734	0.488	0.673	0.940	0.980	0.890	0.950	0.161	0.069	0.140	0.138
BBF08	0.396	0.125	0.162	0.222	0.830	0.640	0.680	0.720	0.123	0.116	0.087	0.087
BBF09	0.201	0.126	-0.042	0.047	0.700	0.650	0.460	0.570	0.014	0.056	0.048	0.060
BBF10	-0.383	-0.392	-0.374	-0.390	0.120	0.120	0.150	0.140	0.114	0.050	0.067	0.060
BBF11.1	0.478	0.471	0.350	0.363	0.880	0.900	0.810	0.810	0.070	0.036	0.043	0.077
BBF12	0.184	0.183	0.143	0.160	0.680	0.690	0.670	0.670	0.090	0.100	0.138	0.079
BBF13	0.144	-0.019	-0.054	-0.099	0.650	0.480	0.450	0.410	0.133	0.033	0.043	0.032
BBF14	0.318	0.286	0.076	0.074	0.790	0.780	0.600	0.600	0.066	0.068	0.075	0.077
BBF14.1	0.607	0.432	0.548	0.571	0.940	0.880	0.920	0.910	0.075	0.071	0.081	0.064
BBF16	0.609	0.456	0.513	0.595	0.950	0.890	0.910	0.920	0.100	0.146	0.090	0.087
BBF17	0.143	-0.046	-0.232	-0.249	0.650	0.440	0.250	0.260	0.073	0.065	0.038	0.047
BBF18	0.089	0.233	0.118	0.058	0.590	0.740	0.650	0.580	0.049	0.094	0.087	0.059
BBF19	0.167	-0.065	-0.122	-0.193	0.670	0.420	0.370	0.310	0.197	0.049	0.020	0.042
BBF19.1	0.252	0.354	0.340	0.518	0.740	0.830	0.800	0.880	0.016	0.099	0.046	0.082
BBF20	0.319	0.194	0.572	0.829	0.790	0.700	0.930	0.980	0.023	0.077	0.073	0.066

BBF21	0.419	0.413	0.343	0.531	0.840	0.870	0.810	0.890	0.022	0.084	0.082	0.064
BBF22	0.404	0.244	0.158	0.215	0.830	0.750	0.680	0.710	0.043	0.049	0.053	0.070
BBF23	0.350	0.319	0.129	0.225	0.810	0.800	0.660	0.720	0.132	0.141	0.080	0.059
BBF24	-0.007	-0.146	-0.216	-0.246	0.490	0.330	0.260	0.260	0.130	0.058	0.045	0.046
BBF25	0.033	0.052	-0.075	-0.056	0.540	0.560	0.430	0.460	0.098	0.085	0.104	0.090
BBF26	-0.060	-0.109	-0.030	-0.207	0.430	0.370	0.470	0.300	0.057	0.047	0.052	0.029
BBF26.1	0.048	0.006	-0.240	-0.037	0.550	0.510	0.240	0.490	0.188	0.096	0.029	0.082
BBF29	0.504	0.400	0.318	0.387	0.890	0.860	0.790	0.820	0.140	0.138	0.074	0.161
BBF30	0.206	0.257	0.162	0.147	0.700	0.760	0.680	0.660	0.118	0.109	0.062	0.134
BBF31	0.498	0.275	0.199	0.131	0.890	0.770	0.710	0.640	0.034	0.115	0.065	0.160
BBF31.1	0.591	0.605	0.506	0.689	0.940	0.950	0.900	0.950	0.107	0.090	0.158	0.056
BBF32	-1.123	-1.051	-0.868	-0.795	0.000	0.000	0.000	0.000	0.064	0.049	0.021	0.060
BBF33	-0.832	-0.758	-0.732	-0.476	0.000	0.000	0.000	0.100	0.200	0.070	0.068	0.149
BBG01	-0.000	0.193	-0.149	-0.066	0.500	0.700	0.340	0.450	0.092	0.348	0.052	0.072
BBG02	0.057	-0.210	-0.180	-0.344	0.560	0.260	0.300	0.180	0.072	0.051	0.035	0.054
BBG03	0.070	-0.020	-0.068	0.105	0.570	0.480	0.430	0.620	0.049	0.087	0.095	0.108
BBG03	-0.398	-0.402	-0.537	-0.552	0.110	0.120	0.060	0.060	0.060	0.038	0.028	0.066
BBG04	0.514	0.324	0.248	0.303	0.900	0.810	0.740	0.770	0.059	0.092	0.057	0.120
BBG05	0.279	-0.071	-0.387	-0.409	0.760	0.410	0.150	0.130	0.100	0.101	0.045	0.047
BBG06	0.245	0.094	0.097	0.094	0.740	0.610	0.630	0.610	0.047	0.066	0.042	0.035
BBG07	0.237	0.029	-0.068	-0.048	0.730	0.540	0.430	0.470	0.079	0.061	0.060	0.037
BBG08	-0.215	-0.201	-0.163	-0.052	0.270	0.270	0.320	0.470	0.154	0.085	0.044	0.083
BBG09	0.258	0.045	0.171	0.104	0.750	0.560	0.690	0.620	0.111	0.051	0.023	0.022
BBG10	-0.530	-0.330	-0.466	-0.349	0.060	0.160	0.100	0.180	0.139	0.183	0.045	0.117
BBG11	0.095	-0.157	-0.234	-0.272	0.600	0.320	0.250	0.240	0.091	0.052	0.086	0.125
BBG12	-0.369	-0.244	-0.413	-0.346	0.130	0.230	0.130	0.180	0.082	0.186	0.027	0.107
BBG13	-0.313	-0.532	-0.645	-0.691	0.180	0.050	0.020	0.000	0.092	0.041	0.046	0.088
BBG14	-0.384	-0.441	-0.501	-0.418	0.120	0.090	0.080	0.130	0.067	0.084	0.034	0.091
BBG15	-0.134	-0.351	-0.470	-0.485	0.350	0.150	0.100	0.090	0.066	0.036	0.062	0.123
BBG16	-0.238	-0.192	-0.227	-0.201	0.250	0.280	0.250	0.300	0.079	0.051	0.041	0.084
BBG17	-0.169	-0.387	-0.415	-0.404	0.310	0.130	0.130	0.140	0.060	0.057	0.059	0.090
BBG18	-0.639	-0.487	-0.666	-0.547	0.030	0.070	0.020	0.060	0.021	0.062	0.064	0.104
BBG19	-0.508	-0.565	-0.531	-0.729	0.060	0.040	0.070	0.000	0.042	0.063	0.174	0.076
BBG20	-0.495	-0.477	-0.569	-0.558	0.070	0.070	0.050	0.050	0.104	0.094	0.043	0.069
BBG21	-0.346	-0.462	-0.593	-0.497	0.150	0.080	0.040	0.080	0.052	0.052	0.043	0.082
BBG22	-0.646	-0.604	-0.728	-0.665	0.030	0.030	0.000	0.010	0.031	0.046	0.059	0.062
BBG23	-0.569	-0.734	-0.716	-0.891	0.050	0.000	0.010	0.000	0.089	0.024	0.122	0.088

BBG24	-0.784	-0.719	-0.790	-0.751	0.010	0.000	0.000	0.000	0.046	0.058	0.087	0.072
BBG25	-0.199	-0.189	-0.238	-0.152	0.280	0.280	0.250	0.350	0.239	0.062	0.038	0.082
BBG26	-0.080	-0.214	-0.250	-0.175	0.400	0.250	0.240	0.330	0.092	0.097	0.138	0.125
BBG27	-0.201	-0.176	-0.305	-0.388	0.280	0.290	0.200	0.150	0.078	0.060	0.089	0.061
BBG28	-0.330	-0.247	-0.364	-0.346	0.170	0.220	0.160	0.180	0.100	0.045	0.083	0.053
BBG29	-0.700	-0.639	-0.712	-0.767	0.020	0.020	0.010	0.000	0.065	0.084	0.039	0.043
BBG30	-0.453	-0.407	-0.461	-0.605	0.090	0.110	0.100	0.030	0.088	0.098	0.056	0.038
BBG31	-0.102	-0.196	-0.354	-0.307	0.380	0.270	0.160	0.200	0.066	0.022	0.038	0.053
BBG32	-0.409	-0.423	-0.484	-0.486	0.110	0.110	0.100	0.090	0.067	0.054	0.050	0.050
BBG33	-0.058	0.009	0.284	0.295	0.430	0.510	0.770	0.770	0.098	0.051	0.073	0.074
BBG34	0.132	0.187	0.109	0.148	0.640	0.700	0.640	0.660	0.104	0.104	0.091	0.092
BBH01	-0.244	-0.346	-0.296	-0.296	0.240	0.150	0.200	0.210	0.126	0.038	0.062	0.063
BBH02	0.059	-0.055	-0.319	0.085	0.570	0.430	0.190	0.610	0.161	0.129	0.057	0.128
BBH03	0.130	-0.049	-0.164	-0.112	0.630	0.440	0.320	0.400	0.115	0.030	0.054	0.060
BBH04	-0.033	-0.074	-0.179	-0.148	0.450	0.410	0.300	0.360	0.049	0.087	0.032	0.047
BBH05	0.045	0.042	-0.018	-0.026	0.550	0.550	0.480	0.500	0.071	0.037	0.092	0.127
BBH06	-0.021	0.059	-0.082	-0.151	0.470	0.570	0.420	0.350	0.104	0.083	0.073	0.050
BBH07	0.431	0.355	0.287	0.283	0.850	0.830	0.770	0.760	0.044	0.138	0.095	0.112
BBH08	0.304	0.163	0.305	0.319	0.780	0.670	0.780	0.780	0.067	0.150	0.133	0.097
BBH09	0.045	-0.017	-0.292	-0.300	0.550	0.480	0.210	0.210	0.037	0.123	0.054	0.095
BBH09.1	0.256	0.330	0.248	0.239	0.750	0.810	0.740	0.730	0.109	0.116	0.048	0.106
BBH10.1	0.636	0.373	0.457	0.537	0.950	0.840	0.870	0.890	0.057	0.091	0.068	0.087
BBH11.1	0.273	0.259	0.218	0.198	0.760	0.760	0.720	0.700	0.158	0.123	0.072	0.056
BBH12	0.349	0.088	0.107	0.123	0.810	0.610	0.640	0.640	0.065	0.064	0.076	0.113
BBH13	0.121	0.347	0.233	0.290	0.630	0.820	0.740	0.760	0.056	0.107	0.082	0.100
BBH14	0.779	0.684	0.503	0.510	0.990	0.980	0.900	0.880	0.083	0.109	0.056	0.092
BBH15	0.568	0.459	0.533	0.547	0.930	0.890	0.920	0.900	0.370	0.116	0.072	0.088
BBH16	0.668	0.483	0.423	0.293	0.960	0.910	0.850	0.770	0.058	0.112	0.068	0.092
BBH16.1	0.626	0.530	0.408	0.456	0.950	0.930	0.840	0.850	0.060	0.106	0.041	0.083
BBH17	0.784	0.506	0.465	0.530	0.990	0.920	0.880	0.890	0.066	0.081	0.037	0.068
BBH18	0.650	0.404	0.416	0.472	0.960	0.860	0.850	0.860	0.110	0.119	0.088	0.058
BBH18.1	0.386	0.136	-0.005	-0.154	0.820	0.650	0.500	0.350	0.059	0.087	0.044	0.045
BBH20	-0.325	-0.314	-0.345	-0.318	0.170	0.170	0.170	0.200	0.109	0.058	0.051	0.064
BBH20.1	0.555	0.488	0.502	0.432	0.920	0.910	0.900	0.840	0.099	0.132	0.140	0.122
BBH24.1	0.666	0.491	0.502	0.592	0.960	0.910	0.900	0.920	0.050	0.066	0.067	0.087
BBH25.1	0.562	0.461	0.479	0.694	0.920	0.890	0.880	0.960	0.062	0.104	0.121	0.113
BBH26	0.365	0.731	0.616	0.622	0.810	0.980	0.950	0.930	0.124	0.127	0.105	0.096

BBH27	0.759	0.474	0.526	0.569	0.980	0.900	0.910	0.910	0.057	0.077	0.078	0.097
BBH28	0.687	0.426	0.374	0.481	0.970	0.870	0.830	0.870	0.040	0.077	0.070	0.089
BBH29	0.609	0.414	0.588	0.529	0.950	0.870	0.940	0.890	0.046	0.135	0.049	0.081
BBH30	0.616	0.496	0.460	0.551	0.950	0.910	0.870	0.900	0.133	0.111	0.061	0.106
BBH31	0.639	0.533	0.664	0.739	0.960	0.930	0.960	0.970	0.263	0.190	0.124	0.098
BBH32	0.763	0.554	0.586	0.815	0.980	0.930	0.940	0.980	0.003	0.180	0.079	0.283
BBH33	-0.033	-0.103	-0.282	-0.190	0.450	0.380	0.210	0.320	0.102	0.083	0.078	0.073
BBH34	0.233	0.055	0.161	0.070	0.730	0.570	0.680	0.590	0.022	0.071	0.066	0.069
BBH35	0.081	-0.051	-0.192	-0.244	0.580	0.440	0.290	0.260	0.139	0.049	0.025	0.083
BBH36.1	0.337	0.060	-0.156	-0.038	0.800	0.580	0.330	0.480	0.064	0.047	0.075	0.129
BBH36.2	0.191	0.138	0.060	0.020	0.690	0.650	0.580	0.540	0.056	0.046	0.054	0.039
BBH37	-0.020	-0.122	-0.285	-0.191	0.470	0.360	0.210	0.310	0.108	0.091	0.047	0.105
BBH38	0.572	0.427	0.484	0.408	0.930	0.870	0.890	0.820	0.087	0.085	0.090	0.056
BBH39	0.663	0.554	0.523	0.522	0.960	0.930	0.910	0.880	0.048	0.071	0.091	0.060
BBH40	0.047	0.004	-0.007	-0.096	0.550	0.510	0.500	0.420	0.104	0.060	0.108	0.073
BBH41	0.409	0.326	0.258	0.620	0.840	0.810	0.750	0.930	0.119	0.154	0.071	0.170
BBH41	-0.242	-0.307	-0.529	-0.558	0.240	0.180	0.070	0.050	0.047	0.089	0.080	0.038
BBI01	0.318	0.245	-0.038	-0.032	0.790	0.750	0.460	0.490	0.102	0.073	0.058	0.061
BBI02	-0.102	-0.223	-0.305	-0.289	0.380	0.250	0.190	0.220	0.158	0.042	0.046	0.040
BBI02.1	0.771	0.557	0.544	0.485	0.980	0.940	0.920	0.870	0.119	0.078	0.056	0.040
BBI02.2	0.187	0.223	0.206	0.805	0.680	0.730	0.720	0.980	0.015	0.045	0.015	0.077
BBI03	0.375	0.401	0.325	0.411	0.820	0.860	0.790	0.830	0.089	0.106	0.126	0.097
BBI04	0.533	0.472	0.398	0.357	0.910	0.900	0.840	0.800	0.111	0.051	0.111	0.070
BBI05	0.801	0.591	0.613	0.789	0.990	0.950	0.950	0.970	0.105	0.180	0.160	0.063
BBI06	0.110	-0.197	-0.214	-0.158	0.610	0.270	0.270	0.340	0.059	0.077	0.045	0.094
BBI07	0.351	0.250	0.252	0.237	0.810	0.750	0.750	0.730	0.033	0.072	0.070	0.021
BBI08.1	0.159	0.035	0.045	-0.040	0.660	0.540	0.560	0.480	0.129	0.108	0.059	0.112
BBI11	0.409	0.430	0.473	0.479	0.840	0.880	0.880	0.860	0.039	0.058	0.040	0.059
BBI12	0.274	0.218	0.179	0.090	0.760	0.720	0.700	0.610	0.085	0.038	0.057	0.060
BBI13	0.510	0.441	0.381	0.391	0.900	0.880	0.830	0.820	0.076	0.070	0.090	0.072
BBI14	0.531	0.493	0.480	0.606	0.910	0.910	0.880	0.930	0.041	0.070	0.101	0.057
BBI15	0.363	0.160	0.074	0.061	0.810	0.670	0.600	0.580	0.118	0.022	0.053	0.050
BBI16	0.243	-0.174	-0.009	-0.299	0.740	0.300	0.490	0.210	0.206	0.122	0.125	0.041
BBI17	0.118	-0.066	-0.137	0.056	0.620	0.420	0.360	0.580	0.117	0.044	0.079	0.079
BBI17.1	0.265	0.229	0.186	0.088	0.750	0.740	0.700	0.610	0.144	0.152	0.095	0.169
BBI18	0.496	0.374	0.413	0.456	0.890	0.840	0.850	0.850	0.081	0.091	0.064	0.078
BBI19	0.616	0.598	0.486	0.562	0.950	0.950	0.890	0.900	0.107	0.258	0.120	0.102

BBI20	0.414	0.182	0.259	0.137	0.840	0.690	0.750	0.650	0.119	0.117	0.085	0.073
BBI21	0.509	0.638	0.505	0.590	0.900	0.960	0.900	0.920	0.137	0.049	0.068	0.037
BBI22	0.507	0.089	-0.111	-0.094	0.890	0.610	0.390	0.420	0.111	0.105	0.030	0.069
BBI23	0.665	0.634	0.474	0.706	0.960	0.960	0.880	0.960	0.167	0.122	0.060	0.131
BBI24	0.284	0.091	-0.078	-0.138	0.760	0.610	0.420	0.370	0.128	0.048	0.073	0.093
BBI25	0.540	0.566	0.437	0.503	0.910	0.940	0.860	0.880	0.134	0.135	0.100	0.117
BBI26	0.118	-0.103	-0.114	0.052	0.620	0.380	0.380	0.580	0.111	0.096	0.056	0.075
BBI27	0.326	0.082	0.065	-0.046	0.790	0.600	0.580	0.470	0.047	0.115	0.087	0.099
BBI28	-0.356	-0.530	-0.397	-0.372	0.140	0.050	0.140	0.160	0.027	0.062	0.033	0.098
BBI29	0.211	-0.063	-0.111	0.085	0.710	0.420	0.390	0.610	0.048	0.075	0.062	0.029
BBI30	0.415	0.274	0.225	0.362	0.840	0.770	0.730	0.810	0.045	0.059	0.070	0.088
BBI31	0.123	-0.169	-0.356	-0.255	0.630	0.300	0.160	0.250	0.029	0.069	0.116	0.135
BBI31.1	0.474	0.348	0.317	0.414	0.870	0.820	0.780	0.830	0.095	0.055	0.072	0.080
BBI33	0.437	0.121	0.077	0.322	0.850	0.640	0.600	0.790	0.088	0.060	0.060	0.077
BBI34	-0.192	-0.170	-0.014	-0.130	0.290	0.300	0.490	0.380	0.032	0.113	0.083	0.043
BBI35	0.401	0.277	0.208	0.022	0.830	0.770	0.720	0.540	0.083	0.052	0.049	0.049
BBI36	-0.140	-0.129	-0.244	-0.001	0.340	0.350	0.240	0.520	0.059	0.039	0.112	0.121
BBI37	0.634	0.683	0.480	0.575	0.950	0.970	0.880	0.910	0.072	0.160	0.104	0.091
BBI38	-0.167	-0.137	-0.027	-0.022	0.320	0.340	0.470	0.500	0.046	0.050	0.015	0.050
BBI39	0.011	0.022	0.182	0.187	0.510	0.530	0.700	0.690	0.026	0.050	0.026	0.051
BBI40	0.343	0.323	0.155	0.214	0.800	0.810	0.680	0.710	0.024	0.078	0.050	0.057
BBI41	0.419	0.257	0.278	0.172	0.840	0.760	0.760	0.680	0.047	0.027	0.089	0.113
BBI42	-0.462	-0.473	-0.417	-0.440	0.080	0.080	0.120	0.120	0.052	0.134	0.055	0.043
BBI43	0.223	-0.030	0.077	0.004	0.720	0.460	0.600	0.520	0.086	0.102	0.110	0.127
BBJ001	-0.116	-0.170	0.064	-0.048	0.370	0.300	0.580	0.470	0.105	0.081	0.182	0.062
BBJ02.1	-0.096	-0.210	-0.441	-0.377	0.390	0.260	0.120	0.160	0.130	0.158	0.067	0.128
BBJ04	0.195	0.287	-0.021	-0.015	0.690	0.780	0.480	0.510	0.055	0.085	0.102	0.147
BBJ05	0.136	-0.084	-0.288	-0.323	0.640	0.400	0.210	0.190	0.044	0.039	0.041	0.047
BBJ07.1	0.205	0.141	-0.182	-0.164	0.700	0.660	0.300	0.340	0.096	0.110	0.060	0.051
BBJ08	-0.284	-0.272	0.076	0.062	0.200	0.200	0.600	0.590	0.052	0.100	0.085	0.122
BBJ09	0.023	-0.138	-0.237	-0.343	0.530	0.340	0.250	0.180	0.109	0.048	0.092	0.084
BBJ10	0.216	0.100	-0.014	0.071	0.710	0.620	0.490	0.590	0.068	0.060	0.091	0.069
BBJ11	0.152	-0.063	-0.027	-0.054	0.650	0.420	0.470	0.460	0.062	0.049	0.043	0.062
BBJ12.1	0.406	0.328	0.062	0.229	0.840	0.810	0.580	0.720	0.112	0.078	0.069	0.072
BBJ13	0.106	-0.060	-0.192	-0.156	0.610	0.430	0.290	0.350	0.065	0.052	0.057	0.037
BBJ15.1	0.232	0.180	-0.019	0.025	0.730	0.690	0.480	0.550	0.053	0.077	0.047	0.059
BBJ16	0.021	-0.183	-0.172	-0.249	0.520	0.290	0.310	0.260	0.121	0.036	0.030	0.031

BBJ17	0.059	0.087	0.041	0.138	0.570	0.600	0.560	0.650	0.023	0.050	0.048	0.055
BBJ18	0.135	0.110	0.230	0.043	0.640	0.630	0.740	0.570	0.105	0.054	0.073	0.043
BBJ19	-0.073	0.008	0.366	0.232	0.410	0.510	0.820	0.730	0.021	0.064	0.045	0.108
BBJ20	0.088	-0.076	-0.000	-0.007	0.590	0.400	0.510	0.510	0.119	0.061	0.066	0.078
BBJ20.1	0.310	0.028	-0.006	-0.028	0.780	0.530	0.500	0.490	0.178	0.088	0.067	0.083
BBJ21.1	0.225	-0.018	0.110	-0.057	0.720	0.480	0.640	0.460	0.194	0.076	0.069	0.073
BBJ23	-0.244	0.045	-0.396	-0.266	0.240	0.560	0.140	0.240	0.209	0.146	0.102	0.129
BBJ24	-0.025	-0.303	-0.392	-0.480	0.470	0.180	0.140	0.090	0.155	0.050	0.031	0.110
BBJ25	-0.209	-0.129	-0.339	-0.377	0.270	0.350	0.170	0.160	0.109	0.114	0.042	0.080
BBJ26	-0.481	-0.625	-0.517	-0.591	0.080	0.020	0.080	0.040	0.038	0.044	0.031	0.053
BBJ27	-0.420	-0.429	-0.460	-0.628	0.100	0.100	0.110	0.020	0.069	0.066	0.076	0.094
BBJ28	0.007	-0.113	-0.166	0.011	0.500	0.360	0.310	0.530	0.122	0.125	0.064	0.125
BBJ29	-0.355	-0.616	-0.642	-0.689	0.140	0.020	0.020	0.010	0.044	0.069	0.063	0.076
BBJ30	0.389	0.116	0.299	0.426	0.830	0.630	0.780	0.840	0.041	0.105	0.049	0.149
BBJ31	-0.821	-0.877	-0.625	-0.856	0.000	0.000	0.030	0.000	0.088	0.022	0.032	0.062
BBJ32	0.262	0.186	0.300	0.341	0.750	0.700	0.780	0.790	0.149	0.148	0.094	0.094
BBJ33	0.248	0.146	0.015	0.199	0.740	0.660	0.520	0.700	0.083	0.091	0.072	0.116
BBJ34	-0.603	-0.603	-0.491	-0.487	0.040	0.030	0.090	0.090	0.077	0.081	0.045	0.042
BBJ35	0.514	0.203	0.141	0.103	0.900	0.710	0.670	0.620	0.047	0.046	0.044	0.049
BBJ36	-0.526	-0.439	-0.415	-0.203	0.060	0.100	0.130	0.300	0.156	0.028	0.064	0.063
BBJ37	-0.020	-0.348	-0.245	-0.378	0.470	0.150	0.240	0.160	0.109	0.038	0.091	0.068
BBJ38	0.260	0.010	-0.229	-0.070	0.750	0.510	0.250	0.440	0.078	0.047	0.046	0.099
BBJ39	0.484	0.175	-0.045	-0.108	0.880	0.690	0.450	0.400	0.042	0.068	0.064	0.095
BBJ39.1	0.453	0.265	0.219	0.228	0.860	0.760	0.730	0.720	0.063	0.086	0.046	0.114
BBJ40	0.821	0.637	0.497	0.512	0.990	0.960	0.900	0.880	0.142	0.162	0.070	0.093
BBJ41	-0.096	-0.009	0.265	0.330	0.390	0.490	0.750	0.790	0.058	0.076	0.040	0.068
BBJ42	0.537	0.182	0.243	0.378	0.910	0.690	0.740	0.810	0.092	0.077	0.070	0.089
BBJ43	-0.563	-0.483	-0.397	-0.416	0.050	0.070	0.140	0.130	0.050	0.097	0.065	0.042
BBJ44	0.303	0.143	0.126	-0.005	0.780	0.660	0.660	0.510	0.079	0.050	0.079	0.034
BBJ45	-0.780	-0.814	-0.543	-0.630	0.010	0.000	0.060	0.020	0.054	0.066	0.042	0.031
BBJ45.1	0.337	0.074	0.024	0.088	0.800	0.590	0.530	0.610	0.112	0.056	0.082	0.076
BBJ46	-0.038	-0.217	-0.002	-0.121	0.450	0.250	0.500	0.390	0.089	0.042	0.041	0.025
BBJ47	0.091	-0.194	-0.262	-0.282	0.590	0.280	0.230	0.230	0.102	0.074	0.045	0.132
BBJ48	-0.129	-0.188	-0.293	-0.275	0.350	0.280	0.210	0.230	0.034	0.046	0.039	0.050
BBJ49	0.348	0.136	0.210	0.277	0.810	0.650	0.720	0.760	0.054	0.044	0.102	0.152
BBJ50	-0.206	-0.226	-0.108	-0.104	0.280	0.240	0.390	0.410	0.030	0.065	0.075	0.049
BBJ51	-0.673	-0.747	-0.625	-0.672	0.020	0.000	0.030	0.010	0.107	0.124	0.126	0.127

BBK001	0.540	0.453	0.665	0.672	0.910	0.890	0.960	0.950	0.076	0.086	0.075	0.206
BBK01	0.397	0.094	0.006	-0.041	0.830	0.610	0.510	0.480	0.141	0.131	0.090	0.119
BBK02.1	-0.166	-0.122	-0.578	-0.498	0.320	0.360	0.050	0.080	0.111	0.111	0.057	0.114
BBK04.1	0.047	-0.057	-0.306	-0.325	0.550	0.430	0.190	0.190	0.048	0.150	0.053	0.035
BBK05	0.605	0.584	0.744	0.712	0.940	0.950	0.970	0.960	0.168	0.115	0.142	0.079
BBK06	0.713	0.506	0.486	0.575	0.980	0.920	0.890	0.910	0.066	0.036	0.090	0.045
BBK07	-0.266	-0.452	-0.373	-0.430	0.220	0.090	0.150	0.120	0.058	0.134	0.140	0.054
BBK08	0.508	0.267	0.332	0.291	0.900	0.770	0.800	0.770	0.042	0.075	0.078	0.061
BBK09	0.277	0.227	0.034	0.130	0.760	0.730	0.540	0.640	0.034	0.060	0.047	0.078
BBK10	0.198	0.071	0.041	0.149	0.700	0.590	0.560	0.660	0.173	0.037	0.044	0.125
BBK12	-0.302	-0.056	-0.108	0.186	0.190	0.430	0.390	0.690	0.108	0.081	0.097	0.137
BBK13	0.310	0.199	0.418	0.296	0.780	0.710	0.850	0.770	0.087	0.053	0.052	0.042
BBK14	0.690	0.677	0.586	0.816	0.970	0.970	0.940	0.980	0.027	0.088	0.135	0.131
BBK15	-0.088	-0.138	-0.093	-0.274	0.400	0.340	0.410	0.240	0.144	0.058	0.141	0.052
BBK16	0.301	0.341	0.321	0.503	0.770	0.820	0.790	0.880	0.104	0.102	0.114	0.031
BBK17	-0.490	-0.581	-0.607	-0.618	0.070	0.030	0.030	0.030	0.022	0.069	0.037	0.059
BBK18	0.541	0.480	0.435	0.641	0.910	0.900	0.860	0.940	0.070	0.107	0.062	0.184
BBK19	-0.301	-0.459	-0.366	-0.457	0.190	0.080	0.160	0.110	0.126	0.063	0.037	0.040
BBK20		0.659	0.434			0.970	0.850			0.308	0.137	
BBK21	-0.049	-0.108	-0.104	-0.041	0.440	0.370	0.390	0.480	0.049	0.063	0.032	0.114
BBK22	0.181	0.291	0.228	0.359	0.680	0.780	0.730	0.800	0.152	0.176	0.023	0.034
BBK23	-0.098	-0.173	0.028	-0.086	0.390	0.300	0.540	0.430	0.086	0.068	0.078	0.123
BBK24	0.381	0.276	0.192	0.278	0.820	0.770	0.710	0.760	0.045	0.199	0.099	0.141
BBK25	0.078	0.025	0.042	-0.229	0.580	0.530	0.560	0.280	0.056	0.124	0.010	0.030
BBK25.1	0.344	0.205	0.132	0.221	0.800	0.710	0.660	0.720	0.279	0.210	0.085	0.142
BBK31	0.388	0.015	0.085	0.274	0.830	0.520	0.610	0.750	0.164	0.045	0.059	0.175
BBK32	-0.125	-0.462	-0.446	-0.475	0.360	0.080	0.110	0.100	0.052	0.093	0.046	0.088
BBK33	0.838	0.732	0.539	0.604	0.990	0.980	0.920	0.930	0.023	0.107	0.171	0.090
BBK34	0.315	0.103	0.155	0.272	0.780	0.620	0.680	0.750	0.112	0.041	0.028	0.104
BBK35	0.211	-0.030	0.070	0.188	0.710	0.460	0.590	0.690	0.103	0.096	0.159	0.112
BBK36	0.205	0.049	0.044	0.011	0.700	0.560	0.560	0.530	0.100	0.096	0.106	0.069
BBK37	0.073	-0.174	-0.380	-0.299	0.580	0.300	0.150	0.210	0.109	0.116	0.052	0.137
BBK38	-0.214	-0.480	-0.350	-0.411	0.270	0.070	0.170	0.130	0.072	0.057	0.047	0.092
BBK39	-0.563	-0.462	-0.503	-0.464	0.050	0.080	0.080	0.110	0.062	0.095	0.051	0.083
BBK40	0.112	-0.003	0.227	0.202	0.610	0.500	0.730	0.700	0.021	0.079	0.084	0.062
BBK41	-0.274	-0.325	-0.431	-0.278	0.210	0.160	0.120	0.230	0.047	0.105	0.055	0.038
BBK42	0.352	0.356	0.096	0.246	0.810	0.830	0.630	0.740	0.062	0.149	0.076	0.119

BBK42.1	0.166	0.079	0.144	0.276	0.660	0.600	0.670	0.750	0.087	0.075	0.087	0.093
BBK44	0.267	0.121	0.073	0.133	0.750	0.640	0.600	0.650	0.053	0.031	0.046	0.052
BBK45	0.031	0.062	0.219	0.418	0.530	0.580	0.730	0.830	0.072	0.028	0.031	0.097
BBK46	-0.273	-0.567	-0.485	-0.495	0.210	0.040	0.090	0.080	0.061	0.006	0.021	0.043
BBK47	-0.589	-0.494	-0.562	-0.552	0.040	0.070	0.050	0.060	0.038	0.109	0.025	0.042
BBK48	-0.396	-0.475	-0.674	-0.572	0.110	0.080	0.010	0.050	0.090	0.189	0.059	0.101
BBK49	-0.475	-0.400	-0.483	-0.440	0.080	0.120	0.100	0.120	0.116	0.129	0.079	0.080
BBK50	-0.202	-0.404	-0.417	-0.243	0.280	0.110	0.130	0.270	0.109	0.138	0.064	0.101
BBK51	0.599	0.612		0.586	0.940	0.950		0.920	0.147	0.120		0.043
BBK52	-0.178	-0.251	-0.308	-0.264	0.310	0.220	0.190	0.250	0.052	0.106	0.059	0.073
BBK52.1	0.616	0.337	0.318	0.782	0.950	0.820	0.790	0.970	0.269	0.295	0.057	0.197
BBK53	-0.119	-0.397	-0.466	-0.379	0.360	0.120	0.100	0.150	0.022	0.053	0.046	0.071
BBK54	0.046	-0.086	-0.141	-0.194	0.550	0.390	0.350	0.310	0.031	0.064	0.033	0.054
BBL01	-0.465	-0.408	-0.458	-0.460	0.080	0.110	0.110	0.110	0.089	0.061	0.034	0.109
BBL02	-0.735	-0.610	-0.601	-0.592	0.010	0.030	0.040	0.040	0.019	0.089	0.025	0.032
BBL03	-0.472	-0.429	-0.495	-0.389	0.080	0.100	0.090	0.140	0.088	0.047	0.078	0.133
BBL04	-0.547	-0.576	-0.665	-0.517	0.050	0.040	0.020	0.070	0.052	0.054	0.078	0.088
BBL05	-0.606	-0.424	-0.536	-0.397	0.040	0.110	0.070	0.140	0.104	0.075	0.023	0.127
BBL06	-0.730	-0.453	-0.776	-0.597	0.010	0.090	0.000	0.040	0.075	0.073	0.020	0.106
BBL07	-0.756	-0.612	-0.582	-0.578	0.010	0.020	0.050	0.040	0.073	0.099	0.036	0.058
BBL08	-0.277	-0.192	-0.443	-0.306	0.210	0.280	0.110	0.200	0.064	0.043	0.051	0.091
BBL09	-0.626	-0.465	-0.632	-0.510	0.040	0.080	0.030	0.070	0.187	0.148	0.056	0.079
BBL10	-0.304	-0.203	-0.295	-0.387	0.190	0.260	0.200	0.150	0.130	0.084	0.139	0.074
BBL11	-0.826	-0.613	-0.748	-0.606	0.000	0.020	0.000	0.030	0.051	0.090	0.032	0.098
BBL12	-0.212	-0.450	-0.597	-0.469	0.270	0.090	0.040	0.100	0.150	0.061	0.064	0.048
BBL13	-0.157	-0.410	-0.382	-0.455	0.330	0.110	0.150	0.110	0.140	0.051	0.054	0.085
BBL14	0.110	0.063	0.027	0.150	0.610	0.580	0.540	0.660	0.109	0.090	0.107	0.064
BBL15	-0.745	-0.686	-0.687	-0.555	0.010	0.010	0.010	0.050	0.087	0.048	0.032	0.074
BBL16	-0.290	-0.270	-0.372	-0.346	0.200	0.200	0.150	0.180	0.031	0.051	0.058	0.088
BBL17	-0.662	-0.600	-0.485	-0.480	0.030	0.030	0.090	0.090	0.116	0.071	0.019	0.052
BBL18	-0.287	-0.178	-0.236	-0.183	0.200	0.290	0.250	0.320	0.079	0.074	0.118	0.106
BBL19	-0.073	-0.258	-0.127	-0.278	0.410	0.210	0.370	0.230	0.158	0.069	0.053	0.059
BBL20	-0.418	-0.276	-0.296	-0.337	0.100	0.190	0.200	0.180	0.043	0.059	0.106	0.022
BBL21	-0.013	-0.312	-0.275	-0.344	0.480	0.170	0.220	0.180	0.240	0.037	0.115	0.104
BBL22	-0.317	-0.398	-0.356	-0.201	0.170	0.120	0.160	0.310	0.051	0.061	0.060	0.135
BBL23	-0.095	-0.220	-0.212	-0.245	0.390	0.250	0.270	0.260	0.034	0.052	0.025	0.066
BBL24	-0.271	-0.193	-0.322	-0.382	0.210	0.280	0.180	0.150	0.132	0.130	0.054	0.102

BBL25		1.058	0.561	0.810		0.990	0.930	0.980		0.041	0.124	0.108
BBL26	0.568	0.420			0.930	0.870			0.264	0.535		
BBL27	0.090	0.180	0.158	0.284	0.590	0.690	0.680	0.760	0.088	0.120	0.053	0.054
BBL28	-0.076	-0.013	0.164	-0.061	0.410	0.490	0.690	0.450	0.010	0.037	0.052	0.042
BBL29		0.795		0.758		0.990		0.970		0.010		0.016
BBL30	0.019	-0.096	-0.030	0.029	0.520	0.380	0.470	0.550	0.054	0.042	0.045	0.064
BBL31	-0.298	-0.269	-0.212	-0.108	0.190	0.200	0.270	0.400	0.037	0.064	0.058	0.036
BBL32	0.033	-0.259	-0.199	-0.172	0.540	0.210	0.280	0.330	0.107	0.062	0.038	0.050
BBL33	0.594	0.743	0.526	0.677	0.940	0.980	0.910	0.950	0.145	0.067	0.093	0.108
BBL34	-0.009	-0.109	-0.139	-0.091	0.490	0.370	0.350	0.420	0.112	0.066	0.065	0.054
BBL35	-0.439	-0.217	-0.143	-0.040	0.090	0.250	0.340	0.480	0.094	0.037	0.042	0.070
BBL36	-0.262	-0.428	-0.587	-0.489	0.220	0.100	0.040	0.080	0.084	0.075	0.036	0.059
BBL37	-0.509	-0.440	-0.454	-0.279	0.060	0.090	0.110	0.230	0.050	0.044	0.102	0.034
BBL38	-0.101	0.101	-0.103	0.053	0.380	0.620	0.400	0.580	0.081	0.193	0.119	0.090
BBL39	-0.158	-0.200	-0.044	-0.044	0.330	0.270	0.450	0.470	0.140	0.044	0.062	0.044
BBL40	-0.106	-0.221	-0.166	-0.166	0.370	0.250	0.320	0.340	0.045	0.051	0.056	0.022
BBL41	0.090	0.120	0.026	-0.096	0.590	0.640	0.540	0.420	0.042	0.088	0.025	0.067
BBL42	-0.162	-0.322	-0.348	-0.318	0.320	0.160	0.170	0.200	0.053	0.034	0.030	0.055
BBL43	-0.853	-0.527	-0.589	-0.540	0.000	0.050	0.040	0.060	0.075	0.107	0.029	0.043
BBM01	-0.397	-0.292	-0.421	-0.512	0.110	0.190	0.120	0.070	0.194	0.190	0.017	0.048
BBM02	-0.802	-0.570	-0.500	-0.465	0.000	0.040	0.080	0.110	0.054	0.046	0.102	0.094
BBM03	-0.172	-0.270	-0.261	-0.131	0.310	0.200	0.230	0.380	0.053	0.033	0.090	0.142
BBM04	-0.276	-0.369	-0.473	-0.435	0.210	0.140	0.100	0.120	0.053	0.109	0.115	0.091
BBM05	-0.601	-0.515	-0.777	-0.650	0.040	0.060	0.000	0.020	0.114	0.047	0.063	0.113
BBM06	-0.830	-0.655	-0.769	-0.659	0.000	0.010	0.000	0.010	0.012	0.050	0.040	0.061
BBM07	-0.606	-0.641	-0.577	-0.647	0.040	0.020	0.050	0.020	0.043	0.056	0.033	0.069
BBM08	-0.344	-0.392	-0.491	-0.505	0.150	0.120	0.090	0.080	0.079	0.036	0.064	0.036
BBM09	-0.196	-0.200	-0.326	-0.265	0.290	0.270	0.180	0.240	0.045	0.050	0.099	0.118
BBM10	-0.360	-0.344	-0.515	-0.448	0.140	0.150	0.080	0.110	0.057	0.054	0.091	0.045
BBM11	-0.754	-0.612	-0.798	-0.659	0.010	0.020	0.000	0.010	0.113	0.085	0.078	0.090
BBM12	-0.442	-0.488	-0.521	-0.420	0.090	0.070	0.070	0.130	0.160	0.052	0.121	0.101
BBM13	-0.477	-0.499	-0.589	-0.586	0.080	0.060	0.040	0.040	0.162	0.087	0.039	0.043
BBM14	-0.135	-0.090	-0.298	-0.331	0.350	0.390	0.200	0.190	0.064	0.098	0.106	0.071
BBM15	-0.707	-0.703	-0.715	-0.555	0.020	0.010	0.010	0.050	0.036	0.045	0.026	0.053
BBM16	-0.362	-0.406	-0.518	-0.479	0.140	0.110	0.070	0.090	0.072	0.043	0.071	0.051
BBM17	-0.499	-0.368	-0.438	-0.427	0.070	0.140	0.120	0.130	0.112	0.137	0.028	0.076
BBM18	-0.381	-0.550	-0.530	-0.446	0.130	0.050	0.070	0.120	0.205	0.047	0.104	0.061

BBM19	-0.215	-0.246	-0.138	-0.363	0.270	0.230	0.350	0.170	0.120	0.040	0.043	0.066
BBM20	-0.700	-0.484	-0.551	-0.552	0.020	0.070	0.060	0.060	0.048	0.044	0.027	0.036
BBM21	-0.412	-0.478	-0.565	-0.538	0.110	0.070	0.050	0.060	0.103	0.050	0.017	0.050
BBM22	-0.452	-0.326	-0.554	-0.537	0.090	0.160	0.060	0.060	0.101	0.035	0.026	0.039
BBM23	-0.026	-0.142	-0.121	-0.149	0.460	0.330	0.380	0.350	0.084	0.044	0.037	0.064
BBM24	-0.074	-0.213	-0.308	-0.163	0.410	0.260	0.190	0.340	0.090	0.111	0.109	0.090
BBM25	-0.104	-0.316	-0.351	-0.403	0.380	0.170	0.170	0.140	0.114	0.064	0.014	0.050
BBM26	-0.041	-0.154	-0.182	-0.054	0.440	0.320	0.300	0.460	0.087	0.115	0.072	0.085
BBM27	-0.202	-0.035	-0.400	-0.291	0.280	0.460	0.140	0.220	0.129	0.164	0.086	0.050
BBM28	-0.405	-0.467	-0.447	-0.300	0.110	0.080	0.110	0.210	0.031	0.059	0.033	0.075
BBM29	-0.516	-0.534	-0.679	-0.746	0.060	0.050	0.010	0.000	0.116	0.055	0.029	0.065
BBM30	-0.105	0.102	-0.002	-0.069	0.370	0.620	0.500	0.450	0.024	0.116	0.050	0.046
BBM31	-0.210	-0.274	-0.253	-0.335	0.270	0.200	0.230	0.190	0.040	0.046	0.037	0.042
BBM32	0.033	0.051	-0.088	0.017	0.540	0.560	0.410	0.530	0.150	0.212	0.122	0.095
BBM33	-0.236	-0.219	-0.022	-0.137	0.250	0.250	0.480	0.370	0.043	0.050	0.126	0.050
BBM34	0.153	-0.024	-0.041	-0.045	0.660	0.470	0.460	0.470	0.128	0.042	0.122	0.133
BBM35	-0.097	-0.218	-0.607	-0.495	0.390	0.250	0.040	0.080	0.089	0.099	0.038	0.053
BBM36	-0.251	-0.470	-0.530	-0.367	0.230	0.080	0.070	0.160	0.061	0.031	0.069	0.110
BBM37	-0.073	-0.136	-0.446	-0.348	0.410	0.340	0.110	0.180	0.050	0.020	0.024	0.065
BBM38	-0.302	-0.313	-0.366	-0.343	0.190	0.170	0.160	0.180	0.048	0.252	0.038	0.069
BBM39	0.482	0.446	0.428	0.548	0.880	0.880	0.850	0.900	0.260	0.084	0.109	0.043
BBM40	0.603	0.485	0.638	0.533	0.940	0.910	0.950	0.890	0.065	0.094	0.088	0.058
BBM41	-0.162	-0.352	-0.433	-0.376	0.320	0.140	0.120	0.160	0.052	0.078	0.069	0.086
BBM42	-0.727	-0.732	-0.638	-0.617	0.020	0.000	0.030	0.030	0.050	0.154	0.037	0.066
BBN01	-0.352	-0.419	-0.561	-0.609	0.150	0.110	0.050	0.030	0.040	0.033	0.014	0.071
BBN02	-0.728	-0.606	-0.610	-0.561	0.020	0.030	0.030	0.050	0.107	0.060	0.048	0.098
BBN03	-0.481	-0.554	-0.533	-0.471	0.080	0.040	0.070	0.100	0.042	0.076	0.041	0.103
BBN04	-0.752	-0.563	-0.516	-0.476	0.010	0.040	0.080	0.100	0.032	0.036	0.044	0.050
BBN05	-0.155	-0.061	-0.302	-0.046	0.330	0.420	0.200	0.470	0.082	0.227	0.091	0.069
BBN06	-0.430	-0.448	-0.532	-0.349	0.100	0.090	0.070	0.180	0.117	0.071	0.075	0.101
BBN07	-0.427	-0.555	-0.565	-0.597	0.100	0.040	0.050	0.040	0.158	0.084	0.058	0.090
BBN08	-0.211	-0.243	-0.337	-0.145	0.270	0.230	0.170	0.360	0.110	0.119	0.126	0.102
BBN09	-0.100	-0.252	-0.262	-0.095	0.380	0.220	0.230	0.420	0.066	0.069	0.113	0.117
BBN10	-0.185	0.027	-0.320	-0.082	0.300	0.530	0.190	0.430	0.075	0.123	0.055	0.107
BBN11	-0.563	-0.507	-0.644	-0.481	0.050	0.060	0.020	0.090	0.096	0.085	0.085	0.119
BBN12	-0.635	-0.574	-0.677	-0.628	0.030	0.040	0.010	0.020	0.044	0.056	0.038	0.042
BBN13	-0.135	-0.140	-0.199	-0.201	0.350	0.330	0.280	0.300	0.063	0.124	0.078	0.117

BBN14	-0.061	-0.259	-0.282	-0.045	0.420	0.210	0.210	0.470	0.082	0.064	0.067	0.121
BBN15	-0.105	-0.460	-0.622	-0.556	0.370	0.080	0.030	0.050	0.270	0.063	0.060	0.128
BBN16	-0.492	-0.373	-0.567	-0.443	0.070	0.130	0.050	0.120	0.120	0.052	0.045	0.044
BBN17	-0.198	-0.257	-0.408	-0.351	0.290	0.220	0.130	0.180	0.073	0.084	0.082	0.154
BBN18	-0.585	-0.517	-0.631	-0.474	0.040	0.060	0.030	0.100	0.061	0.038	0.036	0.087
BBN19	-0.239	-0.261	-0.216	-0.308	0.240	0.210	0.260	0.200	0.123	0.071	0.012	0.055
BBN20	-0.636	-0.394	-0.551	-0.622	0.030	0.120	0.060	0.030	0.088	0.064	0.024	0.016
BBN21	-0.337	-0.393	-0.322	-0.285	0.160	0.120	0.180	0.230	0.108	0.035	0.028	0.080
BBN22	0.045	-0.117	-0.118	-0.102	0.550	0.360	0.380	0.410	0.152	0.100	0.083	0.057
BBN23	-0.051	-0.204	-0.222	-0.170	0.440	0.260	0.260	0.330	0.073	0.030	0.028	0.064
BBN24	-0.437	-0.477	-0.400	-0.494	0.090	0.070	0.140	0.080	0.129	0.065	0.035	0.040
BBN25	-0.073	-0.067	-0.159	-0.119	0.410	0.420	0.320	0.400	0.059	0.102	0.044	0.038
BBN26	0.016	-0.068	-0.251	-0.195	0.520	0.420	0.230	0.310	0.080	0.180	0.072	0.123
BBN27	-0.094	-0.067	0.095	0.096	0.390	0.420	0.620	0.610	0.050	0.043	0.022	0.031
BBN28	0.298	0.306	0.271	0.413	0.770	0.800	0.760	0.830	0.076	0.142	0.105	0.106
BBN29	0.114	-0.184	-0.060	-0.100	0.620	0.290	0.440	0.410	0.102	0.038	0.116	0.075
BBN30	0.073	0.219	0.246	0.296	0.580	0.730	0.740	0.770	0.105	0.118	0.094	0.067
BBN31	0.021	-0.140	-0.160	0.037	0.520	0.340	0.320	0.560	0.049	0.033	0.080	0.143
BBN32	0.492	0.284	0.208	0.373	0.880	0.780	0.720	0.810	0.285	0.154	0.095	0.123
BBN33	0.472	0.519	0.440	0.609	0.870	0.920	0.860	0.930	0.061	0.047	0.028	0.013
BBN34	0.473	0.402	0.328	0.501	0.870	0.860	0.790	0.870	0.022	0.113	0.100	0.070
BBN35	-0.505	-0.601	-0.637	-0.686	0.060	0.030	0.030	0.010	0.097	0.059	0.035	0.059
BBN36	-0.258	-0.305	-0.239	-0.136	0.230	0.180	0.240	0.370	0.087	0.041	0.076	0.096
BBN37	-0.461	-0.342	-0.264	-0.497	0.080	0.150	0.220	0.080	0.059	0.073	0.151	0.095
BBN38	0.449	0.436	0.191	0.355	0.860	0.880	0.710	0.800	0.139	0.220	0.068	0.037
BBN39	0.070	-0.051	0.221	0.086	0.570	0.440	0.730	0.610	0.095	0.091	0.034	0.043
BBN40	0.525	0.712	0.476	0.388	0.910	0.980	0.880	0.820	0.164	0.225	0.041	0.143
BBN41	0.407	0.172	0.052	0.227	0.840	0.680	0.570	0.720	0.076	0.097	0.083	0.124
BBN42	0.471	0.229	0.350	0.481	0.870	0.740	0.810	0.870	0.152	0.368	0.066	0.136
BBN43	-0.486	-0.341	-0.653	-0.505	0.070	0.150	0.020	0.080	0.086	0.096	0.062	0.145
BBO01	-0.695	-0.578	-0.469	-0.584	0.020	0.040	0.100	0.040	0.089	0.057	0.044	0.042
BBO02	-0.378	-0.348	-0.575	-0.428	0.130	0.150	0.050	0.130	0.064	0.063	0.060	0.107
BBO03	-0.791	-0.564	-0.560	-0.489	0.000	0.040	0.050	0.080	0.134	0.101	0.093	0.037
BBO04	-0.628	-0.711	-0.817	-0.782	0.030	0.010	0.000	0.000	0.065	0.075	0.030	0.127
BBO05	-0.355	-0.263	-0.524	-0.122	0.140	0.210	0.070	0.390	0.083	0.101	0.086	0.092
BBO06	-0.789	-0.690	-0.785	-0.640	0.010	0.010	0.000	0.020	0.069	0.096	0.040	0.092
BBO07	-0.918	-0.689	-0.586	-0.544	0.000	0.010	0.040	0.060	0.160	0.085	0.049	0.065

BBO08	0.036	-0.242	-0.415	-0.279	0.540	0.230	0.130	0.230	0.045	0.013	0.036	0.094
BBO09	-0.551	-0.322	-0.496	-0.401	0.050	0.160	0.090	0.140	0.053	0.064	0.037	0.084
BBO10	-0.262	-0.064	-0.395	-0.224	0.220	0.420	0.140	0.280	0.018	0.225	0.048	0.083
BBO11	-0.886	-0.730	-0.481	-0.548	0.000	0.000	0.100	0.060	0.054	0.099	0.087	0.052
BBO12	-0.287	-0.463	-0.544	-0.573	0.200	0.080	0.060	0.050	0.048	0.055	0.046	0.095
BBO13	-0.182	-0.191	-0.290	-0.288	0.310	0.280	0.210	0.220	0.047	0.070	0.055	0.029
BBO14	0.019	-0.278	-0.353	-0.190	0.520	0.190	0.160	0.320	0.080	0.034	0.047	0.063
BBO15	-0.331	-0.232	-0.329	-0.188	0.160	0.240	0.180	0.320	0.132	0.111	0.080	0.085
BBO16	0.017	0.139	-0.148	-0.019	0.520	0.660	0.340	0.500	0.070	0.128	0.077	0.164
BBO17	-0.019	-0.013	-0.226	-0.184	0.480	0.490	0.250	0.320	0.093	0.148	0.119	0.064
BBO18	0.364	0.489	0.357	0.434	0.810	0.910	0.810	0.840	0.105	0.123	0.210	0.104
BBO19	-0.277	-0.135	-0.174	-0.026	0.210	0.340	0.310	0.500	0.001	0.127	0.092	0.104
BBO20	0.137	0.121	-0.056	0.128	0.640	0.640	0.450	0.640	0.123	0.074	0.099	0.138
BBO21	-0.221	-0.102	-0.254	-0.014	0.260	0.380	0.230	0.510	0.067	0.077	0.025	0.132
BBO22	-0.261	-0.285	-0.373	-0.367	0.220	0.190	0.150	0.160	0.060	0.036	0.033	0.111
BBO23	-0.077	-0.251	-0.221	-0.193	0.410	0.220	0.260	0.310	0.052	0.095	0.040	0.025
BBO24	-0.202	-0.250	-0.406	-0.250	0.280	0.220	0.130	0.260	0.019	0.046	0.029	0.082
BBO25	0.298	0.169	0.020	0.184	0.770	0.680	0.530	0.690	0.043	0.107	0.061	0.098
BBO26	-0.111	-0.125	-0.252	-0.104	0.370	0.350	0.230	0.410	0.097	0.073	0.042	0.084
BBO27	0.051	-0.088	0.086	0.232	0.560	0.390	0.610	0.720	0.113	0.045	0.063	0.064
BBO28	-0.103	-0.195	-0.123	-0.137	0.380	0.270	0.370	0.370	0.107	0.043	0.043	0.055
BBO29	-0.228	-0.040	-0.216	-0.079	0.260	0.450	0.260	0.440	0.069	0.104	0.073	0.075
BBO30	0.317	0.335	0.278	0.466	0.780	0.810	0.760	0.850	0.090	0.118	0.061	0.093
BBO31	-0.263	-0.116	-0.150	-0.176	0.220	0.360	0.330	0.330	0.090	0.168	0.044	0.034
BBO32	-0.056	-0.099	0.055	0.106	0.430	0.380	0.570	0.630	0.023	0.043	0.064	0.041
BBO33	0.340	0.244	0.133	0.156	0.800	0.750	0.660	0.670	0.130	0.082	0.053	0.023
BBO34	0.367	0.385	0.277	0.433	0.820	0.850	0.760	0.840	0.144	0.101	0.066	0.112
BBO35		0.777				0.990				0.187		
BBO36	-0.520	-0.520	-0.667	-0.607	0.060	0.060	0.020	0.030	0.103	0.057	0.022	0.081
BBO37	-0.128	-0.082	-0.183	0.032	0.360	0.400	0.300	0.560	0.080	0.146	0.116	0.178
BBO38	-0.484	-0.382	-0.423	-0.472	0.070	0.130	0.120	0.100	0.124	0.124	0.047	0.032
BBO39	0.020	-0.295	-0.353	-0.243	0.520	0.190	0.170	0.270	0.037	0.119	0.048	0.088
BBO39	0.518	0.389	0.492	0.765	0.900	0.850	0.890	0.970	0.107	0.234	0.103	0.177
BBO40	-0.349	-0.381	-0.333	-0.059	0.150	0.130	0.180	0.460	0.127	0.034	0.033	0.094
BBO41												
BBO42	-0.100	-0.175	-0.059	-0.190	0.380	0.300	0.440	0.320	0.204	0.084	0.077	0.083
BBO43	0.005	0.162	0.068	0.100	0.500	0.670	0.590	0.620	0.124	0.195	0.093	0.036

BBO44	-0.570	-0.437	-0.625	-0.655	0.040	0.100	0.030	0.010	0.051	0.091	0.028	0.065
BBP01	-0.359	-0.335	-0.209	-0.332	0.140	0.150	0.270	0.190	0.026	0.035	0.155	0.085
BBP02	-0.428	-0.539	-0.609	-0.545	0.100	0.050	0.030	0.060	0.062	0.046	0.034	0.131
BBP03	-0.280	-0.146	-0.359	-0.281	0.210	0.330	0.160	0.230	0.135	0.088	0.095	0.154
BBP04	-0.620	-0.503	-0.681	-0.678	0.040	0.060	0.010	0.010	0.076	0.075	0.093	0.172
BBP05	-0.243	-0.406	-0.515	-0.537	0.240	0.110	0.080	0.070	0.180	0.087	0.116	0.072
BBP06	-0.738	-0.755	-0.753	-0.777	0.010	0.000	0.000	0.000	0.080	0.109	0.033	0.091
BBP07	-0.751	-0.639	-0.545	-0.509	0.010	0.020	0.060	0.070	0.095	0.053	0.049	0.080
BBP08	-0.253	-0.481	-0.520	-0.466	0.230	0.070	0.070	0.110	0.133	0.046	0.065	0.126
BBP09	-0.698	-0.593	-0.514	-0.501	0.020	0.030	0.080	0.080	0.038	0.090	0.069	0.095
BBP10	-0.382	-0.644	-0.425	-0.593	0.120	0.020	0.120	0.040	0.099	0.061	0.080	0.092
BBP11	-0.821	-0.725	-0.707	-0.651	0.000	0.000	0.010	0.020	0.069	0.112	0.060	0.061
BBP12	-0.504	-0.693	-0.721	-0.742	0.070	0.010	0.010	0.000	0.123	0.084	0.062	0.099
BBP13	-0.458	-0.480	-0.554	-0.491	0.090	0.070	0.060	0.080	0.073	0.076	0.067	0.079
BBP14	-0.046	-0.256	-0.406	-0.248	0.440	0.220	0.130	0.260	0.104	0.072	0.073	0.071
BBP15	-0.774	-0.712	-0.640	-0.506	0.010	0.000	0.020	0.070	0.099	0.068	0.031	0.072
BBP16	-0.416	-0.592	-0.487	-0.453	0.100	0.030	0.090	0.110	0.126	0.085	0.052	0.119
BBP17	-0.797	-0.537	-0.460	-0.430	0.000	0.050	0.100	0.120	0.068	0.061	0.050	0.046
BBP18	-0.317	-0.582	-0.445	-0.502	0.170	0.030	0.110	0.080	0.081	0.083	0.078	0.081
BBP19	-0.232	-0.158	-0.089	-0.207	0.250	0.320	0.410	0.300	0.104	0.178	0.044	0.107
BBP20	-0.325	-0.381	-0.521	-0.386	0.170	0.130	0.070	0.150	0.082	0.151	0.031	0.106
BBP21	-0.413	-0.524	-0.345	-0.295	0.100	0.060	0.170	0.210	0.115	0.063	0.055	0.105
BBP22	-0.480	-0.521	-0.513	-0.219	0.080	0.060	0.080	0.290	0.070	0.042	0.118	0.150
BBP23	0.047	0.100	0.069	0.135	0.550	0.620	0.590	0.650	0.100	0.136	0.127	0.113
BBP24	-0.290	-0.541	-0.459	-0.476	0.200	0.050	0.110	0.100	0.111	0.065	0.042	0.080
BBP25	-0.230	-0.251	-0.199	-0.126	0.250	0.220	0.280	0.390	0.082	0.052	0.041	0.066
BBP26	0.056	-0.159	0.118	0.130	0.560	0.320	0.650	0.640	0.053	0.133	0.148	0.232
BBP27	0.694	0.617	0.495	0.523	0.970	0.960	0.890	0.880	0.150	0.177	0.105	0.055
BBP28	0.088	-0.086	-0.131	-0.043	0.590	0.390	0.360	0.480	0.093	0.126	0.094	0.139
BBP29	-0.347	-0.440	-0.339	-0.288	0.150	0.100	0.170	0.220	0.075	0.069	0.023	0.044
BBP30	0.541	0.503	0.391	0.541	0.920	0.920	0.840	0.890	0.055	0.121	0.064	0.096
BBP31	-0.235	-0.191	-0.141	-0.045	0.250	0.280	0.350	0.470	0.039	0.067	0.044	0.052
BBP32	-0.080	-0.207	-0.059	-0.096	0.400	0.260	0.440	0.420	0.183	0.065	0.073	0.046
BBP33	0.167	0.265	0.039	0.041	0.670	0.760	0.550	0.570	0.091	0.119	0.028	0.016
BBP34	0.086	-0.056	0.094	0.126	0.590	0.430	0.620	0.640	0.177	0.080	0.044	0.072
BBP35	-0.539	-0.574	-0.425	-0.411	0.060	0.040	0.120	0.130	0.212	0.115	0.100	0.048
BBP36	-0.482	-0.502	-0.537	-0.492	0.080	0.060	0.060	0.080	0.108	0.055	0.060	0.078

BBP37	-0.226	-0.007	-0.385	-0.210	0.260	0.490	0.150	0.290	0.090	0.098	0.033	0.095
BBP38	-0.051	-0.118	-0.201	-0.062	0.440	0.360	0.280	0.450	0.017	0.043	0.021	0.064
BBP39	-0.345	-0.191	-0.215	-0.133	0.150	0.280	0.270	0.380	0.067	0.047	0.033	0.014
BBP40	0.052	0.107	0.183	0.326	0.560	0.630	0.700	0.790	0.064	0.133	0.077	0.155
BBP41	-0.252	-0.144	-0.242	-0.015	0.230	0.330	0.240	0.510	0.111	0.093	0.122	0.073
BBP42	-0.637	-0.615	-0.589	-0.576	0.030	0.020	0.040	0.050	0.126	0.163	0.064	0.067
BBQ01	0.310	0.206	0.049	0.263	0.780	0.710	0.570	0.750	0.036	0.131	0.078	0.078
BBQ02	0.422	0.297	0.477	0.622	0.850	0.790	0.880	0.930	0.037	0.086	0.075	0.091
BBQ03	-0.276	-0.193	-0.198	-0.184	0.210	0.280	0.280	0.320	0.135	0.116	0.102	0.129
BBQ04	-0.245	-0.328	-0.191	-0.264	0.240	0.160	0.290	0.250	0.179	0.094	0.084	0.060
BBQ05	0.188	0.081	0.018	0.208	0.680	0.600	0.520	0.710	0.124	0.112	0.115	0.122
BBQ06	-0.455	-0.526	-0.474	-0.455	0.090	0.060	0.100	0.110	0.175	0.101	0.049	0.060
BBQ07	0.269	0.317	0.291	0.527	0.750	0.800	0.770	0.890	0.157	0.154	0.124	0.150
BBQ08	0.272	-0.076	-0.043	-0.228	0.750	0.400	0.460	0.280	0.175	0.025	0.061	0.039
BBQ09	0.495	0.239	0.060	0.120	0.890	0.740	0.580	0.630	0.201	0.110	0.032	0.089
BBQ10	-0.289	-0.372	-0.509	-0.560	0.200	0.130	0.080	0.050	0.133	0.032	0.087	0.117
BBQ12	-0.483	-0.296	-0.428	-0.415	0.070	0.180	0.120	0.130	0.052	0.170	0.098	0.075
BBQ13	-0.874	-0.834	-0.822	-0.856	0.000	0.000	0.000	0.000	0.078	0.072	0.081	0.072
BBQ14	-0.789	-0.658	-0.486	-0.582	0.010	0.010	0.090	0.040	0.068	0.035	0.023	0.110
BBQ15	-0.433	-0.608	-0.536	-0.669	0.090	0.030	0.070	0.010	0.203	0.056	0.057	0.087
BBQ16	-0.635	-0.629	-0.528	-0.576	0.030	0.020	0.070	0.050	0.063	0.081	0.069	0.107
BBQ17	-0.414	-0.429	-0.656	-0.641	0.100	0.100	0.020	0.020	0.129	0.100	0.027	0.070
BBQ18	-0.845	-0.675	-0.639	-0.632	0.000	0.010	0.020	0.020	0.064	0.095	0.038	0.058
BBQ19	-0.539	-0.751	-0.652	-0.682	0.060	0.000	0.020	0.010	0.138	0.088	0.045	0.091
BBQ20	-0.643	-0.560	-0.496	-0.478	0.030	0.040	0.090	0.100	0.018	0.066	0.065	0.080
BBQ21	-0.149	-0.438	-0.305	-0.440	0.330	0.100	0.190	0.120	0.103	0.037	0.076	0.092
BBQ22	-0.925	-0.794	-0.696	-0.609	0.000	0.000	0.010	0.030	0.041	0.079	0.030	0.075
BBQ23	-0.492	-0.665	-0.733	-0.647	0.070	0.010	0.000	0.020	0.106	0.050	0.051	0.086
BBQ24	-0.714	-0.599	-0.452	-0.485	0.020	0.030	0.110	0.090	0.044	0.066	0.066	0.051
BBQ25	-0.212	-0.402	-0.440	-0.335	0.270	0.120	0.120	0.190	0.064	0.062	0.087	0.126
BBQ26	-0.377	-0.355	-0.111	-0.235	0.130	0.140	0.390	0.270	0.156	0.059	0.026	0.054
BBQ27	-0.582	-0.532	-0.483	-0.548	0.040	0.050	0.100	0.060	0.084	0.085	0.044	0.060
BBQ28	-0.334	-0.527	-0.413	-0.344	0.160	0.050	0.130	0.180	0.170	0.031	0.065	0.084
BBQ29	-0.487	-0.663	-0.521	-0.674	0.070	0.010	0.070	0.010	0.072	0.053	0.040	0.060
BBQ30	-0.185	-0.332	-0.183	-0.206	0.300	0.160	0.300	0.300	0.176	0.065	0.039	0.049
BBQ31	-0.182	-0.318	-0.350	-0.193	0.310	0.170	0.170	0.310	0.048	0.107	0.111	0.104
BBQ32	-0.345	-0.433	-0.228	-0.265	0.150	0.100	0.250	0.240	0.105	0.052	0.063	0.051

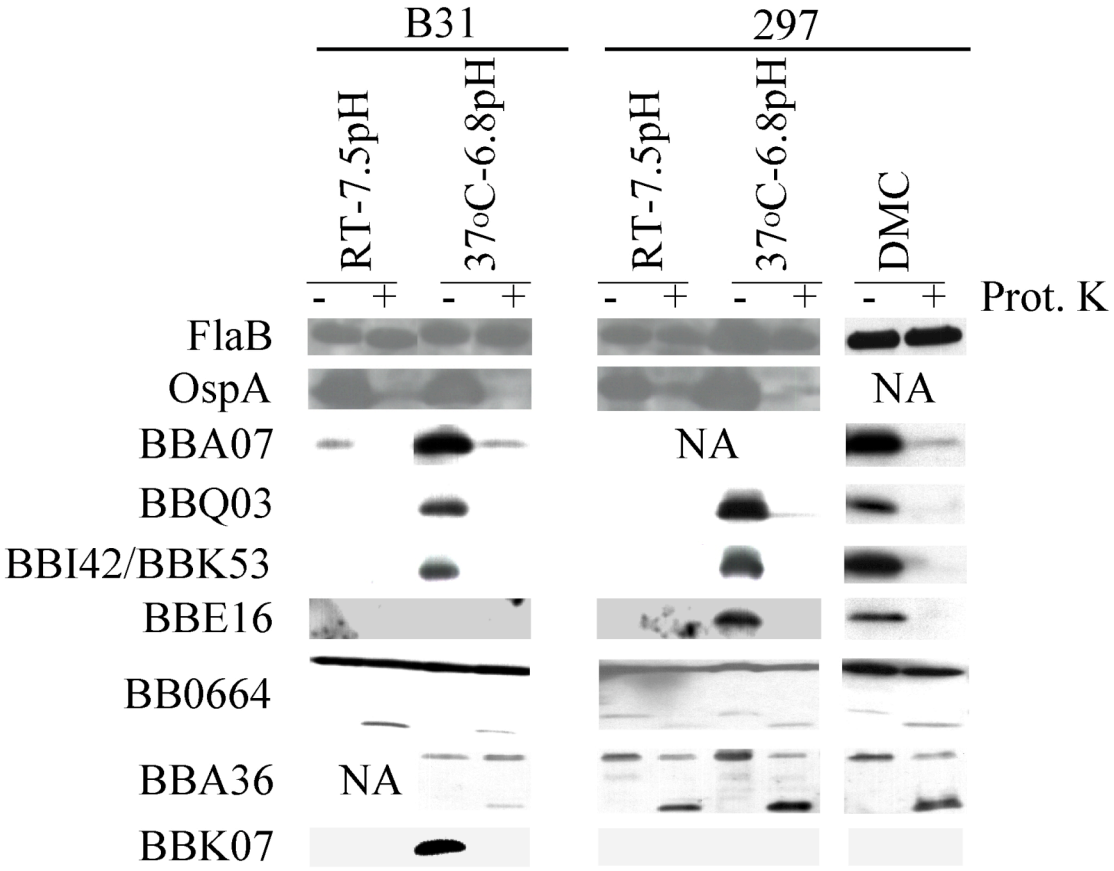
BBQ33	-0.221	-0.274	-0.404	-0.304	0.260	0.200	0.130	0.210	0.054	0.093	0.059	0.094
BBQ34	-0.023	-0.095	-0.194	-0.132	0.470	0.380	0.290	0.380	0.049	0.054	0.049	0.057
BBQ34				0.896				0.980				0.043
BBQ35	0.187	0.142	0.049	0.176	0.680	0.660	0.560	0.680	0.060	0.028	0.050	0.116
BBQ36	0.722	0.607	0.588	0.702	0.980	0.950	0.940	0.960	0.093	0.160	0.067	0.129
BBQ37	-0.299	-0.448	-0.372	-0.387	0.190	0.090	0.150	0.150	0.073	0.098	0.129	0.057
BBQ38	-0.097	-0.227	0.043	0.041	0.390	0.240	0.560	0.570	0.037	0.057	0.045	0.061
BBQ39	-0.245	-0.251	-0.094	-0.109	0.240	0.220	0.400	0.400	0.101	0.071	0.028	0.035
BBQ40	0.008	-0.112	-0.012	0.020	0.510	0.370	0.490	0.540	0.034	0.055	0.060	0.107
BBQ41	0.245	0.152	0.335	0.324	0.740	0.660	0.800	0.790	0.046	0.069	0.026	0.060
BBQ42	0.499	0.947	0.581	0.684	0.890	0.990	0.930	0.950	0.167	0.074	0.096	0.140
BBQ42	0.139	0.049	0.250	0.199	0.640	0.560	0.750	0.700	0.098	0.061	0.061	0.085
BBQ43	-0.541	-0.538	-0.472	-0.430	0.060	0.050	0.100	0.120	0.173	0.095	0.028	0.041
BBQ44	-0.367	-0.362	-0.453	-0.403	0.130	0.140	0.110	0.140	0.174	0.091	0.026	0.081
BBQ45	-0.057	-0.007	-0.103	-0.104	0.430	0.490	0.400	0.410	0.029	0.078	0.103	0.088
BBQ46	0.477	0.428	0.376	0.487	0.870	0.870	0.830	0.870	0.026	0.093	0.083	0.081
BBQ47	-0.105	0.010	-0.082	-0.129	0.370	0.510	0.420	0.380	0.052	0.041	0.108	0.050
BBQ48	0.129	0.132	0.219	0.132	0.630	0.650	0.730	0.640	0.068	0.075	0.039	0.059
BBQ49	-0.548	-0.513	-0.487	-0.399	0.050	0.060	0.090	0.140	0.167	0.083	0.057	0.079
BBQ50	-0.728	-0.518	-0.491	-0.477	0.020	0.060	0.090	0.100	0.144	0.150	0.058	0.052
BBQ51	-0.674	-0.647	-0.458	-0.562	0.020	0.010	0.110	0.050	0.222	0.087	0.036	0.055
BBQ52	-0.657	-0.546	-0.499	-0.614	0.030	0.050	0.080	0.030	0.023	0.080	0.058	0.077
BBQ53	-0.587	-0.552	-0.222	-0.411	0.040	0.040	0.260	0.130	0.204	0.088	0.109	0.070
BBQ54	-0.340	-0.098	-0.091	-0.273	0.160	0.380	0.410	0.240	0.045	0.062	0.199	0.044
BBQ56	0.448	0.619	0.448	0.631	0.860	0.960	0.860	0.940	0.027	0.269	0.055	0.292
BBQ60	-0.249	-0.222	-0.357	-0.303	0.230	0.250	0.160	0.210	0.163	0.099	0.079	0.100
BBQ63	-0.671	-0.571	-0.604	-0.626	0.020	0.040	0.040	0.030	0.124	0.092	0.040	0.058
BBQ65	0.057	0.094	-0.126	0.073	0.560	0.610	0.370	0.600	0.032	0.117	0.081	0.121
BBQ66	0.531	0.285	0.362	0.319	0.910	0.780	0.820	0.780	0.058	0.042	0.082	0.059
BBQ67		0.718	0.513	0.477		0.980	0.910	0.860		0.128	0.066	0.126
BBQ69	0.337	0.376	0.287	0.248	0.800	0.840	0.770	0.740	0.105	0.190	0.064	0.086
BBQ71	0.135	0.170	0.203	0.046	0.640	0.680	0.720	0.570	0.063	0.128	0.156	0.097
BBQ72	0.498	0.401	0.387	0.428	0.890	0.860	0.840	0.840	0.051	0.163	0.115	0.065
BBQ73	0.210	0.184	0.086	0.105	0.710	0.700	0.610	0.620	0.045	0.087	0.065	0.104
BBQ74	-0.190	-0.159	-0.102	-0.182	0.290	0.310	0.400	0.320	0.118	0.081	0.055	0.129
BBQ75	0.530	0.439	0.357	0.332	0.910	0.880	0.810	0.790	0.116	0.108	0.059	0.108
BBQ76	0.691	0.517	0.464	0.478	0.970	0.920	0.870	0.860	0.114	0.074	0.068	0.069

BBQ77	0.343	0.094	0.169	0.027	0.800	0.610	0.690	0.550	0.067	0.073	0.052	0.076
BBQ79	0.514	0.498	0.168	0.420	0.900	0.910	0.690	0.830	0.043	0.145	0.077	0.120
BBQ80	-0.049	-0.182	-0.380	-0.388	0.440	0.290	0.150	0.150	0.071	0.058	0.019	0.053
BBQ81	0.401	0.349	0.126	0.242	0.830	0.820	0.660	0.730	0.058	0.102	0.076	0.141
BBQ82	0.474	0.293	0.143	0.146	0.870	0.780	0.670	0.660	0.055	0.074	0.042	0.092
BBQ83	0.541	0.421	0.446	0.521	0.910	0.870	0.860	0.880	0.101	0.094	0.063	0.092
BBQ84	0.175	0.017	-0.132	-0.172	0.670	0.520	0.360	0.330	0.053	0.101	0.035	0.068
BBQ84.1	0.333	0.232	0.070	0.125	0.800	0.740	0.590	0.640	0.068	0.090	0.015	0.087
BBQ85	-0.019	-0.098	-0.234	-0.251	0.480	0.380	0.250	0.260	0.102	0.062	0.057	0.057
BBQ86	0.483	0.583	0.481	0.549	0.880	0.940	0.880	0.900	0.065	0.081	0.070	0.045
BBQ87	0.302	0.125	-0.091	-0.055	0.770	0.640	0.410	0.460	0.084	0.054	0.074	0.083
BBQ88	-0.365	-0.456	-0.594	-0.540	0.140	0.080	0.040	0.060	0.070	0.095	0.027	0.061
BBQ89	0.098	-0.120	-0.226	-0.203	0.600	0.360	0.250	0.300	0.105	0.021	0.038	0.092
BBR01	-0.776	-0.541	-0.362	-0.481	0.010	0.050	0.160	0.090	0.023	0.055	0.046	0.044
BBR02	-0.415	-0.486	-0.483	-0.627	0.100	0.070	0.100	0.030	0.067	0.044	0.055	0.078
BBR03	-0.552	-0.453	-0.431	-0.405	0.050	0.090	0.120	0.130	0.083	0.042	0.024	0.056
BBR04	-0.165	-0.202	-0.181	-0.187	0.320	0.260	0.300	0.320	0.156	0.136	0.178	0.147
BBR05	-0.633	-0.496	-0.674	-0.633	0.030	0.070	0.010	0.020	0.022	0.030	0.043	0.066
BBR06	-0.756	-0.645	-0.782	-0.746	0.010	0.020	0.000	0.000	0.055	0.060	0.055	0.095
BBR07	-0.752	-0.491	-0.543	-0.509	0.010	0.070	0.060	0.070	0.068	0.037	0.036	0.059
BBR08	-0.189	-0.259	-0.391	-0.419	0.300	0.210	0.150	0.130	0.141	0.049	0.102	0.104
BBR09	-0.622	-0.479	-0.514	-0.527	0.040	0.070	0.080	0.070	0.095	0.091	0.091	0.054
BBR10	-0.245	-0.254	-0.298	-0.485	0.240	0.220	0.200	0.090	0.126	0.056	0.151	0.071
BBR11	-0.669	-0.543	-0.587	-0.587	0.030	0.050	0.040	0.040	0.072	0.080	0.029	0.035
BBR12	-0.683	-0.725	-0.726	-0.701	0.020	0.000	0.000	0.000	0.189	0.068	0.065	0.035
BBR13	-0.234	-0.291	-0.329	-0.288	0.250	0.190	0.180	0.220	0.253	0.125	0.139	0.115
BBR14	-0.307	-0.382	-0.491	-0.482	0.180	0.130	0.090	0.090	0.113	0.031	0.051	0.038
BBR15	-0.478	-0.454	-0.558	-0.549	0.080	0.090	0.060	0.060	0.055	0.028	0.091	0.061
BBR16	-0.486	-0.456	-0.552	-0.454	0.070	0.080	0.060	0.110	0.199	0.074	0.031	0.078
BBR17	-0.366	-0.482	-0.384	-0.413	0.140	0.070	0.150	0.130	0.204	0.072	0.045	0.053
BBR18	-0.578	-0.674	-0.625	-0.617	0.040	0.010	0.030	0.030	0.110	0.082	0.062	0.082
BBR19	-0.168	-0.111	-0.164	-0.219	0.320	0.370	0.320	0.290	0.124	0.052	0.028	0.067
BBR20	-0.749	-0.627	-0.492	-0.719	0.010	0.020	0.090	0.000	0.150	0.078	0.140	0.040
BBR21	0.072	0.079	0.039	-0.014	0.570	0.600	0.550	0.510	0.179	0.132	0.195	0.169
BBR22	-0.555	-0.664	-0.605	-0.596	0.050	0.010	0.040	0.040	0.099	0.058	0.042	0.084
BBR23	-0.070	-0.081	-0.122	-0.226	0.420	0.400	0.370	0.280	0.071	0.066	0.076	0.065
BBR24	-0.557	-0.595	-0.617	-0.636	0.050	0.030	0.030	0.020	0.191	0.051	0.013	0.047

BBR25	-0.320	-0.338	-0.128	-0.287	0.170	0.150	0.370	0.220	0.112	0.048	0.080	0.041
BBR26	-0.505	-0.520	-0.516	-0.520	0.060	0.060	0.080	0.070	0.119	0.051	0.036	0.036
BBR27	0.335	0.353	0.452	0.592	0.800	0.830	0.870	0.920	0.173	0.148	0.031	0.065
BBR28	0.075	-0.203	-0.165	-0.180	0.580	0.260	0.320	0.330	0.169	0.054	0.059	0.106
BBR29	-0.359	-0.452	-0.447	-0.523	0.140	0.090	0.110	0.070	0.099	0.058	0.022	0.055
BBR30	0.547	0.306	0.377	0.467	0.920	0.800	0.830	0.860	0.083	0.056	0.102	0.151
BBR31	0.068	0.217	0.281	0.269	0.570	0.720	0.760	0.750	0.135	0.138	0.032	0.072
BBR32	-0.127	-0.226	-0.099	-0.265	0.360	0.240	0.400	0.240	0.095	0.085	0.114	0.043
BBR33	0.192	-0.095	-0.091	-0.024	0.690	0.380	0.410	0.500	0.446	0.098	0.116	0.052
BBR34	0.226	0.063	0.080	0.328	0.720	0.580	0.600	0.790	0.108	0.055	0.034	0.064
BBR35	0.248	0.216	0.147	0.204	0.740	0.720	0.670	0.700	0.044	0.112	0.028	0.033
BBR36	-0.157	-0.318	-0.586	-0.592	0.330	0.170	0.040	0.040	0.020	0.061	0.073	0.076
BBR37	-0.392	-0.615	-0.726	-0.641	0.120	0.020	0.010	0.020	0.120	0.063	0.036	0.058
BBR38	-0.169	-0.224	-0.516	-0.522	0.320	0.250	0.080	0.070	0.135	0.064	0.015	0.064
BBR39	0.173	0.133	-0.051	0.189	0.670	0.650	0.450	0.700	0.054	0.093	0.081	0.130
BBR40	0.374	0.160	-0.019	-0.027	0.820	0.670	0.480	0.490	0.039	0.071	0.027	0.050
BBR41	-0.383	-0.285	-0.666	-0.362	0.120	0.190	0.020	0.170	0.075	0.057	0.101	0.136
BBR42	0.154	-0.071	-0.059	0.027	0.660	0.410	0.440	0.550	0.050	0.069	0.059	0.134
BBR43	0.096	-0.087	-0.145	0.040	0.600	0.390	0.340	0.560	0.092	0.130	0.079	0.119
BBR44	-0.130	-0.291	-0.441	-0.381	0.350	0.190	0.110	0.150	0.054	0.054	0.027	0.085
BBR45	-0.671	-0.454	-0.662	-0.559	0.030	0.090	0.020	0.050	0.062	0.114	0.042	0.066
BBS01	-0.453	-0.426	-0.586	-0.642	0.090	0.100	0.040	0.020	0.048	0.041	0.027	0.038
BBS02	-0.813	-0.675	-0.673	-0.605	0.000	0.010	0.020	0.030	0.029	0.078	0.015	0.072
BBS03	0.535	0.417	0.448	0.454	0.910	0.870	0.860	0.850	0.090	0.063	0.097	0.047
BBS04	-0.727	-0.588	-0.696	-0.594	0.020	0.030	0.010	0.040	0.020	0.043	0.035	0.084
BBS05	-0.469	-0.433	-0.477	-0.533	0.080	0.100	0.100	0.070	0.068	0.039	0.066	0.078
BBS06	-0.958	-0.719	-0.717	-0.661	0.000	0.000	0.010	0.010	0.087	0.104	0.045	0.044
BBS07	-0.562	-0.544	-0.564	-0.601	0.050	0.050	0.050	0.040	0.051	0.087	0.045	0.060
BBS08	-0.362	-0.415	-0.559	-0.498	0.140	0.110	0.050	0.080	0.086	0.040	0.022	0.068
BBS09	-0.342	-0.386	-0.393	-0.462	0.160	0.130	0.140	0.110	0.158	0.110	0.067	0.086
BBS10	-0.399	-0.256	-0.625	-0.554	0.110	0.220	0.030	0.060	0.063	0.092	0.039	0.133
BBS11	-0.659	-0.571	-0.754	-0.730	0.030	0.040	0.000	0.000	0.057	0.060	0.072	0.089
BBS12	-0.673	-0.582	-0.724	-0.584	0.020	0.030	0.010	0.040	0.050	0.085	0.042	0.067
BBS13	-0.206	-0.395	-0.523	-0.441	0.280	0.120	0.070	0.120	0.122	0.034	0.066	0.030
BBS14	-0.338	-0.405	-0.414	-0.310	0.160	0.110	0.130	0.200	0.070	0.031	0.032	0.050
BBS15	-0.240	-0.174	-0.505	-0.602	0.240	0.300	0.080	0.030	0.128	0.201	0.043	0.048
BBS16	-0.387	-0.384	-0.420	-0.423	0.120	0.130	0.120	0.130	0.106	0.063	0.033	0.054

BBS17	-0.675	-0.606	-0.616	-0.547	0.020	0.030	0.030	0.060	0.109	0.043	0.048	0.058
BBS18	-0.544	-0.428	-0.395	-0.386	0.050	0.100	0.140	0.150	0.195	0.102	0.096	0.106
BBS19	-0.134	-0.228	-0.251	-0.302	0.350	0.240	0.230	0.210	0.043	0.034	0.017	0.079
BBS20	-0.380	-0.338	-0.498	-0.562	0.130	0.150	0.090	0.050	0.093	0.059	0.064	0.035
BBS21	-0.381	-0.443	-0.517	-0.409	0.130	0.090	0.080	0.130	0.125	0.051	0.023	0.108
BBS22	-0.629	-0.469	-0.552	-0.592	0.030	0.080	0.060	0.040	0.059	0.090	0.015	0.050
BBS23	-0.138	-0.306	-0.316	-0.336	0.340	0.180	0.190	0.190	0.104	0.050	0.033	0.034
BBS24	-0.568	-0.534	-0.577	-0.561	0.050	0.050	0.050	0.050	0.129	0.055	0.034	0.050
BBS25	-0.386	-0.455	-0.403	-0.518	0.120	0.090	0.140	0.070	0.271	0.054	0.077	0.040
BBS26	-0.446	-0.328	-0.293	-0.385	0.090	0.160	0.200	0.150	0.125	0.071	0.105	0.094
BBS27	0.176	0.095	-0.064	-0.029	0.670	0.610	0.440	0.490	0.101	0.042	0.067	0.067
BBS28	0.583	0.559	0.695	0.741	0.940	0.940	0.960	0.970	0.102	0.092	0.062	0.081
BBS29	0.004	0.039	0.226	0.250	0.500	0.550	0.730	0.740	0.127	0.107	0.084	0.083
BBS30	-0.503	-0.190	-0.170	-0.273	0.070	0.280	0.310	0.240	0.023	0.055	0.058	0.029
BBS31	-0.381	-0.456	-0.607	-0.484	0.130	0.080	0.030	0.090	0.013	0.088	0.042	0.057
BBS32	0.419	0.391	0.289	0.196	0.840	0.850	0.770	0.700	0.041	0.055	0.048	0.060
BBS33	-0.020	-0.144	0.066	0.096	0.470	0.330	0.590	0.620	0.059	0.038	0.028	0.036
BBS34	-0.384	-0.343	-0.171	-0.321	0.120	0.150	0.310	0.190	0.113	0.047	0.076	0.040
BBS35	-0.072	-0.201	-0.261	-0.410	0.410	0.270	0.230	0.130	0.153	0.024	0.034	0.044
BBS36	0.231	0.279	0.358	0.319	0.730	0.770	0.810	0.780	0.132	0.115	0.009	0.031
BBS37		1.134	1.215	0.985		0.990	0.990	0.990		0.091	0.072	0.117
BBS37	0.146	0.027	0.237	0.034	0.650	0.530	0.740	0.560	0.055	0.097	0.053	0.084
BBS38	0.170	-0.079	-0.445	-0.310	0.670	0.400	0.110	0.200	0.062	0.094	0.091	0.135
BBS39	-0.262	-0.571	-0.606	-0.689	0.220	0.040	0.040	0.010	0.146	0.030	0.032	0.098
BBS40	-0.076	-0.077	-0.222	-0.291	0.410	0.400	0.260	0.220	0.077	0.099	0.118	0.074
BBS41	-0.302	-0.359	-0.260	-0.264	0.190	0.140	0.230	0.250	0.023	0.136	0.047	0.019
BBS42	0.592	0.255	0.100	0.152	0.940	0.750	0.630	0.660	0.170	0.072	0.069	0.079
BBS43	0.778	0.657	0.734	0.587	0.990	0.970	0.970	0.920	0.196	0.156	0.075	0.124
BBS44	-0.058	-0.266	-0.327	-0.215	0.430	0.210	0.180	0.290	0.079	0.089	0.076	0.115
BBS45	-0.442	-0.357	-0.584	-0.556	0.090	0.140	0.050	0.050	0.070	0.107	0.044	0.088
BBT01	0.565	0.404	0.095	0.305	0.930	0.860	0.620	0.780	0.079	0.257	0.180	0.149
BBT02	0.739	0.524	0.527	0.357	0.980	0.920	0.910	0.800	0.115	0.106	0.104	0.082
BBT03	0.161	-0.143	-0.229	-0.133	0.660	0.330	0.250	0.380	0.108	0.075	0.048	0.043
BBT04	0.924	0.555	0.620	0.720	0.990	0.940	0.950	0.960	0.094	0.087	0.068	0.150
BBT05	0.525	0.225	0.222	0.415	0.900	0.730	0.730	0.830	0.065	0.161	0.087	0.131
BBT06	0.018	-0.075	-0.306	-0.258	0.520	0.410	0.190	0.250	0.062	0.116	0.074	0.100
BBT07	0.362	0.114	-0.032	0.076	0.810	0.630	0.470	0.600	0.023	0.046	0.059	0.083

BBU01	0.449	0.177	0.221	0.331	0.860	0.690	0.730	0.790	0.073	0.160	0.069	0.119
BBU02	0.302	0.013	-0.158	-0.035	0.770	0.520	0.330	0.490	0.073	0.096	0.049	0.112
BBU03	0.483	0.371	0.485	0.478	0.880	0.840	0.890	0.860	0.083	0.107	0.082	0.067
BBU04	0.232	0.087	0.070	0.607	0.730	0.610	0.590	0.930	0.119	0.043	0.059	0.096
BBU05	0.053	-0.054	-0.165	0.186	0.560	0.430	0.320	0.690	0.061	0.103	0.024	0.062
BBU06	0.519	0.302	0.424	0.505	0.900	0.790	0.850	0.880	0.100	0.150	0.075	0.099
BBU07	0.507	0.345	0.282	0.292	0.900	0.820	0.770	0.770	0.027	0.108	0.089	0.044
BBU08	0.367	0.196	0.169	0.263	0.820	0.700	0.690	0.750	0.037	0.099	0.074	0.138
BBU09	0.225	0.242	-0.016	0.152	0.720	0.740	0.490	0.660	0.064	0.103	0.076	0.099
BBU10	0.558	0.466	0.545	0.601	0.920	0.890	0.920	0.920	0.117	0.090	0.110	0.079
BBU11	0.012	-0.154	-0.335	-0.205	0.510	0.320	0.180	0.300	0.099	0.110	0.080	0.108
BBU12	0.303	0.207	-0.185	0.014	0.770	0.710	0.290	0.530	0.048	0.077	0.080	0.048
BBU-63	0.456	0.360	0.348	0.480	0.860	0.830	0.810	0.860	0.057	0.158	0.077	0.113



APPENDIX C. Protease accessibility of various *B. burgdorferi* protiens when spirochetes were grown under various culture conditions (top). Evaluations on strain B31 MI were performed on *in vitro*-cultivated spirochetes only, whereas evaluations on strain 297 were performed on both *in vitro*-cultivated spirochetes as well as spirochetes cultivated within DMCs. Each lane was loaded with 5 x 10^7 bacteria that had been subjected to either Proteinase K (Prot. K) (+) or mock treatment (-). Detection (immunoblotting) of the endoflagellar (periplasmic) protein FlaB was used as an indicator of *B. burgdorferi* outer membrane integrity and as a loading control.

APPENDIX D. Evaluation of protective capabilities of selected immunogens from *B. burgdorferi* when mice are needle-challenged with 1 x 10^3 spirochetes

antigen	# mice pos/# mice tested	% reduction in infected mice
OspA	0/5	100
DHFR	5/5	0
BB0664	5/5	0
BBA07	5/5	0
BBA36	5/5	0
BB0070	5/5	0
BBI42/K53	5/5	0
BBQ03	5/5	0
BBK07	5/5	0
BBE17	3/5	40
BBE16	3/5	40

APPENDIX E. Evaluation of protective capabilities of BptA as a vaccinogen when mice are challenged with five (5) *B. burgdorferi*-infected ticks

antigen	# mice pos/# mice tested	% reduction in infected mice
OspA	0/5	100
BBQ03	5/5	0
BBE16	5/5	0

BIBLIOGRAPHY

1. **Ackermann, R., J. Kabatzki, H. P. Boisten, A. C. Steere, S. JHartung, and U. Runne.** 1984. Dtsch. Med. Wochenschr. **109:**92-97.
2. **Afzelius, A.** 1910. Verhandlungen der Dermatologischen Gesellschaft zu Stockholm on October 28, 1909. Arch Dermatol Syph **101:**404.
3. **Aguero-Rosenfeld, M. E., J. Nowakowski, S. Bittker, D. Cooper, R. B. Nadelman, and G. P. Wormser.** 1996. Evolution of the serologic response to *Borrelia burgdorferi* in treated patients with culture-confirmed erythema migrans. J Clin Microbiol **34:**1-9.
4. **Akin, E., G. L. McHugh, R. A. Flavell, E. Fikrig, and A. C. Steere.** 1999. The immunoglobulin (IgG) antibody response to OspA and OspB correlates with severe and prolonged Lyme arthritis and the IgG response to P35 correlates with mild and brief arthritis. Infect Immun **67:**173-81.
5. **Akins, D. R., K. W. Bourell, M. J. Caimano, M. V. Norgard, and J. D. Radolf.** 1998. A new animal model for studying Lyme disease spirochetes in a mammalian host-adapted state. J Clin Invest **101:**2240-50.
6. **Akins, D. R., S. F. Porcella, T. G. Popova, D. Shevchenko, S. I. Baker, M. Li, M. V. Norgard, and J. D. Radolf.** 1995. Evidence for *in vivo* but not *in vitro* expression of a *Borrelia burgdorferi* outer surface protein F (OspF) homologue. Mol Microbiol **18:**507-20.

7. **Alitalo, A., T. Meri, H. Lankinen, I. Seppala, P. Lahdenne, P. S. Hefty, D. Akins, and S. Meri.** 2002. Complement inhibitor factor H binding to Lyme disease spirochetes is mediated by inducible expression of multiple plasmid-encoded outer surface protein E paralogs. J Immunol **169:**3847-53.

8. **Anderson, J. F.** 1989. Epizootiology of Borrelia in *Ixodes* tick vectors and reservoir hosts. Rev Infect Dis **11 Suppl 6:**S1451-9.

9. **Anderson, J. F., S. W. Barthold, and L. A. Magnarelli.** 1990. Infectious but nonpathogenic isolate of *Borrelia burgdorferi*. J Clin Microbiol **28:**2693-9.

10. **Anderson, J. F., R. A. Flavell, L. A. Magnarelli, S. W. Barthold, F. S. Kantor, R. Wallich, D. H. Persing, D. Mathiesen, and E. Fikrig.** 1996. Novel *Borrelia burgdorferi* isolates from *Ixodes scapularis* and *Ixodes dentatus* ticks feeding on humans. J Clin Microbiol **34:**524-9.

11. **Anderson, J. F., L. A. Magnarelli, and J. B. McAninch.** 1988. New *Borrelia burgdorferi* antigenic variant isolated from *Ixodes dammini* from upstate New York. J Clin Microbiol **26:**2209-12.

12. **Anguita, J., S. Samanta, B. Revilla, K. Suk, S. Das, S. W. Barthold, and E. Fikrig.** 2000. *Borrelia burgdorferi* gene expression *in vivo* and spirochete pathogenicity. Infect Immun **68:**1222-30.

13. **Arza, B., J. Felez, P. Fabregas, Y. Laroche, D. Collen, and H. R. Lijnen.** 2000. Plasminogen binding properties of macrophage inflammatory protein (MIP)-2alpha. Thromb Haemost **84:**71-7.

14. **Asbrink, E., E. Brehmer-Anderson, and A. Hovmark.** 1986. Am J Dermatopathology **8:**209-219.

15. **Bacon, R. M., M. A. Pilgard, B. J. Johnson, S. J. Raffel, and T. G. Schwan.** 2004. Glycerophosphodiester phosphodiesterase gene (glpQ) of *Borrelia lonestari* identified as a target for differentiating Borrelia species associated with hard ticks (Acari:Ixodidae). J Clin Microbiol **42:**2326-8.

16. **Bankhead, T., and G. Chaconas.** 2004. Mixing active-site components: A recipe for the unique enzymatic activity of a telomere resolvase. Proc Natl Acad Sci U S A.

17. **Baranton, G., M. Assous, and D. Postic.** 1992. [Three bacterial species associated with Lyme borreliosis. Clinical and diagnostic implications]. Bull Acad Natl Med **176:**1075-85; discussion 1085-6.

18. **Baranton, G., D. Postic, I. Saint Girons, P. Boerlin, J. C. Piffaretti, M. Assous, and P. A. Grimont.** 1992. Delineation of *Borrelia burgdorferi sensu stricto*, *Borrelia garinii* sp. nov., and group VS461 associated with Lyme borreliosis. Int J Syst Bacteriol **42:**378-83.

19. **Barbour, A.** 1984. Isolation and Cultivation of Lyme Disease Spirochetes. Yale J Biol Med **57:**521-525.

20. **Barbour, A. G., R. A. Heiland, and T. R. Howe.** 1985. Heterogeneity of major proteins in Lyme disease borreliae: a molecular analysis of North American and European isolates. J Infect Dis **152:**478-84.

21. **Baril, C., C. Richaud, G. Baranton, and I. S. Saint Girons.** 1989. Linear chromosome of *Borrelia burgdorferi*. Res Microbiol **140:**507-16.

22. **Barthold, S. W., D. S. Beck, G. M. Hansen, G. A. Terwilliger, and K. D. Moody.** 1990. Lyme borreliosis in selected strains and ages of laboratory mice. J Infect Dis **162:**133-8.

23. **Barthold, S. W., and L. K. Bockenstedt.** 1993. Passive immunizing activity of sera from mice infected with *Borrelia burgdorferi*. Infect Immun **61:**4696-702.

24. **Barthold, S. W., M. S. de Souza, J. L. Janotka, A. L. Smith, and D. H. Persing.** 1993. Chronic Lyme borreliosis in the laboratory mouse. Am J Pathol **143:**959-71.

25. **Belisle, J. T., M. E. Brandt, J. D. Radolf, and M. V. Norgard.** 1994. Fatty acids of *Treponema pallidum* and *Borrelia burgdorferi* lipoproteins. J Bacteriol **176:**2151-7.

26. **Benach, J. L., E. M. Bosler, J. P. Hanrahan, J. L. Coleman, G. S. Habicht, T. F. Bast, D. J. Cameron, J. L. Ziegler, A. G. Barbour, W. Burgdorfer, R. Edelman, and R. A. Kaslow.** 1983. Spirochetes isolated from the blood of two patients with Lyme disease. N Engl J Med **308:**740-2.

27. **Bergstrom, S., A. G. Barbour, C. F. Garon, P. Hindersson, I. Saint Girons, and T. G. Schwan.** 1991. Genetics of *Borrelia burgdorferi*. Scand J Infect Dis Suppl **77:**102-7.

28. **Binder, E., R. Doepfmer, and O. Hornstein.** 1955. Experimentelle Ubertragung des Erythema chronicum migrans von Mensch zu Mensch. Hautrazt **6:**494-496.

29. **Blattner, F. R., G. Plunkett, 3rd, C. A. Bloch, N. T. Perna, V. Burland, M. Riley, J. Collado-Vides, J. D. Glasner, C. K. Rode, G. F. Mayhew, J. Gregor, N. W. Davis, H. A. Kirkpatrick, M. A. Goeden, D. J. Rose, B. Mau, and Y. Shao.** 1997. The complete genome sequence of *Escherichia coli* K-12. Science **277:**1453-74.

30. **Blevins, J. S., A. T. Revel, M. J. Caimano, X. F. Yang, J. A. Richardson, K. E. Hagman, and M. V. Norgard.** 2004. The *luxS* gene is not required for *Borrelia burgdorferi* tick colonization, transmission to a mammalian host, or induction of disease. Infect Immun **72:**4864-7.

31. **Bockenstedt, L. K., S. Barthold, K. Deponte, N. Marcantonio, and F. S. Kantor.** 1993. *Borrelia burgdorferi* infection and immunity in mice deficient in the fifth component of complement. Infect Immun **61:**2104-7.

32. **Bockenstedt, L. K., I. Kang, C. Chang, D. Persing, A. Hayday, and S. W. Barthold.** 2001. CD4+ T helper 1 cells facilitate regression of murine Lyme carditis. Infect Immun **69:**5264-9.

33. **Bono, J. L., A. F. Elias, J. J. Kupko, 3rd, B. Stevenson, K. Tilly, and P. Rosa.** 2000. Efficient targeted mutagenesis in *Borrelia burgdorferi*. J Bacteriol **182:**2445-52.

34. **Brandt, M. E., B. S. Riley, J. D. Radolf, and M. V. Norgard.** 1990. Immunogenic integral membrane proteins of *Borrelia burgdorferi* are lipoproteins. Infect Immun **58:**983-91.

35. **Brooks, C. S., P. S. Hefty, S. E. Jolliff, and D. R. Akins.** 2003. Global analysis of *Borrelia burgdorferi* genes regulated by mammalian host-specific signals. Infect Immun **71:**3371-83.

36. **Brown, E. L., R. M. Wooten, B. J. Johnson, R. V. Iozzo, A. Smith, M. C. Dolan, B. P. Guo, J. J. Weis, and M. Hook.** 2001. Resistance to Lyme disease in decorin-deficient mice. J Clin Invest **107:**845-52.

37. **Brusca, J. S., A. W. McDowall, M. V. Norgard, and J. D. Radolf.** 1991. Localization of outer surface proteins A and B in both the outer membrane and intracellular compartments of *Borrelia burgdorferi*. J Bacteriol **173:**8004-8.

38. **Buck, M., M.-T. Gallegos, D. J. Studholme, Y. Guo, and J. D. Gralla.** 2000. The Bacterial Enhancer-Dependent sigma 54 (sigma N) Transcription Factor. J. Bacteriol. **182:**4129-4136.

39. **Bugrysheva, J., E. Y. Dobrikova, H. P. Godfrey, M. L. Sartakova, and F. C. Cabello.** 2002. Modulation of *Borrelia burgdorferi* stringent response and gene expression during extracellular growth with tick cells. Infect Immun **70:**3061-7.

40. **Bugrysheva, J., E. Y. Dobrikova, M. L. Sartakova, M. J. Caimano, T. J. Daniels, J. D. Radolf, H. P. Godfrey, and F. C. Cabello.** 2003. Characterization of the stringent response and rel(Bbu) expression in *Borrelia burgdorferi*. J Bacteriol **185:**957-65.

41. **Bunikis, J., and A. G. Barbour.** 1999. Access of antibody or trypsin to an integral outer membrane protein (P66) of *Borrelia burgdorferi* is hindered by Osp lipoproteins. Infect Immun **67:**2874-83.

42. **Bunikis, J., C. J. Luke, E. Bunikiene, S. Bergstrom, and A. G. Barbour.** 1998. A surface-exposed region of a novel outer membrane protein (P66) of Borrelia *spp.* is variable in size and sequence. J Bacteriol **180:**1618-23.

43. **Bunikis, J., L. Noppa, and S. Bergstrom.** 1995. Molecular analysis of a 66-kDa protein associated with the outer membrane of Lyme disease Borrelia. FEMS Microbiol Lett **131:**139-45.

44. **Burgdorfer, W.** 1986. Discovery of the Lyme disease spirochete: a historical review. Zentralbl Bakteriol Mikrobiol Hyg [A] **263:**7-10.

45. **Burgdorfer, W., A. G. Barbour, S. F. Hayes, J. L. Benach, E. Grunwaldt, and J. P. Davis.** 1982. Lyme disease-a tick-borne spirochetosis? Science **216:**1317-9.

46. **Burgdorfer, W., and J. E. Keirans.** 1983. Ticks and Lyme disease in the United States. Ann Intern Med **99:**121.

47. **Burkot, T. R., G. R. Mullen, R. Anderson, B. S. Schneider, C. M. Happ, and N. S. Zeidner.** 2001. *Borrelia lonestari* DNA in adult *Amblyomma americanum* ticks, Alabama. Emerg Infect Dis **7:**471-3.

48. **Byram, R., P. E. Stewart, and P. Rosa.** 2004. The essential nature of the ubiquitous 26-kilobase circular replicon of *Borrelia burgdorferi*. J Bacteriol **186:**3561-9.

49. **Cabello, F. C., M. Sartakova, and E. Dobrikova.** 2001. Genetic Manipulation of Spirochetes - Light at the End of the Tunnel. Trends in Microbiology **9:**245-8.

50. **Cadavid, D., D. D. Thomas, R. Crawley, and A. G. Barbour.** 1994. Variability of a bacterial surface protein and disease expression in a possible mouse model of systemic Lyme borreliosis. J Exp Med **179:**631-42.

51. **Caimano, M. J., C. H. Eggers, K. R. Hazlett, and J. D. Radolf.** 2004. RpoS is not central to the general stress response in *Borrelia burgdorferi* but does control expression of one or more essential virulence determinants. Infect Immun **72:**6433-45.

52. **Carroll, J. A., C. F. Garon, and T. G. Schwan.** 1999. Effects of Environmental pH on Membrane Proteins in *Borrelia burgdorferi*. Infect. Immun. **67:**3181-3187.

53. **Carroll, J. A., P. E. Stewart, P. Rosa, A. F. Elias, and C. F. Garon.** 2003. An enhanced GFP reporter system to monitor gene expression in *Borrelia burgdorferi*. Microbiology **149:**1819-28.

54. **Casadevall, A., and L.-a. Pirofski.** 2001. Host-Pathogen Interactions: The attributes of Virulence. J Infect Dis **184:**337-44.

55. **Cashel, M., D. R. Gentry, V. J. Hernandez, and D. Vinella.** 1996. in *Escherichia coli and Salmonella* ed. Niedhardt, F. C. (Am. Soc. Microbiol., Washington, DC):1458-1496.

56. **Casjens, S.** 1999. Evolution of the linear DNA replicons of the Borrelia spirochetes. Curr Opin Microbiol **2:**529-534.

57. **Casjens, S., N. Palmer, R. van Vugt, W. M. Huang, B. Stevenson, P. Rosa, R. Lathigra, G. Sutton, J. Peterson, R. J. Dodson, D. Haft, E. Hickey, M. Gwinn, O. White, and C. M. Fraser.** 2000. A bacterial genome in flux: the twelve linear and nine circular extrachromosomal DNAs in an infectious isolate of the Lyme disease spirochete *Borrelia burgdorferi*. Mol Microbiol **35:**490-516.

58. **Casjens, S., R. van Vugt, K. Tilly, P. A. Rosa, and B. Stevenson.** 1997. Homology throughout the multiple 32-kilobase circular plasmids present in Lyme disease spirochetes. J Bacteriol **179:**217-27.

59. **Cassatt, D. R., N. K. Patel, N. D. Ulbrandt, and M. S. Hanson.** 1998. DbpA, but Not OspA, Is Expressed by *Borrelia burgdorferi* during Spirochetemia and Is a Target for Protective Antibodies. Infect. Immun. **66:**5379-5387.

60. **CDC.** 2002. MMWR **52:**741-750.

61. **CDC.** 1995. Recommendations for Test Performance and Interpretation form the Second National Conference on Serological Diagnosis of Lyme Disease. MMWR **44:**590-591.

62. **Coburn, J., W. Chege, L. Magoun, S. C. Bodary, and J. M. Leong.** 1999. Characterization of a candidate *Borrelia burgdorferi* beta3-chain integrin ligand identified using a phage display library. Mol Microbiol **34:**926-40.

63. **Coburn, J., and C. Cugini.** 2003. Targeted mutation of the outer membrane protein P66 disrupts attachment of the Lyme disease agent, *Borrelia burgdorferi*, to integrin alphavbeta3. Proc Natl Acad Sci U S A **100:**7301-6.

64. **Coleman, J. L., J. A. Gebbia, J. Piesman, J. L. Degen, T. H. Bugge, and J. L. Benach.** 1997. Plasminogen is required for efficient dissemination of *B. burgdorferi* in ticks and for enhancement of spirochetemia in mice. Cell **89:**1111-9.

65. **Coleman, J. L., R. C. Rogers, P. A. Rosa, and J. L. Benach.** 1994. Variations in the ospB gene of *Borrelia burgdorferi* result in differences in monoclonal antibody reactivity and in production of escape variants. Infect Immun **62:**303-7.

66. **Cox, D. L., D. R. Akins, K. W. Bourell, P. Lahdenne, M. V. Norgard, and J. D. Radolf.** 1996. Limited surface exposure of *Borrelia burgdorferi* outer surface lipoproteins. Proc Natl Acad Sci U S A **93:**7973-8.

67. **Crother, T. R., C. I. Champion, J. P. Whitelegge, R. Aguilera, X. Y. Wu, D. R. Blanco, J. N. Miller, and M. A. Lovett.** 2004. Temporal analysis of the antigenic composition of *Borrelia burgdorferi* during infection in rabbit skin. Infect Immun **72:**5063-72.

68. **Crother, T. R., C. I. Champion, X. Y. Wu, D. R. Blanco, J. N. Miller, and M. A. Lovett.** 2003. Antigenic composition of *Borrelia burgdorferi* during infection of SCID mice. Infect Immun **71:**3419-28.

69. **Cugini, C., M. Medrano, T. G. Schwan, and J. Coburn.** 2003. Regulation of expression of the *Borrelia burgdorferi* beta(3)-chain integrin ligand, P66, in ticks and in culture. Infect Immun **71:**1001-7.

70. **de Silva, A. M., and E. Fikrig.** 1995. Growth and migration of *Borrelia burgdorferi* in *Ixodes* ticks during blood feeding. Am J Trop Med Hyg **53:**397-404.

71. **de Silva, A. M., S. R. Telford, 3rd, L. R. Brunet, S. W. Barthold, and E. Fikrig.** 1996. *Borrelia burgdorferi* OspA is an arthropod-specific transmission-blocking Lyme disease vaccine. J Exp Med **183:**271-5.

72. **Defoe, G., and J. Coburn.** 2001. Delineation of *Borrelia burgdorferi p66* sequences required for integrin alpha(IIb)beta(3) recognition. Infect Immun **69:**3455-9.

73. **Deibler, R. W., S. Rahmati, and E. L. Zechiedrich.** 2001. Topoisomerase IV, alone, unknots DNA in *E. coli*. Genes Dev **15:**748-61.

74. **Dennis, D. T., T. S. Nekomoto, J. C. Victor, W. S. Paul, and J. Piesman.** 1998. Reported distribution of *Ixodes scapularis* and *Ixodes pacificus* (Acari: Ixodidae) in the United States. J Med Entomol **35:**629-38.

75. **Dunn, J. J., S. R. Buchstein, L. Butler, S. Fisenne, D. S. Polin, B. N. Lade, and B. J. Luft.** 1994. Complete Nucleotide Sequence of a Ciruclar Plasmid from the Lyme disease Spirochete, *Borrelia burgdorferi*. J Bacteriol **176:**2706-2717.

76. **Duray, P. H.** 1989. Histopathology of clinical phases of Lyme disease. Rheum Dis Clin North Am **15:**691-711.

77. **Duray, P. H., and A. C. Steere.** 1988. Clinical pathological correlations of Lyme disease by stage. Ann. Ny. Y. Acad. Med. **53:**65-79.

78. **Eggers, C. H., M. J. Caimano, M. L. Clawson, W. G. Miller, D. S. Samuels, and J. D. Radolf.** 2002. Identification of loci critical for replication and compatibility of a *Borrelia burgdorferi* cp32 plasmid and use of a cp32-based shuttle vector for the expression of fluorescent reporters in the lyme disease spirochaete. Mol Microbiol **43:**281-95.

79. **Eggers, C. H., M. J. Caimano, and J. D. Radolf.** 2004. Analysis of promoter elements involved in the transcriptional initiation of RpoS-dependent *Borrelia burgdorferi* genes. J Bacteriol **186:**7390-402.

80. **Eggers, C. H., S. Casjens, S. F. Hayes, C. F. Garon, C. J. Damman, D. B. Oliver, and D. S. Samuels.** 2000. Bacteriophages of spirochetes. J Mol Microbiol Biotechnol **2:**365-73.

81. **Eggers, C. H., B. J. Kimmel, J. L. Bono, A. F. Elias, P. Rosa, and D. S. Samuels.** 2001. Transduction by phiBB-1, a bacteriophage of *Borrelia burgdorferi*. J Bacteriol **183:**4771-8.

82. **Eicken, C., V. Sharma, T. Klabunde, M. B. Lawrenz, J. M. Hardham, S. J. Norris, and J. C. Sacchettini.** 2002. Crystal structure of Lyme disease variable surface antigen VlsE of *Borrelia burgdorferi*. J Biol Chem **277:**21691-6.

83. **Eisen, M. B., P. T. Spellman, P. O. Brown, and D. Botstein.** 1998. Cluster analysis and display of genome-wide expression patterns. PNAS **95:**14863-14868.

84. **Elias, A. F., J. L. Bono, J. A. Carroll, P. Stewart, K. Tilly, and P. Rosa.** 2000. Altered stationary-phase response in a *Borrelia burgdorferi rpoS* mutant. J Bacteriol **182:**2909-18.

85. **Elias, A. F., J. L. Bono, J. J. Kupko, 3rd, P. E. Stewart, J. G. Krum, and P. A. Rosa.** 2003. New antibiotic resistance cassettes suitable for genetic studies in *Borrelia burgdorferi*. J Mol Microbiol Biotechnol **6:**29-40.

86. **Elias, A. F., P. E. Stewart, D. Grimm, M. J. Caimano, C. H. Eggers, K. Tilly, J. L. Bono, D. R. Akins, J. D. Radolf, T. G. Schwan, and P. Rosa.** 2002. Clonal polymorphism of *Borrelia burgdorferi* strain B31 MI: implications for mutagenesis in an infectious strain background. Infect Immun **70:**2139-50.

87. **England, J. D., R. P. Bohm, Jr., E. D. Roberts, and M. T. Philipp.** 1997. Lyme neuroborreliosis in the rhesus monkey. Semin Neurol **17:**53-6.

88. **Falkow, S.** 1988. Molecular Koch's postulates applied to microbial pathogenicity. Rev Infect Dis **10 Suppl 2:**S274-6.

89. **Figueroa, R., L. A. Bracero, M. Aguero-Rosenfeld, D. Beneck, J. Coleman, and I. Schwartz.** 1996. Confirmation of *Borrelia burgdorferi* spirochetes by polymerase chain reaction in placentas of women with reactive serology for Lyme antibodies. Gynecol Obstet Invest **41:**240-3.

90. **Fikrig, E., S. W. Barthold, F. S. Kantor, and R. A. Flavell.** 1990. Protection of mice against the Lyme disease agent by immunizing with recombinant OspA. Science **250:**553-6.

91. **Fikrig, E., S. W. Barthold, W. Sun, W. Feng, S. R. Telford, 3rd, and R. A. Flavell.** 1997. *Borrelia burgdorferi* P35 and P37 proteins, expressed *in vivo*, elicit protective immunity. Immunity **6:**531-9.

92. **Fikrig, E., L. K. Bockenstedt, S. W. Barthold, M. Chen, H. Tao, P. Ali-Salaam, S. R. Telford, and R. A. Flavell.** 1994. Sera from patients with chronic Lyme disease protect mice from Lyme borreliosis. J Infect Dis **169:**568-74.

93. **Fikrig, E., W. Feng, S. W. Barthold, S. R. Telford, 3rd, and R. A. Flavell.** 2000. Arthropod- and host-specific *Borrelia burgdorferi bbk32* expression and the inhibition of spirochete transmission. J Immunol **164:**5344-51.

94. **Fikrig, E., B. Liu, L. L. Fu, S. Das, J. I. Smallwood, R. A. Flavell, D. H. Persing, R. T. Schoen, S. W. Barthold, and S. E. Malawista.** 1995. An *ospA* frame shift, identified from DNA in Lyme arthritis synovial fluid, results in an outer surface protein A that does not bind protective antibodies. J Immunol **155:**5700-4.

95. **Fikrig, E., H. Tao, S. W. Barthold, and R. A. Flavell.** 1995. Selection of variant *Borrelia burgdorferi* isolates from mice immunized with outer surface protein A or B. Infect Immun **63:**1658-62.

96. **Fikrig, E., S. R. Telford, 3rd, S. W. Barthold, F. S. Kantor, A. Spielman, and R. A. Flavell.** 1992. Elimination of *Borrelia burgdorferi* from vector ticks feeding on OspA-immunized mice. Proc Natl Acad Sci U S A **89:**5418-21.

97. **Fikrig, E., S. R. Telford, 3rd, R. Wallich, M. Chen, Y. Lobet, F. R. Matuschka, R. B. Kimsey, F. S. Kantor, S. W. Barthold, A. Spielman, and et al.** 1995. Vaccination against Lyme disease caused by diverse *Borrelia burgdorferi*. J Exp Med **181:**215-21.

98. **Finlay, B. B., and S. Falkow.** 1989. Common themes in microbial pathogenicity. Microbiol Rev **53:**210-30.

99. **Fischer, J. R., N. Parveen, L. Magoun, and J. M. Leong.** 2003. Decorin-binding proteins A and B confer distinct mammalian cell type-specific attachment by *Borrelia burgdorferi*, the Lyme disease spirochete. Proc Natl Acad Sci U S A **100:**7307-12.

100. **Frank, K. L., S. F. Bundle, M. E. Kresge, C. H. Eggers, and D. S. Samuels.** 2003. aadA confers streptomycin resistance in *Borrelia burgdorferi*. J Bacteriol **185:**6723-7.

101. **Fraser, C. M., S. Casjens, W. M. Huang, G. G. Sutton, R. Clayton, R. Lathigra, O. White, K. A. Ketchum, R. Dodson, E. K. Hickey, M. Gwinn, B. Dougherty, J. F. Tomb, R. D. Fleischmann, D. Richardson, J. Peterson, A. R. Kerlavage, J. Quackenbush, S. Salzberg, M. Hanson, R. van Vugt, N. Palmer, M. D. Adams, J. Gocayne, J. C. Venter, and et al.** 1997. Genomic sequence of a Lyme disease spirochaete, *Borrelia burgdorferi*. Nature **390:**580-6.

102. **Fraser, C. M., S. J. Norris, G. M. Weinstock, O. White, G. G. Sutton, R. Dodson, M. Gwinn, E. K. Hickey, R. Clayton, K. A. Ketchum, E. Sodergren, J. M. Hardham, M. P. McLeod, S. Salzberg, J. Peterson, H. Khalak, D. Richardson, J. K. Howell, M. Chidambaram, T. Utterback, L. McDonald, P. Artiach, C.**

Bowman, M. D. Cotton, J. C. Venter, and et al. 1998. Complete genome sequence of *Treponema pallidum*, the syphilis spirochete. Science **281:**375-88.

103. **Fuchs, R., S. Jauris, F. Lottspeich, V. Preac-Mursic, B. Wilske, and E. Soutschek.** 1992. Molecular analysis and expression of a *Borrelia burgdorferi* gene encoding a 22 kDa protein (pC) in *Escherichia coli*. Mol Microbiol **6:**503-9.

104. **Ge, Y., and N. W. Charon.** 1997. Molecular characterization of a flagellar/chemotaxis operon in the spirochete *Borrelia burgdorferi*. FEMS Microbiol Lett **153:**425-31.

105. **Glickstein, L., B. Moore, T. Bledsoe, N. Damle, V. Sikand, and A. C. Steere.** 2003. Inflammatory cytokine production predominates in early Lyme disease in patients with erythema migrans. Infect Immun **71:**6051-3.

106. **Glockner, G., R. Lehmann, A. Romualdi, S. Pradella, U. Schulte-Spechtel, M. Schilhabel, B. Wilske, J. Suhnel, and M. Platzer.** 2004. Comparative analysis of the *Borrelia garinii* genome. Nucleic Acids Res **32:**6038-46.

107. **Goldstein, S. F., N. W. Charon, and J. A. Kreiling.** 1994. *Borrelia burgdorferi* swims with a planar waveform similar to that of eukaryotic flagella. Proc Natl Acad Sci U S A **91:**3433-7.

108. **Grimm, D., C. H. Eggers, M. J. Caimano, K. Tilly, P. E. Stewart, A. F. Elias, J. D. Radolf, and P. A. Rosa.** 2004. Experimental assessment of the roles of linear plasmids lp25 and lp28-1 of *Borrelia burgdorferi* throughout the infectious cycle. Infect Immun **72:**5938-46.

109. **Grimm, D., A. F. Elias, K. Tilly, and P. A. Rosa.** 2003. Plasmid stability during *in vitro* propagation of *Borrelia burgdorferi* assessed at a clonal level. Infect Immun **71:**3138-45.

110. **Grimm, D., K. Tilly, R. Byram, P. E. Stewart, J. G. Krum, D. M. Bueschel, T. G. Schwan, P. F. Policastro, A. F. Elias, and P. A. Rosa.** 2004. Outer-surface protein C of the Lyme disease spirochete: a protein induced in ticks for infection of mammals. Proc Natl Acad Sci U S A **101:**3142-7.

111. **Gross, D. M., T. Forsthuber, M. Tary-Lehmann, C. Etling, K. Ito, Z. A. Nagy, J. A. Field, A. C. Steere, and B. T. Huber.** 1998. Identification of LFA-1 as a candidate autoantigen in treatment-resistant Lyme arthritis. Science **281:**703-6.

112. **Gross, D. M., A. C. Steere, and B. T. Huber.** 1998. T helper 1 response is dominant and localized to the synovial fluid in patients with Lyme arthritis. J Immunol **160:**1022-8.

113. **Guo, B. P., E. L. Brown, D. W. Dorward, L. C. Rosenberg, and M. Hook.** 1998. Decorin-binding adhesins from *Borrelia burgdorferi*. Mol Microbiol **30:**711-23.

114. **Guo, B. P., S. J. Norris, L. C. Rosenberg, and M. Hook.** 1995. Adherence of *Borrelia burgdorferi* to the proteoglycan decorin. Infect Immun **63:**3467-72.

115. **Haake, D. A., and M. A. Lovett.** 1994. Interjunctional invasion of endothelial cell monolayers. Methods Enzymol **236:**447-63.

116. **Hagman, K. E., P. Lahdenne, T. G. Popova, S. F. Porcella, D. R. Akins, J. D. Radolf, and M. V. Norgard.** 1998. Decorin-binding protein of *Borrelia burgdorferi*

is encoded within a two-gene operon and is protective in the murine model of Lyme borreliosis. Infect Immun **66:**2674-83.

117. **Hagman, K. E., X. Yang, S. K. Wikel, G. B. Schoeler, M. J. Caimano, J. D. Radolf, and M. V. Norgard.** 2000. Decorin-binding protein A (DbpA) of *Borrelia burgdorferi* is not protective when immunized mice are challenged via tick infestation and correlates with the lack of DbpA expression by *B. burgdorferi* in ticks. Infect Immun **68:**4759-64.

118. **Hanson, M. S., D. R. Cassatt, B. P. Guo, N. K. Patel, M. P. McCarthy, D. W. Dorward, and M. Hook.** 1998. Active and passive immunity against *Borrelia burgdorferi* decorin binding protein A (DbpA) protects against infection. Infect Immun **66:**2143-53.

119. **Hayashi, S., and H. C. Wu.** 1990. Lipoproteins in bacteria. J Bioenerg Biomembr **22:**451-71.

120. **Hefty, P. S., S. E. Jolliff, M. J. Caimano, S. K. Wikel, and D. R. Akins.** 2002. Changes in temporal and spatial patterns of outer surface lipoprotein expression generate population heterogeneity and antigenic diversity in the Lyme disease spirochete, *Borrelia burgdorferi*. Infect Immun **70:**3468-78.

121. **Hengge-Aronis, R.** 1996. Back to log phase: sigma S as a global regulator in the osmotic control of gene expression in *Escherichia coli*. Mol Microbiol **21:**887-93.

122. **Herxheimer, K., and K. Harmann.** 1902. Ueber Acrodermatitis chrnica atrophicans. Arch. Derm. Syph. **61:**57-76.

123. **Hodzic, E., S. Feng, K. J. Freet, and S. W. Barthold.** 2003. *Borrelia burgdorferi* population dynamics and prototype gene expression during infection of immunocompetent and immunodeficient mice. Infect Immun **71:**5042-55.

124. **Hollstrom, E.** 1951. Successful treatment of the erythema migrans Afzelius. Acta Dermatolofica Venereologica **31:**235-243.

125. **Hossain, H., H. J. Wellensiek, R. Geyer, and G. Lochnit.** 2001. Structural analysis of glycolipids from *Borrelia burgdorferi*. Biochimie **83:**683-92.

126. **Hovis, K. M., J. V. McDowell, L. Griffin, and R. T. Marconi.** 2004. Identification and characterization of a linear-plasmid-encoded factor H-binding protein (FhbA) of the relapsing fever spirochete *Borrelia hermsii*. J Bacteriol **186:**2612-8.

127. **Howe, T. R., L. W. Mayer, and A. G. Barbour.** 1985. A single recombinant plasmid expressing two major outer surface proteins of the Lyme disease spirochete. Science **227:**645-6.

128. **Hubner, A., A. T. Revel, D. M. Nolen, K. E. Hagman, and M. V. Norgard.** 2003. Expression of a *luxS* gene is not required for *Borrelia burgdorferi* infection of mice via needle inoculation. Infect Immun **71:**2892-6.

129. **Hubner, A., X. Yang, D. M. Nolen, T. G. Popova, F. C. Cabello, and M. V. Norgard.** 2001. Expression of *Borrelia burgdorferi* OspC and DbpA is controlled by a RpoN-RpoS regulatory pathway. Proc Natl Acad Sci U S A **98:**12724-9.

130. **Hudson, C. R., J. G. Frye, F. D. Quinn, and F. C. Gherardini.** 2001. Increased expression of *Borrelia burgdorferi vlsE* in response to human endothelial cell membranes. Mol Microbiol **41:**229-39.

131. **Hughes, C. A., C. B. Kodner, and R. C. Johnson.** 1992. DNA analysis of *Borrelia burgdorferi* NCH-1, the first northcentral U.S. human Lyme disease isolate. J Clin Microbiol **30:**698-703.

132. **Hughes, T. R., M. J. Marton, A. R. Jones, C. J. Roberts, R. Stoughton, C. D. Armour, H. A. Bennett, E. Coffey, H. Dai, Y. D. He, M. J. Kidd, A. M. King, M. R. Meyer, D. Slade, P. Y. Lum, S. B. Stepaniants, D. D. Shoemaker, D. Gachotte, K. Chakraburtty, J. Simon, M. Bard, and S. H. Friend.** 2000. Functional discovery via a compendium of expression profiles. Cell **102:**109-26.

133. **Indest, K. J., J. K. Howell, M. B. Jacobs, D. Scholl-Meeker, S. J. Norris, and M. T. Philipp.** 2001. Analysis of *Borrelia burgdorferi vlsE* gene expression and recombination in the tick vector. Infect Immun **69:**7083-90.

134. **Indest, K. J., R. Ramamoorthy, M. Sole, R. D. Gilmore, B. J. Johnson, and M. T. Philipp.** 1997. Cell-density-dependent expression of *Borrelia burgdorferi* lipoproteins *in vitro*. Infect Immun **65:**1165-71.

135. **Jones, J. D., K. W. Bourell, M. V. Norgard, and J. D. Radolf.** 1995. Membrane topology of *Borrelia burgdorferi* and *Treponema pallidum* lipoproteins. Infect Immun **63:**2424-34.

136. **Jonsson, K., B. P. Guo, H. J. Monstein, J. J. Mekalanos, and G. Kronvall.** 2004. Molecular cloning and characterization of two *Helicobacter pylori* genes coding for plasminogen-binding proteins. Proc Natl Acad Sci U S A **101:**1852-7.

137. **Jonsson, M., and S. Bergstrom.** 1995. Transcriptional and translational regulation of the expression of the major outer surface proteins in Lyme disease Borrelia strains. Microbiology **141 (Pt 6):**1321-9.

138. **Jonsson, M., L. Noppa, A. G. Barbour, and S. Bergstrom.** 1992. Heterogeneity of outer membrane proteins in *Borrelia burgdorferi*: comparison of osp operons of three isolates of different geographic origins. Infect Immun **60:**1845-53.

139. **Kang, M. S., B. K. Lim, I. S. Seong, J. H. Seol, N. Tanahashi, K. Tanaka, and C. H. Chung.** 2001. The ATP-dependent CodWX (HslVU) protease in *Bacillus subtilis* is an N-terminal serine protease. EMBO J **20:**734-42.

140. **Kasinsky, H. E., J. D. Lewis, J. B. Dacks, and J. Ausio.** 2001. Origin of H1 linker histones. Faseb J **15:**34-42.

141. **Katona, L. I., S. Ayalew, J. L. Coleman, and J. L. Benach.** 2000. A bactericidal monoclonal antibody elicits a change in its antigen, OspB of *Borrelia burgdorferi*, that can be detected by limited proteolysis. J Immunol **164:**1425-31.

142. **Kawabata, H., T. Masuzawa, and Y. Yanagihara.** 1993. Genomic analysis of *Borrelia japonica* sp. nov. isolated from *Ixodes ovatus* in Japan. Microbiol Immunol **37:**843-8.

143. **Kawabata, H., S. J. Norris, and H. Watanabe.** 2004. BBE02 disruption mutants of *Borrelia burgdorferi* B31 have a highly transformable, infectious phenotype. Infect Immun **72:**7147-54.

144. **Keane-Meyers, A., and S. P. Nickell.** 1995. Role of IL-4 and INF-Gamma in modulation of immunity to *Borrelia burgdorferi*. J Immunol **155:**2020-2028.

145. **Klezovitch, O., and A. M. Scanu.** 1995. Heterogeneity of lipoprotein (a): growing complexities. Curr Opin Lipidol **6:**223-8.

146. **Kobryn, K., and G. Chaconas.** 2002. ResT, a telomere resolvase encoded by the Lyme disease spirochete. Mol Cell **9:**195-201.

147. **Kraiczy, P., J. Hellwage, C. Skerka, H. Becker, M. Kirschfink, M. M. Simon, V. Brade, P. F. Zipfel, and R. Wallich.** 2004. Complement resistance of *Borrelia burgdorferi* correlates with the expression of BbCRASP-1, a novel linear plasmid-encoded surface protein that interacts with human factor H and FHL-1 and is unrelated to Erp proteins. J Biol Chem **279:**2421-9.

148. **Kraiczy, P., J. Hellwage, C. Skerka, M. Kirschfink, V. Brade, P. F. Zipfel, and R. Wallich.** 2003. Immune evasion of *Borrelia burgdorferi*: mapping of a complement-inhibitor factor H-binding site of BbCRASP-3, a novel member of the Erp protein family. Eur J Immunol **33:**697-707.

149. **Kriuchechnikov, V. N., E. I. Korenberg, S. V. Shcherbakov, V. Kovalevskii Iu, and M. L. Levin.** 1988. [Identification of Borrelia isolated in the USSR from *Ixodes persulcatus* Schulze ticks]. Zh Mikrobiol Epidemiol Immunobiol**:**41-4.

150. **Kusano, S., Q. Ding, N. Fujita, and A. Ishihama.** 1996. Promoter Selectivity of *Escherichia coli* RNA Polymerase ERpo^{70} and ERpoS Holoenzymes. J. Biol. Chem. **271:**1998-2004.

151. **Labandeira-Rey, M., E. A. Baker, and J. T. Skare.** 2001. VraA (BBI16) protein of *Borrelia burgdorferi* is a surface-exposed antigen with a repetitive motif that confers partial protection against experimental Lyme borreliosis. Infect Immun **69:**1409-19.

152. **Labandeira-Rey, M., and J. T. Skare.** 2001. Decreased Infectivity in *Borrelia burgdorferi* Strain B31 Is Associated with Loss of Linear Plasmid 25 or 28-1. Infect. Immun. **69:**446-455.

153. **Lahdenne, P., S. F. Porcella, K. E. Hagman, D. R. Akins, T. G. Popova, D. L. Cox, L. I. Katona, J. D. Radolf, and M. V. Norgard.** 1997. Molecular characterization of a 6.6-kilodalton *Borrelia burgdorferi* outer membrane-associated lipoprotein (lp6.6) which appears to be downregulated during mammalian infection. Infect Immun **65:**412-21.

154. **Lam, T. T., T. P. Nguyen, R. R. Montgomery, F. S. Kantor, E. Fikrig, and R. A. Flavell.** 1994. Outer surface proteins E and F of *Borrelia burgdorferi*, the agent of Lyme disease. Infect Immun **62:**290-8.

155. **Lawrenz, M. B., H. Kawabata, J. E. Purser, and S. J. Norris.** 2002. Decreased electroporation efficiency in *Borrelia burgdorferi* containing linear plasmids lp25 and lp56: impact on transformation of infectious *B. burgdorferi*. Infect Immun **70:**4798-804.

156. **Lawrenz, M. B., R. M. Wooten, J. F. Zachary, S. M. Drouin, J. J. Weis, R. A. Wetsel, and S. J. Norris.** 2003. Effect of complement component C3 deficiency on experimental Lyme borreliosis in mice. Infect Immun **71:**4432-40.

157. **Lee, M. L., F. C. Kuo, G. A. Whitmore, and J. Sklar.** 2000. Importance of replication in microarray gene expression studies: statistical methods and evidence from repetitive cDNA hybridizations. Proc Natl Acad Sci U S A **97:**9834-9.

158. **Li, C., R. G. Bakker, M. A. Motaleb, M. L. Sartakova, F. C. Cabello, and N. W. Charon.** 2002. Asymmetrical flagellar rotation in *Borrelia burgdorferi* nonchemotactic mutants. Proc Natl Acad Sci U S A **99:**6169-74.

159. **Liang, F. T., E. L. Brown, T. Wang, R. V. Iozzo, and E. Fikrig.** 2004. Protective niche for *Borrelia burgdorferi* to evade humoral immunity. Am J Pathol **165:**977-85.

160. **Liang, F. T., M. J. Caimano, J. D. Radolf, and E. Fikrig.** 2004. *Borrelia burgdorferi* outer surface protein (*osp*) B expression independent of *ospA*. Microb Pathog **37:**35-40.

161. **Liang, F. T., M. B. Jacobs, L. C. Bowers, and M. T. Philipp.** 2002. An immune evasion mechanism for spirochetal persistence in Lyme borreliosis. J Exp Med **195:**415-22.

162. **Liang, F. T., A. C. Steere, A. R. Marques, B. J. Johnson, J. N. Miller, and M. T. Philipp.** 1999. Sensitive and specific serodiagnosis of Lyme disease by enzyme-linked immunosorbent assay with a peptide based on an immunodominant conserved region of *Borrelia burgdorferi vlsE*. J Clin Microbiol **37:**3990-6.

163. **Lim, C. J., T. Daws, M. Gerami-Nejad, and J. A. Fuchs.** 2000. Growth-phase regulation of the *Escherichia coli* thioredoxin gene. Biochim Biophys Acta **1491:**1-6.

164. **Ma, Y., K. P. Seiler, K. F. Tai, L. Yang, M. Woods, and J. J. Weis.** 1994. Outer surface lipoproteins of *Borrelia burgdorferi* stimulate nitric oxide production by the cytokine-inducible pathway. Infect Immun **62:**3663-71.

165. **Ma, Y., and J. J. Weis.** 1993. *Borrelia burgdorferi* outer surface lipoproteins OspA and OspB possess B-cell mitogenic and cytokine-stimulatory properties. Infect Immun **61:**3843-53.

166. **Marconi, R. T., D. S. Samuels, and C. F. Garon.** 1993. Transcriptional analyses and mapping of the ospC gene in Lyme disease spirochetes. J Bacteriol **175:**926-32.

167. **Margolis, N., D. Hogan, W. Cieplak, Jr., T. G. Schwan, and P. A. Rosa.** 1994. Homology between *Borrelia burgdorferi* OspC and members of the family of *Borrelia hermsii* variable major proteins. Gene **143:**105-10.

168. **Masuda, Y., K. Miyakawa, Y. Nishimura, and E. Ohtsubo.** 1993. chpA and chpB, *Escherichia coli* chromosomal homologs of the pem locus responsible for stable maintenance of plasmid R100. J. Bacteriol. **175:**6850-6856.

169. **Matuschka, F. R., and A. Speilman.** 1986. Exp. Applied Acarol. **2:**337-353.

170. **McDowell, J. V., J. Wolfgang, E. Tran, M. S. Metts, D. Hamilton, and R. T. Marconi.** 2003. Comprehensive analysis of the factor h binding capabilities of borrelia species associated with lyme disease: delineation of two distinct classes of factor h binding proteins. Infect Immun **71:**3597-602.

171. **Means, R. G., and D. J. White.** 1997. New distribution records of *Amblyomma americanum* (L.) (Acari: Ixodidae) in New York State. J Vector Ecol **22:**133-45.

172. **Metts, M. S., J. V. McDowell, M. Theisen, P. R. Hansen, and R. T. Marconi.** 2003. Analysis of the OspE determinants involved in binding of factor H and OspE-targeting antibodies elicited during *Borrelia burgdorferi* infection in mice. Infect Immun **71:**3587-96.

173. **Michel, H., B. Wilske, G. Hettche, G. Gottner, C. Heimerl, U. Reischl, U. Schulte-Spechtel, and V. Fingerle.** 2003. An *ospA*-polymerase chain reaction/restriction fragment length polymorphism-based method for sensitive detection and reliable differentiation of all European *Borrelia burgdorferi sensu lato* species and OspA types. Med Microbiol Immunol (Berl).

174. **Moore, V. A. t., A. S. Varela, M. J. Yabsley, W. R. Davidson, and S. E. Little.** 2003. Detection of *Borrelia lonestari*, putative agent of southern tick-associated rash illness, in white-tailed deer (*Odocoileus virginianus*) from the southeastern United States. J Clin Microbiol **41:**424-7.

175. **Motaleb, M. A., L. Corum, J. L. Bono, A. F. Elias, P. Rosa, D. S. Samuels, and N. W. Charon.** 2000. *Borrelia burgdorferi* periplasmic flagella have both skeletal and motility functions. Proc Natl Acad Sci U S A **97:**10899-904.

176. **Mullegger, R. R., G. McHugh, R. Ruthazer, B. Binder, H. Kerl, and A. C. Steere.** 2000. Differential expression of cytokine mRNA in skin specimens from patients with erythema migrans or acrodermatitis chronica atrophicans. J Invest Dermatol **115:**1115-23.

177. **Narasimhan, S., M. J. Caimano, F. T. Liang, F. Santiago, M. Laskowski, M. T. Philipp, A. R. Pachner, J. D. Radolf, E. Fikrig, and M. J. Camaino.** 2003. *Borrelia burgdorferi* transcriptome in the central nervous system of non-human primates. Proc Natl Acad Sci U S A **100:**15953-8.

178. **Nguyen, T. P., T. T. Lam, S. W. Barthold, S. R. Telford, 3rd, R. A. Flavell, and E. Fikrig.** 1994. Partial destruction of *Borrelia burgdorferi* within ticks that engorged on OspE- or OspF-immunized mice. Infect Immun **62:**2079-84.

179. **Nocton, J. J., F. Dressler, B. J. Rutledge, P. N. Rys, D. H. Persing, and A. C. Steere.** 1994. Detection of *Borrelia burgdorferi* DNA by polymerase chain reaction in synovial fluid from patients with Lyme arthritis. N Engl J Med **330:**229-34.

180. **Norgard, M. V., L. L. Arndt, D. R. Akins, L. L. Curetty, D. A. Harrich, and J. D. Radolf.** 1996. Activation of human monocytic cells by *Treponema pallidum* and *Borrelia burgdorferi* lipoproteins and synthetic lipopeptides proceeds via a pathway distinct from that of lipopolysaccharide but involves the transcriptional activator NF-kappa B. Infect Immun **64:**3845-52.

181. **Norgard, M. V., B. S. Riley, J. A. Richardson, and J. D. Radolf.** 1995. Dermal inflammation elicited by synthetic analogs of *Treponema pallidum* and *Borrelia burgdorferi* lipoproteins. Infect Immun **63:**1507-15.

182. **Ohnishi, J., J. Piesman, and A. M. de Silva.** 2001. Antigenic and genetic heterogeneity of *Borrelia burgdorferi* populations transmitted by ticks. PNAS **98:**670-675.

183. **Ojaimi, C., C. Brooks, S. Casjens, P. Rosa, A. Elias, A. Barbour, A. Jasinskas, J. Benach, L. Katona, J. Radolf, M. Caimano, J. Skare, K. Swingle, D. Akins, and I. Schwartz.** 2003. Profiling of temperature-induced changes in *Borrelia burgdorferi* gene expression by using whole genome arrays. Infect Immun **71:**1689-705.

184. **Pachner, A. R., D. Cadavid, G. Shu, D. Dail, S. Pachner, E. Hodzic, and S. W. Barthold.** 2001. Central and peripheral nervous system infection, immunity, and inflammation in the NHP model of Lyme borreliosis. Ann Neurol **50:**330-8.

185. **Pachner, A. R., H. Gelderblom, and D. Cadavid.** 2001. The rhesus model of Lyme neuroborreliosis. Immunol Rev **183:**186-204.

186. **Pal, U., X. Li, T. Wang, R. R. Montgomery, N. Ramamoorthi, A. M. Desilva, F. Bao, X. Yang, M. Pypaert, D. Pradhan, F. S. Kantor, S. Telford, J. F. Anderson, and E. Fikrig.** 2004. TROSPA, an *Ixodes scapularis* receptor for *Borrelia burgdorferi*. Cell **119:**457-68.

187. **Pal, U., X. Yang, M. Chen, L. K. Bockenstedt, J. F. Anderson, R. A. Flavell, M. V. Norgard, and E. Fikrig.** 2004. OspC facilitates *Borrelia burgdorferi* invasion of *Ixodes scapularis* salivary glands. J Clin Invest **113:**220-30.

188. **Philipp, M. T., Y. Lobet, R. P. Bohm, Jr., E. D. Roberts, V. A. Dennis, Y. Gu, R. C. Lowrie, Jr., P. Desmons, P. H. Duray, J. D. England, P. Hauser, J. Piesman, and K. Xu.** 1997. The outer surface protein A (OspA) vaccine against Lyme disease: efficacy in the rhesus monkey. Vaccine **15:**1872-87.

189. **Piesman, J.** 1993. Standard system for infecting ticks (Acari: Ixodidae) with the Lyme disease spirochete, *Borrelia burgdorferi*. J Med Entomol **30:**199-203.

190. **Piesman, J., B. S. Schneider, and N. S. Zeidner.** 2001. Use of quantitative PCR to measure density of *Borrelia burgdorferi* in the midgut and salivary glands of feeding tick vectors. J Clin Microbiol **39:**4145-8.

191. **Pollack, R., S. Telford, 3d, and A. Spielman.** 1993. Standardization of medium for culturing Lyme disease spirochetes. J. Clin. Microbiol. **31:**1251-1255.

192. **Porcella, S. F., T. G. Popova, D. R. Akins, M. Li, J. D. Radolf, and M. V. Norgard.** 1996. *Borrelia burgdorferi* supercoiled plasmids encode multicopy tandem open reading frames and a lipoprotein gene family. J Bacteriol **178:**3293-307.

193. **Postic, D., M. V. Assous, P. A. Grimont, and G. Baranton.** 1994. Diversity of *Borrelia burgdorferi sensu lato* evidenced by restriction fragment length polymorphism of rrf (5S)-rrl (23S) intergenic spacer amplicons. Int J Syst Bacteriol **44:**743-52.

194. **Preac-Mursic, V., B. Wilske, G. Schierz, H. W. Pfister, and K. Winhaupl.** 1984. Eur. Journal of Clinical Microbiology **3:**564-565.

195. **Probert, W. S., K. M. Allsup, and R. B. LeFebvre.** 1995. Identification and characterization of a surface-exposed, 66-kilodalton protein from *Borrelia burgdorferi*. Infect Immun **63:**1933-9.

196. **Probert, W. S., and B. J. Johnson.** 1998. Identification of a 47 kDa fibronectin-binding protein expressed by *Borrelia burgdorferi* isolate B31. Mol Microbiol **30:**1003-15.

197. **Probert, W. S., J. H. Kim, M. Hook, and B. J. Johnson.** 2001. Mapping the ligand-binding region of *Borrelia burgdorferi* fibronectin-binding protein BBK32. Infect Immun **69:**4129-33.

198. **Purser, J. E., M. B. Lawrenz, M. J. Caimano, J. K. Howell, J. D. Radolf, and S. J. Norris.** 2003. A plasmid-encoded nicotinamidase (PncA) is essential for infectivity of *Borrelia burgdorferi* in a mammalian host. Mol Microbiol **48:**753-64.

199. **Purser, J. E., and S. J. Norris.** 2000. Correlation between plasmid content and infectivity in *Borrelia burgdorferi*. PNAS **97:**13865-13870.

200. **Radolf, J. D., L. L. Arndt, D. R. Akins, L. L. Curetty, M. E. Levi, Y. Shen, L. S. Davis, and M. V. Norgard.** 1995. *Treponema pallidum* and *Borrelia burgdorferi* lipoproteins and synthetic lipopeptides activate monocytes/macrophages. J Immunol **154:**2866-77.

201. **Radolf, J. D., K. W. Bourell, D. R. Akins, J. S. Brusca, and M. V. Norgard.** 1994. Analysis of *Borrelia burgdorferi* membrane architecture by freeze-fracture electron microscopy. J Bacteriol **176:**21-31.

202. **Radolf, J. D., M. S. Goldberg, K. Bourell, S. I. Baker, J. D. Jones, and M. V. Norgard.** 1995. Characterization of outer membranes isolated from *Borrelia burgdorferi*, the Lyme disease spirochete. Infect Immun **63:**2154-63.

203. **Radolf, J. D., M. V. Norgard, M. E. Brandt, R. D. Isaacs, P. A. Thompson, and B. Beutler.** 1991. Lipoproteins of *Borrelia burgdorferi* and *Treponema pallidum* activate cachectin/tumor necrosis factor synthesis. Analysis using a CAT reporter construct. J Immunol **147:**1968-74.

204. **Revel, A. T., A. M. Talaat, and M. V. Norgard.** 2002. DNA microarray analysis of differential gene expression in *Borrelia burgdorferi*, the Lyme disease spirochete. Proc Natl Acad Sci U S A **99:**1562-7.

205. **Riley, B. S., N. Oppenheimer-Marks, E. J. Hansen, J. D. Radolf, and M. V. Norgard.** 1992. Virulent *Treponema pallidum* activates human vascular endothelial cells. J Infect Dis **165:**484-93.

206. **Rosa, P., D. S. Samuels, D. Hogan, B. Stevenson, S. Casjens, and K. Tilly.** 1996. Directed insertion of a selectable marker into a circular plasmid of *Borrelia burgdorferi*. J Bacteriol **178:**5946-53.

207. **Sadziene, A., A. G. Barbour, P. A. Rosa, and D. D. Thomas.** 1993. An OspB mutant of *Borrelia burgdorferi* has reduced invasiveness *in vitro* and reduced infectivity *in vivo*. Infect Immun **61:**3590-6.

208. **Sadziene, A., P. A. Rosa, P. A. Thompson, D. M. Hogan, and A. G. Barbour.** 1992. Antibody-resistant mutants of *Borrelia burgdorferi*: *in vitro* selection and characterization. J Exp Med **176:**799-809.

209. **Samuels, D. S.** 1995. in *Methods in Molecular Biology* ed. Nickoloff, J. A. (Humana, Totowa, NJ):253-259.

210. **Sartakova, M., E. Dobrikova, and F. C. Cabello.** 2000. Development of an extrachromosomal cloning vector system for use in *Borrelia burgdorferi*. Proc Natl Acad Sci U S A **97:**4850-5.

211. **Sartakova, M. L., E. Y. Dobrikova, M. A. Motaleb, H. P. Godfrey, N. W. Charon, and F. C. Cabello.** 2001. Complementation of a nonmotile *flaB* mutant of *Borrelia burgdorferi* by chromosomal integration of a plasmid containing a wild-type *flaB* allele. J Bacteriol **183:**6558-64.

212. **Sartakova, M. L., E. Y. Dobrikova, D. A. Terekhova, R. Devis, J. V. Bugrysheva, O. V. Morozova, H. P. Godfrey, and F. C. Cabello.** 2003. Novel antibiotic-resistance markers in pGK12-derived vectors for *Borrelia burgdorferi*. Gene **303:**131-7.

213. **Schaible, U. E., S. Gay, C. Museteanu, M. D. Kramer, G. Zimmer, K. Eichmann, U. Museteanu, and M. M. Simon.** 1990. Lyme borreliosis in the severe combined immunodeficiency (scid) mouse manifests predominantly in the joints, heart, and liver. Am J Pathol **137:**811-20.

214. **Schaible, U. E., M. D. Kramer, K. Eichmann, M. Modolell, C. Museteanu, and M. M. Simon.** 1990. Monoclonal antibodies specific for the outer surface protein A (OspA) of *Borrelia burgdorferi* prevent Lyme borreliosis in severe combined immunodeficiency (scid) mice. Proc Natl Acad Sci U S A **87:**3768-72.

215. **Schena, M., D. Shalon, R. W. Davis, and P. O. Brown.** 1995. Quantitative Monitoring of Gene Expression Patterns with a Complementary DNA Microarray. Science **270:**467-470.

216. **Schwan, T., J. Piesman, W. Golde, M. Dolan, and P. Rosa.** 1995. Induction of an Outer Surface Protein on *Borrelia burgdorferi* During Tick Feeding. PNAS **92:**2909-2913.

217. **Schwan, T. G., W. Burgdorfer, and C. F. Garon.** 1988. Changes in infectivity and plasmid profile of the Lyme disease spirochete, *Borrelia burgdorferi*, as a result of *in vitro* cultivation. Infect Immun **56:**1831-6.

218. **Schwan, T. G., and J. Piesman.** 2000. Temporal changes in outer surface proteins A and C of the lyme disease-associated spirochete, *Borrelia burgdorferi*, during the chain of infection in ticks and mice. J Clin Microbiol **38:**382-8.

219. **Schwan, T. G., M. E. Schrumpf, R. H. Karstens, J. R. Clover, J. Wong, M. Daugherty, M. Struthers, and P. A. Rosa.** 1993. Distribution and molecular analysis of Lyme disease spirochetes, *Borrelia burgdorferi*, isolated from ticks throughout California. J Clin Microbiol **31:**3096-108.

220. **Scriminti, R. J.** 1970. Erythema chronicum migrans. Arch. Dermatol. **102:**104-5.

221. **Sellati, T. J., D. A. Bouis, R. L. Kitchens, R. P. Darveau, J. Pugin, R. J. Ulevitch, S. C. Gangloff, S. M. Goyert, M. V. Norgard, and J. D. Radolf.** 1998. *Treponema pallidum* and *Borrelia burgdorferi* lipoproteins and synthetic lipopeptides activate monocytic cells via a CD14-dependent pathway distinct from that used by lipopolysaccharide. J Immunol **160:**5455-64.

222. **Shapiro, E. D., and M. A. Gerber.** 2000. Lyme disease. Clin Infect Dis **31:**533-42.

223. **Shehan, D. C., and B. B. Hrapchak.** 1980. Theory and Practice of Histotechnology, 2nd edition.

224. **Skare, J. T., T. A. Mirzabekov, E. S. Shang, D. R. Blanco, H. Erdjument-Bromage, J. Bunikis, S. Bergstrom, P. Tempst, B. L. Kagan, J. N. Miller, and M. A. Lovett.** 1997. The Oms66 (*p66*) protein is a *Borrelia burgdorferi* porin. Infect Immun **65:**3654-61.

225. **Skare, J. T., E. S. Shang, D. M. Foley, D. R. Blanco, C. I. Champion, T. Mirzabekov, Y. Sokolov, B. L. Kagan, J. N. Miller, and M. A. Lovett.** 1995.

Virulent strain associated outer membrane proteins of *Borrelia burgdorferi*. J Clin Invest **96:**2380-92.

226. **Smolen, J. S.** 1984. [Lyme disease--another tick-borne disease in Austria]. Wien Klin Wochenschr **96:**823-9.

227. **Smoot, L. M., J. C. Smoot, M. R. Graham, G. A. Somerville, D. E. Sturdevant, C. A. L. Migliaccio, G. L. Sylva, and J. M. Musser.** 2001. Global differential gene expression in response to growth temperature alteration in group A Streptococcus. PNAS **98:**10416-10421.

228. **Sperandio, V., A. G. Torres, J. A. Giron, and J. B. Kaper.** 2001. Quorum Sensing Is a Global Regulatory Mechanism in Enterohemorrhagic *Escherichia coli* O157:H7. J. Bacteriol. **183:**5187-5197.

229. **Stanek, G., N. Satz, F. Strle, and B. Wilske.** 1993. Aspects of Lyme borreliosis, Wever, K. & Burgdorfer, W. eds.**:**358--70.

230. **Steere, A. C.** 1993. Current understanding of Lyme disease. Hosp Pract (Off Ed) **28:**37-44.

231. **Steere, A. C.** 2001. Lyme disease. N Engl J Med **345:**115-25.

232. **Steere, A. C.** 1994. Lyme disease: a growing threat to urban populations. Proc Natl Acad Sci U S A **91:**2378-83.

233. **Steere, A. C., J. Coburn, and L. Glickstein.** 2004. The emergence of Lyme disease. J Clin Invest **113:**1093-101.

234. **Steere, A. C., E. Dwyer, and R. Winchester.** 1990. Association of chronic Lyme arthritis with HLA-DR4 and HLA-DR2 alleles. N Engl J Med **323:**219-23.

235. **Steere, A. C., R. L. Grodzicki, A. N. Kornblatt, J. E. Craft, A. G. Barbour, W. Burgdorfer, G. P. Schmid, E. Johnson, and S. E. Malawista.** 1983. The spirochetal etiology of Lyme disease. N Engl J Med **308:**733-40.

236. **Steere, A. C., D. Gross, A. L. Meyer, and B. T. Huber.** 2001. Autoimmune mechanisms in antibiotic treatment-resistant lyme arthritis. J Autoimmun **16:**263-8.

237. **Steere, A. C., S. E. Malawista, J. A. Hardin, S. Ruddy, W. Askenase, and W. A. Andiman.** 1977. Erythema chronicum migrans and Lyme arthritis: the enlarging clinical spectrum. Annals of Internal Medicine **86:**685-98.

238. **Steere, A. C., V. K. Sikand, F. Meurice, D. L. Parenti, E. Fikrig, R. T. Schoen, J. Nowakowski, C. H. Schmid, S. Laukamp, C. Buscarino, and D. S. Krause.** 1998. Vaccination against Lyme disease with recombinant *Borrelia burgdorferi* outer-surface lipoprotein A with adjuvant. Lyme Disease Vaccine Study Group. N Engl J Med **339:**209-15.

239. **Stevenson, B., L. K. Bockenstedt, and S. W. Barthold.** 1994. Expression and gene sequence of outer surface protein C of *Borrelia burgdorferi* reisolated from chronically infected mice. Infect Immun **62:**3568-71.

240. **Stevenson, B., J. L. Bono, A. Elias, K. Tilly, and P. Rosa.** 1998. Transformation of the Lyme disease spirochete *Borrelia burgdorferi* with heterologous DNA. J Bacteriol **180:**4850-5.

241. **Stevenson, B., N. El-Hage, M. A. Hines, J. C. Miller, and K. Babb.** 2002. Differential binding of host complement inhibitor factor H by *Borrelia burgdorferi*

Erp surface proteins: a possible mechanism underlying the expansive host range of Lyme disease spirochetes. Infect Immun **70:**491-7.

242. **Stevenson, B., T. G. Schwan, and P. A. Rosa.** 1995. Temperature-related differential expression of antigens in the Lyme disease spirochete, *Borrelia burgdorferi*. Infect Immun **63:**4535-9.

243. **Stevenson, B., K. Tilly, and P. A. Rosa.** 1996. A family of genes located on four separate 32-kilobase circular plasmids in *Borrelia burgdorferi* B31. J Bacteriol **178:**3508-16.

244. **Stewart, P., R. Byram, D. Grimm, K. Tilly, and P. Rosa.** 2005. The plasmids of *Borrelia burgdorferi*: essential genetic elements of a pathogen. Plasmid **53:**1-13.

245. **Stewart, P. E., G. Chaconas, and P. Rosa.** 2003. Conservation of plasmid maintenance functions between linear and circular plasmids in *Borrelia burgdorferi*. J Bacteriol **185:**3202-9.

246. **Stewart, P. E., R. Thalken, J. L. Bono, and P. Rosa.** 2001. Isolation of a circular plasmid region sufficient for autonomous replication and transformation of infectious *Borrelia burgdorferi*. Mol Microbiol **39:**714-21.

247. **Szeto, J., S. Ramirez-Arcos, C. Raymond, L. D. Hicks, C. M. Kay, and J.-A. R. Dillon.** 2001. Gonococcal MinD Affects Cell Division in *Neisseria gonorrhoeae* and *Escherichia coli* and Exhibits a Novel Self-Interaction. J. Bacteriol. **183:**6253-6264.

248. **Tai, K. F., Y. Ma, and J. J. Weis.** 1994. Normal human B lymphocytes and mononuclear cells respond to the mitogenic and cytokine-stimulatory activities of *Borrelia burgdorferi* and its lipoprotein OspA. Infect Immun **62:**520-8.

249. **Takayama, K., R. J. Rothenberg, and A. G. Barbour.** 1987. Absence of lipopolysaccharide in the Lyme disease spirochete, *Borrelia burgdorferi*. Infect Immun **55:**2311-3.

250. **Talaat, A. M., P. Hunter, and S. A. Johnston.** 2000. Genome-directed primers for selective labeling of bacterial transcripts for DNA microarray analysis. Nat Biotechnol **18:**679-82.

251. **Telford, S. R., 3rd, F. S. Kantor, Y. Lobet, S. W. Barthold, A. Spielman, R. A. Flavell, and E. Fikrig.** 1995. Efficacy of human Lyme disease vaccine formulations in a mouse model. J Infect Dis **171:**1368-70.

252. **Thomas, V., J. Anguita, S. Samanta, P. A. Rosa, P. Stewart, S. W. Barthold, and E. Fikrig.** 2001. Dissociation of infectivity and pathogenicity in *Borrelia burgdorferi*. Infect Immun **69:**3507-9.

253. **Thompson, R. S., W. Burgdorfer, R. Russell, and B. J. Francis.** 1969. Outbreak of tick-borne relapsing fever in Spokane County, Washington. Jama **210:**1045-50.

254. **Tilly, K., A. F. Elias, J. L. Bono, P. Stewart, and P. Rosa.** 2000. DNA exchange and insertional inactivation in spirochetes. J Mol Microbiol Biotechnol **2:**433-42.

255. **Tourand, Y., K. Kobryn, and G. Chaconas.** 2003. Sequence-specific recognition but position-dependent cleavage of two distinct telomeres by the *Borrelia burgdorferi* telomere resolvase, ResT. Mol Microbiol **48:**901-11.

256. **Trueba, G. A., I. G. Old, I. Saint Girons, and R. C. Johnson.** 1997. A cheA cheW operon in *Borrelia burgdorferi*, the agent of Lyme disease. Res Microbiol **148:**191-200.

257. **Varela, A. S., M. P. Luttrell, E. W. Howerth, V. A. Moore, W. R. Davidson, D. E. Stallknecht, and S. E. Little.** 2004. First culture isolation of *Borrelia lonestari*, putative agent of southern tick-associated rash illness. J Clin Microbiol **42:**1163-9.

258. **Wang, G., Y. Ma, A. Buyuk, S. McClain, J. J. Weis, and I. Schwartz.** 2004. Impaired host defense to infection and Toll-like receptor 2-independent killing of *Borrelia burgdorferi* clinical isolates in TLR2-deficient C3H/HeJ mice. FEMS Microbiol Lett **231:**219-25.

259. **Wang, G., A. P. van Dam, I. Schwartz, and J. Dankert.** 1999. Molecular typing of *Borrelia burgdorferi sensu lato*: taxonomic, epidemiological, and clinical implications. Clin Microbiol Rev **12:**633-53.

260. **Weis, J. J., Y. Ma, and L. F. Erdile.** 1994. Biological activities of native and recombinant *Borrelia burgdorferi* outer surface protein A: dependence on lipid modification. Infect Immun **62:**4632-6.

261. **Willett, T. A., A. L. Meyer, E. L. Brown, and B. T. Huber.** 2004. An effective second-generation outer surface protein A-derived Lyme vaccine that eliminates a potentially autoreactive T cell epitope. Proc Natl Acad Sci U S A **101:**1303-8.

262. **Wilske, B., A. G. Barbour, S. Bergstrom, N. Burman, B. I. Restrepo, P. A. Rosa, T. Schwan, E. Soutschek, and R. Wallich.** 1992. Antigenic variation and strain heterogeneity in Borrelia *spp.* Res Microbiol **143:**583-96.

263. **Wilske, B., U. Busch, H. Eiffert, V. Fingerle, H. W. Pfister, D. Rossler, and V. Preac-Mursic.** 1996. Diversity of OspA and OspC among cerebrospinal fluid isolates

of *Borrelia burgdorferi sensu lato* from patients with neuroborreliosis in Germany. Med Microbiol Immunol (Berl) **184:**195-201.

264. **Wilske, B., U. Busch, V. Fingerle, S. Jauris-Heipke, V. Preac Mursic, D. Rossler, and G. Will.** 1996. Immunological and molecular variability of OspA and OspC. Implications for Borrelia vaccine development. Infection **24:**208-12.

265. **Wilske, B., V. Preac-Mursic, U. B. Gobel, B. Graf, S. Jauris, E. Soutschek, E. Schwab, and G. Zumstein.** 1993. An OspA serotyping system for *Borrelia burgdorferi* based on reactivity with monoclonal antibodies and OspA sequence analysis. J Clin Microbiol **31:**340-50.

266. **Wilson, M., J. DeRisi, H.-H. Kristensen, P. Imboden, S. Rane, P. O. Brown, and G. K. Schoolnik.** 1999. Exploring drug-induced alterations in gene expression in *Mycobacterium tuberculosis* by microarray hybridization. PNAS **96:**12833-12838.

267. **Wilson, M. L., and A. Spielman.** 1985. Seasonal activity of immature *Ixodes dammini* (Acari: Ixodidae). J Med Entomol **22:**408-14.

268. **Woods, A. E., and R. C. Ellis.** 1996. Laboratory Histopathology, A Complete Reference.

269. **Xu, Y., C. Kodner, L. Coleman, and R. Johnson.** 1996. Correlation of plasmids with infectivity of *Borrelia burgdorferi sensu stricto* type strain B31. Infect. Immun. **64:**3870-3876.

270. **Yang, X., M. S. Goldberg, T. G. Popova, G. B. Schoeler, S. K. Wikel, K. E. Hagman, and M. V. Norgard.** 2000. Interdependence of environmental factors

influencing reciprocal patterns of gene expression in virulent *Borrelia burgdorferi*. Mol Microbiol **37:**1470-9.

271. **Yang, X., T. G. Popova, M. S. Goldberg, and M. V. Norgard.** 2001. Influence of cultivation media on genetic regulatory patterns in *Borrelia burgdorferi*. Infect Immun **69:**4159-63.

272. **Yang, X., T. G. Popova, K. E. Hagman, S. K. Wikel, G. B. Schoeler, M. J. Caimano, J. D. Radolf, and M. V. Norgard.** 1999. Identification, characterization, and expression of three new members of the *Borrelia burgdorferi* Mlp (2.9) lipoprotein gene family. Infect Immun **67:**6008-18.

273. **Yang, X. F., S. M. Alani, and M. V. Norgard.** 2003. The response regulator Rrp2 is essential for the expression of major membrane lipoproteins in *Borrelia burgdorferi*. Proc Natl Acad Sci U S A **100:**11001-6.

274. **Yang, X. F., A. Hubner, T. G. Popova, K. E. Hagman, and M. V. Norgard.** 2003. Regulation of expression of the paralogous Mlp family in *Borrelia burgdorferi*. Infect Immun **71:**5012-20.

275. **Yang, X. F., U. Pal, S. M. Alani, E. Fikrig, and M. V. Norgard.** 2004. Essential role for OspA/B in the life cycle of the Lyme disease spirochete. J Exp Med **199:**641-8.

276. **Yssel, H., M. C. Shanafelt, C. Soderberg, P. V. Schneider, J. Anzola, and G. Peltz.** 1991. *Borrelia burgdorferi* activates a T helper type 1-like T cell subset in Lyme arthritis. J Exp Med **174:**593-601.

277. **Zhang, J. R., J. M. Hardham, A. G. Barbour, and S. J. Norris.** 1997. Antigenic variation in Lyme disease borreliae by promiscuous recombination of VMP-like sequence cassettes. Cell **89:**275-85.

278. **Zhang, J. R., and S. J. Norris.** 1998. Genetic variation of the *Borrelia burgdorferi* gene *vlsE* involves cassette-specific, segmental gene conversion. Infect Immun **66:**3698-704.

279. **Zhang, J. R., and S. J. Norris.** 1998. Kinetics and *in vivo* induction of genetic variation of *vlsE* in *Borrelia burgdorferi*. Infect Immun **66:**3689-97.

280. **Zhong, J., and A. G. Barbour.** 2004. Cross-species hybridization of a *Borrelia burgdorferi* DNA array reveals infection- and culture-associated genes of the unsequenced genome of the relapsing fever agent *Borrelia hermsii*. Mol Microbiol **51:**729-48.

281. **Zhong, W., T. Stehle, C. Museteanu, A. Siebers, L. Gern, M. Kramer, R. Wallich, and M. M. Simon.** 1997. Therapeutic passive vaccination against chronic Lyme disease in mice. Proc Natl Acad Sci U S A **94:**12533-8.

282. **Zumstein, G., R. Fuchs, A. Hofmann, V. Preac-Mursic, E. Soutschek, and B. Wilske.** 1992. Genetic polymorphism of the gene encoding the outer surface protein A (OspA) of *Borrelia burgdorferi*. Med Microbiol Immunol (Berl) **181:**57-70.

VITA

Andrew "Drew" Thomas Revel was born at St. Mary's Catholic Hospital outside Pueblo Army Depot in Pueblo, Colorado on March 20, 1972, the second child of James Leon and Ellen Louise Wood Revel. He was named after his maternal great-grandfather (Dr. Vernon Andrew Suydam, Ph. D.) and his paternal grandmother (Lorraine Thomas Revel). His sister was born three years prior on March 19, 1969 on Fort Bliss Army Post in El Paso, Texas. Until age five, Drew's family moved often (Aberdeen, Maryland; Auburn, Alabama; and Perry, Georgia) because his father was on active duty in the United States Army, Ordnance Corp. By second grade, Drew's family settled in Dallas, Texas where they lived for ten years. While in Dallas, Drew was awarded the rank of Eagle Scout from the Boy Scouts Of America, as well as first place from the Texas State Science Fair for his two-year investigation on the side effects resulting from the use of the chemotherapeutic agent, Cyclophosphamide. Then in the summer between Drew's junior and senior years in high school, his family moved to Austin, where he graduated in the top 10% of his class from Westwood High School.

While attending Auburn University, Drew was a member of the Army ROTC on a full scholarship. In March of 1995, Drew earned his Bachelor of Science degree in Molecular Biology. For six months after graduation, he worked at G. Heilman Brewing Company in Perry, Georgia as a microbiologist and quality control technician before moving to Washington, D.C. While in Washington, D.C., Drew worked at MedImmune, Inc. as well as attending Johns Hopkins University part time where he earned his Masters of Science

degree in Biotechnology. For nine months after graduating from Johns Hopkins University in August, 1998, Drew was employed by The Institute for Genomic Research in Rockville, Maryland as the Sequencing Core Research and Development / Quality Control team leader.

In June of 1999, Drew then moved to Dallas to enter the Graduate School of Biomedical Sciences at the University of Texas Southwestern Medical School at Dallas. A year later, he joined the Molecular Microbiology Graduate Program. While attending graduate school, he was the recipient of the 2000 Sigma Xi Research Forum Abstract Award and the 2001 S. Edward Sulkin Memorial Scholarship. He was awarded the degree of Doctor of Philosophy in March, 2005. He will be joining the lab of Dr. John J. Mekalanos, Ph. D. at Harvard Medical School as a post-doctoral fellow.

Permanent Address:

18403 Teal Creek Drive

Humble, Texas 72346

This dissertation was typed by Andrew T. Revel.